frontiers | Research Topics

Insights into the role of microorganisms on food quality and food safety

Edited by
Jinxuan Cao, Hongshun Yang, Wei Zhao,
Changyu Zhou and Zhihong Sun

Published in
Frontiers in Microbiology

ISSN 1664-8714
ISBN 978-2-8325-3107-5
DOI 10.3389/978-2-8325-3107-5

About Frontiers

Frontiers is more than just an open access publisher of scholarly articles: it is a pioneering approach to the world of academia, radically improving the way scholarly research is managed. The grand vision of Frontiers is a world where all people have an equal opportunity to seek, share and generate knowledge. Frontiers provides immediate and permanent online open access to all its publications, but this alone is not enough to realize our grand goals.

Frontiers journal series

The Frontiers journal series is a multi-tier and interdisciplinary set of open-access, online journals, promising a paradigm shift from the current review, selection and dissemination processes in academic publishing. All Frontiers journals are driven by researchers for researchers; therefore, they constitute a service to the scholarly community. At the same time, the *Frontiers journal series* operates on a revolutionary invention, the tiered publishing system, initially addressing specific communities of scholars, and gradually climbing up to broader public understanding, thus serving the interests of the lay society, too.

Dedication to quality

Each Frontiers article is a landmark of the highest quality, thanks to genuinely collaborative interactions between authors and review editors, who include some of the world's best academicians. Research must be certified by peers before entering a stream of knowledge that may eventually reach the public - and shape society; therefore, Frontiers only applies the most rigorous and unbiased reviews. Frontiers revolutionizes research publishing by freely delivering the most outstanding research, evaluated with no bias from both the academic and social point of view. By applying the most advanced information technologies, Frontiers is catapulting scholarly publishing into a new generation.

What are Frontiers Research Topics?

Frontiers Research Topics are very popular trademarks of the *Frontiers journals series*: they are collections of at least ten articles, all centered on a particular subject. With their unique mix of varied contributions from Original Research to Review Articles, Frontiers Research Topics unify the most influential researchers, the latest key findings and historical advances in a hot research area.

Find out more on how to host your own Frontiers Research Topic or contribute to one as an author by contacting the Frontiers editorial office: frontiersin.org/about/contact

Insights into the role of microorganisms on food quality and food safety

Topic editors

Jinxuan Cao — Beijing Technology and Business University, China
Hongshun Yang — Jiangnan University (Shaoxing) Industrial Technology Research Institute, China
Wei Zhao — Jiangnan University, China
Changyu Zhou — Ningbo University, China
Zhihong Sun — Inner Mongolia Agricultural University, China

Citation

Cao, J., Yang, H., Zhao, W., Zhou, C., Sun, Z., eds. (2023). *Insights into the role of microorganisms on food quality and food safety*. Lausanne: Frontiers Media SA. doi: 10.3389/978-2-8325-3107-5

Table of contents

frontiers | Frontiers in Microbiology

TYPE Editorial
PUBLISHED 13 July 2023
DOI 10.3389/fmicb.2023.1237508

OPEN ACCESS

EDITED AND REVIEWED BY
Giovanna Suzzi,
University of Teramo, Italy

*CORRESPONDENCE
Ying Wang
✉ wang-ying@btbu.edu.cn

RECEIVED 09 June 2023
ACCEPTED 28 June 2023
PUBLISHED 13 July 2023

CITATION
Cao J, Wang Y, Zhou C and Geng F (2023) Editorial: Insights into the role of microorganisms on food quality and food safety. *Front. Microbiol.* 14:1237508. doi: 10.3389/fmicb.2023.1237508

Editorial: Insights into the role of microorganisms on food quality and food safety

Jinxuan Cao[1], Ying Wang[1]*, Changyu Zhou[2] and Fang Geng[3]

[1]School of Food and Health, Beijing Technology and Business University, Beijing, China, [2]College of Food and Pharmaceutical Sciences, Ningbo University, Ningbo, China, [3]Meat Processing Key Laboratory of Sichuan Province, School of Food and Biological Engineering, Chengdu University, Chengdu, China

KEYWORDS

microorganisms, food quality, food safety, volatile compounds, spoilage

Editorial on the Research Topic
Insights into the role of microorganisms on food quality and food safety

With increasing health awareness, food safety and quality have been a growing demand globally. Food safety and quality depend upon many factors, including microbes in food production, processing, preservation, and storage. On the one hand, microbes such as bacteria, molds, and yeasts have a long history of application in food production, such as in the production of wine, beer, bread, and dairy products. On the other hand, the growth of microorganisms and contamination by microorganisms lead to food spoilage or even foodborne illness, threatening the development of the food industry.

Microorganisms play a crucial role in the production, preservation, and improvement of food. By transforming the chemical constituents of raw materials of plant/animal sources, functional microorganisms, particularly bacteria and yeast, can improve the sensory quality of food, enhance the bioactivity of nutrients, produce antioxidant and antimicrobial compounds, and promote food safety.

The physicochemical properties and the volatile flavor compounds of food are closely related to the nature of microorganisms, especially in fermented food. Liu, Cao et al. utilized a mixture of *yeast* and *Lactobacillus rhamnosus* YL-1 as a starter in the fermentation process of salami sausage, which could effectively decrease the degree of lipid oxidation and result in changes in flavor profiles. The combination of *Lactobacillus fermentum* YZU-06, *Staphylococcus saprophyticus* CGMCC 3475, and leucine has also been applied in the production of fermented sausage, which improves not only the diversity of flavor compounds but also the overall quality of sausages (Liu R. et al.). Liao et al. compared the quality and the main metabolic changes of instant dark teas fermented by different fungi, such as *Aspergillus cristatus*, *Aspergillus niger*, and *Aspergillus tubingensis*, revealing that the chemical constituents of instant dark teas were affected by the fungi. Tao et al. reviewed the utilization of microbiome in the fermentation process, which could remove the unpleasant beany flavors and enhance the aroma profile of plant-based meat analogs. Probiotics make a great

contribution to gut health by improving digestion and enhancing nutrient absorption. Zhu Y. et al. demonstrated that feeding patterns can affect gut microbiota and the metabolites of Tibetan pigs, which further led to changes in meat quality.

The process of fermentation is influenced by several factors such as temperature, time, pH, oxygen levels, and microbial starter cultures. Food quality can be monitored through the regulation of fermentation conditions. Yu et al. found that the temperature of beef aging could affect the microbial community, physiochemical attributes, and flavor profiles of beef. Liu A. et al. observed significant differences between the bacterial community of vinegar from the same day with different fermentation depths, but no apparent difference appeared in the fungal community. In addition, the function of microbiota and volatile flavor compounds were affected by the microbial community at different depths. By comparing the physicochemical properties and microbial community compositions of Jinhua fat ham and lean ham, Zhang et al. explored the potential mechanism of characteristic microorganisms affecting the formation of flavor in lean dry-cured hams.

Spoilage and pathogenic microorganisms are considered one of the main factors threatening food quality and safety (Liu C. et al.; Guo et al.; Fulano et al.). Unscientific storage of food can cause an infestation of harmful microorganisms. For example, various fungal strains have been found in the production and preservation of dark tea, leading to the proliferation of fungi toxins. Xu et al. reviewed the contamination levels of common mycotoxin species, the main microbial sources of mycotoxin, and the possible ways to cause mycotoxin contamination in dark tea, providing a foundation for the prevention of harmful fungi.

To avoid illness and prevent food from spoiling, various technologies of food preservation have been developed to control the growth of microorganisms. Some microorganisms produce antimicrobial compounds and organic acids that inhibit the growth of spoilage-causing bacteria. Chen et al. found that the microbiota, mainly *Lactobacillus*, inhibited the formation of biogenic amines during the traditional fermentation of *Scomber japonicus*. To extend the shelf life of food, packaging materials have been explored to protect food from chemical and microbiological changes. Schmid et al. investigated the contaminating bacterial growth and survival in different fiber-based food packaging materials and evaluated the role of pH as an intrinsic antimicrobial factor. Furthermore, some active substances have been found to have inhibitory effects on the growth and toxicity production of microorganisms. Some *Aspergillus niger* produce ochratoxin A, which has harmful effects on human health, whereas tea polyphenols and epigallocatechin gallate were found to inhibit the growth of *Aspergillus niger* and ochratoxin synthesis, according to Zhao et al.'s study. Based on Propidium Monoazide combined with real-time PCR, Liu, Huang et al. developed a new method for fast detection of the antibacterial and bacteriostatic activity of disinfectants.

In conclusion, this Research Topic explored the beneficial and harmful effects of microorganisms on food quality and safety, highlighting the correlation between microbial community and volatile compounds. The reasonable application of beneficial microorganisms and the regulation of harmful microbial infestation are essential to achieve the desired properties, leading to reliable food products and ensuring food quality, safety, and consistency.

Author contributions

YW, CZ, and FG collected literatures, organized information, and wrote the first draft of the article. JC provided writing ideas and checked and revised the first draft. All authors contributed to the article and approved the submitted version.

Funding

This study was supported by the National Natural Science Foundation of China (No. 41927806), the Fundamental Research Funds for the Central Universities (No. lzujbky-2021-ct04), and the Education Science and Technology Innovation Project of Gansu Province (Grant No. 2021A-008).

Acknowledgments

We deeply thank all the authors and reviewers who have participated in this Research Topic.

Conflict of interest

The authors declare that the research was conducted in the absence of any commercial or financial relationships that could be construed as a potential conflict of interest.

Publisher's note

frontiers | Frontiers in Microbiology

TYPE Original Research
PUBLISHED 02 November 2022
DOI 10.3389/fmicb.2022.1030789

OPEN ACCESS

EDITED BY
Jinxuan Cao,
Beijing Technology and Business University, China

REVIEWED BY
Shengjun Chen,
South China Sea Fisheries Research Institute (CAFS), China
Shiling Lu,
Shihezi University, China
Wenshui Xia,
Jiangnan University, China

*CORRESPONDENCE
Changrong Ou
ouchangrong@nbu.edu.cn

SPECIALTY SECTION
This article was submitted to Food Microbiology, a section of the journal Frontiers in Microbiology

RECEIVED 29 August 2022
ACCEPTED 10 October 2022
PUBLISHED 02 November 2022

CITATION
Chen J, Tang H, Zhang M, Sang S, Jia L and Ou C (2022) Exploration of the roles of microbiota on biogenic amines formation during traditional fermentation of *Scomber japonicus*. *Front. Microbiol.* 13:1030789. doi: 10.3389/fmicb.2022.1030789

Exploration of the roles of microbiota on biogenic amines formation during traditional fermentation of *Scomber japonicus*

Jingyi Chen[1], Haiqing Tang[2], Mengsi Zhang[1], Shangyuan Sang[1] Lingling Jia[1], and Changrong Ou[1,3]*

[1]College of Food and Pharmaceutical Sciences, Ningbo University, Ningbo, China, [2]Faculty of Food Science, Zhejiang Pharmaceutical University, Ningbo, China, [3]Key Laboratory of Animal Protein Food Deep Processing Technology of Zhejiang Province, Ningbo University, Ningbo, China

The influence of microbiota composition and metabolisms on the safety and quality of fermented fish products is attracting increasing attention. In this study, the total viable count (TVC), pH, total volatile base nitrogen (TVB-N) as well as biogenic amines (BAs) of traditional fermented *Scomber japonicus* (*zaoyu*) were quantitatively determined. To comprehend microbial community variation and predict their functions during fermentation, 16S rRNA-based high-throughput sequencing (HTS) and phylogenetic investigation of communities by reconstruction of unobserved states (PICRUSt) were employed, respectively. The fresh samples stored without fermentation were used as controls. TVC and TVB-N values increased rapidly, and the content of BAs exceeded the permissible limit on day 2 in the controls, indicating serious spoilage of the fish. In contrast, a slower increase in TVC and TVB-N was observed and the content of BAs was within the acceptable limit throughout the fermentation of *zaoyu*. Significant differences in microbiota composition were observed between *zaoyu* and the controls. The bacterial community composition of *zaoyu* was relatively simple and *Lactobacillus* was identified as the dominant microbial group. The accumulation of histamine was inhibited in *zaoyu,* which was positively correlated with the relative abundance of *Vibrio*, *Enterobacter*, *Macrococcus*, *Weissella*, et al. based on Redundancy analysis (RDA), while *Lactobacillus* showed a positive correlation with tyramine, cadaverine, and putrescine. Functional predictions, based on Kyoto Encyclopedia of Genes and Genomes (KEGG) pathways analysis, revealed that the relative abundance of metabolic function exhibited a decreasing trend with prolonged fermentation time and the abundance of metabolism-related genes was relatively stable in the later stage of fermentation. Those metabolisms related to the formation of BAs like histidine metabolism and arginine metabolism were inhibited in *zaoyu*. This study has accompanied microbiota analysis and functional metabolism with the accumulation of BAs to trace their correspondences, clarifying the roles of microorganisms in the inhibition of BAs during fermentation of *Scomber japonicus*.

KEYWORDS

fermented *Scomber japonicus* (*zaoyu*), biogenic amines, MiSeq sequencing, microbiota composition, PICRUSt

Introduction

Scomber japonicus is an economically important fish species extensively distributed in the East China Sea, the Yellow Sea, and the Sea of Japan (Yu et al., 2018). It is noted for its pleasant aroma and high nutritional value, whereas it is rich in free histidine in muscle tissues, which is commonly implicated in incidents of histamine poisoning (Visciano et al., 2012). Hence the preservation of *Scomber* has been a quite challenging issue. Fermentation plays a vital role around the world for the preservation of aquatic products, such as *Narezushi* in Japan (Doi et al., 2021), *Gravlax* in Northern Europe (Wiernasz et al., 2020) and *zaoyu* in China. *Zaoyu* is a traditional fermented product made by mixing fish and fermented rice, then sealed in the vessel for a long-term fermentation under anaerobic conditions, which is usually made from several marine species such as *Scomber japonicus, Miichthys miiuy, Trichiurus lepturus, Muraenesox cinereus*, and freshwater species (Chen et al., 2021). The fermentation process imparts a distinctive flavor to the final products. Typically high levels of biogenic amines (BAs) have been found in some fermented fish products like fish sauce (Kuda et al., 2012) and dried fish (Huang et al., 2010), owing to the availability of amino acids, which may be the potential precursors of BAs. However, it's worth noting that the formation of BAs was inhibited during the preparation of *zaoyu*.

BAs are low molecular weight organic bases with biological activity that are formed by microbial decarboxylase of the corresponding amino acid or transamination of aldehydes and ketones by amino acid transaminases (Zhai et al., 2012). The intake of foods with high concentration of BAs could provoke those adverse reactions like migraine, brain hemorrhage, heart failure, hypertension, urticaria, and headache as well (Rice et al., 1976). The most common sources of BAs intoxication are histamine (His) and tyramine (Tyr) (Smith, 1981), produced by the decarboxylation of histidine and tyrosine, respectively. Putrescine (Put) and cadaverine (Cad) could enhance histamine toxicity through interfering with the histamine detoxification system (Kim et al., 2009). The formation of BAs in fermented foods might result from a complex process and could be influenced by many factors and their interactions (Sang et al., 2020).

Spontaneously fermented fish has a unique flavor, while it is restricted by the relatively long production period and the risk of spoilage is higher. Hence the inoculum of suitable microorganisms, defined as starter cultures, has become a widely adopted approach in fermented food. Bover-Cid et al. have shown that the incorporation of pure or mixed amine-negative starter cultures is capable of inhibiting microorganisms with amino acid-decarboxylase activity in fermented products (Bover-Cid et al., 2000; Hu et al., 2007). However, the use of commercial starter cultures may reduce the microbial diversity of fermented food, and the dominant bacteria may inhibit the growth of other microorganisms including those contributing to the flavor formation. *Zaoyu* is produced on the basis of the traditional fermentation method, mostly relying on the community of autochthonous microorganisms from fermented rice. The addition of fermented rice as natural starter culture differs from spontaneous fermentation, which could not only promote the appearance of dominant bacteria, but also be used as the supplementary substrate for carbon sources during traditional fermentation (Bassi et al., 2015). Besides, figuring out the microbiota composition of *zaoyu* is vital for the application of synthetic microbial community (SMC) in fermented foods, which could construct a controllable and stable microbial interaction network and might serve as a potential strategy to control the quality of fermented fish in the future (Han et al., 2022).

Dynamic changes and interactions of the microbiota during fermentation were found to play a critical role in the quality characterization. Since spoilage potentials and metabolic characteristics of different microbes vary significantly and could be affected by microbial interactions (Lu et al., 2018). High-throughput sequencing (HTS) with the properties of high flux and short experimental cycle has recently been applied to the analysis of microbial systems in different food matrices, such as fish sauce (Wang et al., 2018), reef fishes (Gao et al., 2020), and Pacific white shrimp (Guan et al., 2021). A great potential of HTS is facilitating the exploration of the relationships between the microbiota composition and specific variables like BAs (Hao and Sun, 2020), salinity (Mengjuan et al., 2021). Phylogenetic investigation of communities by reconstruction of unobserved states (PICRUSt), a technique predicting metagenomes based on 16S rRNA gene data and a reference genome database (Yan et al., 2019), provides a great amount of information about the genetic profile and metabolic potential of microbiota composition. Combined with both technologies could determine the dynamic changes of microbial community in *zaoyu* and get a comprehensive view of the role that fermentation played in inhibiting the accumulation of BAs from the perspective of microorganism.

The aim of this study is to explore microbial succession during fermentation of *Scomber japonicus* and demonstrate the correlation among the microbiota composition, functional

metabolism and the formation of BAs. The microbiota composition of *zaoyu* also may serve as a promising model system to study eco-evolutionary dynamics, such multidisciplinary approach is expected to improve the property and quality of fermented foods.

Materials and methods

Source of samples

Fresh *Scomber japonicus* was obtained from a local market in Ningbo, Zhejiang Province, China, and filleted to collect the dorsal muscle. The dorsal muscle was cut with a knife into blocks of 7 × 7 × 4 cm and were cleaned with tap water and mixed with 12% saline marinate in a barrel for 3 h, then drained the water for 12 h. *Zaoyu* was prepared according to the traditional techniques by mixing fresh fish with fermented rice and were neatly stacked layer-by-layer in a barrel for fermentation. Then *Zaoyu* samples were collected at 0, 1, 2, 4, 6 and 8 days of the fermentation stages for further analysis as experimental group. The fresh *Scomber japonicus* stored at 28°C under the same conditions were used as controls, and fermented rice was collected as the other controls named Z. All of the experiments were conducted in three replications.

Methods

Enumeration of cultivable microbes

The TVC was determined based on the National Standards of the People's Republic of China (GB 4789.2-2016). Briefly, an aliquot of 2.5g fish filets was collected in an aseptic manner, put into aseptic bag, and homogenized in 22.5 ml of physiological saline for 2 min. The homogenates were serially diluted with sterile physiological saline (1:10), and 1.0 ml aliquots of the dilutes were poured onto a 15–20 ml of plate count agar medium to obtain a mixture. Colonies on the plates were identified posterior to incubation under 30°C for 72 h. The total number of the colony was described as lg CFU/g.

Determination of physicochemical indices.

The water content was measured with a moisture analyzer (MB27; OHAUS, American). An aliquot of 2.0 g samples was homogenized in 20 ml of distilled water at room temperature and then recorded *via* a digital pH meter (PHS-2F, Leici, Shanghai, China). TVB-N levels were identified *via* a semi-micro determination of nitrogen approach as per the Chinese Standard (GB 5009.288-2016). All samples for analysis were ground individually using a meat grinder. An aliquot of 4.0 g ground filets was taken into a beaker, blended with 20 ml distilled water, then impregnated still for 30 min and shook the beaker every 10 min. Next, the solution was filtered through the filter paper, then 5 ml of filtrate was made alkaline by adding 5 ml of 10 g/L Magnesia (MgO). Steam distillation was distilled for 5 min using a Kjeldahl distillation unit. The distillate was absorbed by 10 ml of 20 g/L boric acid, and titrated with 0.01 mol/L HCl. The result stated for each sample is the mean value of two measurements, TVB-N content was calculated and expressed with a unit of mg/100 g.

Determination of biogenic amines

The separation and quantification of BAs were carried out according to the liquid chromatography–tandem mass spectrometry method (Waters Alliance e2695) using 1,7-diaminoheptane as internal standard. For the analysis, 2 g of sample was ground in a Waring blender for 60 s and thoroughly homogenized with 20 ml of distilled water. The obtained homogenate was decanted into centrifuge tubes and added acetonitrile (20 ml), ethanol (3 ml), n-hexane (5 ml), followed by centrifugation (5,000 rpm, 5 min). The supernatant was collected and cleaned with methylene chloride (2 × 2 ml) twice. The solution was then filtered with 0.45 μm filter paper and diluted 1:4 with pure water before injection in the column equipped with ACQUITY HSS T3 (100 mm × 2.1 mm, 1.8 μm; Waters Technologies (Shanghai) Limited). The mobile phases of LC–MS/MS were A: 2 mM/L ammonium acetate, and B: methanol containing 0.1% formic acid. The flow rate was 0.2 ml/min.

Total DNA extraction, PCR reaction and MiSeq sequencing

Total genomic DNA was extracted from the muscle of mackerel samples (10 g) with the instructions of the E.Z.N.A® Bacterial DNA kit following the manufacturer's instructions. DNA samples were then stored at −80°C before amplification. The V3-V4 (341F: 5′-CCTACGGGNGGCWGCAG-3′, 806R: 5′-GGACTACNNGGGTATCTAAT-3′) hypervariable regions of the bacterial 16S rRNA genes were, respectively, amplified using the genomic DNA extracts for each sample. The reactions mixture (25 μl) included 2.5 μl of 10 × PCR buffer, 2.0 μl of dNTP, 0.5 μl of each primer, 1.0 μl of DNA, 0.5 μl of TaqE and 18 μl of ddH_2O. PCR reactions were conducted in a Thermal Cycler under the following conditions: initial denaturation at 95°C for 3 min, followed by 30 cycles of denaturation at 95°C for 30 s, primer annealing at 57°C for 1 min, and extension at 72°C for 45 s, and a final extension step at 72°C for 10 min. The PCR products and expected size were checked by 1% agarose gel electrophoresis and were purified with a quick gel extraction kit. The concentration and quality of amplicons were measured using a NanoDrop-1000 spectrophotometer. Sequencing was performed on an Illumina MiSeq platform at Novogene Bioinformatics Technology Co. Ltd.

Statistical analysis

The bioinformatics analysis was performed with QIIME 2 (2021.11). Then quality filter, denoising, merging, and chimera removal were conducted by the DADA2 plugin. The sequences were clustered at the level of 97% similarity and the representative sequence of each operational taxonomic unit (OTU) was annotated by Silva database. Analysis of α-diversity

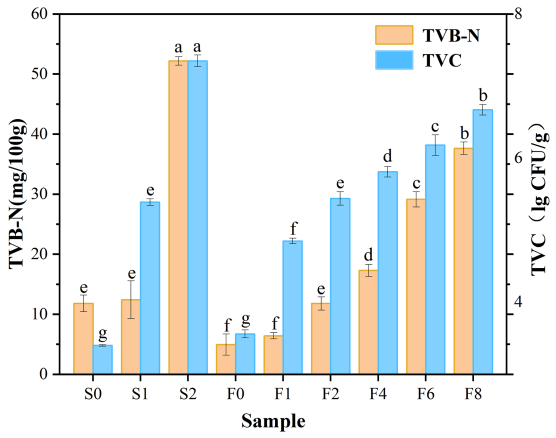

FIGURE 1
Changes in TVB-N and TVC values. Notes: S0, S1, S2 denote the controls on day 0, 1, 2, respectively; F0, F1, F2, F4, F6, F8 denote *zaoyu* on day 0, 1, 2, 4, 6, 8, respectively; Z denotes the fermented rice. Different letters (a, b, c etc.) indicate significantly different means at $p<0.05$ (analysis of variance; ANOVA). The same below.

and β-diversity was completed based on the platform of Personalbio.[1] The Linear discriminant analysis Effect Size (LEfSe) tool[2] was used to analyze the different species among the sample groups. Phylogenetic investigation of communities by reconstruction of unobserved states (PICRUSt) software and database was used to obtain Kyoto Encyclopedia of Genes and Genomes (KEGG) pathway information. Redundancy analysis (RDA) on interrelationships between microbiota composition and BAs was analyzed by canoco5. Physiochemical properties of samples were analyzed, expressed on mean ± standard deviation. One-way analysis of variance (ANOVA) with Tukey pairwise comparisons at $p < 0.05$ was used to assess the significance between alpha diversity indices and relative abundance rates among each group using SPSS16.0.

Results

Microbiological and chemical analysis

As shown in Figure 1, an increase in TVB-N value was observed during both storage and fermentation, which was in agreement with the microbial load. TVC values in the controls displayed an obvious upward trend and exceeded 7.0 lg CFU/g on day 2, which is the largest value that marine species are suitable for human consumption proposed by the ICMSF (ICMSF, 1986), and this observation was consistent with the trend in TVB-N value. Owing to the degradation of amino acids by microorganisms, the initial TVB-N value increased from 11.79 mg/100 g to 52.18 mg/100 g on day 2 of storage, which exceeded the upper acceptability limit of TVB-N in marine species of 30 mg/100 g according to the Chinese Standard GB/T 2733-2015, indicating it was already in a seriously spoiled state. Whereas it was observed that the amount of TVB-N increased relatively slighter in *zaoyu*, and TVC increased at a slower rate, being 6.67 lg CFU/g on the 8th day of fermentation, According to the microbial analysis below, the dominant microorganism was identified as *Lactobacillus*, which meant that the fermentation inhibited the growth of spoilage microorganisms. The formation of nitrogenous compounds in aquatic products is closely correlated with microbial metabolism indeed (Yu et al., 2019). The lower TVB-N and TVC values may be attributed to that the growth of some microorganisms is partially inhibited by the roles of fermentation. In addition, salting could also be an effective operation for inactivating microbes in the initial fermentation stage (Han et al., 2004).

Physicochemical features

The changes in moisture and pH were displayed in Figure 2. The increase in pH value during storage reflected the accumulation of TVB-N from bacterial activity and protein degradation (Moradi et al., 2019). In general, no significant changes in pH of *zaoyu* samples were observed. The initial pH presented a decreasing trend and reached a relatively stable value with slight fluctuation in the later period of fermentation. The decrease of pH was supposedly the result of the production of organic acids by fermentation (Jung et al., 2013), which was associated with the growth of *Lactobacillus*. The microbiota composition reached equilibrium in the late fermentation stage, which was also reflected in the pH changes. The slight increase in water content of *zaoyu* in the early stage may be attributed to the rehydration of the semi-dried fish soaked in the fermented rice, and the decrease on day 4 may be attributed to the changes in the water holding capacity of protein.

BAs analysis

Totally 8 BAs were detected, including His, Tyr, Put, Cad, 2-Phenethylamine (2-Phe), spermidine (Spd), spermine (Spm) and tryptamine (Try), while octopamine (Oct) was not detected in any samples analyzed (Table 1). His, Cad and Put were the major amines in the spoilage of *Scomber japonicus*, among which His was the most dominant and increased rapidly, reaching 479.64 mg/kg on day 2 of storage, which far exceeded the limit level suggested by the U.S. Food and Drug Administration (FDA; 50 mg/kg). Compared with the controls, the content of His in *zaoyu* increased slightly and was below

1 https://www.genescloud.cn
2 http://huttenhower.sph.harvard.edu/galaxy/root?tool_id=PICRUSt_normalize

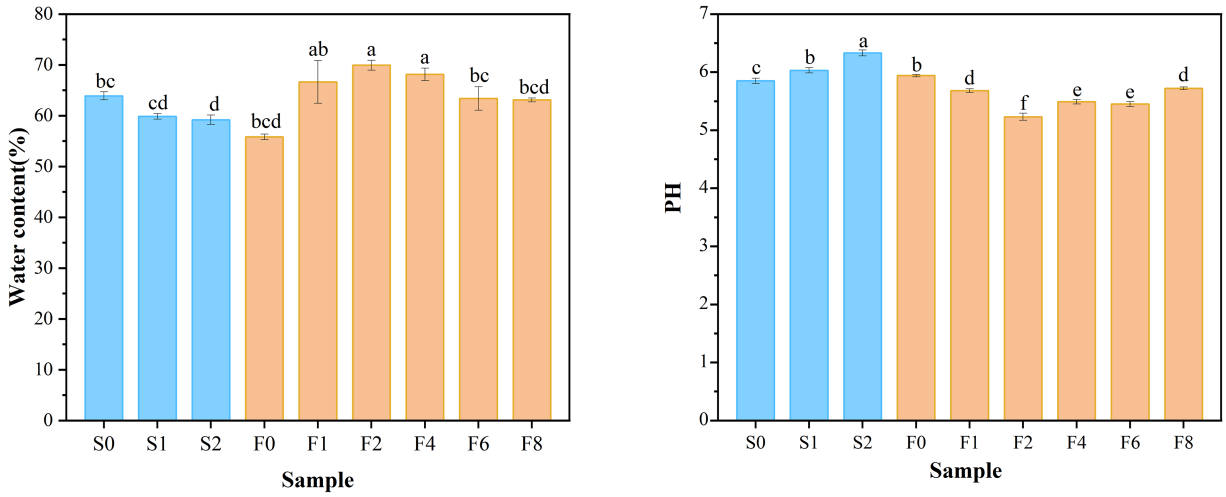

FIGURE 2
Variation in water content and pH.

TABLE 1 Changes in the content of BAs.

Sample	Content of biogenic amines (mg/kg)								
	His	Cad	Put	Phe	Oct	Tyr	Spd	Try	Spm
S0	ND	ND	ND	ND	ND	0.06 ± 0.02^{C}	1.57 ± 0.39^{BC}	0.04 ± 0.02^{D}	1.97 ± 0.59^{A}
S1	145 ± 39.23^{C}	10.42 ± 1.85^{C}	ND	ND	ND	6.45 ± 2.77^{C}	1.04 ± 0.16^{CD}	0.03 ± 0.00^{D}	2.28 ± 0.87^{B}
S2	479.64 ± 46.95^{B}	100.01 ± 5.92^{B}	15.52 ± 2.18^{D}	ND	ND	ND	0.65 ± 0.12^{D}	0.03 ± 0.00^{D}	2.10 ± 0.09^{B}
F0	ND	ND	5.82 ± 0.09^{D}	ND	ND	ND	1.44 ± 0.19^{BC}	0.01 ± 0.00^{D}	2.19 ± 0.33^{B}
F1	ND	ND	8.40 ± 0.44^{D}	ND	ND	26.53 ± 3.68^{B}	2.26 ± 0.18^{A}	2.18 ± 0.35^{D}	2.07 ± 0.03^{B}
F2	5.01 ± 0.16^{A}	12.3 ± 0.66^{C}	132.41 ± 3.28^{C}	3.95 ± 0.15^{C}	ND	87.91 ± 4.65^{A}	1.7 ± 0.1^{AB}	11.41 ± 0.94^{C}	1.88 ± 0.06^{B}
F4	0.95 ± 0.06^{A}	8.47 ± 0.25^{C}	134.3 ± 10.82^{C}	3.90 ± 0.38^{C}	ND	74.28 ± 4.53^{C}	1.81 ± 0.45^{AB}	10.76 ± 2.26^{C}	1.73 ± 0.07^{B}
F6	12.36 ± 0.64^{A}	313.25 ± 24.96^{A}	282.33 ± 23.62^{B}	9.71 ± 1.04^{B}	ND	99.01 ± 6.04^{A}	1.88 ± 0.11^{AB}	17.80 ± 1.39^{B}	1.71 ± 0.04^{B}
F8	4.38 ± 0.37^{A}	287.58 ± 25.22^{A}	342.99 ± 37.84^{A}	14.21 ± 0.27^{A}	ND	92.81 ± 6.93^{A}	1.23 ± 0.03^{BCD}	27.88 ± 0.43^{A}	1.73 ± 0.00^{B}

Values with different capital letters are significantly different ($p < 0.05$). S0, S1, S2 denote the controls on day 0, 1, 2, respectively; F0, F1, F2, F4, F6, F8 denote *zaoyu* on day 0, 1, 2, 4, 6, 8, respectively; Z denotes the fermented rice, and the same below. The same below.

the allowable limit (50 mg/kg) suggested by FDA, indicating that the formation of His or the growth of microorganisms involved in the accumulation of His was inhibited during fermentation.

Put, Cad and Tyr were relatively abundant BAs in *zaoyu* samples, and the content kept an upward trend during fermentation. Whereas the content of Tyr was still lower than the potentially dangerous level of 100–800 mg/kg (Elena et al., 2014), and neither legal limits nor toxic dose has been established for Put and Cad. A combination of Put and Cad has been suggested as an acceptable index in fresh meat, whereas it has proven not suitable to apply to fermented products (Ruiz-Capillas and Jiménez-Colmenero, 2004). The content of Spd and Spm in *zaoyu* was nearly unchanged, indicating that both BAs had negligible correlation with microorganisms. They are often considered to be physiological polyamines in organisms related to variety, location and physiological status (Önal, 2007). Zhai et al. have shown that Spm and Spd cannot be used as indicators for the evaluation of spoilage in fish fermentation (Zhai et al., 2012).

Sequencing results and diversity indices

The number of reads per sample ranged from 16,154 to 36,342, 1,690 OTUs were obtained based on 97% similarity threshold. Alpha diversity indices were compared in different samples (Table 2). The coverage of sequences was over 0.99, showing that the data of amplicon sequencing with sufficient authenticity and depth. Shannon and Simpson are two main indices which comprehensively take the richness and evenness of microbial community of samples into account (Aregbe

TABLE 2 Alpha diversity of bacterial community.

Sample	Shannon		Simpson		Chao1		ACE		Good coverage	
	Mean	SD	Mean	SD	Mean	SD	Mean	SD	Mean	SD
F0	3.77^{c}	0.25	0.92^{c}	0.02	388.97^{f}	44.20	376.07	39.73	0.9983^{a}	4.02E-04
F1	1.97^{b}	0.29	0.73^{b}	0.03	158.63^{bc}	39.23	151.30^{bc}	31.76	0.9995^{cde}	1.59E-04
F2	2.13^{b}	0.23	0.76^{b}	0.03	115.44^{ab}	21.57	115.64^{ab}	21.19	0.9997^{def}	1.17E-04
F4	1.45^{a}	0.05	0.67^{a}	4.70E-03	111.79^{ab}	11.97	112.87^{ab}	12.23	0.9998^{def}	1.46E-04
F6	2.10^{b}	0.07	0.76^{b}	0.01	87.23^{a}	9.12	87.55^{a}	9.20	0.9998^{ef}	1.06E-04
F8	1.52^{a}	0.07	0.67^{a}	0.01	61.61^{a}	9.37	61.48^{a}	9.10	0.9999^{f}	6.22E-05
S0	3.89^{c}	0.08	0.93^{cd}	0.01	347.78^{f}	30.96	344.86^{f}	28.84	0.9991^{bc}	2.63E-04
S1	3.89^{c}	0.20	0.96^{e}	0.01	224.28^{de}	47.54	222.78^{de}	52.55	0.9990^{b}	2.28E-04
S2	3.81^{c}	0.04	0.95^{de}	3.85E-03	183.33^{cd}	8.29	178.56^{cd}	12.35	0.9992^{bc}	1.79E-04
Z	3.98^{c}	0.24	0.96^{e}	0.01	252.82^{e}	49.54	249.48^{ef}	55.96	0.9994^{cd}	1.52E-04

Values with different lowercase letters are significantly different ($p < 0.05$).

et al., 2019). In general, the four indices of bacterial communities presented a decreasing trend during fermentation, indicating that the richness of bacterial community decreased over time and a subset of bacteria became dominant in samples.

Beta-diversity analysis of bacterial community

An NMDS (Non-metric Multidimensional Scaling analysis) ordination biplot demonstrated clear clustering of microbiota composition (Figure 3). Every point represented a sample, and the higher similarity of microbial community was, the closer the sample points were. Overall, the microbiota composition was different between fermentation and storage categories. *Zaoyu* samples on day 0 were distinct from the samples on day 1, revealing that the bacterial community changed significantly in the early fermentation. The closer distance between samples in the later fermentation stage (F2, 4, 6, 8) indicated that their bacterial community was more similar. As the fermentation system established, a dynamic and stable environment was gradually formed, leading to the similarity of microbiota composition (Shen et al., 2021).

The distinct flora of *Scomber japonicus* during different fermentation periods could be obtained based on the Lefse (Linear discriminant analysis effect size) analysis demonstrated in Figure 3B, showing those microorganisms meeting the linear discriminant analysis significance threshold of 4.0. The results revealed that the biomarkers of different samples were significantly different. The biomarker of samples of F1 was *Psychrobacter* spp., and samples of F0 featured a higher abundance of *Bacillus* spp. Compared with the controls, *zaoyu* had greater proportions of *Lactobacillus* spp. and *Lactococcus* spp. belonging to the *Lactobacillales*. These key representative bacterial taxa contributed to the differences of microbiota composition in different samples.

Taxonomic composition of bacterial communities

To explore microbial community succession during fermentation of *Scomber japonicus*, the microbial taxonomic compositions of samples were determined at the phylum (Figure 3A) and genus (Figure 3B) levels, respectively. Among the phylum, Firmicutes and Proteobacteria possessed the highest abundance throughout the fermentation. Such results were found in other fermented seafood, like Yu-lu (Wang et al., 2018), and tilapia sausage (Li et al., 2022). As fermentation progressed, the relative abundance of Firmicutes presented an increasing trend, while the bacteria from Proteobacteria and Actinobacteria were inhibited and presented in minor percentages (Figure 4).

Analysis at genus level showed that the type of bacterial community in *zaoyu* samples was significantly lower than that of the controls, indicating that the microbial community is relatively simple during fermentation, which was in accord with the analysis of alpha diversity. *Vibrio, Psychrobacter,* and *Acinetobacter* were dominant bacterial species in the storage of *Scomber japonicus* and they were active in inducing fish spoilage, among which *Enterobacteriaceae* and *Vibrio*, two typical spoilage microorganisms playing a vital role in the formation of BAs (Kim et al., 2009), were inhibited during fermentation. The relative abundance of *Vibrio, Acinetobacter,* and *Psychrobacter* decreased rapidly along with the fermentation, whereas the relative abundance of *Lactobacillus* increased and quickly occupied the dominant position in *zaoyu*.

Correlation between microbial community and BAs

The RDA results demonstrated the relationship between the accumulation of BAs and bacterial community. The blue arrows expressed 7 BAs, and the red represented core microbes. The

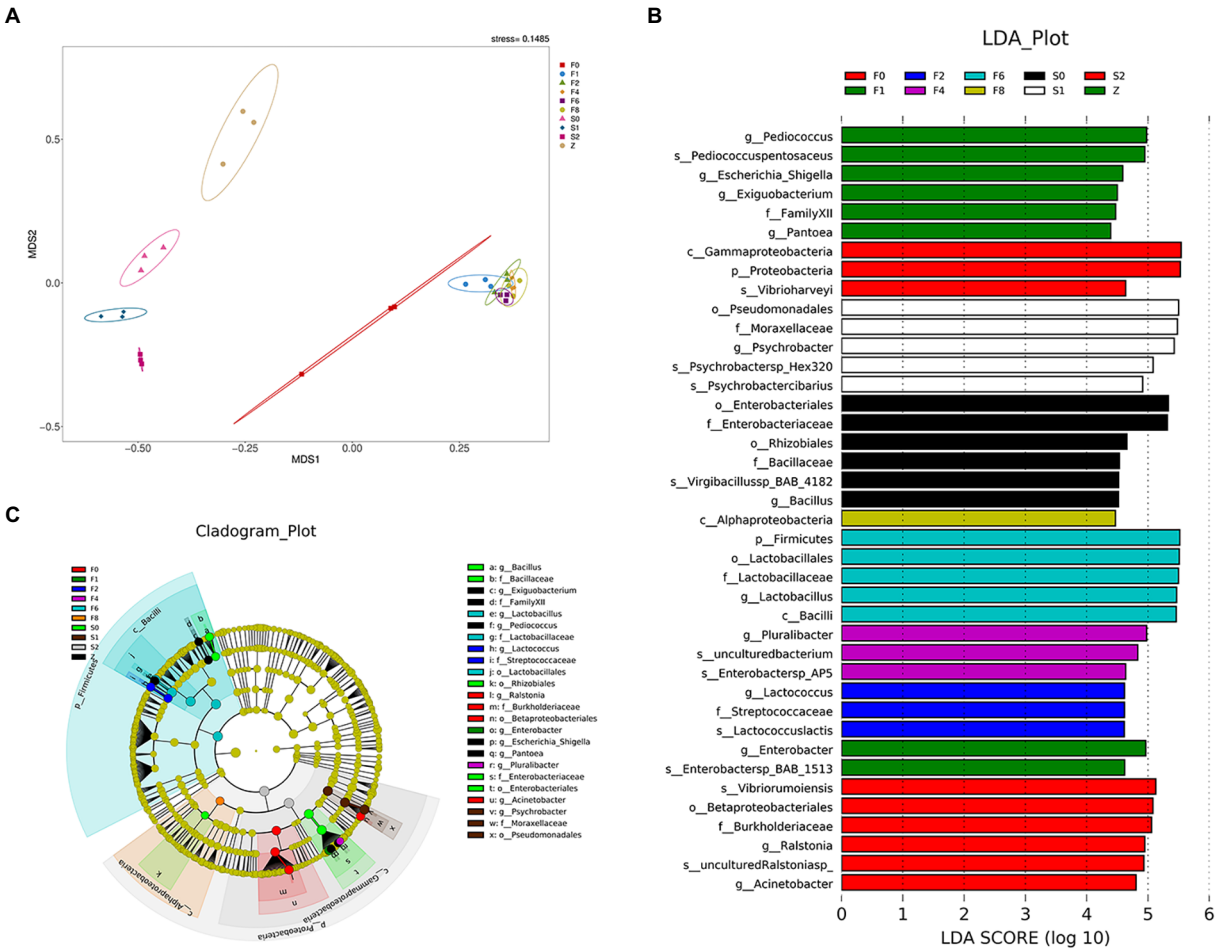

FIGURE 3
The analysis of differences of species diversity. **(A)** Two-dimensional NMDS of microbiota compositions of samples, **(B)** horizontal bar chart, **(C)** microbiota cladogram produced by LEfSe.

length of arrows determined the degree of importance, and the angle between the lines indicated the correlation between them. An acute angle indicated a positive correlation, while an obtuse angle indicated a negative correlation. Changes in bacterial communities were significantly correlated with the formation of different BAs. As shown in Figure 5, the accumulation of His was positively correlated with the relative abundance of *Vibrio, Enterobacter, Macrococcus,* and *Weissella,* et al., while negatively correlated with *Lactobacillus* spp. and *Pediococcus* spp. *Lactobacillus* presented positive relation to Cad, Tyr, Put and Try but negatively related to the growth of some microorganisms which was positively related to the formation of His including *Klebsiella, Acinetobacter, Vibrio,* and *Enterobacter.* These results indicated that diverse microbes like *Vibrio* spp., *Enterobacter* spp., *Macrococcus* spp., *Weissella* spp., and *Weissella* spp. belonging to gram-negative bacteria might facilitate the accumulation of His, and *Lactobacillus* may have an inhibition effect on His production by some microorganisms.

Potential metabolic prediction By PICRUSt-KEGG

Since the type and abundance of metabolic pathways of microbiota determines the process of fermentation and food spoilage, the prediction of metabolic profiles may provide useful information on the potential of metabolic activities (Zhuang et al., 2020a). A total of 328 KEGG Orthology (KO) categories were obtained by assigning homologous sequences in metagenomes based on KEGG gene and pathway database. There were 12 genes related to metabolism during fermentation and storage (Figure 6A). Notably, carbohydrate metabolism presented the most enrichment among the 12 pathways, amino acid and energy metabolism were also important throughout the fermentation. Amino acid metabolism plays an important role in the spoilage of fish due to its producing carbon skeletons, especially keto acids like pyruvic acid and oxoglutarate for microbial activities and biosynthesis (Zhuang et al., 2020c).

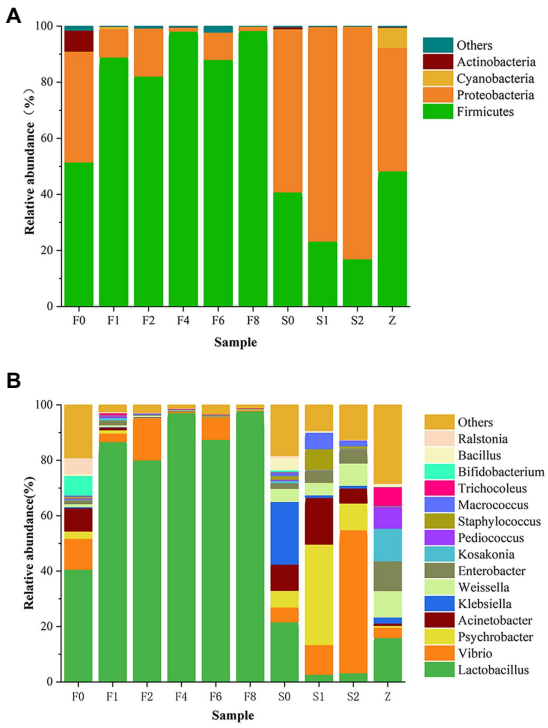

FIGURE 4
Relative abundance at the phylum level **(A)** and the genus level **(B)** of bacterial community.

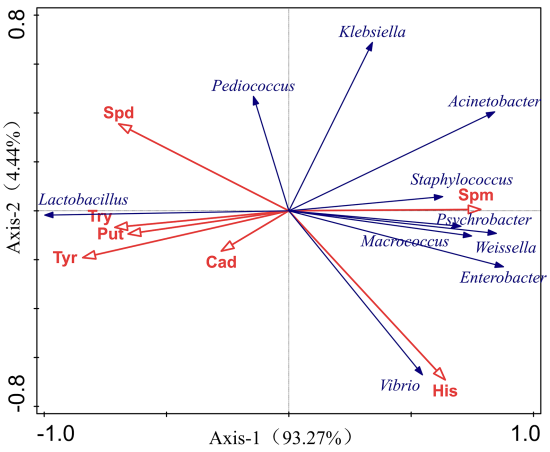

FIGURE 5
RDA for relationship between BAs and microbiota composition based on the top 10 dominant microbes at genus levels.

Figure 6B showed the relative abundance of carbohydrate metabolism, amino acid metabolism, and energy metabolism of samples. Considering that all *zaoyu* samples in this study were collected in the early fermentation stage of *Scomber japonicus,* the relative gene abundance of the three metabolisms during fermentation was relatively low and changed slightly. The changes of microbiota composition may explain well why the relative enrichment levels of the metabolism-related genes decreased first, then in equilibrium during fermentation. LAB as dominant bacteria in the process of fermentation inhibited the growth of other microorganisms and caused bacteria type single.

To analyze and compare the distribution characteristics of microbial metabolism, a heatmap that represented the related gene abundances of metabolism was constructed in Figure 7, which successfully visualized the dynamic changes of various metabolisms. These main metabolic pathways presented a decreasing trend in controls, however, the changes of the metabolic features in *zaoyu* were more stable. In amino acid metabolism, histidine is a precursor substance of His, and Tyr was formed by decarboxylation of tyrosine, whereas several amino acid metabolisms including histidine, glycine, serine, and threonine metabolism were obviously inhibited during fermentation. Hence the formation of BAs in *zaoyu* was inhibited. In addition, the proteins and lipids during fermentation were mainly hydrolyzed by enzymes produced by microbial metabolism, so the relative abundance of enzyme-related genes related to amino acid metabolism was the highest in the whole process.

In carbohydrate metabolism, the main metabolic types were pyruvate metabolism, amino sugar and nucleotide sugar metabolism, as well as glycolysis. Glycolysis and pyruvate metabolism imparted a sweet taste to fermented rice, which is an essential factor affecting the flavor formation of *zaoyu*. Glycolysis is one of the most common carbohydrate metabolic pathways in bacterial communities. Pyruvate produced by glycolysis is oxidized by bacteria to acetyl-CoA for TCA cycling (Bomberg et al., 2016), and TCA cycle provides a source of many amino acid metabolisms such as lysine and glutamate.

Discussion

The quality of *zaoyu* is closely associated with the complex metabolism of microbiota. Microbiota composition of fish flesh undergoes massive changes throughout storage and fermentation, reflected as the changes of bacterial alpha-diversity based on Shannon, Chao1, Simpson, Ace indices and the differences of dominant bacteria. It's noteworthy that despite the highest alpha diversity in fresh samples, most species have no effect on the fermentation process due to that they originated from processing tools and environment, while these exogenous microorganisms could be inhibited under continuous fermentation and certain salt concentrations (Shen et al., 2021). Noticeable differences were observed between *zaoyu* and the controls. The bacterial diversity was relatively low in *zaoyu*, which may be attributed to the presence of dominant microorganisms such as LAB with the ability of acid tolerance. Numerous studies have shown that the presence of dominant microorganisms in aquatic products during storage or processing inhibited the growth of other

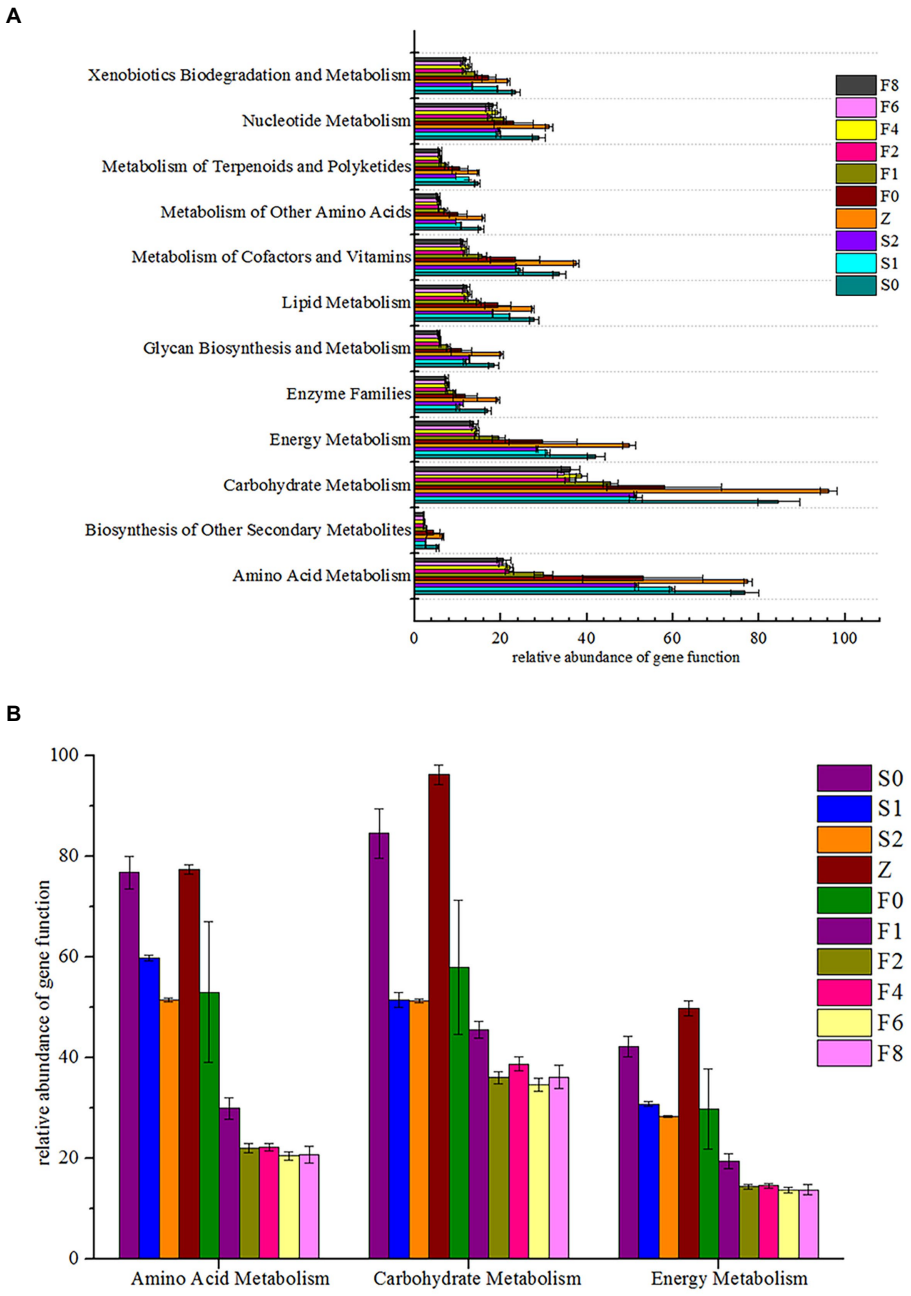

FIGURE 6
Functional genes related to metabolism. **(A)** distribution of KEGG pathways, **(B)** amino acid metabolism, carbohydrate metabolism and energy metabolism.

microorganisms and led to a decrease in microbial diversity (Silbande et al., 2016).

The relationship between microbiota and quality of fermented seafood remained not comprehensively clear though, there has been increasing interests in forging bonds between microbiota composition and different quality indices like BAs as well as exploring the potential role of relevant microorganisms (Bover-Cid et al., 2003; Hao and Sun, 2020). Different microbes may excrete different amino acid decarboxylases to produce specific BAs, and some could also produce amine oxidases to degrade BAs in turn (Lu et al., 2018). In fermented foods, the mutual growth and interaction of LAB and yeast are universal as the growth environment is analogous (Wang et al., 2022). The majority of LAB is able to contribute to the flavor formation of fermented foods and displays some specific metabolic cross-feeding with yeast (Mukisa et al., 2017). Thus, LAB plays a solemn role in the effective fermentation of seafood. In the process of

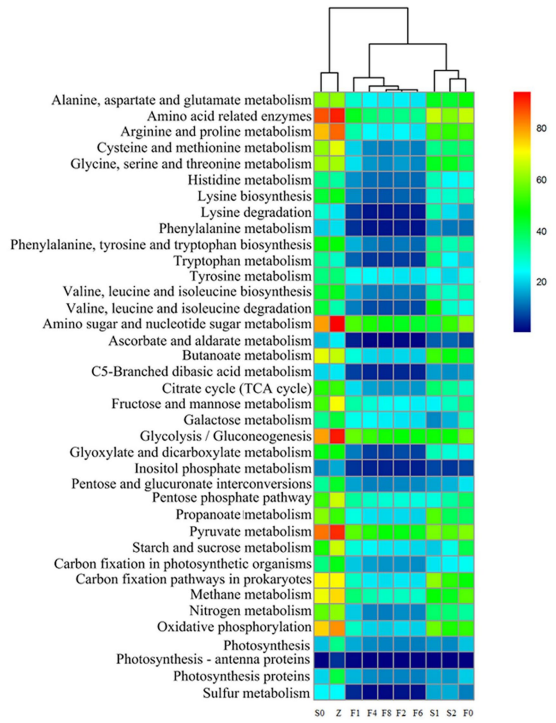

FIGURE 7
Functional prediction of amino acids, carbohydrates and energy metabolism of the microbiota.

fermentation, diverse microbial interactions are thought to be more like those of an evolutionary community able to adapt to the raw material (Alekseeva et al., 2021), when microbiota have adapted to the acidic conditions, it shifts sequentially to a more acidic-tolerant group that is more adaptable to the acidic (Wang et al., 2022). *Lactobacillus* spp. occupied the dominant position throughout the whole fermentation, which is due to that it is a facultative anaerobe with the ability to survive under hypoxic and acid conditions, thus it is not restricted by the fermentation environment and maintains a constant quantity. Besides, arginine degradation has been regarded a significant source of cell energy for *Lactobacillus*, thus it could obtain energy from the formation of Put and thus keep more energetic advantages in bacterial competition (Zhuang et al., 2022). *Lactobacillus* could utilize carbohydrates in *zaoyu* to generate a large amount of lactic acid, and inhibit the growth of other spoilage bacteria like *Vibrio*, thereby reducing the content of BAs (Khouadja et al., 2017).

As the most important type of BA in the spoilage of *Scomber japonicas*, the formation of His is mainly caused by the secretion of histidine decarboxylase by some microorganisms with the ability of histidine decarboxylation to produce free histidine (Kuda et al., 2012). Some species with the ability to degrade *in vitro* Tyr and His, such as *Lactobacillus plantarum, Lactobacillus pentosus, Lactobacillus sakei, Pediococcus acidilactici*, belong to the *Lactobacillus* spp. and *Pediococcus* spp. that occupied the dominant proportions in *zaoyu* samples (Arena and Manca de Nadra, 2001; Emmanuel et al., 2010), this observation is consistent with the results of RDA analysis in this study. Therefore, it is speculated that the growth of dominant microorganisms leads to antagonism between microorganisms and thus inhibits the growth of histamine-forming bacteria. Furthermore, LAB also shows a stimulative effect on the formation of BAs. *Lactococcus, Lactobacillus, Enterococcus,* and *Pediococcus* are considered as strong producers of BAs (Ladero et al., 2012). Tyr is one of the most common and abundant BA in fermented meat products (Ruiz-Capillas and Jiménez-Colmenero, 2004), in which LAB strains of *Enterococcus faecalis, Enterococcus faecium*, and *Enterococcus durans* strains are strong tyramine-producers (Özogul and Hamed, 2017). Put could be produced through the catabolism of agmatine, a decarboxylated derivative of arginine through the agmatine deiminase (AGDI) pathway (del Rio et al., 2015). Species like *Lactobacillus brevis, Lactobacillus curvatus,* and *Enterococcus faecalis* have been reported to be able to produce putrescine *via* AGDI.

Proteobacteria was one of the predominant bacterial phyla during storage, many studies have shown that Proteobacteria is the main bacterial species in the process of seafood spoilage and plays an essential role in its quality changes (Chaiyapechara et al., 2012). It was reported that the formation of TVB-N was mainly related to *Pseudomonas* and *Enterobacteriaceae,* which were responsible for the enzymatic decarboxylation of specific amino acids (Li et al., 2019), hence it was also responsible for the accumulation of BAs. The microbial populations in the controls increased significantly and were mainly dominated by spoilage bacteria, including *Psychrobacter, Klebsiella, Vibrio,* and *Acinetobacter,* which was actively associated with the accumulation of His based on RDA analysis. The synergistic action of various microorganisms during fermentation promotes the production of Put and Cad. LAB could degrade arginine and its amino acid-derived ornithine, and then the degradation products are metabolized by *Enterobacteriaceae* to produce Put (Arena and Manca de Nadra, 2001), which may cause a symbiotic relationship between them, thus leading to a rapid increase in Put during fermentation. Kim et al. have revealed that many stains of *Enterobacter* spp. were identified as amine-forming bacteria with strong decarboxylation activity, being strong producers of Put and Cad (Kim et al., 2009). It's noted that *Aeromonas* belonging to the *Vibrio* specie could be active in producing Cad (Zhuang et al., 2020b), which may be responsible for the relatively high content of Cad in control samples. Most Proteobacteria, including *Enterobacter*, *Salmonella*, *Vibrio,* etc. are gram-negative bacteria, indicating that the spoilage of *Scomber japonicus* is more suitable for gram-negative bacteria. *Vibrio* also may reduce trimethylamine oxides to the fishy smelling compound trimethylamine (TMA), and most strains also produce H_2S (Lin et al., 2021). *Macrococcus caseolyticus* and *Staphylococcus sciuri*, two

histamine-producing bacteria (HPB) reported before (Zhou et al., 2012), belonging to *Macrococcus* and *Staphylococcus*, respectively, were inhibited during fermentation, which could be potentially associated with the reduction of His in the whole fermentation. *Staphylococcus* has exhibited high esterase and lipase activities, and *Micrococcus* has the ability of lipolysis in fermented fish products. It could decompose proteins, free amino acids and fats fatty acids into some small molecules such as aldehydes and ketone, promoting the formation of product flavor (Lin et al., 2021).

Combined with the analysis of metabolic pathways, the metabolism of carbon and nitrogen source compounds plays an essential role during spoilage and fermentation of fish. Microbial catabolism of nitrogen-containing compounds and carbon sources could be related through biochemical reactions like amino acid transamination, which crosslinks various metabolic pathways into a complex network (Zhuang et al., 2020a). Carbohydrate metabolism and amino acid metabolism are primary metabolic pathways during storage and fermentation. The muscles of fish are rich in amino acids, providing sufficient substrate for the microorganisms. Previous studies have shown that proteins could be hydrolyzed into peptides and amino acids by microbial protease (Masniyom, 2011; Zhuang et al., 2019), then metabolized into a variety of BAs and ammonia metabolized through transamination, deamination, and decarboxylation (Biji et al., 2016). In this study, the abundance of metabolic pathways related to the formation of biogenic amines and sulfide in zaoyu was lower compared with the controls, such as phenylalanine, tyrosine and tryptophan metabolism, and these metabolisms have been reported to be associated with *Enterobacteriaceae* and *Pseudomonas* (Li et al., 2019).

Carbohydrate metabolism not only provides building blocks for the construction and assembly of complex macromolecules in cells, including nucleic acids, proteins and lipids, but is also used to generate energy required for microbial growth (Wu et al., 2021). Carbohydrates could be used as an energy source for LAB, belonging to the phylum Firmicutes which is the main microorganism of carbohydrate metabolism during fermentation (Stellato et al., 2016). LAB could compete and inhibit competitors by the rapid utilization of abundant carbohydrates with the accumulation of organic acids (Wang et al., 2022). Lactate is the main product of metabolism when the fermentable carbohydrates are abundant and generally remains the major metabolite of most LAB growing aerobically (Gänzle, 2015). A large amount of LAB produced carbon dioxide making the fermentation environment anaerobic, then synthesized pyruvic acid by anaerobic respiration. Therefore, pyruvate metabolism is the primary metabolic type of anaerobic respiration, mainly in the late stage of fermentation. Oxidative phosphorylation is a crucial type of energy metabolism in fermentation and is considered one of the most vital metabolic pathways in bacterial communities (Bomberg et al., 2016). However, further research is needed on the relationship between the metabolic pathways of exact metabolism and microbes in *zaoyu*.

Conclusion

In this study, we characterized the complex microbiota composition during fermentation of *Scomber japonicus* using metagenomics and explored the relationships among the microbiota composition, functional metabolisms, and the formation of 8 BAs. This study revealed that the accumulation of His was inhibited and it was positively correlated with the relative abundance of *Vibrio, Enterobacter, Weissella,* et al., but negatively related to *Lactobacillus* spp. and *Pediococcus* spp., suggesting that *Lactobacillus* spp. and *Pediococcus* spp. may improve the safety of the *zaoyu* from a microbial point of view, which provided theoretical basis for the control of BAs during fermentation of *Scomber japonicus*. The predicted metabolic pathways revealed that some metabolisms related to the formation of BAs were inhibited throughout the fermentation. Nevertheless, the obtained functional profiles are merely rough functional hierarchy levels, detailed analyses of specific metabolic pathway and the roles of certain microorganism on the formation mechanisms of BAs are needed to be further elucidated.

Data availability statement

The data presented in the study are deposited in the NCBI repository, accession number: PRJNA876092.

Author contributions

JC performed the formal analysis, data visualization, and finished the final manuscript. HT contributed to the conception and design of the study. MZ finished the experiment. SS contributed significantly to analysis and manuscript revision. LJ helped to perform the analysis with constructive discussions. CO and HT contributed to the conception and design of the study. All authors contributed to the article and approved the submitted version.

Funding

This work was supported by the National Key Research and Development Program of China under Grant 2019YFD0901705.

Conflict of interest

The authors confirm that they have no known competing financial interests or personal relationships which could influence the work reported in this paper.

Publisher's note

All claims expressed in this article are solely those of the authors and do not necessarily represent those of their affiliated organizations, or those of the publisher, the editors and the reviewers. Any product that may be evaluated in this article, or claim that may be made by its manufacturer, is not guaranteed or endorsed by the publisher.

Supplementary material

The Supplementary material for this article can be found online at: https://www.frontiersin.org/articles/10.3389/fmicb.2022.1030789/full#supplementary-material

References

Alekseeva, A. Y., Groenenboom, A. E., Smid, E. J., and Schoustra, S. E. (2021). Eco-evolutionary dynamics in microbial communities from spontaneous fermented foods. *Int. J. Environ. Res. Public Health* 18:10093. doi: 10.3390/ijerph181910093

Aregbe, A. Y., Mu, T., and Sun, H. (2019). Effect of different pretreatment on the microbial diversity of fermented potato revealed by high-throughput sequencing. *Food Chem.* 290, 125–134. doi: 10.1016/j.foodchem.2019.03.100

Arena, M. E., and Manca de Nadra, M. C. (2001). Biogenic amine production by lactobacillus. *Eur. J. Appl. Microbiol.* 90, 158–162. doi: 10.1046/j.1365-2672.2001.01223.x

Bassi, D., Puglisi, E., and Cocconcelli, P. S. (2015). Comparing natural and selected starter cultures in meat and cheese fermentations. *Curr. Opin. Food Sci.* 2, 118–122. doi: 10.1016/j.cofs.2015.03.002

Biji, K. B., Ravishankar, C. N., Venkateswarlu, R., Mohan, C. O., and Gopal, T. K. (2016). Biogenic amines in seafood: a review. *J. Food Sci. Technol.* 53, 2210–2218. doi: 10.1007/s13197-016-2224-x

Bomberg, M., Lamminmäki, T., and Itävaara, M. (2016). Microbial communities and their predicted metabolic characteristics in deep fracture groundwaters of the crystalline bedrock at Olkiluoto. *Finland. Biogeosci.* 13, 6031–6047. doi: 10.5194/bg-13-6031-2016

Bover-Cid, S., Hernández-Jover, T., Miguélez-Arrizado, M. J., and Vidal-Carou, M. C. (2003). Contribution of contaminant enterobacteria and lactic acid bacteria to biogenic amine accumulation in spontaneous fermentation of pork sausages. *Eur. Food Res. Technol.* 216, 477–482. doi: 10.1007/s00217-003-0691-6

Bover-Cid, S., Hugas, M., Izquierdo-Pulido, M., and Vidal-Carou, M. C. (2000). Reduction of biogenic amine formation using a negative amino acid-decarboxylase starter culture for fermentation of Fuet sausages. *J. Food Prot.* 63:237. doi: 10.1089/10665270050081559

Chaiyapechara, S., Rungrassamee, W., Suriyachay, I., Kuncharin, Y., Klanchui, A., Karoonuthaisiri, N., et al. (2012). Bacterial community associated with the intestinal tract of *P. monodon* in commercial farms. *Microb. Ecol.* 63, 938–953. doi: 10.1007/s00248-011-9936-2

Chen, Z., Tang, H., Ou, C., Xie, C., Cao, J., and Zhang, X. (2021). A comparative study of volatile flavor components in four types of zaoyu using comprehensive two-dimensional gas chromatography in combination with time-of-flight mass spectrometry. *J. Food Process. Preserv.* 45:e15230. doi: 10.1111/JFPP.15230

del Rio, B., Linares, D. M., Ladero, V., Redruello, B., Fernández, M., Martin, M. C., et al. (2015). Putrescine production via the agmatine deiminase pathway increases the growth of Lactococcus lactis and causes the alkalinization of the culture medium. *Appl. Microbiol. Biotechnol.* 99, 897–905. doi: 10.1007/s00253-014-6130-8

Doi, R., Wu, Y., Kawai, Y., Wang, L., Zendo, T., Nakamura, K., et al. (2021). Transition and regulation mechanism of bacterial biota in Kishu saba-narezushi (mackerel narezushi) during its fermentation step. *J. Biosci. Bioeng.* 132, 606–612. doi: 10.1016/j.jbiosc.2021.09.002

Elena, B., Vita, K., Grazina, J., Daiva, V., and Zita, M. (2014). Solid state fermentation with lactic acid bacteria to improve the nutritional quality of lupin and soya bean. *J. Sci. Food Agric.* 95, 1336–1342. doi: 10.1002/jsfa.6827

Emmanuel, C., Niels, M., Monika, C., Sylvie, P., Hein, T., and Lolkema, J. S. (2010). Origin of the putrescine-producing ability of the coagulase-negative bacterium Staphylococcus epidermidis 2015B. *Appl. Environ. Microbiol.* 76, 5570–5576. doi: 10.1128/AEM.00441-10

Gänzle, M. G. (2015). Lactic metabolism revisited: metabolism of lactic acid bacteria in food fermentations and food spoilage. *Curr. Opin. Food Sci.* 2, 106–117. doi: 10.1016/j.cofs.2015.03.001

Gao, Y., Zou, K., Zhou, L., Huang, X., Li, Y., Gao, X., et al. (2020). Deep insights into gut microbiota in four carnivorous coral reef fishes from the South China Sea. *Microorgansims.* 8:426. doi: 10.3390/microorganisms8030426

Guan, W., Li, K., Zhao, S., and Li, K. (2021). A high abundance of Firmicutes in the intestine of chinese mitten crabs (*Eriocheir sinensis*) cultured in an alkaline region. *AMB Express* 11:141. doi: 10.1186/S13568-021-01301-W

Han, B., Cao, C., Rombouts, F. M., and Nout, M. J. R. (2004). Microbial changes during the production of Sufu––a Chinese fermented soybean food. *Food Control* 15, 265–270. doi: 10.1016/s0956-7135(03)00066-5

Han, J., Kong, T., Wang, Q., Jiang, J., Zhou, Q., Li, P., et al. (2022). Regulation of microbial metabolism on the formation of characteristic flavor and quality formation in the traditional fish sauce during fermentation: a review. *Crit. Rev. Food Sci. Nutr.* 21-20. doi: 10.1080/10408398.2022.2047884

Hao, Y., and Sun, B. (2020). Analysis of bacterial diversity and biogenic amines content during fermentation of farmhouse sauce from Northeast China. *Food Control* 108:106861. doi: 10.1016/j.foodcont.2019.106861

Hu, Y., Xia, W., and Liu, X. (2007). Changes in biogenic amines in fermented silver carp sausages inoculated with mixed starter cultures. *Food Chem.* 104, 188–195. doi: 10.1016/j.foodchem.2006.11.023

Huang, Y. R., Liu, K. J., Hsieh, H. S., Hsieh, C. H., Hwang, D. F., Tsai, Y. H., et al. (2010). Histamine level and histamine-forming bacteria in dried fish products sold in Penghu Island of Taiwan. *Food Control* 21, 1234–1239. doi: 10.1016/j.foodcont.2010.02.008

ICMSF (1986). *Microorganisms in Foods. 2: Sampling for Microbiological Analysis: Principles and Specific Applications, 2nd ed.* Univ. of Toronto Press, Toronto.

Jung, J. Y., Lee, S. H., Lee, H. J., and Jeon, C. O. (2013). Microbial succession and metabolite changes during fermentation of saeu-jeot: traditional Korean salted seafood. *Food Microbiol.* 34:360. doi: 10.1016/j.fm.2013.01.009

Khouadja, S., Haddaji, N., Hanchi, M., and Bakhrouf, A. (2017). Selection of lactic acid bacteria as candidate probiotics for Vibrio parahaemolyticus depuration in pacific oysters (Crassostrea gigas). *Aquac. Res.* 48, 1885–1894. doi: 10.1111/are.13026

Kim, M. K., Mah, J. H., and Hwang, H. J. (2009). Biogenic amine formation and bacterial contribution in fish, squid and shellfish. *Food Chem.* 116, 87–95. doi: 10.1016/j.foodchem.2009.02.010

Kuda, T., Izawa, Y., Ishii, S., Takahashi, H., Torido, Y., and Kimura, B. (2012). Suppressive effect of Tetragenococcus halophilus, isolated from fish-nukazuke, on histamine accumulation in salted and fermented fish. *Food Chem.* 130, 569–574. doi: 10.1016/j.foodchem.2011.07.074

Ladero, V., Fernandez, M., Calles-Enriquez, M., Sanchez-Liana, E., Canedo, E., Martin, M. C., et al. (2012). Is the production of the biogenic amines tyramine and putrescine a species-level trait in enterococci? *Food Microbiol.* 30, 132–138. doi: 10.1016/j.fm.2011.12.016

Li, N., Zhang, Y., Wu, Q., Gu, Q., Chen, M., Zhang, Y., et al. (2019). High-throughput sequencing analysis of bacterial community composition and quality characteristics in refrigerated pork during storage. *Food Microbiol.* 83, 86–94. doi: 10.1016/j.fm.2019.04.013

Li, C., Zhao, Y., Wang, Y., Li, L., Huang, J., Yang, X., et al. (2022). Contribution of microbial community to flavor formation in tilapia sausage during fermentation with Pediococcus pentosaceus. *LWT – Food Sci. Technol.* 154:112628. doi: 10.1016/J.LWT.2021.112628

Lin, F., Nianchu, T., Ruijie, L., Mengyue, G., Zhangtie, W., Yiwen, G., et al. (2021). The relationship between flavor formation, lipid metabolism, and microorganisms in fermented fish products. *Food Funct.* 12, 5685–5702. doi: 10.1039/D1FO00692D

Lu, L., Liying, R., Ji, A., Wen, Z., Chen, S., Ling, W., et al. (2018). Biogenic amines analysis and microbial contribution in traditional fermented food of Douchi. *Sci. Rep.* 8:12567. doi: 10.1038/s41598-018-30456-z

Masniyom, P. (2011). Deterioration and shelf-life extension of fish and fishery products by modified atmosphere packaging. *Songklanakarin J. Sci. Technol.* 33, 181–192.

Mengjuan, C., Yeyou, Q., Fangming, D., Hui, Z., Rongrong, W., Pao, L., et al. (2021). Illumina MiSeq sequencing reveals microbial community succession in salted peppers with different salinity during preservation. *Food Res. Int.* 143:110234. doi: 10.1016/J.FOODRES.2021.110234

Moradi, M., Tajik, H., Almasi, H., Forough, M., and Ezati, P. (2019). A novel pH-sensing indicator based on bacterial cellulose nanofibers and black carrot anthocyanins for monitoring fish freshness. *Carbohydr. Polym.* 222:115030. doi: 10.1016/j.carbpol.2019.115030

Mukisa, I. M., Byaruhanga, Y. B., Muyanja, C. M. B. K., Langsrud, T., and Narvhus, J. A. (2017). Production of organic flavor compounds by dominant lactic acid bacteria and yeasts from Obushera, a traditional sorghum malt fermented beverage. *Food Sci. Nutr.* 5, 702–712. doi: 10.1002/fsn3.450

Önal, A. (2007). A review: current analytical methods for the determination of biogenic amines in foods. *Food Chem.* 103, 1475–1486. doi: 10.1016/j.foodchem.2006.08.028

Özogul, F., and Hamed, I. (2017). The importance of lactic acid bacteria for the prevention of bacterial growth and their biogenic amines formation: a review. *Crit. Rev. Food Sci. Nutr.* 58, 1660–1670. doi: 10.1080/10408398.2016.1277972

Rice, S. L., Eitenmiller, R. R., and Koehler, P. E. (1976). Biologically active amines in food: a review. *J. Milk Food Technol.* 39, 353–358. doi: 10.4315/0022-2747-39.5.353

Ruiz-Capillas, C., and Jiménez-Colmenero, F. (2004). Biogenic amines in meat and meat products. *Crit. Rev. Food Sci. Nutr.* 44, 489–499. doi: 10.1080/10408690490489341

Sang, X., Li, K., Zhu, Y., Ma, X., and Hou, H. (2020). The impact of microbial diversity on biogenic amines formation in grasshopper sub shrimp paste during the fermentation. *Front. Microbiol.* 11:782. doi: 10.3389/fmicb.2020.00782

Shen, Y., Wu, Y., Wang, Y., Li, L., and Yang, S. (2021). Contribution of autochthonous microbiota succession to flavor formation during Chinese fermented mandarin fish (*Siniperca chuatsi*). *Food Chem.* 348:129107. doi: 10.1016/j.foodchem.2021.129107

Silbande, A., Adenet, S., Smith-Ravin, J., Joffraud, J.-J., Rochefort, K., and Leroi, F. (2016). Quality assessment of ice-stored tropical yellowfin tuna (*Thunnus albacares*) and influence of vacuum and modified atmosphere packaging. *Food Microbiol.* 60, 62–72. doi: 10.1016/j.fm.2016.06.016

Smith, T. A. (1981). Amines in food. *Food Chem.* 6, 169–200. doi: 10.1016/0308-8146(81)90008-X

Stellato, G., Storia, A. L., Filippis, F. D., Borriello, G., Villani, F., and Ercolini, D. (2016). Overlap of spoilage microbiota between meat and meat processing environment in small-scale vs large-scale retail distribution. *Appl. Environ. Microbiol.* 82, 4045–4054. doi: 10.1128/AEM.00793-16

Visciano, P., Schirone, M., Tofalo, R., and Suzzi, G. (2012). Biogenic amines in raw and processed seafood. *Front. Microbiol.* 3:188. doi: 10.3389/fmicb.2012.00188

Wang, Y., Li, C., Li, L., Yang, X., Wu, Y., Zhao, Y., et al. (2018). Effect of bacterial community and free amino acids on the content of biogenic amines during fermentation of Yu-lu, a Chinese fermented fish sauce. *J. Aquat. Food Prod. Technol.* 27, 496–507. doi: 10.1080/10498850.2018.1450573

Wang, Y., Zhang, C., Liu, F., Jin, Z., and Xia, X. (2022). Ecological succession and functional characteristics of lactic acid bacteria in traditional fermented foods. *Crit. Rev. Food Sci. Nutr.* 11–15. doi: 10.1080/10408398.2021.2025035

Wiernasz, N., Leroi, F., Chevalier, F., Cornet, J., Cardinal, M., Rohloff, J., et al. (2020). Salmon gravlax biopreservation with lactic acid bacteria: a Polyphasic approach to assessing the impact on organoleptic properties, microbial ecosystem and Volatilome composition. *Front. Microbiol.* 10:3103. doi: 10.3389/fmicb.2019.03103

Wu, Y., Xia, M., Zhao, N., Tu, L., Xue, D., Zhang, X., et al. (2021). Metabolic profile of main organic acids and its regulatory mechanism in solid-state fermentation of Chinese cereal vinegar. *Food Res. Int.* 145:110400. doi: 10.1016/J.FOODRES.2021.110400

Yan, L., Liu, S., Liu, Q., Zhang, M., Liu, Y., Wen, Y., et al. (2019). Improved performance of simultaneous nitrification and denitrification via nitrite in an oxygen-limited SBR by alternating the DO. *Bioresour. Technol.* 275:153. doi: 10.1016/j.biortech.2018.12.054

Yu, W., Guo, A., Zhang, Y., Chen, X., Qian, W., and Li, Y. (2018). Climate-induced habitat suitability variations of chub mackerel *Scomber japonicus* in the East China Sea. *Fish. Res.* 207, 63–73. doi: 10.1016/j.fishres.2018.06.007

Yu, D., Wu, L., Regenstein, J. M., Jiang, Q., Yang, F., Xu, Y., et al. (2019). Recent advances in quality retention of non-frozen fish and fishery products: a review. *Crit. Rev. Food Sci. Nutr.* 60, 1747–1759. doi: 10.1080/10408398.2019.1596067

Zhai, H., Yang, X., Li, L., Xia, G., Cen, J., Huang, H., et al. (2012). Biogenic amines in commercial fish and fish products sold in southern China. *Food Control* 25, 303–308. doi: 10.1016/j.foodcont.2011.10.057

Zhou, W., Tang, H., He, L., Yang, H., and Ou, C. (2012). Screening and identification of histamine-producing bacteria from chub mackerel meat. *Food Sci.* 33, 225–229.

Zhuang, S., Hong, H., Zhang, L., and Luo, Y. (2020a). Spoilage-related microbiota in fish and crustaceans during storage: research progress and future trends. *Compr. Rev. Food Sci. Food Saf.* 20, 252–288. doi: 10.1111/1541-4337.12659

Zhuang, S., Li, Y., Hong, H., Liu, Y., Shu, R., and Luo, Y. (2020b). Effects of ethyl lauroyl arginate hydrochloride on microbiota, quality and biochemical changes of container-cultured largemouth bass (*Micropterus salmonides*) fillets during storage at 4°C. *Food Chem.* 324:126886. doi: 10.1016/j.foodchem.2020.126886

Zhuang, S., Li, Y., Jia, S., Hong, H., Liu, Y., and Luo, Y. (2019). Effects of pomegranate peel extract on quality and microbiota composition of bighead carp (*Aristichthys nobilis*) fillets during chilled storage. *Food Microbiol.* 82, 445–454. doi: 10.1016/j.fm.2019.03.019

Zhuang, S., Liu, X., Li, Y., Zhang, L., Hong, H., Liu, J., et al. (2020c). Biochemical changes and amino acid deamination & decarboxylation activities of spoilage microbiota in chill-stored grass carp (*Ctenopharyngodon idella*) fillets. *Food Chem.* 336:127683. doi: 10.1016/j.foodchem.2020.127683

Zhuang, S., Tan, Y., Hong, H., Li, D., Zhang, L., and Luo, Y. (2022). Exploration of the roles of spoilage bacteria in degrading grass carp proteins during chilled storage: A combined metagenomic and metabolomic approach. *Food Res. Int.* 152:110926. doi: 10.1016/J.FOODRES.2021.110926

frontiers | Frontiers in Microbiology

TYPE Methods
PUBLISHED 08 November 2022
DOI 10.3389/fmicb.2022.1051162

OPEN ACCESS

EDITED BY
Jinxuan Cao,
Beijing Technology and Business University, China

REVIEWED BY
Caili Fu,
National University of Singapore Suzhou Research Institute (NUSRI), China
Md. Ashrafudoulla,
Chung-Ang University, South Korea

*CORRESPONDENCE
Yao Yang
cranny_yang@hotmail.com

†These authors have contributed equally to this work and share first authorship

SPECIALTY SECTION
This article was submitted to Food Microbiology, a section of the journal Frontiers in Microbiology

RECEIVED 22 September 2022
ACCEPTED 24 October 2022
PUBLISHED 08 November 2022

CITATION
Liu Y, Huang S, Zhou J, Zhang C, Hu F, Xiao Y, Qiu H and Yang Y (2022) A new method for the rapid detection of the antibacterial and bacteriostatic activity of disinfectants based on Propidium Monoazide combined with real-time PCR. *Front. Microbiol.* 13:1051162. doi: 10.3389/fmicb.2022.1051162

A new method for the rapid detection of the antibacterial and bacteriostatic activity of disinfectants based on Propidium Monoazide combined with real-time PCR

Yanrong Liu[1†], Shuting Huang[2†], Jungui Zhou[1], Chi Zhang[1], Feijie Hu[1], Youyu Xiao[1], Haopu Qiu[1] and Yao Yang[2*]

[1]Key Laboratory of Biotoxin Analysis and Assessment for State Market Regulation, Nanjing Institute of Product Quality Inspection, Nanjing, China, [2]School of Food Science and Pharmaceutical Engineering, Nanjing Normal University, Nanjing, China

Rapid detection of antibacterial and bacteriostatic properties is an important part of the quality and safety supervision of disinfectants. In this study, propidium monoazide (PMA) was used in combination with real-time PCR (PMA-qPCR) to detect the antibacterial and bacteriostatic activity of disinfectants against three commonly used indicator bacteria, *Escherichia coli*, *Staphylococcus aureus*, and *Candida albicans*, utilizing specifically designed primers. The method for preparing membrane-damaged bacteria was optimized to improve the ability of the PMA dye to distinguish between live and dead indicator bacteria. Finally, this method could simultaneously detect viable numbers of the indicator bacteria after the disinfectants were used. The R^2 values of the PMA-qPCR standard curves were 0.9986, 0.9980, and 0.9962 for *E. coli*, *S. aureus*, and *C. albicans*, respectively, and the detection range was 10^3~10^6CFU/ml, showing no significant difference in accuracy compared to that of the plate counting method ($p > 0.05$). The method established here is the first application of PMA-qPCR to detect the antibacterial and bacteriostatic activity of disinfectants. This technique markedly simplifies the detection steps of antibacterial and bacteriostatic activity, reduces the detection time (3h compared to 48~72h for the plate counting method), improves the quality supervision efficiency of disinfectants, and guarantees healthy and safe lives.

KEYWORDS

disinfectants, antibacterial and bacteriostatic activity, PMA-qPCR method, homogenization method, rapid detection

Introduction

The novel coronavirus has caused a worldwide infection since its outbreak in 2019, and the situation remains dire. The market share of disinfectants has proliferated to maximize people's health status; however, their quality control is facing an unprecedented challenge. Disinfectants products include disinfectant solution, disinfection devices (including

biological indicators, chemical indicators, and packaging for sterilized items), hygiene products, and single-use medical supplies (Fathizadeh et al., 2020). Disinfectants are widely used to ensure the quality and safety of medical devices, human life, and drinking water. Supervision of the product quality and safety of disinfectants, especially research on the rapid detection methods of antibacterial and bacteriostatic activity of disinfectants, is an important scientific issue related to health and the harmonious development of society (Rutala and Weber, 2016).

Disinfection refers to the elimination, removal, and suppression of pathogens and other harmful microorganisms in the environment. The evaluation of the effectiveness of disinfectants often relies on laboratory cultures because of the invisibility of microorganisms to the naked eye. The current national standards for the antibacterial and bacteriostatic activity of disinfectants are based on the indicator bacteria plate count method (China Technical Standard For Disinfection 2002), with the following main indicators: *Escherichia coli* 8099 stands for enteric bacteria, *Staphylococcus aureus* ATCC 6538 stands for septic cocci in bacterial colonies, and *Candida albicans* ATCC 10231 stands for pathogenic fungi. The specific method of this assay is to perform a plate count of the indicator bacteria from the treated samples and calculate the bactericidal inhibition rate from the difference in the number of viable bacteria compared to that of the control samples. The plate count method is simple, but the number of steps and workload is large, the turnaround time for test results is approximately 48 h (bacteria) to 72 h (yeast), and many sublethal indicator bacteria cannot form colonies because of the limitations of the culture environment (Kumar and Ghosh, 2019). Therefore, the plate count method cannot provide rapid evaluation of the antibacterial and bacteriostatic performance of disinfectants.

In recent years, real-time PCR (qPCR) has been widely used for the rapid quantitative detection of microorganisms (Kumar and Ghosh, 2019). The principle of this method is to amplify specific target microorganism genes by designing fluorescent dyes or fluorescence-labeled specific primers, and then determining the number of microorganisms in the sample by quantifying the initial template of the PCR reaction. The qPCR method, a detection technique that does not depend on microbial culture, drastically reduces the detection time; however, the nucleic acid detection method does not distinguish between dead and live bacteria (Zhao et al., 2017). Therefore, conventional qPCR methods are limited in the detection of the antibacterial and bacteriostatic activity of disinfectants.

Ethidium monoazide (EMA) and propidium monoazide (PMA) are a class of photoreactive dyes with a high affinity for DNA (van Frankenhuyzen et al., 2011). They are embedded in double-stranded DNA under intense visible light to form a covalently linked chemical modification that cannot be amplified by PCR. Because EMA and PMA are completely impermeable to cell membranes, this property allows them to be used in combination with qPCR to distinguish between dead and live bacteria. Recently, researchers have found that EMA treatment causes the loss of genomic DNA in live bacteria; therefore, PMA dyes have been chosen more often for this type of study (van Frankenhuyzen et al., 2011). Currently, PMA dye combined with fluorescent qPCR (PMA-qPCR) is widely used as a rapid detection method in food, medicine, and the environment. It detects not only bacteria, such as *E. coli* (Miotto et al., 2020; Deshmukh et al., 2021), *Salmonella* (Techathuvanan and D'Souza, 2020), *Lactobacillus* (Yang et al., 2021), *Vibrio* (Copin et al., 2021), and *Listeria monocytogenes* (Kragh et al., 2020), but also fungi, such as *C.albicans* (Asadzadeh et al., 2018), and even virus (Zeng et al., 2022).

The present study is the first application of PMA dye combined with qPCR for the rapid detection of the antibacterial and bacteriostatic activity of disinfectants. In contrast to the existing PMA-qPCR method, by optimizing the conditions, we aimed to develop a reaction system in which one product to be tested simultaneously acts on multiple indicator bacteria and completes the specific quantitative detection of multiple live indicator bacteria. This method may significantly improve the detection efficiency of the antibacterial and bacteriostatic activity of disinfectants and provide a practical basis for PMA-qPCR for the detection of live bacteria in mixed samples.

Materials and methods

Microorganisms and culture conditions

The bacterial strains and the culture media used in this study are listed in Table 1. The indicator strains were grown in the corresponding culture medium (Table 1).

Species-specific general primers and Probes designed

Specific primers were designed based on the gene sequences of the three indicator bacteria, and the corresponding probe primers were synthesized to improve the specificity of detection of the target indicator bacteria. The primers for amplifying the target sequences of *E. coli* were named EC-F, EC-R, and EC-P, the primers for amplifying the target sequences of *S. aureus* were named SA-F, SA-R, and SA-P, and the primers for amplifying the target sequences of *C. albicans* were named CA-F, CA-R, and CA-P. The results are listed in Table 2. The primer probes were synthesized by Bioengineering (Shanghai).

DNA extraction

For bacterial DNA extraction, cells were first lysed by the homogenization method and then extracted using phenol:chloroform:isopentyl alcohol (25,24,1), which is consistent

TABLE 1 Reference strains and specific primers verified by qPCR.

Strain	Culture medium	Culture temperature	Ct values		
			Primer of EC	Primer of SA	Primer of CA
Escherichia coli ATCC 8099	Nutrient agar	36°C	15.08 ± 0.15	–	–
Staphylococcus aureus ATCC 6538	Nutrient agar	36°C	–	14.64 ± 0.50	–
Candida albicans ATCC 10231	Sabouraud's agar	36°C	–	36.11 ± 0.17	9.08 ± 0.15
Enterobacter aerogenes ATCC 13048	Nutrient agar	36°C	35.64 ± 0.18	–	–
Staphylococcus epidermidis CMCC(B)26,069	Nutrient agar	36°C	–	35.92 ± 0.12	–
Salmonella ATCC 14028	Nutrient agar	36°C	35.28 ± 0.34	36.11 ± 0.03	35.13 ± 0.25
Pseudomonas aeruginosa ATCC 27853	Nutrient agar	36°C	–	–	–
Pseudomonas fluorescens ATCC 13525	Nutrient agar	36°C	–	–	–
Bacillus subtilis ATCC 6633	Nutrient agar	36°C	36.21 ± 0.54	36.77 ± 0.14	34.71 ± 0.56
Listeria monocytogenes ATCC 19111	BHI agar	36°C	–	–	–
Saccharomyces cerevisiae ATCC9763	Sabouraud's agar	36°C	35.31 ± 0.31	36.17 ± 0.12	34.86 ± 0.16

"–" indicates that no band is amplified.

TABLE 2 The primer used in this study.

Name of the primer	Primer sequence	Product size	Reference gene	References
EC-F	5′-gcgggtatttggctacgtaacga-3'	109 bp	*lacY*	Yuan et al. (2018)
EC-R	5′-ccagcagcagggcatttttc-3′			
EC-P	5'-VIC-tgcgccactgatcat-MGB-3′			
SA-F	5′-tagggatggctatcagtaatgttt-3′	105 bp	GenBank ID: DQ507382.1	Zhang et al. (2015)
SA-R	5′-ctatttacgccgttacctgtttgt-3′			
SA-P	5'-CY5-agaacaatacacaaagagg-MGB-3′			
CA-F	5′-cagaagtgacaggaacagcaatca-3′	94 bp	*sapI*	Lin et al. (2021)
CA-R	5′-gccactggacaaatcattttcg-3′			
CA-P	5'-FAM-ccactgtatttagctttgtca-MGB-3′			

with our previous reports (Yang et al., 2021). The DNA concentration was measured using a microspectrophotometer.

Quantitative qPCR analysis

The qPCR reaction system was (20 μl):2× SYBR Premix ExTaq 10 μl, 0.4 μl each of upstream and downstream primers and probe primer (10 μmol·L-1), 2 μl of template DNA (10 ng·μL-1), and dd H2O was added to 20 μl. A negative control reaction was set without DNA.

The amplification conditions were: pre-denaturation at 95°C for 30 s, denaturation at 95°C for 5 s, annealing at 58°C for 30 s, and extension at 72°C for 30 s for 40 cycles. The fluorescence signal was collected at the time of warming to establish a melting curve.

Specificity and sensitivity of qPCR

Primer specificity was verified by extracting genomic DNA from the three experimental strains and eight reference strains mentioned above, amplifying the samples by qPCR using the three primers mentioned above, and determining the specificity of the primers based on the results of the amplified Ct values (Zhai et al., 2019).

Primer amplification efficiency was verified by taking 1 ml of the prepared experimental broth with OD600 ≈ 1 (refer to live cells at the beginning of the exponential phase), and the number of viable bacteria in the experimental broth was determined by plate counting (Kragh et al., 2020). At the same time, whole genomic DNA was extracted, and gradient dilutions (10^1 to 10^6 dilutions) were prepared to obtain samples with different initial

DNA concentrations. The samples were amplified by qPCR using the above primers, and the linear equation of the Ct value versus initial DNA concentration was plotted to calculate the qPCR amplification efficiency E value ($E = 10^{-1/slope}$). Three replicates were performed for each qPCR sample.

Killing method for obtaining the dead cells of indicator bacteria

Heating methods

One milliliter of the experimental bacterial solution with OD600 ≈ 1 prepared as above was placed in a 1.5 ml centrifuge tube, washed twice in phosphate buffer solution (PBS), and resuspended in 1 ml of PBS buffer. The bacteria were treated in a water bath at 100°C for 15 min for heat lethality, and the untreated suspension was used as the control group. Three replicates were performed for each sample.

Homogenization (mechanical) method

One milliliter of the experimental bacterial solution with OD600 ≈ 1 prepared as described above was placed in a 1.5 ml centrifuge tube, washed twice in PBS buffer, and resuspended in 1 ml of PBS buffer. The homogenization program was set to a homogenization speed of 6.0 m/s, working time of 30 s, and interval of 30 s. A total of 15, 20, 25, 30, and 35 cycles were performed, with the untreated bacterial suspension as the control group. Three replicates were performed for each sample.

The samples obtained using the above method were directly coated with 200 μl of the corresponding solid medium plates and incubated at 37°C for 24 ~ 48 h. These results were used to determine the effectiveness of the preparation of membrane-damaged bacteria. Three replicates were performed for each sample.

PMA treatment for PMA-qPCR

The working concentration of PMA dye-treated samples (experimental bacterial solution or samples to be examined) in this study was 40 μg/ml (Zhao et al., 2019; Yang et al., 2021). The PMA was well mixed with the samples, incubated for 5 min protected from light, followed by 15 min of light reaction time, and the PMA-treated samples were analyzed in a PMA-Lite LED Photolysis Device (BIOTIUM, E90002, USA).

Construction of PMA-qPCR standard curve

One milliliter of the experimental bacterial solution with OD600 ≈ 1 prepared by the above method was collected by centrifugation at 12,000 × *g* for 1 min, washed twice with PBS buffer solution, and resuspended in an equal volume of PBS buffer solution. The suspensions were divided equally into two groups: one group without any treatment, that is, the live group, and one group with membrane-damaged bacteria prepared first according to the optimized method, followed by PMA treatment. DNA was extracted from both groups, and the DNA of the live group was diluted in a gradient ($10^0 \sim 10^6$ times) with the DNA of the membrane-damaged group. The Ct values were obtained by qPCR amplification using the designed primers. Ct values were obtained using an ABI 7500 FAST fluorescent quantitative PCR instrument. Three replicates were performed for each sample. A standard curve of Ct values versus the initial DNA concentration of live bacteria after PMA treatment was plotted.

Testing of disinfection products

The disinfectant products tested were: Refreshing Hand sanitizer, produced by Shanghai Jahwa United for germicidal experiments; Willows Foam Antibacterial Hand sanitizer, produced by Willis (Guangzhou) Household Products for germicidal experiments; Jierou sanitary wipes, produced by Zhongshun Jierou (Sichuan) Paper for sterilization experiments; Vida sanitary wipes, produced by Vida Paper (Beijing) for germicidal experiments; 84 disinfectants, produced by Jiangsu Atef 84 for sterilization experiments; and Hand disinfectant, produced by Nanjing Zhuhai Biotechnology for sterilization experiments.

Handwash inhibition test

A 10 g sample of hand sanitizer was weighed, added to an equal mass of PBS (0.03 mol/l, pH 7.2), homogenized, and prepared to obtain the sample solution to be tested.

Plate counting detection refers to China Standard GB15979-2002: Hygienic standard for disposable sanitary products. The PMA-qPCR method was slightly modified on the basis of the plate counting method, as follows: the 24 h slant culture of a single indicator bacterium was washed with PBS to make a bacterial concentration of approximately $5 \times 10^5 \sim 4.5 \times 10^6$ CFU/ml suspension; the three indicator bacterial suspensions were mixed in equal volumes; 300 μl of the mixed suspension was added to 5 ml of the sample solution, and 300 μl of the control sample was added to 5 ml of PBS for the control group. After 2 min, the experimental and control samples (0.5 ml) were placed in a test tube containing 5 ml of PBS and mixed well to terminate the inhibition experiment. The experimental and control samples were treated with PMA, and DNA was extracted and subjected to qPCR assays. The Ct values were recorded, and the number of viable bacteria in the sample solution was calculated using the PMA-qPCR standard curve.

Germicidal test of sanitary wipes

The neutralizing agent was identified according to China Standard GB15979-2002: Hygienic standard for disposable sanitary products, and the neutralizing agent of the sanitary wipes

used in this study was determined to be "Tryptic Soybean Peptone Liquid Medium (TSB) containing 1% sodium thiosulfate and 1% Tween 80." The PMA-qPCR method was modified slightly by mixing three indicator bacterial suspensions in equal volumes, each with a concentration of $5\times10^5\sim4.5\times10^6$ CFU/ml. Next, 300 µl of the indicator bacterial suspension was added dropwise to the control sample. After the reaction was terminated by the neutralizer, the samples of the experimental group and the control group were treated with PMA, and DNA was extracted and subjected to qPCR. Ct values were recorded, and the number of viable bacteria in the samples was calculated using the PMA-qPCR standard curve.

Sterilization experiments with disinfectants

The neutralizer identification test was performed according to China Technical Standard For Disinfection 2002, and the neutralizer used in this study for the 84 disinfectant samples was PBS containing 0.5% sodium thiosulfate, 0.2% lecithin, and 2% Tween 80″. The disinfectant sample to be tested was prepared using sterile hard water at a concentration of 1.25 times the concentration to be tested.

The PMA-qPCR method was slightly modified in the experimental method, and the indicator bacterial suspension was mixed with three types of suspensions in equal volumes, and the concentration of each indicator suspension was approximately 3×10^8 CFU/ml to 1.5×10^9 CFU/ml. The samples were treated with PMA, and DNA was extracted and subjected to qPCR. Ct values were recorded, and the number of viable bacteria in the samples was calculated using the PMA-qPCR standard curve.

Statistical analysis

The experiments were repeated three times with all indicators in three parallel groups. The results are expressed as $x\pm s$. The SPSS software (version 2.0) was used for the statistical analysis of the experimental data. The two groups were analyzed using independent samples *t*-test, and the significance level was set at 0.05.

Results

Primer specificity validation

The specificity of qPCR primers was verified according to a previously described method. The qPCR results obtained for the Ct values are shown in Table 1. DNA from the three target indicator bacteria were successfully amplified using the corresponding primers, with Ct values ranging from 9.08 ± 0.15 to 15.08 ± 0.15 (Table 1). Moreover, amplification of other indicator bacteria and reference strains using the target primers was unsuccessful, illustrating the specificity of the qPCR primers.

Validation of primer amplification efficiency

The experimental bacterial solutions prepared at OD600 ≈ 1 for the indicator bacteria were subjected to plate colony counting. The results showed that the experimental concentrations of the three different indicator bacteria, *E. coli*, *S. aureus*, and *C. albicans*, were 1.1×10^9, 5.6×10^8, and 4.5×10^8 CFU/ml, respectively. The genomic DNA of the three indicator bacteria was then extracted separately, diluted in a gradient to obtain $10^2\sim10^9$ CFU/ml bacterial DNA concentrations, and used sequentially as templates for qPCR amplification. The Ct values of the single indicator bacteria were plotted against a standard curve of $\log_{10}$ CFU/mL, and the experimental results are shown in Table 3.

The results showed that DNA from the three indicator bacteria was successfully amplified using the corresponding qPCR in the range of $10^3\sim10^6$ CFU/ml, and the amplification efficiency was in the range of 90 ~ 105%.

Based on these results, we concluded that the qPCR primers had good specificity and high amplification efficiency. To further improve the detection efficiency, three indicator bacteria primers were added to the qPCR system simultaneously in the actual disinfectant sample testing to achieve a one-step detection of different indicator bacteria.

Preparation of membrane-damaging bacteria

Heating method

The three indicator bacteria were treated separately in a 100°C water bath for 15 min, and the samples before and after treatment were subjected to plate counting and qPCR. In addition, the heated samples were subjected to PMA treatment and subsequent qPCR analysis; the results are shown in Table 4.

The heating method was effective for fragmenting all three indicator bacteria, and no colonies grew on the corresponding plates after heating (Table 4). However, qPCR showed that the Ct values changed before and after the heat treatment, especially for S. aureus and C. albicans. The ΔCt values were 6.24 and 4.87 before and after treatment, respectively, which is highly variable,

TABLE 3 The amplification efficiency of qPCR.

Indicator bacteria	Equation of linear regression	R^2 value	Detection range ($\log_{10}$CFU/mL)	*E* value[a]
Escherichia coli	$y=-3.4571x+37.1901$	0.9993	3 ~ 6	94.65%
Staphylococcus aureus	$y=-3.7889x+42.3801$	0.9995	3 ~ 6	93.62%
Candida albicans	$y=-3.1250x+36.4680$	0.9991	3 ~ 6	92.95%

[a]*E*-value = $10^{(-1/\text{slope})}$.

and it was seen that the heat treatment caused different degrees of damage to the DNA of all three indicator bacteria, which affected the amplification of PCR reactions. Although the Ct values of qPCR were further reduced after PMA treatment, it could not be determined whether heat treatment influenced the PMA-bound DNA. Therefore, the heating method is not applicable for the preparation of membrane-damaged bacteria. Currently, the heating method has been used in many PMA-qPCR studies for the preparation of membrane-damaged bacteria; however, optimization of the heat treatment conditions needs to be performed according to different target strains. Because the goal of the current study was to detect three indicator bacteria simultaneously, the generality of membrane-damaged bacterial preparations was required; therefore, no further attempts to optimize the heat treatment method were made.

Homogenization (mechanical) method

To determine the appropriate homogenization intensity that could simultaneously target the three indicator bacteria, a one-way experiment on the number of homogenization cycles was conducted, and the results are shown in Table 5.

The homogenization method did not have consistent fragmentation effects for the three different indicator bacteria (Table 5). The gram-negative bacterium *E. coli* has a sparse cell wall, is easily fragmented, and was completely fragmented after 15 homogenization cycles, whereas the gram-positive bacterium *S. aureus* and *C. albicans* required increased mechanical fragmentation intensity owing to their dense cell walls. According to the experimental results, the final condition of the homogenization crushing treatment was determined as 6.0 m/s (work 30 s and stop 30 s) per cycle for 35 cycles.

The three indicator bacteria were homogenized and separately fragmented. The samples were subjected to qPCR before and after treatment, and homogenized samples were subjected to PMA and subsequent qPCR analyses. Table 6 presents the results.

The Ct values of qPCR before and after homogenization of the three indicator bacteria were not significantly different, which revealed that this treatment did not affect the amplification of genomic DNA of the strains involved in subsequent PCR reactions (Table 6). In addition, the Ct values of qPCR after PMA treatment were significantly lower than those before PMA treatment, with ΔCt values of 12.83, 12.73, and 11.10 for *E. coli*, *S. aureus*, and *C. albicans*, respectively, indicating that PMA could distinguish between live and membrane-damaged bacteria. These results fully illustrated the feasibility of PMA-qPCR for the quantification of viable bacteria among the three indicator bacteria.

Construction of PMA-qPCR standard curve

Standard curves of PMA-qPCR for the three indicator bacteria were established according to the methods described above (Table 7). The results show that the standard curves had a good linear relationship, and all of the concentration ranges of the detected *E. coli*, *S. aureus*, and *C. albicans* were $10^3 \sim 10^6$ CFU/ml, respectively, which met the requirements for antibacterial and bacteriostatic effects of disinfectants (China Standard GB15979-2002: Hygienic standard for disposable sanitary products).

Testing of disinfection products

The antibacterial and bacteriostatic activity of the three disinfectants were tested using the PMA-qPCR method and were compared with those of the corresponding national standards adopted for plate counting.

Figure 1 shows the qPCR amplification curves of the three indicator bacteria treated with PMA after exposure to the test product. Compared with that of the control sample (three indicator bacteria in contact with PBS), the amplification curve of the experimental sample showed a significant backward shift, that is, a significant increase in the Ct value. This result indicates that PMA effectively differentiated the live and dead bacteria in the experimental sample, which enabled subsequent qPCR to successfully quantify the live bacteria of the three indicator bacteria in the sample and finally achieved rapid detection of the bacteriostatic properties of the product. More importantly, as shown in Figure 1, the simultaneous addition of the designed primers and probes for the three indicator bacteria to the qPCR system enabled the concurrent quantitative detection of three different indicator bacteria in the experimental samples. In total, the results show that this method can successfully detect the

TABLE 4 Experimental results of the heating treated samples.

Indicator bacteria	Plate count (log_{10}CFU/mL)		qPCR (Ct value)		PMA-qPCR (Ct value)
	Before heating	After heating	Before heating	After heating	After heating
Escherichia coli	8.87 ± 0.57	–	11.92 ± 0.17	12.62 ± 0.34	20.66 ± 0.43
Staphylococcus aureus	6.14 ± 0.35	–	12.62 ± 0.68	18.86 ± 0.21	20.17 ± 0.28
Candida albicans	4.14 ± 0.46	–	14.37 ± 0.19	19.24 ± 0.38	21.11 ± 0.37

"–" indicates that no clone growth.

quantification of three indicator bacteria in one sample, which has not been reported yet.

In the present study, the established PMA-qPCR method was applied to test six disinfectants in three categories, hand sanitizers, sanitary wipes, and disinfection solutions, as shown in Figure 2. There was no significant difference between the PMA-qPCR and plate counting methods in the quantitative detection of the three indicator bacteria after contact with disinfectants. This result illustrates that the PMA-qPCR method established here is accurate and appropriate for detecting the antibacterial and bacteriostatic activity of disinfectants.

Discussion

According to China Technical Standard For Disinfection 2002, the plate counting method is the national standard detection method for the numerical detection of viable microorganisms in disinfectants. This method is simple; however, test results depend on the growth of microorganisms, which takes approximately 48 h (bacteria) to 72 h (yeast). In addition, owing to the limitations of the culture medium and conditions, the plate counting method can only detect bacteria suitable for growth under the corresponding culture conditions. Many indicator bacteria in a sublethal state (VBNC) cannot form colonies in conventional culture media (Li et al., 2017; Golpayegani et al., 2019). Therefore, it is difficult to evaluate the number of indicator bacteria before and after sterilization using daily chemical disinfectants.

At the same time, antibacterial and bacteriostatic activity tests of disinfectants usually require two to three indicator bacteria: *S. aureus*, *E. coli*, and *C. albicans* (Jampilek, 2018). During detection, the same product to be tested needs to be applied to different indicator bacteria and the quantitative detection of each indicator bacteria after treatment. In conclusion, current national standard methods are unable to rapidly evaluate the antibacterial and bacteriostatic activity of disinfectants. To date, no other methods have been developed to detect the antibacterial and bacteriostatic activity of disinfectants.

Currently, PMA combined with qPCR is primarily used for microbial detection in food, medicine, and the environment. However, there are no reports on the antibacterial and bacteriostatic activity detection of disinfectants. The standard curve of PMA-qPCR was drawn by preparing the membrane-damaged bacteria of the target microorganism using the DNA from the membrane-damaged bacteria to conduct a gradient dilution of its living bacterial DNA, and then drawing it according to the Ct value of the qPCR reaction. Therefore, the preparation method of membrane-damaged bacteria is the key to distinguishing between live and dead bacteria of the target microorganism by PMA dye, and it also determines the accuracy of PMA-qPCR for the detection of living target microorganisms. Heating is the most commonly reported method for preparing membrane-damaged bacteria (Chen et al., 2011; Løvdal et al., 2011; Ditommaso et al., 2015). However, we showed that although the heating method had a good crushing effect on the three indicator bacteria, there was no colony growth on

TABLE 5 Optimization results of the homogenization method.

Indicator bacteria	Cycles				
Plate counting result					
(log_{10}CFU/mL)	15	20	25	30	35
Escherichia coli	–	–	–	–	–
Staphylococcus aureus	4.58 ± 0.12	2.83 ± 0.28	1.73 ± 0.25	–	–
Candida albicans	4.08 ± 0.34	2.64 ± 0.23	1.92 ± 0.18	1.62 ± 0.26	–

"-" indicates that no clone growth.

TABLE 6 qPCR results of homogenization treated samples.

Indicator bacteria	qPCR (Ct value)		PMA-qPCR (Ct value)	ΔCt[a]
	Before homogenization	After homogenization	After homogenization	Before and after PMA treatment
Escherichia coli	11.84 ± 0.13	9.82 ± 0.33	24.67 ± 0.23	12.83
Staphylococcus aureus	12.43 ± 0.58	12.48 ± 0.19	25.16 ± 0.21	12.73
Candida albicans	14.07 ± 0.16	14.21 ± 0.28	25.17 ± 0.47	11.1

[a]ΔCt = Ct value of PMA-qPCR - Ct value of the control group.

the corresponding plates after heat treatment. Moreover, the qPCR results (Table 4) showed that Ct values changed before and after treatment, especially for *S. aureus* and *C. albicans*, where the ΔCt values were 6.24 and 4.87 before and after heat treatment, respectively. These results revealed that the treatment caused different degrees of DNA damage in the three indicator bacteria and affected the amplification of the PCR reaction. Therefore, the heating method was not suitable for the preparation of membrane-damaged bacteria in this study. In addition, three indicator bacteria with membrane damage were prepared using the optimized homogenization method and analyzed using PMA treatment and qPCR. The results showed that the ΔCt values of qPCR before and after PMA treatment of the three indicator bacteria were 12.83, 12.73, and 11.10 for *E. coli*, *S. aureus*, and *C. albicans*, respectively (Table 6). PMA can clearly distinguish between living and membrane-damaged bacteria. It is worth noting that the preparation method of membrane-damaged bacteria in the current study can be applied to indicator bacteria for antibacterial and bacteriostatic activity detection of three disinfectants simultaneously, providing favorable conditions for the simultaneous detection of antibacterial and bacteriostatic activity of one disinfectant against multiple indicator bacteria.

Finally, the PMA-qPCR quantitative detection method established herein was used to rapidly detect the antibacterial and bacteriostatic activity of the six disinfectants in three categories. The quantitative detection results of living bacteria before and after contact with the indicator bacteria of each disinfectant was not significantly different from those of the plate counting method, and the detection time was shortened to 3 h compared to 48 ~ 72 h for the plate counting method

TABLE 7 PMA-qPCR standard curves of three indicator bacteria.

Indicator bacteria	Equation of linear regression	R^2 value	Detection range (log_{10}CFU/mL)
Escherichia coli	$y = -3.3559x + 36.7329$	0.9986	3 ~ 6
Staphylococcus aureus	$y = -3.238x + 38.8192$	0.998	3 ~ 6
Candida albicans	$y = -3.168x + 36.5982$	0.9962	3 ~ 6

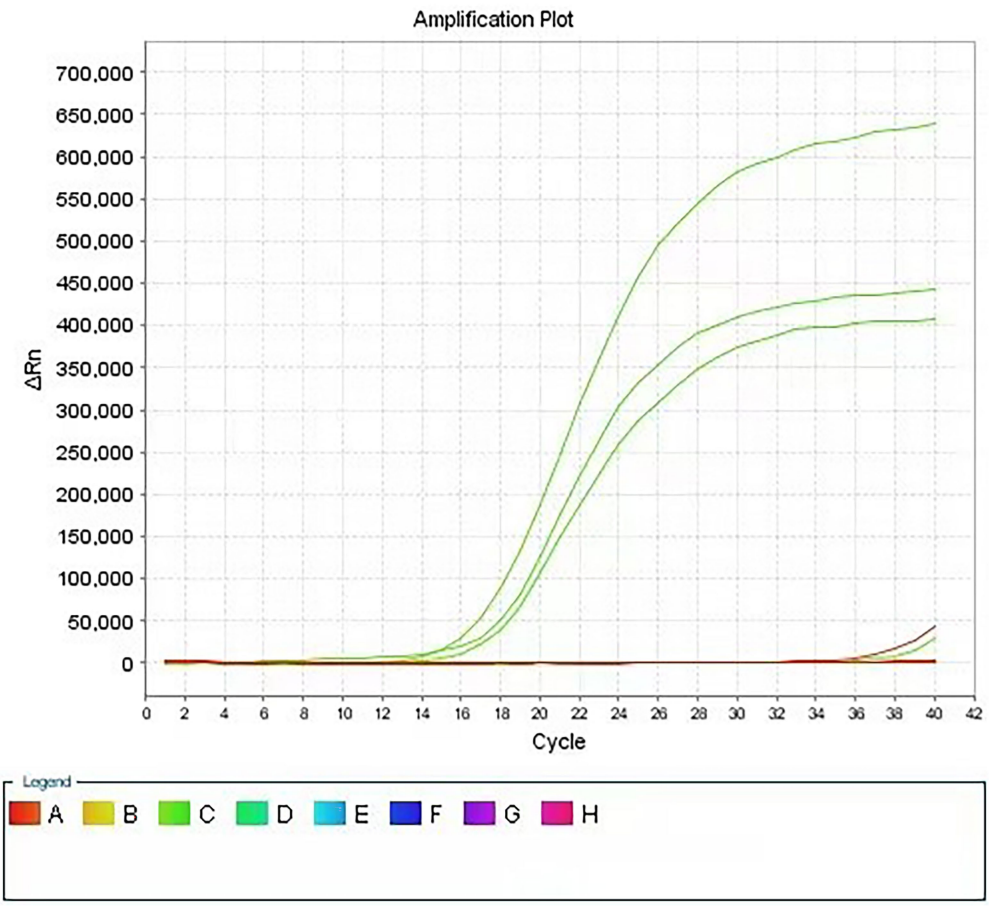

FIGURE 1
Amplification curve of PMA-qPCR assay for disinfectant products. Using specific primers for three indicator bacteria, real-time quantitative detection of three indicator bacteria was realized in the same reaction system.

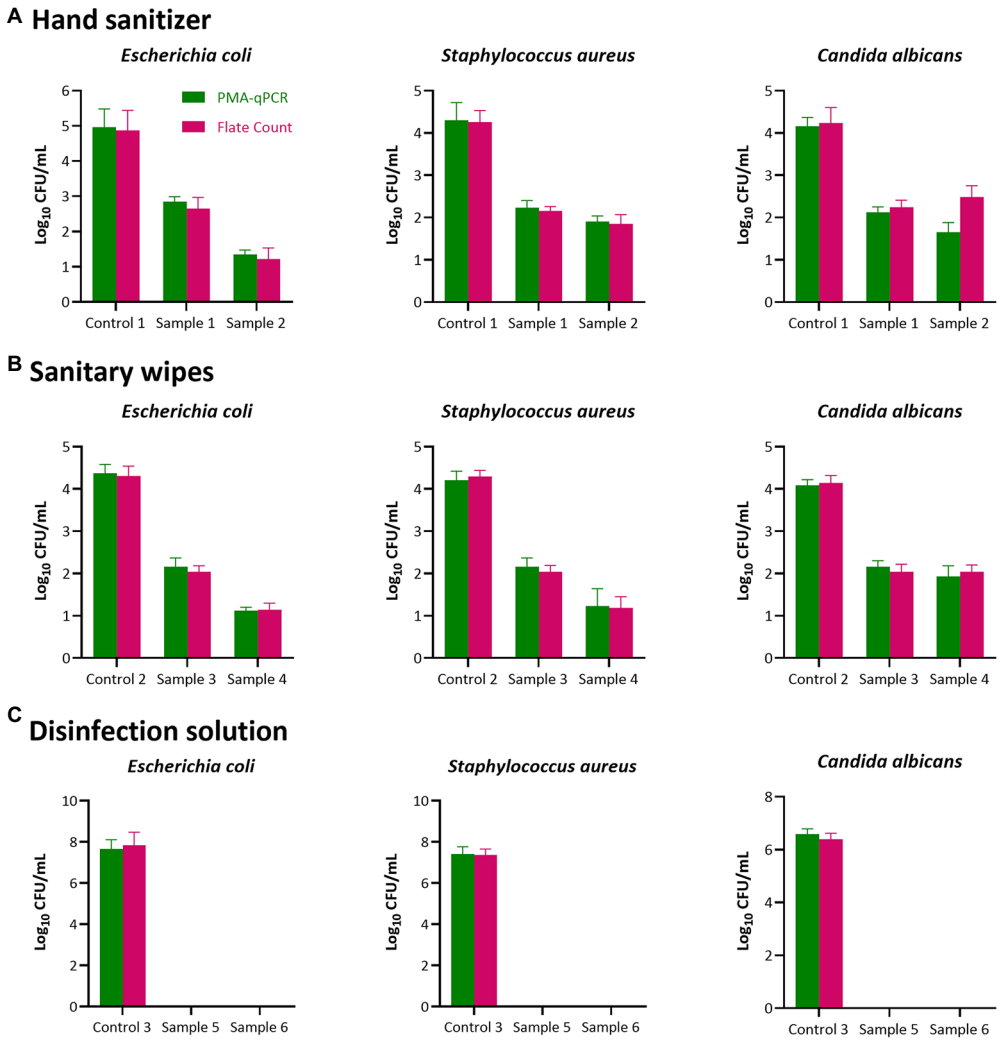

FIGURE 2
Antibacterial and Bacteriostatic activity test results of disinfectant products. Two individual methods (plate count in MRS agar and PMA-qPCR) were used to detect the antibacterial and bacteriostatic activity of the six disinfectants in three categories [**(A)**, Hand sanitizer; **(B)**, Sanitary wipes and **(C)**, Disinfection solutions)] Results represent the mean value of three repeats ± SD. No significant difference between the PMA-qPCR and plate counting methods in the quantitative detection of the three indicator bacteria after contact with disinfectants ($p > 0.05$).

(Figure 2). The present study markedly improves the detection efficiency of the antibacterial and bacteriostatic activity of disinfectants and their quality supervision efficiency (Drauch et al., 2020; Filipe et al., 2021). The PMA-qPCR method established here also provides the potential for detecting live mixed bacteria in complex samples.

Conclusion

The current study is the first application of PMA-qPCR for the rapid detection of the antibacterial and bacteriostatic activity of disinfectants. There was no significant difference between the method established here and the plate counting method in the rapid detection of the antibacterial and bacteriostatic activity of the six disinfectants in the three categories, indicating the high accuracy of this method. In addition, this method inspects disinfectants in a reaction system concurrently to carry out quarantine on three commonly used indicator bacteria/antimicrobial resistance testing. Furthermore, it significantly simplifies the testing steps, reduces the testing time, improves the quality of disinfectant regulatory efficiency, and safeguards people's health and safety.

Data availability statement

The original contributions presented in the study are included in the article/supplementary material, further inquiries can be directed to the corresponding author.

Author contributions

YL, SH, JZ, CZ, FH, YX, HQ, and YY participated in the design and discussion of the study. YL and SH carried out the experiments. YL, SH, and YY wrote the manuscript. JZ, CZ, FH, YX, HQ, and YY discussed, revised, and edited the manuscript. All authors have read and approved the final version to be published.

Funding

This work was supported by the State Administration for Market Regulation Foundation of China [Grant number 2020MK136], and the Key Laboratory of Biotoxin Analysis and Assessment for State Market Regulation.

Conflict of interest

The authors declare that the research was conducted in the absence of any commercial or financial relationships that could be construed as a potential conflict of interest.

Publisher's note

All claims expressed in this article are solely those of the authors and do not necessarily represent those of their affiliated organizations, or those of the publisher, the editors and the reviewers. Any product that may be evaluated in this article, or claim that may be made by its manufacturer, is not guaranteed or endorsed by the publisher.

References

Asadzadeh, M., Ahmad, S., Al-Sweih, N., and Khan, Z. J. M. P. (2018). Rapid and accurate identification of Candida Albicans and Candida dubliniensis by real-time PCR and melting curve analysis. *Med Princ Pract.* 27, 543–548. doi: 10.1159/000493426

Chen, S., Wang, F., Beaulieu, J. C., Stein, R. E., Ge, B. J. A., and Microbiology, E. (2011). Rapid detection of viable salmonellae in produce by coupling propidium monoazide with loop-mediated isothermal amplification. *Appl Environ Microbiol.* 77, 4008–4016. doi: 10.1128/AEM.00354-11

Copin, S., Mougin, J., Raguenet, V., Robert-Pillot, A., Midelet, G., Grard, T., et al. (2021). Ethidium and propidium monoazide: comparison of potential toxicity on vibrio sp viability. *Letters in Applied Microbiology* 72, 245–250. doi: 10.1111/lam.13412

Deshmukh, R., Bhand, S., and Roy, U. J. I. J. O. M. (2021). BCIG-SMAC medium and PMA-qPCR for differential detection of viable Escherichia coli in potable water. *Iran J Microbiol.* 13, 624–631. doi: 10.18502/ijm.v13i5.7427

Ditommaso, S., Giacomuzzi, M., Ricciardi, E., Zotti, C. M. J. M., and Probes, C. (2015). Viability-qPCR for detecting legionella: comparison of two assays based on different amplicon lengths. *Molecular and Cellular Probes* 29, 237–243. doi: 10.1016/j.mcp.2015.05.011

Drauch, V., Ibesich, C., Vogl, C., Hess, M., and Hess, C. J. I. J. O. F. M. (2020). *In-vitro* testing of bacteriostatic and bactericidal efficacy of commercial disinfectants against salmonella Infantis reveals substantial differences between products and bacterial strains. *Int J Food Microbiol.* 328:108660. doi: 10.1016/j.ijfoodmicro.2020.108660

Fathizadeh, H., Maroufi, P., Momen-Heravi, M., Dao, S., Köse, Ş., Ganbarov, K., et al. (2020). Protection and disinfection policies against SARS-CoV-2 (COVID-19). *Infez Med.* 28, 185–191.

Filipe, H. A., Fiuza, S. M., Henriques, C. A., and Antunes, F. E. J. I. J. O. P. (2021). Antiviral and antibacterial activity of hand sanitizer and surface disinfectant formulations. *Int J Pharm.* 609:121139. doi: 10.1016/j.ijpharm.2021.121139

Golpayegani, A., Douraghi, M., Rezaei, F., Alimohammadi, M., and Nodehi, R. N. J. J.Engineering (2019). Propidium monoazide–quantitative polymerase chain reaction (PMA-qPCR) assay for rapid detection of viable and viable but non-culturable (VBNC) Pseudomonas aeruginosa in swimming pools. *J Environ Health Sci Eng.* 17, 407–416. doi: 10.1007/s40201-019-00359-w

Jampilek, J. J. C. M. C. (2018). Design and discovery of new antibacterial agents advances, perspectives, challenges. *Curr Med Chem.* 25, 4972–5006. doi: 10.2174/0929867324666170918122633

Kragh, M. L., Thykier, M., and Hansen, L. T. J. F. M. (2020). A long-amplicon quantitative PCR assay with propidium monoazide to enumerate viable listeria monocytogenes after heat and desiccation treatments. *Food Microbiol.* 86:103310. doi: 10.1016/j.fm.2019.103310

Kumar, S. S., and Ghosh, A. R. J. M. (2019). Assessment of bacterial viability: a comprehensive review on recent advances and challenges. *Microbiology* 165, 593–610. doi: 10.1099/mic.0.000786

Li, Y., Yang, L., Fu, J., Yan, M., Chen, D., and Zhang, L. J. M. P. (2017). The novel loop-mediated isothermal amplification based confirmation methodology on the bacteria in viable but non-Culturable (VBNC) state. *Microb Pathog.* 111, 280–284. doi: 10.1016/j.micpath.2017.09.007

Lin, X., Jin, X., Du, W., Shan, X., Huang, Q., Fu, R., et al. (2021). Quantitative and specific detection of viable pathogens on a portable microfluidic chip system by combining improved propidium monoazide (PMAxx) and loop-mediated isothermal amplification (LAMP). *Anal. Methods* 13, 3569–3576. doi: 10.1039/D1AY00953B

Løvdal, T., Hovda, M. B., Björkblom, B., and Møller, S. G. J. J. O. M. M. (2011). Propidium monoazide combined with real-time quantitative PCR underestimates heat-killed listeria innocua. *J Microbiol Methods*. 85, 164–169. doi: 10.1016/j.mimet.2011.01.027

Miotto, M., Barretta, C., Ossai, S. O., Da Silva, H. S., Kist, A., Vieira, C. R. W., et al. (2020). Optimization of a propidium monoazide-qPCR method for Escherichia coli quantification in raw seafood. *International Journal of Food Microbiology* 318:108467. doi: 10.1016/j.ijfoodmicro.2019.108467

Rutala, W. A., and Weber, D. J. J. I. D. C. (2016). Disinfection and sterilization in health care facilities: an overview and current issues. *Infect Dis Clin North Am.* 30, 609–637. doi: 10.1016/j.idc.2016.04.002

Techathuvanan, C., and D'souza, D. H. J. J. O. F. S. (2020). Propidium monoazide for viable salmonella enterica detection by PCR and LAMP assays in comparison to RNA-based RT-PCR, RT-LAMP, and culture-based assays. *J Food Sci.* 85, 3509–3516. doi: 10.1111/1750-3841.15459

Van Frankenhuyzen, J. K., Trevors, J. T., Lee, H., Flemming, C. A., and Habash, M. B. J. J. O. M. M. (2011). Molecular pathogen detection in biosolids with a focus on quantitative PCR using propidium monoazide for viable cell enumeration. *Journal of Microbiological Methods* 87, 263–272. doi: 10.1016/j.mimet.2011.09.007

Yang, Y., Liu, Y., Shu, Y., Xia, W., Xu, R., and Chen, Y. J. F. A. M. (2021). Modified PMA-qPCR method for rapid quantification of viable lactobacillus spp. in fermented dairy products. *Food Analytical Methods* 14, 1908–1918. doi: 10.1007/s12161-021-02022-3

Yuan, Y., Zheng, G., Lin, M., and Mustapha, A. J. W. R. (2018). Detection of viable Escherichia coli in environmental water using combined propidium monoazide staining and quantitative PCR. *Water Res.* 145, 398–407. doi: 10.1016/j.watres.2018.08.044

Zeng, D., Qian, B., Li, Y., Zong, K., Peng, W., Liao, K., et al. (2022). Prospects for the application of infectious virus detection technology based on propidium monoazide in African swine fever management. *Front Microbiol.* 13:1025758. doi: 10.3389/fmicb.2022.1025758

Zhai, L., Li, J., Tao, T., Lu, Z., Lv, F., and Bie, X. J. C. J. O. M. (2019). Propidium monoazide real-time PCR amplification for viable Salmonella species and Salmonella Heidelberg in pork. *Can J Microbiol.* 65, 477–485. doi: 10.1139/cjm-2018-0547

Zhang, Z., Liu, W., Xu, H., Aguilar, Z. P., Shah, N. P., and Wei, H. J. J. O. D. S. (2015). Propidium monoazide combined with real-time PCR for selective detection of viable Staphylococcus aureus in milk powder and meat products. *Journal of Dairy Science* 98, 1625–1633. doi: 10.3168/jds.2014-8938

Zhao, Y., Chen, H., Liu, H., Cai, J., Meng, L., Dong, L., et al. (2019). Quantitative polymerase chain reaction coupled with sodium dodecyl sulfate and propidium monoazide for detection of viable Streptococcus agalactiae in milk. *Front Microbiol.* 10:661. doi: 10.3389/fmicb.2019.00661

Zhao, X., Zhong, J., Wei, C., Lin, C.-W., and Ding, T. J. F. I. M. (2017). Current perspectives on viable but non-culturable state in foodborne pathogens. *Front. Microbiol.* 8:580. doi: 10.3389/fmicb.2017.00580

frontiers | Frontiers in Microbiology

TYPE Mini Review
PUBLISHED 01 December 2022
DOI 10.3389/fmicb.2022.1070773

OPEN ACCESS

EDITED BY
Changyu Zhou,
Ningbo University,
China

REVIEWED BY
Hao Dong,
Zhongkai University of Agriculture and Engineering, China
Zhang Jiamin,
Chengdu University,
China
Liao Guozhou,
Yunnan Agricultural University,
China

*CORRESPONDENCE
Tian Zhong
tzhong@must.edu.mo
Xi Yu
xyu@must.edu.mo

†These authors have contributed equally to this work

SPECIALTY SECTION
This article was submitted to Food Microbiology, a section of the journal Frontiers in Microbiology

RECEIVED 15 October 2022
ACCEPTED 11 November 2022
PUBLISHED 01 December 2022

CITATION
Tao A, Zhang H, Duan J, Xiao Y, Liu Y, Li J, Huang J, Zhong T and Yu X (2022) Mechanism and application of fermentation to remove beany flavor from plant-based meat analogs: A mini review. *Front. Microbiol.* 13:1070773. doi: 10.3389/fmicb.2022.1070773

Mechanism and application of fermentation to remove beany flavor from plant-based meat analogs: A mini review

Anqi Tao[1†], Hongyu Zhang[1†], Junnan Duan[1†], Ying Xiao[1,2], Yao Liu[3], Jianwei Li[4], Jieyu Huang[4], Tian Zhong[1*] and Xi Yu[1,2*]

[1]Faculty of Medicine, Macau University of Science and Technology, Macau, Macau SAR, China, [2]Guangdong-Hong Kong-Macao Joint Laboratory for Contaminants Exposure and Health, School of Environmental Science and Engineering, Institute of Environmental Health and Pollution Control, Guangdong University of Technology, Guangzhou, China, [3]School of Pharmacy and Food Science, Zhuhai College of Science and Technology, Zhuhai, China, [4]Macau Uni-Win Biotechnology Co., Ltd, Macau, Macau SAR, China

Over the past few decades, there has been a noticeable surge in the market of plant-based meat analogs (PBMA). Such popularity stems from their environmentally friendly production procedures as well as their positive health effects. In order to meet the market demand, it is necessary to look for plant protein processing techniques that can help them match the quality of conventional meat protein from the aspects of sensory, quality and functionality. Bean proteins are ideal options for PBMA with their easy accessibility, high nutrient-density and reasonable price. However, the high polyunsaturated lipids content of beans inevitably leads to the unpleasant beany flavor of soy protein products, which severely affects the promotion of soy protein-based PBMA. In order to solve this issue, various methods including bleaching, enzyme and fermentation etc. are developed. Among these, fermentation is widely investigated due to its high efficiency, less harm to the protein matrix, targeted performance and low budget. In addition, proper utilization of microbiome during the fermentation process not only reduces the unpleasant beany flavors, but also enhances the aroma profile of the final product. In this review, we provide a thorough and succinct overview of the mechanism underlying the formation and elimination of beany flavor with associated fermentation process. The pros and cons of typical fermentation technologies for removing beany flavors are discussed in alongside with their application scenarios. Additionally, the variations among different methods are compared in terms of the strains, fermentation condition, target functionality, matrix for application, sensory perception etc.

KEYWORDS

beany-flavor, plant-based meat analogs, fermentation, soy proteins, pea proteins, off-flavor

Introduction

The Food and Agriculture Organization of the United Nations estimates that in 2019, humans consumed about 3.25 million tons of meat; demand for meat is expected to increase by another 12% by 2029; and by 2050, demand for meat will increase by about 70%. If traditional meat production and management patterns remain unchanged, an additional 30%–50% of the land will be needed for livestock and meat production by then (Chen et al., 2019). Moreover, such situation of undersupply can be further intensified by natural disasters showing up every now and then. Animal diseases such as African swine fever and avian influenza in 2018 caused an increasing number of small and medium-sized livestock companies to exit the market. During the Coronavirus Disease 2019 (COVID-19) pandemic, the meat, poultry, and animal product processing plants were the sectors most affected, which leads to imbalance between global supply and demand for meat products (Chen and Yang, 2021). This situation has now triggered an increase in the price of traditional meat products. The global agriculture and meat industry is facing serious challenges considering factors such as increasing pressure on the natural environment, population growth, consumer trends in health and environmental protection, and food innovation (Kumar et al., 2017). To relieve the supply pressure of meat products, the development of plant-based meat analogs (PBMA) can be an effective way to address the imbalance between meat production and consumption (Taufik et al., 2019; Sun et al., 2022).

Recent PBMA research and development has been focusing on utilizing raw materials such as soy and pea proteins to mimic the flavor, smell, appearance and texture of traditional meats. It is beneficial for the whole mankind not only in terms of promoting a sustainable development, but also from a nutrition aspect (Kyriakopoulou et al., 2021). Compared to traditional meat, the energy, land, and water consumption of plant-based meat is much lowered. That is why this new star can effectively mitigate carbon emissions and moderate global environmental change (Pimentel and Pimentel, 2003). Many epidemiological studies have shown that long-term meat consumption, especially red and processed meats, increases the incidence of digestive cancer, cardiovascular disease and hypercholesterolemia (Cordelle et al., 2022). Conversely pieces of evidence support the health benefits of consuming a plant-based diet and increasing the intake of legumes. Significantly reduces the incidence of heart disease, high blood pressure, stroke, and type 2 diabetes (Polak et al., 2015).

Nevertheless, despite the many benefits of PBMA, their market share is still low at around 1% (Choudhury et al., 2020). The major bottleneck for developing ideal products which can cater the public lies in the texture as well as the taste. Other problems include high energy consumption of the production line, rough finished products and premature control technology. Currently, the key problem with the flavor of PBMA is that soy and pea proteins have an unpleasant beany-flavor which hinders consumer preference and acceptability (Mittermeier-Kleßinger et al., 2021). Flavorings are added during the production process to cover the off flavors as a current mainstream solution. However, the addition of extra seasonings may also have an impact on the overall taste and bring about adverse health issues for the consumers. Other methods to reduce the beany flavor include temperature control, enzyme treatment, acid–base treatment, supercritical CO_2 extraction, new cultivars breeding, genetic engineering, etc. (Zhang et al., 2012). However, some of these methods have hidden risks for food safety and quality, while the high cost and extra energy consumption also bring about new problems (Kumari et al., 2015; Nedele et al., 2021; Korma et al., 2022). Therefore, searching for novel technology to remove beany off-flavors instead of covering them is significant to improve the overall taste and future development of PBMA (Sun et al., 2022).

Recently, through the effort of modern microbiologists, it is more and more revealed that fermentation using microorganisms can effectively remove the beany flavor from next-generation plant-based food products such as PBMA. Moreover, a new aromatic taste can be developed during the fermentation to mask or cover the beany flavor sometimes (Wang Z. et al., 2022). Other than that, fermentation has many additional benefits, such as adjusting the gut microbiota and remediating the detriment on the gut epithelium caused by food additives (Yu and Zuo, 2021). This review discusses the mechanism of the formation of beany odors, the mechanism of using fermentation to remove them, and the applications and the differences of various traditional and newly emerged techniques. In the end, summary and discussion are made about the possibilities to utilize and improve current fermentation technique to better develop our food for future signatured by PBMA.

The formation of beany flavor

Unsaturated fatty acids are the main cause of beany flavor formation in legume-based foods. The formation of off-flavor compounds usually results from the oxidation of unsaturated fatty acids and the hydrolysis of lipids (Jelen, 2011). Legume seeds contain a large amount of unsaturated fatty acids, the most abundant being oleic acid, linolenic acid, and linoleic acid (Khrisanapant et al., 2019). The oxidation mechanism generally consists of three categories: automatic oxidation, photo-oxidation, and enzymatic oxidation (Wang Y. Q. et al., 2022).

Automatic oxidation

As shown in the yellow route in Figure 1, automatic oxidation is a free radical chain reaction involving oxygen and unsaturated lipids (Wang Y. Q. et al., 2022). Principally, reactive singlet oxygen attacks H, forming α-methylene near the double bonds, thus forming alkyl radicals (R·). After that, further oxygen absorption leads to the formation of peroxyl radicals (ROO·) and hydrogen peroxide, which ends up with a wide range of volatile and non-volatile secondary products, odor compounds (Wang et al.,

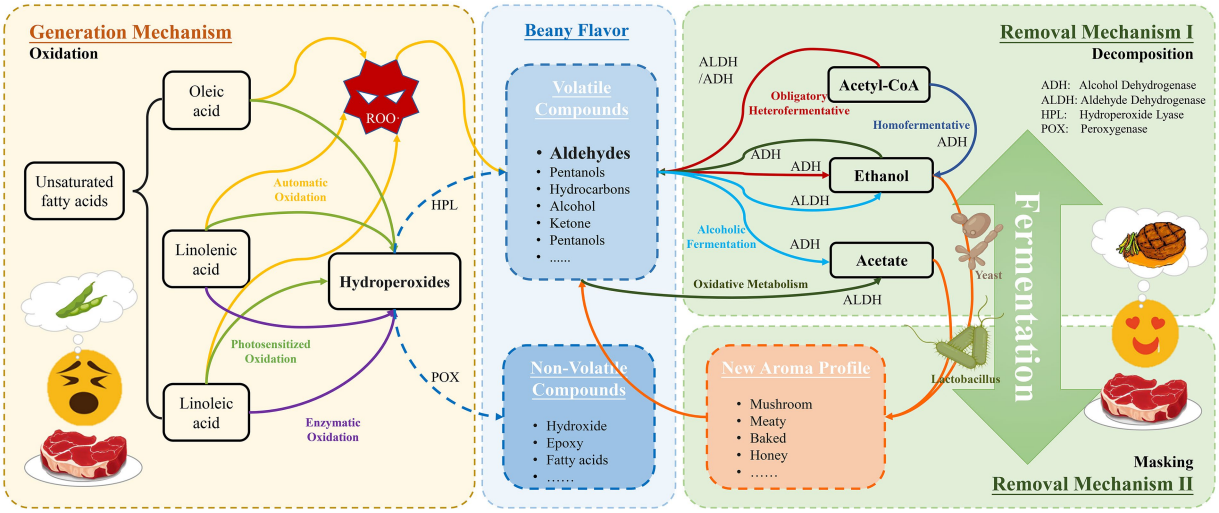

FIGURE 1
The generation and removal mechanism of beany-flavor.

2021). Once the chain reaction starts, it is very difficult to be stopped. Therefore, preventing chain reaction initiation is the most effective way to control autoxidation.

Photosensitized oxidation

The left green route in Figure 1 displays the photosensitized oxidation, which differs from automatic oxidation in that during photosensitized oxidation, highly reactive singlet oxygen directly attacks the double bonds of unsaturated fatty acids, resulting in oxygen binding directly to the fatty acids in the formation of hydrogen peroxide. Singlet oxygen is more significant for photosensitized oxidation in the oxidation process than automatic oxidation (Hammond and White, 2011).

Enzymatic oxidation

As illustrated in the purple route in Figure 1, enzymatic oxidation is the main reason to produce most volatiles in legumes, which is the primary way in which off-flavor is generated. Lipoxygenase (LOX) is a major element of enzymatic oxidation (Roland et al., 2017). LOX belongs to the family of nonheme iron-containing enzymes that can effectively catalyze the deoxygenation of polyunsaturated fatty acids (PUFAs) such as linoleic acid (18:2) and linolenic acid (18:3), to produce hydroperoxyl derivative (Alhendi et al., 2018). Because oxidation reactions usually occur in specific regions and oxygen is generally bound within C9 and C13 (Gardner, 1991), Soy LOX isoenzymes are classified into three types: 9-, 13- and 9-/13-LOXs. For example, soy LOX-1 is a 13-LOX, LOX-2 is a 9-/13-LOX, and soy LOX-3 is a 9-LOX or 9-/13-LOX (Wang Y. Q. et al., 2022).

After the formation of hydrogen peroxide derivatives through three processes: automatic oxidation, photosensitized oxidation and enzymatic oxidation. As shown in Figure 1, the main volatile flavor compounds, and nonvolatile lipid oxidation products were produced through three different oxidation mechanisms (Roland et al., 2017; Zhang et al., 2020). Hydroperoxide lyase (HPL), alcohol dehydrogenase (ADH), and peroxygenase (POX) will further catalyze the generation of products and aggregation, resulting in beany flavor. Hydroperoxide lyase (HPL) reacts with hydroperoxyl derivative to form volatiles such as C6 aldehydes and C9 aldehydes, and in the presence of ADH, these aldehydes are reacted to the corresponding alcohols, such as alcohols and acids. And hydroperoxyl derivative forms non-volatile lipid oxidation products such as hydroxy, epoxy, and fatty acids in the presence of POX (Wang Y. Q. et al., 2022).

Therefore, in order to control the production of beany flavor, we have to control the oxidation and degradation of unsaturated fatty acids. In the automatic oxidation process, the concentration of oxygen is extremely important, the higher the concentration of oxygen, the faster the rate of automatic oxidation (Wang et al., 2021). On the contrary, in the photosensitized oxidation process, the oxygen concentration has little effect, and the number and distribution of unsaturated double bonds have a significant effect (Wang et al., 2020). And in the enzymatic reaction process, lox is its limiting factor (Roland et al., 2017; Wang et al., 2021).

The mechanism underlying the fermentation removal of beany off-flavor

There are currently two major types of methods to remove beany flavor from plants. The first way is to use enzymes to

decompose the components that produce the beany flavor in plants and use enzymes to decompose the precursor substances of the plants that produce the beany flavor (Zhu and Damodaran, 2018; Fischer et al., 2022). The second way is to generate new aromatic profile which can mask the original beany flavor.

Direct decomposition of compounds with beany off-flavor

It was found that ADH and aldehyde dehydrogenase (ALDH) had the most obvious effect on the removal of beany flavor. Because the selection of compounds involved in the beany flavor included nine aldehydes, one furan, four alcohols, four ketones, three sulfides, and five pyrazines, the compound with the greatest effect on "beany" are aldehydes (Xu et al., 2020). ADH converts aldehydes to primary alcohols and ketones to secondary alcohols. ALDH converts aldehydes to carboxylic acids. Reduces beany flavor by converting odorous compounds (aldehydes and ketones) to less odorous products (alcohols and carboxylic acids; Shi et al., 2021).

As illustrated in the upper right of Figure 1, there are five main ways they remove the beany flavor: (a) The blue route illustrates the homofermentation: For the catabolism that occurs in this type of fermentation, ADH does not participate in basal metabolism, but plays a role in the mixed acid pathway. Such as *Lactobacillus acidophilus* and *Streptococcus thermophiles* (Shi et al., 2021). (b) Obligatory heterofermentative Lactic acid bacteria illustrated with the red route (LAB): such as *L. fermentum*. ADH is present in metabolism as a constitutive enzyme as well as an aldehyde/alcohol dehydrogenase (Ortakci et al., 2015; Verce et al., 2020). (c) Facultative heterofermentative LAB: Only the heterofermentative pathway is inducible. Such as *L. plantarum*. Its basic metabolism is the homofermentative pathway (Prückler et al., 2015). (d) Alcoholic fermentation illustrated with the cyan route: ADH and aldehyde dehydrogenase are present in the catabolism of the strain as constitutive enzymes. For example *Saccharomyces cerevisiae* (Mizuno et al., 2006). (e) Oxidative metabolism. "Oxidative fermentation" is the incomplete oxidation of substrates, carried by the dehydrogenases of the respiratory chain, resulting in the extracellular accumulation of oxidized products. The "oxidative system" is located in the cytoplasmic membrane and is connected to the respiratory chain, for example, *Gluconobacter suboxydans* (Deppenmeier and Ehrenreich, 2009; Lynch et al., 2019).

Breaking down beany flavor precursors in plants

Previous studies have indicated that the beany flavor in legumes is primarily the result of interactions between lipid oxidation products, proteins, and phytochemicals. Lipid-derived off-flavors are believed to be the main cause of beany flavor. Among them, the precursors of the flavor of legumes are mainly phospholipids (PLs) and free fatty acids (FFAs).

Phospholipase can be used to remove such precursors, among which the combined phospholipase A2 (PLA2) and cyclodextrin mixed with soybean meal in a water bath and it is found that the removal rate of phospholipids is more effective (Zhu and Damodaran, 2018).

In previous studies, it was found that the principle of removing beany flavor was mainly divided into two steps: hydrolyzing PLA 2 to decompose PL, and then removing the hydrolyzed product by forming an inclusion complex through β-cyclodextrin (β-CD). PLA2 selectively cleaves the ester bond of the acyl chain at the sn-2 position of PL and generates Lyso-PL and FFA. The product is a non-polar material. β-CD is a cyclic non-reducing oligosaccharide. Its special construction makes its inner cavity hydrophobic. β-CD and other cyclodextrins can form water-soluble inclusion complexes with insoluble non-polar substances. The water-soluble inclusion compound can be dissolved into the supernatant by a polar solvent such as deionized water, so as to achieve the effect of separation from soybean flour.

Additional studies have shown that after the application of Alcalase, papain or a combination of enzymes, the acidic subunits of β-conglycinin and glycinin disappear completely, resulting in the removal of some of the precursors of the beany flavor, thereby reducing the beany flavor (Meinlschmidt et al., 2016).

Odor masking and transformation

As shown in the low right of Figure 1, some strains can produce new aldehydes with aroma after fermentation while reducing the content of compounds with beany smell. In this way, the new aroma can mask the original beany smell to further enhance the total aroma profile of the product. For example, phenylacetaldehyde produced by fermentation of *L. rhamose* L08 can bring floral and honey-like aromas (Pei et al., 2022). And the main contributors to the aroma profile of *A. aegerita* fermented soy beverages remain soy-derived compounds. At the same time, ethyl esters and lactones were produced during fermentation, which resulted in increased fruity, floral, and creamy/dairy aromas present in cheese aromas and altered the overall aroma of the samples (Nedele et al., 2022a). Other scents include milky, nutty, and more.

Application of microorganisms to remove beany flavor

In recent years, fermentation has become the primary method employed in many studies to reduce the beany flavor due to its various advantages. Several strains are discussed below that have shown potential to remove or cover the beany flavor in bean protein-based products (Table 1).

TABLE 1 Application of fermentation methods for removing beany flavor.

	Matrices	Strains	Fermentation conditions	Method	Function	Sensory perception	References
Lactobacillus	Mung bean	LAB (*L. plantarum*)	37 ± 1°C 48 h	Biotransformation	Transform aldehydes into esters.	The esters give the fermented products a pleasant fruity odor.	Yi et al. (2021)
	Lupinus angustifolius L.	Five lactic acid bacteria	28°C 48 h	Decomposition and masking	Reduce aldehydes, especially hexanal, which possesses "green" odor; Create new pleasant aromatic compounds.	Increase sourness and "vinegar" odor; Reduce the "beany" flavor as well as the unpleasant off flavor.	Laaksonen et al. (2021)
	Pea flour (*Pisum sativum* L.)	*L. rhamnosus* L08	37°C 2 days	Decomposition and masking	Increase the variety of acids and esters; Reduce the unpleasant flavor compounds such as nonanal, decanal, octanal, 1-hexanol and 2-ethyl-1-hexanol; Produce phenylethyl aldehyde that could bring pleasant aromas.	Reduce the unpleasant beany flavor; Produce floral and honey-like aromas.	Pei et al. (2022)
	Pea protein isolates	*L. plantarum*, *L. casei* and mixed strains of probiotics	37°C 5, 10, 15, 20, 25, and 30 h Anaerobic conditions	Decomposition	Remove around 42% aldehyde and 64% ketone content; Produce a small amount of alcohol.	Decrease the overall unpleasant aroma and flavor intensity.	Shi (2020)
	Lupin protein extracts (LPE)	*L. plantarum* L1047 and *Pediococcus pentosaceus* P113	–	Decomposition and masking	Decrease the concentration of n-hexanal and prevent its re-formation; Change the aroma profile which may mask off-flavors.	The more pleasant odor of the fermented protein extracts, compared to the unfermented protein extracts is explained by its different aroma profile.	Schindler et al. (2011)
	Soymilk	*Lactobacilli* and *Streptococci*	37°C 12 h	Decomposition	Reduce or even eliminate the concentrations of volatile components that have been associated with the beany flavor of soymilk, such as methanol, acetaldehyde, ethanol, and hexanal.	The heat treatment applied to the soymilk in the present study would certainly cause a severe cooked flavor. Thus, the resulting fermented product would not have been suitable for sensory analysis.	Blagden and Gilliland (2005)
	Pea protein isolates (PPI)	*L. plantarum*	37°C 30 h Anaerobic conditions	Decomposition	Eliminate aroma compounds that belong to the aldehyde, ketone, and alcohol groups.	Reduce the off-flavor ("hay" and "green" like aroma); Improve the aroma profile.	Shi et al. (2021)
	Pea (*Pisum sativum*) protein extract	*L. plantarum* L1047 or *P. pentosaceus* P113	37°C 48 h	Decomposition and masking	Decrease the n-hexanal content; Reduce or mask undesirable green notes.	Improve the aroma profile.	Schindler et al. (2012)

(Continued)

10.3389/fmicb.2022.1070773

TABLE 1 (Continued)

	Matrices	Strains	Fermentation conditions	Method	Function	Sensory perception	References
	Lupin protein isolate	*Lactobacilli*	30°C (*L. parabuchneri*, *L. brevis*) 37°C (*L. helveticus*, *L. delbrueckii*, *L. sakei sub* sp. *carnosus*, *L. reuteri*, *S. xylosus*) 42°C (*L. amylolyticus*) 36–48 h	Decomposition and masking	Decrease the n-hexanal content; Reduce or mask undesirable green notes.	Reduce the intensity of characteristic aroma impression (pea-like, green bell pepper-like) from 4.5 to 1.0.	Schlegel et al. (2019)
Yeast	Okara	Yeast (*Lindnera saturnus*)	30°C 48 h Solid-state fermentation	Biotransformation	Aldehydes are reduced into alcohols by yeast alcohol dehydrogenase or oxidized into acids by yeast aldehyde dehydrogenase, and finally form esters *via* enzymatic reactions.	Transform the aroma profile of okara from a green, grassy off-flavor into a markedly fruity and sweet aroma.	Vong and Liu (2018)
	Soybean residue (okara)	Four "dairy yeasts" (*Geotrichum candidum*, *Yarrowia lipolytica*, *Debaryomyces hansenii* and *Kluyveromyces lactis*) and six "wine yeasts" (*Saccharomyces cerevisiae*, *Lachancea thermotolerans, Metschnikowia pulcherrima*, *Pichia kluyveri, Torulaspora delbrueckii,* and *Williopsis saturnus*)	30°C 72 h Solid-state fermentation	Biotransformation	Oxidize the undesirable aldehydes into fatty acids, or reduce them into alcohols, and finally yield esters; Yeast proteinases and peptidases break down the protein in okara. Yeasts degrade the free amino acids to yield higher alcohols and esters.	The final fermented okara had a very strong fruity and estery character.	Vong and Liu (2017)
	Soy (tofu) whey	commercial non-*Saccharomyces* yeasts (*T. delbrueckii*; *L. thermotolerans*; *M. pulcherrima*; *P. kluyveri* and *W. saturnus*)	20°C 3 days	Decomposition & Masking	Metabolize endogenous carbonyls and alcohols to low or trace levels; Produce new alcohols, esters and acids to enrich aroma profiles that were unique to each non-*Saccharomyces* yeast.	Each yeast produced different levels of different volatile compounds that can contribute to the different aroma profiles of the fermented whey.	Chua et al. (2018)
Edible Basidiomycetes	Soybean products (soy drink and soy protein isolate)	*Lycoperdon pyriforme*	24°C 28 h In darkness	Biotransformation	Saturated aldehydes were metabolized by the fungus to their corresponding alcohols; Di-unsaturated aldehydes were synthesized to a non-volatile product.	Impart slightly bitter almond-like, fungal and nutty odor notes without recognition of the soy product off-flavors.	Nedele et al. (2022b)

(Continued)

10.3389/fmicb.2022.1070773

TABLE 1 (Continued)

	Matrices	Strains	Fermentation conditions	Method	Function	Sensory perception	References
	Okara	*Wolfiporia cocos CGMCC 5.55*, *W. cocos CGMCC 5.528*, *W. cocos CGMCC 5.78* and *Tremella fuciformis CGMCC 5.466*	25 ± 1°C 7 days	Decomposition & Masking	Decrease the content of off-flavor compounds like hexanal; New aromatic compounds were generated.	All fermented products had very little characteristics of beany flavor, and a fragrant, floral, and sweet aroma was present.	Wang Z. et al. (2022)
	Soy drink	*Agrocybe aegerita*	24°C 75 h In darkness	Decomposition and masking	Many typical soybean off-flavor contributors were reduced in their intensity such as green aldehydes; Synthesize ethyl esters and lactone, which change the overall aroma of the sample.	Produce a natural and vegan cheese aroma; Decrease the off-flavor in soybean-based products; Produce a sweet, floral and fruity flavor impression.	Nedele et al. (2022a)
	Soy drink	*L. pyriforme*	24°C 28 h In darkness	Decomposition & Masking	Increase aroma compounds such as 1-octen-3-one with a mushroom-like odor and benzyl alcohol with a sweetish flavor; Decrease most of the key aroma compounds with a green off-flavor.	The aroma of soy drink turned from green, beany, and oat-like to oat-like, mushroom-like, and almond-like.	Nedele et al. (2021)
Co-fermentation	Soybean (soymilk)	Three isolated new yeasts (*K. marxianus* SP-1, *Candida ethanolica* ATW-1, and *P. amenthionina* Y) and a commercial yeast (*K. marxianus* K) along with five strains of lactic acid bacteria (LAB)	36°C 5 h LAB and yeast ratio (5:2, v/v)	Biotransformation	Transform aldehydes into either acids, alcohols and esters.	Remove the beany flavor; Produce rich aromatic components; Improved the flavor and taste of drinks.	Korma et al. (2022)
	Okara (soybean residue)	Probiotic (*L. paracasei*) and yeast (*L. saturnus*)	30°C 48 h (viable cell count ratio of probiotic:yeast was about 100:1)	Biotransformation	Produce large amounts of esters to give a natural fruity aroma.	Give a natural fruity aroma.	Vong and Liu (2019)
	Pea protein-based product	Lactic acid bacteria and yeasts	pH 7.1 ± 0.1 to 4.55 30°C to 4°C	Decomposition & Masking	Degrade many off-flavor compounds; Trigger the generation of esters compounds with fruity and floral notes.	Reduce the concentration of pea off-notes; Generate new notes that could modify the perception of sensory defects; Improve the aroma quality of fermented beverages.	El Youssef et al. (2020)

(Continued)

10.3389/fmicb.2022.1070773

TABLE 1 (Continued)

Matrices	Strains	Fermentation conditions	Method	Function	Sensory perception	References
Okara	Compound probiotics (*L. plantarum*, *L. acidophiluss*, *Bifidobacterium lactis*, *L. casei* and *B. longum*, *S. cerevisiae* and *Hansenula* sp.) and mixed yeast (*S. cerevisiae* and *Hansenula* sp.)	28°C for 1 day 37°C for 2 days Anaerobic conditions Solid-state fermentation	Biotransformation	Convert aldehydes into alcohols and esters, among other compounds to improve the flavor of okara.	Give the okara a pleasant smell and taste. Sensory acceptability is greatly improved compared to unfermented okara.	Shi et al. (2020)

Lactobacillus

Lactic fermentation might be a promising strategy to improve the aroma profile of plant-based food products as it results in a reduction or covering of undesirable flavors. Some *Lactobacillus* strains can reduce or eliminate aroma compounds that have been linked with the beany flavor which are members of the aldehyde, ketone, and alcohol groups. Several authors demonstrated how fermentation with lactic acid bacteria in pea, lupin protein extract, and soymilk, respectively, reduced the concentration of hexanal, which is primarily responsible for the greeny and beany off-flavor (Blagden and Gilliland, 2005; Schindler et al., 2011, 2012; Shi, 2020). Other researches have shown that lactic fermentation can produce higher aldehydes, alcohols, acids, and ester compounds through further biotransformation to cover the beany flavors (Schindler et al., 2011; Shi et al., 2021; Yi et al., 2021). Lipid degradation, which also contributes to the creation of the odors found in fermented foods, takes place concurrently with this biotransformation. For instance, *L. rhamnosus* L08 fermentation produced phenylethyl aldehyde that could bring floral and honey-like aromas, phenylethyl alcohol that exhibits a fresh bread-like, rose-like aroma, and several esters with floral and fruity fragrances, which had the effect of covering undesirable flavors (Pei et al., 2022).

Yeast

Some yeasts are also used to modify the odor characteristics of plant-based products by biotransformation. The products of yeast fermentation often carry a pleasant flavor profile of alcohols and esters. Chua et al. fermented soy whey samples using five commercial non-*Saccharomyces* yeasts. Volatile compounds such as ethanol and 2-phenylethanol were found in the fermented products, giving them a rose-like aromatic character (Chua et al., 2018). Other studies used yeasts to ferment okara and obtained a very strong fruity and estery character since most of the undesirable aldehydes were reduced into alcohols and esters by the yeasts fermentation (Vong and Liu, 2017; Vong and Liu, 2018).

Unfortunately, although fermentation with lactic acid bacteria or yeasts reduces the beany flavor substances, the fermentation process of certain strains inevitably produces acids such as lactic acid and hexanoic acid, causing strong sour and wine flavors, which to some extent aggravate the undesirable flavor of the bean protein-based product (Laaksonen et al., 2021; Nedele et al., 2021; Wang Z. et al., 2022). Thus, the optimization of fermentation conditions is required to prevent the creation of unpleasant flavor compounds.

Edible basidiomycetes

In the food processing industry, edible fungi are common fermentation strains. Among them, basidiomycetes have garnered

increasing interest due to their abundance, diversity, accessibility, and nutritional benefits (Mahboubi et al., 2017; Sun et al., 2020; Bentil, 2021). While most conventional starter cultures mainly produce primary metabolites, basidiomycetes are noted for their sensory modification of various food products (Nedele et al., 2021; Rigling et al., 2021; Nedele et al., 2022a). They are able to modify the flavor because their highly sophisticated secretomes produce abundant natural flavor molecules (Bouws et al., 2008). The scientists used four types of edible fungi to reduce the beany flavor and gain new aromatic flavors of okara. These new flavors contain benzene, ethanol, and linalool, which are probably byproducts of enzymatic events occurring during the growth and metabolism of edible fungi. In addition to adding floral, sweet, and orange fragrances, the presence of these compounds can disguise the flavor characteristics of some unwanted components (Wang Z. et al., 2022). Apart from that, recent studies have confirmed that by using a unique fermentation procedure with *Lycoperdon pyriforme*, the beany flavor of soy beverages was diminished while the nutritional profile was maintained. During this fermentation process, aldehydes, the main off-flavor contributors, were decreased and some pleasant aroma components were created, imparting the finished product an almond- and nutty-like smell (Nedele et al., 2021, 2022b). Therefore, it can be expected that the edible basidiomycetes are likely to be a promising strain for flavor improvement in plant-based foods. Further research is required to ascertain which kind of strains can successfully grow in the various sources of legume dietary fiber systems as well as what fermentation conditions can facilitate the aroma profile improvement.

Conclusion and outlook

In summary, oxidation of unsaturated fatty acids and hydrolysis of lipids are the primary causes of undesirable flavor in a plant protein-base food. At present, masking, biotransformation and enzymatic degradation are the main mechanisms and approaches for removing the beany flavor. Several species of microorganisms including lactobacillus, yeast, and edible basidiomycetes were demonstrated to reduce the level of beany flavor compounds by converting them into less impacting compounds or covering them with new pleasant compounds formed during fermentation. However, different fermentation approaches will produce different final flavor characteristics due to the different metabolic pathways and capacities of the strains. Thus, the strains utilized have a significant impact on how the fermentation affects the fragrance profile of the plant proteins. It should be noted that no technique is perfect, and each method has its own inherent advantages and drawbacks.

In order to further improve the flavor quality of plant-based meat analogs, future product development and application research can mainly focus on the following aspects: (a) Fermentation using some strains may produce products with high acidity, which may not be preferred by consumers. More research is needed to select suitable strains and optimize fermentation process to meet the preferences of consumers (Laaksonen et al., 2021). (b) Aside from legume proteins, other ingredients including microalgae, konjac, and edible mushrooms could be promising substitutes for meat analogs due to their superior production capabilities and high nutritional content. Scientists can process these ingredients using fermentation method to explore the next generation of meat analogs (Jiménez-Colmenero et al., 2012; Fu et al., 2021; Yuan et al., 2022). (c) The fermentation process produces amino acids, sugars, and a series of precursors for Maillard reactions. Therefore, if the fermentation process is properly designed and oriented, it will effectively promote the Maillard reaction, providing better flavor and taste to plant-based meat analogs and eliminating the beany flavor. (d) The metabolomic pathway of fermentation process should be further investigated to demonstrate how the beany flavor is decomposed with the aid of mass spectrometry, nuclear magnetic resonance or isotopic labeling experiments (Ran et al., 2022). And the influence of more volatile compounds exist at low amounts should be further studied to confirm their effect on the aroma change of the fermented product. Improvements of current fermentation techniques will benefit from the results of such research. (e) There is still a lack of comprehensive research on the application of fermentation to remove beany flavor from plant-based meat analog. Not only the technological aspects, but also the safety concerns should be taken into consideration. Possible safety problems such as microbiological stability, allergenic potential and heavy metal and toxic substance contamination during fermentation should be investigated to develop safe and efficient fermentation protocols for the production of plant-based meat analogs.

Author contributions

XY and TZ contributed to conception and design of the study. AT, HZ, and JD wrote the first draft of the manuscript. YX, YL, JL, and JH helped review and revise the manuscript. All authors contributed to the article and approved the submitted version.

Funding

This work was supported by the Science and Technology Development Funds, Macau SAR (0024/2022/A and 0004/2021/ITP), the Science and Technology Planning Project of Guangdong Province (2020B1212030008), Innovation Cultivation Project of Zhuhai College of Science and Technology (2019XJCQ006), and the Open Fund of Guangdong-Hong Kong-Macao Joint Laboratory for Contaminants Exposure and Health (GHMJLCEH-05).

Conflict of interest

JL and JH were employed by Macau Uni-Win Biotechnology Co., Ltd.

The remaining authors declare that the research was conducted in the absence of any commercial or financial relationships that could be construed as a potential conflict of interest.

Publisher's note

References

Alhendi, A., Yang, W., and Sarnoski, P. J. (2018). The effect of solution properties on the photochemical ability of pulsed light to inactivate soybean lipoxygenase. *Int. J. Food Eng.* 14:14. doi: 10.1515/ijfe-2018-0086

Bentil, J. A. (2021). Biocatalytic potential of basidiomycetes: relevance, challenges and research interventions in industrial processes. *Sci. Afr.* 11:e00717. doi: 10.1016/j.sciaf.2021.e00717

Blagden, T. D., and Gilliland, S. E. (2005). Reduction of levels of volatile components associated with the "beany" flavor in soymilk by lactobacilli and streptococci. *J. Food Sci.* 70, M186–M189. doi: 10.1111/j.1365-2621.2005.tb07148.x

Bouws, H., Wattenberg, A., and Zorn, H. (2008). Fungal secretomes - Nature's toolbox for white biotechnology. *Appl. Microbiol. Biotechnol.* 80, 381–388. doi: 10.1007/s00253-008-1572-5

Chen, A., He, H., Wang, J., Li, M., Guan, Q., and Hao, J. (2019). A study on the arable land demand for food security in China. *Sustainability* 11:4769. doi: 10.3390/su11174769

Chen, J., and Yang, C.-C. (2021). The impact of COVID-19 on the revenue of the livestock industry: a case study of China. *Animals* 11:3586. doi: 10.3390/ani11123586

Choudhury, D., Singh, S., Seah, J. S. H., Yeo, D. C. L., and Tan, L. P. (2020). Commercialization of plant-based meat alternatives. *Trends Plant Sci.* 25, 1055–1058. doi: 10.1016/j.tplants.2020.08.006

Chua, J.-Y., Lu, Y., and Liu, S.-Q. (2018). Evaluation of five commercial non-saccharomyces yeasts in fermentation of soy (tofu) whey into an alcoholic beverage. *Food Microbiol.* 76, 533–542. doi: 10.1016/j.fm.2018.07.016

Cordelle, S., Redl, A., and Schlich, P. (2022). Sensory acceptability of new plant protein meat substitutes. *Food Qual. Prefer.* 98:104508. doi: 10.1016/j.foodqual.2021.104508

Deppenmeier, U., and Ehrenreich, A. (2009). Physiology of acetic acid bacteria in light of the genome sequence of Gluconobacter oxydans. *Microbial Physiol.* 16, 69–80. doi: 10.1159/000142895

El Youssef, C., Bonnarme, P., Fraud, S., Péron, A.-C., Helinck, S., and Landaud, S. (2020). Sensory improvement of a pea protein-based product using microbial co-cultures of lactic acid bacteria and yeasts. *Foods* 9:349. doi: 10.3390/foods9030349

Fischer, E., Cayot, N., and Cachon, R. (2022). Potential of microorganisms to decrease the "beany" off-flavor: a review. *J. Agric. Food Chem.* 70, 4493–4508. doi: 10.1021/acs.jafc.1c07505

Fu, Y., Chen, T., Chen, S. H. Y., Liu, B., Sun, P., Sun, H., et al. (2021). The potentials and challenges of using microalgae as an ingredient to produce meat analogues. *Trends Food Sci. Technol.* 112, 188–200. doi: 10.1016/j.tifs.2021.03.050

Gardner, H. W. (1991). Recent investigations into the lipoxygenase pathway of plants. Biochimica et Biophysica Acta (BBA)-lipids and lipid. *Metabolism* 1084, 221–239. doi: 10.1016/0005-2760(91)90063-N

Hammond, E. G., and White, P. J. (2011). A brief history of lipid oxidation. *J. Am. Oil Chem. Soc.* 88, 891–897. doi: 10.1007/s11746-011-1761-8

Jelen, H. (2011). *Food flavors: Chemical, sensory and technological properties*. Boca Raton: CRC press.

Jiménez-Colmenero, F., Cofrades, S., Herrero, A. M., Fernández-Martín, F., Rodríguez-Salas, L., and Ruiz-Capillas, C. (2012). Konjac gel fat analogue for use in meat products: comparison with pork fats. *Food Hydrocoll.* 26, 63–72. doi: 10.1016/j.foodhyd.2011.04.007

Khrisanapant, P., Kebede, B., Leong, S. Y., and Oey, I. (2019). A comprehensive characterisation of volatile and fatty acid profiles of legume seeds. *Foods* 8:651. doi: 10.3390/foods8120651

Korma, S. A., Li, L., Ghamry, M., Zhou, Q., An, P., Abdrabo, K. A., et al. (2022). Effect of co-fermentation system with isolated new yeasts on soymilk: microbiological, physicochemical, rheological, aromatic, and sensory characterizations. *Braz. J. Microbiol.* 53, 1549–1564. doi: 10.1007/s42770-022-00773-7

Kumar, P., Chatli, M., Mehta, N., Singh, P., Malav, O., and Verma, A. K. (2017). Meat analogues: health promising sustainable meat substitutes. *Crit. Rev. Food Sci. Nutr.* 57, 923–932. doi: 10.1080/10408398.2014.939739

Kumari, S., Dahuja, A., Vinutha, T., Lal, S. K., Kar, A., and Rai, R. D. (2015). Changes in the levels of off-flavor generation in soybean through biotic elicitor treatments. *J. Agric. Food Chem.* 63, 700–706. doi: 10.1021/jf505199a

Kyriakopoulou, K., Keppler, J. K., and van der Goot, A. J. (2021). Functionality of ingredients and additives in plant-based meat analogues. *Foods* 10:600. doi: 10.3390/foods10030600

Laaksonen, O., Kahala, M., Marsol-Vall, A., Blasco, L., Järvenpää, E., Rosenvald, S., et al. (2021). Impact of lactic acid fermentation on sensory and chemical quality of dairy analogues prepared from lupine (Lupinus angustifolius L.) seeds. *Food Chem.* 346:128852. doi: 10.1016/j.foodchem.2020.128852

Lynch, K. M., Zannini, E., Wilkinson, S., Daenen, L., and Arendt, E. K. (2019). Physiology of acetic acid bacteria and their role in vinegar and fermented beverages. *Compr. Rev. Food Sci. Food Saf.* 18, 587–625. doi: 10.1111/1541-4337.12440

Mahboubi, A., Ferreira, J. A., Taherzadeh, M. J., and Lennartsson, P. R. (2017). Value-added products from dairy waste using edible fungi. *Waste Manag.* 59, 518–525. doi: 10.1016/j.wasman.2016.11.017

Meinlschmidt, P., Schweiggert-Weisz, U., and Eisner, P. (2016). Soy protein hydrolysates fermentation: effect of debittering and degradation of major soy allergens. *LWT* 71, 202–212. doi: 10.1016/j.lwt.2016.03.026

Mittermeier-Kleßinger, V. K., Hofmann, T., and Dawid, C. (2021). Mitigating off-flavors of plant-based proteins. *J. Agric. Food Chem.* 69, 9202–9207. doi: 10.1021/acs.jafc.1c03398

Mizuno, A., Tabei, H., and Iwahuti, M. (2006). Characterization of low-acetic-acid-producing yeast isolated from 2-deoxyglucose-resistant mutants and its application to high-gravity brewing. *J. Biosci. Bioeng.* 101, 31–37. doi: 10.1263/jbb.101.31

Nedele, A.-K., Bär, A., Mayer, N., Schiebelbein, R., and Zhang, Y. (2022a). Characterization of cheesy odor formed during fermentation of soy drink with Agrocybe aegerita. *Food Chem.* 381:132170. doi: 10.1016/j.foodchem.2022.132170

Nedele, A.-K., Gross, S., Rigling, M., and Zhang, Y. (2021). Reduction of green off-flavor compounds: comparison of key odorants during fermentation of soy drink with Lycoperdon pyriforme. *Food Chem.* 334:127591. doi: 10.1016/j.foodchem.2020.127591

Nedele, A.-K., Schiebelbein, R., Bär, A., Kaup, A., and Zhang, Y. (2022b). Reduction of aldehydes with green odor in soy products during fermentation with Lycoperdon pyriforme and analysis of their degradation products. *Food Res. Int.* 152:110909. doi: 10.1016/j.foodres.2021.110909

Ortakci, F., Broadbent, J. R., Oberg, C. J., and McMahon, D. J. (2015). Growth and gas production of a novel obligatory heterofermentative Cheddar cheese nonstarter lactobacilli species on ribose and galactose. *J. Dairy Sci.* 98, 3645–3654. doi: 10.3168/jds.2014-9293

Pei, M., Zhao, Z., Chen, S., Reshetnik, E. I., Gribanova, S. L., Li, C., et al. (2022). Physicochemical properties and volatile components of pea flour fermented by lactobacillus rhamnosus L08. *Food Biosci.* 46:101590. doi: 10.1016/j.fbio.2022.101590

Pimentel, D., and Pimentel, M. (2003). Sustainability of meat-based and plant-based diets and the environment. *Am. J. Clin. Nutr.* 78, 660S–663S. doi: 10.1093/ajcn/78.3.660S

Polak, R., Phillips, E. M., and Campbell, A. (2015). Legumes: health benefits and culinary approaches to increase intake. *Clin. Diabetes* 33, 198–205. doi: 10.2337/diaclin.33.4.198

Prückler, M., Lorenz, C., Endo, A., Kraler, M., Dürrschmid, K., Hendriks, K., et al. (2015). Comparison of homo- and heterofermentative lactic acid bacteria for implementation of fermented wheat bran in bread. *Food Microbiol.* 49, 211–219. doi: 10.1016/j.fm.2015.02.014

Ran, X., Yang, Z., Chen, Y., and Yang, H. (2022). Konjac glucomannan decreases metabolite release of a plant-based fishball analogue during in vitro digestion by affecting amino acid and carbohydrate metabolic pathways. *Food Hydrocoll.* 129:107623. doi: 10.1016/j.foodhyd.2022.107623

Rigling, M., Yadav, M., Yagishita, M., Nedele, A.-K., Sun, J., and Zhang, Y. (2021). Biosynthesis of pleasant aroma by enokitake (Flammulina velutipes) with a potential use in a novel tea drink. *LWT* 140:110646. doi: 10.1016/j.lwt.2020.110646

Roland, W. S., Pouvreau, L., Curran, J., van de Velde, F., and de Kok, P. M. (2017). Flavor aspects of pulse ingredients. *Cereal Chem.* 94, 58–65. doi: 10.1094/CCHEM-06-16-0161-FI

Schindler, S., Wittig, M., Zelena, K., Krings, U., Bez, J., Eisner, P., et al. (2011). Lactic fermentation to improve the aroma of protein extracts of sweet lupin (Lupinus angustifolius). *Food Chem.* 128, 330–337. doi: 10.1016/j.foodchem.2011.03.024

Schindler, S., Zelena, K., Krings, U., Bez, J., Eisner, P., and Berger, R. G. (2012). Improvement of the aroma of pea (Pisum sativum) protein extracts by lactic acid fermentation. *Food Biotechnol.* 26, 58–74. doi: 10.1080/08905436.2011.645939

Schlegel, K., Leidigkeit, A., Eisner, P., and Schweiggert-Weisz, U. (2019). Technofunctional and sensory properties of fermented Lupin protein isolates. *Foods* 8:678. doi: 10.3390/foods8120678

Shi, Y. *Reducing off-flavour in plant protein isolates by lactic acid fermentation [text]* (2020).

Shi, Y., Singh, A., Kitts, D. D., and Pratap-Singh, A. (2021). Lactic acid fermentation: a novel approach to eliminate unpleasant aroma in pea protein isolates. *LWT* 150:111927. doi: 10.1016/j.lwt.2021.111927

Shi, H., Zhang, M., Wang, W., and Devahastin, S. (2020). Solid-state fermentation with probiotics and mixed yeast on properties of okara. *Food Biosci.* 36:100610

Sun, A., Wu, W., Soladoye, O. P., Aluko, R. E., Bak, K. H., Fu, Y., et al. (2022). Maillard reaction of food-derived peptides as a potential route to generate meat flavor compounds: a review. *Food Res. Int.* 151:110823. doi: 10.1016/j.foodres.2021.110823

Sun, Y., Zhang, M., and Fang, Z. (2020). Efficient physical extraction of active constituents from edible fungi and their potential bioactivities: a review. *Trends Food Sci. Technol.* 105, 468–482. doi: 10.1016/j.tifs.2019.02.026

Taufik, D., Verain, M. C., Bouwman, E. P., and Reinders, M. J. (2019). Determinants of real-life behavioural interventions to stimulate more plant-based and less animal-based diets: a systematic review. *Trends Food Sci. Technol.* 93, 281–303. doi: 10.1016/j.tifs.2019.09.019

Verce, M., De Vuyst, L., and Weckx, S. (2020). Comparative genomics of lactobacillus fermentum suggests a free-living lifestyle of this lactic acid bacterial species. *Food Microbiol.* 89:103448. doi: 10.1016/j.fm.2020.103448

Vong, W. C., and Liu, S.-Q. (2017). Changes in volatile profile of soybean residue (okara) upon solid-state fermentation by yeasts. *J. Sci. Food Agric.* 97, 135–143. doi: 10.1002/jsfa.7700

Vong, W. C., and Liu, S.-Q. (2018). Bioconversion of green volatiles in okara (soybean residue) into esters by coupling enzyme catalysis and yeast (Lindnera saturnus) fermentation. *Appl. Microbiol. Biotechnol.* 102, 10017–10026. doi: 10.1007/s00253-018-9396-4

Vong, W. C., and Liu, S.-Q. (2019). The effects of carbohydrase, probiotic lactobacillus paracasei and yeast Lindnera saturnus on the composition of a novel okara (soybean residue) functional beverage. *LWT* 100, 196–204. doi: 10.1016/j.lwt.2018.10.059

Wang, Z., Gao, T., He, Z., Zeng, M., Qin, F., and Chen, J. (2022). Reduction of off-flavor volatile compounds in okara by fermentation with four edible fungi. *LWT* 155:112941. doi: 10.1016/j.lwt.2021.112941

Wang, Y., Guldiken, B., Tulbek, M., House, J. D., and Nickerson, M. (2020). Impact of alcohol washing on the flavour profiles, functionality and protein quality of air classified pea protein enriched flour. *Food Res. Int.* 132:109085. doi: 10.1016/j.foodres.2020.109085

Wang, Y. Q., Tuccillo, F., Lampi, A. M., Knaapila, A., Pulkkinen, M., Kariluoto, S., et al. (2022). Flavor challenges in extruded plant-based meat alternatives: a review. *Compr. Rev. Food Sci. Food Saf.* 21, 2898–2929. doi: 10.1111/1541-4337.12964

Wang, B., Zhang, Q., Zhang, N., Bak, K. H., Soladoye, O. P., Aluko, R. E., et al. (2021). Insights into formation, detection and removal of the beany flavor in soybean protein. *Trends Food Sci. Technol.* 112, 336–347. doi: 10.1016/j.tifs.2021.04.018

Xu, M., Jin, Z., Gu, Z., Rao, J., and Chen, B. (2020). Changes in odor characteristics of pulse protein isolates from germinated chickpea, lentil, and yellow pea: role of lipoxygenase and free radicals. *Food Chem.* 314:126184. doi: 10.1016/j.foodchem.2020.126184

Yi, C., Li, Y., Zhu, H., Liu, Y., and Quan, K. (2021). Effect of lactobacillus plantarum fermentation on the volatile flavors of mung beans. *LWT* 146:111434. doi: 10.1016/j.lwt.2021.111434

Yu, X., and Zuo, T. (2021). *Food additives*, Cooking and Processing: Impact on the Microbiome. Frontiers Media SA; p. 731040–7310488.

Yuan, X., Jiang, W., Zhang, D., Liu, H., and Sun, B. (2022). Textural, sensory and volatile compounds analyses in formulations of sausages analogue elaborated with edible mushrooms and soy protein isolate as meat substitute. *Foods* 11:52. doi: 10.3390/foods11010052

Zhang, Y., Guo, S., Liu, Z., and Chang, S. K. (2012). Off-flavor related volatiles in soymilk as affected by soybean variety, grinding, and heat-processing methods. *J. Agric. Food Chem.* 60, 7457–7462. doi: 10.1021/jf3016199

Zhang, C. M., Hua, Y. F., Li, X. F., Kong, X. Z., and Chen, Y. M. (2020). Key volatile off-flavor compounds in peas (Pisum sativum L.) and their relations with the endogenous precursors and enzymes using soybean (Glycine max) as a reference. *Food Chem.* 333:127469. doi: 10.1016/j.foodchem.2020.127469

Zhu, D., and Damodaran, S. (2018). Removal of off-flavour-causing precursors in soy protein by concurrent treatment with phospholipase A2 and cyclodextrins. *Food Chem.* 264, 319–325. doi: 10.1016/j.foodchem.2018.05.045

frontiers | Frontiers in Microbiology

TYPE Original Research
PUBLISHED 02 December 2022
DOI 10.3389/fmicb.2022.1076123

OPEN ACCESS

EDITED BY
Jinxuan Cao,
Beijing Technology and Business University, China

REVIEWED BY
Lv Zengpeng,
China Agricultural University, China
Kai Zhang,
Qingdao Agricultural University, China

*CORRESPONDENCE
Shanlong Tang
tangshanlong01@126.com
Basang-wangdui
bw0891@163.com

SPECIALTY SECTION
This article was submitted to Food Microbiology, a section of the journal Frontiers in Microbiology

RECEIVED 21 October 2022
ACCEPTED 17 November 2022
PUBLISHED 02 December 2022

CITATION
Zhu Y, Cidan-yangji, Sun G, Luo C, Duan J, Shi B, Ma T, Tang S, Zhong R, Chen L, Basang-wangdui and Zhang H (2022) Different feeding patterns affect meat quality of Tibetan pigs associated with intestinal microbiota alterations. *Front. Microbiol.* 13:1076123. doi: 10.3389/fmicb.2022.1076123

Different feeding patterns affect meat quality of Tibetan pigs associated with intestinal microbiota alterations

Yanbin Zhu[1], Cidan-yangji[1], Guangming Sun[1], Chengzeng Luo[2,3], Jiujun Duan[2], Bin Shi[1], Teng Ma[2], Shanlong Tang[2]*, Ruqing Zhong[2], Liang Chen[2], Basang-wangdui[1]* and Hongfu Zhang[2]

[1]Institute of Animal Husbandry and Veterinary Medicine, Tibet Academy of Agriculture and Animal Husbandry Sciences, Lhasa, China, [2]The State Key Laboratory of Animal Nutrition, Institute of Animal Sciences, Chinese Academy of Agricultural Sciences, Beijing, China, [3]College of Animal Science, Xinjiang Agricultural University, Urumqi, China

This study aimed to investigate the effects of different feeding patterns on meat quality, gut microbiota and its metabolites of Tibetan pigs. Tibetan pigs with similar body weight were fed the high energy diets (**HEP**, 20 pigs) and the regular diets (**RFP**, 20 pigs), and free-ranging Tibetan pigs (**FRP**, 20 pigs) were selected as the reference. After 6 weeks of experiment, meat quality indexes of semitendinosus muscle (**SM**) and cecal microbiota were measured. The results of meat quality demonstrated that the shear force of pig SM in FRP group was higher than that in HEP and RFP groups ($p<0.001$); the pH-value of SM in HEP pigs was higher at 45min ($p<0.05$) and lower at 24h ($p<0.01$) after slaughter than that in FRP and RFP groups; the SM lightness (L^* value) of FRP pigs increased compared with RFP and HEP groups ($p<0.001$), while the SM redness (a^* value) of FRP pigs was higher than that of RFP group ($p<0.05$). The free fatty acid (**FA**) profile exhibited that the total FAs and unsaturated FAs of pig SM in HEP and RFP groups were higher than those in FRP group ($p<0.05$); the RFP pigs had more reasonable FA composition with higher n-3 polyunsaturated FAs (**PUFAs**) and lower n-6/n-3 PUFA ratio than HEP pigs ($p<0.05$). Based on that, we observed that Tibetan pigs fed high energy diets (HEP) had lower microbial α-diversity in cecum ($p<0.05$), and distinct feeding patterns exhibited a different microbial cluster. Simultaneously, the short-chain FA levels in cecum of FRP and RFP pigs were higher compared with HEP pigs ($p<0.05$). A total of 11 genera related to muscle lipid metabolism or meat quality, including *Alistipes*, *Anaerovibrio*, *Acetitomaculun*, etc., were identified under different feeding patterns ($p<0.05$). Spearman correlation analysis demonstrated that alterations of free FAs in SM were affected by the genera *Prevotellaceae_NK3B31_group*, *Prevotellaceae UCG-003* and *Christensenellaceae_R-7_group* ($p<0.05$). Taken together, distinct feeding patterns affected meat quality of Tibetan pigs related to gut microbiota alterations.

KEYWORDS

Tibetan pigs, meat quality, intestinal microbiota, feeding patterns, long-chain fatty acid

Introduction

Tibetan pig is a rare plateau pig species, mostly living in the alpine and cold areas of semi-farming and semi-grazing (Yang et al., 2021). In addition to its developed cardiopulmonary function, strong lipid-settling ability, and ability to endure plateau anoxic environments, it has a high level of cold or stress resistance, delicious meat, and has a lot of fat between the muscles (Fan et al., 2016; Luo et al., 2022; Niu et al., 2022). In recent years, with the increasing demand for ecological, green and high-quality pork products, Tibetan pig breeding industry has attracted widespread attention.

The traditional way of feeding Tibetan pigs is grazing, which mainly relies on grass, fruits, roots and other food sources of grassland and understory, and rarely supplements with refined feed, so the breeding cost is low (Wang et al., 2013). Understory resources are abundant in summer and autumn, and a lot of nutrients can be obtained by Tibetan pigs; however, in winter and spring with cold climate, the food resources are gradually reduced, and the nutrients that can be absorbed are limited, far from meeting the growth needs of pigs (Zhang et al., 2019; Yang et al., 2021). This traditional feeding pattern seriously slows down the growth and development of pigs and reduces the production performance of Tibetan pigs. Changing the traditional breeding way, therefore, adopting the appropriate house feeding pattern is the only way for the development of industrialization of Tibetan pigs. However, whether changing the way of Tibetan pig breeding will change the quality of meat products needs further verification, especially the effects of diet transformation on Tibetan pork quality from extensive farming to fine farming needing to be clarified.

In recent years, with the depth exploration of microbial functions, gut-brain axis, gut-liver axis and other signaling pathways mediated by microorganisms and their metabolites (especially short-chain fatty acids) have been confirmed to be involved in the host's energy metabolism (Morais et al., 2021; Wang et al., 2021). The microbiota-gut-skeletal muscle axis has also been gradually confirmed, and dietary components (including dietary fiber) can change the gut microbiota to regulate the glucose and lipid metabolism of the host skeletal muscle, resulting in the improvement of their meat quality (Sonnenburg and Backhed, 2016; Chen et al., 2022). Therefore, it is a new idea to regulate skeletal muscle metabolism by altering intestinal microbiota or its metabolites through diet and other factors, ultimately improving muscle production and quality.

Therefore, this study aimed to explore the effects of different feeding patterns on meat quality of Tibetan pigs, and analyze the role of cecal microorganisms and their metabolites short-chain fatty acids (**SCFAs**), which is expected to provide a theoretical basis for large-scale breeding of Tibetan pigs, and provide a reference for selecting specific feeding patterns according to different market orientation and demand structure to achieve accurate pig breeding.

Materials and methods

Ethics approval

The experimental protocol (Ethics Approval Code: IAS2021-241) was reviewed and approved by the Institutional Animal Care and Use Committee of the Institute of Animal Sciences, Chinese Academy of Agricultural Sciences (Beijing, China).

Animals, experimental design, and sample collection

This experiment was conducted in the research farm (Shannan District, Tibet, China) of Institute of Animal Husbandry and Veterinary Medicine, Tibet Academy of Agriculture and Animal Husbandry Sciences. A total of 40 house-feeding Tibetan pigs [initial body weight (**IBW**) = 22.4 ± 1.7 kg] with the same genetic background were allotted to 2 pens randomly and each pen was regarded as one dietary treatment. During the 42-day experimental period, Tibetan pigs were fed the regular Tibetan pig diets (**RFP** group) and the high energy content diets (**HEP** group; Table 1). All pigs were allowed to free access to feed and water. Diets were formulated to meet or exceed the vitamins and minerals of pigs according to the nutrient requirements of swine (GB/T 39235–2020). At the same time, another 20 free-ranging Tibetan pigs (IBW = 21.3 ± 1.0 kg) were selected and set as the reference (**FRP** group).

At the end of this experiment (day 42), 7 randomly selected pigs of each treatment were sacrificed by electric stunning and carcass weight (**CW**) of each pig was recorded. An incubation period of 3 h at room temperature was followed by centrifugation at 3,000 rpm for 10 min after drawing blood from the jugular vein with a sterilized syringe. We aliquoted and stored the serum samples at −80°C for subsequent analysis. The semitendinosus muscle (**SM**) samples (approximately 1 g) were collected into 2-mL sterile tubes for free fatty acids analysis. Aseptically collected chyme from the cecum was sequenced for microbial 16S rRNA genes and analyzed for SCFA levels. All samples of SM and cecum

TABLE 1 Composition and nutrient level of experimental diet (as fed-basis).

Ingredients	RFP diet	HEP diet
Corn	32.14	66.4
Soybean meal	7.5	15.5
Wheat bran	7.26	15
Alfalfa	50	0
Limestone	1	1
CaHPO4	0.5	0.5
NaCl	0.3	0.3
L-Lys (70%)	0.2	0.2
Choline chloride	0.1	0.1
Premix[1]	1	1
Total	100	100
Calculated nutrient levels %		
CP	15.37	14.83
DE, MJ/kg	9.77	13.9
SID Thr	0.43	0.43
SID Trp	0.12	0.13
SID Lys	0.64	0.75
SID Met	0.2	0.23
Ca	1.09	0.56
TP	0.42	0.46
STTD P	0.25	0.25

[1]Provided the following quantities per kg of diet: vitamin A, 9140 IU; vitamin D_3, 4,405 IU; vitamin E, 11 IU; menadione sodium bisulfite, 7.30 mg; riboflavin, 9.15 mg; D-pantothenic acid, 18.33 mg; niacin, 73.50 mg; choline chloride, 1,285 mg; vitamin B_{12}, 200 μg; biotin, 900 μg; thiamine mononitrate, 3.67 mg; folic acid, 1,650 μg; pyridoxine hydrochloride, 5.50 mg; I, 1.85 mg; Mn, 110.10 mg; Cu, 7.40 mg; Fe, 73.50 mg; Zn, 73.50 mg; Se, 500 μg.

RFP: feeding the regular Tibetan pig diets; HEP: feeding the high energy content diets. CP: crude protein; DE: digestible energy; SID AA: standardized ileal digestible amino acid; TP: total phosphorus; STTD P: standardized total tract digestibility of phosphorus.

digesta were immediately frozen in liquid nitrogen and stored at −80°C.

Analysis of serum metabolites

Concentrations of low-density lipoprotein cholesterol (**LDL-C**, Cat # A113-2-1), alanine aminotransferase (**ALT**, Cat # C009-3-1), alkaline phosphatase (**ALP**, Cat # A112-1-1) and high-density lipoprotein cholesterol (**HDL-C**, Cat # A086-1-1) in serum were measured by commercial assay kits from Nanjing Jiancheng Bioengineering Institute (Nanjing, China).

Measurement of meat quality index

Meat color and pH value of SM samples were directly measured by OPTO-STAR and pH-STAR (Matthäus, Germany) according to the manufacturer's instructions at 45 min and 24 h postmortem, respectively. The shear force value of SM samples was obtained by the Warner-Bratzler meat shear machine (Salter 235, Manhattan, Kansas, United States) following the procedure described by Lang et al. (2020).

Detection of free fatty acids in meat

Freeze-dried and ground SM samples were used to analyze medium- and long-chain fatty acid contents. Firstly, lipids were extracted from SM samples by the chloroacetyl-methanol (1:10, v/v) procedure. Hexanes were added for methylation at 80°C water incubation for 4 h. Then, the gas chromatography was utilized to detect the profile of free fatty acids in samples by targeted metabolomics according to the description by Tang et al. (2020).

Quantification of short-chain fatty acids

Approximately 1 g of cecal chyme was collected and immersed in 10 mL of ddH_2O in 15-mL screw-capped vials, after which it was shaken for 30 min and set aside at 4°C overnight. For the analysis of SCFA concentration, the mixture was centrifuged at 10000 rpm for 10 min. The concentration was determined using gas chromatography according to Tang et al. (2021b).

Microbial 16S rRNA gene sequencing analysis

Each sample contained approximately 0.5–1 g of cecal chyme, from which the manufacturer's instructions of the E.Z.N.A.® soil DNA Kit (D5625-02, Omega Bio-Tek Inc., Norcross, GA, United States) were followed to extract microbial community genomic DNA. A 1% agarose gel electrophoresis and NanoDrop2000 spectrophotometer (Thermo Fisher Scientific, Waltham, MA, United States) were used separately to determine the purity and DNA concentration. These primers [338F (5'-ACTCCTACGGGAGGCAGCAG-3′) and 806R (5'-GGACTACHVGGGTWTCTAAT-3′)] were used to amplify the V3-V4 regions of the 16S rRNA gene of bacteria. As described by Tang et al. (2021a), the reaction system, measuring amplified fragments, and purification were conducted according to their methods.

We obtained microbial sequence data from Majorbio Bio-Pharm Technology Co. Ltd. (Shanghai, China). Sequences were analyzed and classified into operational taxonomic units (**OTUs**; 97% identity). Additionally, QIIME (Version 174 1.7.0) generated alpha-diversity coverage based on the Ace, Chao and Sobs index within each sample, and an unweighted UniFrac distance based on Bray-Curtis distance was computed and PCoA was used to visualize beta-diversity. The significant difference between treatments at the phylum and genus level was tested by the Kruskal-Wallis H test (nonparametric test) with corrected

p-value (FDR) < 0.05. Unless otherwise noted, the microbial data were analyzed on the Majorbio I-Sanger Cloud Platform.[1]

Statistical analysis

One-way ANOVA analysis of the data on CW, serum metabolites, meat quality index, free fatty acids in meat, SCFAs in cecal chyme and microbial alpha-diversity (including Ace, Chao and Sobs index) was used to test for differences among 3 groups using the SPSS software (version 23.0, IBM, Armonk, NY, United States). The least significant difference (LSD) as a post-hoc multiple comparison method was used to compare results between every 2 of 3 distinct groups. The correlation matrix between cecal microbes and free fatty acids or SCFAs was generated using Spearman's correlation coefficient on the Majorbio I-Sanger Cloud Platform. All the above data were drawn using GraphPad 7.0. Lastly, the results were presented as means ± SE with $p < 0.05$ being regarded as statistically significant.

Results

Carcass weight and serum metabolites

The IBW and CW, as well as HDL-C, LDL-C, ALT and ALP in serum were shown in Figure 1. The CW and LDL-C of HEP pigs were significantly higher than those of the FRP or RFP pigs ($p < 0.01$), whereas no significant changes in CW and LDL-C were found between FRP and RFP pigs ($p > 0.05$; Figures 1B,D). The HDL-C of HEP pigs was significantly improved compared with the FRP pigs ($p < 0.05$), and the HDL-C of RFP pigs had an increased trend compared with the FRP pigs ($p = 0.058$; Figure 1C). The ALP of HEP pigs was significantly higher compared with the FRP or RFP pigs ($p < 0.05$), whereas no significant change in ALP was found between FRP and RFP pigs ($p > 0.05$; Figure 1F). In addition, no significant difference was observed in ALT among three group pigs ($p > 0.05$; Figure 1E).

Alterations in meat quality

The meat color, pH value, and shear force of SM were shown in Table 2. The L^* (45 min), L^* (24 h) and shear force of SM in FRP pigs were significantly higher than that in RFP and HEP pigs ($p < 0.001$), whereas no significant changes in L^* (45 min), L^* (24 h) and shear force were found between HEP and RFP pigs ($p > 0.05$). The a^* (45 min) and a^* (24 h) of RFP pigs were significantly lower compared with FRP pigs ($p < 0.05$). The b^* (45 min) and pH_{45min} of HEP pigs were the highest, being significantly more elevated than those of RFP and FRP pigs ($p < 0.05$). However, the b^* (24 h) and pH_{24h} of HEP pigs were the lowest and were significantly lower than that of the FRP pigs ($p < 0.01$).

Concentrations of free fatty acids in meat

The concentrations of free fatty acids in SM were shown in Figure 2. The concentrations of saturated fatty acid (**STA**, $p < 0.05$; Figure 2A), monounsaturated fatty acid (**MUFA**, $p = 0.081$; Figure 2B), total fatty acid (**TFA**, $p = 0.065$; Figure 2D) and n-3 polyunsaturated fatty acid (**PUFA**, $p < 0.01$; Figure 2F) in SM of RFP pigs were higher compared with FRP pigs, and the n-3 PUFA in RFP pigs was still higher than that in HEP pigs ($p < 0.01$; Figure 2F). The concentrations of PUFA ($p = 0.062$, Figure 2C) and n-6 PUFA ($p = 0.056$, Figure 2E) in HEP pigs had an increased trend compared with the FRP pigs. In addition, the ratio of n-6/n-3 PUFA in HEP pigs was significantly higher compared with the FRP and RFP pigs ($p < 0.01$), whereas no significant change in the ratio was found between FRP and RFP pigs ($p > 0.05$; Figure 2G).

As data shown in Table 3, the concentrations of C6:0, C20:2, C20:5 n3 and C22:0 of SM in FRP pigs were higher than that in HEP pigs ($p < 0.05$). The concentrations of C12:0, C14:0, C16:0, C17:0, C17:1, C18:0, C18:3 n3, C20:0, C20:1 n9, and C20:3 n3 of SM in RFP pigs were significantly higher compared with the FRP pigs ($p < 0.05$), whereas no significant change in concentrations of C12:0, C14:0, C16:0, C17:0, C17:1, C18:3 n3, and C20:1 n9 were found between HEP and RFP pigs ($p > 0.05$). The concentrations of C14:1 and C18:2,cis(n6) of SM in FRP pigs were lower compared with the RFP and HEP pigs, and significantly lower than that in the HEP pigs ($p < 0.05$). In addition, the concentration of C20:4 n6 of RFP pigs was the highest among three group pigs, and significantly higher than that in the HEP pigs ($p < 0.05$).

Concentrations of short-chain fatty acids in cecal chyme

The concentrations of SCFAs in cecal chyme were shown in Figure 3. The levels of acetic acid and butyric acid in RFP pigs were higher than that in FRP and HEP pigs ($p < 0.05$), whereas no significant changes of that were found between HEP and FRP pigs ($p > 0.05$). The levels of propionic acid and total SCFAs in cecal chyme of FRP or RFP pigs were higher compared with HEP pigs ($p < 0.01$). The concentrations of isobutyrate, isovalerate and valerate in RFP pigs were lower compared with FRP or HEP pigs ($p < 0.05$).

Variations in cecal microbes

The fresh cecal chyme was obtained from FRP, RFP and HEP pigs, and 16 s rRNA gene sequencing analysis was performed. The

1 https://cloud.majorbio.com

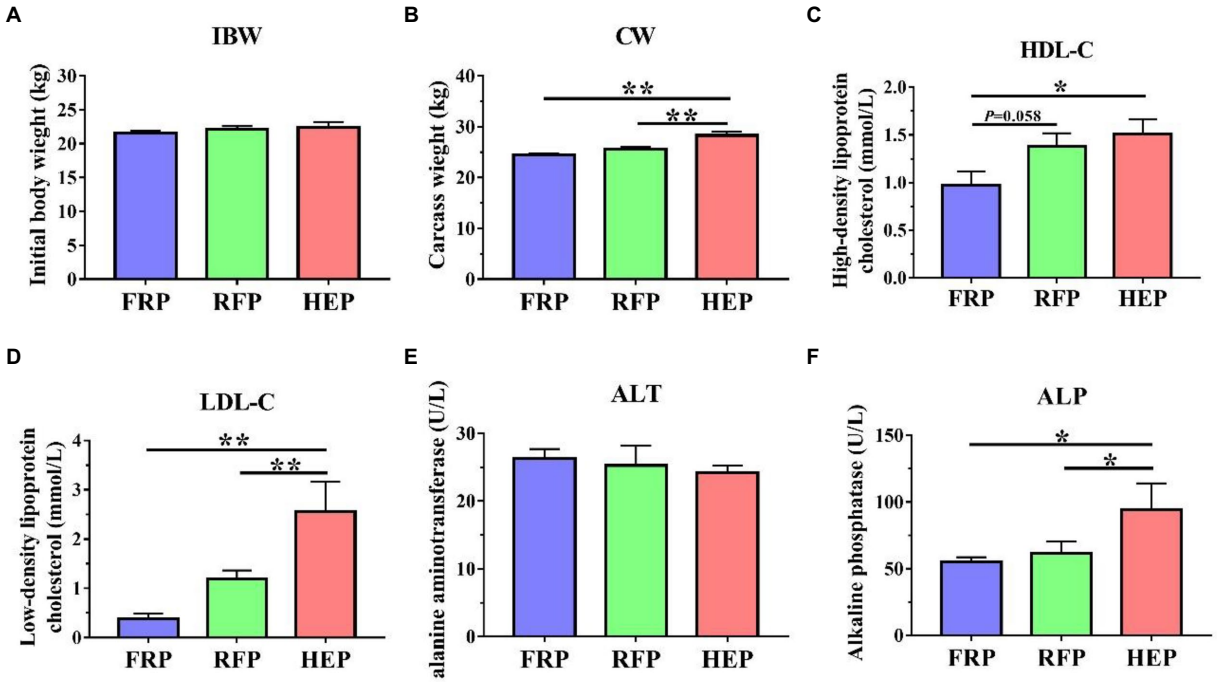

FIGURE 1
Effects of different feeding patterns on the CW, and HDL-C, LDL-C, ALT ALP in serum of Tibetan pigs. **(A)** The initial body weight (IBW) of Tibetan pigs. **(B)** The carcass weight (CW) of Tibetan pigs. **(C)** The content of high-density lipoprotein cholesterol (HDL-C) in serum of Tibetan pigs. **(D)** The content of low-density lipoprotein cholesterol (LDL-C) in serum of Tibetan pigs. **(E)** The activity of alanine aminotransferase (ALT) in serum of Tibetan pigs. **(F)** The activity of alkaline phosphatase (ALP) in serum of Tibetan pigs. Data are expressed as mean±SE (n=6–7). * and ** indicates p <0.05 and p <0.01, respectively. FRP: free-ranging Tibetan pigs; RFP: feeding the regular Tibetan pig diets; HEP: feeding the high energy content diets.

TABLE 2 The meat quality of semitendinosus muscle.

Items		FRP	RFP	HEP	*p* value
Meat color	L^* (45 min)	44.5610 ± 0.85633^a	36.9057 ± 1.52944^b	38.4371 ± 0.56005^b	<0.001
	L^* (24 h)	46.0100 ± 0.56874^a	40.4414 ± 0.81403^b	39.7986 ± 0.86017^b	<0.001
	a^* (45 min)	24.8580 ± 0.70553^a	22.5186 ± 0.44134^b	22.9286 ± 0.46605^{ab}	0.022
	a^* (24 h)	21.3890 ± 0.53471^a	19.5286 ± 0.43414^b	19.9100 ± 0.57722^{ab}	0.042
	b^* (45 min)	2.0830 ± 0.07926^b	3.0314 ± 0.24751^b	4.2529 ± 0.59320^a	<0.001
	b^* (24 h)	7.5190 ± 0.50205^a	5.7529 ± 0.85541^{ab}	4.2486 ± 0.67026^b	0.006
pH values	pH_{45min}	6.3522 ± 0.04099^b	6.3457 ± 0.07211^b	6.5614 ± 0.03508^a	0.012
	pH_{24h}	5.6833 ± 0.06254^a	5.6071 ± 0.06672^a	5.3829 ± 0.03797^b	0.005
Shear force (N)		56.6240 ± 1.78240^a	46.6219 ± 2.29898^b	42.2857 ± 2.85427^b	<0.001

Values in the same row with different superscripts (a, b) are significantly different (p < 0.05) (n = 6–7). L^* (45 min) or L^* (24 h): the lightness of meat color after slaughter 45 min or 24 h; a^* (45 min) or a^* (24 h): the redness of meat color after slaughter 45 min or 24 h; b^* (45 min) or b^* (24 h): the yellowness of meat color after slaughter 45 min or 24 h; pH_{45min} or pH_{24h}: the pH value of meat after slaughter 45 min or 24 h. FRP: free-ranging Tibetan pigs; RFP: feeding the regular Tibetan pig diets; HEP: feeding the high energy content diets.

Ace (Figure 4A), Chao (Figure 4B) and Sobs index (Figure 4C) of cecal chyme microbes at OTU level in HEP pigs were significantly lower than that in FRP pigs (p < 0.05), and extremely significantly lower than that in RFP pigs (p < 0.01). The PCoA analysis based on Bray-Curtis distance revealed that beta-diversity shifted due to distinct feeding patterns and notable differences were observed in the cecal chyme at the OTU level (Figure 4D). There were 1103 (208), 1138 (232) and 1009 (214) OTUs (genera) obtained from FRP, RFP and HEP pigs, respectively, of which 778 (181) were common OTUs (genera) among the three different feeding patterns (Figure 4E).

Microbial community composition at the phylum and genus level of the three feeding patterns was presented in Figure 5. The cecal chyme samples comprised five major phyla including *Firmicutes*, *Bacteroidota*, *Spirochaetota*, *Actinobacteria* and *Proteobacteria*, and the *Firmicutes* and *Bacteroidetes* were the most

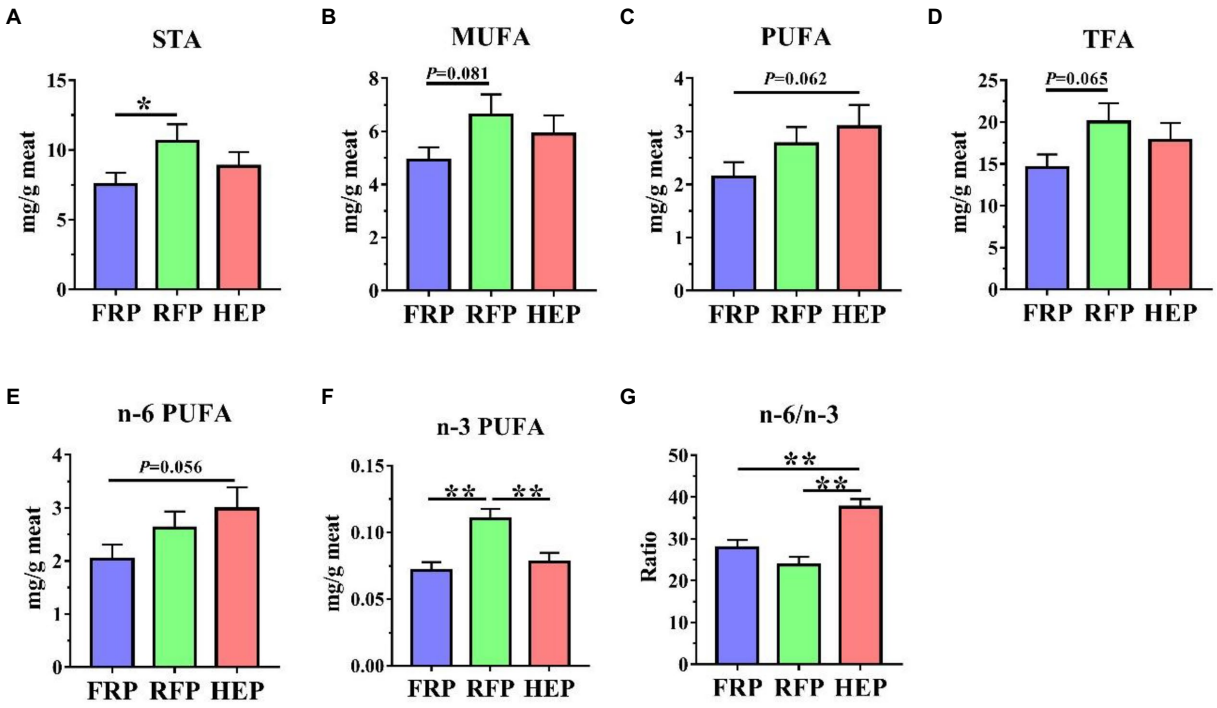

FIGURE 2
Effects of different feeding patterns on concentrations of fatty acids in semitendinosus muscle (SM) of Tibetan pigs. The concentrations of saturated fatty acid (STA, **A**), monounsaturated fatty acid (MUFA, **B**), polyunsaturated fatty acid (PUFA, **C**), total fatty acid (TFA, **D**), n-6 PUFA **(E)**, n-3 PUFA **(F)** and n-6/n-3 PUFA ratio **(G)** in SM of Tibetan pigs, respectively. Data are expressed as mean±SE (n=6–7). * and ** indicates p<0.05 and p<0.01, respectively. FRP: free-ranging Tibetan pigs; RFP: feeding the regular Tibetan pig diets; HEP: feeding the high energy content diets.

predominant phyla in the cecal chyme of FRP, RFP and HEP pigs (Figure 5A). In addition, there were also significant differences in the abundance of *Firmicutes* and *Bacteroidota*, as well as the ratio of *Firmicutes* to *Bacteroidota* among three groups ($p < 0.01$; Figure 5B). At the genus level, the top three most abundant genera in different feeding patterns, in turn, were *norank_f_p-251-o5, Prevotellaceae_UCG-003* and *Rikenellaceae_RC9_gut_group* (Figures 5C,D). The *Prevotellaceae_UCG-003* was extremely significantly enriched in the FRP pigs ($p < 0.01$); the *Parabacteroides, Clostridium_sensu_stricto_1, Clostridium_sensu_stricto_6,* and *Anaerovibrio* were extremely significantly enriched in the RFP pigs ($p < 0.01$); and *Lactobacillus* was extremely significantly enriched in the HEP pigs ($p < 0.01$; Figure 5E).

Correlation between microbiota and free fatty acids in meat or SCFAs in cecal chyme

Spearman's correlation analysis between microbiota and free fatty acids or SCFAs were shown in Figure 6. The relative abundance of *Christensenellaceae_R-7_group* was positively associated with the levels of STA, MUFA, PUFA, TFA, n-6 PUFA and n-6/n-3 ratio in SM, except for n-3 PUFA ($p < 0.05$, Figure 6A). The relative abundance of *Terrisporobacter* and *norank_f_Eubacterium_coprostanoligenes_group* were positively associated with the ratio of n-6/n-3 in SM ($p < 0.05$), whereas the ratio of n-6/n-3 in SM was negatively correlated with the relative abundance of *norank_f_bacteroidales_RF16_group* and *norank_f_p-251-o5* ($p < 0.05$; Figure 6A). In addition, we found that the concentrations of PUFA and n-6 PUFA in SM were negatively correlated with the relative abundance of *Prevotallaceae_UCG-003* ($p < 0.05$, Figure 6A). The concentrations of valerate and total SCFAs were positively associated with the relative abundance of *Rikenellaceae_RC9_gut_group* and *norank_f_Eubacterium_coprostanoligenes_group*, respectively ($p < 0.05$, Figure 6B). However, the concentration of butyrate was negatively correlated with the relative abundance of *norank_f_Eubacterium_coprostanoligenes_group* ($p < 0.01$, Figure 6B).

Discussion

Tibetan pig breeding, not only the focus of the development of agriculture and animal husbandry with local characteristics, but also a crucial industry for people in Tibetan areas to get rid of poverty and become rich, is a vital part of traditional animal husbandry in Tibet. As is known to all, the traditional Tibetan pig breeding method is mainly grazing with a long breeding cycle, which cannot be scientifically managed to maximize the utilization of Tibetan pig resources (Wang et al., 2013; Yang et al., 2021). House feeding can provide full mixed diet for Tibetan pigs without

TABLE 3 The concentrations of free fatty acids in semitendinosus muscle.

Items	FRP	RFP	HEP	*p*-value
C6:0	0.0071 ± 0.00070^{a}	0.0055 ± 0.00010^{ab}	0.0045 ± 0.00030^{b}	0.011
C8:0	0.0029 ± 0.00015	0.0032 ± 0.00020	0.0031 ± 0.00018	0.557
C10:0	0.0133 ± 0.00113	0.0160 ± 0.00163	0.0148 ± 0.00166	0.405
C12:0	0.0086 ± 0.00106^{b}	0.0141 ± 0.00173^{a}	0.0150 ± 0.00202^{a}	0.013
C14:0	0.1224 ± 0.01747^{b}	0.2197 ± 0.02990^{a}	0.2199 ± 0.03506^{a}	0.017
C14:1	0.0041 ± 0.00024^{b}	0.0052 ± 0.00038^{ab}	0.0066 ± 0.00094^{a}	0.01
C16:0	4.9156 ± 0.54760^{b}	7.6975 ± 0.94717^{a}	6.6303 ± 0.83387^{ab}	0.042
C16:1	0.3261 ± 0.03787	0.4642 ± 0.05147	0.5347 ± 0.09375	0.055
C17:0	0.0363 ± 0.00603^{b}	0.0636 ± 0.01085^{a}	0.0397 ± 0.00570^{ab}	0.045
C17:1	0.0271 ± 0.00416^{b}	0.0467 ± 0.00718^{a}	0.0329 ± 0.00465^{ab}	0.047
C18:0	1.5339 ± 0.15239^{b}	2.1517 ± 0.24149^{a}	1.5179 ± 0.13221^{b}	0.042
C18:1,trans(n9)	0.0419 ± 0.11920	0.0310 ± 0.01596	0.0056 ± 0.00555	0.128
C18:1,cis(n9)	3.9440 ± 0.43034	5.8624 ± 0.69633	5.1484 ± 0.60341	0.062
C18:2,trans(n6)	0.2908 ± 0.08110	0.6042 ± 0.08765	0.5198 ± 0.10835	0.056
C18:2,cis(n6), LA	1.5852 ± 0.15389^{b}	1.9638 ± 0.23539^{ab}	2.4176 ± 0.30595^{a}	0.047
C18:3 n6	0.0092 ± 0.00068	0.0075 ± 0.00057	0.0100 ± 0.00171	0.269
C18:3 n3, ALA	0.0207 ± 0.00257^{b}	0.0357 ± 0.00374^{a}	0.0277 ± 0.00379^{ab}	0.014
C20:0	0.0488 ± 0.00784^{b}	0.1306 ± 0.02530^{a}	0.0802 ± 0.12700^{b}	0.004
C20:1 n9	0.1001 ± 0.00947^{b}	0.1833 ± 0.02523^{a}	0.1453 ± 0.01975^{ab}	0.009
C20:2	0.0196 ± 0.00238^{a}	0.0152 ± 0.00141^{ab}	0.0090 ± 0.00171^{b}	0.007
C20:3 n6	0.0466 ± 0.00487	0.0356 ± 0.00348	0.0363 ± 0.00498	0.18
C20:4 n6, ARA	0.0061 ± 0.00131^{ab}	0.0137 ± 0.00538^{a}	0.0011 ± 0.00059^{b}	0.029
C20:3 n3	0.0273 ± 0.00153^{b}	0.0463 ± 0.00507^{a}	0.0308 ± 0.00153^{b}	<0.001
C20:5 n3, EPA	0.0158 ± 0.00092^{a}	0.0154 ± 0.00030^{a}	0.0128 ± 0.00066^{b}	0.035
C22:0	0.4347 ± 0.05281^{a}	0.2681 ± 0.01530^{b}	0.2646 ± 0.03119^{b}	0.013
C22:1	0.0007 ± 0.00052	<0.00001	<0.00001	0.296
C22:2	0.0160 ± 0.00144	0.0142 ± 0.00060	0.0120 ± 0.00142	0.129
C22:6 n3, DHA	0.0111 ± 0.00209	0.0128 ± 0.00266	0.0067 ± 0.00204	0.213
C24:0	0.0478 ± 0.00379	0.0419 ± 0.00202	0.0385 ± 0.00428	0.2
C24:1	0.0253 ± 0.00242	0.0242 ± 0.00123	0.0211 ± 0.00244	0.421

Values in the same row with different superscripts (a, b) are significantly different ($P < 0.05$) ($n = 6–7$). The results were expressed as free fatty acid (mg) per 1 g of freeze-dried meat. C6:0: caproic acid; C8:0: octanoic acid; C10:0: decanoic acid; C12:0: lauric acid; C14:0: myristic acid; C14:1: tetradecenoic acid; C16:0: palmitic acid; C16:1: palmitoleic acid; C17:0: margaric acid; C17:1: margaroleic acid; C18:0: stearic acid; C18:1,trans(n9): elaidic acid; C18:1,cis(n9): oleic acid; C18:2,trans(n6): trans-linoleic acid n6; C18:2,cis(n6): linoleic acid n6; C18:3 n6: gamma-linolenic acid; C18:3 n3: alpha-linolenic acid; C20:0: arachidic acid; C20:1 n9: eicosenoic acid n9; C20:2: eicosadienoic acid; C20:3 n6: eicosatrienoic acid n6; C20:4 n6: arachidonic acid n6; C20:3 n3: eicosatrienoic acid n3; C20:5 n3: eicosapentaenoic acid n3; C22:0: behenic acid; C22:1: cetoleic acid; C22:2: docosadienoic acid; C22:6 n3: docosahexaenoic acid n3; C24:0: lignoceric acid; C24:1: nervonic acid. FRP: free-ranging Tibetan pigs; RFP: feeding the regular Tibetan pig diets; HEP: feeding the high energy content diets.

foraging and less exercise, which is conducive to muscle and fat deposition (Zhang et al., 2019). In this study, the carcass weight of Tibetan pigs in HEP group was significantly higher than those in RFP and FRP groups, indicating that the house feeding pattern with whole mixed diet was beneficial to promote the growth of Tibetan pigs and produce more meat, which was consistent with the results of Zhang et al. (2019).

The serum lipid-related metabolites may reflect the overall metabolic state to a certain extent (Tang et al., 2021b). The HDL-C, mainly synthesized in the liver, is an anti-atherogenic lipoprotein that transports cholesterol from extrahepatic tissues to the liver for metabolism and is excreted from the body by bile (Rigotti et al., 2003). By contrast, the LDL-C is a lipoprotein particle that carries cholesterol into peripheral tissue cells (van der Wulp et al., 2013). In this study, it was found that the levels of HDL-C and LDL-C in Tibetan pig varies due to the different energy intake of feeding patterns. The contents of LDL-C and HDL-C in serum of HEP group pigs were the highest, indicating that cholesterol turnover and metabolism in liver were increased. Similar results were also found in broilers with increased dietary energy levels causing elevated serum HDL and LDL levels (Hu et al., 2021). In addition, it was found in this study that the serum ALP level of Tibetan pigs under different feeding patterns was within the normal range (40–160 U/L), but the ALP level in Tibetan pigs fed high energy content diet was significantly higher than that in Tibetan pigs fed regular diet or free-ranging, meaning that the liver metabolic process was significantly enhanced (Siller and Whyte, 2018).

Tibetan pork, as an ecological, green and high-quality pork product, has attracted public attention. Meat quality is a crucial

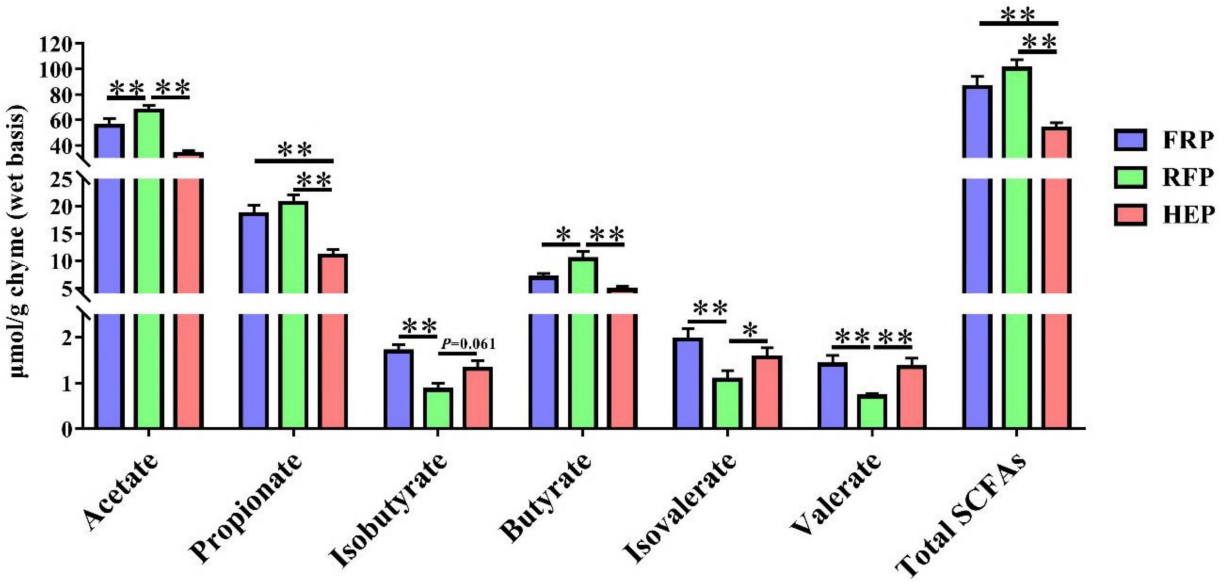

FIGURE 3
Effects of different feeding patterns on concentrations of short-chain fatty acid (SCFA), including acetate acid, propionic acid, isobutyric acid, butyric acid, isovaleric acid, valeric acid and total SCFAs in cecal chyme of Tibetan pigs. Data are expressed as mean±SE (n=6–7). * and ** indicates p<0.05 and p<0.01, respectively. FRP: free-ranging Tibetan pigs; RFP: feeding the regular Tibetan pig diets; HEP: feeding the high energy content diets.

economic trait, which directly affects consumers' preference for pork, and different meat quality characteristics are applied to different meat processing methods (Modzelewska-Kapitula et al., 2012; Wang et al., 2022a). For example, tender meat is suitable for grilling, while chewy meat is better for braising. This study showed that differences in energy intake levels caused by different feeding patterns did result in alterations in meat quality (including tenderness, pH value, meat color, medium and long-chain fatty acid content). We observed that the shear force of Tibetan pork in the grazing group was significantly higher than those of the other two groups, and the meat color was brighter and redder (L^* and a^* values). The type and composition of muscle fibers were closely related to meat quality, and the type I myofiber was more enriched in the muscle of grazing Tibetan pigs due to frequent exercise and running (Jackson et al., 2015). The meat color depends on the content of myoglobin in the muscle (Bekhit and Faustman, 2005), and the free-range Tibetan pork was red and bright because of increased type I myofiber, oxidative myofiber, with high content of myoglobin (Ryu and Kim, 2005). The reason why Tibetan pork became dark red with the increase of exposure time under any feeding pattern was that oxymyoglobin (bright red) was oxidized to methemoglobin (brown) (Bekhit and Faustman, 2005). In addition, the researcher believed that the glycolytic myofiber (type IIb) has a faster maturation rate than the oxidative myofiber (type I), so the higher proportion of type I myofiber exhibited a higher shear force in muscle (Seideman, 1986), which provided a reasonable explanation for the alterations of pork tenderness under different feeding pattern in this experiment. Generally, meat with a $pH_{45min} \geq 6$ measured after 45 min of slaughter is considered as high-quality meat, and meat with a $pH_{24h} > 6$ measured after 24 h is considered as dark firm dry meat (Yin, 2011). Hence, from the point of view of pH value, we found high quality of Tibetan pork in any feeding pattern, and the highest pH_{24h} was found in the free-ranging group. Due to the high proportion of type I myofiber with low glycogen content and weak glycolytic ability (Yin, 2011) in free-ranging Tibetan pigs, the lactic acid production was low, finally leading to higher pH_{24h} in muscle. Intriguingly, the pH value of Tibetan pigs in free-ranging group and regular diet feeding group at 45 min was lower than that of Tibetan pigs in high energy group, which might be closely related to dietary fiber content.

Additionally, fatty acids are essential for human health with various physiological functions (Calder, 2015). We observed that the total fatty acids and unsaturated fatty acids in meat of Tibetan pigs fed high energy diets and regular diets were significantly higher than those in free-ranging Tibetan pigs, indicating the crucial roles of energy intake level for the fatty acid content in meat (Wang et al., 2020). It is widely recognized that n-6 PUFAs have potentially negative effects, while n-3 PUFAs [especially eicosapentaenoic acid (**EPA**) and docosahexaenoic acid (**DHA**)] have significant positive effects on human health (Jeromson et al., 2015; Sears and Perry, 2015). Meanwhile, researchers have demonstrated that n-3 PUFA exhibited curative effects on bronchial asthma, neuropsychiatric disorders and cognitive brain function in children and can also prevent future cardiovascular events in adults (Ciccone et al., 2013). The fatty acid composition, especially n-3 PUFA, is

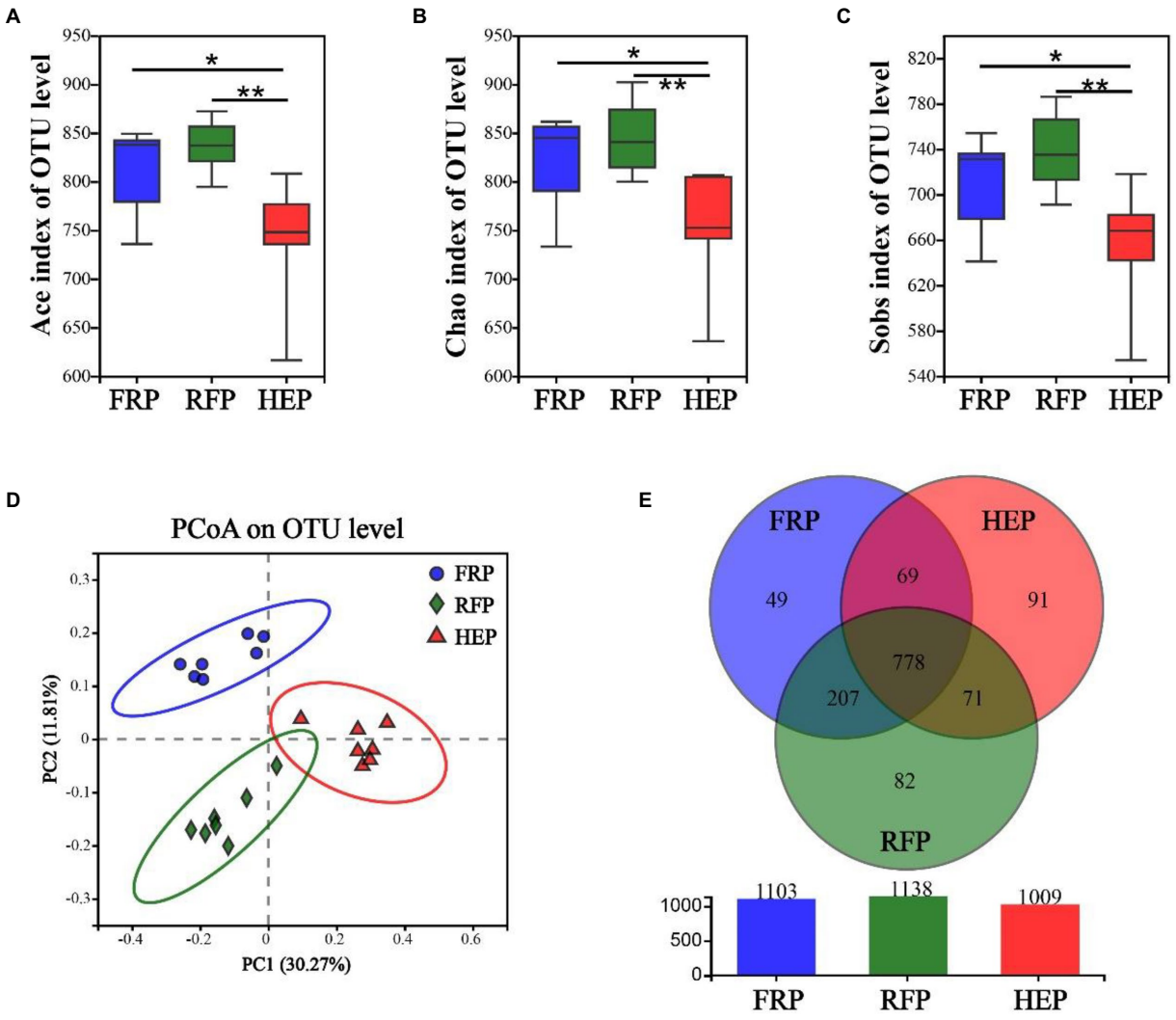

FIGURE 4
Effects of different feeding patterns on gut microbiota diversity of Tibetan pigs. The Ace **(A)**, Chao **(B)** and Sobs index **(C)** of microbiota in cecal chyme. Data are expressed as minimum to maximum (n =7). * and ** indicates p<0.05 and p<0.01, respectively. **(D)** PCoA analysis of microbiota in cecal chyme at the OTU level based on the Bray-Curtis distance. **(E)** The Venn figure of microbiota in cecal chyme. FRP: free-ranging Tibetan pigs; RFP: feeding the regular Tibetan pig diets; HEP: feeding the high energy content diets.

modulated by altering dietary lipid intake and absorption levels (Poorghasemi et al., 2013). In this study, Tibetan pigs fed regular diets had more reasonable fatty acid composition with higher n-3 PUFAs and lower n-6/n-3 PUFA ratio than high energy intake Tibetan pigs. In addition to n-3 PUFAs, other fatty acids including C18:3n-3 (alpha-linolenic acid, **ALA**), C20:5n-3 (EPA) and C22:6n-3 (DHA) also have health benefits in preventing brain, retina and cardiovascular diseases (Howe et al., 2006). In this research, the higher content of EPA in free-ranging and regular diets group pork might be closely related to the alterations of gut microbiota caused by fiber intake (Chen et al., 2022). For other unsaturated fatty acids [linoleic acid (**LA**), ALA and arachidonic acid (**ARA**)] that are beneficial to human beings, different feeding patterns have their own advantages.

In recent years, the interaction between gut microbiota and muscle has been confirmed by more and more studies, and the importance of its microbiota-gut-muscle axis has been fully recognized (Ticinesi et al., 2019). Gut microbiota can affect skeletal muscle metabolism and muscle fiber phenotype (Lahiri et al., 2019; Nay et al., 2019), and several species of bacteria also have similar effects on regulating skeletal muscle metabolism (Ni et al., 2019; Scheiman et al., 2019). Hence, we analyzed the microbial composition in the cecum of Tibetan pigs, and the results exhibited that the microbial community was obviously divided into three different clusters under different feeding patterns, and the microbial diversity in the cecum of Tibetan pigs fed high energy diets was significantly reduced due to the lack of fiber in the diets (Pu et al., 2022). Besides, microbiota-derived SCFA was affected by dietary fiber intake (Pu et al., 2022), which

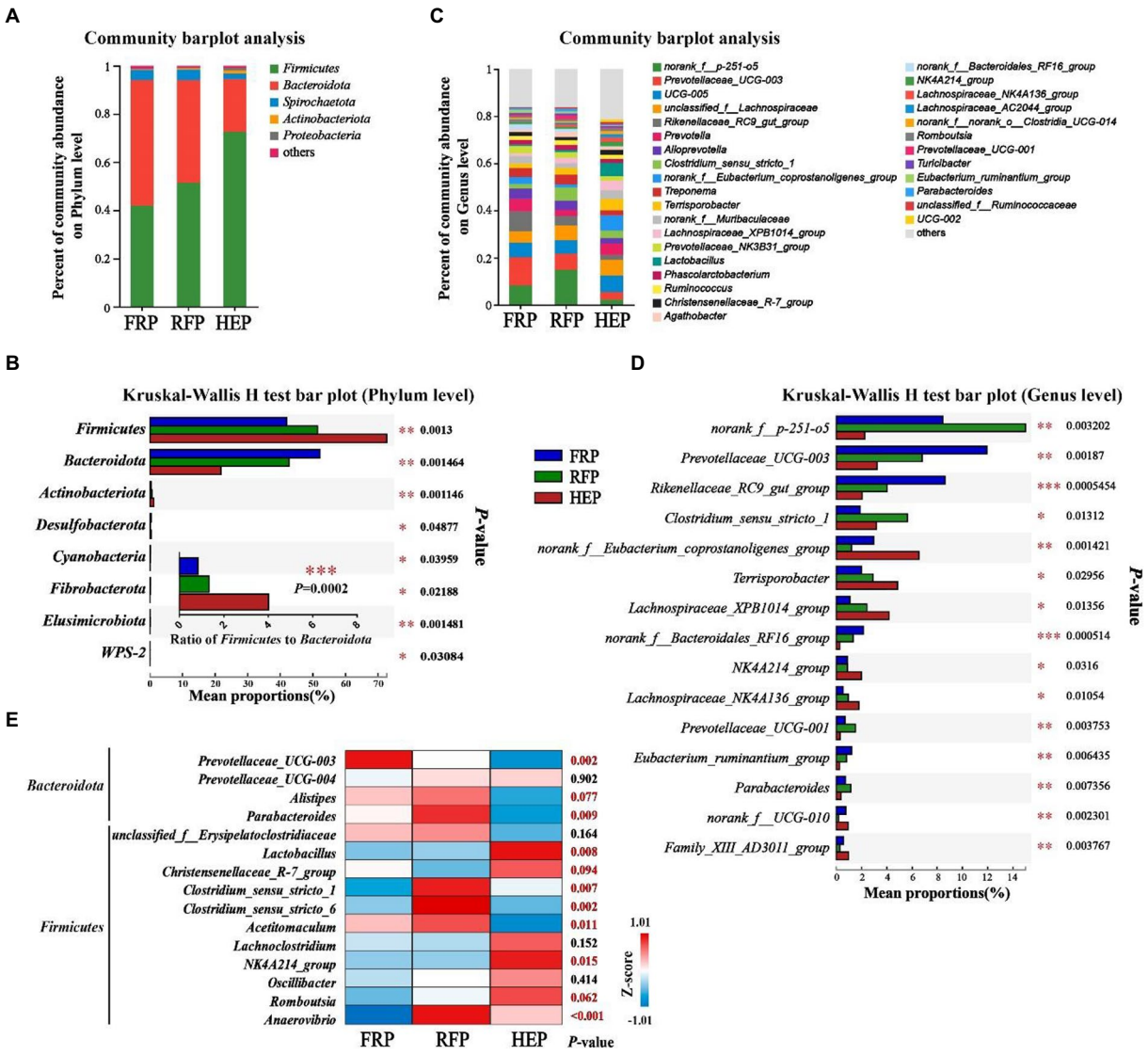

FIGURE 5
Effects of different feeding patterns on gut microbiota community composition in the cecal chyme of Tibetan pigs. The relative abundances of microbiota in cecal chyme at the phylum **(A)** or genus level **(C)**. Analysis of variance in the gut microbiota with significant differences at the phylum **(B)** and genus level (the top 15 genera, **D**). **(E)** heat map of the different enrichment of bacteria related to meat quality among three groups. Data are expressed as mean value (n =7). *, ** and *** indicates p<0.05, p<0.01 and p<0.001, respectively. FRP: free-ranging Tibetan pigs; RFP: feeding the regular Tibetan pig diets; HEP: feeding the high energy content diets.

was consistent with the results that the content of SCFAs (especially acetic acid, propionic acid, and butyric acid) was higher in the cecum of Tibetan pigs in free-ranging and regular diet groups with more fiber intake in this study. The results of Spearman correlation analysis suggested that the genera *Prevotellaceae UCG-003*, *norank_f_Eubacterium_coprostanoligenes_group*, *Rikenellaceae_RC9_gut_group* and *norank_f_p-251-o5* were significantly correlated with the production of SCFA in intestinal tract of Tibetan pigs. It has been reported that SCFA infusion from ileum inhibited the expression of fatty acid synthase and acetyl-CoA carboxylase in longissimus dorsi muscle and altered meat quality after antibiotic clearance of endogenous SCFA-produced microbiota in hindgut of pigs (Jiao et al., 2021). Feeding alfalfa and SCFA in goats significantly increased the content of C16:0 and C18:0 in meat (Wang et al., 2022b), which was highly similar to the results of this experiment. Simultaneously, increasing evidence confirmed that gut microbes (for example, *Parabacteroides*, *Unclassified Erysipelotrichaceae*, *Prevotellaceae UCG-001*, *Butyrivibrio*, *Alistipes*, *Phocaeicola*, *Acetitomaculun*, *Corynebacterium*, *Anaerovibrio*, *Lachnoclostridium_1*) affect lipid deposition and fatty acid content in skeletal muscle by altering lipid metabolism (Chen et al., 2022). A total of 11 genera related to lipid metabolism, including *Unclassified_f_Erysipelotrichaceae*,

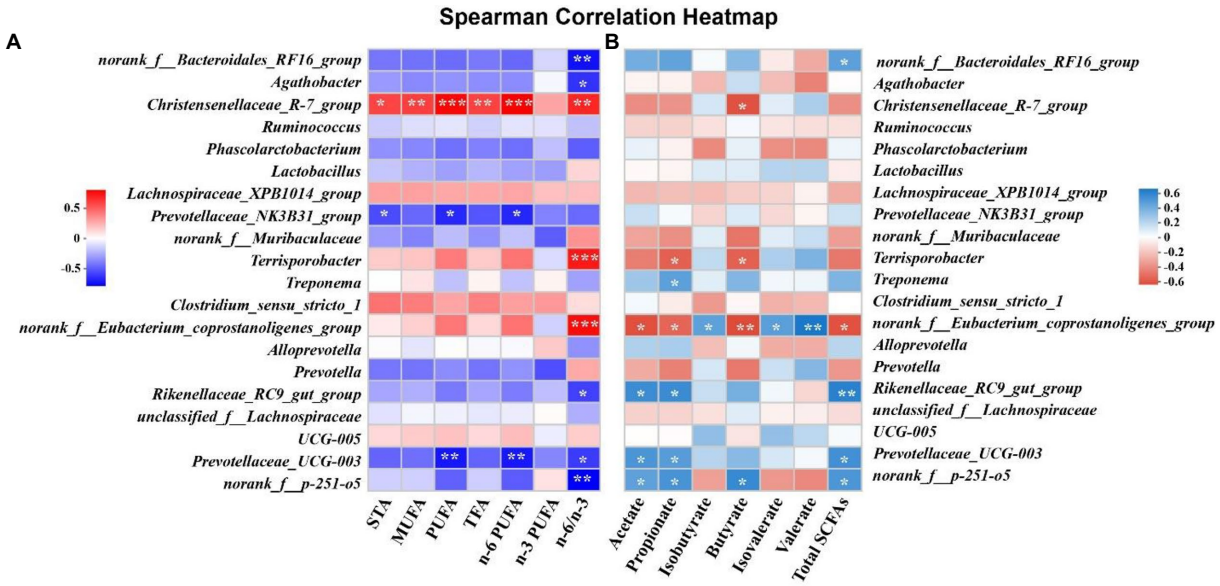

FIGURE 6
The correlation matrix of cecal genera, free fatty acids and short-chain fatty acids (SCFAs). **(A)** The correlation between cecal genera and free fatty acids in semitendinosus muscle. **(B)** The correlation between cecal genera and SCFAs in cecal chyme. *, ** and *** indicates $p<0.05$, $p<0.01$ and $p<0.001$, respectively. STA, saturated fatty acid; MUFA, monounsaturated fatty acid; PUFA, polyunsaturated fatty acid; TFA, total fatty acid.

Alistipes, *Anaerovibrio*, *Acetitomaculun*, etc., were identified under different feeding patterns in this study. Among that, the high content of C18:1 cis-9 and C18:2n-6 trans in Tibetan pork with higher energy intake (REP and HEP group pigs) might be caused by the increased abundance of *Anaerovibrio* bacteria in intestinal tract (Wang et al., 2019). Besides, the high content of saturated fatty acids in Tibetan pork with higher energy intake was also closely related to the probiotic and antioxidant effects of *Lactobacillus* (*Lactobacillus johnsonii*) in intestinal tract (Wang et al., 2017). In this study, Spearman correlation analysis demonstrated that alterations in the content of medium or long-chain fatty acids in meat were affected by the genera *Prevotellaceae_NK3B31_group*, *Prevotellaceae UCG-003* and *Christensenellaceae_R-7_group*. In addition to the bacteria related to lipid metabolism, this study also found that the bacteria *Prevotella* and *Clostridium* related to meat quality (Fang et al., 2017) changed significantly in the cecum of Tibetan pigs under different feeding patterns.

Conclusion

Taken together, our results demonstrated that high energy feeding pattern for house feeding improved carcass weight and enhanced feeding efficiency of Tibetan pigs, yet distinct feeding patterns affected meat quality of Tibetan pigs closely associated with altering gut microbiota, which could provide a reference for choosing specific feeding pattern based on various market orientation and demand to achieve precision breeding.

Data availability statement

The datasets presented in this study can be found in online repositories. The names of the repository/repositories and accession number(s) can be found at: https://www.ncbi.nlm.nih.gov, PRJNA899682.

Ethics statement

The animal study was reviewed and approved by the Institutional Animal Care and Use Committee of the Institute of Animal Sciences, Chinese Academy of Agricultural Sciences (Ethics Approval Code: IAS2021-241).

Author contributions

YZ, CL, ST, and RZ designed the research. YZ, Cy, CL, GS, BS, and JD conducted the experiments. YZ and ST analyzed the data. YZ, RZ, Bw, and ST wrote the paper and revised the manuscript. YZ, TM, RZ, LC, and HZ provided the funding and supervision. All authors contributed to the article and approved the submitted version.

Funding

This study was funded by the Tibet Science and Technology Projects (XZ-2019-NK-NS-003), the National Key Research and Development Program of China (2022YFD1600201), and

Agricultural Science and Technology Innovation Program (CAAS-ZDRW202006-02, ASTIPIAS07).

Conflict of interest

The authors declare that the research was conducted in the absence of any commercial or financial relationships that could be construed as a potential conflict of interest.

Publisher's note

All claims expressed in this article are solely those of the authors and do not necessarily represent those of their affiliated organizations, or those of the publisher, the editors and the reviewers. Any product that may be evaluated in this article, or claim that may be made by its manufacturer, is not guaranteed or endorsed by the publisher.

References

Bekhit, A. E., and Faustman, C. (2005). Metmyoglobin reducing activity. *Meat Sci.* 71, 407–439. doi: 10.1016/j.meatsci.2005.04.032

Calder, P. C. (2015). Functional roles of fatty acids and their effects on human health. *JPEN J. Parenter. Enteral Nutr.* 39, 18S–32S. doi: 10.1177/0148607115595980

Chen, B., Li, D., Leng, D., Kui, H., Bai, X., and Wang, T. (2022). Gut microbiota and meat quality. *Front. Microbiol.* 13:951726. doi: 10.3389/fmicb.2022.951726

Ciccone, M. M., Scicchitano, P., Gesualdo, M., Zito, A., Carbonara, S., Ricci, G., et al. (2013). The role of omega-3 polyunsaturated fatty acids supplementation in childhood: a review. *Recent Pat. Cardiovasc. Drug Discov.* 8, 42–55. doi: 10.2174/1574890111308010006

Fan, B., Zhang, H., Bai, J., Liu, X., Li, Y., Wang, X., et al. (2016). Pathogenesis of highly pathogenic porcine reproductive and respiratory syndrome virus in Chinese Tibetan swine. *Res. Vet. Sci.* 108, 33–37. doi: 10.1016/j.rvsc.2016.07.012

Fang, S., Xiong, X., Su, Y., Huang, L., and Chen, C. (2017). 16S rRNA gene-based association study identified microbial taxa associated with pork intramuscular fat content in feces and cecum lumen. *BMC Microbiol.* 17:162. doi: 10.1186/s12866-017-1055-x

Howe, P., Meyer, B., Record, S., and Baghurst, K. (2006). Dietary intake of long-chain omega-3 polyunsaturated fatty acids: contribution of meat sources. *Nutrition* 22, 47–53. doi: 10.1016/j.nut.2005.05.009

Hu, X., Li, X., Xiao, C., Kong, L., Zhu, Q., and Song, Z. (2021). Effects of dietary energy level on performance, plasma parameters, and central AMPK levels in stressed broilers. *Front Vet Sci.* 8:681858. doi: 10.3389/fvets.2021.681858

Jackson, J. R., Kirby, T. J., Fry, C. S., Cooper, R. L., McCarthy, J. J., Peterson, C. A., et al. (2015). Reduced voluntary running performance is associated with impaired coordination as a result of muscle satellite cell depletion in adult mice. *Skelet. Muscle* 5:41. doi: 10.1186/s13395-015-0065-3

Jeromson, S., Gallagher, I. J., Galloway, S. D., and Hamilton, D. L. (2015). Omega-3 fatty acids and skeletal muscle health. *Mar. Drugs* 13, 6977–7004. doi: 10.3390/md13116977

Jiao, A., Diao, H., Yu, B., He, J., Yu, J., Zheng, P., et al. (2021). Infusion of short chain fatty acids in the ileum improves the carcass traits, meat quality and lipid metabolism of growing pigs. *Anim Nutr.* 7, 94–100. doi: 10.1016/j.aninu.2020.05.009

Lahiri, S., Kim, H., Garcia-Perez, I., Reza, M. M., Martin, K. A., Kundu, P., et al. (2019). The gut microbiota influences skeletal muscle mass and function in mice. *Sci. Transl. Med.* 11:662. doi: 10.1126/scitranslmed.aan5662

Lang, Y., Zhang, S., Xie, P., Yang, X., Sun, B., and Yang, H. (2020). Muscle fiber characteristics and postmortem quality of longissimus thoracis, psoas major and semitendinosus from Chinese Simmental bulls. *Food Sci. Nutr.* 8, 6083–6094. doi: 10.1002/fsn3.1898

Luo, C., Sun, G., Duan, J., Han, H., Zhong, R., Chen, L., et al. (2022). Effects of high-altitude hypoxic environment on colonic inflammation, intestinal barrier and gut microbiota in three-way crossbred commercial pigs. *Front. Microbiol.* 13:521. doi: 10.3389/fmicb.2022.968521

Modzelewska-Kapitula, M., Dabrowska, E., Jankowska, B., Kwiatkowska, A., and Cierach, M. (2012). The effect of muscle, cooking method and final internal temperature on quality parameters of beef roast. *Meat Sci.* 91, 195–202. doi: 10.1016/j.meatsci.2012.01.021

Morais, L. H., Schreiber, H. L. T., and Mazmanian, S. K. (2021). The gut microbiota-brain axis in behaviour and brain disorders. *Nat. Rev. Microbiol.* 19, 241–255. doi: 10.1038/s41579-020-00460-0

Nay, K., Jollet, M., Goustard, B., Baati, N., Vernus, B., Pontones, M., et al. (2019). Gut bacteria are critical for optimal muscle function: a potential link with glucose homeostasis. *Am. J. Physiol. Endocrinol. Metab.* 317, E158–E171. doi: 10.1152/ajpendo.00521.2018

Ni, Y., Yang, X., Zheng, L., Wang, Z., Wu, L., Jiang, J., et al. (2019). Lactobacillus and Bifidobacterium improves physiological function and cognitive ability in aged mice by the regulation of gut microbiota. *Mol. Nutr. Food Res.* 63:e1900603. doi: 10.1002/mnfr.201900603

Niu, H., Feng, X. Z., Shi, C. W., Zhang, D., Chen, H. L., Huang, H. B., et al. (2022). Gut bacterial composition and functional potential of Tibetan pigs under semi-grazing. *Front. Microbiol.* 13:850687. doi: 10.3389/fmicb.2022.850687

Poorghasemi, M., Seidavi, A., Qotbi, A. A., Laudadio, V., and Tufarelli, V. (2013). Influence of dietary fat source on growth performance responses and carcass traits of broiler chicks. *Asian-Australas J Anim Sci.* 26, 705–710. doi: 10.5713/ajas.2012.12633

Pu, G., Hou, L., Du, T., Wang, B., Liu, H., Li, K., et al. (2022). Effects of short-term feeding with high fiber diets on growth, utilization of dietary fiber, and microbiota in pigs. *Front. Microbiol.* 13:963917. doi: 10.3389/fmicb.2022.963917

Rigotti, A., Miettinen, H. E., and Krieger, M. (2003). The role of the high-density lipoprotein receptor SR-BI in the lipid metabolism of endocrine and other tissues. *Endocr. Rev.* 24, 357–387. doi: 10.1210/er.2001-0037

Ryu, Y. C., and Kim, B. C. (2005). The relationship between muscle fiber characteristics, postmortem metabolic rate, and meat quality of pig longissimus dorsi muscle. *Meat Sci.* 71, 351–357. doi: 10.1016/j.meatsci.2005.04.015

Scheiman, J., Luber, J. M., Chavkin, T. A., MacDonald, T., Tung, A., Pham, L. D., et al. (2019). Meta-omics analysis of elite athletes identifies a performance-enhancing microbe that functions via lactate metabolism. *Nat. Med.* 25, 1104–1109. doi: 10.1038/s41591-019-0485-4

Sears, B., and Perry, M. (2015). The role of fatty acids in insulin resistance. *Lipids Health Dis.* 14:121. doi: 10.1186/s12944-015-0123-1

Seideman, S. C. (1986). Methods of expressing collagen characteristics and their relationship to meat tenderness and muscle fiber types. *J. Food Sci.* 51, 273–276. doi: 10.1111/j.1365-2621.1986.tb11107.x

Siller, A. F., and Whyte, M. P. (2018). Alkaline phosphatase: discovery and naming of our favorite enzyme. *J. Bone Miner. Res.* 33, 362–364. doi: 10.1002/jbmr.3225

Sonnenburg, J. L., and Backhed, F. (2016). Diet-microbiota interactions as moderators of human metabolism. *Nature* 535, 56–64. doi: 10.1038/nature18846

Tang, S., Xie, J., Wu, W., Yi, B., Liu, L., and Zhang, H. (2020). High ammonia exposure regulates lipid metabolism in the pig skeletal muscle via mTOR pathway. *Sci. Total Environ.* 740:139917. doi: 10.1016/j.scitotenv.2020.139917

Tang, S., Zhang, S., Zhong, R., Su, D., Xia, B., Liu, L., et al. (2021a). Time-course alterations of gut microbiota and short-chain fatty acids after short-term lincomycin exposure in young swine. *Appl. Microbiol. Biotechnol.* 105, 8441–8456. doi: 10.1007/s00253-021-11627-x

Tang, S., Zhong, R., Yin, C., Su, D., Xie, J., Chen, L., et al. (2021b). Exposure to high aerial ammonia causes hindgut dysbiotic microbiota and alterations of microbiota-derived metabolites in growing pigs. *Front. Nutr.* 8:689818. doi: 10.3389/fnut.2021.689818

Ticinesi, A., Lauretani, F., Tana, C., Nouvenne, A., Ridolo, E., and Meschi, T. (2019). Exercise and immune system as modulators of intestinal microbiome: implications for the gut-muscle axis hypothesis. *Exerc. Immunol. Rev.* 25, 84–95.

van der Wulp, M. Y., Verkade, H. J., and Groen, A. K. (2013). Regulation of cholesterol homeostasis. *Mol. Cell. Endocrinol.* 368, 1–16. doi: 10.1016/j.mce.2012.06.007

Wang, H., He, Y., Li, H., Wu, F., Qiu, Q., Niu, W., et al. (2019). Rumen fermentation, intramuscular fat fatty acid profiles and related rumen bacterial populations of Holstein bulls fed diets with different energy levels. *Appl. Microbiol. Biotechnol.* 103, 4931–4942. doi: 10.1007/s00253-019-09839-3

Wang, Y., Li, T., Chen, X., Liu, C., Jin, X., Tan, H., et al. (2022b). Preliminary investigation of mixed orchard hays on the meat quality, fatty acid profile, and gastrointestinal microbiota in goat kids. *Animals (Basel).* 12:780. doi: 10.3390/ani12060780

Wang, S., Li, J., Wang, H., Han, S., Guo, C., and Wang, Y. (2013). A review on Tibetan swine(a)-carcass, meat quality, basic nutrition component, amino acids, fatty acids, inosine monophosphate and muscle fiber. *Agric Sci & Technol.* 14: 1369–1374, 1391. doi: 10.16175/j.cnki.1009-4229.2013.10.030

Wang, H., Ni, X., Liu, L., Zeng, D., Lai, J., Qing, X., et al. (2017). Controlling of growth performance, lipid deposits and fatty acid composition of chicken meat through a probiotic, lactobacillus johnsonii during subclinical *Clostridium perfringens* infection. *Lipids Health Dis.* 16:38. doi: 10.1186/s12944-017-0408-7

Wang, B., Shen, C., Cai, Y., Liu, D., and Gai, S. (2022a). The purchase willingness of consumers for red meat in China. *Meat Sci.* 192:108908. doi: 10.1016/j.meatsci.2022.108908

Wang, R., Tang, R., Li, B., Ma, X., Schnabl, B., and Tilg, H. (2021). Gut microbiome, liver immunology, and liver diseases. *Cell. Mol. Immunol.* 18, 4–17. doi: 10.1038/s41423-020-00592-6

Wang, Y., Wang, Q., Dai, C., Li, J., Huang, P., Li, Y., et al. (2020). Effects of dietary energy on growth performance, carcass characteristics, serum biochemical index, and meat quality of female Hu lambs. *Anim Nutr.* 6, 499–506. doi: 10.1016/j.aninu.2020.05.008

Yang, L., Wang, G., Zhou, J., Yang, Y., Pan, H., Zeng, X., et al. (2021). Exploration of the potential for efficient fiber degradation by intestinal microorganisms in Diqing Tibetan pigs. *Fermentation.* 7:275. doi: 10.3390/fermentation7040275

Yin, J. (2011). *Animal Muscle and Meat Quality*. China Agricultural University Press, Beijing.

Zhang, P., Shang, P., Zhang, B., Zhang, J., Wang, L., Zhang, H., et al. (2019). Comparison of slaughtering performance and meat quality of Tibetan pigs under indoor feeding and grazing conditions. *Chinese J of Anim Sci.* 55, 107–109. doi: 10.19556/j.0258-7033.2019-03-107

frontiers | Frontiers in Microbiology

TYPE Original Research
PUBLISHED 06 December 2022
DOI 10.3389/fmicb.2022.1073950

OPEN ACCESS

EDITED BY
Jinxuan Cao,
Beijing Technology and Business University, China

REVIEWED BY
Xinlin Wei,
Shanghai Jiao Tong University, China
Bin Wang,
Shihezi University, China

*CORRESPONDENCE
Yao Zou
zouyao82@163.com
Ming-Zhi Zhu
mzzhucn@hotmail.com
Wei Xu
xuweianti@sicau.edu.cn

SPECIALTY SECTION
This article was submitted to Food Microbiology, a section of the journal Frontiers in Microbiology

RECEIVED 19 October 2022
ACCEPTED 17 November 2022
PUBLISHED 06 December 2022

CITATION
Zhao Y-Q, Jia W-B, Liao S-Y, Xiang L, Chen W, Zou Y, Zhu M-Z and Xu W (2022) Dietary assessment of ochratoxin A in Chinese dark tea and inhibitory effects of tea polyphenols on ochratoxigenic *Aspergillus niger*. *Front. Microbiol.* 13:1073950. doi: 10.3389/fmicb.2022.1073950

Dietary assessment of ochratoxin A in Chinese dark tea and inhibitory effects of tea polyphenols on ochratoxigenic *Aspergillus niger*

Yi-qiao Zhao[1], Wen-bao Jia[1], Si-yu Liao[1], Lin Xiang[1], Wei Chen[1], Yao Zou[1]*, Ming-Zhi Zhu[2]* and Wei Xu[1]*

[1]College of Horticulture, Tea Refining and Innovation Key Laboratory of Sichuan Province, Sichuan Agricultural University, Chengdu, China, [2]Key Laboratory of Tea Science of Ministry of Education, National Research Center of Engineering Technology for Utilization of Functional Ingredients From Botanicals, College of Horticulture, Hunan Agricultural University, Changsha, China

In recent years, there has been an increasingly heated debate on whether Chinese dark tea is contaminated with mycotoxins and whether it poses health risks to consumers. In this study, a rapid method based on high-performance liquid chromatography was used to detect ochratoxin A (OTA) in Chinese dark tea samples from different regions of China and different years. Of the 228 Chinese dark tea samples tested, 21 were detected for OTA contamination, with a concentration ranging from 2.51±0.16 to 12.62±0.72 μg/kg. Subsequently, a dark tea drinking risk assessment was conducted, and the hazard quotient for each group was far below the acceptable level of 1.0. Of the 12 *Aspergillus* spp. strains isolated, one strain of *Aspergillus niger* had the ability to produce OTA. We also found that tea polyphenols and epigallocatechin gallate inhibited the growth of ochratoxin-producing *Aspergillus niger* and the expression of non-ribosomal peptide synthetase *(NRPS)*, a key gene for ochratoxin synthesis. Thus, OTA contamination of dark tea is at an acceptable risk level, and the inhibition of ochratoxigenic *Aspergillus niger* by polyphenols provides new insights into the safety of dark tea consumption.

KEYWORDS

hazard quotient, Ochratoxin A contamination, risk assessment, polyphenols, non-ribosomal peptide synthetase

Introduction

Dark tea, which is highly preferred in China, is a unique type of solid fermentation tea (Wang et al., 1991). There are various types of dark tea available in different regions of China, and the major types are Kang brick tea in Sichuan, Fu brick tea in Hunan and Shaanxi, Ripe Pu-erh tea in Yunnan, and Qing brick tea in Hubei (Wang R. et al., 2018). The unique flavor qualities and health benefits of dark tea are attributed to pile-fermentation, which is a special process in dark tea processing. *Aspergillus niger* is the

dominant fungus in the pile-fermentation processing (Ou, 2017; Xiong, 2017), and parts of *Aspergillus niger* have the ability to produce ochratoxin A (OTA; Sánchez-Hervás et al., 2008; Iqbal et al., 2014; Wang et al., 2016; Deng et al., 2020). Recent reports have shown that *Aspergillus niger* isolated from dark tea can produce OTA. This implies that there is a possibility of dark tea contamination by OTA (Zhou et al., 2015; Zhao et al., 2021).

With the increasing consumption of dark tea, the study of OTA determination and risk assessment for dark tea is imminent. Numerous studies (Haas et al., 2013; Liu et al., 2016, 2017; Mo et al., 2016; Ye et al., 2020) regarding OTA determination in dark tea have been conducted, the concentrations ranging from 0.22 to 94.7 μg/kg, but a larger number and more representative samples of dark tea should be investigated. Risk assessment of OTA in dark tea has been carried out in some studies (Ye et al., 2020; Yan et al., 2021), and the results showed that there is no observed risk concern to consumers as the hazard quotient (HQ) was below 1.0. In addition, large amounts of tea consumption data are urgently required to generate a more accurate assessment.

Ochratoxin A, a group of secondary metabolites produced by the fungi *Aspergillus* (Wang Y. et al., 2018), is nephrotoxic, hepatotoxic, immunotoxic, genotoxic, neurotoxic, and teratogenic (Chen et al., 2018). This compound is widely found in cereal products, wine, coffee, tea, and even meat products (Duarte et al., 2010; Kumar et al., 2020). OTA contamination is an increasing concern worldwide because of its harmful effects on human health. The cluster of genes involved in OTA synthesis in *Aspergillus niger* has been extensively investigated, and the results suggest that polyketide synthase (*PKS*), non-ribosomal peptide synthetase (*NRPS*), cytochrome p450 (*P450*), basic leucine zipper (*BZIP*), and halogenase (*HAL*) may be key genes of the OTA synthesis gene cluster in *Aspergillus niger* (Karolewiez and Geisen, 2005; O'Callaghan et al., 2003; Pel et al., 2007).

Previous studies (Zhang et al., 2016; Zhao et al., 2021) have shown that OTA-producing fungi in dark tea are characterized by various fungal species and high detection frequencies; however, the detection rate and content of OTA in dark tea samples were lower than expected. This may be due to the ability of tea polyphenols (TPs) to inhibit the production of OTA by OTA-producing fungi. Many studies have shown that TPs can inhibit fungal production of mycotoxins (Mo et al., 2013; Wu Q., 2013; Li et al., 2015).

In this study, we used a rapid high-performance liquid chromatography (HPLC)-based assay to detect OTA in dark tea samples from different years obtained from six different regions of China. The OTA contamination levels of dark tea obtained in this study and the consumer data on dark tea consumption across the country were used to assess the risk of dark tea consumption. In addition, 12 *Aspergillus* spp. strains were isolated from tea samples containing OTA, and one strain of *Aspergillus niger* had the ability to produce OTA. We also investigated the inhibitory effects of different concentrations of TPs and epigallocatechin gallate (EGCG) on the growth of OTA-producing *Aspergillus niger* (AN3) isolated from tea samples containing OTA, and the mechanism of inhibition of their toxin production by TPs and EGCG.

Materials and methods

Materials and reagents

Kang brick tea from Sichuan, Fu brick tea from Hunan and Shaanxi, Ripe Pu-erh tea from Yunnan, Qing brick tea from Hubei, and Liu Bao tea from Guangxi (Figure 1), with 228 samples of different vintage dark tea that were randomly purchased from tea markets, tea retail outlets, and online shops (March 2021–September 2021). The samples were stored in a clean and air-ventilated environment prior to the analysis.

Ochratoxin α (OTα), OTA, and ochratoxin B (OTB) were purchased from Pribolab Pte Ltd. (Qingdao, China). TPs and EGCG were purchased from Hunan Sunfull Bio-tech Co., Ltd. (Changsha, China). Chromatographic-grade methanol, acetonitrile, and glacial acetic acid were provided by Chengdu Kelong Co. Ltd. (Chengdu, China).

Sample preparation and HPLC system and operating conditions

The tea sample was prepared by extracting 1.0 g of crushed dark tea with 10.0 ml of a methanol-formic acid (25:1 v/v) solution. The solution was mixed using a stirrer for 2 min and further extracted using ultrasonic bathing for 10 min. It was then centrifuged at 4,000 rpm for 10 min, the supernatant was filtered through filter paper, and the volume was fixed to 4.0 ml. The filtrate was filtered through a 0.45 μm organic filter membrane before HPLC analysis.

The filtrate was measured on an Agilent 1260Infinity II (Agilent Technologies Co. Ltd., Palo Alto, CA, United States) HPLC system equipped with a fluorescence detector.

For HPLC analysis of dark tea, OTA was separated using a C_{18} column (5 μm, 250 × 4.6 mm; Phenomenex, Torrance, CA, United States). Separation was performed at 30°C, and the injection volume was 10.0 μl. The mobile phase was composed of water-glacial acetic acid(98:2 v/v; phase A) and acetonitrile (phase B), and gradient elution was as follows: 0–10 min, 88–80% A, 12–20% B; 10–12 min, 80–70% A, 20–30% B; 12–19 min, 70–50% A, 30–50% B; 19–31 min, 50–0% A, 50–100% B; 31–40 min, 0–88% A, 100–12% B; 40–45 min, 88% A, 12% B.

For the HPLC analysis of the liquid culture, OTα, OTA, and OTB were separated using a Pribolab ODS C_{18} column (2.5 μm, 150 × 4.6 mm), water-glacial acetic acid (98:2 v/v; phase A) and acetonitrile (phase B), and isocratic elution (50:50).

Method validation

Recovery rates were evaluated by adding three concentrations (5, 10, and 20 μg·kg^{-1}) of OTA to non-toxic tea samples. Recovery was determined by comparing the average peak areas of the spiked samples with those of the standard solutions. Linearity was calculated by peak areas and concentrations of the OTA standard (1, 5, 10, 20,

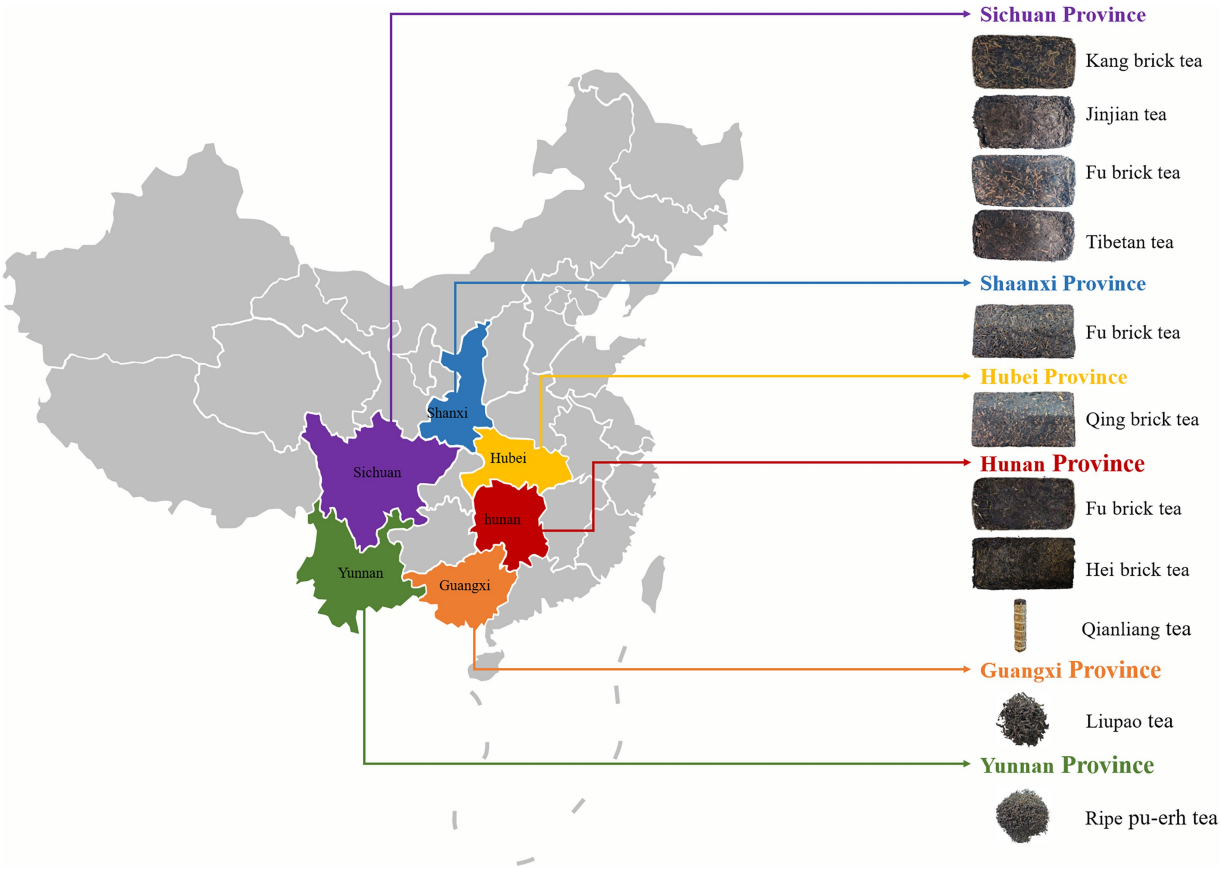

FIGURE 1
The samples of dark tea.

and 30 μg·L^{-1}) using HPLC. The limit of detection (LOD) and limit of quantification (LOQ) were determined by analyzing the lowest OTA in the tea samples. The LOD and LOQ were calculated based on a signal-to-noise ratio (S/N) of three (3:1) and 10 times (10:1) the background chromatographic noise, respectively.

Tea consumption questionnaire

Tea consumption data were obtained through a questionnaire with a total of 446 participants, who were selected randomly from Sichuan, Chongqing, Hunan, Guangdong, Yunnan, and Inner Mongolia. The participants were questioned about their sex, age, weight, city, brewing volume, and proportion of drinking volume to brewing volume.

Health risk assessment

Deterministic risk assessment

The dietary risk of mycotoxin exposure from drinking dark tea was assessed based on contamination levels and consumption data. The health neoplastic risk of OTA was assessed based on the HQ (IARC, 1993). A HQ value of <1.0 indicates that the population is not at risk of exposure (WHO, 2005; EFSA, 2013). The average daily intake of ADD (μg·kg^{-1}·day^{-1}) and the HQ values were calculated using the following equations:

$$ADD = C * CA/BW$$

$$HQ = ADD/RfD$$

Here, C is the average mycotoxin concentration in dark tea (μg·kg^{-1}), CA is the amount of dark tea consumed (g·person^{-1}·day^{-1}), BW is the average body weight of the population (kg), ADD is the average daily intake of OTA, and RfD is the provisional maximum tolerable daily intake (PMTDI) suggested by the World Health Organization (WHO).

For the risk assessment, average and heavy tea consumers (95% of tea consumers) were evaluated. We used 0 (lower limit), 1/2 LOD (middle limit), and LOD (upper limit; GEMS/Food-EURO, 1995) as the three possible scenarios for the risk assessment. In addition, we explored extreme exposure scenarios, that is, the mean and maximum OTA contamination values of all tea samples contained in this study for neoplastic risk assessment.

Probabilistic risk estimation

Deterministic risk assessment methods ignore the variability and uncertainty of data and fail to reflect the differences among individuals. Probabilistic risk assessment compensates for the shortcomings of deterministic risk assessment by quantifying variability and uncertainty and is now the main tool for dietary exposure assessment. Probabilistic assessment requires assessment of all risk factors in the population, such as data on the body weight of all individuals in the assessment population, assessment of tea consumption data, and data on the OTA content of the tea. Therefore, a large data resource is necessary to carry out accurate probabilistic assessments. The variability of exposure factors (i.e., OTA contamination, body weight, and tea consumption) was assessed for each assessment group through Monte Carlo simulations using the Crystal Ball (*Version 11.2*) software to determine the best-fit distribution. Sensitivity analyses were performed using the Crystal Ball software to assess the contribution of each exposure factor to neoplastic risk. A total of 10,000 iterations were performed using the Monte Carlo simulation. The lower, middle, and upper limits as well as the average and maximum (extreme case) contamination exposures were determined separately.

Isolation of fungal strains in tea samples containing OTA

Fungal strains in tea samples containing OTA from six regions (Sichuan, Hunan, Yunnan, Shaanxi, Guangxi, and Hubei) were isolated. The toxin-producing abilities of the isolated fungal strains were analyzed, and those with toxin-producing abilities were identified by phylogenetic analysis of partial β-tubulin (*BenA*; *Bt2a*:GGTAACCAAATCGGTGCTGCTTTC, *Bt2b*:ACCCTCAGTGTAGTGACCCTTGGC), partial calmodulin (CaM; *CF1L*:GCCGACTCTTTGACYGARGAR, *CF1M*:AGGCCGAYTCTYTGACYGA, *CF4*:TTTYTGCATCATRAGYTGGAC), and RNA polymerase beta gene (*RPB2*; *fRPB2-5F*:GAYGAYMGWGATCAYTTYGG, *fRPB2-7cR*:CCCATRGCTTGYTTRCCCAT), which were then used in subsequent experiments.

Inhibition of TPs and EGCG on *Aspergillus niger* AN3

Growth inhibition

Tea polyphenols and EGCG were added to CYB medium separately so that the concentrations of TPs and EGCG in the medium were 0, 10, 25, 50, and 75 mg/ml. After incubation at 28°C for 7 days, the growth of *A. niger* AN3 was observed.

Inhibition of the mechanism of toxicity production

The cultures were expanded at 50 mg/ml concentrations of TPs and EGCG for 3 and 7 days, respectively, and then detected for OTα, OTA, and OTB in the culture broth. RNA of *A. niger* AN3 was extracted, reverse-transcribed, and subjected to RT-PCR.

The relative expression levels of *PKS*, *NRPS*, *P450*, *BZIP*, and *HAL*, the key genes for OTA synthesis in *A. niger* AN3 under TPs and EGCG treatment conditions, were measured, and the β-tubulin gene was used as an internal reference for normalization of gene expression.

DNA extraction and RNA preparation

DNA of *A. niger* AN3 was extracted using the Fungi Genomic DNA Extraction Kit (D2300, Solarbio, Co., Ltd., China) according to the manufacturer's instructions. The total DNA was eluted in 100 μl of elution buffer. To measure the expression of *PKS*, *NRPS*, *P450*, *BZIP*, and *HAL*, total RNA was extracted by Total RNA Extraction Kit (Solarbio, Co., Ltd., China). RNA was reverse-transcribed using FastKing RT-qPCR Kit (Tiangen Biotech Co., Ltd., Beijing, China). All the primers for PCR and qPCR were designed by Sangon Biotech Co., Ltd. (Shanghai, China).

Statistical analysis

All experiments were performed with three replicates. The variability of exposure factors, sensitivity, and the Monte Carlo simulation were performed using the Crystal Ball Version 11.2 (Oracle Corp., Redwood, CA, United States). The significant differences based on one-way analysis followed by the Duncan's Multiple Range Test were performed using SPSS Statistics Version 25.0 (IBM Corp., Armonk, NY, United States).

Results

Method validation

Chromatograms of OTA in dark tea sample are shown in Figure 2B. The determination coefficient was $R^2 > 0.9991$, and the regression equation (OTA concentration = $6.53 \times 10^{-2} \times$ peak area-0.0369) showed suitable linearity from 1 to 30 ng/ml. LOD and LOQ of OTA using the current method were 0.39 and 1.30 μg/kg, respectively. Under the different spiked concentrations, the recoveries by the method used in this study ranged from 78.8 ± 1.3 to 103.6 ± 9.4%. It is shown that the present method was suitable for fermented tea sample determination.

OTA concentration in dark tea

A total of 228 dark tea samples from six regions (Figure 2A) were tested (Supplementary Table S1), and 21 samples contained OTA, as shown in Table 1; the occurrence of OTA was 9.2% (21/228), with concentrations ranging from 2.51 ± 0.16 to 12.62 ± 0.72 μg/kg.

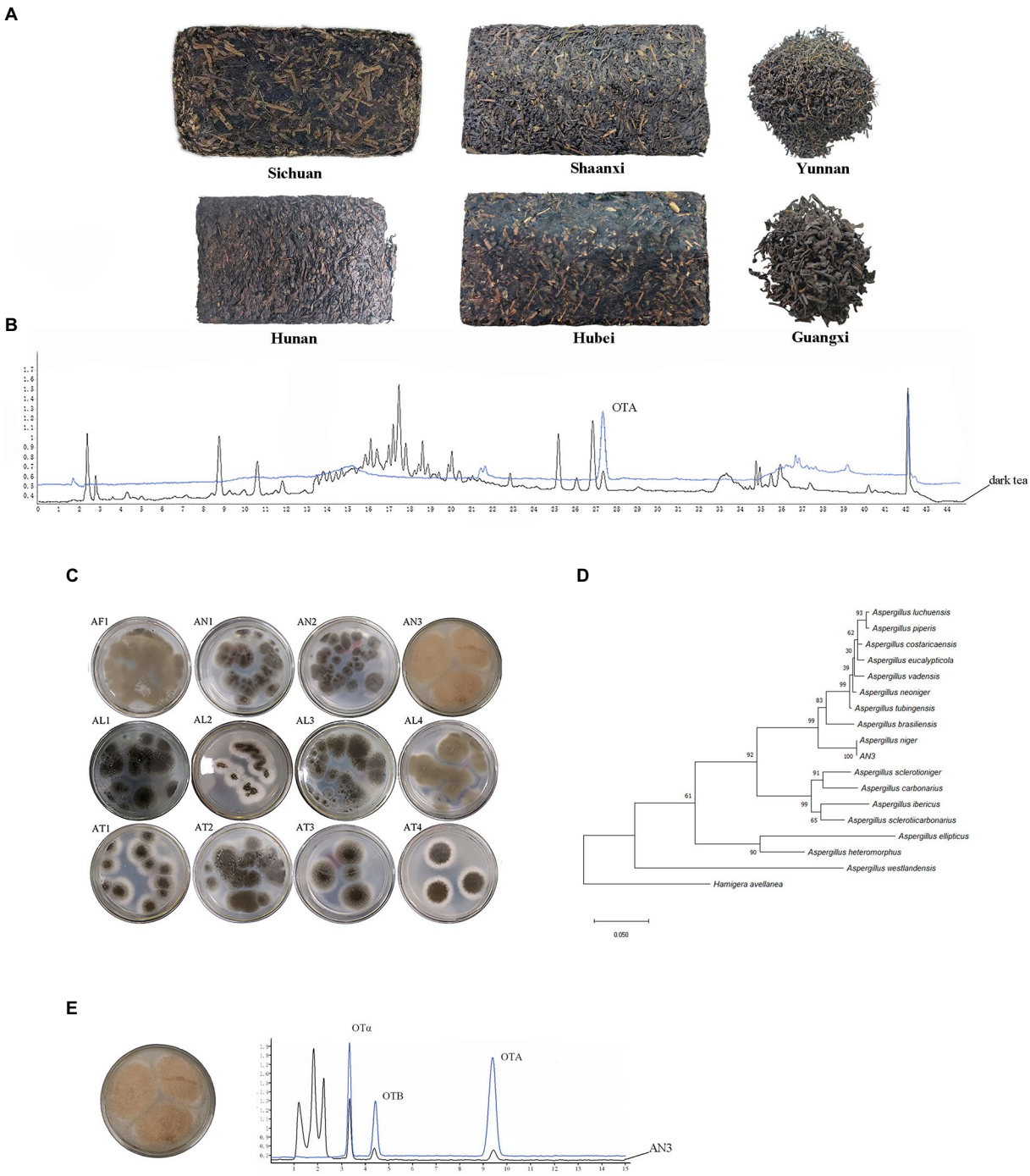

FIGURE 2
OTA detection in dark tea samples and isolation of OTA-producing fungal strains. **(A)** Tea samples from six different regions. **(B)** Chromatograms of OTA in dark tea sample. **(C)** *Aspergillus* fungal strains isolated from tea samples containing OTA. **(D)** Phylogenetic tree of *A. niger* AN3 based on combined sequences of *BenA*, *CaM*, and *RPB2* gene. **(E)** OTA-producing fungi, *A. niger* AN3 and Chromatograms of OTA-producing fungi.

Dark tea consumption

A total of 236 males and 210 females participated in the questionnaire survey. We grouped consumers by gender and age into two groups for males and two groups for females and five age groups: <21 years, 21–30 years, 31–40 years, 41–50 years, and 50 years and above. The average total black tea consumption was 7.02 g per day. Weight and dark tea consumption data for each group are presented in Supplementary Table S2.

TABLE 1 OTA concentrations above LOQ of dark tea samples from different regions and years.

No.	Year	Region	Type	Concentration (μg/kg)
GX38	2016	Guangxi	Liupao tea	4.59 ± 3.02
HN2	2019	Hunan	Dark tea	9.75 ± 1.65
HB10	2000	Hunan	Dark tea	2.63 ± 0.67
HB13	2015	Hunan	Fu brick tea	6.80 ± 0.59
HN16	2014	Hunan	Tianjian tea	3.92 ± 0.49
HN17	2017	Hunan	Qing brick tea	2.79 ± 0.61
HN22	2018	Hunan	Fu brick tea	4.72 ± 0.24
HN24	2012	Hunan	Fu brick tea	2.76 ± 0.36
SC9	2014	Sichuan	Kang brick tea	4.61 ± 0.70
SC12	2016	Sichuan	Jinjian tea	5.38 ± 2.47
SC13	2016	Sichuan	Kang brick tea	9.83 ± 1.54
SC15	2018	Sichuan	Kang brick tea	7.60 ± 1.00
SC18	2014	Sichuan	Jinjian tea	5.75 ± 2.01
SC24	2017	Sichuan	Kang brick tea	3.90 ± 0.12
SC30	2015	Sichuan	Kang brick tea	4.55 ± 0.62
SC36	2017	Sichuan	Dark tea	7.74 ± 0.94
SC38	2021	Sichuan	Dark tea	5.36 ± 0.29
SC39	2021	Sichuan	Kang brick tea	12.62 ± 0.72
SC44	2021	Sichuan	Tibetan tea	5.61 ± 2.88
SX1	2018	Shannxi	Fu brick tea	3.52 ± 0.07
YN30	2020	Yunnan	Ripe Pu-erh tea	2.51 ± 0.16

Risk assessment

Deterministic risk assessment

The OTA deterministic risk assessment was based on OTA exposure contamination data from 228 dark tea samples and tea consumption data from 446 respondents obtained in this study. In the deterministic risk assessment, consumers with average and heavy tea consumption (95% tea consumption) were considered to have average and heavy OTA exposure, respectively. In addition, the mean of all tea samples containing OTA levels in this study and the maximum OTA contamination level was considered extreme cases for exposure assessment. The WHO PMTDI value for OTA is 0.0143 μg/kg b.w. (JECFA, 2002). The risk factor was calculated by comparing the exposure data with the WHO-recommended PMTDI values. The deterministic potential neoplastic risk was assessed based on the exposure calculations, and the detailed results are shown in Table 2.

The results of the deterministic risk assessment indicated that the maximal HQ values for lower bound (LB), middle bound (MB), and upper bound (UB) were 5.313×10^{-3}, 7.147×10^{-3}, and 8.980×10^{-3} for average-intake consumers (>50 age group), respectively. The maximal HQ values for LB, MB, and UB were 1.130×10^{-2}, 1.520×10^{-2}, and 1.910×10^{-2}, respectively, for heavy-intake consumers (31–40 years).

The maximal HQ values for all the groups were below 1.0, indicating no neoplastic risk. In the two extremes of exposure, the mean and maximal OTA levels in all tea samples containing OTA in this study, the maximal HQ values were 5.768×10^{-2} and 1.309×10^{-1}, respectively, both below 1.0, indicating no neoplastic risk.

Probabilistic risk assessment

Probabilistic estimation was performed using the OTA pollution exposure concentrations, tea consumption, and consumer weight. First, the best-fit distributions of the exposure factors for different scenarios were examined. As shown in Supplementary Table S3, the best-fit distributions for the OTA contamination concentrations under the LB, MB, and UB scenarios were all minimum extreme value distributions, the best-fit distribution for body weight was a gamma distribution, and the best-fit distribution for daily tea consumption was a maximum extreme value distribution. Probabilistic risks were estimated for each group and the results are presented in Table 2.

The results of the neoplastic risk assessment showed that the HQ values for LB, MB, and UB were 5.131×10^{-2}, 5.205×10^{-2}, and 5.285×10^{-2}, respectively, for heavy-intake consumers. The HQ values of 1.053×10^{-1} and 2.389×10^{-1} for heavy-intake consumers for the two extreme OTA exposure scenarios of average and maximum contamination concentrations, respectively, were also below 1.0, indicating no neoplastic risk. The results of deterministic and probabilistic risk assessments indicate that there was no OTA neoplastic risk from dark tea consumption. Sensitivity analysis showed that OTA contamination was the first key factor in the exposure assessment, with an R of 0.496 for the UB case and 0.472 for the UB case, with daily tea intake as the second influencing factor, as shown in Supplementary Table S4.

Isolation of OTA-producing fungi

A total of 12 *Aspergillus* fungal strains (Figure 2C) were isolated from tea samples containing OTA from six different regions of China (Sichuan, Hunan, Yunnan, Hubei, Shaanxi, and Guangxi). Only one strain (AN3) has the capacity to produce OTA. The maximum likelihood tree based on combined sequences of *BenA*, *CaM*, and *RPB2* gene (Figure 2D) showed that AN3 was closely related to *Aspergillus niger* (the partial *BenA*, *CaM*, and *RPB2* gene sequences were deposited in GenBank under accession numbers OP682803, OP682804, and OP682805, respectively). Therefore, the AN3 was identified as *Aspergillus niger*. The Chromatograms of OTA-producing fungi are shown in Figure 2E.

Inhibitory effects of TPs and EGCG on growth and toxicity production

The growth of *A. niger* AN3 after the addition of different concentrations of TPs and EGCG in the CYB medium for 7 days is shown in Figure 3. The inhibition of *A. niger* AN3 growth at low concentrations (0, 10, and 25 mg/ml) of TPs was not significant. The growth of *A. niger* AN3 was strongly inhibited at higher

TABLE 2 Deterministic and probabilistic risk assessments of OTA in dark tea.

Group	Average-intake consumers					Heavy-intake consumers				
	LB	MB	UB	AVE	MAX	LB	MB	UB	AVE	MAX
(A) Deterministic risk assessment of OTA in dark tea										
All	4.005×10^{-3}	5.387×10^{-3}	6.769×10^{-3}	4.348×10^{-2}	9.864×10^{-2}	1.142×10^{-2}	1.536×10^{-2}	1.930×10^{-2}	1.239×10^{-1}	2.812×10^{-1}
Male	$\mathbf{4.230\times10^{-3}}$	$\mathbf{5.690\times10^{-3}}$	$\mathbf{7.151\times10^{-3}}$	$\mathbf{4.593\times10^{-2}}$	$\mathbf{1.042\times10^{-1}}$	$\mathbf{2.035\times10^{-3}}$	$\mathbf{2.738\times10^{-3}}$	$\mathbf{3.441\times10^{-3}}$	$\mathbf{2.210\times10^{-2}}$	$\mathbf{5.014\times10^{-2}}$
Female	3.675×10^{-3}	4.944×10^{-3}	6.212×10^{-3}	3.990×10^{-2}	9.053×10^{-2}	1.322×10^{-2}	1.779×10^{-2}	2.235×10^{-2}	1.436×10^{-1}	3.257×10^{-1}
<21	1.426×10^{-3}	1.918×10^{-3}	2.410×10^{-3}	1.548×10^{-2}	3.512×10^{-2}	6.394×10^{-3}	8.601×10^{-3}	1.081×10^{-2}	6.942×10^{-2}	1.575×10^{-1}
21–30	2.586×10^{-3}	3.479×10^{-3}	4.371×10^{-3}	2.808×10^{-2}	6.370×10^{-2}	1.126×10^{-2}	1.515×10^{-2}	1.904×10^{-2}	1.223×10^{-1}	2.775×10^{-1}
31–40	4.566×10^{-3}	6.142×10^{-3}	7.718×10^{-3}	4.957×10^{-2}	1.125×10^{-1}	$\mathbf{1.130\times10^{-2}}$	$\mathbf{1.520\times10^{-2}}$	$\mathbf{1.910\times10^{-2}}$	$\mathbf{1.227\times10^{-1}}$	$\mathbf{2.783\times10^{-1}}$
41–50	5.044×10^{-3}	6.786×10^{-3}	8.527×10^{-3}	5.477×10^{-2}	1.243×10^{-1}	1.051×10^{-2}	1.414×10^{-2}	1.777×10^{-2}	1.141×10^{-1}	2.589×10^{-1}
>50	$\mathbf{5.313\times10^{-3}}$	$\mathbf{7.147\times10^{-3}}$	$\mathbf{8.980\times10^{-3}}$	$\mathbf{5.768\times10^{-2}}$	$\mathbf{1.309\times10^{-1}}$	1.108×10^{-2}	1.490×10^{-2}	1.873×10^{-2}	1.203×10^{-1}	2.729×10^{-1}
(B) Probabilistic risk assessment of OTA in dark tea										
all	2.106×10^{-2}	2.137×10^{-2}	2.169×10^{-2}	4.322×10^{-2}	9.805×10^{-2}	4.783×10^{-2}	4.853×10^{-2}	4.927×10^{-2}	9.815×10^{-2}	2.227×10^{-1}
male	$\mathbf{2.113\times10^{-2}}$	$\mathbf{2.143\times10^{-2}}$	$\mathbf{2.176\times10^{-2}}$	$\mathbf{4.335\times10^{-2}}$	$\mathbf{9.836\times10^{-2}}$	4.524×10^{-2}	4.589×10^{-2}	4.659×10^{-2}	9.282×10^{-2}	2.106×10^{-1}
female	2.043×10^{-2}	2.072×10^{-2}	2.104×10^{-2}	4.191×10^{-2}	9.509×10^{-2}	$\mathbf{4.902\times10^{-2}}$	$\mathbf{4.973\times10^{-2}}$	$\mathbf{5.049\times10^{-2}}$	$\mathbf{1.006\times10^{-1}}$	$\mathbf{2.282\times10^{-1}}$
<21	8.623×10^{-3}	8.748×10^{-3}	8.882×10^{-3}	1.769×10^{-2}	4.014×10^{-2}	2.864×10^{-2}	2.906×10^{-2}	2.950×10^{-2}	5.877×10^{-2}	1.333×10^{-1}
21–30	7.017×10^{-3}	7.119×10^{-3}	7.227×10^{-3}	1.440×10^{-2}	3.267×10^{-2}	2.001×10^{-2}	2.030×10^{-2}	2.061×10^{-2}	4.106×10^{-2}	9.315×10^{-2}
31–40	2.070×10^{-2}	2.101×10^{-2}	2.133×10^{-2}	4.249×10^{-2}	9.639×10^{-2}	4.944×10^{-2}	5.016×10^{-2}	5.092×10^{-2}	1.014×10^{-1}	2.302×10^{-1}
41–50	2.406×10^{-2}	2.441×10^{-2}	2.478×10^{-2}	4.937×10^{-2}	1.120×10^{-1}	4.821×10^{-2}	4.892×10^{-2}	4.966×10^{-2}	9.893×10^{-2}	2.245×10^{-1}
>50	$\mathbf{2.522\times10^{-2}}$	$\mathbf{2.559\times10^{-2}}$	$\mathbf{2.598\times10^{-2}}$	$\mathbf{5.176\times10^{-2}}$	$\mathbf{1.174\times10^{-1}}$	$\mathbf{5.131\times10^{-2}}$	$\mathbf{5.205\times10^{-2}}$	$\mathbf{5.285\times10^{-2}}$	$\mathbf{1.053\times10^{-1}}$	$\mathbf{2.389\times10^{-1}}$

Deterministic risk assessment of OTA in dark tea. Average-intake consumers: average tea consumption, heavy-intake consumers: 95th percentile of tea consumption. LB (lower bound) indicates that 0 was used as the contamination value for undetected samples in the risk assessment. MB (middle bound) indicates that the 1/2 LOD value of the corresponding study was used as the contamination value for undetected samples in the risk assessment. UB (upper bound) indicates that the LOD value of the corresponding study was used as the contamination value for undetected samples in the risk assessment. AVE, the average contamination value in this study, was selected as the contamination value for the extreme-case risk assessment. Max, the maximum contamination value in this study, was selected as the contamination value for terrible case risk assessment. Values with bold font are the maximal HQ to each comparison group.

concentrations of TPs (50 mg/ml), and it was inhibited almost completely at higher concentrations of TPs (75 mg/ml). The growth of *A. niger* AN3 was not significantly inhibited at low concentrations of EGCG (0, 10, and 25 mg/ml), whereas it was inhibited at higher concentrations of EGCG (50 and 75 mg/ml) but not completely, and *A. niger* AN3 was still able to grow at higher concentrations of EGCG.

The growth of *A. niger* AN3 was inhibited with increasing concentrations of TPs and EGCG. In the detection of OTA production, we found that no OTA was detected in *A. niger* AN3 under the treatment culture conditions with TPs and EGCG, both at low and high concentrations. After 3 and 7 days of incubation with the addition of TPs and EGCG, although *A. niger* AN3 was able to grow at lower concentrations, OTA production was not detected.

Mechanism of inhibition of toxicity production by TPs and EGCG

The concentrations of OTα, OTA, and OTB in the cultures after 3 and 7 days of incubation are presented in Table 3. We found no detectable production of OTA under either TPs or EGCG treatment. Under TPs treatment conditions, the OTα content at 7 days of culture was higher than that at 3 days of culture. However, we found that OTα levels were lower under TPs treatment than in the blank control, and no OTα production was detected under EGCG treatment. We speculated that this may be due to the inhibition of OTα production by TPs and EGCG through the inhibition of *A. niger* AN3 growth and its conversion to other substances, such as OTB and OTB ethyl ester.

Meanwhile, we observed that OTB levels at 7 days were higher than those at 3 days. However, unlike OTα, OTB levels were higher in the TPs treatment culture than in the blank control. This is probably due to the inhibition of OTα synthesis in favor of OTB. After EGCG treatment, OTα, OTA, and OTB were not detected. We speculated that EGCG may inhibit mycotoxin production by inhibiting their growth. We also found lower levels of OTA after 7 days incubation than after 3 days incubation, and Varga et al. (2000) suggested that *Aspergillus niger* may secrete enzymes to degrade OTA into other products, or in the case of nutrient deficiency, OTA is consumed as a supplementary nitrogen source.

The OTA synthesis pathway has not been completely resolved and only a few predicted pathways are available. The major OTA synthesis pathways postulated by Huff and Hamilton (1979) and Harris and Mantle (2001) are shown in Figure 3. We found a significant reduction ($p < 0.01$) in the relative expression of *NRPS* by real-time fluorescence quantification of genes critical for possible OTA synthesis in *A. niger* AN3. No OTA production was detected in any of the cultures, suggesting that TPs and EGCG inhibit the expression of *NRPS* and thus may suppress OTA toxin synthesis. Moreover, TPs and EGCG may inhibit the growth of *A. niger* AN3 through other pathways, thus suppressing OTA production.

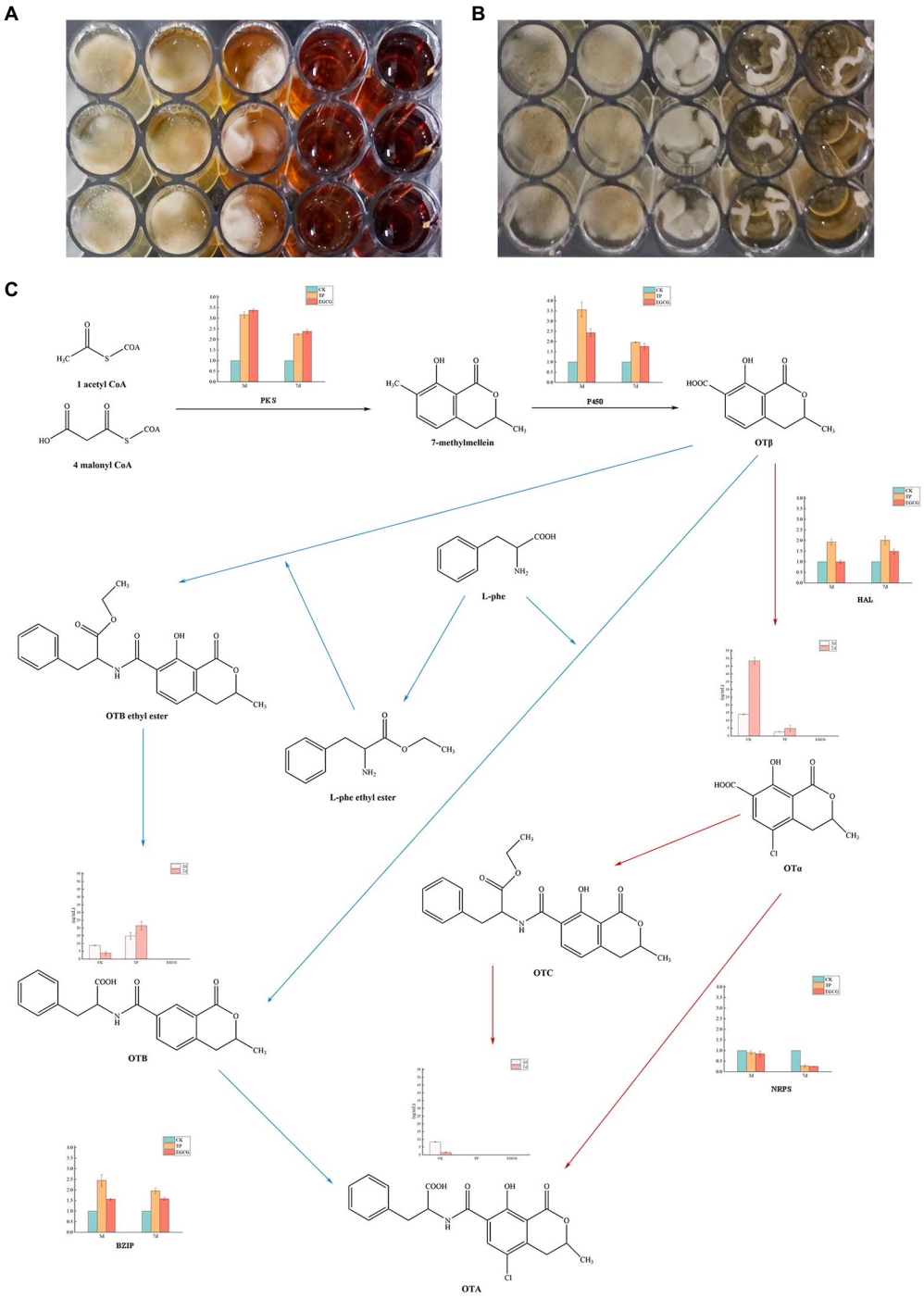

FIGURE 3
Inhibitory effects of TPs and EGCG on *Aspergillus niger*. **(A)** Growth of *A. niger* AN3 in medium containing TPs. **(B)** Growth of *A. niger* AN3 in medium containing EGCG. **(C)** OTA synthesis pathway and expression of OTA synthesis-related genes and concentrations of OTα, OTA, and OTB in *A. niger* AN3 (*BZIP*, a pathway-specific regulator that controls OTA production by regulating the *PKS*, *P450*, *HAL*, and *NRPS*).

Discussion

Mycotoxin contamination in dark tea has been a topical issue for researchers and consumers in recent years, whether it is the presence of mycotoxins in dark tea affects people's health or the residual mycotoxins having an impact on consumers' health. Many studies have suggested the possibility of mycotoxin contamination in dark tea; aflatoxins (Wu J., 2013; Cui et al., 2020), ochratoxins (Liu et al., 2016; Mo et al., 2016), vomitoxins (Liu et al., 2017; Hu et al., 2019), and citrinins (Li et al., 2020)

TABLE 3 Concentrations of OTα, OTA, and OTB after treatment with different concentrations of TPs and EGCG.

Treatment	Concentrations (mg/ml)	OTα (ng/ml)	OTB (ng/ml)	OTA (ng/ml)
CK	/	48.54 ± 2.09	3.81 ± 1.21	1.55 ± 0.34
tea polyphenols	10	19.58 ± 1.40	13.44 ± 0.93	ND
	25	19.68 ± 1.32	2.94 ± 0.97	ND
	50	15.78 ± 0.67	ND	ND
	75	29.14 ± 2.16	ND	ND
EGCG	10	94.76 ± 2.57	4.75 ± 0.17	ND
	25	15.15 ± 7.89	2.60 ± 0.67	ND
	50	ND	ND	ND
	75	ND	ND	ND

CK represents a blank control without added tea polyphenols and EGCG.

have been detected in dark tea samples. In contrast to other studies, 228 dark tea samples from different regions and years were investigated, demonstrating a wide and better representative origin, and 9.2% of the samples contained OTA. Haas et al. (2013) investigated 36 Ripe Pu-erh tea samples, and OTA was detected in four samples at concentrations of 0.65, 0.65, 14.8, and 94.7 μg/kg, with a detection rate of 11%. Mo et al. (2016) conducted a survey of 100 tea samples and four samples with OTA concentrations ranging from 0.22 to 0.44 μg/kg. Liu et al. (2016) surveyed 25 fermented tea samples, and one Hunan Fu brick tea sample was found to be contaminated by OTA at 4.2 μg/kg. Liu et al. analyzed 61 dark tea samples (Liu et al., 2017) using Quick Easy Cheap Effective Rugged Safe-ultra-high-performance liquid chromatography–tandem mass spectrometry and OTA was detected in five samples, including two samples of Ripe Pu-erh tea (6.7 and 2.5 μg/kg), one sample of Hunan dark tea (4.0 μg/kg), and two samples of Guangxi Liu Bao tea (0.9 and 1.3 μg/kg). Another more comprehensive survey involving 108 dark tea samples was conducted by Ye et al. (2020), which showed that five samples were contaminated by OTA with an average concentration of 0.66 μg/kg and a maximum concentration of 36.4 μg/kg. The presence of OTA in these dark tea samples could be attributed to two reasons. First, the dark tea may have been infested with exogenous ochratoxigenic fungi during the fermentation process. Second, some of the dark tea samples were stored for a long period or under unfavorable environmental conditions during the storage process, which contributed to the OTA contamination of dark tea.

There are some differences between the results of this study and those of others, which may be due to differences in the source of the samples or the detection methods. Combined with the above findings, it can be inferred that dark tea can be contaminated by OTA, which poses a potential health hazard to consumers. Therefore, it is expected that more researchers will conduct assessments on OTA contamination in dark tea.

Despite the risk of mycotoxin contamination in dark tea, studies by Cui et al. (2020), Ye et al. (2020), and Yan et al. (2021) show that the consumption of dark tea does not pose a significant health risk to consumers. Yan et al. (2021) assessed neoplastic risk based on the results of the Malir study (OTA level of 250 μg/kg; Malir et al., 2014), and only consumers with moderate and heavy tea consumption had maximal HQ values close to 1 or ≥1, indicating a potential neoplastic risk. However, the results of the study used a very extreme scenario. With the exception of Malir's findings (Malir et al., 2014), other researchers have reported OTA exposure values well below 250 μg/kg. The results of this study are similar to those of other researchers, which also showed that OTA exposure from dark tea consumption posed no health risks to the population. However, there are limitations to the dark tea sample and consumer tea consumption data in this study. It is expected that more researchers will focus on mycotoxins in dark tea in the future to obtain better and more accurate results.

Some studies show that TPs have a significant inhibitory effect on aflatoxin synthesis (Mo et al., 2013; Wu Q., 2013), and the presence of antioxidants also inhibits the synthesis of aflatoxin B_1 (Zhao, 2014). Zhang (2014) suggested that quercetin, a polyphenol in tea leaves, is an active factor in inhibiting the growth and toxicity of *Aspergillus flavus*, and that this substance induces downregulation of the expression of *AflS* and *AflR* by activating the antioxidant system transcription factor *Yap1*. Few studies have been conducted on the inhibition of OTA production by bioactive components. The results of Jiang et al. (2022) show that five genes in the OTA biosynthesis gene cluster, in particular the global regulator *LaeA* that regulates OTA biosynthesis, was markedly downregulated by eugenol. In this study, the evaluation of the inhibitory ability of TPs and EGCG at different concentrations in a co-cultivation system with *A. niger* AN3 showed that TPs and EGCG have significant inhibitory effects on *A. niger* AN3 under liquid culture conditions. *A. niger* AN3 was able to grow at lower concentrations but without OTA production, which prompted us to question whether TPs and EGCG inhibited the expression of key genes related to OTA synthesis in *A. niger* AN3. Further studies revealed that TPs and EGCG may have inhibited the production of OTA by *A. niger* AN3 by suppressing the expression of *NRPS*, a key gene for OTA synthesis. In this study, TPs and EGCG were found to inhibit *NRPS* expression in *A. niger* AN3; however, the principle of inhibition has not yet been identified, and further studies are required. Further research on the inhibition of OTA synthesis by biologically active ingredients is expected. Effective methods to control OTA contamination in tea include preventing toxin production and degrading pre-existing fungal toxins. Strictly regulated management during tea production and processing is the best way to prevent OTA contamination; however, if contamination has already occurred, appropriate methods need to be employed to remove it or reduce its toxicity. The results of this study indicate that TPs and EGCG can inhibit the growth and toxicity of *A. niger* AN3, providing new insights and ideas for the prevention of OTA contamination.

Conclusion

In recent years, dark tea consumption has gradually increased. However, the contamination of dark tea with mycotoxins has received considerable attention from consumers and researchers. In this study, a rapid HPLC method using OTA was used to determine mycotoxins in dark tea with superior sensitivity and satisfactory recovery. A validated method was used to determine the contamination levels of OTA in 228 Chinese dark teas, and the proportion of tea samples containing OTA was 9.2%. The results of the deterministic and probabilistic risk assessments indicated that there was no neoplastic risk to human health from OTA exposure due to dark tea consumption. No consumption risk was observed for Chinese dark tea, and the results are important for consumers in countries that enjoy Chinese dark tea. Furthermore, 12 *Aspergillus* spp. strains were isolated from tea samples containing OTA, where only one strain of *A. niger* had the ability to produce OTA. The inhibitory effects of TPs and EGCG on growth and OTA production may provide new ideas for the detoxification of ochratoxins, but the most effective way to avoid OTA contamination of dark tea is to avoid the infestation of harmful microorganisms at the source during production, processing, and storage.

Data availability statement

The data presented in the study are deposited in the https://www.ncbi.nlm.nih.gov/ repository, accession number: OP682803, OP682804, and OP682805.

Author contributions

Y-qZ: conceptualization, methodology, formal analysis, and writing of the original draft. W-bJ: software investigation. S-yL and LX: software and validation. WC: methodology and validation. YZ and M-ZZ: writing—review and editing. WX: conceptualization, methodology, formal analysis, writing—review and editing, and funding acquisition. All authors contributed to the article and approved the submitted version.

Funding

This work was supported by the National Key R&D Program of China (2019YFC0840503), Sichuan Province S&T Project (2021ZHFP0021), and Sichuan Agricultural University I&T Program (202210626034), Natural Science Foundation of China (32002095 and 32172217), Hunan "Three Top" Innovative Talents Project (2022RC1142), Natural Science Foundation of Hunan Province for Outstanding Young Scholars (2022JJ20028), and Changsha City Outstanding Innovative Youth Training Program (kq2107015).

Conflict of interest

The authors declare that the research was conducted in the absence of any commercial or financial relationships that could be construed as a potential conflict of interest.

Publisher's note

All claims expressed in this article are solely those of the authors and do not necessarily represent those of their affiliated organizations, or those of the publisher, the editors and the reviewers. Any product that may be evaluated in this article, or claim that may be made by its manufacturer, is not guaranteed or endorsed by the publisher.

Supplementary material

The Supplementary material for this article can be found online at: https://www.frontiersin.org/articles/10.3389/fmicb.2022.1073950/full#supplementary-material

References

Chen, W., Li, C., Zhang, B., Zhou, Z., Shen, Y., Liao, X., et al. (2018). Advances in biodetoxification of ochratoxin a-a review of the past five decades. *Front. Microbiol.* 9:1386. doi: 10.3389/fmicb.2018.01386

Cui, P., Yan, H., Granato, D., Ho, C., Ye, Z., Wang, Y., et al. (2020). Quantitative analysis and dietary risk assessment of aflatoxins in chinese post-fermented dark tea. *Food Chem. Toxicol.* 146:111830. doi: 10.1016/j.fct.2020.111830

Deng, X., Tu, Q., Wu, X., Huang, G., Shi, H., Li, Y., et al. (2020). Research progress on the safety risk of ochratoxin a in tea. *Sci. Technol. Food Ind.* 42, 405–412. doi: 10.13386/j.issn1002-0306.2020070080

Duarte, S. C., Pena, A., and Lino, C. M. (2010). A review on ochratoxin a occurrence and effects of processing of cereal and cereal derived food products. *Food Microbiol.* 27, 187–198. doi: 10.1016/j.fm.2009.11.016

EFSA (2013). Scientific opinion on risks for animal and public health related to the presence of nivalenol in food and feed. *EFSA J.* 11:3262. doi: 10.2903/j.efsa.2013.3262

GEMS/Food-EURO (1995). Second workshop on reliable evaluation of low-level contamination of food, 26–27

Haas, D., Pfeifer, B., Reiterich, C., Partenheimer, R., Reck, B., and Buzina, W. (2013). Identification and quantification of fungi and mycotoxins from pu-erh tea. *Int. J. Food Microbiol.* 166, 316–322. doi: 10.1016/j.ijfoodmicro.2013.07.024

Harris, J. P., and Mantle, P. G. (2001). Biosynthesis of ochratoxins by aspergillus ochraceus. *Phytochemistry* 58, 709–716. doi: 10.1016/S0031-9422(01)00316-8

Hu, L., Shi, Z., Zhao, L., Liu, X., Dong, Y., Jiang, M., et al. (2019). Simultaneous detection and analysis of 16 kinds of mycotoxins in pu-erh tea. *Acta Agric. Zhejiang.* 31, 1700–1708. doi: 10.3969/j.issn.1004-1524.2019.10.16

Huff, W. E., and Hamilton, P. B. (1979). Mycotoxins - their biosynthesis in fungi: ochratoxins - metabolites of combined pathways. *J. Food Prot.* 42, 815–820. doi: 10.4315/0362-028X-42.10.815

IARC (1993). "Monographs on the evaluation of carcinogenic risks to humans," in *Some Naturally Occurring Substances: Food Items and Constituents, Heterocyclic Aromatic Amines and Mycotoxins*, vol. *56* (World Health Organization: Lyon, France).

Iqbal, S. Z., Nisar, S., Asi, M. R., and Jinap, S. (2014). Natural incidence of aflatoxins, ochratoxin a and zearalenone in chicken meat and eggs. *Food Control* 43, 98–103. doi: 10.1016/j.foodcont.2014.02.046

JECFA (2002). 56 st report of jecfa-evaluation of certain mycotoxins in food. Geneva: World Health Organization.

Jiang, N., Wang, L., Jiang, D., Wang, M., Liu, H., Yu, H., et al. (2022). Transcriptomic analysis of inhibition by eugenol of ochratoxin a biosynthesis and growth of aspergillus carbonarius. *Food Control* 135:108788. doi: 10.1016/j.foodcont.2021.108788

Karolewiez, A., and Geisen, R. (2005). Cloning a part of the ochratoxin a biosynthetic gene cluster of *penicillium nordicum* and characterization of the ochratoxin polyketide synthase gene. *Syst. Appl. Microbiol.* 28, 588–595. doi: 10.1016/j.syapm.2005.03.008

Kumar, P., Mahato, D. K., Sharma, B., Borah, R., Haque, S., Mahmud, M. M. C., et al. (2020). Ochratoxins in food and feed: occurrence and its impact on human health and management strategies. *Toxicon* 187, 151–162. doi: 10.1016/j.toxicon.2020.08.031

Li, Z., Mao, Y., Teng, J., Xia, N., Huang, L., Wei, B., et al. (2020). Evaluation of mycoflora and citrinin occurrence in chinese liupao tea. *J. Agric. Food Chem.* 68, 12116–12123. doi: 10.1021/acs.jafc.0c04522

Li, H., Tan, Y., Chen, Z., Qu, J., Chen, Y., and Fang, X. (2015). Effect of Yunnan large-leaf *camellia sinensis* extract on growth and aflatoxin production of *aspergillus flavus*. *Mod. Food Sci. Technol.* 31, 101–106. doi: 10.13982/j.mfst.1673-9078.2015.11.017

Liu, Y., Chen, J., Tan, G., Liu, Z., and Li, X. (2017). Determination of ten mycotoxins in fermented dark tea by quechers-ultra-high-performance liquid chromatography-tandem mass spectrometry. *Mod. Food Sci. Technol.* 33, 280–288. doi: 10.13982/j.mfst.1673-9078.2017.7.039

Liu, Y., Tan, G., Liu, Z., Li, X., and Chen, J. (2016). Determination of various mycotoxins in fermented tea by ultra-high performance liquid chromatography-tandem mass spectrometry. *Mod. Food Sci. Technol.* 32, 322–327. doi: 10.13982/j.mfst.1673-9078.2016.8.049

Malir, F., Ostry, V., Pfohl-Leszkowicz, A., Toman, J., Bazin, I., and Roubal, T. (2014). Transfer of ochratoxin a into tea and coffee beverages. *Toxins* 6, 3438–3453. doi: 10.3390/toxins6123438

Mo, J., Gong, Q., Zhou, H., Bai, X., Tan, J., Peng, Z., et al. (2016). Determination of ochratoxin a in tea by high performance liquid chromatography-tandem mass spectrometry. *J. Food Saf. Qual.* 7, 182–187. doi: 10.19812/j.cnki.jfsq11-5956/ts.2016.01.037

Mo, H. Z., Zhang, H., Wu, Q. H., and Hu, L. B. (2013). Inhibitory effects of tea extract on aflatoxin production by aspergillus flavus. *Lett. Appl. Microbiol.* 56, 462–466. doi: 10.1111/lam.12073

O'Callaghan, J., Caddick, M. X., and Dobson, A. D. W. (2003). A polyketide synthase gene required for ochratoxin a biosynthesis in *aspergillus ochraceus*. *Microbiology* 149, 3485–3491. doi: 10.1099/mic.0.26619-0

Ou, H. (2017). Isolation and identification of microbial from liupao tea and study on the influence of superiority strains of tea compounds. Master's thesis. Guang Zhou, South China Agricultural University.

Pel, H. J., de Winde, J. H., Archer, D. B., Dyer, P. S., Hofmann, G., Schaap, P. J., et al. (2007). Genome sequencing and analysis of the versatile cell factory *aspergillus Niger* cbs 513.88. *Nat. Biotechnol.* 25, 221–231. doi: 10.1038/nbt1282

Sánchez-Hervás, M., Gil, J. V., Bisbal, F., Ramón, D., and Martínez-Culebras, P. V. (2008). Mycobiota and mycotoxin producing fungi from cocoa beans. *Int. J. Food Microbiol.* 125, 336–340. doi: 10.1016/j.ijfoodmicro.2008.04.021

Varga, J., Rigó, K., and Téren, J. (2000). Degradation of ochratoxin a by *aspergillus* species. *Int. J. Food Microbiol.* 59, 1–7. doi: 10.1016/S0168-1605(00)00230-0

Wang, Z., Shi, Z., Liu, Z., Huang, J., and Wen, Q. (1991). On the mechanism of fu brick tea quality and flavour formation. *J. Tea Sci.* 11, 49–55.

Wang, Y., Wang, L., Liu, F., Wang, Q., Selvaraj, J., Xing, F., et al. (2016). Ochratoxin a producing fungi, biosynthetic pathway and regulatory mechanisms. *Toxins* 8:83. doi: 10.3390/toxins8030083

Wang, Y., Wang, L., Wu, F., Liu, F., Wang, Q., Zhang, X., et al. (2018). A consensus ochratoxin a biosynthetic pathway: insights from the genome sequence of *aspergillus ochraceus* and a comparative genomic analysis. *Appl. Environ. Microbiol.* 84, e1009–e1018. doi: 10.1128/AEM.01009-18

Wang, R., Xiao, M., Li, D., Ling, T., and Xie, Z. (2018). Recent advance on quality characteristics and health effects of dark tea. *J. Tea Sci.* 38, 113–124.

WHO (2005). Total diet studies: a recipe for safer food

Wu, J. (2013). Study on pu'er tea quality formation and state of mycotoxins during the aging process. Master's thesis. Nan Chang, Nan Chang University.

Wu, Q. (2013). Study on components of inhibiting production of aflatoxin in tea and related characteristic. Master's thesis. Yang Ling, Northwest A & F University.

Xiong, Y. (2017). Study on microbial diversity of Sichuan dark tea during post-fermentation and airborne microbial in fermentation workshop. Master Master's thesis. Ya An, Sichuan Agricultural University.

Yan, H., Zhang, L., Ye, Z., Wu, A., Yu, D., Wu, Y., et al. (2021). Determination and comprehensive risk assessment of dietary exposure to ochratoxin a on fermented teas. *J. Agric. Food Chem.* 69, 12021–12029. doi: 10.1021/acs.jafc.1c04824

Ye, Z., Wang, X., Fu, R., Yan, H., Han, S., Gerelt, K., et al. (2020). Determination of six groups of mycotoxins in chinese dark tea and the associated risk assessment. *Environ. Pollut.* 261:114180. doi: 10.1016/j.envpol.2020.114180

Zhang, H. (2014). Polyphenols changes in tea fermentation and the inhibitory effect on aflatoxin production. Doctor Master's thesis. Yang Ling, Northwest A&F University.

Zhang, Y., Skaar, I., Sulyok, M., Liu, X., Rao, M., and Taylor, J. W. (2016). The microbiome and metabolites in fermented pu-erh tea as revealed by high-throughput sequencing and quantitative multiplex metabolite analysis. *PLoS One* 11:e157847. doi: 10.1371/journal.pone.0157847

Zhao, X. (2014). Mechanistic study on the inhibition of aflatoxin biosynthesis by gallic acid based on rna-seq data, 249.

Zhao, Z., Lou, Y., Shui, Y., Zhang, J., Hu, X., Zhang, L., et al. (2021). Ochratoxigenic fungi in post-fermented tea and inhibitory activities of *bacillus* spp. from post-fermented tea on ochratoxigenic fungi. *Food Control* 126:108050. doi: 10.1016/j.foodcont.2021.108050

Zhou, C., Chen, W., Wu, Z., Zhang, M., Guan, J., Li, T., et al. (2015). Research on identification, function and safety of *aspergillus Niger*, apreponderant fungus during the fermentative process of pu'er tea. *J. Food Saf. Qual.* 6, 1006–1010. doi: 10.19812/j.cnki.jfsq11-5956/ts.2015.03.048

frontiers | Frontiers in Microbiology

TYPE Original Research
PUBLISHED 20 December 2022
DOI 10.3389/fmicb.2022.1100889

OPEN ACCESS

EDITED BY
Zhihong Sun,
Inner Mongolia Agricultural University, China

REVIEWED BY
Chunsheng Li,
South China Sea Fisheries Research Institute (CAFS), China
İsmail Akyol,
Ankara University, Turkey

*CORRESPONDENCE
Jianxin Sui
✉ suijianxin@ouc.edu.cn

†These authors have contributed equally to this work and share first authorship

SPECIALTY SECTION
This article was submitted to Food Microbiology, a section of the journal Frontiers in Microbiology

RECEIVED 17 November 2022
ACCEPTED 05 December 2022
PUBLISHED 20 December 2022

CITATION
Liu C, Wang G, Han X, Cao L, Wang K, Lin H and Sui J (2022) Heterologous expression and activity verification of ornithine decarboxylase from a wild strain of *Shewanella xiamenensis*. *Front. Microbiol.* 13:1100889. doi: 10.3389/fmicb.2022.1100889

Heterologous expression and activity verification of ornithine decarboxylase from a wild strain of *Shewanella xiamenensis*

Chang Liu†, Guiyuan Wang†, Xiangning Han, Limin Cao, Kaiqiang Wang, Hong Lin and Jianxin Sui*

College of Food Science and Engineering, Ocean University of China, Qingdao, Shandong, China

Shewanella xiamenensis is widely found in spoilage fish, shrimp and other seafoods. Under suitable conditions, ornithine can be synthesized into putrescine, which may spoil food or endanger health. Our research used a wild strain of *Shewanella xiamenensis* isolated from "Yi Lu Xian" salted fish (a salting method for sea bass) as a research object. According to the database of National Center of Biotechnology Information (NCBI), the target ornithine decarboxylase (ODC) gene SpeF was successfully amplified using the wild strain of *Shewanella xiamenensis* as the template. Sequencing alignment showed that the SpeF of the wild strain had more than 98% homology compared with the standard strain. The amino acid substitution occurred in the residues of 343, 618, 705, and 708 in the wild strain. After optimizing the expression conditions, a heterologous expression system of ODC was constructed to achieve a high yield of expression. The amount of 253.38 mg of ODC per liter of LB broth was finally expressed. High performance liquid chromatography (HPLC) and subsequent ODC activity verification experiments showed that hetero-expressed ODC showed a certain enzyme activity for about 11.91 ± 0.38 U/mg. Our study gives a new way to the development of a low-cost and high-yield strategy to produce ODC, providing experimental materials for further research and elimination of putrescine in food hazards.

KEYWORDS

***Shewanella xiamenensis*, ornithine decarboxylase, heterologous expression, HPLC, enzymatic activity**

1 Introduction

Putrescine is one of the most common biogenic amines that has many physiological activities, such as promoting the formation of biofilms (Bjornsdottir-Butler et al., 2018; Bao et al., 2021), affecting cell growth (Bogdanović et al., 2020) and the synthesis of ferro-carriers (Bujnakova et al., 2014; Bustin et al., 2020), and is commonly found in meat, fermented products and seafood (Costantini et al., 2013; Chmiel et al., 2020;

Cagiada et al., 2021). More importantly, a high concentration of putrescine not only affects the sensory characteristics of food, but also causes toxicological reactions. Putrescine can enhance the toxic effect of histamine, causing headaches, nausea, vomiting, and other adverse reactions (Huang et al., 2015; Hofmann et al., 2020; Fu et al., 2021). Therefore, putrescine is an important spoilage indicator in food (Kanjee et al., 2011).

Putrescine in food is mainly produced by specific microorganisms (Luqman, 2012; Lotfi et al., 2017; Mühlmann et al., 2017; Li et al., 2021), and is produced mainly in two pathways, including the ornithine decarboxylation (ODC) pathway and the arginine decarboxylation (ADC) pathway (Önal et al., 2013; Nakamura et al., 2019; Omer et al., 2021). In the study of putrescine production by *Chlamydomonas*, the ODC activity is almost 5 times than that in ADC activity, and is, undoubtedly, the main pathway of putrescine synthesis (Ramos-Molina et al., 2015; Rio et al., 2018). In the ODC pathway, three synthases including SpeC, SpeF, and PotE are involved in the putrescine production. Among them, it is found that the SpeF of ornithine into putrescine is widely regarded as the main pathway of putrescine production. Therefore, putrescine formation could be affected by inhibiting the synthesis or supply of ornithine (Rio et al., 2018, 2019). Although it has been shown that ODC produced by microbial systems converts ornithine to putrescine, there is no study on the ODC acting *in vitro*.

The wild strain of *Shewanella xiamenensis* used in this study was isolated from the "Yi Lu Xian" salting process in our previous research. According to our previous research, this wild strain of *Shewanella xiamenensis* could produce putrescine in the presence of only glucose, ornithine, and NaCl. The ODC system responsible for putrescine production in *Shewanella xiamenensis* remained unknown. Therefore, the SpeF gene of this wild strain was selected for producing the heterologous ODC, and the target gene was amplified by using the designed specific primers. The heterologous expression system was optimized to achieve a high yield of ODC expression. Hetero-expressed ODC was then used to verify its ODC activity by High performance liquid chromatography (HPLC) and other experiments *in vitro*. We hope this study gives a new way to the development of a low-cost and high-yield strategy to produce putrescine for further investigation, contributes to a broader understanding of the production mechanism of biogenic amines in the food system and provides theoretical support for effectively ensuring the safety of seafood.

2 Materials and methods

2.1 Materials and instruments

BL21 (DE3) competent cells, plasmid pET-30a, and specific primers were synthesized and purchased in Beijing Genomics institution Co., Ltd. (China). Eight biogenic amines standards and dansulfonyl chloride were purchased from Sigma Co., Ltd. (USA). Methanol and acetonitrile (Chromatographic use) was purchased from Tedia Co., Ltd. (USA). Broad-spectrum protein Marker (11–180 KDa), L (+) -Ornithine hydrochloride, pyridoxal 5-phosphatemonohydrate and 5X protein loading buffer were purchased from Solarbio Co., Ltd. (China).

2.2 Gene synthesis and the construction of recombinant strains

The gene sequence of standard strain of *Shewanella xiamenensis* (Gene ID: 75190569), used for the comparison with the wild strain of *Shewanella xiamenensis* in our research, was obtained from the National Center of Biotechnology Information (NCBI) database (Romano et al., 2012). The specific primers for amplifying the speF gene were designed. Single colonies of the experimental strain were selected and picked up in sterile ultrapure water and heated at 100°C for 15 min to obtain the complete genome of the experimental strain. The obtained whole genome was used as the DNA template, and the target gene SpeF with the cloned gene size of 2,163 bp was amplified by designing the specific primers, including primer-forward (5′-TAA TTG GGT GGG CAG CAT-3′) and primer-reverse (5′-TGC ACC ATC CAG CTT ACT CA-3′) (Sakamoto et al., 2012). PCR conditions were set as follows: 95°C for 5 min, later, 95°C for 15 s, 55°C for 15 s, and 72°C for 30 s for 35 cycles and finally extension at 72°C for 5 min. Nucleic acid electrophoresis was used to isolate PCR products. Later, the PCR products were sent to Tsingke company (Qingdao, China) for further sequencing and analyzing. The pET-30a expression vector with 6 × His tag was used for the heterologous expression. After analyzing the gene sequencing, *Sac*I (5′-GAGCT′C-3′), and *Eco*RI (5′-G′AATTC-3′) were selected as restriction sites. The target gene was cloned by the method of double enzyme digestion and T4 ligase to construct the recombinant plasmid.

The recombinant plasmid was then transferred to BL21 competent by thermal transformation. In brief, 10 μL of plasmid was added to 100 μL of competent cells. After standing on ice for 30 min, the transform system was treated in a water bath with 42°C for 45 s and placed on ice for another 2 min. Later, 1 mL of LB liquid medium was added and cultured at 37°C for 60 min with shaking at 220 rpm. The components were then plated on LB agar plates containing 50 μL/mL kanamycin for growing at 37°C for 16 h. Clones were randomly selected from the plate for further culturing, plasmid extraction, and sequencing. Clones with correct sequencing results were identified as positive clones and stored for the further expression use.

2.3 Expression and purification of recombinant ODC

Freshly transformed *E. coli* BL21 cells were inoculated into 10 mL of LB broth containing 50 μg/mL kanamycin and cultured overnight (16 h) at 37°C with shaking at 200 rpm. Afterward, the 5 mL of medium was transformed into 1,000 mL of LB broth containing 50 μg/mL kanamycin and cultured at 37°C for 4 h. Different induced temperatures, culturing time and concentrations of isopropyl-β-D-thiogalactoside (IPTG) were investigated for the best condition of heterologous expression (Santiyanont et al., 2019). The cells were obtained by centrifugation at 4,000 rpm for 30 min and then resuspended in PBS buffer at 4°C (0.01 M, pH 7.4). After breaking by a low-temperature high-pressure cell crusher for 10 min, the soluble protein containing 6 × His-tag was then separated by the centrifugation at 4°C and 13,000 rpm for 20 min.

The nickel immobilized metal ion affinity chromatography (IMAC) Ni-NTA resin column was used for the purification of recombinant protein (Smart-lifesciences, China). After washing by binding buffer (50 mmol/L Tris, 500 mmol/L NaCl, pH 8.0), the soluble protein containing 6 × His-tag was loaded onto the column. After collecting the flow-through sample, the column was washed with a fivefold column volume of PBS (0.01 M, pH 7.4) to remove the non-specific binding proteins. Later, the column was washed with the binding buffer containing 10, 20, 50, 100, and 200 mM of imidazole, and the recombinant protein was then eluted by the binding buffer containing 500 mM imidazole. Finally, the eluted protein was dialyzed by the binding buffer at 4°C and changed every 8 h and repeated three times to remove the imidazole.

2.4 SDS-PAGE of purified ODC

Pre-fabricated protein electrophoresis gel was used for SDS-PAGE verification. The protein samples were mixed with 5 × protein loading buffer and heated with boiling water for 7 min. After electrophoresis under the voltage of 120 V for about 60 min, the G250 gel solution and the decolorizing solution (methanol, acetic acid and ultrapure water with a ratio of 1:12:17) were used for dyeing and decolorization of gel to observe the electrophoresis bands, respectively.

2.5 Determination of ODC activity

2.5.1 Preliminary treatment

The L (+)—ornithine hydrochloride and Pyridoxal 5-phosphatemonohydrate were used as a substrate and a coenzyme to determine the activity of ODC, respectively. The reaction solution (2,000 μL) was prepared containing 1,500 μL Hepes buffer solution (10 mM, pH 6.8–8.0) of dissolved

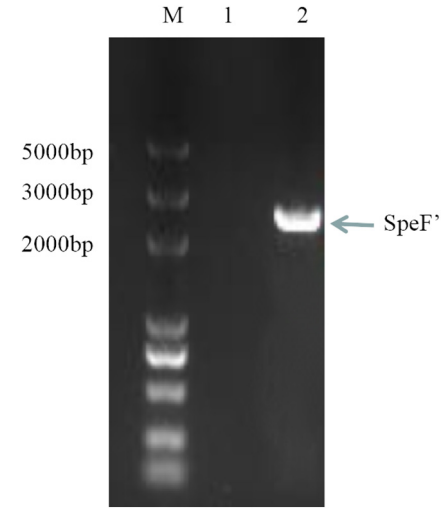

FIGURE 1
SpeF amplicon obtained from the polymerase chain reaction. Lane M: DNA Marker (5,000 bp). Lane 1: negative control (no DNA template added). Lane 2: SpeF amplicon gene from the wild strain of *Shewanella xiamenensis*.

L (+)—ornithine hydrochloride (10 mM) and pyridoxal 5-phosphatemonohydrate (1 mM) and 500 μL enzyme solution. The whole reaction process was conducted in a sterile environment and all solutions were treated with 0.22 μm sterile membranes. After incubation at 37°C for 4 h, the reaction was terminated by adding 2 mL of 5% (v/v) TCA. The mixture was centrifuged at 8,000 rpm for 20 min. A control group (No ODC added) was used to eliminate the effect of environmental implications. The supernatant was collected for further HPLC determination.

2.5.2 High performance liquid chromatography (HPLC)

The putrescine needs to be derived before the determination of HPLC since it has no UV absorption peak. The method of derivation and determination of putrescine was referred to Fu's research (Soleymani and Mostafaie, 2019). In brief, 1 mL of saturated $NaHCO_3$ was added into the supernatant, adjusting the pH value to 9.0 by using the 1 M NaOH. Then, 1 mL of dansulfonyl chloride (10 mg/mL) was added and mixed in a water bath at 60°C for 20 min. After that, 3 mL of ether was added for extraction. After shaking and standing for 10 min, the upper organic phase was transferred and dried by nitrogen. Later, 0.9 ml of acetonitrile and 0.1 mL of ammonia were added for re-dissolution, followed by passing through a 0.22 μm filter membrane. By comparing the chromatogram with the standard product, the type of amines produced by amine-producing was determined. During the HPLC detection, acetonitrile and ultra-pure water were used as the mobile phase A and mobile phase B. C18 column (5 μm × 250 mm × 4.6 mm) was used for detection

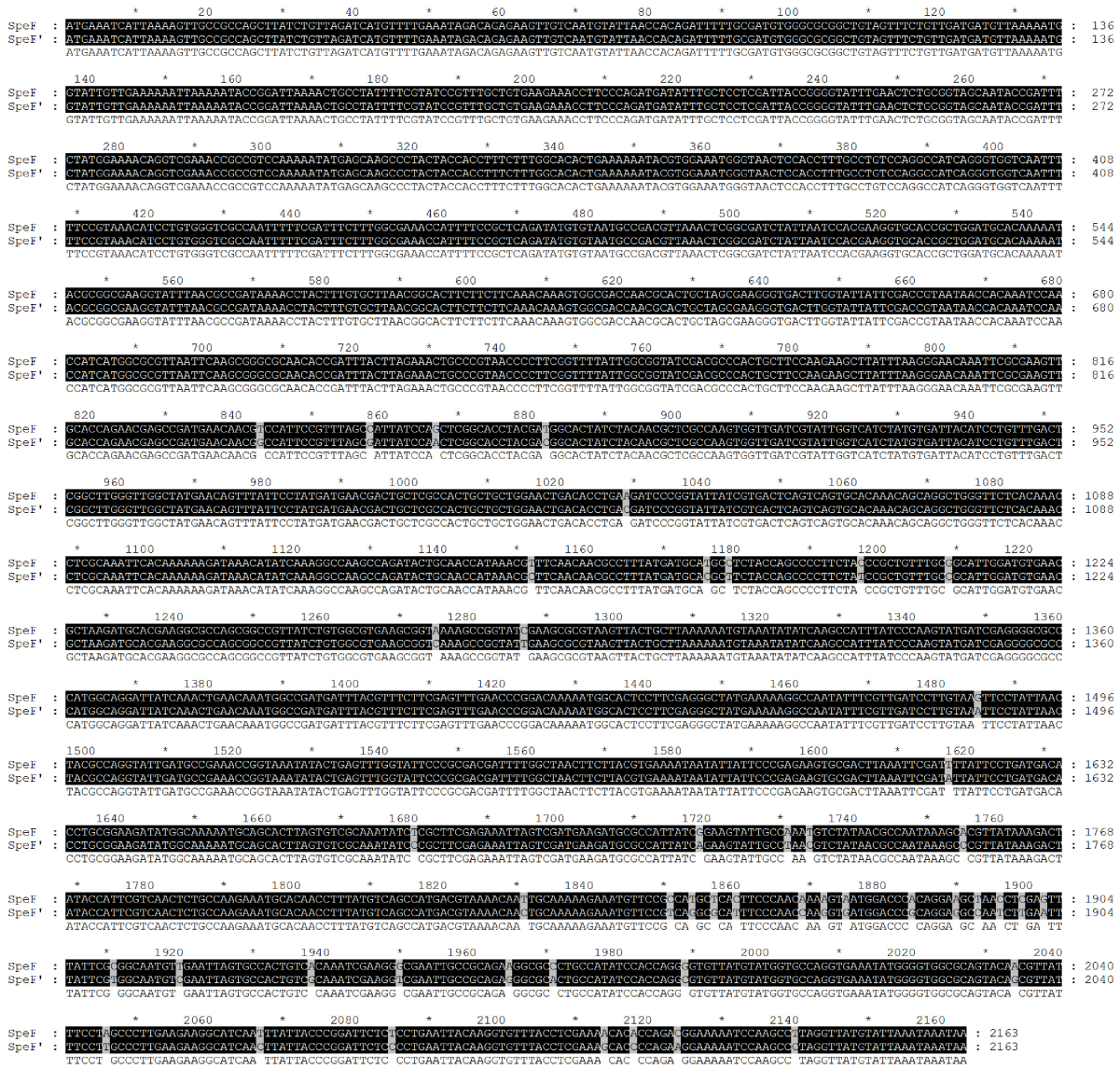

FIGURE 2
Nucleotide sequence alignment of PCR product amplified by a wild strain of *Shewanella xiamenensis*, which was named as SpeF', and ornithine decarboxylation gene from NCBI database, which was named as SpeF.

under the temperature of 40°C and the detection wavelength of 254 nm. The flow rate and the sample size were set at 1 mL/min and 20 μL, respectively. Eight bioamine standard solutions were mixed with the concentrations of 0, 0.2, 1, 5, 10, and 20 mg/L for subsequent derivative steps and bioamine standard curve comparison.

2.5.3 The calculation of ODC activity

The enzyme activity is defined as the amount of substrate converted into product per minute per milligram of the protein, as shown in the following formula. Protein concentration in the following formula was determined by Bradford's method.

$$Enzymatic\ activity = \frac{The\ molar\ amount\ of\ the\ substrate\ converted\ into\ pruduct\ (mol)}{The\ weight\ of\ protein\ (mg) \times Reaction\ time\ (min)}$$

2.6 Data analysis

All data in this study were processed by SPSS (Version 20.0; SPSS Inc., Chicago, USA). Comparisons were made using a one-way analysis of variance (ANOVA). $p < 0.05$ was considered

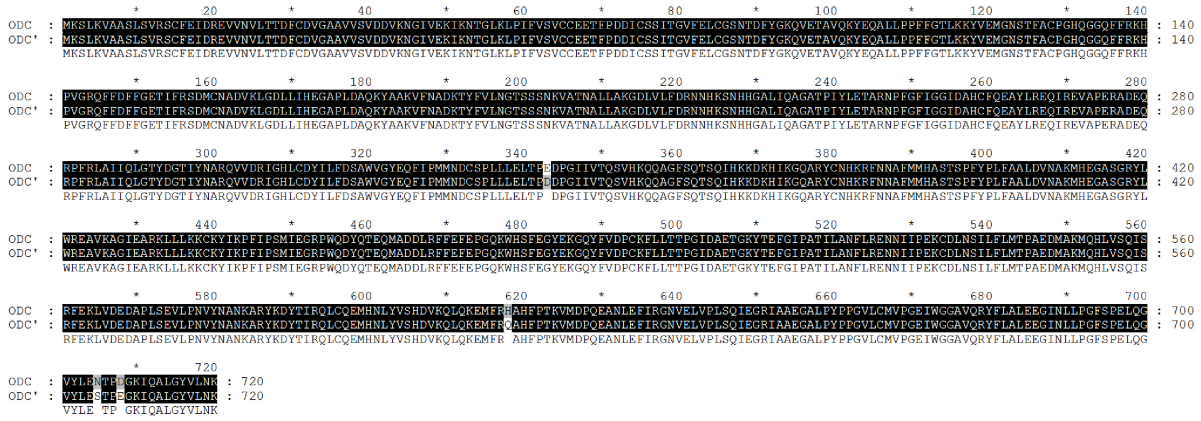

FIGURE 3
Amino acid sequence alignment of PCR product amplified by a wild strain of *Shewanella xiamenensis*, which was named as ODC', and ornithine decarboxylation gene from NCBI database, named as ODC.

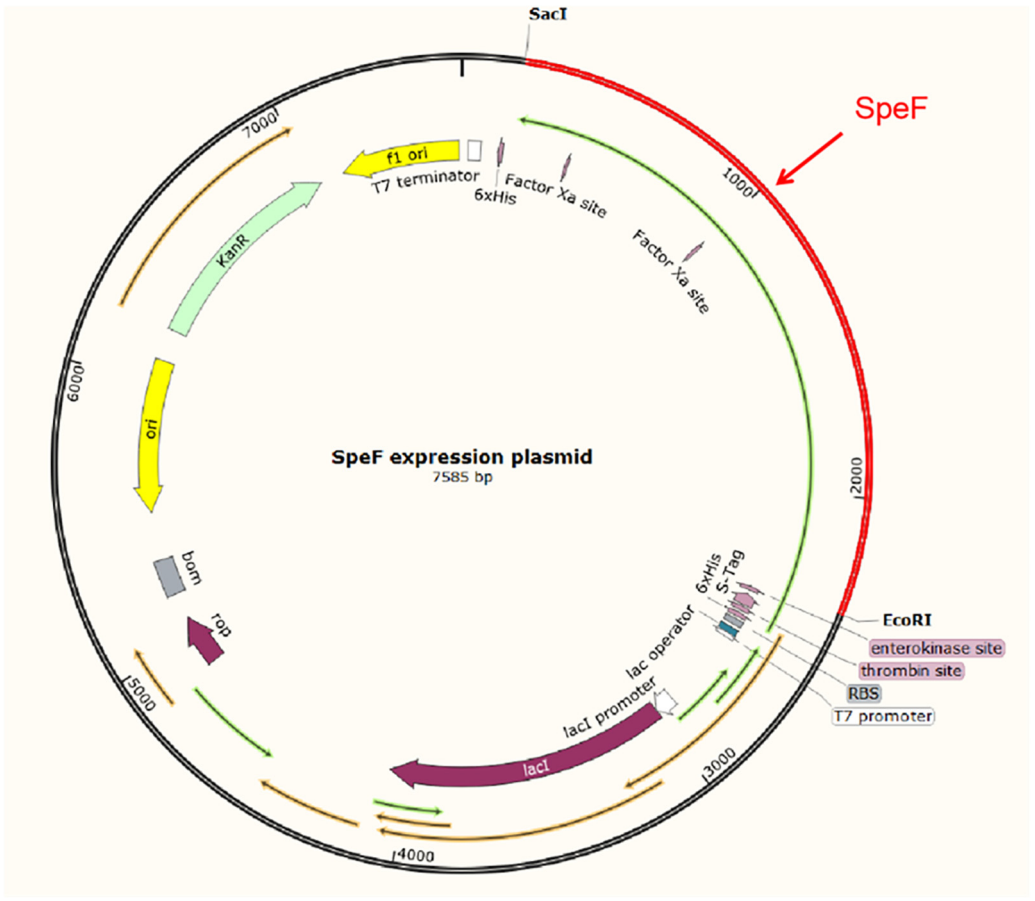

FIGURE 4
The schematic diagram of the pET-30a-SpeF recombinant plasmid. The *Sac*I and *Eco*RI were selected as restriction sites.

a statistically significant difference. Duncan's test was used to evaluate the statistical significance of differences. OriginLab (Version 8.1; OriginLab Inc., Massachusetts, USA) and Adobe Photoshop (Version 19.1.3; Adobe Systems Incorporated Inc., USA) were used for data processing, spectrum analysis, and chart making.

10.3389/fmicb.2022.1100889

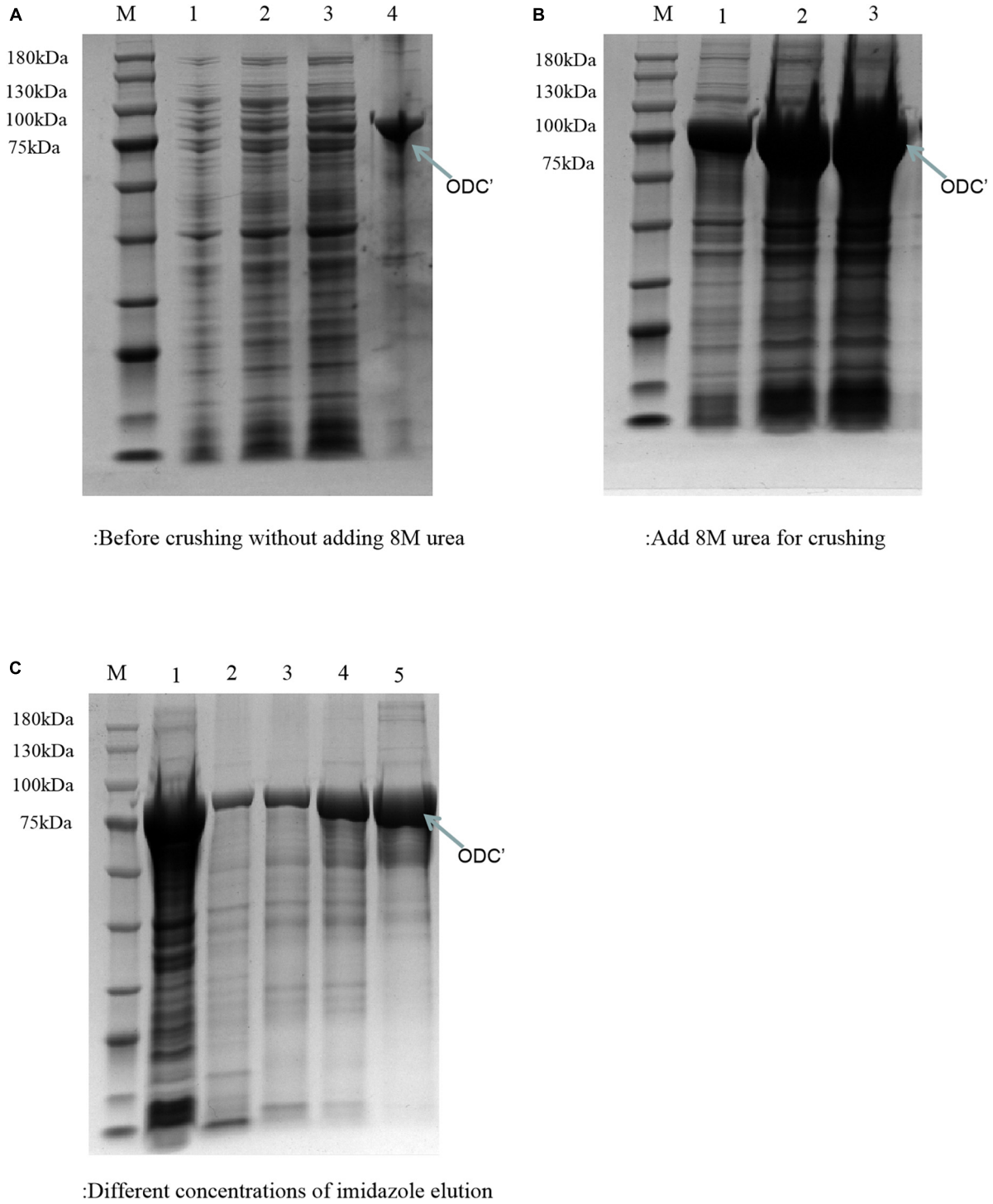

FIGURE 5
SDS-PAGE analysis of ODC under the express condition of 1 M IPTG at 25°C for 12 h. M represented the protein marker (180 kDa). **(A)** Represented the components before adding 8 M urea. Lanes 1–3 represented the supernatant of crushed cells centrifuge precipitate with different volumes (1, 3, and 5 μL), respectively. Lane 4 represented the precipitate of crushed cells. **(B)** Represented the components after adding 8 M urea. Lanes 1–3 represented the precipitated solutions with different volumes (1 μL, 3 μL, 5 μL), respectively. **(C)** SDS-PAGE verification of the different concentrations of imidazole eluents. Lane 1 represented the supernatant after breaking by a low-temperature high-pressure cell crusher. Lanes 2–5 represented the eluents of different concentrations of imidazole (20, 50, 100, and 200 mM), respectively.

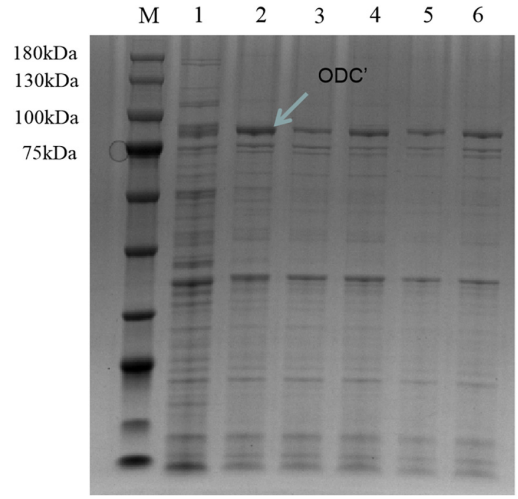

FIGURE 6
SDS-PAGE verification of hetero-expression ODC under the inducement condition at 20°C for 14 h. M represented the protein marker (180 kDa). Line 1 represented hetero-expression ODC with no inducement. Lines 2–6 represented the hetero-expression ODC induced with 0.05, 0.1, 0.3, 0.5, and 0.7 mM IPTG, respectively.

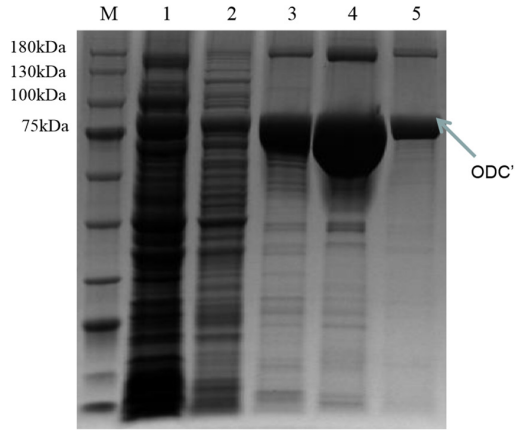

FIGURE 7
SDS-PAGE verification of the different concentrations of imidazole eluents after the inducement of at 20°C for 14 h with the final concentration IPTG of 0.05 mM. M represented the protein marker (180 kDa). Lane 1 represented the supernatant after breaking by a low-temperature high-pressure cell crusher. Lanes 2–5 represented the eluents of different concentrations of imidazole (20 mM, 50 mM, 100 mM, 200 mM), respectively.

3 Results and discussion

3.1 The cloning of ODC coding sequence

The standard ODC sequence is available with the gene ID 58507711 in the NCBI database, with the predicted molecular mass and pI value of the ODC being 80 kDa and 5.81, respectively. As shown in **Figure 1**, the ODC encoding gene SpeF from the wild strain was successfully amplified by PCR reaction using the designed primers, while the target band was bright, with a molecular band between 2,000 and 3,000 bp. After sequence analyzing and comparing with the speF gene of standard *Shewanella xiamenensis* on NCBI, the similarity between PCR product and SpeF gene was 98%, with 48 bases different from the standard speF gene sequence, as shown in **Figure 2**. After converting into the amino acid sequences, the similarity between ODC from wild strain and standard ODC was about 99%. Four amino acid sites were substituted with ODC in the standard strain (**Figure 3**). Glutamate was replaced by aspartic acid at residue 343, glutamine was replaced by histidine at residue 618, asparagine was replaced by serine at position 705, and aspartic acid was replaced with glutamic acid at residue 708, which might affect the type and arrangement of amino acids, protein structure and activity (Taylor and Eitenmiller, 1986; Tassoni et al., 2018; Sunde et al., 2021). However, from the perspective of the characteristics of amino acids, the properties of these substituting amino acids were similar compared to the original amino acids, except for the glutamine replaced by histidine at residue 618. ExPasy was used to predict the properties of the expressed protein. According to the prediction results, the molecular weight of the expressed protein was 81.064 kDa, with a theoretical pI value of 5.81, which showed a high similarity to standard ODC. The ExPasy also provided some other theoretical information about the protein, including 88 negatively charged residues (Asp + Glu) and 74 positively charged residues (Arg + Lys). The instability index (II) was 37.35, indicating that the protein was relatively stable. The aliphatic index and grand average of hydropathicity (GRAVY) were 82.50 and 0.230, respectively. Therefore, it was considered that these four sites were not able enough to affect the activity of ODC. Later, the ODC sequence of wild strain was considered to be introduced into the expression plasmid pET-30a for further heterologous expression.

3.2 Heterologous expression and purification of ODC

The theoretical plasmid diagram is shown in **Figure 4**. After the recombinant plasmid was successfully constructed and introduced into the BL21 competent cells, the positive clone with correct sequence results was used for subsequent heterologous expression experiments. At first, a high final concentration of IPTG (1 M), culturing at 25°C for 12 h was used as the induction condition to express the ODC protein. SDS-PAGE result showed that the expressed proteins existed in the precipitation as inclusion bodies (**Figures 5A, B**). This may be because the molecular weight of expressed ODC is

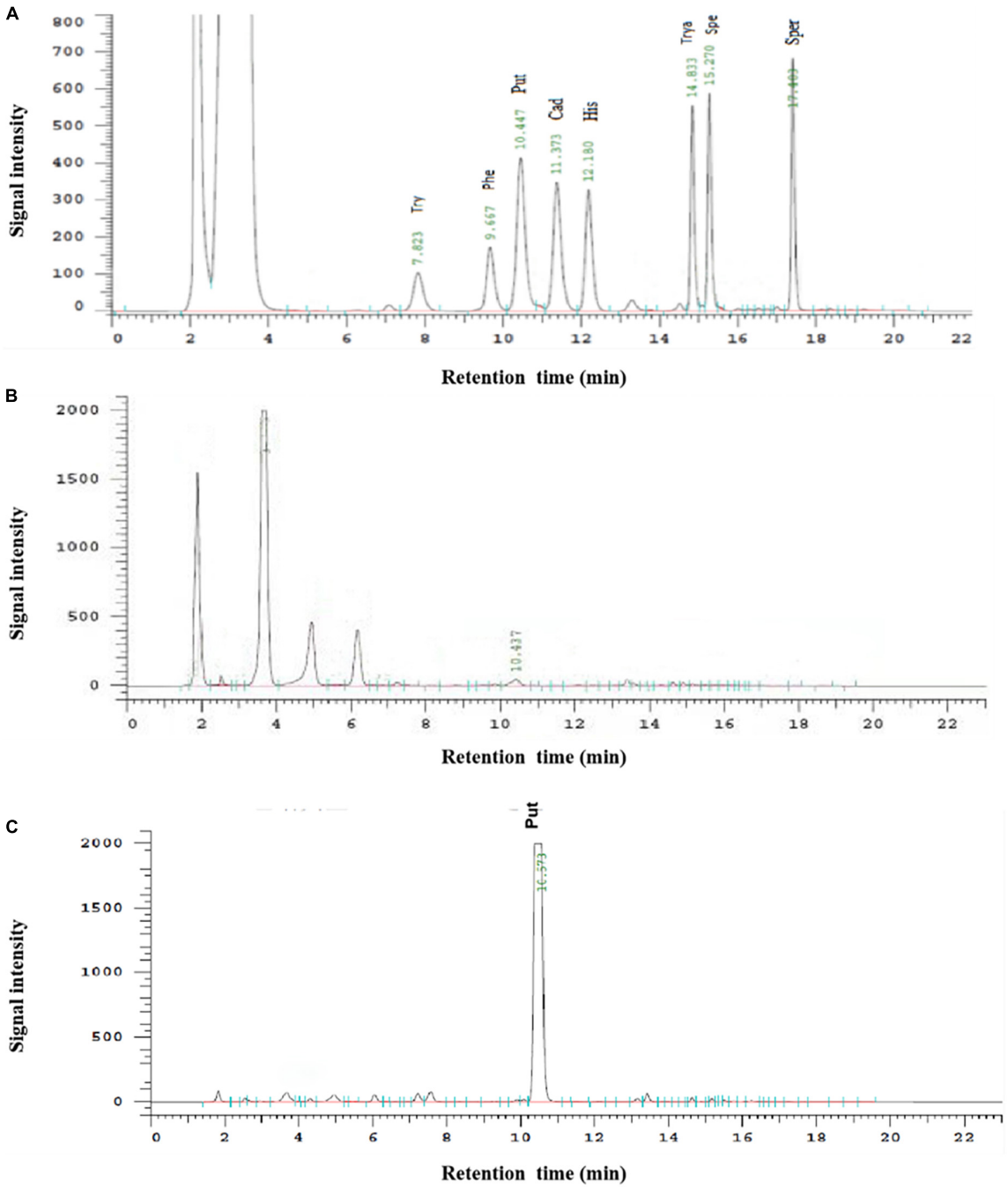

FIGURE 8
The HPLC determination of biogenic amines. **(A)** Represented the HPLC determination result of the mixture of eight biogenic amines standards. **(B)** Represented the HPLC determination result of the negative control. **(C)** Represented the HPLC determination result of hetero-expressed ODC.

about 80 kDa, macromolecular protein usually requires lower temperature and a longer time to complete its structure, and the IPTG with too much high concentration is not conducive to the structural integrity of ODC (Valle et al., 2020; Wang et al., 2020). Therefore, a high urea concentration was used to dissolve the protein after being purified by Ni-NTA resin column with gradient concentrations of imidazole. The SDS-PAGE result showed that the target protein band was bright with a correct molecular weight of 80 kDa (**Figure 5C**), which was consistent with the previously reported ODC size (Wang et al., 2016). However, after the renaturation with arginine and glutamine, the renatured protein did not show the apparent activity of

ODC. This may be due to the fact that although the molecular weight of the expressed protein is correct, the two subunits that play an essential role may not be fully renatured to the complete structure and show their ODC activity through the existing renaturation methods (Zare and Ghazali, 2017).

Therefore, the induced expression strategy of the ODC protein was changed. The inducement conditions of 20°C for 14 h was selected by evaluating the effect of different IPTG concentration (0, 0.05, 0.1, 0.3, 0.5, and 0.7 mM) on protein expression. As shown in **Figure 6**, SDS-PAGE results showed that the target protein band was most obvious under the induction condition of the final concentration of 0.05 mM IPTG, indicating the best induction condition of ODC protein expression. As shown in **Figure 7**, after being purified by Ni-NTA resin column with gradient concentrations of imidazole, the recombinant ODC eluted by 200 mmol/L imidazoles showed an obvious band on SDS-PAGE verification with the molecular weight of 80 kDa. The protein was freeze-dried to calculate the expression yield and the result showed that 253.8 ± 2.4 mg ODC protein could be obtained per liter of LB broth.

3.3 The determination of ODC activity

The determination of putrescine by HPLC has the advantages of simplicity, rapidity, high sensitivity, and good reproducibility (Zhang et al., 2019). As shown in **Figure 8A**, all eight biogenic amines standards could be separated well within 20 min, and each peak was symmetrical without baseline drift during the HPLC determination. Therefore, this method can be used for the quantitative analysis of putrescine. As can be seen from **Figures 8B, C**, there was only one peak of putrescine and no peak of other biogenic amines in the liquid chromatography in the experimental group while the negative group without ODC showed no significant bioamine peaks. After calculating, the standard curve of putrescine is y = 35753x-4057.3 (R^2 > 99.9%), which showed the high accuracy and good repeatability, and could be used for quantitative analysis of putrescine content. By comparing the standard curve, it can be calculated that the expressed protein had a certain specific activity of ODC and could be quantified to 11.91 ± 0.38 U/mg, indicating that the expressed protein in our study has the ability to convert ornithine into putrescine.

4 Conclusion

In this study, the SpeF gene encoding ODC isolated from a wild strain was successfully amplified. By comparing to the NCBI database, SpeF showed high similarity of standard SpeF with four amino acid differences compared to the standard strain. After constructing and optimizing the heterologous expression system, the final concentration of 0.05 mM IPTG at 20°C for 14 h was selected for the best inducement condition. The ODC was expressed with a high yield of 253.8 ± 2.4 mg per liter of fermentation broth with a molecular weight of about 80 kDa, which was consistent with the previously reported ODC size. The HPLC determination and further experiments demonstrated that the hetero-expressed ODC in our research could convert L-ornithine to putrescine in a buffer system containing only L-ornithine and coenzyme with an enzyme activity of 11.91 ± 0.38 U/mg.

Data availability statement

The data presented in this study are deposited in the NCBI repository, accession number: OP985534.

Author contributions

CL and GW wrote the manuscript and made the figures under the supervision and revision of XH, LC, KW, HL, and JS. All authors contributed to the article and approved the submitted version.

Funding

This work was financially supported by the National Key R&D Program of China (grant no. 2018YFD0901005) and the Fundamental Research Funds for the Central Universities (grant no. 202042011).

Conflict of interest

The authors declare that the research was conducted in the absence of any commercial or financial relationships that could be construed as a potential conflict of interest.

Publisher's note

References

Bao, X., Wang, F., Yang, R., Zhang, Y., Fu, L., and Wang, Y. (2021). Ornithine decarboxylation system of shewanella baltica regulates putrescine production and acid resistance. *J. Food Prot.* 84, 303–309. doi: 10.4315/JFP-20-227

Bjornsdottir-Butler, K., Abraham, A., Harper, A., Dunlap, P., and Benner, R. (2018). Biogenic amine production by and phylogenetic analysis of 23 *Photobacterium* species. *J Food Prot.* 81, 1264–1274. doi: 10.4315/0362-028X.JFP-18-022

Bogdanović, T., Petričević, S., Brkljača, M., Listeš, I., and Pleadin, J. (2020). Biogenic amines in selected foods of animal origin obtained from the croatian retail market. *Food Addit. Contam.* 37, 815–830. doi: 10.1080/19440049.2020.1726503

Bujnakova, D., Strakova, E., and Kmet, V. (2014). *In vitro* evaluation of the safety and probiotic properties of *Lactobacilli* isolated from chicken and calves. *Anaerobe* 29, 118–127.

Bustin, S., Mueller, R., and Nolan, T. (2020). Parameters for successful PCR primer design. *Methods Mol. Biol.* 2065, 5–22.

Cagiada, M., Johansson, K., Valanciute, A., Nielsen, S., Hartmann-Petersen, R., Yang, J., et al. (2021). Understanding the origins of loss of protein function by analyzing the effects of thousands of variants on activity and abundance. *Mol. Biol. Evol.* 38, 3235–3246. doi: 10.1093/molbev/msab095

Chmiel, M., Roszko, M., Hać-Szymańczuk, E., Adamczak, L., Florowski, T., Pietrzak, D., et al. (2020). Time evolution of microbiological quality and content of volatile compounds in chicken fillets packed using various techniques and stored under different conditions. *Poult. Sci.* 99, 1107–1116. doi: 10.1016/j.psj.2019.10.045

Costantini, A., Pietroniro, R., Doria, F., Pessione, E., and Garcia-Moruno, E. (2013). Putrescine production from different amino acid precursors by lactic acid bacteria from wine and cider. *Int. J. Food Microbiol.* 165, 11–17. doi: 10.1016/j.ijfoodmicro.2013.04.011

Fu, Q., Zheng, H., Han, X., Cao, L., and Sui, J. (2021). Development of a highly sensitive HPLC method for the simultaneous determination of eight biogenic amines in aquatic products. *Acta Chromatogr.* 33, 378–386.

Hofmann, M., Campo, J., Sobrado, P., and Tischler, D. (2020). Biosynthesis of desferrioxamine siderophores initiated by decarboxylases: A functional investigation of two lysine/ornithine-decarboxylases from *Gordonia rubripertincta* CWB2 and *Pimelobacter simplex* 3E. *Arch. Biochem. Biophys.* 689:108429. doi: 10.1016/j.abb.2020.108429

Huang, J., Jones, B., and Kazlauskas, R. (2015). Stabilization of an α/β-hydrolase by introducing proline residues: Salicylic acid binding protein 2 from tobacco. *Biochemistry* 54, 4330–4341. doi: 10.1021/acs.biochem.5b00333

Kanjee, U., Gutsche, I., Ramachandran, S., and Houry, W. (2011). The enzymatic activities of the *Escherichia coli* basic aliphatic amino acid decarboxylases exhibit a pH zone of inhibition. *Biochemistry* 50, 9388–9398. doi: 10.1021/bi201161k

Li, B., Liang, J., Hanfrey, C., Phillips, M., and Michael, A. (2021). Discovery of ancestral L-ornithine and L-lysine decarboxylases reveals parallel, pseudoconvergent evolution of polyamine biosynthesis. *J. Biol. Chem.* 297:101219. doi: 10.1016/j.jbc.2021.101219

Lotfi, H., Hejazi, M., Heshmati, M., Mohammadi, S., and Zarghami, N. (2017). Optimizing expression of antiviral cyanovirin-N homology gene using response surface methodology and protein structure prediction. *Cell. Mol. Biol.* 63, 96–105. doi: 10.14715/cmb/2017.63.9.17

Luqman, S. (2012). Ornithine decarboxylase: A promising and exploratory candidate target for natural products in cancer chemoprevention. *Asian Pac. J. Cancer Prev.* 13, 2425–2427. doi: 10.7314/apjcp.2012.13.5.2425

Mühlmann, M., Forsten, E., Noack, S., and Büchs, J. (2017). Optimizing recombinant protein expression via automated induction profiling in microtiter plates at different temperatures. *Microb. Cell Fact.* 16:220. doi: 10.1186/s12934-017-0832-4

Nakamura, A., Ooga, T., and Matsumoto, M. (2019). Intestinal luminal putrescine is produced by collective biosynthetic pathways of the commensal microbiome. *Gut Microbes* 10, 159–171. doi: 10.1080/19490976.2018.1494466

Omer, A., Mohammed, R., Ameen, P., Abas, Z., and Ekici, K. (2021). Presence of biogenic amines in food and their public health implications: A review. *J. Food Prot.* 84, 1539–1548.

Önal, A., Tekkeli, S., and Önal, C. (2013). A review of the liquid chromatographic methods for the determination of biogenic amines in foods. *Food Chem.* 138, 509–515.

Ramos-Molina, B., López-Contreras, A., Lambertos, A., Dardonville, C., Cremades, A., and Peñafiel, R. (2015). Influence of ornithine decarboxylase antizymes and antizyme inhibitors on agmatine uptake by mammalian cells. *Amino Acids* 47, 1025–1034. doi: 10.1007/s00726-015-1931-3

Rio, B., Alvarez-Sieiro, P., Redruello, B., Martin, M., Fernandez, M., Ladero, V., et al. (2018). Lactobacillus rossiae strain isolated from sourdough produces putrescine from arginine. *Sci. Rep.* 8:3989. doi: 10.1038/s41598-018-22309-6

Rio, B., Redruello, B., Linares, D., Ladero, V., Ruas-Madiedo, P., Fernandaz, M., et al. (2019). The biogenic amines putrescine and cadaverine show *in vitro* cytotoxicity at concentrations that can be found in foods. *Sci. Rep.* 9:120. doi: 10.1038/s41598-018-36239-w

Romano, A., Trip, H., Mulder, N., Lonvaud-Funel, A., Lolkema, J., and Lucas, P. (2012). Evidence of two functionally distinct ornithine decarboxylation system in lactic acid bacteria. *Appl. Environ. Microbiol.* 78:1953–61. doi: 10.1128/AEM.07161-11

Sakamoto, A., Terui, Y., Yamamoto, T., Kasahara, T., Nakamura, M., Tomitori, H., et al. (2012). Enhanced biofilm formation and/or cell viability by polyamines through stimulation of response regulators UvrY and CpxR in the two-component signal transducing systems, and ribosome recycling factor. *Int. J. Biochem. Cell Biol.* 44, 1877–1886.

Santiyanont, P., Chantarasakha, K., Tepkasikul, P., Srimarut, Y., Mhuantong, W., Tangphatsornruang, S., et al. (2019). Dynamics of biogenic amines and bacterial communities in a Thai fermented pork product NHAM. *Food Res. Int.* 119, 110–118. doi: 10.1016/j.foodres.2019.01.060

Soleymani, B., and Mostafaie, A. (2019). Analysis of methods to improve the solubility of recombinant bovine sex determining region Y protein. *Rep. Biochem. Mol. Biol.* 8, 227–235.

Sunde, H., Ryder, K., Bekhit, A., and Carne, A. (2021). Analysis of peptides in a sheep beta lactoglobulin hydrolysate as a model to evaluate the effect of peptide amino acid sequence on bioactivity. *Food Chem.* 365:130346. doi: 10.1016/j.foodchem.2021.130346

Tassoni, A., Awad, N., and Griffiths, G. (2018). Effect of ornithine decarboxylase and norspermidine in modulating cell division in the green alga *Chlamydomonas reinhardtii*. *Plant Physiol. Biochem.* 123, 125–131. doi: 10.1016/j.plaphy.2017.12.014

Taylor, S., and Eitenmiller, R. (1986). Histamine food poisoning: Toxicology and clinical aspects. *Crit. Rev. Toxicol.* 17, 91–128. doi: 10.3109/10408448609023767

Valle, A., Seip, B., Cervera-Marzal, I., Sacheau, G., Seefeldt, A., and Innis, C. (2020). Ornithine capture by a translating ribosome controls bacterial polyamine synthesis. *Nat. Microbiol.* 5, 554–561.

Wang, S., Liang, H., Liu, L., Jiang, X., Wu, S., and Gao, H. (2020). Promiscuous enzymes cause biosynthesis of diverse siderophores in *Shewanella oneidensis*. *Appl. Environ. Microbiol.* 86:e00030–20. doi: 10.1128/AEM.00030-20

Wang, Y., Kim, S., Natarajan, R., Heindl, J., Bruger, E., Water, C., et al. (2016). Spermidine inversely influences surface interactions and planktonic growth in *Agrobacterium tumefaciens*. *J. Bacteriol.* 198, 2682–2691. doi: 10.1128/JB.00265-16

Zare, D., and Ghazali, H. (2017). Assessing the quality of sardine based on biogenic amines using a fuzzy logic model. *Food Chem.* 221, 936–943. doi: 10.1016/j.foodchem.2016.11.071

Zhang, J., Hu, J., Wang, S., Lin, X., Liang, H., Li, S., et al. (2019). Developing and validating a UPLC-MS method with a stagetip-based extraction for the biogenic amines analysis in fish. *J. Food Sci.* 84, 1138–1144. doi: 10.1111/1750-3841.14597

frontiers | Frontiers in Microbiology

TYPE Original Research
PUBLISHED 22 December 2022
DOI 10.3389/fmicb.2022.1091486

OPEN ACCESS

EDITED BY
Jinxuan Cao,
Beijing Technology and Business University, China

REVIEWED BY
Mingzhi Zhu,
Hunan Agricultural University, China
Hai Yu,
Yangzhou University, China
Dengyong Liu,
Bohai University, China

*CORRESPONDENCE
Baozhong Sun
baozhongsun@163.com

†These authors have contributed equally to this work and share first authorship

SPECIALTY SECTION
This article was submitted to Food Microbiology, a section of the journal Frontiers in Microbiology

RECEIVED 07 November 2022
ACCEPTED 24 November 2022
PUBLISHED 22 December 2022

CITATION
Yu H, Zhang S, Liu X, Lei Y, Wei M, Liu Y, Yang X, Xie P and Sun B (2022) Comparison of physiochemical attributes, microbial community, and flavor profile of beef aged at different temperatures. *Front. Microbiol.* 13:1091486. doi: 10.3389/fmicb.2022.1091486

Comparison of physiochemical attributes, microbial community, and flavor profile of beef aged at different temperatures

Haojie Yu[1†], Songshan Zhang[1†], Xiaochang Liu[1], Yuanhua Lei[1], Meng Wei[1,2], Yinchu Liu[1], Xiaodong Yang[1], Peng Xie[1] and Baozhong Sun[1*]

[1]Institute of Animal Sciences, Chinese Academy of Agricultural Sciences, Beijing, China, [2]Chemical Engineering Institute, Shijiazhuang University, Shijiazhuang, China

Beef aging for tenderness and flavor development may be accelerated by elevated temperature. However, little to no research has been undertaken that determines how this affects other important meat quality characteristics and microbial community. This study aims to decrease aging time by increasing temperature. Beef were aged and vacuum packaged at 10 and 15°C, and the effects of increased temperature on meat physiochemical attributes, microbial community, and flavor profile were monitored. The shear force decreased with aging in all temperature and showed the higher rate at elevated temperatures compare to 4°C. The beef aged at elevated temperatures (10 or 15°C) for 5 days showed equivalent shear force value to the beef aged at 4°C for 10 days ($p > 0.05$), however, the final tenderness was not affected by the elevated temperature. The beef aged at elevated temperatures showed a significantly higher cooking loss and less color stability compared to 4°C ($p < 0.05$). The total volatile basic nitrogen and aerobic plate count increased ($p < 0.05$) faster at elevated temperatures compare to 4°C. Carnobacterium, Lactobacillus and Hafnia–Obesumbacterium were the dominant genus in the beef samples aged at 4, 10, and 15°C, respectively. In addition, the contents of isobutyraldehyde, 3-methylbutyraldehyde, 2-methylbutyraldehyde, and 3-methylbutanol were higher than aged at 4°C ($p < 0.05$). Therefore, these results suggest that application of elevated aged temperatures could shorten required aging time prior while not adversely affecting meat quality. In turn, this will result in additional cost savings for meat processors.

KEYWORDS

aged beef, temperature, tenderness, microbial community, vacuum packaged, flavor analysis

Introduction

Tenderness is the major eating quality of beef, and consumers are willing to pay a higher price for the beef that is guaranteed to be tender (Marino et al., 2013). In the beef industry, aging is widely used to improve tenderness, which can be affected by complex changes during

muscle metabolism after slaughter (Colle and Doumit, 2017). The aging of beef is essential to provide a tender product and influenced by temperature. Beef were usually aged for 14 days at 4°C by processors (Kilgannon et al., 2019). However, this conventional aging temperature takes considerable refrigerated space requirements, operational losses, and energy (Wahlgren, 1994). Koohmaraie (1992) demonstrated that decreasing aging temperature reduced the autolysis of key muscle proteins and increasing aging temperature could improve tenderness. Consequently, aging temperature determined tenderization rates. When beef was aged at higher temperatures, beef tenderness improved largely within a shorter period (Kim et al., 2018). Pierson (1976) found that aging beef at an elevated temperature (20°C versus 3°C) for short periods (3–5 days) increasesd muscle tenderness. Meanwhile, Devine (1994) found that higher aging temperatures of approximately 10–15°C resulted in the highest degree of meat tenderness with the lowest muscle shortening and maximum aging potential.

Higher aging temperatures can increase beef tenderness within less aging time, meanwhile the proliferation of microorganisms in beef is promoted, which can lead to a significant reduction in shelf life (Zhu et al., 2004). Discoloration, off-odors, and slime formation caused by the deteriorative effects of microbial growth makes meat unacceptable to consumers (Esteves et al., 2021). Microbial growth is closely related to temperature. For example, total viable bacterial counts in beef stored at 10°C for 72 h increased by 2 log CFU/cm^2, whereas those in beef stored at 5°C increased by 0.4 log CFU/cm^2 (Kinsella et al., 2009). Moreover, Gribble et al. (2014a) reported that the counts of lactic acid bacteria (LAB), *Enterobacteriaceae*, and *Brochothrix thermosphacta* increased with the prolongation of storage time regardless of the experimental temperature (−1.5, 0, 2, and 7°C). Vacuum packaging is often used to prolong the shelf life of beef, given that storage under anaerobic conditions proved to be very effective in extending the shelf life of various perishable foods (Mansur et al., 2019). Devine (1994) reported that temperatures of 10 and 15°C resulted in better tenderness of aged beef but the effect of higher aging temperatures on the color, microbial community, and flavor of beef were not evaluated.

This study aims to address the paucity of data on the effects of high temperatures on meat quality traits, microbial load, and flavor parameters and to provide a theoretical basis for shortening the aging time of beef.

Materials and methods

Sample preparation

Longissimus dorsi muscles were collected from six Simmental cattle (24 ± 1 months old, 470 ± 30 Kg) in a commercial abattoir and transferred to the laboratory in an ice box within 2 h. All beef were rinsed with sterile water to remove stains and blood, and then dried with sterilized paper towels. The muscles were cut into 300 g samples (6 cm × 6 cm × 10 cm) and vacuum packaged at the O_2-transmission rate of 40 cm^3/m^2/day and 85% relative humidity. Samples were divided into three groups, and aged at respective temperature (4, 10, or 15°C). Samples were analyzed at different time points (0, 2, 4, 6, 8, 10, 14, and 18 day for 4°C, 1, 2, 3, 4, 5, 6, 8, 10, 12, and 14 day for 10°C; 0, 1, 2, 3, 4, 5, 6, and 7 days for 15°C). The temperature was monitored continuously by using remote temperature recorders with high precision control. Each analysis was performed using triplicate samples.

Cooking loss and shear force measurement

The beef samples (3 cm × 3 cm × 6 cm) were packaged and cooked in a water bath at 80°C to achieve a core temperature of approximately 70°C. After cooking, the samples were cooled at 4°C until the core temperature cooled down to 10°C, surface-blotted with paper towels, and reweighed for weight loss. Cooking loss was determined by calculating the weight difference of the samples before and after cooking and expressed as the percentage of initial weight. Shear force values of samples (1.0 cm × 1.0 cm × 3.0 cm) weredetermined across the longitudinal direction of muscle fibers by a texture analyzer (TA-XT plus) attached with a Warner-Bratzler blade (V-notch, HDP/BSW). The cutting line was positioned to avoid fatty and connective tissues and was perpendicular to the muscle fiber direction. The shear force value was calculated as the mean of the maximum force and expressed as in Newtons (N).

Instrumental color measurement

The surface color of the beef samples was measured on each analysis day after the samples were blooming for 30 min at room temperature. The lightness (L^*), redness (a^*), and yellowness (b^*) of the beef samples were measured by a spectrophotometer (model CR-410, Minplta, Tokyo, Japan) with a diameter of 8 mm. The instrument was set for illuminant D65 and calibrated with a standard white plate before measurement. Measurements were taken in triplicate at different locations within each sample.

Total volatile basic nitrogen measurements

Briefly, 10 g of raw meat (free of subcutaneous fat) was weighed into a closed glass vessel with 75 ml of distilled water with intermittent shaking for 30 min (room temperature). Immediately prior to distillation, 1 g of magnesium oxide was added to the sample, and the sample was steam distilled for 5 min. The distillate was condensed into a receiving flask containing boric acid (20 g/L) with a mixed indicator solution of bromocresol green/methyl red. The solution was back-titrated with 0.01 M hydrochloric acid solution, and TVB-N was calculated as mg/100 g raw meat.

Microbiological analysis

A total of 25 g of samples from the top surface (depth: 0.5 cm) were blended in 225 ml of 0.85% sterile saline solution for 90 s in a stomacher (Ningbo Jiangnan Instrument Factory) at room temperature. Samples for microbial testing were prepared in a series of decimal dilutions by using sterile saline. Plate count agar (PCA) was used for total viable counts (TVCs). Violet red bile glucose agar (VRBA) was used for *Enterobacteriaceae* counts. Rogosa and Sharpe agar (MRS) was utilized for LAB counts. Cephalothin–sodium fusidate–cetrimide (CFC) agar with CFC-selective supplement was applied to determine *Pseudomonas* spp. counts. Streptomycin thallous acetate agar (STAA) with STAA selective supplement was employed for *Brochothrix thermosphacta* counts. Each diluent (0.1 ml) was spread on the selective medium agar in triplicate. CFC and STAA plates were incubated at 25°C for 48 h. PCA and MRS plates were incubated at 30°C for 48 h, and VRBA plates were incubated for 24 h at 37°C. The number of colonies was counted and expressed as colony forming units per gram (log CFU/g).

Microbial-community analysis

DNA extraction and PCR

Total microbial genomic DNA was extracted from the beef samples using the E.Z.N.A.® soil DNA Kit (Omega Bio-tek, Norcross, GA, United States) in accordance with the manufacturer's instructions. The quality and concentration of DNA were determined using 1.0% agarose gel electrophoresis and a NanoDrop® ND-2000 spectrophotometer (Thermo Scientific Inc., United States). The DNA samples were kept at −80°C prior to further use. The hypervariable V3–V4 region of the bacterial 16S rRNA gene was amplified with primer pairs 338F (5′-ACTCCTACGGGAGGCAGCAG-3′) and 806R (5′-GGACTACHVGGGTWTCTAAT-3′) using an ABI GeneAmp® 9,700 PCR thermocycler (ABI, CA, United States). The PCR reaction mixture included 4 µl of 5 × Fast Pfu buffer, 2 µl of 2.5 mM dNTPs, 0.8 µl of each primer (5 µM), 0.4 µl of Fast Pfu polymerase, 10 ng of template DNA, and ddH_2O to the final volume of 20 µl. The PCR amplification cycling conditions were as follows: initial denaturation at 95°C for 3 min, followed by 27 cycles of denaturation at 95°C for 30 s; annealing at 55°C for 30 s and extension at 72°C for 45 s; a single extension cycle at 72°C for 10 min; and a final cycle at 4°C. All samples were amplified in triplicate. The PCR product was extracted from 2% agarose gel and purified by using the AxyPrep DNA Gel Extraction Kit (Axygen Biosciences, Union City, CA, United States) in accordance with the manufacturer's instructions and quantified using Quantus™ Fluorometer (Promega, United States).

Illumina MiSeq sequencing

Purified amplicons were pooled in equimolar amounts and paired-end sequenced on an Illumina MiSeq PE300 platform/NovaSeq PE250 platform (Illumina, San Diego, United States) in accordance with the standard protocols by of Majorbio Bio-Pharm Technology Co. Ltd. (Shanghai, China).

Flavor analysis

The volatile compounds present in beef samples were identified and quantified by a GC–IMS flavor analyzer (FlavourSpec®, Shandong, China) equipped with a syringe and an autosampler unit for headspace analysis. Briefly, 2 g of homogenized beef sample was transferred into a 20 ml headspace vial, incubated at 60°C for 20 min, the vial was put in an incubator and shook at 500 rpm to facilitate the emitting of volatiles into headspace, the vial was sealed by using a magnetic cap with a silicone septum. The temperature of head space injection needle was 60°C and the injection volume was 500 µl. The analytical conditions for this test are as follows: Chromatographic column type: MXT-5, 15 m, 0.53 mmID, 1.0 µm df (RESTEK, United States), to separate the volatile components and coupled to ion mobility spectrometry (IMS); carrier/drift gas: N_2, with the flow ramp starting at 2 ml/min for 2 min, then increasing to 20 ml/min in 8 min and increasing to 130 ml/min in10 min, finally 130 ml/min for 5 min, introducing the sample into the capillary; column syringe temperature: 85°C. The total GC runtime was 25 min, triplicate injections and analysis of samples were performed.

Statistical analysis

All experiments were performed in triplicate. The mean values and standard errors of the means were recorded, outlying observations were identified, and implausible values were verified with the original source or coded as missing. Differences between treatments were analyzed through Tukey's test. Statistical analyses were conducted at a 95% confidence level. Bioinformatics analysis was carried out on the microbiota by using the Majorbio Cloud platform on the basis of OTU information; rarefaction curves; and alpha diversity indices, including observed OTUs. The analytical software Laboratory Analytical Viewer and the built-in NIST and IMS databases of the GC–IMS Library Search software were used for the qualitative analysis of characteristic volatile compounds. One-way ANOVA was used to estimate the difference between means ($p < 0.05$).

Results and discussion

Cooking loss and shear force

Cooking loss is the water loss from the meat due to protein denaturation during cooking (Kim et al., 2019). Figure 1A illustrates the effect of different aging temperatures on cooking

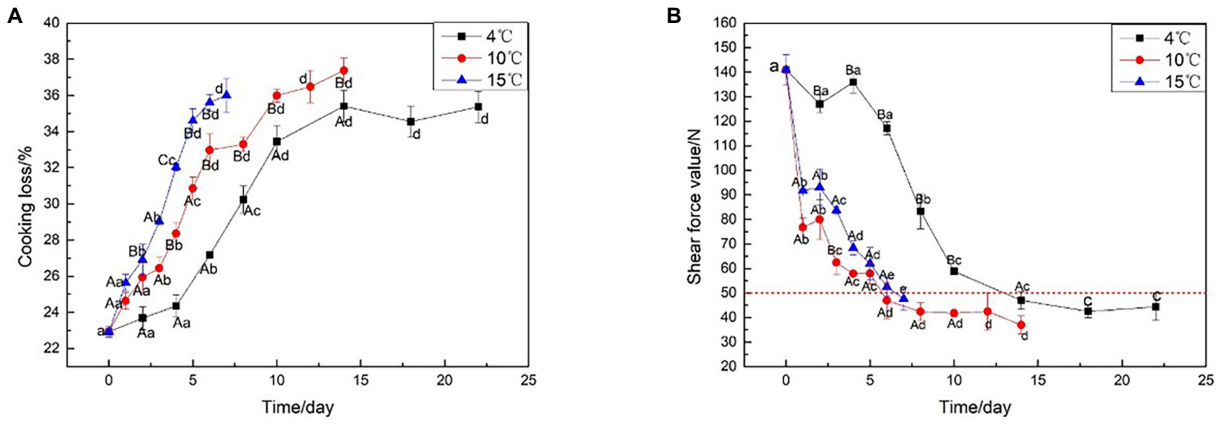

FIGURE 1
Cooking loss and Shear force analysis on beef samples aging at 4, 10, and 15°C. **(A)** Cooking loss, **(B)** Shear force analysis.

loss, which tended to increase as the beef aged: the higher the aging temperature, the higher the cooking loss. In particular, the cooking loss aged at 15°C always higher than aged at 4°C ($p < 0.05$). Similarly, the interaction of aging temperature had an effect on the Warner-Bratzler shear force (WBSF) of the beef ($p < 0.05$). Figure 1B shows that with the prolongation of aging time, the shear force values show a decreasing trend whether it is decreased at 4, 10, or 15°C; specifically, aging affected the shear force values of all the beef samples with the meat becoming increasingly tender at each time point ($p < 0.05$). The beef aged at elevated temperatures (10 or 15°C) for 5 days had equivalent shear force values as the beef aged at 4°C for 10 days ($p > 0.05$). The beef aged at 15°C for 3 days had equivalent shear force values to beef aged at 4°C for 8 days ($p > 0.05$). This indicated that the aging period could be shortened by placing the meat at a slightly higher temperature than the typical meat aging temperature (4°C). However, the final tenderness is not affected by the elevated temperature. Aging at 4°C resulted in no significant reduction in shear force values before 6 days due to lower temperatures, however, the shear force values of the beef aged at 10 and 15°C decreased rapidly to 47.9 and 47.1 N, respectively, at the same stage of aging. At 14 days after aging at 4°C, the beef samples had an average WBSF value of less than 50 N. Aging at 10°C and 15°C required about 6 days, to achieve the same results, likely due to the enhancement in proteolytic enzyme activity, proteolysis *via* calpains, and collagen fiber breakdown from lysosomal enzyme activity at high temperatures (Kim et al., 2016). Furthermore, when the beef shear force under 50 N, the change is no longer significant. The time point could be considered as the end of beef aging, to save aging time and energy consumption.

Surface color

Meat color is a direct estimate of meat freshness and wholesomeness for consumers, who often associate discoloration with spoilage (Li et al., 2015). The L^*, a^*, and b^* color attributes of beef samples are shown in Figures 2A–C. The L^* value decreased with the extension of aging time. Groups aged at higher temperatures presented significantly decreased L^* values compared with those aged at 4°C. a^* is the most important color parameter for fresh meat (Yim et al., 2016). Generally, the higher a^* value, the fresher the meat. Figure 2B shows that a^* decreased with the extension of aging time. At the same aging time, the a^* values of samples aged at 10°C and 15°C were lower than those of samples aged at 4°C, indicating that the higher temperature, the more unfavorable a^* value of beef. With the progression of aging, the b^* value increased, and the b^* value of samples aged at 15 and 10°C was significantly higher than that of the samples aged at 4°C ($p < 0.05$). Furthermore, aged at 4°C for 14 days had equivalent b^* values as the beef aged at elevated temperatures (10 and 15°C) for 5 days, indicating that the higher temperature, the more unfavorable the effect on meat color.

TVB-N analysis

TVB-N refers to the combined action of endogenous enzymes and bacteria in the muscle during the storage of animal food (Holman et al., 2021). It is highly temperature-sensitive and increases rapidly with small increases in storage temperature (Frank et al., 2019). The trend of TVB-N during aging at 4, 10, and 15°C was shown in Figure 2D. During aging at 4°C, the TVB-N content increased from the initial 4.6 to 12.5 mg/100 g after 14 days ($p < 0.05$). In vacuum-packaged beef aged at 4°C, it increased to 15 mg/100 g in approximately 16 days. During aging at 10°C, the TVB-N content increased to 13.4 mg/100 g after 10 days and continued to increase to 15 mg/100 g on the next day. The TVB-N content exceeded 15 mg/100 g after 5 days of aging at 15°C, indicating that the TVB-N values of beef increased rapidly at high temperatures, rose slowly in the early stages of storage, then rapidly increased.

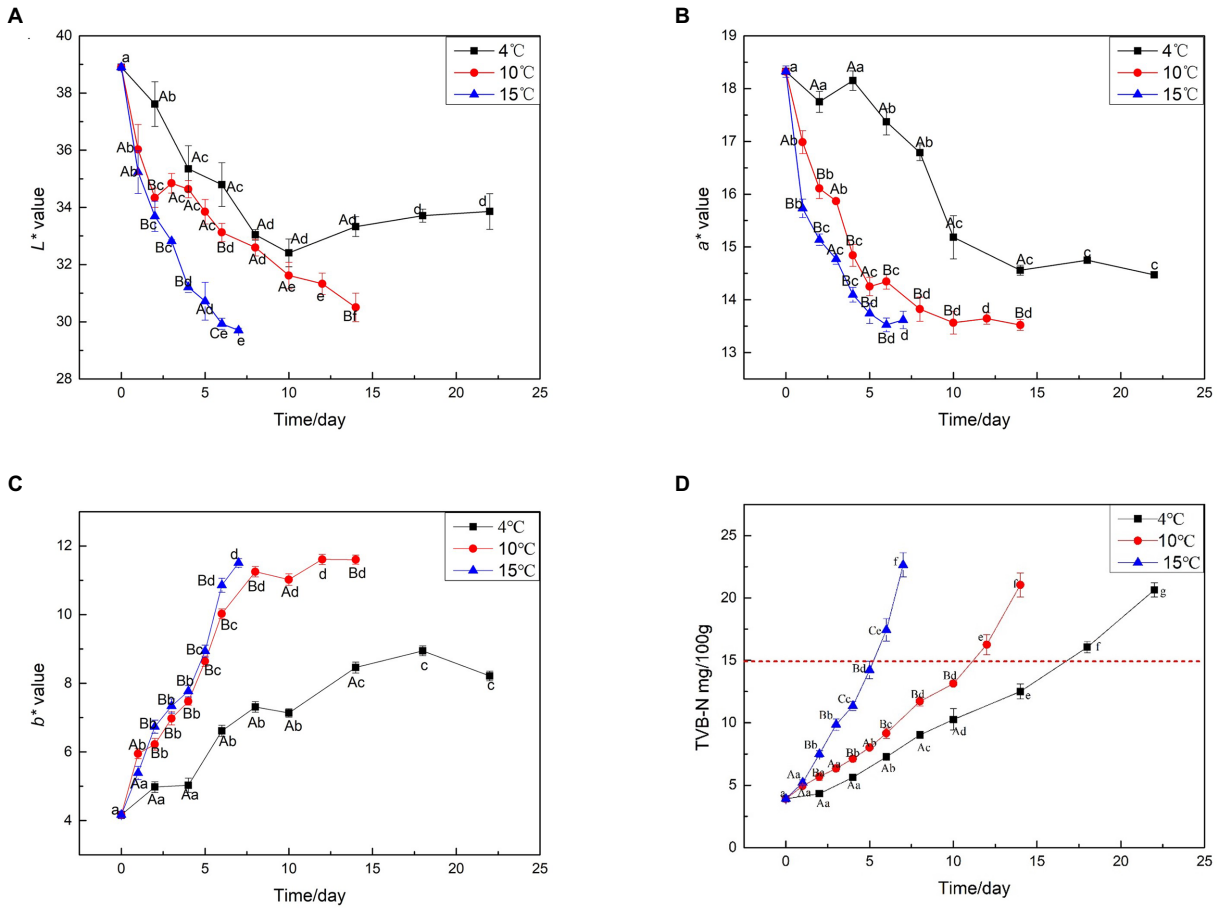

FIGURE 2
Surface color and TVB-N analysis on beef samples aging at 4, 10, and 15°C. **(A)** L* value, **(B)** a* value, **(C)** b* value, **(D)** TVB-N value.

Microbial counts

The changes in the microbial counts of beef samples aged at different temperatures are shown in Table 1. Temperature appears to be the most important factor that influences the spoilage and safety of meat (Kennedy et al., 2005). Significant aging time and temperature interactions affected the TVC and growth of *Pseudomonas*, *Brochothrix thermosphacta*, LAB, and *Enterobacteriaceae* ($p < 0.05$). Initially, microorganisms were present at low levels. The TVC in unaged beef samples was 3.1 ± 0.01 log CFU/g, indicating that the sample is of good quality (Yang et al., 2018). In beef samples aged at 4°C, TVCs increased slowly at the beginning of aging but increased rapidly on day 6 and exceeded 5.8 log CFU/g by day 14, at which the shear force value reduced to less than 50 N. During aging at 10°C, the microbial counts exceeded 7.0 log CFU/g on day 10, and when the shear value started to drop below 50 N on day 6, the corresponding microbial count was 6.0 log CFU/g. Similarly, during aging at 15°C, the shear value of beef started below 50 N on day 5, corresponding to the microbial count of 6.3 log CFU/g that did not exceed 7.0 log CFU/g (Yang et al., 2016). A TVC total of 7.0 log CFU/g is recommended as the load limit at the end of the shelf life for red meat, According to the microbial colony counts, the shelf life of beef samples as the aged temperature increased. In order to the quality and safety of beef, it could be consider transferring the beef to 4°C storage when the shear value of beef is reduced 50 N to extend the shelf life, which is also our next research program. *Pseudomonas*, *Brochothrix thermosphacta*, *Enterobacteriaceae*, and *Lactobacillus* increased with a trend similar to the trend shown by the total number of colonies. LAB was the dominant population in the vacuum-packaged beef samples in this study. Similarly, Gribble et al. (2014b) LAB, *Enterobacteriaceae*, and *Pseudomonas* spp. populations increased when the beef was subjected to higher aging temperatures.

Bacterial flora analysis

Overall structural changes in beef bacterial communities

In this study, high-throughput sequencing technology was used to investigate the microbiota found in beef samples collected

10.3389/fmicb.2022.1091486

TABLE 1 Microbial counts of beef samples under different aging temperature.

Colony counts (lg CFU/g)	Temperature	Aging time(days)										
		0	1	2	3	4	5	6	8	10	14	18
Total viable counts	4°C	3.1 ± 0.01	/	3.4 ± 0.05	/	3.9 ± 0.09	/	4.4 ± 0.05	4.8 ± 0.02	5.4 ± 0.05	5.8 ± 0.07	6.9 ± 0.05
	10°C		3.9 ± 0.12	4.3 ± 0.08	4.7 ± 0.04	5.2 ± 0.03	5.8 ± 0.11	6.0 ± 0.05	6.7 ± 0.21			
	15°C		4.1 ± 0.11	4.9 ± 0.04	5.3 ± 0.32	5.9 ± 0.14	6.3 ± 0.26					
Pseudomonas spp	4°C	2.0 ± 0.08	/	2.7 ± 0.05	/	2.9 ± 0.06	/	3.2 ± 0.03	3.7 ± 0.06	4.2 ± 0.04	4.4 ± 0.03	4.6 ± 0.04
	10°C		2.7 ± 0.03	3.5 ± 0.05	4.2 ± 0.11	4.7 ± 0.09	5.3 ± 0.10	5.7 ± 0.11	5.9 ± 0.14			
	15°C		2.4 ± 0.11	3.4 ± 0.14	3.8 ± 0.05	4.5 ± 0.03	5.9 ± 0.15					
B. thermosphacta	4°C	2.7 ± 0.01	/	3.0 ± 0.05	/	3.5 ± 0.02	/	4.3 ± 0.05	4.7 ± 0.06	5.1 ± 0.03	5.8 ± 0.06	5.9 ± 0.04
	10°C		3.8 ± 0.14	4.4 ± 0.13	5.0 ± 0.05	5.2 ± 0.06	5.4 ± 0.08	5.8 ± 0.03	5.8 ± 0.10			
	15°C		3.1 ± 0.19	3.9 ± 0.06	4.7 ± 0.05	5.1 ± 0.23	5.7 ± 0.31					
Lactic acid	4°C	2.5 ± 0.03	/	2.8 ± 0.06	/	3.6 ± 0.11	/	4.6 ± 0.05	5.1 ± 0.04	5.5 ± 0.06	6.3 ± 0.05	6.6 ± 0.06
bacteria	10°C		3.5 ± 0.03	4.2 ± 0.07	4.9 ± 0.01	5.4 ± 0.02	5.5 ± 0.05	6.2 ± 0.03	6.5 ± 0.09			
	15°C		3.8 ± 0.14	4.3 ± 0.11	5.6 ± 0.16	6.3 ± 0.09	6.7 ± 0.03					
Enterobacteriaceae	4°C	1.4 ± 0.07	/	1.7 ± 0.06	/	1.9 ± 0.02	/	2.3 ± 0.05	2.4 ± 0.04	3.2 ± 0.08	3.7 ± 0.05	4.2 ± 0.05
	10°C		1.7 ± 0.10	2.2 ± 0.03	2.5 ± 0.06	3.2 ± 0.04	3.3 ± 0.27	3.5 ± 0.18	3.7 ± 0.07			
	15°C		2.3 ± 0.04	2.7 ± 0.22	3.3 ± 0.14	3.7 ± 0.17	4.1 ± 0.15					

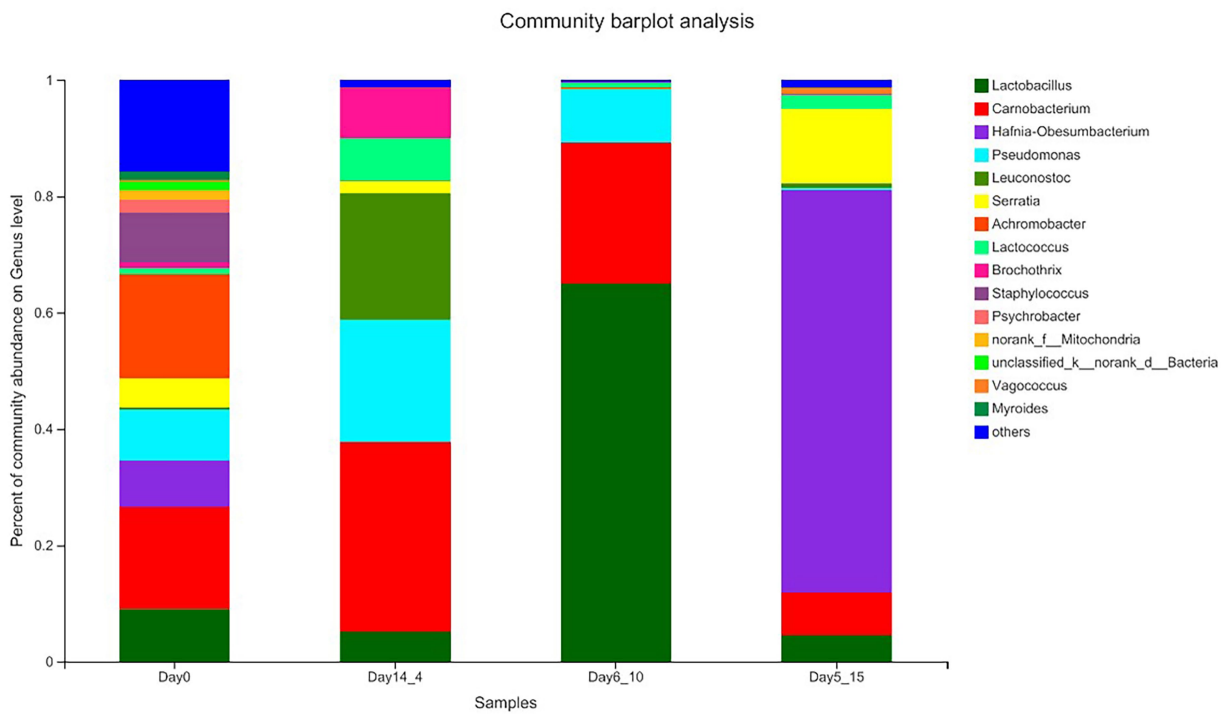

FIGURE 3
Relative abundance (%) of the top bacterial genera (Genus level) found on beef samples aging 14days at 4°C, aging 6days at 10°C, and aging 5days at 15°C.

at 14 days of aging at 4°C (Day14_4), 6 days of aging at 10°C (Day6_10), and 5 days of aging at 15°C (Day5_15).

The results of the species annotations were as follows: domain: 1, kingdom: 1, phylum: 30, class: 69, order: 168, family: 269, genus: 454, species: 649, OTU: 974. The top five phylum included Firmicutes, Proteobacteria, Actinobacteriota, Bacteroidota, and unclassified_k__norank_d__Bacteria. The top five genera included *Lactobacillus*, *Carnobacterium*, *Hafnia–Obesumbacterium*, *Pseudomonas*, and *Achromobacter*. Figure 3 shows the percentage of the most abundant bacterial genera in Day14_4, Day6_10, 5 Day5_15 and 0 day beef samples because these points of time corresponded to shear values that started

below 50 N. In the Day_0 sample, the dominant bacterial genera were *Vagococcus* and *Carnobacterium,* with average relative abundances of 17.95 and 17.60%, respectively, followed by *Lactobacillus*, *Pseudomonas*, *Staphylococcus*, *Hafnia–Obesumbacterium*, and *Serratia* with abundances ranging from 5.00 to 9.06%. *Leuconostoc*, *Brochothrix*, *Lactococcus*, and *Mitochondria* were also present in beef samples at abundances ranging from 0 to 5.00%. Chaillou et al. (2015) stated that these bacteria mainly originated from the meat processing environments, such as soil or water. In the sample aged at 4°C for 14 days, *Carnobacterium*, *Pseudomonas*, and *Leuconostoc* were the dominant genera. *Carnobacterium* increased to 32.55%, *Pseudomonas* increased from 8.78 to 21.01%, and *Cryptococcus* increased from 0.39 to 21.74% in the sample aged at 4°C for 14 days relative to those in the Day_0 sample. These species belong to the genus *Cryophilus* and exhibit good growth performance at low temperatures (Kaur et al., 2021). The genus *Lactobacillus* was clearly the dominant bacterial community in the Day6_10 sample and showed a seven-fold increase relative to that in the Day_0 sample and accounted for 65.02% of the total number of bacteria. This genus showed better growth performance at 10°C than at other temperatures. In the Day5_15 sample, the genus *Hafnia–Obesumbacterium* predominated, with its content reaching 69.24%, far exceeding the number of other genera. This result is a good indication that the structure of the flora in beef is affected by temperature. Low temperatures significantly favored the growth of LAB (*Carnobacterium* and *Leuconostoc*), whereas higher temperatures favored members of the phylum Proteobacteria (*Hafnia*). Given that the dominant genera often develop into specific spoilage bacteria, these results provide ideas for the precise prevention and control of spoilage bacteria in high-temperature aging.

Heatmap analysis of beef bacterial communities

A genus-level clustering heatmap based on the top 30 genera in terms of relative abundance was constructed to analyze and compare the composition and dynamic changes in microbial communities in different samples (Figure 4). The horizontal coordinate is the sample name, the vertical coordinate is the genus name, and the color gradient of the color block shows the variation in the abundance of the different species in the sample, with the values represented by the color gradient on the right-hand side of the graph. The heatmap demonstrated that in the day 0 sample,

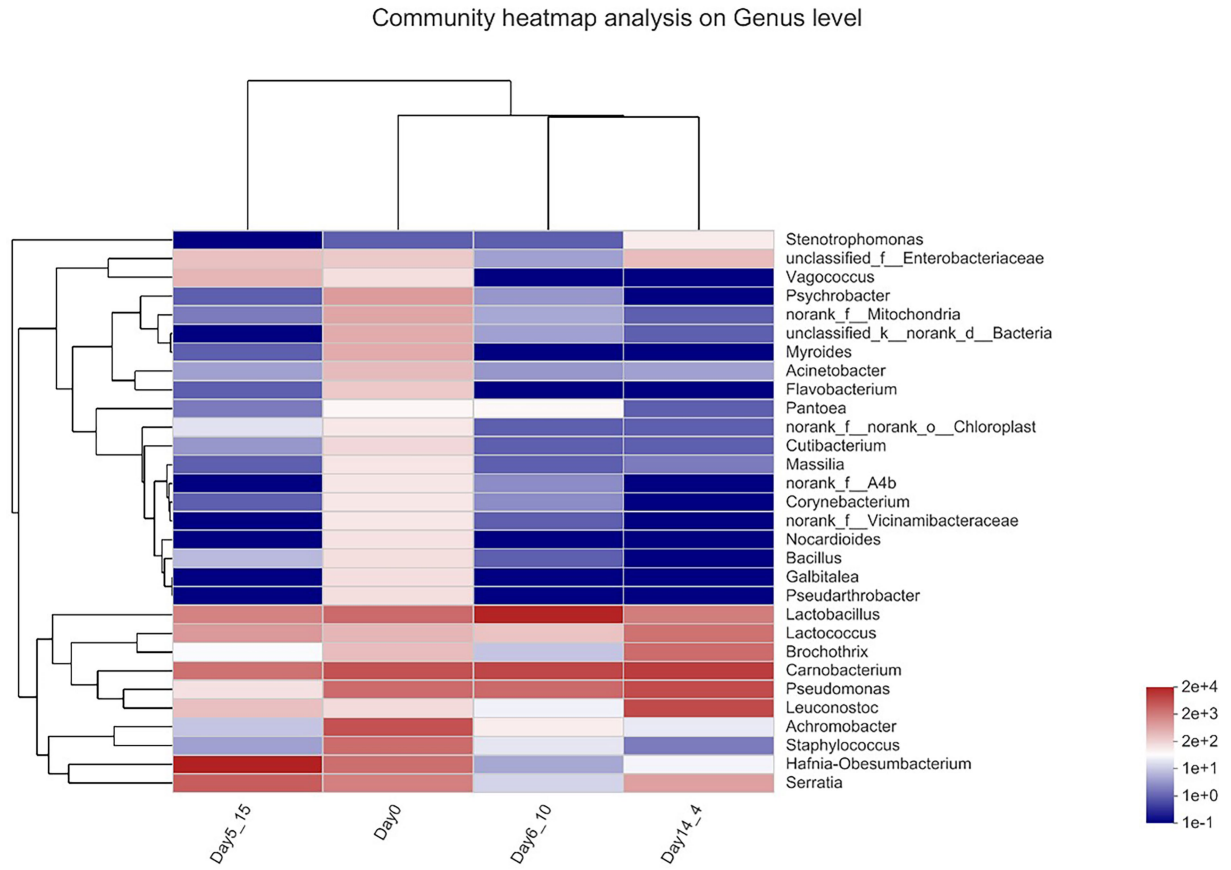

FIGURE 4
Heatmap of bacterial genera in beef samples found on beef samples aging 14days at 4°C, aging 6days at 10°C and aging 5days at 15°C.

Carnobacterium and *Vagococcus* clustered together with high relative OTU abundances during aging. *Carnobacterium*, *Pseudomonas*, and *Leuconostoc* clustered together with high relative OTU abundances in Day14_4. *Lactobacillus* clustered together with high relative OTU abundance on Day6_10 during aging. *Hafnia–Obesumbacterium* was present at higher relative contents in the Day5_15 sample. The bacterial compositions that gradually stabilized at late storage stages were generally dominated by bacteria that contribute largely to meat spoilage (Nychas et al., 2008).

Characteristic volatile fingerprints

A characteristic fingerprint corresponding to each aging temperature was established by using gallery plots, and the difference and specific distribution of volatile compounds between different aging temperatures were compared intuitively (Figure 5). The Gallery Plot plugin of LAV software was used to compare the differences in the volatile compounds in beef samples at aged at different temperatures comprehensively. The colors of the plots indicated the signal strengths of the compounds: the darker the signal, the weaker the signal intensity and vice versa (Huang et al., 2022). The signal intensities of most volatile compounds significantly increased after aging at high temperatures, indicating that the levels of most volatile compounds were positively correlated with the aging temperature.

As shown in Figure 5, all the peaks to be analyzed in the obtained two-dimensional GC–IMS spectrum were automatically generated on the basis of fingerprints. Each row in the figure represents all signal peaks selected in a beef sample, and each column in the figure represents the signal peaks of the same volatile organic compounds in different beef samples. The substances in the red box in the picture had the highest content on 0 day compared to other groups. This substance included benzaldehyde, which decreased during aging at 4, 10, or 15°C. Benzaldehyde, is found in hyacinth, lemongrass, and rockrose and is a volatile compound that potentially results from the Strecker degradation of tyrosine, which has a bitter almond, cherry, and associated with a strong almond odor (Ma et al., 2012), if the level are raised too high, the undesirable flavor may result. The content of the substances in the yellow box in Figure 5 increased significantly in the 4°C_14D sample ($p < 0.05$). These substances included 2-heptanone, isobutyl butyrate, 1-octen-3-ol, and 1-pentanol. 2-Heptanone can produce a buttery, creamy, and cheesy aroma; it can be used as a spice raw material and is critical to aging flavor (Resconi et al., 2012). Isobutyl butyrate exists in pineapples and other fruits naturally and has a pleasant aroma. It is potentially a characteristic compound of fresh beef. 1-Octen-3-ol is positively correlated with umami flavor and is a volatile

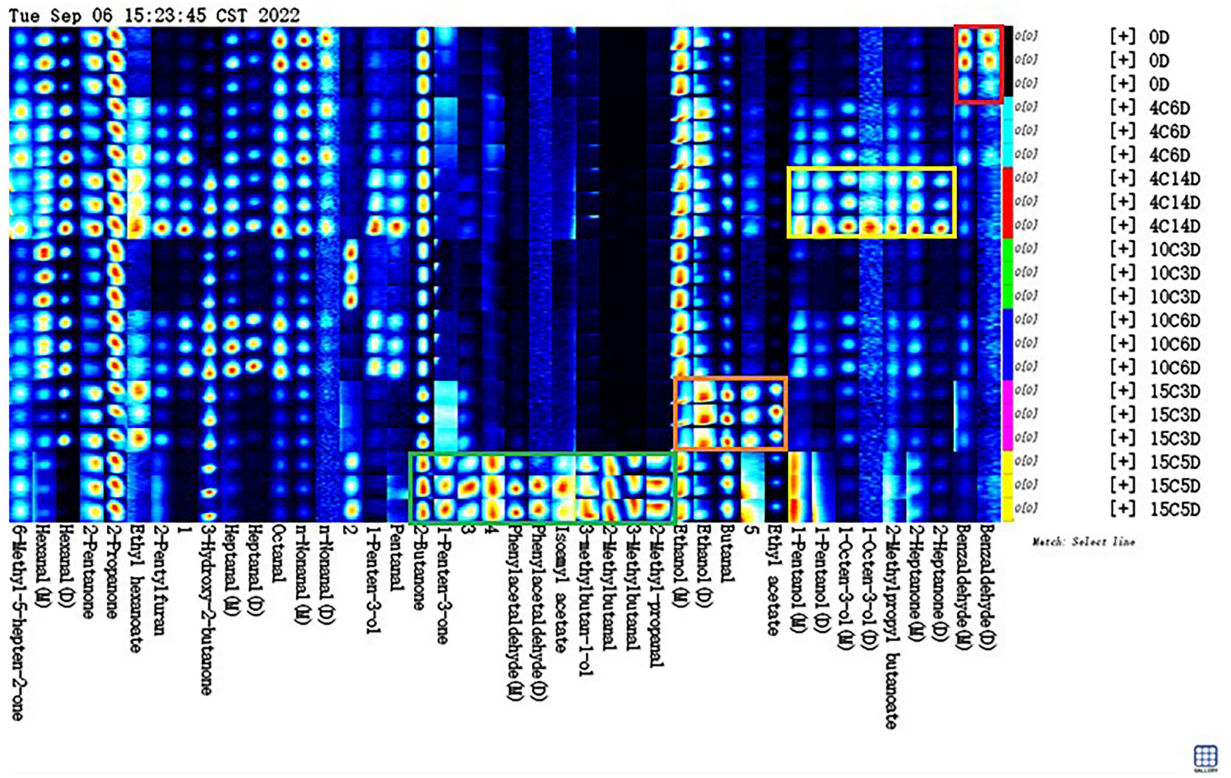

FIGURE 5
Fingerprint spectra of volatile compounds in beef samples different stages aging at 4, 10, and 15°C.

alcohol with a mushroom-like aroma that is found in dry-cured ham and dry sausage (Tansawat et al., 2013). Positive attributes, such as umami and juicy flavors in grain-fed steaks, are correlated with 1-octen-3-ol (Song et al., 2011). 1-Pentanol has a strong, sweet, balsamic aroma (Liu et al., 2022). Meanwhile, the dominant bacterial community was *Carnobacterium*, including that could produce these VOCs at low temperatures. The substances in the orange box in Figure 5 have the highest content in the 15C_3D sample. They included butanal and ethanol. Butanal is found in many essential oils, such as flowers, fruits, and dairy products, and has an ethereal fragrance when extremely diluted (Lee et al., 2019). Ethanol is the main component of wine, ethanol can also be used to make acetic acid, beverages, baked goods, and it generally have a low odour threshold, and thus they partly contribute to the flavour of cooked beef, what's more, butanal and ethanol was found to decrease or remain stable at chill temperatures, whilst an increase was observed at elevated temperatures in vacuum packaged conditions. The substances in the green box in Figure 5 have the highest content in the 15C_5D sample compare to other groups. They included 2-methylbutanal, 3-methylbutanal, 3-methylbutanol, 2-methyl-propanal, isoamyl acetate, phenylacetaldehyde and 1-penten-3-one, and 2-butanone. 2-Methylbutanal is described as having a brothy, grainy or boiled meat aroma, which improves the sensory value of products (Lee et al., 2021). 3-Methylbutanal is a colorless and transparent liquid that is used as an intermediate in the production of flavors (Mansur et al., 2019). 2-Methylbutanal and 3-methylbutanal are Strecker degradation products of isoleucine and leucine, respectively (Saraiva et al., 2014). 2-Methyl-propanal is used in the synthesis of cellulose esters and flavors and is commonly applied in baked goods and meat products (Utama et al., 2018). Aldehydes, in general, are unstable and can easily react with other compounds to produce compounds with different flavors, it have a low odor-detection threshold; hence, even a trace amount can contribute to meat flavor, and, consequently, they are the most interesting of the lipid-derived volatiles (Legako et al., 2016). Isoamyl acetate has banana and pear aromas and is widely used in the production of various fruity edible flavors (Ercolini et al., 2009). Phenylacetaldehyde is naturally found in chicken, bread, rose oil, and citrus oil and confers beef with a clear and evocative aroma that differs in accordance with quality grade; specifically, it is higher in prime and low-choice steaks than in standard steaks (Zhu et al., 2016). 1-Penten-3-one is mainly used as a spice for food and in onion, garlic, and mustard flavoring; it has been identified as the main contributor to the integral flavor of beef due to its high odor activity values (Vilar et al., 2022). 2-Butanone is an intermediate in the preparation of pharmaceuticals, fragrances, antioxidants, and certain catalysts (Pavlidis et al., 2019). Meanwhile, the dominant bacterial community was *Hafnia–Obesumbacterium*, which can use the nutrients in beef to produce these compounds (Argyri et al., 2015). It could conclude that different aging temperatures produce different flavor profiles, on the one hand, these compounds could be formed protein degradation or oxidation of fatty acids; on the other hand, some bacteria studied in this work have probably contributed to different levels in the accumulation/depletion of the measured metabolic compounds.

Conclusion

The results suggested that high-temperature (10 and 15°C) aging had a significantly shorter aging time than conventional aging (4°C) without affecting the safety of the product. This statement is supported by the practical equivalence of the surface color, TVB-N content, microbial counts, and flavor traits of the beef samples aged at high temperatures to those of the control samples. In this study, combining the total number of colonies and shear force values, it could be suggested that the aging time should be set 6 days at 10°C or 5 days at 15°C. On the basis of this new information, the beef industry is recommended to adopt shorter aging periods using slightly elevated temperatures 10 °C or and 15°C to capitalize on the advantages of a condensed aging period.

Data availability statement

The raw data supporting the conclusions of this article will be made available by the authors, without undue reservation.

Author contributions

BS, SZ, and XL designed the study. MW, YLe, and XY carried out the sample processing. HY performed the experimental data analysis and wrote the manuscript. All authors have read and agreed to the published version of the manuscript. All authors contributed to the article and approved the submitted version.

Funding

This work was financially supported by the National Natural Science Foundation of China (No. 32072143), the Major Public Welfare Projects of Henan Province (No. 201300111200), the Agriculture Research System of China (No. CARS-37), the Special Basic Research Fund for Central Public Research Institutes (No. 2021-YWF-ZYSQ-07), and Science and Technology Plan Project of Tibet Autonomous Region (XZ202101YD0019C).

Acknowledgments

I gratefully acknowledge the help of my supervisor, Professor Sun, who has offered me valuable suggestions in the academic

studies. Moreover, I would like to give my deeper thanks to my friends, XL, YLe, MW, and YLi.

Conflict of interest

The authors declare that the research was conducted in the absence of any commercial or financial relationships that could be construed as a potential conflict of interest.

Publisher's note

References

Argyri, A. A., Mallouchos, A., Panagou, E. Z., and Nychas, G. E. (2015). The dynamics of the HS/SPME–GC/MS as a tool to assess the spoilage of minced beef stored under different packaging and temperature conditions. *Int. J. Food Microbiol.* 193, 51–58. doi: 10.1016/j.ijfoodmicro.2014.09.020

Chaillou, S., Chaulot-Talmon, A., Caekebeke, H., Cardinal, M., Christieans, S., Denis, C., et al. (2015). Origin and ecological selection of core and food-specific bacterial communities associated with meat and seafood spoilage. *ISME J.* 9, 1105–1118. doi: 10.1038/ismej.2014.202

Colle, M. J., and Doumit, M. E. (2017). Effect of extended aging on calpain-1 and -2 activity in beef longissimus lumborum and semimembranosus muscles. *Meat Sci.* 131, 142–145. doi: 10.1016/j.meatsci.2017.05.014

Devine, W. T. (1994). Effect of rigor temperature on muscle shortening and tenderisation of restrained and unrestrained beef m. longissimus thoracicus et lumborum. *Meat Sci.* 51, 61–72.

Ercolini, D., Russo, F., Nasi, A., Ferranti, P., and Villani, F. (2009). Mesophilic and psychrotrophic bacteria from meat and their spoilage potential in vitro and in beef. *Appl. Environ. Microbiol.* 75, 1990–2001. doi: 10.1128/AEM.02762-08

Esteves, E., Whyte, P., Mills, J., Brightwell, G., Gupta, T. B., and Bolton, D. (2021). An investigation into the anaerobic spoilage microbiota of beef carcass and rump steak cuts using high- throughput sequencing. *FEMS Microbiol. Lett.* 368, 1–10. doi: 10.1093/femsle/fnab109

Frank, D., Zhang, Y., Li, Y., Luo, X., Chen, X., Kaur, M., et al. (2019). Shelf life extension of vacuum packaged chilled beef in the Chinese supply chain. A feasibility study. *Meat Sci.* 153, 135–143. doi: 10.1016/j.meatsci.2019.03.006

Gribble, A., Mills, J., and Brightwell, G. (2014a). The spoilage characteristics of *Brochothrix thermosphacta* and two psychrotolerant Enterobacteriaceae in vacuum packed lamb and the comparison between high and low pH cuts. *Meat Sci.* 97, 83–92. doi: 10.1016/j.meatsci.2014.01.006

Gribble, A., Mills, J., and Brightwell, G. (2014b). The spoilage characteristics of *Brochothrix thermosphacta* and two psychrotolerant Enterobacteriacae in vacuum packed lamb and the comparison between high and low pH cuts. *Meat Sci.* 97, 83–92. doi: 10.1016/j.meatsci.2014.01.006

Holman, B. W. B., Bekhit, A. E. A., Waller, M., Bailes, K. L., Kerr, M. J., and Hopkins, D. L. (2021). The association between total volatile basic nitrogen (TVB-N) concentration and other biomarkers of quality and spoilage for vacuum packaged beef. *Meat Sci.* 179:108551. doi: 10.1016/j.meatsci.2021.108551

Huang, Q., Dong, K., Wang, Q., Huang, X., Wang, G., An, F., et al. (2022). Changes in volatile flavor of yak meat during oxidation based on multi-omics. *Food Chem.* 371:131103. doi: 10.1016/j.foodchem.2021.131103

Kaur, M., Williams, M., Bissett, A., Ross, T., and Bowman, J. P. (2021). Effect of abattoir, livestock species and storage temperature on bacterial community dynamics and sensory properties of vacuum packaged red meat. *Food Microbiol.* 94:103648. doi: 10.1016/j.fm.2020.103648

Kennedy, J., Jackson, V., Blair, I. S., McDowell, D. A., Cowan, C., and Bolton, D. J. (2005). Food safety knowledge of consumers and the microbiological and temperature status of their refrigerators. *J. Food Prot.* 68, 1421–1430. doi: 10.4315/0362-028x-68.7.1421

Kilgannon, A. K., Holman, B. W. B., Mawson, A. J., Campbell, M., Collins, D., and Hopkins, D. L. (2019). The effect of different temperature-time combinations when ageing beef: sensory quality traits and microbial loads. *Meat Sci.* 150, 23–32. doi: 10.1016/j.meatsci.2018.11.023

Kim, M., Choe, J., Lee, H. J., Yoon, Y., Yoon, S., and Jo, C. (2019). Effects of aging and aging method on physicochemical and sensory traits of different beef cuts. *Food Sci. Anim. Resour.* 39, 54–64. doi: 10.5851/kosfa.2019.e3

Kim, Y. H. B., Kemp, R., and Samuelsson, L. M. (2016). Effects of dry-aging on meat quality attributes and metabolite profiles of beef loins. *Meat Sci.* 111, 168–176. doi: 10.1016/j.meatsci.2015.09.008

Kim, S. Y., Yong, H. I., Nam, K. C., Jung, S., Yim, D., and Jo, C. (2018). Application of high temperature (14°C) aging of beef M. semimembranosus with low-dose electron beam and X-ray irradiation. *Meat Sci.* 136, 85–92. doi: 10.1016/j.meatsci.2017.10.016

Kinsella, K. J., Prendergast, D. M., McCann, M. S., Blair, I. S., McDowell, D. A., and Sheridan, J. J. (2009). The survival of *Salmonella enterica* serovar Typhimurium DT104 and total viable counts on beef surfaces at different relative humidities and temperatures. *J. Appl. Microbiol.* 106, 171–180. doi: 10.1111/j.1365-2672.2008.03989.x

Koohmaraie, M. (1992). Effect of pH, temperature, and inhibitors on autolvsis and catalvtic activitv of bovine a skeletal muscfe μ-calpain. *J. Anim. Sci.* 1:2.

Lee, J., Featherstone, A., Nayga, R., and Han, D. (2019). The long-run and short-run effects of ethanol production on U.S. beef producers. *Sustainability* 11:1685. doi: 10.3390/su11061685

Lee, D., Lee, H. J., Yoon, J. W., Kim, M., and Jo, C. (2021). Effect of different aging methods on the formation of aroma volatiles in beef strip loins. *Foods* 10:146. doi: 10.3390/foods10010146

Legako, J. F., Dinh, T. T. N., Miller, M. F., Adhikari, K., and Brooks, J. C. (2016). Consumer palatability scores, sensory descriptive attributes, and volatile compounds of grilled beef steaks from three USDA quality grades. *Meat Sci.* 112, 77–85. doi: 10.1016/j.meatsci.2015.10.018

Li, S., Zamaratskaia, G., Roos, S., Båth, K., Meijer, J., Borch, E., et al. (2015). Inter-relationships between the metrics of instrumental meat color and microbial growth during aerobic storage of beef at 4°C. *Acta Agric. Scand. Sect. A Anim. Sci.* 65, 97–106. doi: 10.1080/09064702.2015.1072579

Liu, C., Hou, Y., Su, R., Luo, Y., Dou, L., Yang, Z., et al. (2022). Effect of dietary probiotics supplementation on meat quality, volatile flavor compounds, muscle fiber characteristics, and antioxidant capacity in lambs. *Food Sci. Nutr.* 10, 2646–2658. doi: 10.1002/fsn3.2869

Ma, Q. L., Hamid, N., Bekhit, A. E. D., Robertson, J., and Law, T. F. (2012). Evaluation of pre-rigor injection of beef with proteases on cooked meat volatile profile after 1day and 21days post-mortem storage. *Meat Sci.* 92, 430–439. doi: 10.1016/j.meatsci.2012.05.006

Mansur, A. R., Seo, D., Song, E., Song, N., Hwang, S. H., Yoo, M., et al. (2019). Identifying potential spoilage markers in beef stored in chilled air or vacuum packaging by HS-SPME-GC-TOF/MS coupled with multivariate analysis. *LWT* 112:108256. doi: 10.1016/j.lwt.2019.108256

Mansur, A. R., Song, E., Cho, Y., Nam, Y., Choi, Y., Kim, D., et al. (2019). Comparative evaluation of spoilage-related bacterial diversity and metabolite profiles in chilled beef stored under air and vacuum packaging. *Food Microbiol.* 77, 166–172. doi: 10.1016/j.fm.2018.09.006

Marino, R., Albenzio, M., Della Malva, A., Santillo, A., Loizzo, P., and Sevi, A. (2013). Proteolytic pattern of myofibrillar protein and meat tenderness as affected by breed and aging time. *Meat Sci.* 95, 281–287. doi: 10.1016/j.meatsci.2013.04.009

Nychas, G. E., Skandamis, P. N., Tassou, C. C., and Koutsoumanis, K. P. (2008). Meat spoilage during distribution. *Meat Sci.* 78, 77–89. doi: 10.1016/j.meatsci.2007.06.020

Pavlidis, D. E., Mallouchos, A., Ercolini, D., Panagou, E. Z., and Nychas, G. E. (2019). A volatilomics approach for off-line discrimination of minced beef and pork meat and their admixture using HS-SPME GC/MS in tandem with multivariate data analysis. *Meat Sci.* 151, 43–53. doi: 10.1016/j.meatsci.2019.01.003

Pierson, C. J. (1976). Effect of postmortem aging time and temperature on pH, tenderness and soluble collagen fractions in bovine longissimus muscle. *J. Anim. Sci.* 43, 1206–1210.

Resconi, V. C., Escudero, A., Beltrán, J. A., Olleta, J. L., Sañudo, C., and Mar Campo, M. D. (2012). Color, lipid oxidation, sensory quality, and aroma compounds of beef steaks displayed under different levels of oxygen in a modified atmosphere package. *J. Food Sci.* 77, S10–S18. doi: 10.1111/j.1750-3841.2011.02506.x

Saraiva, C., Oliveira, I., Silva, J. A., Martins, C., Ventanas, J., and García, C. (2014). Implementation of multivariate techniques for the selection of volatile compounds

as indicators of sensory quality of raw beef. *J. Food Sci. Technol.* 52, 3887–3898. doi: 10.1007/s13197-014-1447-y

Song, S., Zhang, X., Hayat, K., Liu, P., Jia, C., Xia, S., et al. (2011). Formation of the beef flavour precursors and their correlation with chemical parameters during the controlled thermal oxidation of tallow. *Food Chem.* 124, 203–209. doi: 10.1016/j.foodchem.2010.06.010

Tansawat, R., Maughan, C. A. J., Ward, R. E., Martini, S., and Cornforth, D. P. (2013). Chemical characterisation of pasture- and grain-fed beef related to meat quality and flavour attributes. *Int. J. Food Sci. Technol.* 48, 484–495. doi: 10.1111/j.1365-2621.2012.03209.x

Utama, D. T., Lee, S. G., Baek, K. H., Jang, A., Pak, J. I., and Lee, S. K. (2018). Effects of high-pressure processing on taste-related ATP breakdown compounds and aroma volatiles in grass-fed beef during vacuum aging. *Asian Australas J. Anim. Sci.* 31, 1336–1344. doi: 10.5713/ajas.17.0677

Vilar, E. G., O'Sullivan, M. G., Kerry, J. P., and Kilcawley, K. N. (2022). Volatile organic compounds in beef and pork by gas chromatography-mass spectrometry: a review. *Sep. Sci. Plus* 5, 482–512. doi: 10.1002/sscp.202200033

Wahlgren, N. M. (1994). Effect of rigor temperature on muscle shortening and tenderisation of restrained and unrestrained beef m. longissimus thoracicus et lumborum. *Meat Sci.* 51, 61–72. doi: 10.1016/s0309-1740(98)00098-9

Yang, X., Zhang, Y., Zhu, L., Han, M., Gao, S., and Luo, X. (2016). Effect of packaging atmospheres on storage quality characteristics of heavily marbled beef longissimus steaks. *Meat Sci.* 117, 50–56. doi: 10.1016/j.meatsci.2016.02.030

Yang, X., Zhu, L., Zhang, Y., Liang, R., and Luo, X. (2018). Microbial community dynamics analysis by high-throughput sequencing in chilled beef longissimus steaks packaged under modified atmospheres. *Meat Sci.* 141, 94–102. doi: 10.1016/j.meatsci.2018.03.010

Yim, D., Jo, C., Kim, H. C., Seo, K. S., and Nam, K. (2016). Application of electron-beam irradiation combined with aging for improvement of microbiological and physicochemical quality of beef loin. *Korean J. Food Sci. Anim. Resour.* 36, 215–222. doi: 10.5851/kosfa.2016.36.2.215

Zhu, M. J., Mendonca, A., and Ahn, D. U. (2004). Temperature abuse affects the quality of irradiated pork loins. *Meat Sci.* 67, 643–649. doi: 10.1016/j.meatsci.2004.01.005

Zhu, Q., Zhang, S., Wang, M., Chen, J., and Zheng, Z. P. (2016). Inhibitory effects of selected dietary flavonoids on the formation of total heterocyclic amines and 2-amino-1-methyl-6-phenylimidazo[4,5-b]pyridine (PhIP) in roast beef patties and in chemical models. *Food Funct.* 7, 1057–1066. doi: 10.1039/c5fo01055a

frontiers | Frontiers in Microbiology

TYPE Original Research
PUBLISHED 16 January 2023
DOI 10.3389/fmicb.2022.1113848

OPEN ACCESS

EDITED BY
Changyu Zhou,
Ningbo University, China

REVIEWED BY
Lujuan Xing,
Nanjing Agricultural University, China
Peijun Li,
Hefei University of Technology, China

*CORRESPONDENCE
Jing Wang
✉ wangjing@th.btbu.edu.cn

SPECIALTY SECTION
This article was submitted to Food Microbiology, a section of the journal Frontiers in Microbiology

RECEIVED 01 December 2022
ACCEPTED 28 December 2022
PUBLISHED 16 January 2023

CITATION
Liu Y, Cao Y, Yohannes Woldemariam K, Zhong S, Yu Q and Wang J (2023) Antioxidant effect of yeast on lipid oxidation in salami sausage.
Front. Microbiol. 13:1113848.
doi: 10.3389/fmicb.2022.1113848

Antioxidant effect of yeast on lipid oxidation in salami sausage

Yingli Liu[1], Yating Cao[1], Kalekristos Yohannes Woldemariam[1,2], Shengjie Zhong[1], Qinglin Yu[1] and Jing Wang[1]*

[1]China-Canada Joint Lab of Food Nutrition and Health (Beijing), Key Laboratory of Special Food Supervision Technology for State Market Regulation, Beijing Engineering and Technology Research Center of Food Additives, Beijing Technology and Business University, Beijing, China, [2]Delisi Group Co., Ltd., Weifang, China

Salami is a kind of fermented meat product with rich nutrition and unique flavor. Because it is rich in fat, it is easy to oxidize to produce bad flavor. Compared with the way of adding artificial or natural antioxidants to reduce the degree of sausage oxidation, the antioxidant characteristics of developing the starter itself deserve more attention. In this study, firstly the antioxidant activities of 5 strains of yeast were measured *in vitro*, and then the mixture of yeast and Lactobacillus rhamnosus YL-1 was applied to fermented sausage model. The effect of the starter in the sausage model was investigated through physicochemical parameters, degree of fat oxidation, free fatty acid content, and though volatile flavor compound analysis, sensory evaluation and various indexes after storage were observed. Metagenomics was used to explore metabolic pathways, functional genes and key enzymes related to lipid oxidizing substances in sausage in yeast. The results showed that Wickerhamomyces anomalus Y12-3 and Y12-4 had strong tolerance to H2O2, and had higher SOD and CAT enzyme activities. The addition of yeast effectively reduced the material value of peroxidation value and active thiobarbiturate in salami. In flavor analysis, the content of flavor compounds associated with lipid oxidation, such as hexanal, heptanal, nonanal and (E)-2-decenal were significantly lower with the use of Debaryomyces hansenii Y4-1 and Y12-3. Meanwhile, the possible pathways of yeast metabolism of flavor substances related to lipid oxidation (mainly aldehydes) were discussed with the help of metagenomic techniques. According to the results of metagenomics, fatty acid degradation (ko00071) metabolic pathway was related to the degradation of aldehydes through aldehyde dehydrogenase, which was the potential key enzyme.

KEYWORDS

yeast, lipid oxidation, salami, volatile compounds, antioxidant potential

1. Introduction

Fermented sausage refers to the meat products with long shelf life, unique flavor, texture, and color made by mixing raw meat with starter, seasoning and spices under specific temperature and humidity conditions and pouring them into casings (Huang and Huan, 2016). The important components in fermented meat products (protein and fat) are easily oxidized and degraded in the process of production and processing, thus affecting the quality of products. In the process of fermentation and maturation, proteins were hydrolyzed into short peptides and free amino acids, which are degraded into aldehydes, acids and esters under the action of microorganisms. Moderate degradation of protein can improve the nutritional value and flavor of the product, while excessive oxidation of protein will adversely affect the texture, water retention and flavor of meat, and oxidative induction of protein may also affect the digestibility

and reduce the nutritional value of meat products (Berardo et al., 2015). During fermentation process besides the protein hydrolysis the lipid oxidation hydrolysis also plays an important role in the production of flavor compounds. In addition to directly producing volatile flavor compounds such as hexanal, 2-nonenal, 2, 4-nonadienal, ethyl butyrate and 1-octene-3-ol, lipid oxidation degradation products can further participate in the Maillard reaction, thus giving fermented meat products unique and rich flavor (Liu et al., 2021b). Moderate fat oxidation can improve the meat flavor, quality, but excessive oxidation results in rancidity, loss of color and texture, and shorten the shelf life. It also affects consumer acceptance and highly contribute to the production of toxic substances such as malondialdehyde, amyl aldehyde, 4-hydroxy nonyl aldehyde which are a big concern to human health (Cao et al., 2019). Therefore, in processing and circulation of fermented meat products, keeping the balance of protein and fat hydrolysis and oxidation is a big concern.

The application of synthetic antioxidants is widely used technique, while it has its own drawbacks as mainly it is in general synthetic and are mainly a concern related to the cause of cancer. Among some of these antioxidants are butylated hydroxytoluene (BHT), butylated hydroxyanisole (BHA), and tert-butylhydroquinone (TBHQ) are mainly a concern to cancer while the use of ascorbic acid is considered to be the safest (Seo et al., 2021). With the decrease in synthetic antioxidants application, the screening and application of starter cultures for fermented sausage production with antioxidant capacity are attracting more and more attention. Zhang et al. (2017) measured the antioxidant activity of lactic acid bacteria isolated from fermented sour meat, among which, *L. curvatus* SR6 had high 2-diphenyl-1-picrylhydrazyl (DPPH) free radical scavenging and reducing ability, and *L. paracasei* SR10-1 had high hydroxyl free radical scavenging activity and lipid peroxidation inhibition ability. Coppola et al. (1997) isolated 138 strains of *Staphylococcus* and *Micrococcus* from molisana, a traditional Italian fermented sausage, all of which had Catalase activity test (CAT) activity and moreover could reduce nitrate to nitrite in most strains. Perea-Sanz et al. (2020) found that sausages inoculated with *D. Hansenii* maintained a lower degree of thiobarbituric acid reactive substances (TBARS), while inhibiting nitrite oxidation and promoting the formation of flavor substances such as 3-methylbutanal in sausages. This makes *D. Hansenii* as one of the potential strains that can be applied as a starter culture in fermented sausage products. Even though it has a big potential, the study on the antioxidant activity is very limited.

Although some strains such as Lactobacillus (Zhang et al., 2017), Staphylococcus (Coppola et al., 1997), Aspergillus (Arora and Chandra, 2010), Yeast (Banwo et al., 2021), and other microorganisms also show some antioxidant potential, while there is still lack of systematic and in-depth research in the antioxidant activity of starters applicable in fermented sausage production. Based on the understanding of this point, the antioxidant activities of five yeast strains were measured in vitro first. Considering the lack of acid producing and bacteriostatic effects of lactic acid bacteria, if yeast is used alone for sausage production, it will lead to quality and safety problems in the sausage. Therefore, lactic acid bacteria and yeast were mixed together to apply to fermented salami sausage. At the same time, lactic acid bacteria used alone is set as the experimental control to obtain more accurate results. The yeast antioxidant activity, degree of lipid oxidation and volatile flavor components of sausage after fermentation and storage were detected. The possible pathway of yeast metabolism of fatty acid through aldehydes degradation was analyzed by metagenomic technology.

2. Materials and methods

2.1. Yeast strains and culture media

Six species of starter cultures, designated *Debaryomyces hansenii* Y3-1, *Debaryomyces hansenii* Y4-1, *Wickerhamomyces anomalus* Y12-2, *Wickerhamomyces anomalus* Y12-3, *Wickerhamomyces anomalus* Y12-4, and *Lactobacillus rhamnosus* YL-1 were previously isolated from traditional fermented foods (Liu et al., 2015). They were stored at the School of Food and Health, Beijing Technology and Business University (BTBU), Beijing, China. *L. rhamnosus* YL-1 has been proved to have strong acid production capacity; in addition, it has been shown to contribute to good flavor formation. YL-1 were stored in glycerin and Man-Rogosa-Sharpe (MRS) broth medium mixture at −80°C until use, whereas yeasts were stored at −80°C on the glycerin and yeast-peptone-dextrose (YPD) broth medium mixture until use.

2.2. Determination of tolerance of hydrogen peroxide

After activation, the yeast was inoculated with the same OD value (OD600 = 1.0) into the sterilized YPD liquid medium which added H_2O_2 solution (the final concentration of H_2O_2 was 0.0, 2.0, 4.0, 6.0, or 8.0 mmol/L), and cultured at 28°C and 150 rpm for 24 h. The absorbance A_x of culture medium was measured at wavelength 600 nm (Yang et al., 2012). The group without H_2O_2 solution was used as blank control with the absorbance labeled as A_0. The same volume of liquid medium YPD was used as blank-zero with absorbance labeled as A_j. The survival rate of yeast was calculated according to the following formula.

$$\text{Survival Fraction (SF)} = \frac{\text{Ax}-\text{Aj}}{\text{A0}-\text{Aj}} \times 100\% \quad (1)$$

2.3. Determination of antioxidant activity of yeast *in vitro*

After yeast strains were activated twice on YPD plate, single colonies were selected and inoculated into 50 mL YPD liquid medium, and cultured overnight at 28°C and 150 rpm. Then, the fermentation broth was transferred to 50 mL YPD liquid medium with the same OD value (OD_{600} = 1.0), and cultured at 28°C and 150 rpm for 72 h.

After the end of fermentation, the fermentation liquid was centrifuged (4°C, 20700 × *g*, 5 min). The precipitation was washed with sterile deionized water and the yeast concentration was adjusted to 10^9 CFU/mL. At the same time, a part of cell suspension was taken for ultrasonic crushing for 40 min (650 W, 30 s on, 30 s off) under ice bath condition. After crushing, the mixture was centrifuged (4°C, 20700 × *g*, 5 min), and the supernatant was taken as the sample of intracellular cell-free extracts (Chen et al., 2015). The above two

samples were used for the determination of subsequent antioxidant experiments.

2.4. Free radical scavenging capacity

The hydroxyl free radical scavenging rate and superoxide anion free radical scavenging rate of each component of yeast fermentation for 72 h were determined by referring to the method of hydroxyl free radical determination kit and superoxide anion free radical determination kit (Nanjing Jiancheng Technology Co., Ltd., Nanjing, China).

2.5. Total antioxidant capacity and antioxidant enzyme activity

The total antioxidant capacity and antioxidant enzyme activity was conducted using the manual for T-AOC kit and Glutathione peroxidase (GPX) kit which were purchased from Nanjing Jiancheng Technology Co., Ltd. The catalase activity test was performed using Catalase (CAT) kit and the superoxide dismutase activity was conducted following Superoxide dismutase (SOD) kit purchased from Beijing Solarbio Technology Co., Ltd.

2.6. Sausage manufacture

The sausage was divided into following seven batches: batch CK (without inoculation), batch LGG inoculated with about 10^7 CFU/g of *L. rhamnosus* YL-1, batch S1 inoculated with about 10^7 CFU/g of *L. rhamnosus* YL-1 and 10^6 CFU/g of *D. hansenii* Y3-1, batch S2 inoculated with about 10^7 CFU/g of *L. rhamnosus* YL-1 and 10^6 CFU/g of *D. hansenii* Y4-1, batch S3 inoculated with about 10^7 CFU/g of *L. rhamnosus* YL-1 and 10^6 CFU/g of *W. anomalus* Y12-2, batch S4 inoculated with about 10^7 CFU/g of *L. rhamnosus* YL-1 and 10^6 CFU/g of *W. anomalus* Y12-3, batch S5 inoculated with about 10^7 CFU/g of *L. rhamnosus* YL-1 and 10^6 CFU/g of *W. anomalus* Y12-4. The formulation of the sausages was modified based on the formulation of Huang et al. (2020), Liu et al. (2021a). In detail it includes 80% lean pork meat, 20% pork back fat, 3% NaCl, 0.3% sucrose, 0.3% black pepper, 0.3% white pepper, 0.2% glucose, 0.1% garlic powder, 0.05% D-sodium erythorbate, and 0.015% sodium nitrite. Lean meat, fat, ingredients, and starter cultures were mixed with a blender at 4°C. The mixture was then stuffed into a collagen casing (200 g of meat-mixture for each sausage), and placed in a fermentation chamber.

All sausages were fermented for 20 h at 23°C with 80% relative humidity (RH) and for 24 h at 21°C with 65% RH. Then the sausages are ripened for 24 h at 20°C with 67% RH, 24 h at 19°C with 69% RH, 24 h at 18°C with 71% RH, 24 h at 16°C with 73% RH, 24 h at 15°C with 74% RH, 24 h at 14°C with 76% RH, 24 h at 12°C with 77% RH, and kept at 10°C with 73% RH until the end of 23 days. The samples in storage were kept sealed in the dark at room temperature until 60 days, others sausage was vacuum packaged and frozen at -80°C for subsequent analyses. At each corresponding fermentation time (0, 5, 10, 16, 23, and 60 days), three randomly selected sausages of each treatment were used to analyze pH, a_w, POV, TBARS, free fatty acids measurement, volatile compound analysis and sensory analysis.

2.7. Determination of physical and chemical properties of sausage

According to the method of Beck et al. (2021), the pH, and water activity a_w were measured during sausage ripening using a pH meter (Testo 205, AG, Testo, Lenzkirch, Germany) and an Aqualab 4TE water activity meter (Decagon Devices Inc., Pullman, WA, United States), respectively.

2.8. Determination of the peroxide value

Peroxide values for sausages were determined using the method of Vareltzis et al. (2008) with a few modifications. Take an appropriate amount. A broken sausage samples 2.5 g was transferred into a 50 mL centrifuge tube and, add 3 times of petroleum ether with respect to the sample weight, mixed well and left for extraction for 12 h. The sample solution is filtered by a funnel containing anhydrous sodium sulfate, and the filtrate is evaporated under reduced pressure at 39°C, and the residue is the sample to be tested.

The 1 mL of samples to be tested and 50 μL ferrous chloride (3.5 g/L) solution were transferred to centrifugal tube, then the volume was adjusted to 10 mL by mixture of dichloromethane:methanol (v :v = 7:3). Add 50 μL 30% potassium thiocyanate solution, mixed well and the mixture was allowed to stand for 5 min at room temperature. The absorbance of the supernatant was measured at wavelength 500 nm, mixture of dichloromethane:methanol (v :v = 7:3) was used to zero the instrument. POV value was calculated by standard curve, and the result was expressed as meq/kg sample.

$$\mathrm{POV} = \frac{\mathrm{C}}{\mathrm{m} \times 111.68} \tag{2}$$

Where, C is the mass of iron obtained against the standard curve, expressed in μg, m is the mass of the sample which represented by 1 mL of samples to be tested, expressed in g, and 116.68 is the conversion factor.

2.9. Determination of thiobarbituric acid reactive substances

The TBARS was conducted following the method of Filho et al. (2021) with some modifications. In detail adding 5.00 g of broken sausage sample into 100 mL conical flask containing 50 mL of 75.00 g/L trichloroacetic acid solution (including 1.00 g/L ethylenediaminetetraacetic acid disodium). The mixture sealed and shake well then incubated in a thermostatic oscillator at 50°C for 30 min. The mixture is filtrated when it cools to room temperature and 5 mL of filtrate was transferred into a tube containing 5 mL of 2.88 g/L thiobarbituric acid (TBA) solution. The sample solution mixed, sealed, allowed to react in a 90°C-water bath for 30 min. After reaction take the tube out, and allowed to cool to room temperature. The absorbance of the cooled reaction solution was

measured at 532 nm. The content of TBARS was determined by comparing the standard curve of malondialdehyde, which was expressed as mg of malondialdehyde /1.00 kg sausage sample (mg/kg).

2.10. Determination of free fatty acid

By referring to Feng et al. (2015) with some modifications, the lipids and free fatty acids were extracted and separated. In detail, 5.0 g of broken sausage samples were placed in 100 mL beaker, then add 60 mL of chloroform/methanol solution (v:v = 2:1). After mixing, the samples were homogenized (6000 rpm, 20 s) and broken twice in ice bath. The homogenates was made to stand in a fume hood for 1 h and then filtered. Filtrate was collected and 0.2-fold volume of 0.9% normal saline was added. The mixture was centrifuged for 10 min at 3000 × *g*, 4°C. The underlying organic phase was collected and evaporated into oil droplets in a vacuum at 44°C to serve as a lipid extraction sample.

Free fatty acids were separated as follows. The 100 mg lipids were weighed in a 2 mL centrifuge tube and dissolved using 1 mL chloroform and vortexed for mixing. The mixture was transferred to an aminopropyl-silica gel cartridges (SPE columns, Kangyuan Techbio Biological Technology Co., Ltd.) which activated with 1 mL chloroform. After activation, the free fatty acids in the SPE column were eluted with 3 mL 2 % acetic acid-diethyl ether solution.

The separated free fatty acid solution was dried by blowing dry nitrogen. The dried sample is mixed with 20 μL 2, 2-dimethoxy-propane (to absorb trace water produced in the process of methyl esterification) and 2 mL 14 % boron trifluoride-methanol solution, mixed and reacted in water bath at 60°C for 1 h. After methyl esterification and cooling, 1 mL n-heptane and 1 mL ultrapure water were added and dissolved using vortex. After standing for stratification, the upper organic phase was collected and dried with a nitrogen blower. Then the final volume was made up to 0.5 mL by n-heptane, then detected using GC-MS (Gas-chromatography-mass-spectrometry) detection.

The free fatty acids were separated and identified by GC-MS (8890 GC System, 5977B MSD) equipped with a DB-WAX capillary column (30 m × 250 μm × 0.25 μm, Agilent Technologies, Santa Clara, CA, United States). The GC conditions were as follows: Helium (purity of 99.99%) was used as a carrier gas at a constant flow rate of 1.0 mL/min. The inlet temperature was set to 250°C with a solvent delay of 2 min, kept at 1 μL for injection volume, and the split ratio was 5:1. The column initial temperature was 100°C, increased to 200°C at a rate of 10°C/min for 5 min, then further increased to 220°C at a rate of 1°C/min for 5 min (Huang et al., 2013).

The MS conditions were as follows. The auxiliary heater temperature and ion source temperature were respectively set to 240°C and 230°C, and the four-stage rod temperature was 150°C. MS fragmentation was detected in electron-impact (EI) mode (ionization energy of 70 eV) with an acquisition range from 40 to 500 m/z in full-scan mode. The experimental results were qualitatively analyzed by Supelco 37 Component FAME Mix (Supelco, Bellefonte, PA, United States; catalog No. 47885-U) and NIST 14 library, and quantitatively analyzed by peak area method.

2.11. Determination of volatile compounds

The Solid phase micro-extraction (SPME) method was used to extract and quantitate the aroma compounds according to the method of Li et al. (2015). Briefly, 3.0 g of minced sausage was weighed precisely and placed in a 20 ml headspace vial. Immediately after, 1 μL of internal standard (o-Dichlorobenzene, 1.306 μg/μL in methanol) injected quickly, The vial was placed in an HH-series digital constant-temperature water bath and incubated at 60°C for 30 min. Then volatile compounds were extracted with a extraction head (DVB/CAR/PDMS, 50/30 μm) for 30 min at 60°C.

Volatile compounds in sausage were separated and identified by GC-MS (8890 GC System, 5977B MSD) equipped with a InertCap WAX capillary column (60 m × 0.25 mm × 0.25 μm; GL Sciences, Tokyo, Japan). The GC conditions were as follows: Helium (purity of 99.999%) was used as a carrier gas at a constant flow rate of 1.6 mL/min. The inlet temperature was set to 250°C with desorbed 5 min. The column initial temperature was kept at 40°C for 3 min, increased to 180°C at a rate of 3°C/min for 3 min, then to 230°C at a rate of 10°C/min for 5 min. The ion source temperature was set to 230°C. MS fragmentation was detected in electron-impact (EI) mode (ionization energy of 70 eV) with an acquisition range from 45 to 500 m/z in full-scan mode (Martín et al., 2003). The retention time was calculated and compared with NIST 14 library to identify the peaks, and the ratio of peak area to internal standard peak area was calculated to determine the quantity.

2.12. Sensory analysis

Sensory evaluation of seven groups of sausage samples was carried out after fermentation. Sensory assessment was performed by 39 trained team members. Sausage samples are sliced into 2 mm slices and placed on white plates. Samples were randomly labeled with three digits, and each sample was evaluated three times. Cleanse the palate between samples was performed by ingesting salt-free biscuits and water. Odor (cheese, fruity, rancid, oily), texture, taste (sour, salty, mellow), and overall acceptability of the samples were evaluated according to a 7-point scale from 1 to 7, in which odor and taste indicators were scored according to the intensity of perception from low to high, and liking index was scored according to the degree of liking (Liu et al., 2018).

2.13. Metagenomic sequencing

The S4 group (Y12-3) and S5 group (Y12-4) of fermented sausages were selected for metagenomic sequencing in this experiment. After they were matured (23 days), they were crushed by a crusher and stored at −80°C for standby. Metagenomic sequencing was performed by the Shanghai Majorbio Bio-Pharm Technology Co., Ltd.

2.14. Statistical analysis

Three replicates were set for each treatment in this experiment. SPSS 25.0 (SPSS Inc., Chicago, IL, United States) were used for

statistical significance analysis of experimental data, and GraphPad Prism (Prism v8.0, GraphPad) was used for drawing.

3. Results and discussion

3.1. Comparison of tolerance of different yeast to H_2O_2

As an important eukaryote, yeast is faced with various pressures such as oxidative stress during its growth. H_2O_2 is a strong oxidant, which can be converted into hydroxyl radical under the catalysis of metal ions, and because of its toxicity to proteins, lipids, DNA, RNA, and other molecules, so the resistance of yeast to oxidative stress (such as H_2O_2) can reflect its antioxidant properties.

The effects of different concentrations of H_2O_2 on the survival rate of yeast strains were shown in **Figure 1**. Compared with the SF (100%) of the control group, the Y12-4 increased to a certain extent after 24 h treatment with 2.0 mM H_2O_2, which may be due to CAT in the yeast cells decomposed H_2O_2 into O_2, thereby promoting its growth. This conclusion is similar to that of Wang et al. (2020). In contrast, the SF of the other four yeast strains was inhibited at 2.0 mM H_2O_2. Growth of all yeasts was inhibited when the concentration of H_2O_2 reached 6 mM. Among them, Y12-4 has the highest SF (58.89%), followed by Y3-1 (25.94%) and Y12-3 (24.29%). When the concentration of H_2O_2 was 8 mM, the SF of Y12-4 remained 9.64%. In conclusion, Y12-4 was the most tolerant to H_2O_2, followed by Y3-1 and Y12-3. While, strains Y4-1 and Y12-2 were the most sensitive to H_2O_2.

3.2. Comparison of free radical scavenging ability of different yeasts

Hydroxyl free radicals are an extremely active reactive oxygen species with strong oxidation capacity, which can easily cause damage to macromolecules of biological cells, thus affecting the normal function of cells. The hydroxyl radical scavenging ability of the intact cell suspension and the broken cell-free extracts of 5 yeast strains was measured, and the results were shown in **Figure 2A**. The hydroxyl radical scavenging capacity of 5 yeast strains was significantly different ($p < 0.05$). The hydroxyl radical scavenging rate of the intact cell suspension exceeded 45%, while that in the broken cell-free extracts was between 28 and 44 %. Among them, the intact cell suspension scavenging rate of Y12-4 was the highest, reaching 55.27%, and the scavenging rate in the broken cell-free extracts of Y4-1 was the highest, reaching 43.23%. Overall, the hydroxyl radical scavenging rates of Y3-1 and Y12-2 were significantly lower than that of other strains ($p < 0.05$).

Superoxide anion radical (O_2^-) is a relatively weak oxidant. Although it cannot directly induce the oxidation of lipids, it can undergo Fenton reaction in the presence of metal ions, forming strongly oxidized hydroxyl radicals and then participate in oxidation. The same way with the hydroxyl free radical scavenging activity the superoxide anion radical scavenging ability was measured for five yeast strains with whole cell and broken cell as shown in **Figure 2B**. The scavenging ability of superoxide anion radical of 5 yeast strains was significantly different ($p < 0.05$). In terms of different components, contrary to the results of hydroxyl radical scavenging ability, the scavenging rate of broken cell-free extracts exceeded 51%, which was stronger than that of intact cell suspension. The scavenging rate of Y12-2 broken supernatant was the highest, reaching 57.48%. The scavenging rate of superoxide anion free radicals in intact bacterial suspension was 30−42%, and the scavenging rate of Y3-1 intact bacterial suspension was 41.90%, which was significantly higher than that of other strains ($p < 0.05$).

In conclusion, there were significant differences in the free radical scavenging activities of intact cell suspension and broken cell-free extracts of different yeasts. The free radical scavenging activity of intact cell suspension may be related to its antioxidant substances (such as enzymes, polyphenols, and other yeast secretions) and polysaccharide proteins on the cell wall surface (Jaehrig et al., 2008). Li et al. (2012) found that Polysaccharides or proteins on the surface of intact cells of plantarum C88 participate in the DPPH scavenging effect. After removing these compounds, the DPPH scavenging ability of suspension is significantly reduced. The free radical scavenging activity of the broken supernatant may be attributed to the role of GSH-Px, SOD, CAT and other antioxidant enzymes. In general, the hydroxyl free radical scavenging ability of intact cell suspension is higher than that of the corresponding broken cell-free extracts, which may be due to the thick cell wall of yeast, and makes it difficult for ultrasonic crushing to release all the antioxidant substances stored in the cells into the supernatant, so that the free radical scavenging activity of the broken cell-free extracts is lower.

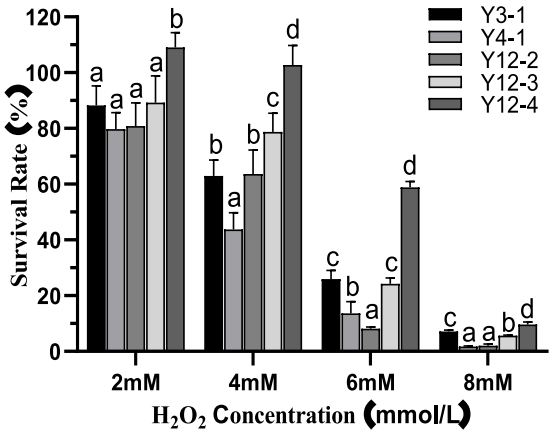

FIGURE 1
Survival rate of yeast at different concentrations of H_2O_2. Different letters (a–d) indicated that there was significant difference in survival rate between different yeast groups at the same H_2O_2 concentration ($p < 0.05$).

3.3. Comparison of total antioxidant capacity of different yeasts

The total antioxidant capacity (T-AOC) is the result of the combined action of antioxidant enzymes and non-enzymatic antioxidant substances in the tested samples, as well as the ability to scavenge free radicals, chelate metal ions and decompose peroxide. The T-AOC of the broken cell-free extracts of 5 yeast strains was measured, and the results were shown in **Figure 3**. All the broken cell-free extracts of different yeast had a certain total antioxidant capacity,

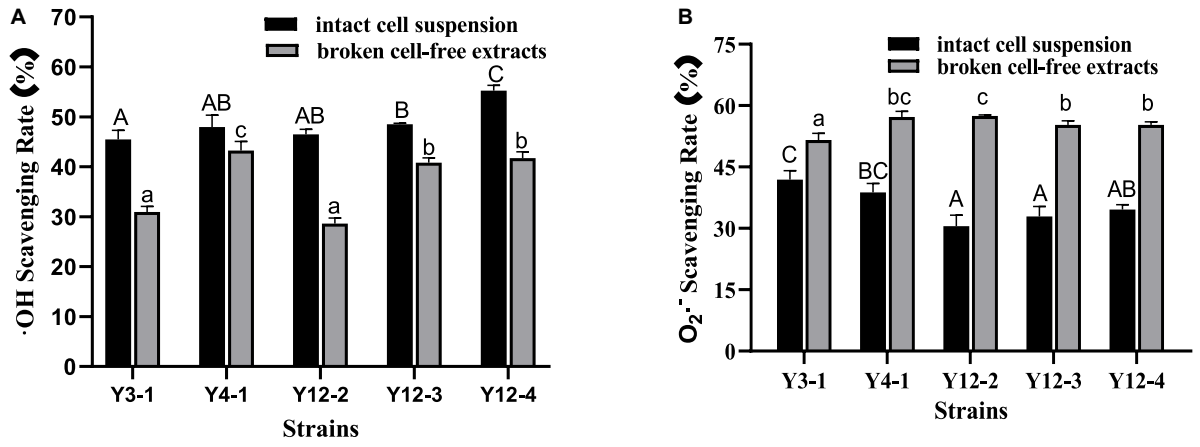

FIGURE 2
Free radical scavenging rate of different yeasts. **(A)** • OH Scavenging Rate; **(B)** O_2 • $^-$ Scavenging Rate. Different capital letters indicated that there was significant difference in free radical scavenging rate among different intact cell suspension ($p < 0.05$). Different lowercase letters indicated that there was significant difference in the free radical scavenging rate among different broken cell-free extracts ($p < 0.05$).

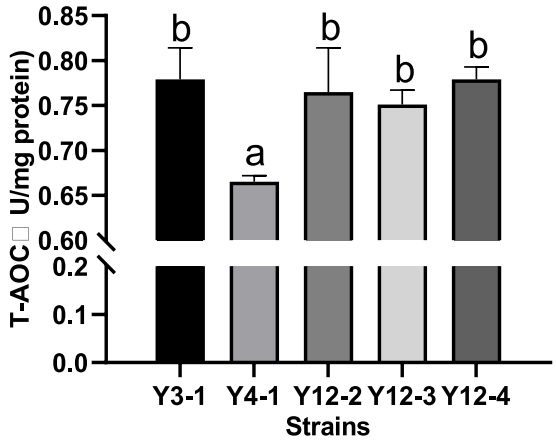

FIGURE 3
Determination of total antioxidant capacity (T–AOC) of different yeasts. Different letters indicated significant difference in total antioxidant capacity among different strains ($p < 0.05$).

indicating that there were substances with antioxidant activity in the supernatant after crushing. However, except Y4-1, which had a low total antioxidant activity (0.779 U/mg protein), the total antioxidant capacity of other strains higher and had no significant difference ($p < 0.05$).

3.4. Comparison of main antioxidant enzyme activities of different yeasts

Antioxidant enzymes, mainly including CAT, SOD, and GPX, play an important role in scavenging free radicals. The higher the enzyme activity, the stronger the antioxidant capacity. The activity results of main antioxidant enzymes in the broken cell-free extracts of these 5 yeast strains are shown in Table 1.

Catalase activity test can catalyze the decomposition of H_2O_2 into H_2O and O_2. In this study, the CAT enzyme activity of these 5 strains ranged from 88.31 to 100.44 U/mg protein of which Y12-4 had the highest enzyme activity, reaching 100.44 ± 2.08 U/mg protein ($p < 0.05$), which was consistent with its H_2O_2 tolerance. Superoxides in almost all cells and cellular organisms are eliminated by SOD. In this study, the SOD activity of these 5 strains ranged from 3.85 to 10.04 U/mg protein, and Y12-4 had the highest SOD activity, reaching 10.04 ± 0.24 U/mg protein ($p < 0.05$). GPX is an important hydroxyl radical scavenger. GPX activity wasn't detected in all yeast strains except Y12-2, which may be due to the sensitivity of the detection method is low or the GPX activity is too low to be detected.

Each yeast strain has its own advantages and disadvantages in different *in vitro* antioxidant test indexes, and there is a lager differences between the *in vitro* antioxidant test conditions and the actual application environment of fermented sausage. For example, its inhibition or promotion of lipid and protein oxidation in fermented sausage is also related to lipase and protease activities and metabolic regulation. Therefore, all the 5 yeast strains were applied to the production of fermented sausage to further explore their effects on lipid oxidation, free fatty acid changes and volatile flavor substances.

3.5. Analysis of pH value of fermented sausage in each group

LAB produces a large amount of lactic acid through carbohydrate metabolism at initial stage of sausage fermentation, rapidly reducing the pH value of sausage, thus inhibiting the growth of spoilage organisms and promoting the formation of flavor and color of sausage.

As shown in Figure 4, the pH value of ground meat on 0 days was about 5.8. On the 5th day of fermentation, the pH value of the sausage group with *L. rhamnosus* YL-1 was decreased to about 4.9, which was significantly lower than that of the blank group CK ($p < 0.05$), indicating that YL-1 had good acid-producing capacity in the sausage. When the sausages were matured after 23 days of fermentation, there was no significant difference ($p < 0.05$) in pH value of fermented sausage groups except for CK group and S1 group, which was around 5.6 and 5.2, respectively. The increase of pH value in S1 group may

TABLE 1 The main antioxidant enzyme activities in the broken cell-free extracts (*U/mg protein*).

	Y3-1	Y4-1	Y12-2	Y12-3	Y12-4
CAT	91.70 ± 3.05ab	93.09 ± 0.28b	88.31 ± 1.10a	92.12 ± 0.99b	100.44 ± 2.08c
SOD	7.36 ± 0.28c	5.13 ± 0.54b	3.85 ± 0.62a	6.75 ± 0.25c	10.04 ± 0.24 days
GPX	n.d.	n.d.	Trace	n.d.	n.d.

Different lowercase letters indicated that there was significant difference in antioxidant enzyme activity among different strains ($p < 0.05$). n.d., indicates no detection.

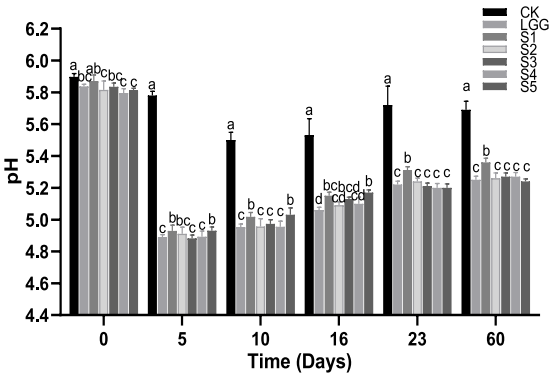

FIGURE 4
Evolution of pH value during the ripening of the different samples of sausage. Different letters indicate that there is significant difference in pH value between different groups of fermented sausage at the same time ($p < 0.05$).

be related to the metabolism of lactic acid by *D. hansenii* Y3-1 (He et al., 2017). On the whole, the pH value of fermented sausage in each group showed a process of first decreasing and then slowly increasing (after 10 days of fermentation). This may be due to the degradation of the protein in fermented sausage by microorganisms or endogenous protease to produce basic amino acids, biological amines and TVB-N, resulting in a slow increase in pH value (Liu et al., 2013).

3.6. Analysis of a_w value of fermented sausage in each group

The a_w directly affects the growth and metabolism of microorganisms. It is generally believed that when a_w is lower than 0.90, it can effectively inhibit the growth of spoilage and pathogenic bacteria (Leistner and Gould, 2002). As shown in **Figure 5**, the initial a_w values of the 5 groups of sausage samples were all around 0.97. With the progress of fermentation, the water was gradually lost and the a_w value showed a trend of slow decline. At the end of 23rd days of fermentation, the a_w value dropped to below 0.78 in all groups. From the point of different starter groups at about the 10 days, the a_w of fermented sausage in LGG, S1, S2, and S4 groups were significantly lower than that in CK group ($p < 0.05$). This may be caused by the fact that lactic acid produced by *L. rhamnosus* at the initial stage of fermentation reduced the pH value of the sausage system, made myosin close to the isoelectric point, changed its binding ability with water, and thus promotes water loss (Hu et al., 2021). At the end of the 23rd day of fermentation, the drying speed of the CK control group may be too fast due to the high pH value, low gelatinization degree of protein and loose texture. While there was a significant difference between the mixed starter culture group and the a_w of the LGG group, which may be because the yeast mainly grew on the surface of the sausage or the outside of the meat filling during the fermentation process, thus controlling the loss of the moisture activity of the mixed starter culture fermented sausage was significantly higher than that of the LGG group (Ramos-Moreno et al., 2021).

3.7. Analysis of POV value of fermented sausage in each group

The determination of POV reflects the extent to which sample fat is oxidized to hydroperoxide, and is applicable to the determination of meat product quality at the initial stage of oxidation. As shown in **Figure 6**, POV value rose at first in the whole process of sausage fermentation and storage. With a trend of decreased slightly at 16–23 days of fermentation, and then increases again at 23–60 days. This is mainly because the hydroperoxide of fat is extremely unstable in the process of lipid oxidation, which is easy to further oxidize to form small molecular compounds such as aldehydes and ketones, thus affecting the accuracy of POV value (Zhang et al., 2021). Kim et al. (2010) also obtained similar results when exploring the influence of different addition forms of garlic and BHA on emulsion-type sausage quality. Between different starter groups, the POV value of fermented sausage in S5 group (with yeast added) was significantly lower than that in LGG group (without yeast added) at 23rd days ($p < 0.05$). In the sausage samples stored for 60 days, the POV value of fermented sausage in S1, S3, S4, and S5 groups was significantly lower than that in CK and LGG groups ($p < 0.05$), indicating that the addition of yeast had a certain inhibitory effect on the change of sausage POV.

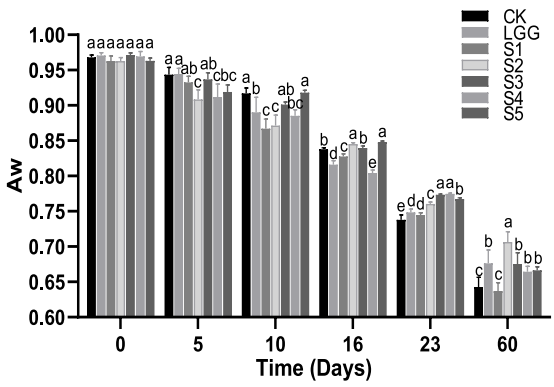

FIGURE 5
Evolution of a_w value during the ripening of the different samples of sausage. Different letters indicate that a_w value of fermented sausage in different groups has significant difference at the same time ($p < 0.05$).

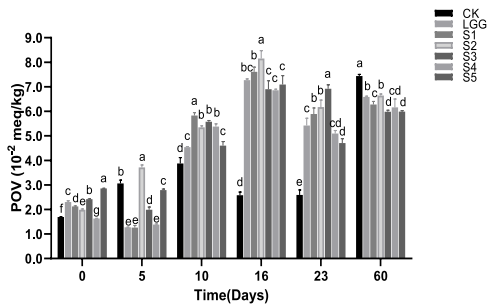

FIGURE 6
Evolution of peroxide value (POV) value during the ripening of the different samples of sausage. Different letters indicate that POV values of different groups of fermented sausage have significant difference at the same time ($p < 0.05$).

3.8. Analysis of TBARS value of fermented sausage in each group

Thiobarbituric acid (TBA) is the most commonly used method to evaluate the fat oxidation of meat products. TBARS value represent the contents of all substances that can react with TBA in meat products, mainly the content of malondialdehyde, the secondary product of lipid oxidation, and is a direct indicator of the degree of oxidative deterioration of meat products. Its results are highly related to the sensory quality and the degree of fat oxidation of meat products. Tarladgis et al. (1960) found that the TBARS value was highly correlated with the odor evaluation results of sensory reviewers, with a correlation coefficient of 0.89, and when the TBARS value ranged from 0.5 to 1.0, the reviewers could perceive the rancidity taste.

As shown in **Figure 7**, TBARS values show an overall upward trend in the whole process of sausage fermentation and storage. However, TBARS in CK, S3, S4, and S5 groups were slightly reduced on the 23rd day, which may be due to the fact that malondialdehyde reacted with protein in a binding state and was not detected. Except S2 group, the TBARS of sausage in all groups reached the maximum value at 60 days. The TBARS values of S1, S2, S3, S4, and S5 sausage in yeast group were 1.25, 0.50, 0.79, 1.07, and 0.70 mg MDA/kg sausage, respectively. It was significantly lower than that of 2.45 and 3.60 mg MDA/kg sausage in CK and LGG groups ($p < 0.05$), indicating that yeast supplementation could inhibit the increase of TBARS value of sausage.

3.9. Analysis of free fatty acid content of fermented sausage in each group

Free fatty acids (FFA) play an important role as precursors to the formation of flavor substances in fermented sausage. The release of a certain amount of FFA during sausage fermentation is conducive to the formation of special flavor of sausage. The effect of different starter on lipid hydrolysis of fermented sausage could be evaluated by measuring the content of FFA in each group. As shown in **Table 2**, 7 types of saturated fatty acids (SFA), 4 types of monounsaturated fatty acids (MUFA) and 4 types of polyunsaturated fatty acids (PUFA) were detected, respectively in each group of the fermented sausage, and the types of FFA did not change between the groups, which means that microbial fermentation only improved the degree of hydrolysis of FFA, but didn't change the way of lipid hydrolysis. Chen et al. (2017) also reached a similar conclusion when exploring the effects of bacterial fermentation on lipid decomposition and lipid oxidation in Harbin dry sausage.

The CK group is the sausage without inoculating the starters. Compared with the content of fatty acids in the meat mince used for the sausage making, the changes of these two groups are not obvious, with total fatty acids contents of 22.876 mg/g fat and 22.967 mg/g fat, respectively. While total fatty acids contents in LGG, S1, S2, and S5 groups increased to 29.343, 26.588, 24.330, and 36.106 mg/g fat, respectively, indicating that the addition of starter, especially Y12-4, was beneficial to the hydrolytic release of free fatty acids. While for S3 and S4 groups they did not increase the content of free fatty acids in fermented sausages after inoculation, which may be related to the lipase activity of Y12-2 and Y12-3 strains. Another aspect may also be that during the ripening process of sausage fermentation, a large number of unsaturated fatty acids are oxidized to lipid carbonyl compounds, and at the same time, alcohols, aldehydes and ketones are produced, which can form peroxides through free radical chain reaction. These secondary reactions produce a large number of volatile compounds, thereby reducing the content of free fatty acids. According to the proportion of different fatty acids in total fatty acids, the contents of SFA and MUFA were about 38 %, higher than PUFA (22−25 %). Compared with CK group, the proportion of SFA in S1, S2, S3, S4, and S5 groups added with starter decreased, while the proportion of PUFA increased. It is generally believed that the addition of starter is conducive to the hydrolysis of lipids into short-chain volatile fatty acids and other substances, endowing sausages with special flavor, promoting the degradation of SFA and the release of MUFA and PUFA (Hu et al., 2021). According to the types of fatty acids, palmitic acid, stearic acid, oleic acid and linoleic acid were relatively higher in all sausage samples, accounting for about 89% of the total fatty acids, which were the main components of FFA in fermented sausage.

3.10. Analysis of volatile flavor substance of fermented sausage in different groups

The determination results of flavor substances in sausage samples are shown in **Table 4**. A total of 75 volatile flavor substances were

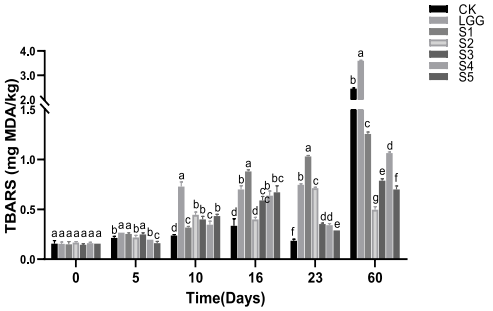

FIGURE 7
Evolution of thiobarbituric acid reactive substances (TBARS) value during the ripening of the different samples of sausage. Different letters indicate that there are significant differences in TBARS values between different groups at the same time ($p < 0.05$).

TABLE 2 Changes of free fatty acids (FFA) content in different fermented sausage samples.

Time (d)	0	23						
FFA (mg/g fat)	Meat mince	CK	LGG	S1	S2	S3	S4	S5
C10:0	0.122 ± 0.006b	0.119 ± 0.006b	0.136 ± 0.006b	0.129 ± 0.009b	0.135 ± 0.005b	0.136 ± 0.013b	0.129 ± 0.004b	0.172 ± 0.004a
C12:0	0.017 ± 0.003cd	0.015 ± 0.008d	0.031 ± 0.005b	0.022 ± 0.003bcd	0.028 ± 0.003bc	0.029 ± 0.004b	0.022 ± 0.002bcd	0.065 ± 0.006a
C14:0	0.498 ± 0.076d	0.538 ± 0.064cd	0.692 ± 0.007b	0.659 ± 0.045b	0.617 ± 0.038bc	0.594 ± 0.049bcd	0.536 ± 0.017cd	1.011 ± 0.069a
C16:0	4.818 ± 0.433d	4.981 ± 0.335cd	6.183 ± 0.062b	5.564 ± 0.226bc	5.276 ± 0.221cd	4.749 ± 0.117d	4.814 ± 0.614d	7.587 ± 0.345a
C17:0	0.098 ± 0.004c	0.086 ± 0.007d	0.136 ± 0.003a	0.121 ± 0.007b	0.095 ± 0.006cd	0.070 ± 0.001e	0.054 ± 0.006f	0.131 ± 0.003ab
C18:0	3.144 ± 0.334b	3.155 ± 0.212b	4.165 ± 0.144a	3.427 ± 0.196b	3.207 ± 0.194b	2.650 ± 0.019c	2.341 ± 0.181c	4.536 ± 0.178a
C20:0	0.098 ± 0.001b	0.096 ± 0.004b	0.117 ± 0.003a	0.097 ± 0.003b	0.096 ± 0.003b	0.088 ± 0.001c	0.080 ± 0.004d	0.102 ± 0.002b
C16:1	0.677 ± 0.046b	0.689 ± 0.071b	0.866 ± 0.016b	0.800 ± 0.051b	0.796 ± 0.045b	0.772 ± 0.050b	0.756 ± 0.089b	1.425 ± 0.229a
C17:1	0.094 ± 0.008c	0.084 ± 0.013cd	0.128 ± 0.001b	0.126 ± 0.006b	0.093 ± 0.007c	0.080 ± 0.002cd	0.071 ± 0.009d	0.162 ± 0.016a
C18:1n9c	7.395 ± 0.811d	7.739 ± 0.572cd	9.840 ± 0.128b	8.730 ± 0.408c	8.046 ± 0.420cd	7.295 ± 0.148d	7.220 ± 0.671d	12.013 ± 0.713a
C20:1	0.250 ± 0.012c	0.264 ± 0.021c	0.360 ± 0.006a	0.310 ± 0.016b	0.293 ± 0.019b	0.249 ± 0.003c	0.212 ± 0.014d	0.298 ± 0.000b
C18:2n6c	5.054 ± 0.584c	4.690 ± 0.415c	5.963 ± 0.062b	5.797 ± 0.374b	5.039 ± 0.309c	4.943 ± 0.187c	4.535 ± 0.156c	7.642 ± 0.476a
C18:3n3	0.306 ± 0.026cd	0.255 ± 0.032d	0.350 ± 0.006bc	0.398 ± 0.038b	0.304 ± 0.021cd	0.343 ± 0.024bc	0.278 ± 0.034cd	0.514 ± 0.068a
C20:2	0.226 ± 0.008cde	0.202 ± 0.018de	0.299 ± 0.012b	0.272 ± 0.029bc	0.248 ± 0.019cd	0.217 ± 0.009de	0.188 ± 0.026e	0.369 ± 0.042a
C20:4n6	0.079 ± 0.004b	0.054 ± 0.006b	0.077 ± 0.016b	0.136 ± 0.018a	0.057 ± 0.007b	0.068 ± 0.004b	0.061 ± 0.003b	0.079 ± 0.026b
SFA	8.795 (38.45%)	8.990 (39.14%)	11.460 (39.06%)	10.019 (37.68%)	9.454 (38.86%)	8.316 (37.32%)	7.976 (37.45%)	13.604 (37.68%)
MUFA	8.416 (36.79%)	8.776 (38.21%)	11.194 (38.15%)	9.966 (37.48%)	9.228 (37.93%)	8.396 (37.68%)	8.259 (38.78%)	13.898 (38.49%)
PUFA	5.665 (24.76%)	5.201 (22.65%)	6.689 (22.8%)	6.603 (24.83%)	5.648 (23.21%)	5.571 (25%)	5.062 (23.77%)	8.604 (23.83%)
Total FFA	22.876	22.967	29.343	26.588	24.330	22.283	21.297	36.106

Values in brackets of SFA, MUFA, and PUFA indicate the proportion of such fatty acids in total free fatty acids (%). Different lower case letters indicate that there is a significant difference in the content of this fatty acid between different groups of fermented sausages ($p < 0.05$).

10.3389/fmicb.2022.1113848

TABLE 3 Changes of key volatile flavor compounds OAV in different fermented sausage samples.

	Volatile compounds	Threshold value (μ g/kg)	OVA						
			CK	LGG	S1	S2	S3	S4	S5
1	Hexanal	5.00	7.94 ± 0.21	90.79 ± 2.03	19.53 ± 0.17	5.77 ± 0.76	27.35 ± 1.58	9.42 ± 0.86	30.04 ± 1.77
2	Heptanal	2.80	—	20.83 ± 1.50	—	—	8.95 ± 0.40	—	10.22 ± 0.75
3	Nonanal	1.10	12.63 ± 2.00	55.97 ± 4.31	18.79 ± 0.46	14.04 ± 0.56	18.10 ± 0.99	12.12 ± 1.29	21.29 ± 1.88
4	*(E)*-2-octenal	3.00	—	10.69 ± 1.17	—	—	—	—	—
5	*(E)*-2-nonenal	0.19	—	74.45 ± 4.23	—	—	—	—	—
6	*(E,E)*-2,4-decadienal	0.03	—	122.4 ± 10.98	48.69 ± 4.99	22.50 ± 7.27	40.40 ± 3.71	27.41 ± 2.55	56.61 ± 2.01
7	Hexanol	5.60	0.42 ± 0.04	1.28 ± 0.12	1.41 ± 0.11	0.94 ± 0.03	1.93 ± 0.21	1.27 ± 0.09	2.13 ± 0.09
8	1-octene-3-ol	1.50	2.10 ± 0.17	46.16 ± 4.38	6.20 ± 0.33	3.05 ± 0.30	8.97 ± 0.32	3.93 ± 0.14	12.26 ± 1.22
9	1-heptanol	5.40	0.18 ± 0.04	1.87 ± 0.19	1.07 ± 0.06	0.77 ± 0.11	1.28 ± 0.09	0.94 ± 0.04	1.58 ± 0.19
10	Linalool	0.22	424.05 ± 24.32	389.44 ± 3.04	438.04 ± 12.04	427.18 ± 3.30	374.86 ± 23.42	379.39 ± 2.16	433.17 ± 36.13
11	Ethyl caproate	5.00	1.45 ± 0.12	—	1.77 ± 0.20	1.30 ± 0.12	1.66 ± 0.08	1.58 ± 0.05	2.11 ± 0.08
12	Ethyl octanoate	19.30	0.25 ± 0.02	—	0.40 ± 0.01	0.32 ± 0.02	0.84 ± 0.05	0.38 ± 0.04	1.05 ± 0.04
13	Acetoin	14.00	4.29 ± 0.15	11.19 ± 0.14	6.69 ± 0.30	4.89 ± 0.31	5.82 ± 0.48	4.58 ± 0.42	7.22 ± 0.31
14	α-pinene	14.00	20.88 ± 0.93	17.9 ± 0.05	26.65 ± 2.29	17.14 ± 0.92	14.67 ± 1.36	20.49 ± 1.32	19.17 ± 1.10
15	β-pinene	140.00	2.75 ± 0.14	2.14 ± 0.01	3.00 ± 0.29	2.26 ± 0.10	1.94 ± 0.24	2.39 ± 0.16	2.41 ± 0.14
16	δ-3-carene	770.00	1.88 ± 0.10	1.29 ± 0.06	1.73 ± 0.15	1.47 ± 0.12	1.42 ± 0.24	1.40 ± 0.01	1.78 ± 0.09
17	Sabinene	980.00	0.94 ± 0.07	0.67 ± 0.01	1.16 ± 0.01	0.87 ± 0.07	0.77 ± 0.06	0.98 ± 0.06	0.91 ± 0.06
18	Limonene	200.00	10.45 ± 0.69	9.24 ± 0.17	11.70 ± 1.10	9.39 ± 0.61	8.36 ± 0.46	9.34 ± 0.62	9.90 ± 0.50
19	Styrene	3.60	0.62 ± 0.07	0.65 ± 0.08	1.39 ± 0.10	0.94 ± 0.13	1.47 ± 0.14	1.12 ± 0.02	1.23 ± 0.14
20	β-caryophyllene	64.00	10.61 ± 1.14	9.82 ± 0.70	9.96 ± 0.72	12.97 ± 1.18	9.43 ± 0.49	8.57 ± 0.63	10.23 ± 0.64
21	Allyl methyl sulfide	22.00	4.64 ± 0.22	1.89 ± 0.37	5.39 ± 0.62	5.33 ± 0.45	3.13 ± 0.01	5.16 ± 0.12	1.97 ± 0.07
22	2-pentyl furan	5.80	—	2.95 ± 0.33	—	—	—	—	—
23	*p*-cymene	5.01	96.11 ± 6.52	94.85 ± 1.93	114.70 ± 0.84	92.59 ± 7.47	84.54 ± 5.20	91.64 ± 5.47	95.17 ± 6.01

10.3389/fmicb.2022.1113848

TABLE 4 Changes of volatile flavor substances content in different fermented sausage samples.

	Volatile compounds	Odor	Threshold value (μg/kg)	Probable origin	Sausage samples (μg/kg)							
					CK	LGG	S1	S2	S3	S4	S5	SEM
Aldehydes												
1	Hexanal	Grass, tallow, fat	5.00	Lipid oxidation	39.69 ± 1.06	453.95 ± 10.13	97.66 ± 0.84	28.84 ± 3.82	136.73 ± 7.89	47.12 ± 4.28	150.22 ± 8.85	30.24
2	Heptanal	Fat, citrus, rancid	2.80	Lipid oxidation	—	58.31 ± 4.21	—	—	25.05 ± 1.11	—	28.62 ± 2.09	5.24
3	*(E)*-2-hexenal	Apple, green	88.70	Lipid oxidation	—	14.4 ± 1.32	—	—	—	—	—	0.93
4	Nonanal	Fat, citrus, green	1.10	Lipid oxidation	13.89 ± 2.20	61.57 ± 4.75	20.67 ± 0.50	15.45 ± 0.62	19.91 ± 1.09	13.33 ± 1.42	23.42 ± 2.06	3.48
5	*(E)*-2-octenal	Green, nut, fat	3.00	Lipid oxidation	—	32.06 ± 3.5	—	—	—	—	—	2.48
6	Benzaldehyde	Almond, burnt sugar	750.89	Amino acid degradation	—	13.78 ± 0.96	9.31 ± 0.33	12.86 ± 0.94	14.33 ± 0.69	9.56 ± 0.02	13.38 ± 1.30	0.54
7	*(E)*-2-nonenal	Cucumber, fat, green	0.19	Lipid oxidation	—	14.15 ± 0.80	—	—	—	—	—	0.57
8	*(E)*-2-decenal	Tallow	17.00		1.16 ± 0.11	7.58 ± 0.01	1.56 ± 0.57	1.10 ± 0.07	1.58 ± 0.30	0.98 ± 0.22	1.97 ± 0.15	0.45
9	Phenylethanal	Hawthorne, honey, sweet	6.30	Amino acid degradation	—	1.14 ± 0.21	—	—	—	—	—	0.15
10	2-undecenal	Sweet			—	1.94 ± 0.00	—	—	—	—	0.61	0.44
11	*(E,E)*-2,4-decadienal	Fried, wax, fat	0.03		—	3.30 ± 0.30	1.31 ± 0.13	0.61 ± 0.20	1.09 ± 0.10	0.74 ± 0.07	1.53 ± 0.05	0.21
	Total				54.74 ± 3.37	662.18 ± 26.19	130.51 ± 2.37	58.86 ± 5.65	198.69 ± 11.18	71.73 ± 6.01	219.75 ± 14.5	33.00
Alcohols												
12	Ethanol	Sweet	950000.00	Carbohydrate fermentation	44.25 ± 5.58	34.6 ± 4.49	94.14 ± 3.44	81.49 ± 4.39	40.51 ± 2.57	54.74	47.96 ± 1.88	5.57
13	2-heptanol	Mushroom	65.24	Lipid β oxidation	0.25 ± 0.10	2.07 ± 0.17	3.37 ± 0.19	2.87 ± 0.06	2.28 ± 0.19	2.34 ± 0.20	1.92 ± 0.13	0.20
14	Hexanol	Resin, flower, green	5.60	Lipid oxidation	2.34 ± 0.24	7.17 ± 0.68	7.92 ± 0.62	5.26 ± 0.19	10.81 ± 1.17	7.12 ± 0.53	11.95 ± 0.49	0.79
15	2-octanol	Mushroom, fat	7.80	Lipid oxidation		0.24 ± 0.05	0.19 ± 0.06	0.17 ± 0.01	0.30 ± 0.05	0.18 ± 0.08	0.17 ± 0.00	0.02
16	1-octene-3-ol	Mushroom	1.50	Lipid β oxidation	3.16 ± 0.25	69.25 ± 6.57	9.31 ± 0.49	4.57 ± 0.45	13.46 ± 0.49	5.89 ± 0.22	18.39 ± 1.83	4.73
17	1-heptanol	Chemical, green	5.40	Lipid oxidation	0.98 ± 0.24	10.11 ± 1.02	5.77 ± 0.34	4.17 ± 0.58	6.92 ± 0.47	5.08 ± 0.19	8.52 ± 1.00	0.69
18	2-ethyl-1-hexanol	Rose, green	25482.20	Lipid oxidation	49.41 ± 2.84	40.46 ± 1.31	55.49 ± 2.00	35.10 ± 1.88	31.13 ± 3.40	36.08 ± 1.86	52.28 ± 4.18	1.97
19	*(E)*-2-hepten-1-ol	Pungent, fatty, plastic	4172.00		—	—	—	—	0.67 ± 0.02	0.41 ± 0.03	0.79 ± 0.10	0.06

(Continued)

10.3389/fmicb.2022.1113848

TABLE 4 (Continued)

	Volatile compounds	Odor	Threshold value (μg/kg)	Probable origin	Sausage samples (μg/kg)							
					CK	LGG	S1	S2	S3	S4	S5	SEM
20	2-nonanol	Cucumber	58.00		—	0.83 ± 0.07	1.4 ± 0.11	1.09 ± 0.02	0.97 ± 0.13	0.96 ± 0.02	0.43 ± 0.01	0.08
21	2,3-butanediol	Fruit, onion	20000.00	Carbohydrate fermentation	51.65 ± 2.86	—	44.55 ± 1.77	21.59 ± 2.07	46.58 ± 5.05	5.77 ± 1.12	6.24 ± 0.08	5.26
22	Linalool	Flower, lavender	0.22	Spices	93.29 ± 5.35	85.68 ± 0.67	96.37 ± 2.65	93.98 ± 0.73	82.47 ± 5.15	83.47 ± 0.47	95.3 ± 7.95	1.58
23	Octanol	Chemical, metal, burnt	125.80	Lipid oxidation	2.77 ± 0.28	8.76 ± 0.86	4.07 ± 0.25	3.47 ± 0.24	4.66 ± 0.16	2.17 ± 0.16	4.36 ± 0.53	0.42
24	α-terpineol	Oil, anise, mint	1200.00	Spices	11.61 ± 1.93	11.99 ± 0.66	11.18 ± 0.73	10.30 ± 0.62	11.10 ± 1.64	11.77 ± 0.50	13.25 ± 0.74	0.32
25	Myrtenol	Sweet, mint, medical	7.00		0.48 ± 0.05	0.55 ± 0.11	0.62 ± 0.01	0.39 ± 0.03	0.43 ± 0.03	0.73 ± 0.11	0.55 ± 0.05	0.03
26	Benzylalcohol	Sweet, flower	2546.21	Amino acid degradation	0.87 ± 0.07	1.22 ± 0.16	1.83 ± 0.15	1.82 ± 0.11	1.85 ± 0.20	1.46 ± 0.10	2.31 ± 0.16	0.11
27	Phenethylalcohol	Honey, spice, rose, lilac	564.23	Smoking	5.31 ± 0.52	6.53 ± 0.51	13.62 ± 0.61	13.16 ± 0.64	13.36 ± 0.75	11.91 ± 0.61	19.48 ± 1.51	1.04
	Total				266.37 ± 20.31	279.46 ± 17.33	349.83 ± 13.42	279.43 ± 12.02	267.5 ± 21.47	230.08 ± 6.2	283.9 ± 20.64	14.76
Acids												
28	Acetic acid	Sour	99000.00	Carbohydrate fermentation	43.17 ± 2.81	191.18 ± 6.10	242.04 ± 2.63	213.12 ± 1.80	247.98 ± 50.83	156.09 ± 14.11	196.84 ± 10.58	15.56
29	Propionic acid	Pungent, rancid, soy	2190.00	Lipid oxidation	—	—	3.32 ± 0.23	3.44 ± 0.34	3.66 ± 0.31	1.28 ± 0.26	2.46 ± 0.23	0.23
30	Butyric acid	Rancid, cheese, sweat	2400.00	Lipid oxidation	13.92 ± 0.47	37.35 ± 2.36	54.05 ± 3.21	53.6 ± 2.26	51.15 ± 6.76	40.39 ± 3.39	58.99 ± 5.75	3.33
31	Isovaleric acid	Sweat, acid, rancid	490.00	Amino acid degradation	5.55 ± 0.55	6.18 ± 0.58	15.33 ± 0.53	8.18 ± 0.36	11.44 ± 1.24	8.22 ± 1.74	10.87 ± 0.61	0.78
32	Pentanoic acid	Sweat	11000.00	Lipid oxidation	0.44 ± 0.06	2.51 ± 0.04	1.61 ± 0.10	2.41 ± 0.24	4.2 ± 0.51	2.44 ± 0.18	5.29 ± 0.58	0.40
33	Caproic acid	Sweat	890.00	Lipid oxidation	1.9 ± 0.21	19.18 ± 2.88	12.02 ± 0.54	12 ± 1.15	15.27 ± 1.32	11.43 ± 0.86	22.11 ± 0.75	1.47
34	Heptanoic acid	Rancid, sour, cheesy, sweat	640.00	Lipid oxidation	—	2.66 ± 0.11	2.73 ± 0.21	2.88 ± 0.13	3.94 ± 0.44	3.05 ± 0.15	5.29 ± 0.57	0.26
35	Octanoic acid	Sweat, cheese	3000.00	Lipid oxidation	0.89 ± 0.02	6.81 ± 0.32	5.88 ± 0.54	5.68 ± 0.29	9.44 ± 0.92	7.09 ± 0.01	15.99 ± 2.64	1.19
36	Nonanoic acid	Green, fat	4600.00	Lipid oxidation	0.49 ± 0.01	1.74 ± 0.17	2.22 ± 0.15	2.97 ± 0.21	4.03 ± 0.33	3.09 ± 0.69	10.49 ± 2.95	0.89
37	Decanoic acid	Rancid, fat	10000.00	Lipid oxidation	—	2.4 ± 0.03	2.85 ± 0.24	3.18 ± 0.24	5.24 ± 0.42	3.08 ± 0.37	8.13 ± 2.88	0.74
	Total				66.36 ± 4.13	270.01 ± 12.59	342.05 ± 8.38	307.46 ± 7.02	356.35 ± 63.08	236.16 ± 21.76	336.46 ± 27.54	24.57

(Continued)

10.3389/fmicb.2022.1113848

TABLE 4 (Continued)

	Volatile compounds	Odor	Threshold value (μg/kg)	Probable origin	Sausage samples (μg/kg)							
					CK	LGG	S1	S2	S3	S4	S5	SEM
Esters												
38	Methyl hexanoate	Fruit, fresh, sweet	70.00		11.91 ± 2.93	—	22.89 ± 0.40	11.20 ± 0.82	—	18.31 ± 1.76	—	1.60
39	Ethyl caproate	Apple peel, fruit	5.00	Esterase activity	7.25 ± 0.61	—	8.84 ± 1.00	6.48 ± 0.59	8.32 ± 0.38	7.88 ± 0.25	10.57 ± 0.41	0.32
40	Ethyl lactate	Fruit	50000.00		1.17 ± 0.18	3.67 ± 0.03	4.68 ± 0.12	6.01 ± 0.80	5.12 ± 0.41	5.10 ± 0.34	6.17 ± 0.47	0.45
41	Methyl octanoate	Orange	200.00	Esterase activity	—	4.75 ± 0.62	4.85 ± 0.00	2.60 ± 0.15	4.23 ± 0.10	4.01 ± 0.29	4.21 ± 0.08	0.20
42	Butyl hexanoate	Fruit	10000.00		0.71 ± 0.11	—	—	—	—	—	—	0.06
43	Ethyl octanoate	Fruit	19.30	Esterase activity	4.81 ± 0.44	—	7.75 ± 0.24	6.27 ± 0.29	16.22 ± 1.00	7.33 ± 0.71	20.25 ± 0.78	1.53
44	Ethyl nonanoate	Fruity, rose, waxy, wine	377.00		0.93	1.45 ± 0.03	0.82 ± 0.56	—	0.43 ± 0.06	0.63 ± 0.01	1.70 ± 0.03	0.16
45	γ-hexalactone	Sweet, coumarin	260.00	Lipid oxidation	0.19	0.36 ± 0.03	0.32 ± 0.03	0.27 ± 0.06	—	—	0.30 ± 0.10	0.02
46	γ-nonalactone	Coconut, peach	9.70		0.37 ± 0.06	1.05 ± 0.02	1.10 ± 0.10	1.24 ± 0.04	1.73 ± 0.08	1.07 ± 0.06	1.88 ± 0.12	0.11
	Total				27.34 ± 4.33	11.28 ± 0.73	51.25 ± 2.45	34.07 ± 2.75	36.05 ± 2.03	44.33 ± 3.42	45.08 ± 1.99	3.23
Ketones												
47	2-nonanone	Hot milk, soap, green	41.00	Lipid β oxidation	5.59 ± 0.43	—	—	—	—	—	—	0.22
48	Piperitone	Mint, fresh	680.00		1.23 ± 0.05	1.19 ± 0.08	1.32 ± 0.04	1.35 ± 0.08	1.27 ± 0.15	1.47 ± 0.09	1.38 ± 0.09	0.03
49	DL-carvone	Mint, basil, fennel	27.00		0.56 ± 0.01	0.83 ± 0.08	0.48 ± 0.09	0.42 ± 0.01	0.84 ± 0.08	0.53 ± 0.02	0.58 ± 0.06	0.04
50	Acetoin	Butter, cream	14.00	Carbohydrate fermentation	60.13 ± 2.09	156.72 ± 1.91	93.63 ± 4.21	68.51 ± 4.29	81.45 ± 6.74	64.07 ± 5.92	101.08 ± 4.36	6.67
	Total				67.51 ± 2.58	158.74 ± 2.07	95.43 ± 4.34	70.28 ± 4.38	83.56 ± 6.97	66.07 ± 6.03	103.04 ± 4.51	9.00
Terpenes												
51	α-pinene	Pine, turpentine	14.00	Spices	292.27 ± 13.04	250.63 ± 0.75	373.08 ± 32	240.02 ± 12.88	205.37 ± 19.04	286.85 ± 18.43	268.35 ± 15.44	11.40
52	β-pinene	Pine, resin, turpentine	140.00	Spices	384.37 ± 20.03	299.76 ± 1.68	419.58 ± 40.01	315.93 ± 14.46	271.52 ± 34.04	334 ± 22.51	337.72 ± 19.01	11.22
53	δ-3-carene	Lemon, resin	770.00		1445.16 ± 79.51	993.24 ± 49.07	1329.65 ± 117.93	1130.71 ± 88.87	1092.93 ± 184.61	1079.57 ± 4.63	1373.1 ± 71.94	39.59

(Continued)

10.3389/fmicb.2022.1113848

TABLE 4 (Continued)

	Volatile compounds	Odor	Threshold value (μg/kg)	Probable origin	Sausage samples (μg/kg)							
					CK	LGG	S1	S2	S3	S4	S5	SEM
54	Sabinene	Pepper, turpentine, wood	980.00	Spices	925.03 ± 65.23	658.18 ± 9.21	1139.96 ± 7.93	848.04 ± 65.04	751.56 ± 58.69	964.74 ± 60.42	892.36 ± 63.16	31.06
55	α-terpinene	Lemon	80.00	Spices	36.80 ± 4.12	31.00 ± 1.61	59.13 ± 5.72	47.33 ± 3.14	40.74 ± 3.63	45.64 ± 3.17	47.55 ± 3.40	2.07
56	Limonene	Lemon, orange	200.00	Spices	2090.01 ± 137.5	1847.49 ± 33.96	2340.64 ± 219.39	1878.23 ± 122.99	1671.00 ± 91.50	1868.14 ± 124.24	1979.72 ± 100.26	50.03
57	β-phellandrene	Mint, turpentine	500.00	Spices	91.63 ± 8.75	65.48 ± 2.15	112.04 ± 12.16	81.27 ± 6.19	71.57 ± 4.77	87.37 ± 5.03	88.53 ± 5.42	3.14
58	γ-terpinene	Gasoline, turpentine	1000.00	Spices	33.9 ± 4.62	33.28 ± 2.23	40.47 ± 1.40	34.21 ± 2.78	23.63 ± 0.19	35.68 ± 2.37	27.10 ± 2.56	1.22
59	(Z)-β-ocimene	Citrus, herb, flower	34.00	Spices	9.38 ± 1.14	6.02 ± 0.04	10.05 ± 0.08	8.86 ± 0.60	9.59 ± 1.08	9.52 ± 0.52	8.01 ± 0.73	0.32
60	Styrene	Balsamic, gasoline	3.60	Spices	2.25 ± 0.24	2.33 ± 0.30	5.00 ± 0.35	3.38 ± 0.48	5.30 ± 0.51	4.02 ± 0.07	4.44 ± 0.49	0.29
61	Terpinolene	Pine, plastic	200.00	Spices	95.88 ± 12.55	68.06 ± 3.19	117.31 ± 9.46	96.93 ± 8.65	79.59 ± 3.28	98.84 ± 9.77	98.18 ± 6.24	3.33
62	α-p-dimethylstyrene	Citrus, pine	85.00		26.69 ± 0.96	25.42 ± 2.53	31.68 ± 1.66	29.91 ± 0.29	26.25 ± 3.52	27.11 ± 0.57	30.43 ± 1.31	0.63
63	δ-elemene	Wood		Spices	48.16 ± 5.11	46.63 ± 3.65	50.88 ± 4.36	57.66 ± 5.37	65.55 ± 13.05	48.40 ± 2.21	54.95 ± 2.89	1.99
64	β-caryophyllene	Wood, spice	64.00	Spices	679.23 ± 72.74	628.61 ± 44.65	637.20 ± 45.95	829.81 ± 75.50	603.47 ± 31.34	548.22 ± 40.17	654.56 ± 41.18	19.99
65	α-humulene	Wood	160.00	Spices	36.2 ± 5.9	32.8 ± 2.94	32.61 ± 1.78	45.83 ± 5.44	32.58 ± 2.51	27.14 ± 0.48	35.95 ± 2.49	1.34
66	δ-cadinene	Thyme, medicine, wood		Spices	6.18 ± 0.18	6.02 ± 0.50	5.66 ± 1.18	7.10 ± 0.38	4.88 ± 0.31	4.45 ± 0.01	6.33 ± 0.60	0.22
67	Caryophyllene oxide	Herb, sweet, spice	410.00		1.71 ± 0.23	2.63 ± 0.19	1.49 ± 0.12	1.21 ± 0.10	1.14 ± 0.15	0.74 ± 0.01	1.28 ± 0.13	0.12
	Total				6204.85 ± 431.85	4997.58 ± 158.65	6706.43 ± 501.48	5656.43 ± 413.16	4956.67 ± 452.22	5470.43 ± 294.61	5908.56 ± 337.25	303.49
Others												
68	Allyl methyl sulfide	Garlic, onion	22.00		102.04 ± 4.94	41.61 ± 8.03	118.55 ± 13.71	117.26 ± 9.88	68.82 ± 0.14	113.56 ± 2.54	43.39 ± 1.57	7.67
69	2-pentyl furan	Green bean, butter	5.80	Lipid oxidation	—	17.10 ± 1.94	—	—	—	—	—	1.37
70	p-cymene	Solvent, gasoline, citrus	5.01		481.51 ± 32.66	475.18 ± 9.67	574.63 ± 4.21	463.88 ± 37.43	423.53 ± 26.04	459.12 ± 27.42	476.82 ± 30.10	10.22

(Continued)

10.3389/fmicb.2022.1113848

TABLE 4 (Continued)

	Volatile compounds	Odor	Threshold value (μg/kg)	Probable origin	Sausage samples (μg/kg)						
					CK	LGG	S1	S2	S3	S4	S5	SEM
71	D-camphor	Camphor, minty, phenolic, herbal	1360.00		5.22 ± 0.16	5.1 ± 0.79	5.78 ± 0.50	4.66 ± 0.23	5.08 ± 0.28	5.62 ± 0.16	5.59 ± 0.50	0.11
72	Borneol	Camphor	180.00		0.26 ± 0.07	0.33 ± 0.06	0.33 ± 0.05	0.52 ± 0.05	0.49 ± 0.05	0.41 ± 0.04	0.47 ± 0.03	0.02
73	Phenol	Phenol	58585.25	Amino acid degradation	0.88 ± 0.07	0.91 ± 0.01	0.9 ± 0.12	0.84 ± 0.01	0.96 ± 0.11	0.75 ± 0.05	0.82 ± 0.03	0.02
74	p-cresol	Medicine, phenol, smoke	3.90		1.82 ± 0.07	1.66 ± 0.05	1.99 ± 0.11	2.16 ± 0.07	2.16 ± 0.17	1.89 ± 0.07	2.64 ± 0.32	0.07
75	Meta-cresol	Fecal, plastic	15.00		4.87 ± 0.11	4.64 ± 0.45	5.26 ± 0.35	5.11 ± 0.10	4.81 ± 0.41	4.43 ± 0.15	6.01 ± 0.54	0.12
	Total				596.6 ± 38.08	546.53 ± 21	707.44 ± 19.05	594.43 ± 47.77	505.85 ± 27.2	585.78 ± 30.43	535.74 ± 33.09	41.99

SEM is the Standard Error of Mean (SEM) of the same volatile compound content in different groups of sausage samples.

analyzed, including 11 aldehydes, 16 alcohols, 10 acids, 9 esters, 4 ketones, 17 terpenes, and 8 other types. The content of terpenes was obviously higher, more than 70% in each sample group, followed by other, acids, alcohols and aldehydes, esters and ketones were relatively less. CK group had the least kinds of flavor compounds (59 substances) in sausages in each group, while LGG and S5 had 67 substances, S1, S3, and S4 had 65 substances, and S2 had 64 substances.

Aldehydes mainly come from the automatic oxidation of unsaturated fatty acids such as oleic acid and linoleic acid and the degradation of amino acids. They have low threshold value. Therefore, although the total content of aldehydes is low, they are of great significance to the formation of sausage flavor. The total content of aldehydes in LGG group was the highest (662.18 ± 26.19 μg/kg), which was much higher than S2 group (58.86 ± 5.65 μg/kg) and S4 group (71.73 ± 6.01 μg/kg). Hexanal, as the aldehyde with the highest proportion, was considered to be positively correlated with the degree of fat oxidation (Olivares et al., 2011). The content of hexaldehyde in S1−S5 groups was 97.66 ± 0.84, 28.84 ± 3.82, 136.73 ± 7.89, 47.12 ± 4.28, and 150.22 ± 8.85 μg/kg, which was much lower than 453.95 ± 10.13 μg/kg in LGG group. The results showed that LGG group had the highest lipid oxidation degree, while yeast fermentation effectively inhibited the production of hexanal, which had good antioxidant effect, consistent with the results of POV value and TBARS. In addition, heptanal, nonanal, (*E*)-2-decenal also found the same change. (*E*)-2-hexenal, (*E*)-2-octenal, (*E*)-2-nonenal and phenylacetaldehyde only detected in LGG group.

The OAV value of flavor compounds can directly reflect the contribution of compounds to the formation of sausage flavor. It is generally believed that flavor compounds with OAV ≥ 1 are the key flavor compounds of the product, and the higher the OAV value, the stronger the contribution. **Table 3** collated the key flavor compounds in the 23 days sausage sample. It isn't difficult to find that the OVA value of aldehydes was high, which plays an important role in the flavor formation of sausage. Among them, hexanal, heptanal, nonanal, (*E*)-2-octenal, (*E*)-2-nonenal, (*E,E*)-2, 4-decadienal are the key flavor aldehydes, which have grass, rancid, fat, nut, cucumber and fried flavor, respectively.

The formation of alcohols is mainly related to microbial carbohydrate fermentation, such as ethanol and 2, 3-butanediol. However, it is difficult to have a significant impact on the overall flavor of sausage because of their high threshold. Some alcohols are associated with fat β-oxidation and auto-oxidation, such as 1-octene-3-ol (with mushroom flavor), which has higher content in LGG group. On the whole, the content of alcohols in S1 group was higher, which may be related to the strong carbohydrate capacity of Y3-1. Among the key flavor alcohols, hexanol, 1-octene-3-ol and 1-heptanol are mainly derived from lipid oxidation and β-oxidation, and have resin, mushroom and pharmaceutical flavor, respectively, while linalool is mainly derived from spice and has flower flavor.

The contents of acids, especially acetic acid and butyric acid, in the sausage samples inoculated with starter were much higher than those in the CK group. Acetic acid is mainly produced by the metabolism of carbohydrates by microorganisms, and butyric acid is thought to be related to the automatic oxidation of fat. Similar to alcohols, acids also had higher thresholds, and no key flavor acids were found in OVA analysis.

The production of esters is mainly affected by microbial esterase activity, and most of them are aromatic. Esters generated by short-chain fatty acids mostly have fruit flavor, while esters generated by

TABLE 5 Changes of volatile flavor compounds in fermented sausage samples after storage.

	Volatile compounds	Odor	Threshold value (μg/kg)	Probable origin	0 day	23 days			60 days			
					CK	LGG	S4	S5	LGG	S4	S5	SEM
Aldehydes												
1	Hexanal	Grass, tallow, fat	5.00	Lipid oxidation	—	453.95 ± 10.13	47.12 ± 4.28	150.22 ± 8.85	540.59 ± 4.72	272.83 ± 22.84	227.12 ± 10.42	41.31
2	Heptanal	Fat, citrus, rancid	2.80	Lipid oxidation	—	58.31 ± 4.21	—	28.62 ± 2.09	74.74 ± 1.61	41.23 ± 3.24	39.13 ± 2.10	4.47
3	*(E)*-2-hexenal	Apple, green	88.70	Lipid oxidation	—	14.40 ± 1.32	—	—	12.91 ± 1.24	5.86 ± 0.73	5.68 ± 0.45	1.32
4	Octanal	Fat, soap, lemon, green	0.59	Lipid oxidation	—	—	—	—	95.94 ± 22.21	51.64 ± 2.74	51.78 ± 3.90	7.56
5	(Z)-2-heptenal		56.00	Lipid oxidation	—	—	—	—	143.37 ± 13.14	56.53 ± 4.72	56.08 ± 5.21	13.49
6	Nonanal	Fat, citrus, green	1.10	Lipid oxidation	1.56 ± 0.31	61.57 ± 4.75	13.33 ± 1.42	23.42 ± 2.06	76.76 ± 0.31	41.36 ± 2.59	43.89 ± 2.56	4.98
7	*(E)*-2-octenal	Green, nut, fat	3.00	Lipid oxidation	—	32.06 ± 3.5	—	—	56.66 ± 5.10	—	—	6.29
8	*(E,E)*-2,4-heptadienal	Fatty, green, cinnamon	57.00		—	—	—	—	2.13 ± 0.19	—	—	0.13
9	Benzaldehyde	Almond, burnt sugar	750.89	Amino acid degradation	4.05 ± 0.61	13.78 ± 0.96	9.56 ± 0.02	13.38 ± 1.30	17.83 ± 0.41	15.83 ± 1.44	17.41 ± 1.64	0.71
10	*(E)*-2-nonenal	Cucumber, fat, green	0.19	Lipid oxidation	—	14.15 ± 0.8	—	—	24.94 ± 1.95	—	—	2.72
11	*(E)*-2-decenal	Tallow	17.00			7.58 ± 0.01	0.98 ± 0.22	1.97 ± 0.15	12.3 ± 1.16	5.54 ± 0.45	5.33 ± 0.34	0.94
12	Phenylethanal	Hawthorne, honey, sweet	6.30	Amino acid degradation		1.14 ± 0.21	—	—	—	—	—	0.15
13	Ethyl benzaldehyde	Sweet	13.00						3.63 ± 0.26			0.18
14	2-undecenal	Sweet			—	1.94 ± 0.00	—	0.61	5.32 ± 0.49	2.29 ± 0.09	2.55 ± 0.21	0.42
15	*(E,E)*-2,4-decadienal	Fried, wax, fat	0.03		—	3.30 ± 0.30	0.74 ± 0.07	1.53 ± 0.05	13.44 ± 2.21	4.84 ± 0.69	4.07 ± 0.61	1.16
16	Hexadecanal	Cardboard			—	—	—	—	1.73 ± 0.11	4.24 ± 0.79	4.49 ± 0.28	0.47
	Total				5.61 ± 0.92	662.18 ± 26.19	71.73 ± 6.01	219.75 ± 14.5	1082.29 ± 55.11	502.19 ± 40.32	457.53 ± 27.72	69.92
Alcohols												
17	Ethanol	Sweet	950000.00	Carbohydrate fermentation	—	34.6 ± 4.49	54.74	47.96 ± 1.88	33.26 ± 7.42	33.89 ± 6.61	26.30 ± 9.73	2.90
18	2-heptanol	Mushroom	65.24	Lipid β oxidation	—	2.07 ± 0.17	2.34 ± 0.20	1.92 ± 0.13	1.03 ± 0.15	1.95 ± 0.21	1.54 ± 0.17	0.11
19	Hexanol	Resin, flower, green	5.60	Lipid oxidation	0.78 ± 0.13	7.17 ± 0.68	7.12 ± 0.53	11.95 ± 0.49	13.26 ± 1.22	39.10 ± 2.92	38.83 ± 1.19	3.66
20	2-octanol	Mushroom, fat	7.80	Lipid oxidation	—	0.24 ± 0.05	0.18 ± 0.08	0.17 ± 0.00	—	—	—	0.02

(Continued)

10.3389/fmicb.2022.1113848

TABLE 5 (Continued)

	Volatile compounds	Odor	Threshold value (μg/kg)	Probable origin	0 day	23 days			60 days			
					CK	LGG	S4	S5	LGG	S4	S5	SEM
21	1-octene-3-ol	Mushroom	1.50	Lipid β oxidation	0.98 ± 0.08	69.25 ± 6.57	5.89 ± 0.22	18.39 ± 1.83	120.99 ± 7.96	54.81 ± 3.63	55.62 ± 4.92	9.11
22	1-heptanol	Chemical, green	5.40	Lipid oxidation	—	10.11 ± 1.02	5.08 ± 0.19	8.52 ± 1.00	13.19 ± 1.04	16.92 ± 2.08	20.42 ± 0.61	1.21
23	2-ethyl-1-hexanol	Rose, green	25482.20	Lipid oxidation	30.28 ± 1.1	40.46 ± 1.31	36.08 ± 1.86	52.28 ± 4.18	20.56 ± 2.81	20.64 ± 1.38	27.52 ± 1.91	2.78
24	*(E)*-2-hepten-1-ol	Pungent, fatty, plastic	4172.00		—	—	0.41 ± 0.03	0.79 ± 0.1	—	—	—	0.10
25	2-nonanol	Cucumber	58.00		—	0.83 ± 0.07	0.96 ± 0.02	0.43 ± 0.01	—	—	—	0.10
26	2,3-butanediol	Fruit, onion	20000.00	Carbohydrate fermentation	—	—	5.77 ± 1.12	6.24 ± 0.08	—	39.44 ± 4.05	35.08 ± 2.00	5.31
27	Linalool	Flower, lavender	0.22	Spices	57.80 ± 1.47	85.68 ± 0.67	83.47 ± 0.47	95.30 ± 7.95	86.55 ± 5.95	96.56 ± 5.33	105.72 ± 4.64	2.06
28	Octanol	Chemical, metal, burnt	125.80	Lipid oxidation	0.33 ± 0.17	8.76 ± 0.86	2.17 ± 0.16	4.36 ± 0.53	9.33 ± 0.84	5.98 ± 0.69	6.04 ± 0.04	0.61
29	α-terpineol	Oil, anise, mint	1200.00	Spices	7.82 ± 0.71	11.99 ± 0.66	11.77 ± 0.50	13.25 ± 0.74	11.75 ± 1.11	13.43 ± 0.67	13.23 ± 2.88	0.36
30	Myrtenol	Sweet, mint, medical	7.00		—	0.55 ± 0.11	0.73 ± 0.11	0.55 ± 0.05	0.65 ± 0.08	0.65 ± 0.12	—	0.03
31	Benzylalcohol	Sweet, flower	2546.21	Amino acid degradation	0.48 ± 0.05	1.22 ± 0.16	1.46 ± 0.10	2.31 ± 0.16	1.31 ± 0.31	2.06 ± 0.10	2.2 ± 0.02	0.11
32	Phenethylalcohol	Honey, spice, rose	564.23	Smoking	0.31 ± 0.01	6.53 ± 0.51	11.91 ± 0.61	19.48 ± 1.51	3.88 ± 0.65	8.32 ± 0.35	8.50 ± 1.19	1.15
	Total				98.78 ± 3.72	279.46 ± 17.33	230.08 ± 6.20	283.90 ± 20.64	315.76 ± 29.54	333.75 ± 28.14	341.00 ± 29.3	15.24
Acids												
33	Acetic acid	Sour	99000.00	Carbohydrate fermentation	—	191.18 ± 6.10	156.09 ± 14.11	196.84 ± 10.58	185.09 ± 0.57	187.10 ± 17.7	194.98 ± 18.58	4.46
34	Propionic acid	Pungent, rancid, soy	2190.00	Lipid oxidation	—	—	1.28 ± 0.26	2.46 ± 0.23	4.03 ± 0.30	3.45 ± 0.28	2.95 ± 0.40	0.25
35	Butyric acid	Rancid, cheese, sweat	2400.00	Lipid oxidation	1.71 ± 0.81	37.35 ± 2.36	40.39 ± 3.39	58.99 ± 5.75	47.97 ± 2.96	63.52 ± 2.88	63.96 ± 2.46	2.72
36	Isovaleric acid	Sweat, acid, rancid	490.00	Amino acid degradation	—	6.18 ± 0.58	8.22 ± 1.74	10.87 ± 0.61	—	—	—	0.82
37	Pentanoic acid	Sweat	11000.00	Lipid oxidation	—	2.51 ± 0.04	2.44 ± 0.18	5.29 ± 0.58	9.65 ± 0.42	8.42 ± 0.29	8.39 ± 0.15	0.76
38	Caproic acid	Sweat	890.00	Lipid oxidation	0.87 ± 0.3	19.18 ± 2.88	11.43 ± 0.86	22.11 ± 0.75	88.12 ± 3.21	64.46 ± 2.84	70.46 ± 1.76	7.32
39	Heptanoic acid	Rancid, sour, cheesy, sweat	640.00	Lipid oxidation	—	2.66 ± 0.11	3.05 ± 0.15	5.29 ± 0.57	6.98 ± 0.52	8.62 ± 0.6	8.23 ± 0.62	0.59
40	Octanoic acid	Sweat, cheese	3000.00	Lipid oxidation	0.31 ± 0.01	6.81 ± 0.32	7.09 ± 0.01	15.99 ± 2.64	24.55 ± 1.32	31.44 ± 2.31	32.24 ± 2.94	2.70

(Continued)

10.3389/fmicb.2022.1113848

TABLE 5 (Continued)

	Volatile compounds	Odor	Threshold value (μg/kg)	Probable origin	0 day	23 days			60 days			
					CK	LGG	S4	S5	LGG	S4	S5	SEM
41	Nonanoic acid	Green, fat	4600.00	Lipid oxidation	1.61 ± 0.18	1.74 ± 0.17	3.09 ± 0.69	10.49 ± 2.95	11.18 ± 3.15	15.49 ± 1.45	12.94 ± 1.82	1.32
42	Decanoic acid	Rancid, fat	10000.00	Lipid oxidation	—	2.4 ± 0.03	3.08 ± 0.37	8.13 ± 2.88	13.49 ± 1.00	21.56 ± 2.90	24.14 ± 1.58	2.15
	Total				4.50 ± 1.30	270.01 ± 12.59	236.16 ± 21.76	336.46 ± 27.54	391.06 ± 13.45	404.06 ± 31.25	418.29 ± 30.31	25.28
Esters												
43	Methyl hexanoate	Fruit, fresh, sweet	70.00		0.89 ± 0.5	—	18.31 ± 1.76	—	—	—	—	1.02
44	Ethyl caproate	Apple peel, fruit	5.00	Esterase activity	—	—	7.88 ± 0.25	10.57 ± 0.41	—	—	—	0.61
45	Ethyl lactate	Fruit	50000.00		—	3.67 ± 0.03	5.10 ± 0.34	6.17 ± 0.47	3.44 ± 0.17	5.10 ± 0.50	3.71 ± 0.32	0.27
46	Methyl octanoate	Orange	200.00	Esterase activity	1.57 ± 0.10	4.75 ± 0.62	4.01 ± 0.29	4.21 ± 0.08	4.11 ± 0.35	4.17 ± 0.35	4.76 ± 0.34	0.10
47	Ethyl octanoate	Fruit	19.30	Esterase activity	—	—	7.33 ± 0.71	20.25 ± 0.78	—	33.86 ± 1.42	34.01 ± 1.50	3.07
48	Ethyl nonanoate	Fruity, rose, waxy, wine	377.00		—	1.45 ± 0.03	0.63 ± 0.01	1.7 ± 0.03	1.83 ± 0.28	1.29 ± 0.93	—	0.18
49	γ-hexalactone	Sweet, coumarin	260.00	Lipid oxidation	—	0.36 ± 0.03	—	0.3 ± 0.1	1.5 ± 0.13	1.71 ± 0.08	1.29 ± 0.16	0.17
50	γ-nonalactone	Coconut, peach	9.70		—	1.05 ± 0.02	1.07 ± 0.06	1.88 ± 0.12	1.61 ± 0.03	3.54 ± 0.36	3.35 ± 0.15	0.26
	Total				2.46 ± 0.6	11.28 ± 0.73	44.33 ± 3.42	45.08 ± 1.99	12.49 ± 0.96	49.67 ± 3.64	47.12 ± 2.47	4.27
Ketones												
51	Piperitone	Mint, fresh	680.00		0.68 ± 0.07	1.19 ± 0.08	1.47 ± 0.09	1.38 ± 0.09	1.52 ± 0.07	1.66 ± 0.07	1.71 ± 0.16	0.05
52	DL-carvone	Mint, basil, fennel	27.00		0.33 ± 0.02	0.83 ± 0.08	0.53 ± 0.02	0.58 ± 0.06	1.28 ± 0.04	1.09 ± 0.13	0.76 ± 0.10	0.06
53	Acetoin	Butter, cream	14.00	Carbohydrate fermentation	6.42 ± 0.38	156.72 ± 1.91	64.07 ± 5.92	101.08 ± 4.36	—	—	—	13.64
	Total				7.43 ± 0.47	158.74 ± 2.07	66.07 ± 6.03	103.04 ± 4.51	2.80 ± 0.11	2.75 ± 0.20	2.47 ± 0.26	12.46
Terpenes												
54	α-pinene	Pine, turpentine	14.00	Spices	73.64 ± 6.59	250.63 ± 0.75	286.85 ± 18.43	268.35 ± 15.44	328.58 ± 53.06	344.37 ± 15.44	374.00 ± 24.60	11.35
55	β-pinene	Pine, resin, turpentine	140.00	Spices	112.30 ± 9.09	299.76 ± 1.68	334.00 ± 22.51	337.72 ± 19.01	375.35 ± 16.7	409.00 ± 16.06	407.52 ± 23.75	10.23
56	δ-3-carene	Lemon, resin	770.00		558.34 ± 50.50	993.24 ± 49.07	1079.57 ± 4.63	1373.1 ± 71.94	1197.6 ± 23.69	1567.96 ± 190.84	1692.08 ± 75.63	62.96
57	Sabinene	Pepper, turpentine, wood	980.00	Spices	51.78 ± 16.14	658.18 ± 9.21	964.74 ± 60.42	892.36 ± 63.16	743.99 ± 115.18	1025.37 ± 27.42	1050.91 ± 34.82	34.14
58	α-terpinene	Lemon	80.00	Spices	11.32 ± 1.24	31.00 ± 1.61	45.64 ± 3.17	47.55 ± 3.40	29.42 ± 2.81	49.52 ± 2.09	59.25 ± 0.13	2.63

(Continued)

10.3389/fmicb.2022.1113848

TABLE 5 (Continued)

	Volatile compounds	Odor	Threshold value (μg/kg)	Probable origin	0 day	23 days			60 days			
					CK	LGG	S4	S5	LGG	S4	S5	SEM
59	Limonene	Lemon, orange	200.00	Spices	668.46 ± 48.21	1847.49 ± 33.96	1868.14 ± 124.24	1979.72 ± 100.26	2093.74 ± 174.12	2294.97 ± 83.77	2303.58 ± 150.27	48.58
60	β-phellandrene	Mint, turpentine	500.00	Spices	25.55 ± 1.42	65.48 ± 2.15	87.37 ± 5.03	88.53 ± 5.42	74.35 ± 4.2	91.78 ± 7.78	114.07 ± 8.67	3.80
61	γ-terpinene	Gasoline, turpentine	1000.00	Spices	8.11 ± 0.58	33.28 ± 2.23	35.68 ± 2.37	27.1 ± 2.56	38.41 ± 1.42	39.74 ± 4.96	47.05 ± 4.20	1.70
62	(Z)-β-ocimene	Citrus, herb, flower	34.00	Spices	1.50 ± 0.50	6.02 ± 0.04	9.52 ± 0.52	8.01 ± 0.73	4.08 ± 0.79	7.15 ± 1.48	10.16 ± 0.06	0.48
63	Styrene	Balsamic, gasoline	3.60	Spices	1.01 ± 0.15	2.33 ± 0.30	4.02 ± 0.07	4.44 ± 0.49	3 ± 0.47	5.53 ± 0.24	4.77 ± 0.27	0.28
64	Terpinolene	Pine, plastic	200.00	Spices	35.85 ± 1.90	68.06 ± 3.19	98.84 ± 9.77	98.18 ± 6.24	81.63 ± 11.73	110.50 ± 5.38	120.17 ± 4.81	4.08
65	α-p-dimethylstyrene	Citrus, pine	85.00		14.71 ± 1.03	25.42 ± 2.53	27.11 ± 0.57	30.43 ± 1.31	28.88 ± 1.44	30.31 ± 1.41	30.63 ± 3.86	0.67
66	δ-elemene	Wood		Spices	15.00 ± 2.93	46.63 ± 3.65	48.40 ± 2.21	54.95 ± 2.89	54.86 ± 4.74	60.35 ± 5.25	68.53 ± 3.19	1.90
67	β-caryophyllene	Wood, spice	64.00	Spices	286.46 ± 57.41	628.61 ± 44.65	548.22 ± 40.17	654.56 ± 41.18	759.46 ± 44.52	755.29 ± 63.33	802.57 ± 41.99	22.39
68	α-humulene	Wood	160.00	Spices	16.64 ± 2.97	32.8 ± 2.94	27.14 ± 0.48	35.95 ± 2.49	39.52 ± 3.85	40.25 ± 3.73	45.1 ± 1.67	1.39
69	δ-cadinene	Thyme, medicine, wood		Spices	3.08 ± 0.16	6.02 ± 0.50	4.45 ± 0.01	6.33 ± 0.60	6.60 ± 0.39	7.51 ± 0.42	7.50 ± 0.53	0.27
70	Caryophyllene oxide	Herb, sweet, spice	410.00		0.36 ± 0.06	2.63 ± 0.19	0.74 ± 0.01	1.28 ± 0.13	3.16 ± 0.27	1.91 ± 0.48	2.20 ± 0.22	0.19
	Total				1884.11 ± 200.88	4997.58 ± 158.65	5470.43 ± 294.61	5908.56 ± 337.25	5862.63 ± 459.38	6841.51 ± 430.08	7140.09 ± 378.67	273.69
Others												
71	Allyl methyl sulfide	Garlic, onion	22.00		72.10 ± 4.10	41.61 ± 8.03	113.56 ± 2.54	43.39 ± 1.57	22.50 ± 13.85	53.63 ± 3.42	27.77 ± 17.35	8.56
72	2-pentyl furan	Green bean, butter	5.80	Lipid oxidation	—	17.10 ± 1.94	—	—	58.18 ± 2.30	40.17 ± 2.16	42.55 ± 3.18	4.01
73	p-cymene	Solvent, gasoline, citrus	5.01		183.45 ± 23.56	475.18 ± 9.67	459.12 ± 27.42	476.82 ± 30.10	533.19 ± 27.55	556.53 ± 13.34	573.53 ± 35.92	11.53
74	D-camphor	Camphor, minty, phenolic, herbal	1360.00		2.30 ± 0.53	5.10 ± 0.79	5.62 ± 0.16	5.59 ± 0.5	8.50 ± 0.28	7.18 ± 0.32	7.12 ± 0.38	0.28
75	Borneol	Camphor	180.00		0.22 ± 0.08	0.33 ± 0.06	0.41 ± 0.04	0.47 ± 0.03	0.41 ± 0.03	0.38 ± 0.03	0.34 ± 0.11	0.02
76	Phenol	Phenol	58585.25	Amino acid degradation	0.41 ± 0.04	0.91 ± 0.01	0.75 ± 0.05	0.82 ± 0.03	0.24 ± 0.13	1.13 ± 0.15	1.05 ± 0.07	0.07
77	p-cresol	Medicine, phenol, smoke	3.90		1.55 ± 0.11	1.66 ± 0.05	1.89 ± 0.07	2.64 ± 0.32	1.52 ± 0.14	2.85 ± 0.19	2.79 ± 0.32	0.14
78	Meta-cresol	Fecal, plastic	15.00		4.26 ± 0.24	4.64 ± 0.45	4.43 ± 0.15	6.01 ± 0.54	5.12 ± 0.27	6.56 ± 0.45	6.85 ± 0.57	0.25
	Total				264.29 ± 28.66	546.53 ± 21.00	585.78 ± 30.43	535.74 ± 33.09	629.66 ± 44.55	668.43 ± 20.06	662.00 ± 57.90	30.49

SEM is the Standard Error of Mean (SEM) of the same volatile compound content in different groups of sausage samples.

10.3389/fmicb.2022.1113848

long-chain fatty acids mostly have fat flavor. It is easily to find from Table 4 that, the addition of yeast facilitates the formation of esters. The content of esters in S1 group was the highest (51.25 ± 2.45 μg/kg), which may be related to the high content of acids and alcohols in S1 group, and then promoted the formation of esters. Cano-García et al. (2014) also reached a similar conclusion when exploring the influence of *D. hansenii* on aroma substances of fermented sausage. Among the key flavor esters, ethyl caproate and ethyl octanoate had fruit flavor, which were detected in all groups except LGG.

Ketones may be derived from lipid oxidation or raw meat. Four ketones were detected in 7 groups of sausage samples, of which 2-nonanone (related to lipid β oxidation) was only detected in CK group. 3-hydroxy-2-butanone (acetoin) was detected in all groups, OVA > 1, and the highest content in LGG group. It was associated with microbial carbohydrate fermentation, and had a pleasant buttery odor and was thought to contribute significantly to the formation of sausage flavor.

Alkenes accounted for the highest proportion of the flavor substances, mainly from the use of spices, and α-pinene (pine), β-pinene (pine resin), δ-3-carene (lemon), sabinene (pepper), limonene (lemon), and β-caryophyllene (wood) were relatively high. In addition, a certain amount of allyl methyl sulfide, 2-pentyl furan, *p*-cymene and *D*-camphor were also detected in various sausage samples. 2-pentyl furan is related to the automatic oxidation of fat and is a secondary oxidation product of linoleic acid, which exists in most preserved meat products (Shahidi and Wanasundara, 1998). *p*-cymene had a citrus flavor and had little difference in content among different groups, which might be derived from the use of spices in sausage making process.

3.11. Analysis of sensory evaluation of fermented sausage in each group

Although many literatures have indicated that moderate fat oxidation can improve the flavor and quality of fermented meat products, excessive oxidation will produce rancidity and rancid taste, shorten the shelf life, and ultimately affect the acceptance of products. However, there is no clear definition of the highest sensory acceptance of products at what level of fat oxidation, and fermented sausage is a relatively complex system. Therefore, it is difficult to explore the effect of different yeast on the actual sensory quality of fermented sausage by analyzing the degree of lipid oxidation and the content of flavor substances. The sensory evaluation results of 7 groups of fermented sausages by 39 professionally trained food students are shown in Figure 8.

The higher cheese flavor in the LGG group may be partly due to higher levels of 3-hydroxy-2-butanone (cheese, butter flavor). The fruit flavor in the yeast groups were significantly higher than that of LGG group and CK group, and the rancid taste and oily taste were decreased. The score of S4 group was the lowest (1.23 ± 1.22 and 1.21 ± 1.15), and that of LGG group was the highest (1.56 ± 1.59 and 1.95 ± 1.73), which were consistent with the previous content of aldehydes in volatile flavor substances, indicating that the use of yeast improved the production of flavor substances related to lipid oxidation. In terms of sour taste, the LGG group scored the highest, while the yeast group scored lower, which may be related to the yeast's ability to utilize and metabolize organic acids. In terms of odor (comprehensive score), taste (comprehensive score) and mellow taste, compared with LGG group, scores of yeast groups had increased except S1 group. It is generally believed that yeast plays an important role in the formation of flavor substances such as short peptides and esters during the maturation of fermented meat products due to its ability to decompose protein and fat.

In terms of overall taste, the overall taste of S4 and S5 was higher, reaching 3.67 ± 1.20 and 4.13 ± 1.28, while the overall taste of LGG group and CK group was lower, partly due to the stimulating sour taste of LGG group and the single taste of CK group. S5 group has good performance in mellow taste, appearance color, odor, texture and taste, indicating that this group is the most popular. In addition, S4 group performed well in appearance color, smell and taste, and there was no significant difference in the content of volatile flavor aldehydes between group S4 and S2 (the lowest group). Therefore,

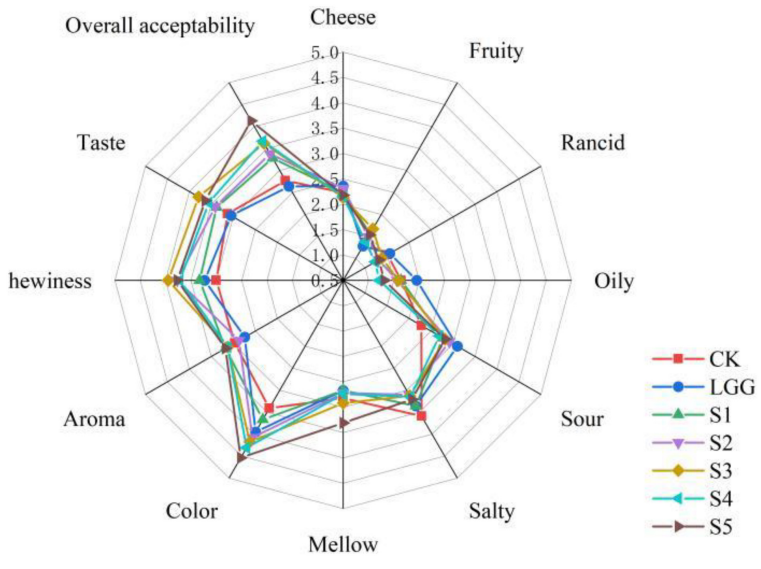

FIGURE 8
Radar image of sensory evaluation scores of different fermented sausage samples.

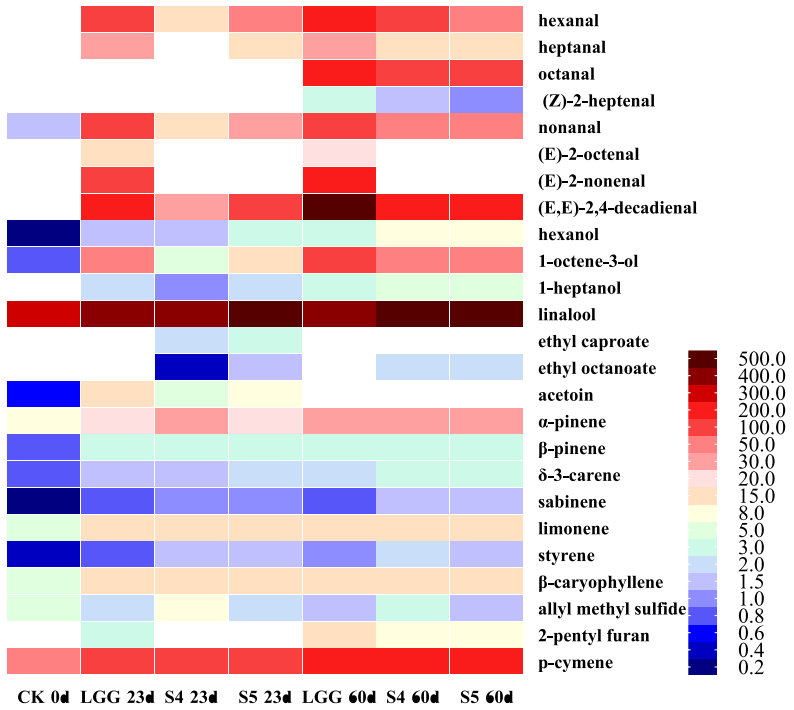

FIGURE 9
OAV heat map of key volatile flavor compounds in different fermented sausage samples after storage.

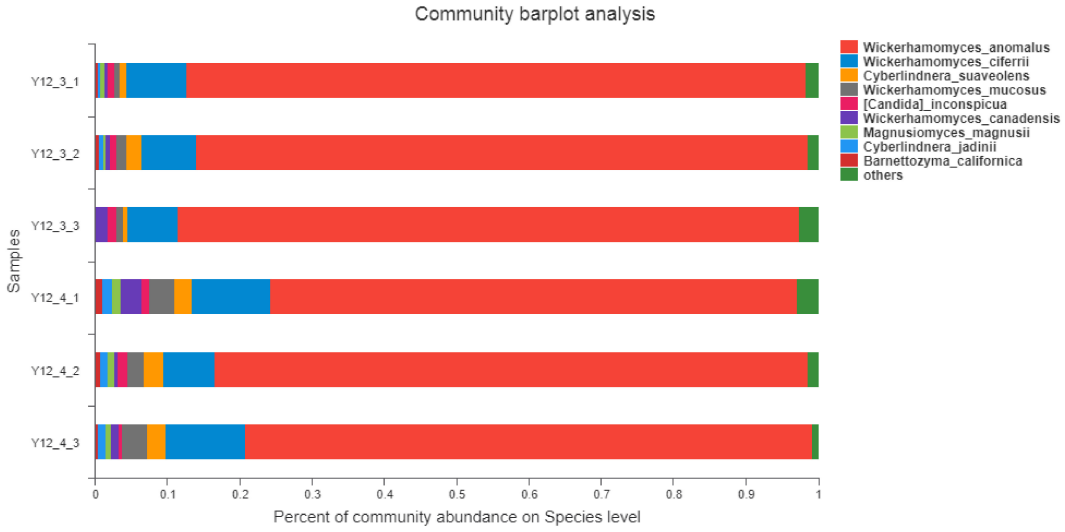

FIGURE 10
Community abundance at species level of fungi in fermented sausage.

the S4 and S5 groups of sausage samples were selected to analyze the flavor substances and metagenomic related indicators of sausage samples after storage.

3.12. Analysis of volatile flavor compounds in fermented sausage after storage

Based on above fat oxidation, volatile flavor compounds analysis and sensory evaluation results, two groups of sausage samples S4 and S5 with low fat oxidation level and excellent sensory scores were screened out. At the same time, the volatile flavor substances of the sausage samples of LGG group stored until 60 days and 0 day of CK were measured. The results were compared based on the 23rd day results, as shown in Table 5. A total of 78 volatile flavor compounds were identified in stored sausage samples, including 16 aldehydes, 16 alcohols, 10 acids, 8 esters, 3 ketones, 17 terpenes, and 8 others.

Compared with the results on day 23, 5 aldehydes were increased, which were octanal, (*Z*)-2-heptenal, (*E,E*)-2, 4-heptadienal, ethyl benzaldehyde and hexadecanal, which were mainly related to the automatic oxidation of fat. Moreover, the proportion of aldehydes

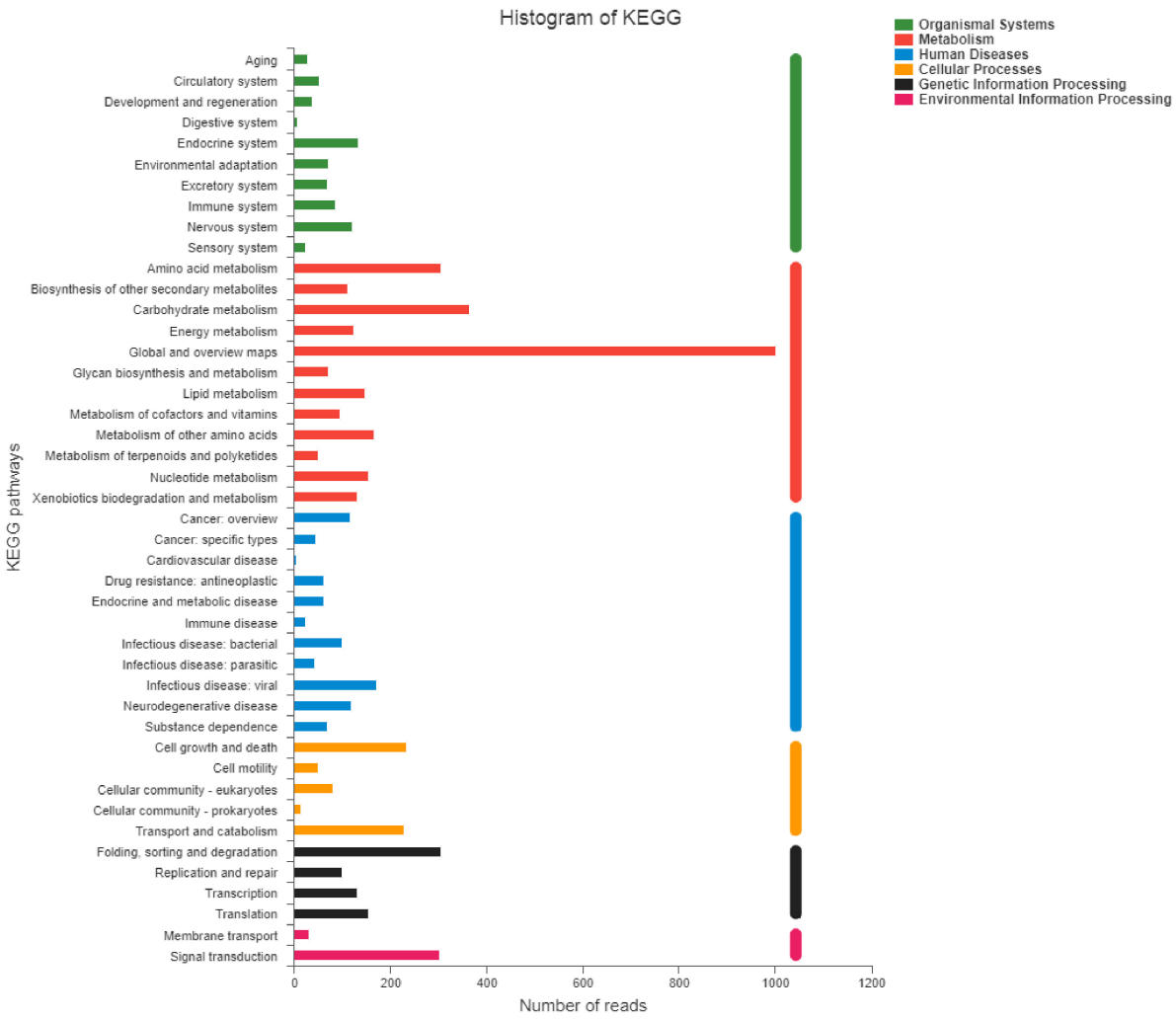

FIGURE 11
Pathway classification statistics of *Wickerhamomyces anomalus* Y12-3.

in total volatile components increased significantly, indicating that the oxidation degree of fat in sausage increased with the increase of storage time, which was consistent with the previous results of POV and TBARS values of sausage samples after storage. Compared with fresh sausage, the types and proportions of other volatile compounds in stored sausage didn't change significantly. According to the sausage sample groups, 43 flavor compounds were detected in the CK- 0 d group, with the least species. 67, 65, and 67 flavor compounds were detected in LGG-23d, S4-23d, and S5-23d, respectively, and 68, 66 and 64 flavor compounds were detected in LGG-60d, S4-60d, and S5-60d, respectively.

Compared with the fresh samples at day 23, the content of aldehydes in the stored samples at day 60 was significantly increased, and the total content of aldehydes in LGG-60d group was 1082.29 ± 55.11 μg/kg, significantly higher than LGG-23d (662.18 ± 26.19 μg/kg), S4-60d (502.19 ± 40.32 μg/kg), and S5-60d (457.53 ± 27.72 μg/kg). It should be noted that the aldehydes content of the S4 group with lower aldehydes content at day 23 exceeded that of the S5 group at day 60. The contents of almost all aldehydes increased after storage, and the content of LGG-60 d group was much higher than that of yeast group, among which the contents of hexanal, octanal, nonanal, (*E*)-2-octenal, (*E*)-2-decenal, (*E,E*)-2, 4-decadienal were significantly different. According to the OAV thermal map analysis (**Figure 9**), it was not difficult to find that the OAV of aldehydes changed significantly (blue indicated lower OAV value, while red indicated higher OAV value), indicating that aldehydes had an important contribution to the formation of unpleasant odor. Octanal and (*Z*)-2-heptenal were the newly added key flavor aldehydes.

The contents of alcohols in samples increased slightly after storage, and the contents of group S4-60d were the highest, reached up to 333.75 ± 28.14 μg/kg. The contents of ethanol and 2-ethyl-1-hexanol decreased after storage, while the contents of hexanol, 1-octene-3-ol, 1-heptanol and 2, 3-butanediol increased after storage. The concentration of 1-octene-3-ol increased by 9.3 times and 3.0 times in S4-60d and S5-60d, respectively. 1-octene-3-ol has a mushroom flavor at low concentration, but is considered to be the main component of peculiar smell at high concentration (Zhou et al., 2020). The variation of linalool content may be related to the water loss of sausages after storage, which was verified by the variation of a_w.

The content of acids in samples was increased after storage, some acid substances had obvious changes, such as butyric acid, pentanoic acid, caproic acid, heptanoic acid, octanoic acid, nonanoic

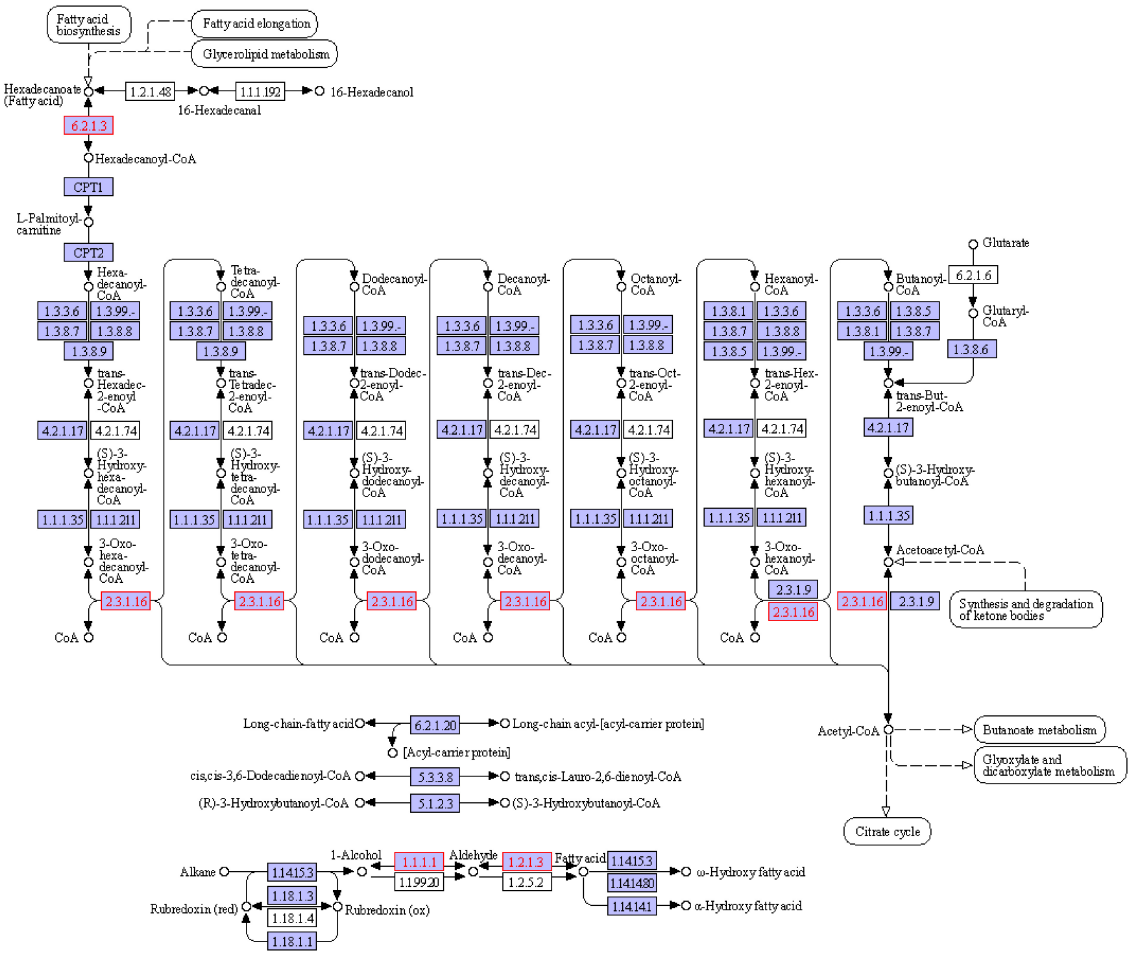

FIGURE 12
Diagram of fatty acid degradation metabolic pathway.

TABLE 6 Key genes and enzymes involved in the degradation of fatty acid in *Wickerhamomyces anomalus* Y12-3.

KEGG gene	KO	KEGG pathway	KEGG enzyme	Enzyme
ppa:PAS_c hr3_0987	K00128	ko00010, ko00053, ko00071, ko00280, ko00310, ko00330, ko00340, ko00380, ko00410, ko00561, ko00620, ko00625, ko00903, ko00981	1.2.1.3	Aldehyde dehydrogenases
kmx:KLM A_70312	K01897	ko00061, ko00071, ko02024, ko03320, ko04146, ko 04216, ko04714, ko04920	6.2.1.3	Long chain acyl-coA synthase

acid and decanoic acid, but still did not reach the odor threshold, so further discussion is not required. The total content of esters did not change significantly in the samples after storage, among which methyl caproate and ethyl caproate were difficult to be detected after storage, while that of ethyl caproate increased. Wu et al. (2019) found that the content of esters decreased at first and then increased during the storage of air-dried sausage, which may be related to the formation of esters through Maillard reaction during storage.

Acetoin, the highest content of ketones, was only detected in fresh and mature samples, but not detected after storage, while the contents of other ketones did not change significantly. The content of terpenes in all sample groups was increased, mainly from the use of spices. The main reason for the increase in content is related to the water loss in the storage process of sausage. Among the other compounds, the content of 2-pentyl furan (related to lipid oxidation) increased in all groups, similar to the change of aldehydes, the content of 2-pentyl furan in LG-60d group was the highest, reaching 58.18 ± 2.3 μ g/kg.

3.13. Exploration of functional genes related to lipid oxidation in yeast

Based on the results of previous determination of volatile flavor compounds in salami, combined with OAV values and possible production pathways of flavor compounds, hexanal, heptanal, nonanal, (*E*)-2-decenal, (*E,E*)-2, 4-decdienal and other flavor compounds related to fat oxidation were selected as the flavor compounds to focus on. The fungal community composition of the samples can be used to analyze the community abundance of fermented sausage at the level of fungal species. The relative abundance of 9 fungi was greater than 0.01 % in the colony structure of fermented sausage, as shown in **Figure 10**. Among them, *Wickerhamomyces anomalus*, *Wickerhamomyces ciferrii*, *Cyberlindnera suaveolens*, and *Wickerhamomyces mucosus* accounted for about 95 %. The proportion of *W. anomalus* in group Y12-3 was higher than that in Y12-4, and the repeatability was better. Therefore,

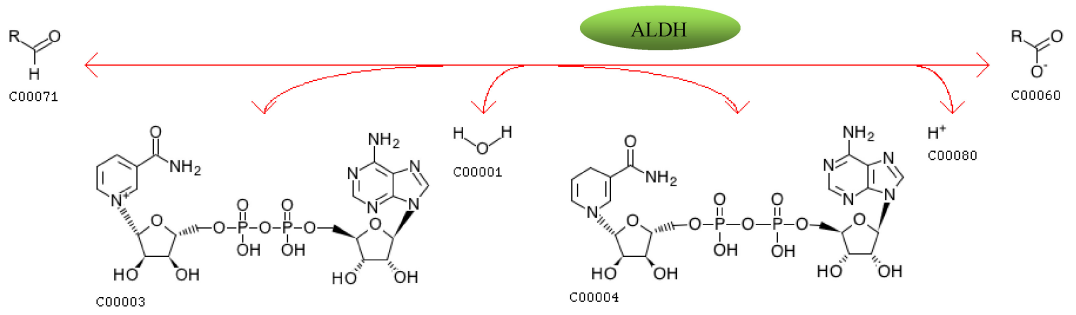

FIGURE 13
The oxidation equation of aldehydes catalyzed by aldehyde dehydrogenase.

the subsequent analysis of functional genes in Y12-3 group could reduce the influence of fungi such as *W. ciferrii* on characteristic flavor substances to a certain extent. The *W. anomalus* Y12-3 gene set was constructed, which was conducted KEGG function annotation and Pathway classification statistics, and the results were shown in **Figure 11**.

The Level 2 functional genes belonging to the same Level 1 were represented in the same color, with the functional gene names for different levels 2 on the vertical axis and the abundance values for the functional gene on the horizontal axis. The abundance of genes related to Metabolism was significantly higher in all six metabolic pathways. Secondary KEGG annotation was performed on genes related to metabolic pathways, of which global and overview maps abundance were the highest, followed by Carbohydrate metabolism, Amino acid metabolism, Metabolism of other amino acids, Nucleotide metabolism, and Lipid metabolism. Meanwhile, the existence of Aldehyde Dehydrogenase (ALDH) function gene could be annotated in the Y12-3 gene set through KEGG database comparison, which was related to Aldehyde metabolism.

Aldehyde Dehydrogenase refers to a class of aldehyde dehydrogenases that rely on NAD(P)+ to catalyze the oxidation of aldehydes. The reaction pathway of its catalytic oxidation of aldehydes is shown in **Figure 11**. Aldehydes, $NAD(P)^+$ and H_2O undergo redox reactions under the catalysis of ALDH to produce carboxylate, NAD(P)H and H^+. Xu et al. (2020) analyzed the effects of 8 *W. anomalus* strains on lipid oxidation of 4°C frozen surimi and found that the addition of yeasts J3, J7, J8, J9, J12, and J18 could significantly reduce the content of TBARS in surimi ($p < 0.05$), and the scavenging rate was proportional to the activity of ALDH. Ziegler and Vasiliou (1999) summarized the research status of ALDH super family and indicated that ALDH super family members can catalyze exogenous and endogenous aldehydes in a broad spectrum. ALDH1A1, ALDH1A2, ALDH1A3, ALDH3B1, and ALDH8A1 can effectively reduce aldehydes produced by lipid peroxidation such as 4-hydroxynonenal, propanal, hexanal, octanal, n-decanal, benzaldehyde, and malondialdehyde.

Aldehyde Dehydrogenase plays the function of metabolic aldehydes through Fatty acid degradation (Pathway ID: ko00071), and the related genes identified include aldehyde dehydrogenase (ppa:PAS_chr3_0987) and long-chain acyl-CoA synthase (kmx:KLMA_70312), as shown in **Figure 12** and **Table 6**. Alcohols form their corresponding aldehydes under the action of alcohol dehydrogenase (EC: 1.1.1.1), and the aldehydes can produce corresponding fatty acids under the action of ALDH. Meanwhile, it should be noted that the above two processes are reversible reactions. According to the results of volatile flavor substances in 23 days sausage samples, except for caproic acid and valeric acid, the content of acids related to lipid oxidation in S4 group was higher than that in LGG group, which verified the possibility that Y12-3 could reduce the content of aldehydes in sausage by metabolizing aldehydes through ALDH (**Figure 13**).

4. Conclusion

The antioxidant capacity of five yeast strains isolated from fermented food was evaluated *in vitro* based on H_2O_2 tolerance, DPPH radical, superoxide anion radical, hydroxyl radical scavenging activity of each cell component (complete bacterial suspension, supernatant after crushing), all these five strains showed the potential of antioxidant activity. However, more attention should be paid to the antioxidation of starter in sausage and whether yeast still retains strong antioxidation after long storage. Considering if yeast is used alone for sausage production without the acid producing and bacteriostatic effects of lactic acid bacteria, it will lead to quality and safety problems in the sausage. *Lactobacillus rhamnosus* YL-1 is a strain screened in our laboratory with strong acid production, nitrite degradation and bacteriostatic effect, and it was mixed with yeast together to apply to fermented salami sausage. At the same time, it could be used alone as the experimental control (LGG group) to obtain more accurate results. Compared with LGG group, the addition of yeast effectively reduced the POV value and TBARS value of sausage, especially in Y12-3 and Y12-4 groups. The analysis results of volatile flavor substances showed that the aldehyde content of LGG group added with lactic acid bacteria alone was significantly higher than that of other groups. After the co fermentation with yeast, the aldehyde content was significantly reduced, especially Y12-3 and Y4-1 groups. The content of flavor substances related to lipid oxidation in Y12-3 group, such as hexanal (fat flavor), heptaldehyde (rancid flavor), *(E)*-2-nonenal (yellow melon flavor), *(E, E)*-2,4-decadienal (fried flavor), was significantly reduced. This result was also supported by sensory evaluation. In Y12-3 group, the scores of putrid taste and oily taste were significantly lower, and the overall acceptance was good, and the oxidation of fat was still effectively inhibited at 60 days. Species and functional contribution analysis showed that yeast Y12-3 contributed the most to the overall function of fungi, and its genes involved in the metabolic pathway were the most abundant at KEGG level1, mainly involved in the

global and overview map, carbohydrate metabolism and amino acid metabolism. Two genes related to fatty acid degradation of aldehydes (ko00071) pathway were found by Y12-3 gene mining. As the key enzyme of aldehyde metabolism, ALDH can direct catalytic aldehyde oxidative dehydrogenation to generate acid substances, which can be used as the follow-up and enzyme activity and gene regulation object, further clarify its role in aldehyde metabolism.

Yeast can be used as a potential antioxidant starter in the production of fermented sausage. The research and development of sausage has practical application value by exploring the antioxidant effect of the starter itself. In the above research, although the metagenomics technology was used to analyze the composition of fungal colonies and predict the gene function, the metabolic pathway of yeast to the lipid oxidation related flavor substances in salami sausage was obtained, and the related enzymes were speculated, the activity of aldehyde dehydrogenase in yeast still needs further verification and reasonable regulation.

Data availability statement

The original contributions presented in this study are included in the article/supplementary material, further inquiries can be directed to the corresponding author.

Author contributions

YL designed and drafted the manuscript. YC carried out the physicochemical properties test and sausage making. KY performed the analysis of microbial populations part and provided helpful feedback and revised the manuscript. SZ performed analysis of volatile flavor compounds. QY helped in antioxidant activities of yeast strains measurement *in vitro*. JW assisted in securing funding and managed the project. All authors contributed to the article and approved the submitted version.

Funding

This work was supported by the National Natural Science Foundation of China (No. 31972111).

Conflict of interest

KY works at the postdoctoral workstation jointly held by Beijing Technology and Business University and Delisi Group Co., Ltd.

The remaining authors declare that the research was conducted in the absence of any commercial or financial relationships that could be construed as a potential conflict of interest.

Publisher's note

All claims expressed in this article are solely those of the authors and do not necessarily represent those of their affiliated organizations, or those of the publisher, the editors and the reviewers. Any product that may be evaluated in this article, or claim that may be made by its manufacturer, is not guaranteed or endorsed by the publisher.

References

Arora, D. S., and Chandra, P. (2010). Assay of antioxidant potential of two *Aspergillus* isolates by different methods under various physio-chemical conditions. *Braz. J. Microbiol.* 41, 765–777. doi: 10.1590/S1517-83822010000300029

Banwo, K., Alonge, Z., and Sanni, A. I. (2021). Binding capacities and antioxidant activities of lactobacillus plantarum and pichia kudriavzevii against cadmium and lead toxicities. *Biol. Trace Elem. Res.* 199, 779–791. doi: 10.1007/s12011-020-02164-1

Beck, P. H. B., Matiucci, M. A., Neto, A. A. M., and Feihrmann, A. C. (2021). Sodium chloride reduction in fresh sausages using salt encapsulated in carnauba wax. *Meat Sci.* 175:108462. doi: 10.1016/j.meatsci.2021.108462

Berardo, A., Claeys, E., Vossen, E., Leroy, F., and De Smet, S. (2015). Protein oxidation affects proteolysis in a meat model system. *Meat Sci.* 106, 78–84. doi: 10.1016/j.meatsci.2015.04.002

Cano-García, L., Rivera-Jiménez, S., Belloch, C., and Flores, M. (2014). Generation of aroma compounds in a fermented sausage meat model system by *Debaryomyces hansenii* strains. *Food Chem.* 151, 364–373. doi: 10.1016/j.foodchem.2013.11.051

Cao, C., Feng, M., Sun, J., Xu, X., and Zhou, G. (2019). Effect of functional starter culture on antioxidant and volatile compound in fermented sausages. *Food Sci.* 40, 106–113. doi: 10.7506/spkx1002-6630-20190513-129

Chen, Q., Kong, B., Han, Q., Xia, X., and Xu, L. (2017). The role of bacterial fermentation in lipolysis and lipid oxidation in harbin dry sausages and its flavour development. *LWT* 77, 389–396. doi: 10.1016/j.lwt.2016.11.075

Chen, Q., Kong, B., Sun, Q., Dong, F., and Liu, Q. (2015). Antioxidant potential of a unique lab culture isolated from harbin dry sausage: in vitro and in a sausage model. *Meat Sci.* 110, 180–188. doi: 10.1016/j.meatsci.2015.07.021

Coppola, R., Iorizzo, M., Saotta, R., Sorrentino, E., and Grazia, L. (1997). Characterization of micrococci and staphylococci isolated from soppressata molisana, a southern italy fermented sausage. *Food Microbiol.* 14, 47–53. doi: 10.1006/fmic.1996.0062

Feng, L., Deng, S., Huang, M., Xu, X., and Zhou, G. (2015). Effect of palatase on lipid hydrolysis, lipid oxidation and sensory attributes of chinese sausage. *Food Sci.* 36, 51–58. doi: 10.7506/spkx1002-6630-201501010

Filho, P. R. C. D., Araújo, I. B., Raúl, L. J., Maciel, M. I. S., Shinohara, N. K. S., and Gloria, M. B. A. (2021). Stability of refrigerated traditional and liquid smoked catfish (*Sciades herzbergii*) sausages. *J. Food Sci.* 86, 2939–2948. doi: 10.1111/1750-3841.15811

He, P. H., She, X., Qian, Y., Yang, J. T., and Rao, Y. (2017). Research advances of spoilage microorganisms and their preventive measures in fermented vegetables. *Sci. Technol. Food Industry* 38, 374–378. doi: 10.13386/j.issn1002-0306.2017.11.064

Hu, G., Wang, D., Zhao, L., Su, L., Tian, J., and Ye, J. (2021). Effects of ripening time on meating quality and flavor compounds of fermented mutton sausages. *J Chinese Inst. Food Sci. Technol.* 21, 194–202. doi: 10.16429/j.1009-7848.2021.02.024

Huang, L., and Huan, Y. J. (2016). Effect of antioxidant starter cultures on lipid oxidation of sausage during fermentation. *Food Fermentation Indust.* 42, 38–44.

Huang, L., Xiong, Y. L., Kong, B., Huang, X., and Li, J. (2013). Influence of storage temperature and duration on lipid and protein oxidation and flavour changes in frozen pork dumpling filler. *Meat Sci.* 95, 295–301. doi: 10.1016/j.meatsci.2013.04.034

Huang, P., Shao, X., Zhu, M., Xu, B., Chen, C., and Li, P. (2020). Sucrose enhances colour formation in dry sausages by up-regulating gene expression of nitric oxide synthase in *Staphylococcus vitulinus*. *Int. J. Food Microbiol.* 315:108419. doi: 10.1016/j.ijfoodmicro.2019.108419

Jaehrig, S. C., Rohn, S., Kroh, L. W., Wildenauer, F. X., Lisdat, F., Fleischer, L., et al. (2008). Antioxidative activity of (1→3), (1→6)-β-d-glucan from *Saccharomyces cerevisiae* grown on different media. *LWT - Food Sci. Technol.* 41, 868–877. doi: 10.1016/j.lwt.2007.06.004

Kim, Y. J., Nahm, B. A., and Choi, I. H. (2010). An evaluation of the antioxidant and antimicrobial effectiveness of different forms of garlic and bha in emulsion-type sausages during refrigerated storage. *J. Muscle Foods.* 21, 813–825. doi: 10.1111/j.1745-4573.2010.00221.x

Leistner, L., and Gould, G. W. (2002). *Hurdle Technologies: Combination Treatments for Food Stability, Safety and Quality*. Berlin: Springer.

Li, S., Zhao, Y., Zhang, L., Zhang, X., Huang, L., Li, D., et al. (2012). Antioxidant activity of Lactobacillus plantarum strains isolated from traditional Chinese fermented foods. *Food Chem.* 135, 1914–1919.

Li, W. C., Liu, Y. L., Zhang, H. J., and Wang, J. (2015). Hs-spme-gc/ms analysis of volatile components in two salami sausages. *Sci. Technol. Food Indust.* 36:9. doi: 10.13386/j.issn1002-0306.2015.07.054

Liu, D., Liang, L., Xia, W., Regenstein, J. M., and Zhou, P. (2013). Biochemical and physical changes of grass carp (*Ctenopharyngodon idella*) fillets stored at -3 and 0°c. *Food Chem.* 140, 105–114. doi: 10.1016/j.foodchem.2013.02.034

Liu, Y., Li, W., Zhang, H., Wang, J., and Sun, B. (2015). Screening of aroma-producing yeast strains from traditional fermented food and research on their aroma-production and fermentation characteristics. *J. Chinese Inst. Food Sci. Technol.* 15, 63–70. doi: 10.16429/j.1009-7848.2015.04.008

Liu, Y., Mao, H., Li, W., Wei, J., Wang, J., Gong, L., et al. (2018). Screening of lactic acid bacteria and effect of its interaction with yeast on the quality of dry fermented sausage. *J. Chinese Inst. Food Sci. Technol.* 18, 96–108. doi: 10.16429/j.1009-7848.2018.09.013

Liu, Y., Wan, Z., Yohannes, K. W., Yu, Q., Yang, Z., Li, H., et al. (2021a). Functional characteristics of lactobacillus and yeast single starter cultures in the ripening process of dry fermented sausage. *Front. Microbiol.* 11:611260. doi: 10.3389/fmicb.2020.611260

Liu, Y., Yu, Q., Zhen, W., Li, H., Liu, J., and Wang, J. (2021b). Effect of antioxidant activity of starter cultures on the quality of fermented meat products: a review. *Food Sci.* 42, 302–312. doi: 10.7506/spkx1002-6630-20200704-052

Martín, A., Córdoba, J. J., Benito, M. J., Aranda, E., and Asensio, M. A. (2003). Effect of *Penicillium* chryso genum and *Debaryomyces hansenii* on the volatile compounds during controlled ripening of pork loins. *Int. J. Food Microbiol.* 84, 327–338. doi: 10.1016/S0168-1605(02)00474-9

Olivares, A., Navarro, J. L., and Flores, M. (2011). Effect of fat content on aroma generation during processing of dry fermented sausages. *Meat Sci.* 87, 264–273. doi: 10.1016/j.meatsci.2010.10.021

Perea-Sanz, L., López-Díez, J. J., Belloch, C., and Flores, M. (2020). Counteracting the effect of reducing nitrate/nitrite levels on dry fermented sausage aroma by *Debaryomyces hansenii* inoculation. *Meat Sci.* 164:108103. doi: 10.1016/j.meatsci.2020.108103

Ramos-Moreno, L., Ruiz-Perez, F., Rodriguez-Castro, E., and Ramos, J. (2021). *Debaryomyces hansenii* is a real tool to improve a diversity of characteristics in sausages and dry-meat products. *Microorganisms* 9:1512. doi: 10.3390/microorganisms9071512

Seo, J. K., Parvin, R., Park, J., and Yang, H. S. (2021). Utilization of astaxanthin as a synthetic antioxidant replacement for emulsified sausages. *Antioxidants* 10:407. doi: 10.3390/antiox10030407

Shahidi, F., and Wanasundara, U. N. (1998). Omega-3 fatty acid concentrates: nutritional aspects and production technologies. *Trends Food Sci. Technol.* 9, 230–240.

Tarladgis, B. G., Watts, B. M., Younathan, M. T., and Dugan, L. (1960). A distillation method for the quantitative determination of malonaldehyde in rancid foods. *J. Am. Oil Chem. Soc.* 37, 44–48.

Vareltzis, P., Hultin, H. O., and Autio, W. R. (2008). Hemoglobin-mediated lipid oxidation of protein isolates obtained from cod and haddock white muscle as affected by citric acid, calcium chloride and ph. *Food Chem.* 108, 64–74. doi: 10.1016/j.foodchem.2007.10.043

Wang, Y., Ouyang, D., Tang, W., Liu, S. B., Gu, Y., and He, Z. G. (2020). Studies on the antioxidant activities of six red yeasts. *Biotechnol. Bull.* 36, 156–164. doi: 10.13560/j.cnki.biotech.bull.1985.2020-0406

Wu, Q., Zhou, H., Li, S., Zhu, N., Zhang, S., Zhao, B., et al. (2019). Changes in volatile flavour compounds during storage and analysis of off-flavour substances in air-dried sausage. *Food Sci.* 40, 208–216. doi: 10.7506/spkx1002-6630-20190217-078

Xu, L., Guo, W., Liu, W., Fu, X., Wu, Y., Luo, F., et al. (2020). Metabolites analysis for cold-resistant yeast (*Wickerhamomyces anomalus*) strains own antioxidant activity on cold stored fish mince. *Food Chem.* 303:125368. doi: 10.1016/j.foodchem.2019.125368

Yang, Y., Fan, F., Zhuo, R., Ma, F., Gong, Y., Wan, X., et al. (2012). Expression of the laccase gene from a white rot fungus in pichia pastoris can enhance the resistance of this yeast to h2o2-mediated oxidative stress by stimulating the glutathione-based antioxidative system. *Appl. Environ. Microbiol.* 78, 5845–5854. doi: 10.1128/AEM.00218-12

Zhang, N., Li, Y., Wen, S., Sun, Y., Chen, J., Gao, Y., et al. (2021). Analytical methods for determining the peroxide value of edible oils: a mini-review. *Food Chem.* 358:129834. doi: 10.1016/j.foodchem.2021.129834

Zhang, Y., Hu, P., Lou, L., Zhan, J., Fan, M., Li, D., et al. (2017). Antioxidant activities of lactic acid bacteria for quality improvement of fermented sausage. *J. Food Sci.* 82, 2960–2967. doi: 10.1111/1750-3841.13975

Zhou, H., Zhao, B., Wu, Q., Li, S., Pan, X., Zhu, N., et al. (2020). Changes in odor-active compounds and analysis of off-flavor compounds in chinese sausage added with black and white pepper during storage. *Food Science.* 41, 162–171. doi: 10.7506/spkx1002-6630-20200315-236

Ziegler, T. L., and Vasiliou, V. (1999). Aldehyde dehydrogenase gene superfamily. *Adv. Exp. Med. Biol.* 463, 255–263. doi: 10.1007/978-1-4615-4735-8_32

frontiers | Frontiers in Microbiology

TYPE Original Research
PUBLISHED 26 January 2023
DOI 10.3389/fmicb.2023.1099906

OPEN ACCESS

EDITED BY
Changyu Zhou,
Ningbo University,
China

REVIEWED BY
Govindaraj Dev Kumar,
University of Georgia,
Griffin Campus,
United States
Haytham M. M. Ibrahim,
Egyptian Atomic Energy Authority,
Egypt

*CORRESPONDENCE
Clemens Kittinger
✉ clemens.kittinger@medunigraz.at

SPECIALTY SECTION
This article was submitted to
Food Microbiology,
a section of the journal
Frontiers in Microbiology

RECEIVED 16 November 2022
ACCEPTED 09 January 2023
PUBLISHED 26 January 2023

CITATION
Schmid PJ, Maitz S, Plank N, Knaipp E, Pölzl S and Kittinger C (2023) Fiber-based food packaging materials in view of bacterial growth and survival capacities.
Front. Microbiol. 14:1099906.
doi: 10.3389/fmicb.2023.1099906

Fiber-based food packaging materials in view of bacterial growth and survival capacities

Paul Jakob Schmid, Stephanie Maitz, Nadine Plank, Elisabeth Knaipp, Sabine Pölzl and Clemens Kittinger*

Diagnostic and Research Institute of Hygiene, Microbiology and Environmental Medicine, Diagnostic and Research Center for Molecular Biomedicine, Medical University of Graz, Graz, Austria

Understanding interactions of bacteria with fiber-based packaging materials is fundamental for appropriate food packaging. We propose a laboratory model to evaluate microbial growth and survival in liquid media solely consisting of packaging materials with different fiber types. We evaluated food contaminating species (*Escherichia coli*, *Staphylococcus aureus*, *Bacillus cereus*), two packaging material isolates and bacterial endospores for their growth abilities. Growth capacities differed substantially between the samples as well as between bacterial strains. Growth and survival were strongest for the packaging material entirely made of recycled fibers (secondary food packaging) with up to 10.8 $\log_{10}$ CFU/ml for the packaging isolates. Among the food contaminating species, *B. cereus* and *E. coli* could grow in the sample of entirely recycled fibers with maxima of 6.1 $\log_{10}$ and 8.6 $\log_{10}$ CFU/mL, respectively. *Escherichia coli* was the only species that was able to grow in bleached fresh fibers up to 7.0 $\log_{10}$ CFU/mL. *Staphylococcus aureus* perished in all samples and was undetectable after 1–6 days after inoculation, depending on the sample. The packaging material strains were isolated from recycled fibers and could grow only in samples containing recycled fibers, indicating an adaption to this environment. Spores germinated only in the completely recycled sample. Additionally, microbial digestion of cellulose and xylan might not be a crucial factor for growth. This is the first study describing bacterial growth in food packaging materials itself and proposing functionalization strategies toward active food packaging through pH-lowering.

KEYWORDS

food packaging, food contamination, bacterial growth, packaging material, cellulose, survival, endospores

1. Introduction

One essential function of food packaging is to protect food from chemical, physical or microbiological changes to extend the shelf life and thereby ensure the quality of the food as well as preserve the consumer's health. In recent years, extensive research on active food packaging has aimed to provide new materials to maintain microbial food integrity beyond traditional packaging systems (Norrrahim et al., 2021). However, many active food packaging strategies are still in their infancy, demand complex functionalization and therefore can only address single steps in the food supply chain (Azevedo et al., 2022). In contrast, the sources of microbial contaminants are manifold and may occur in all steps of food production, transportation, storage and preparation. A large number of different packaging materials are already used in this field to meet the requirements of product quality and safety. However, these established materials are often poorly investigated from the aspect of active food packaging. Fiber-based packaging materials stand out as cost-effective, biodegradable and sustainable solution in the food packaging field due to renewable raw materials

with a large degree of recycling possibilities. Furthermore, a huge diversity of different fiber types and a variety of formulations allow the production of packaging materials for any kind of application. Moreover, a microbiological superiority of fiber-based food packaging materials against plastic packaging has been shown more than once (Patrignani et al., 2016; Siroli et al., 2017). The beneficial effect of fiber-based packaging materials on the cross-contamination potential for stored food has been explained by the capability of entrapping microorganisms within the fiber-network together with a faster loss of viability compared to plastic surfaces (Siroli et al., 2017), indicating active food packaging properties. Nevertheless, little is known about the interactions of microorganisms with the surrounding matrix of fiber packaging due to the high diversity of different types of packaging. While factors affecting a potential transfer of bacteria to contact surfaces have already been assessed (Maitz et al., 2022), the knowledge about microbial growth and survival in food packaging materials needs to be extended. Previous research on the interactions of bacteria with fiber-based packaging materials has largely dealt with fermentation strategies to produce energy carriers such as hydrogen and methane (Ntaikou et al., 2009; Brummer et al., 2014; Asato et al., 2016; Poladyan et al., 2020), or bioplastics (Abdelmalek et al., 2022). These studies usually aimed to optimize waste treatment and used packaging material waste, which was physiochemically treated prior to microbial digestion. Other research focused on spatial interactions and therefore growth media were supplemented to promote microbial growth at the expense of assessing growth capacities (Suominen et al., 1997; Hol et al., 2019). Numerous studies have been conducted on microbial growth in packaged foods, but to our knowledge, no study has ever examined bacterial growth capacities in the food packaging material itself, although fiber-based packaging materials have been postulated to provide a thriving environment for bacteria (Brandwein et al., 2016). More knowledge in this field may contribute to improved types and applications of fiber-based packaging in the food sector as well as point out novel strategies for functionalization. Therefore, this research aimed to evaluate the growth capacities of certain bacterial species in four artificial growth media using only fiber-based packaging materials as a basis, differing in recycled fiber content and fiber bleaching. The tested bacterial strains are related to various food packaging issues either by representing species likely responsible for cross-contamination events, common food contaminants or packaging-inherent microorganisms. *Escherichia coli* (*E. coli*) and *Staphylococcus aureus* (*S. aureus*) are two examples of food-contaminating species responsible for several severe food-borne outbreaks in the last decades (Hennekinne et al., 2012; Yang et al., 2017). The presence of bacteria in fiber-based packaging materials has been intensively studied covering the raw materials, the manufacturing environment and the final product (Väisänen et al., 1998; Zumsteg et al., 2017). Studies on packaging materials revealed a predominance of Gram-positive, mesophilic, endospore-forming bacteria, mostly belonging to the family of Bacillaceae (Suihko et al., 2004; Lalande et al., 2014), including food relevant *Bacillus cereus* (*B. cereus*) (Schmid et al., 2021). Within the last years, the COVID-19 pandemic has drawn public attention to possible cross-contamination events through packaging materials (De Oliveira et al., 2021). However, this cross-contamination involves not only virus particles, but also bacteria in particular when it comes to food contamination. Although hardly any risk for food contamination emanates from the packaging inherent bacteria (Ekman et al., 2009), two members of the Bacillaceae were isolated from a packaging material sample for a more comprehensive study. Furthermore, spore suspensions of *Bacillus subtilis* (*B. subtilis*) and *B. cereus* were tested for their germination and growth capabilities. Both, *B. subtilis* and *B. cereus* are also considered as food spoilage agents (Stenfors Arnesen et al., 2008; Moschonas et al., 2021), especially the latter being known for causing foodborne infections and intoxications. In addition, we investigated factors that can promote or preclude growth, survival and decrease of microorganisms in fiber-based packaging materials by examining cellulose- and xylan-degrading properties of the microorganisms tested and evaluating the role of the pH as intrinsic antimicrobial factor of different packaging materials.

2. Materials and methods

2.1. Samples

In this study, four different cellulose-based fiber materials (PM 1–4) manufactured from three European packaging facilities were included. The samples were provided by industrial partners and were taken by instructed workers after manufacturing, wrapped in aluminum foil and sent to laboratory in sealed plastic bags. All samples came from the food packaging sector with different applications as defined by the manufacturer (Table 1).

2.2. Bacterial strains

The bacterial reference strains used in this study are listed in Table 2. Additionally, a spore suspension of *B. cereus* DSM 345 was prepared using sporulation agar according to EN ISO 7932:2004/prA1:2018 (International Organization for Standardization, 2020). After incubation at 30°C for 5 days, the spores were harvested with 5 ml Sörensen's Phosphate Buffer including KH_2PO_4 (0.067 mol/l, Merck KGaA, Darmstadt, Germany) and $Na_2HPO_4 \cdot 2\,H_2O$ (0.067 mol/l, Merck KGaA) adjusted to a pH of 7. Afterwards, the spore suspension was centrifuged (4,200 rpm, 15 min, 4°C) and the pellet was washed with Sörensen's Phosphate Buffer up to four times until high purity of spores was verified using a light microscope. The spore suspension was finally stored in ddH_2O at −80°C. In order to investigate growth capacities and

TABLE 1 Packaging material samples.

Sample	Fiber type	Packaging type	Application
PM 1	Fresh fibers, bleached	Primary food packaging	Direct food contact (dry/moist/fatty)
PM 2	50% recycled fibers	Primary food packaging	Direct food contact (dry/moist/fatty) direct contact with food products that must be peeled or washed before consumption
PM 3	100% recycled fibers	Secondary food packaging	No direct food contact
PM 4	Fresh fibers, unbleached	Primary food packaging	Direct food contact (dry/moist/fatty)

Samples and corresponding information about the fiber type, food packaging type and application according to the manufacturers' specifications.

TABLE 2 Bacterial reference strains used in this study.

Bacterial strain	Origin
Escherichia coli DSM 1576	German Collection of Microorganisms and Cell Cultures GmbH (DSMZ), Braunschweig, Germany
Staphylococcus aureus DSM 799	DSMZ, Germany
Bacillus cereus DSM 345	DSMZ, Germany
Bacillus subtilis (BGA) spore suspension	Merck KGaA, Darmstadt, Germany
Cellulomonas uda DSM 20108	DSMZ, Germany

characteristics of packaging material inherent bacteria, two bacterial strains (strain 3.1, strain 3.2) were isolated from PM 3, identified on species level by MALDI-TOF (VITEK® MS, bioMérieux Marcy-l'Étoile, France) and 16S rRNA gene sequencing and included in all experiments. In brief, one gram of packaging material was disintegrated with 99 ml of 0.9% saline solution in sterile plastic bags using a Bagmixer (Interscience, St. Nom la Bretèche, France), followed by plating 500 µl on tryptic soy agar (TSA, Oxoid Deutschland GmbH, Wesel, Germany) and incubation at 37°C for 24 h. Two different colonies were randomly picked. For the species identification, strains were grown on COL-S blood agar (Becton Dickinson Austria GmbH, Vienna, Austria) at 37°C overnight, followed by MALDI-TOF identification and 16S rRNA gene sequencing using primer pairs 8FPLm and 806R for the 5′ fragment of the 16S rRNA gene (Relman, 1993). The INVISORB Spin DNA Extraction Kit (Invitek Molecular, Berlin, Germany) was used for DNA purification and amplification products were sent to Eurofins Genomics Germany GmbH (Ebersberg, Germany) for sequencing. Species affiliation was performed using the BLAST Sequence Analysis Tool (Altschul et al., 1990).

2.3. Growth and survival experiments

For preparation of media used to investigate microbial growth, one gram of a packaging material sample was evenly homogenized with 99 ml of 0.9% saline solution in sterile plastic bags using a Bagmixer. Subsequently, the fiber suspension was transferred into an Erlenmeyer flask and sterilized by autoclaving at 121°C. For pH measurements, 10 ml of the packaging material medium were centrifuged at 4,200 rpm for 15 min followed by pH determination in the supernatant using a pH meter (Orion 3 Star, Fisher Scientific (Austria) GmbH, Vienna, Austria). To study the influence of pH in PM 4, the 0.9% saline solution was replaced with phosphate buffered saline (PBS, Merck KGaA) in all steps of the experiment. The sterile packaging material media were inoculated with one of the following species: *E. coli*, *S. aureus*, *B. cereus*, as well as the two packaging material isolates. For this purpose, overnight cultures were grown in tryptic soy broth (TSB, Oxoid Deutschland GmbH) at 30°C (*B. cereus* and the isolated strains) or at 37°C (*E. coli* and *S. aureus*). Afterwards, the optical density at 600 nm (OD_{600}) of the bacterial suspension was measured, followed by three washing steps in sterile 0.9% saline solution and centrifugation at 4,200 rpm for 15 min each to remove remaining traces of TSB. Then, the bacterial suspension was adjusted to an OD_{600} of 0.5 in sterile 0.9% saline solution. Generally, a bacterial suspension with OD_{600} of 0.5 equals approximately 8 $\log_{10}$ CFU/mL including species and strain variations. To study both eventual growth and survival, packaging material media were inoculated with bacterial cells in order to reach a final cell density of approximately 1 to 3 $\log_{10}$ colony forming units (CFU) /mL and 5 to 7 $\log_{10}$ CFU/mL, respectively, in the culture flask. All dilutions were performed with 0.9% sterile saline solution. After inoculation, the flasks were shaken at 120 rpm for 5 min in order to ensure even distribution of the spiked-in bacteria, immediately followed by initial determination of the microbial count and verification of the inoculum size. To determine the bacterial count, pour plate method was performed in which 1 ml was transferred either directly from the culture flask or appropriately diluted into a sterile petri dish and covered with 15 ml warm TSA. Bacterial counts were performed in technical triplicates. Agar plates were incubated at 30 or 37°C for 24 h and CFU were counted. The culture flasks were then incubated at 30 to 37°C with 50 rpm shaking. Further determinations of the bacterial count were performed after 1, 2, 3, 6, and 7 days of incubation. In addition, we inoculated the packaging material media with bacterial spore suspensions of *B. cereus* DSM 345 and *B. subtilis* subsp. *spizizenii* according to the protocol described before. All experiments were performed in biological duplicates.

As a contamination control, sterile medium was included for each packaging material medium to verify proper autoclaving. After each growth experiment, the correct presence of inoculated species was verified by streaking the packaging medium on COL-S agar and subsequent MALDI-TOF identification. Spore germination was assessed by selected microscopic examination of the growth media. For this purpose, 5 to 10 ml of culture medium were pelleted and microscopically examined with the Zeiss Axio Lab.A1 microscope (Carl Zeiss AG, Oberkochen, Germany) and image capture software ZEN version 3.2 (Carl Zeiss AG).

The data was analyzed and visualized in GraphPad Prism version 7.0.0 for Windows (GraphPad Software, San Diego, United States).

2.4. Determination of cellulose- and xylan-digestion abilities

To test potential cellulose digestion by the tested bacteria, we evaluated two carboxymethyl cellulose (CMC) media for CMC-assays previously described (Amore et al., 2013). For the CMC medium A, 5 g sodium CMC, (Sigma-Aldrich, Merck KGaA), 5 g Bacto™ tryptone (Thermo Fisher Scientific, Vienna, Austria) 4 ml micro salt solution consisting of 46.12 µl H_3PO_4 (Merck KGaA), 11.12 mg $FeSO_4$ (Merck KGaA), 5.94 mg $ZnSO_4$ (Merck KGaA), 0.436 mg $CuSO_4$ (Merck KGaA), 2.5 mg $MnSO_4$ (Merck KGaA), 0.6 mg $Co(NO_3)_2$ (Merck KGaA), 0.6 mg Na_2MoO_4 (Merck KGaA) and 1.24 mg H_3BO_3 (Merck KGaA) in 1000 ml dH_2O, as well as 5 g NaCl (Carl Roth GmbH +Co. KG, Karlsruhe, Germany), 2 g $(NH_4)H_2PO_4$ (Merck KGaA), and 15 g agar-agar (Carl Roth GmbH +Co. KG) were dissolved in 1 l deionized water by heating to 60°C, succeeded by autoclaving and agar plate preparation. For CMC medium B, 0.02% Remazol Brilliant Blue R (Merck KGaA) were added after autoclaving. Remazol Brilliant Blue R was intended for visualization of cellulose and xylan degradation indicated by a halo zone around colonies as mentioned by Amore et al. (2013). TSA was supplemented with 5% CMC as an additional medium, in case CMC medium A and B did not result in growth. All bacterial strains included in this study were grown on TSA and then streaked on CMC medium A and B and incubated at 30°C for 4 days. If colonies were found, they were picked and a bacterial suspension equal to McFarland standard 0.5 was prepared and diluted 10^{-3}. Then one µL was spotted on CMC medium A and incubated for another 4 days at 30°C. After incubation, the CMC medium A was stained by flooding the agar plate with 0.1%

aqueous Congo red solution (Carl Roth GmbH +Co. KG) for 10 min and subsequent two times washing with 5 M NaCl to visualize cellulose degradation indicated by a clear halo around the colonies (Amore et al., 2015). Halo zones were measured by taking the total diameter including colony and halo minus the diameter of the colony. All strains were tested in triplicates. For xylan digestion assay, 1,000 ml ready-to-use TSA base were prepared according to manufacturer's protocol and supplemented with 5 g of birch wood xylan (Carl Roth GmbH +Co. KG) before autoclaving and agar plate preparation. All bacterial strains were pre-grown on TSA, then a bacterial suspension equal to McFarland 0.5 was prepared and one µL was spotted on xylan medium and incubated at 30°C for 4 days. Afterwards, the agar plates were stained with 0.1% Congo red and washed with 5 M NaCl. If possible, halo diameters on xylan plates were measured as for CMC plates. As a control, bacterial strains were grown in medium A without CMC and TSA and then stained.

3. Results

3.1. Growth and survival studies on bacterial food contaminants in packaging material media

The critical food contaminants *E. coli*, *S. aureus* and *B. cereus* were spiked in four different sterilized and homogenized packaging material samples to evaluate their growth and survival capacities in this environment. Monitoring over 7 days of the spiked growth media revealed distinct differences in the growth capacities of the test strains depending on the type of fiber-based packaging material used (Figure 1). Microbial growth and survival was primarily associated with the 100% recycled fibers medium and the bleached fresh fibers medium, whereas the media composed of 50% recycled fibers and unbleached fresh fibers, respectively, resulted in both, lower microbial survival and no observable growth. For growth evaluation, the above listed bacterial species were added to the samples in quantities leading to bacterial counts ranging from 1 to 3 $\log_{10}$ CFU/mL (low inoculum) at the beginning of incubation. As a result, *E. coli* (Figure 1A) was able to grow in the PM 1 (fresh fibers, bleached) and PM 3 (100% recycled fibers) media and no growth but a decrease in the number of bacteria was seen for PM 2 (50% recycled fibers) and PM 4 (fresh fibers, unbleached). Thereby, *E. coli* reached a maximum bacterial count of 8.6 $\log_{10}$ CFU/mL in PM 3 within 3 days and 7.0 $\log_{10}$ CFU/mL in PM 1 after 7 days. In contrast, *S. aureus* decreased in all tested media and no growth was observed (Figure 1B). *Bacillus cereus* could only grow in the 100% recycled fibers medium PM 3 reaching a maximum of 6.1 $\log_{10}$ CFU/mL (Figure 1C). Furthermore, it remained at stable bacterial counts in PM 1, while decreasing in PM 2 and PM 4. In addition to growth, survival was evaluated at an initially added bacterial level of 5 to 7 $\log_{10}$ CFU/mL (high inoculum) to better visualize a potential decrease. Growth of *E. coli* even continued to be observed in PM 3 at high inoculation levels up to 9.9 $\log_{10}$ CFU/mL (Figure 1D). No significant changes in bacterial counts were observed in PM 1 and PM 2 suggesting stable survival in these media. In PM 4 however, *E. coli* could not sustain and was completely eliminated within 2 days. No survival was observed for *S. aureus* in any of the media tested (Figure 1E), which corresponds to the observations in the growth experiments with lower spike-in levels. Nevertheless, incubation in PM3 resulted in longer survival and a slower decline for *S. aureus*. Similar to the growth results, *B. cereus* was able to survive in PM 1 and PM 3 without major changes in bacterial numbers (Figure 1F), but decreased in PM 2 and PM 4 without disappearing completely. As a control, the bacterial counts of each inoculum were determined prior to inoculation of the media. For each bacterial species, correct inoculations were observed with deviations of less than 1-$\log_{10}$ in the final medium to the inoculum. After each growth and survival experiment, the presence of the inoculated species was also correctly confirmed by MALDI-TOF identification.

3.2. Identification of packaging material isolates

To investigate the interaction of typical packaging material bacteria with different types of packaging materials, two isolates from PM 3 (100% recycled fibers) were collected, identified on species level and then tested for their growth and survival capacities. The MALDI-TOF identification revealed *Bacillus firmus* and *Bacillus circulans* for the two isolates, which was confirmed by 16S rRNA gene sequencing giving *Cytobacillus* (*C.*) *firmus* and *Nialla* (*N.*) *circulans* as a result. *Cytobacillus firmus* and *Niallia circulans* are both Gram-positive, rod-shaped endospore forming bacteria from the Firmicutes. For both species, new genera were recently proposed separating them from the genus *Bacillus* (Gupta et al., 2020; Patel and Gupta, 2020).

3.3. Growth and survival studies on packaging material isolates

Both strains, *C. firmus* and *N. circulans*, were isolated from PM 3 and showed strong growth in the PM 3 based medium consisting exclusively of recycled fibers (Figures 2A,B). When added to the PM 3 medium at low initial spike-in counts (low inoculum) *C. firmus* and *N. circulans* reached maxima of 10.8 $\log_{10}$ CFU/mL and 10.2 $\log_{10}$ CFU/mL, respectively, after 6 days of incubation, which clearly exceeded the growth capacities of tested *E. coli* and *B. cereus* strains in this packaging material medium. Moreover, microbial growth of *C. firmus* and *N. circulans* was also observed in the PM 2 medium composed of 50% recycled fibers, reaching up to 5.6 $\log_{10}$ CFU/mL after 6 days and 6.0 $\log_{10}$ CFU/mL after 3 days of incubation, respectively. No growth could be observed for *C. firmus* and *N. circulans* in PM 1 and PM 4 media, both consisting of fresh fibers, which may indicate a specific interaction of these two isolates with packaging materials containing recycled fibers. Interestingly, in PM 4, *C. firmus* was already undetectable directly after inoculation at time point 0, which pointed toward an antimicrobial effect that emanates from this packaging material type. The inoculum control revealed a bacterial count of 3.2 $\log_{10}$ CFU/mL present in the medium after inoculation, thus, a 3-$\log_{10}$ reduction (99.9%) of *C. firmus* was observed in PM 4. This immediate antimicrobial effect in the PM 4 medium could also be seen for *N. circulans*, which was reduced from 1.5 $\log_{10}$ CFU/mL after inoculation to a mean count of below 0 $\log_{10}$ CFU/mL (n = 2) at time point 0, followed by a complete elimination. When added to the PM 3 medium at high initial spike-in counts for survival monitoring (high inoculum), *C. firmus* und *N. circulans* reached comparable counts of CFU/mL as in the growth experiments (Figures 2C,D).

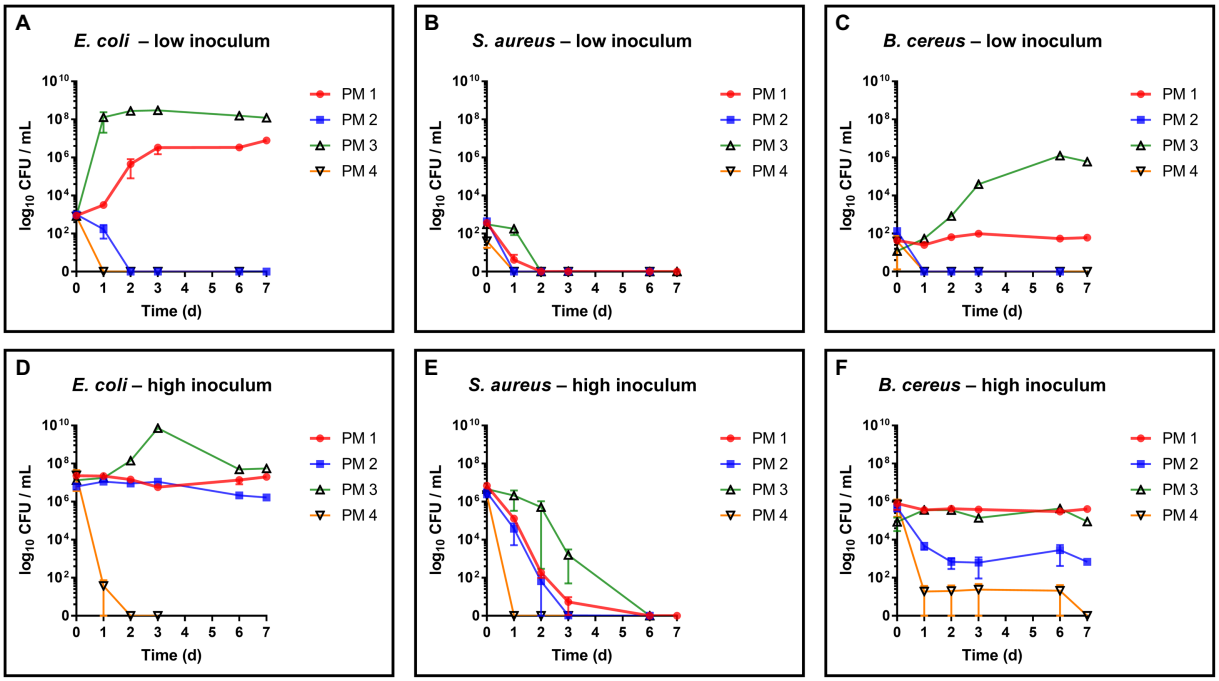

FIGURE 1
Evaluation of growth and survival of food contaminating species. Growth and survival were evaluated over time in liquid media solely consisting homogenized packaging materials. PM 1 (red) consists of bleached fresh fibers, PM 2 (blue) consists of 50% recycled fibers, PM 3 (green) consists of 100% recycled fibers, and PM 4 (yellow) consists of unbleached fresh fibers. **(A)** *E. coli*, low inoculum (1 to 3 $\log_{10}$ CFU/mL), **(B)** *S. aureus*, low inoculum, **(C)** *B. cereus*; low inoculum, **(D)** *E. coli*, high inoculum (5 to 7 $\log_{10}$ CFU/mL), **(E)** *S. aureus*, low inoculum, and **(F)** *B. cereus* high inoculum. All experiments were performed in biological duplicates. The mean with range is plotted.

Therefore, it confirms the extend of growth potential. Reduced growth of *C. firmus* and *N. circulans* was observed in PM 2 medium, confirming the extent of growth potential in this medium determined by the previous growth experiment. Unlike the food contaminants *E. coli* and *B. cereus*, the PM 3 isolates *C. firmus* and *N. circulans* could not sustain in PM 1 consisting of fresh fibers. While *C. firmus* has already disappeared completely after 1 day of incubation, *N. circulans* decreased notably but remained detectable in the medium for up to 7 days at levels below 1 $\log_{10}$ CFU/mL. Incubation in PM 4 medium resulted in a reduction of *C. firmus*, but it was still detectable at levels below 1 $\log_{10}$ CFU/mL (Figure 2C). As for the growth experiment, an immediate antimicrobial effect was seen if comparing the inoculation of PM 4 to 7.1 $\log_{10}$ CFU/mL final concentration with the detected number 3 $\log_{10}$ CFU/mL ($n = 2$) at time point 0 (after 5 min), which corresponds to a 4-$\log_{10}$ reduction (99.99%) of inoculated bacteria (Figure 3). Although a continuous decrease over time could not be observed for *N. circulans* in PM 4 (Figure 2D), a discrepancy between inoculated bacteria and detected bacteria after 5 min was present. The inoculated bacteria of 5.5 $\log_{10}$ CFU/mL final concentration in the medium were reduced to 3.3 $\log_{10}$ CFU/mL, corresponding to a 2-$\log_{10}$ reduction (99%) (Figure 3). The low-level survival of *C. firmus* and *N. circulans* throughout the incubation period resembled the observations for *B. cereus* in PM 2 and PM 4 (Figure 1F), suggesting a connection to the presence of endospores. Correct inoculations with *C. firmus* and *N. circulans* were observed for PM 1 and PM 2 with deviations of less than 1-$\log_{10}$. Inoculation of PM 3 tended to be more unstable which resulted in deviations of less than 2-$\log_{10}$ (Data not shown). After each growth and survival experiment, the presence of the inoculated species was also correctly confirmed by MALDI-TOF identification.

3.4. Germination and growth capabilities of *Bacillus subtilis* and *Bacillus cereus* endospores

The germination capacity of free bacterial endospores was assessed by including a commercial *B. subtilis* subsp. *spizizenii* spore suspension as well as a laboratory made spore suspension of *B. cereus* into our growth and survival experiments. For both strains, spore germination and subsequent growth was exclusively observed in PM 3 medium (100% recycled fibers) (Figures 4A,B). This is in accordance with the results from the growth experiments with vegetative *B. cereus*, whereas lower bacterial counts were detected with a maximum of 5.8 $\log_{10}$ CFU/mL (Figure 4A). In sharp contrast to vegetative *B. cereus* cells, no decrease was observed in PM 2 and PM 4, pointing to the increased stability of bacterial endospores compared to vegetative cells. Nevertheless, neither PM 1, PM 2 nor PM 4 allowed microbial growth when bacterial endospores were added. The inoculation with *B. subtilis* endospores resulted in comparable observations as for *B. cereus* endospores (Figure 4B). Growth of *B. subtilis* was exclusively observed in PM 3 medium, but at both low and high bacterial inoculum up to 8.3 $\log_{10}$ CFU/mL (Figure 4C) and 8.4 $\log_{10}$ CFU/mL (Figure 4D), respectively. Neither growth nor decrease of *B. subtilis* was seen in PM 1, PM 2 and PM 4 suggesting only a stable survival of dormant bacterial endospores (Figures 4C,D). This suggestion is supported by the correct identification of *B. subtilis*

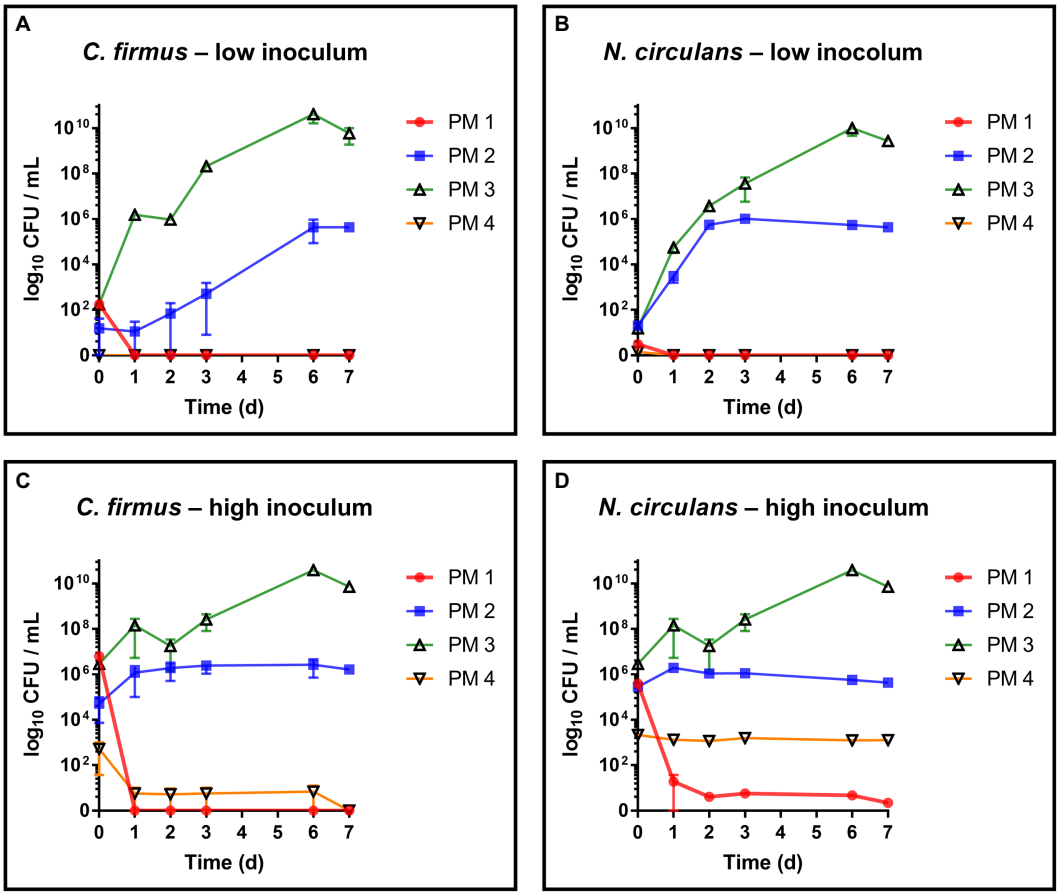

FIGURE 2
Evaluation of growth and survival of packaging material isolates. Growth and survival were evaluated over time in liquid media solely consisting homogenized packaging materials. PM 1 (red) consists of bleached fresh fibers, PM 2 (blue) consists of 50% recycled fibers, PM 3 (green) consists of 100% recycled fibers, and PM 4 (yellow) consists of unbleached fresh fibers. **(A)** *Cytobacillus firmus* (*C. firmus*), low inoculum (1–3 $\log_{10}$ CFU/mL), **(B)** *Niallia circulans* (*N. circulans*), low inoculum, **(C)** *Cytobacillus firmus* (*C. firmus*), high inoculum (5–7 $\log_{10}$ CFU/mL), **(D)** *Niallia circulans* (*N. circulans*), high inoculum. All experiments were performed in biological duplicates. The mean with range is plotted.

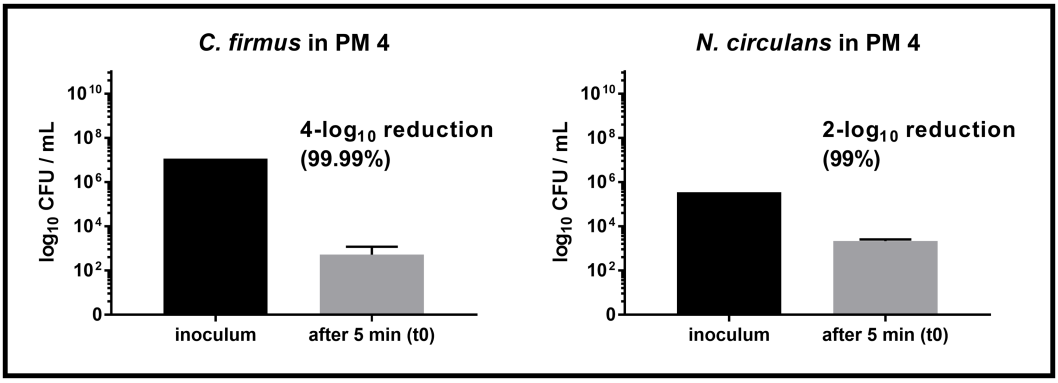

FIGURE 3
Comparison of inoculum and recovery in PM4. Comparison of the inoculum (initially spiked-in) and bacterial count after 5min (t0) in the packaging material medium PM 4. Substantial reduction was only observed for *Cytobacillus firmus* (*C. firmus*, left) and *Niallia circulans* (*N. circulans*, right). Inoculum was prepared once (initially spiked-in). Inoculation of PM 4 and CFU counting after 5min (t0) was done in biological duplicates. The mean with standard deviation is plotted.

subsp. *spizizenii* and *B. cereus* using MALDI-TOF after completion of the experiments, as well as the generally correct inoculation with *B. subtilis* and *B. cereus* spores with deviations of less than 1-$\log_{10}$. A deviation of more than 1-$\log_{10}$ was observed for the growth experiment inoculation of PM 3 with *B. cereus* spores (Data not shown), however, without major effects due to growth in PM 3

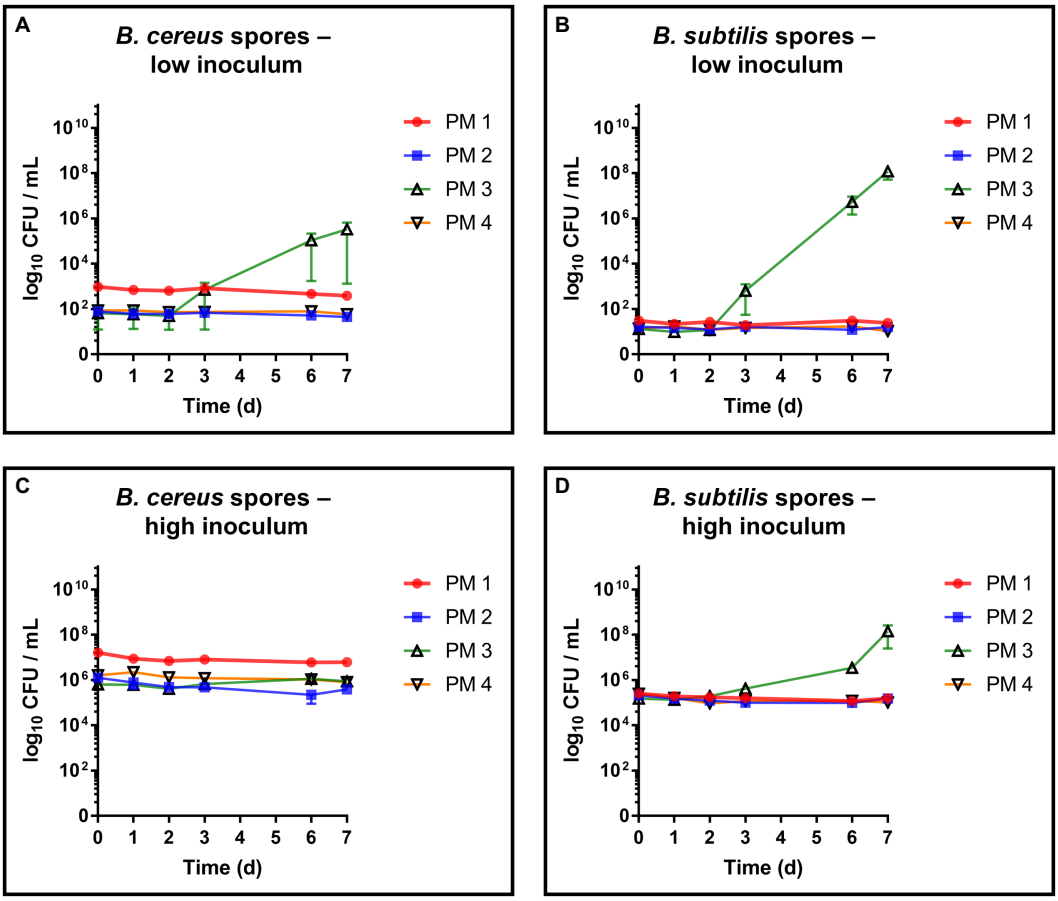

FIGURE 4
Evaluation of spore germination and growth capabilities. Spore germination and growth capabilities of *B. cereus* and *B. subtilis* endospores were evaluated over time in different liquid media solely consisting homogenized packaging materials. PM 1 (red) consists of bleached fresh fibers, PM 2 (blue) consists of 50% recycled fibers, PM 3 (green) consists of 100% recycled fibers, and PM 4 (yellow) consists of unbleached fresh fibers. **(A)** *Bacillus cereus* endospores, low inoculum (1–3 $\log_{10}$ CFU/mL), **(B)** *Bacillus subtilis* endospores, low inoculum, **(C)** *Bacillus cereus* endospores, high inoculum (5–7 $\log_{10}$ CFU/mL), and **(D)** *Bacillus subtilis* endospores, high inoculum. All experiments were performed in biological duplicates. The mean with range is plotted.

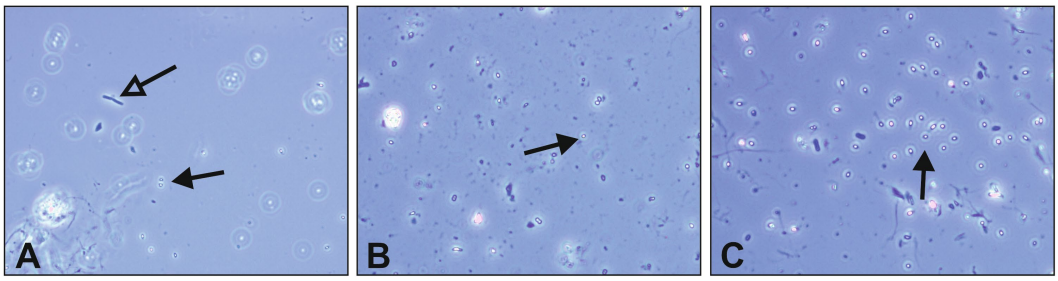

FIGURE 5
Microscopic evaluation of *Bacillus cereus* endospore germination. Endospore germination was evaluated in liquid growth media solely based on different packaging materials. Spore germination was visually assessed in pelleted media using phase-contrast microscopy after 7 days of incubation at 30°C. Dormant bacterial spores are indicated with black arrows, while vital cells emerging from germination are indicated with empty arrows. **(A)** *Bacillus cereus* spores and vital bacterial cell in PM 1, **(B)** *Bacillus cereus* spores in PM 2, and **(C)** *Bacillus cereus* spores in PM 4. The packaging material medium PM 3 was excluded due to pronounced bacterial growth during incubation, making germination evaluation redundant.

medium. Microscopic examination of pelleted growth media confirmed the limited potential of bacterial spores to germinate in PM 1, PM 2 and PM 4 (Figure 5). Germination of *B. cereus* spores was only observed very occasionally in PM 1 (Figure 5A), whereas no germination of *B. subtilis* was found in PM 1, PM 2 and PM 4.

3.5. Bacterial digestion of carboxymethyl cellulose and xylan

To investigate cellulolytic and hemicellulolytic properties, all strains were plated on two different media containing sodium carboxymethyl

cellulose (CMC medium A and B) as well as one xylan-containing medium. Regarding the digestion of CMC, bacterial growth was only observed on medium A, whereas no colonies were detected on medium B indicating growth inhibition emanating from Remazol Brilliant Blue (Table 3). After spot inoculation and staining of CMC medium A, halos were observed for *B. cereus* and *B. subtilis* indicating bacterial cellulose degradation, including a double halo for *B. subtilis* (Figure 6). The evaluation of halo zones revealed large activity for *B. subtilis* (8.3 mm inner halo and 12.3 mm outer halo) and *B. cereus* (7.7 mm) compared to the positive control *Cellulomonas uda* (2.7 mm). However, bacterial growth of *C. uda* was noticeably slower, which resulted in very small colonies and compared to the large colonies of *B. cereus* and *B. subtilis*. Moreover, *C. firmus* turned out to be a more fastidious species and cellulolytic properties could not be assessed on CMC medium A. However, incubation on TSA supplemented with CMC resulted in bacterial growth, but no signs of cellulose degradation, while the control strain *C. uda* showed degradation on this medium. On xylan medium, all strains except for *C. firmus* were able to grow. After Congo red stain, clear halos were visible only for *B. subtilis* (16.7 mm) as well as for the positive control *C. uda* (8.7 mm) indicating digestion of the hemicellulose xylan. Incubation on control media without supplements (CMC or xylan) did not lead to halo formation on the respective media. Based on the results from previous growth experiments in packaging material media, no association could be established between the cellulolytic or xylanolytic properties and the specific microbial growth in packaging material.

3.6. Influence of the pH value of the packaging material on bacterial growth

Although the exact compositions of the packaging materials are not known, a potential factor for observed antimicrobial activity in PM 4 could be determined by pH measurement of the media. The pH for growth media made of PM 1, PM 2 and PM 3 were 6.32, 7.98 and 8.21, respectively, and thus did not deviate widely from neutral pH. In contrast, PM 4 medium showed a considerably lower pH of 4.46, which provides harsh conditions for microbial growth. In order to dissect the detrimental effects of pH in homogenized PM 4, the sample was additionally homogenized with PBS to maintain a neutral pH of 7.40 and inoculated with the test strains for growth monitoring. Growth experiments revealed a stable survival of *E. coli* instead of rapid decrease (Figure 7A) and prolonged survival of *S. aureus* in PM 4 with PBS (Figure 7B). For members of the Bacillaceae (*B. cereus*, *N. circulans*, and *C. firmus*) the stabilizing effect of buffered growth medium could not be confirmed as the decrease of bacterial counts did not change notably compared to PM 4 with 0.9% NaCl (saline) solution (Figures 7C–E). However, the instant reduction of *C. firmus* and *N. circulans* in PM 4 homogenized with saline solution was not observed when PBS was used, giving evidence for the immediate effect of the pH on bacterial survival (Figure 7F). Furthermore, pH did not change significantly over incubation period in bacterial cultures of the Bacillaceae contradicting pH as the sole factor for antimicrobial activity.

4. Discussion

The awareness of food safety continues to grow and, as a result, there is a demand for appropriate food packaging that ensures the microbial integrity of food. Fiber-based packaging materials are widely used as primary food packaging (Deshwal et al., 2019) e.g. as bags for baked goods, pizza boxes, fast food containers, and especially cardboard crates for fruits and vegetables, as well as for secondary and tertiary food packaging applications. However, the effects of bacterial growth within these packaging materials have been scarcely studied. The curious lack of information regarding the microbial integrity of fiber-based packaging materials compared to other packaging systems has already been stated (Brandwein et al., 2016). A recent study investigating storage effects of fiber-based food packaging products on the microbial load reported significant reductions after 6 months of storage at 4°C (Zaidi et al., 2022). However, this long-term study lacked in more comprehensive investigations such as growth promoting temperatures, spiking with external microorganisms, and different time points. Our unique study contributes to fulfill this gap of knowledge by investigating the growth and survival of different species in fiber-based packaging materials, especially since all the packaging materials included are actually used in the food packaging sector (Table 1). These materials generally contain low quantities of bacteria per gram (Hladíková et al., 2015; Maitz et al., 2022), also supporting the need for growth studies in terms of food safety. Furthermore, our findings show possibilities to improve product safety but also storability and shelf life of both, packaged food and packaging material itself. It was suggested that certain packaging types select for and enrich certain microorganisms (Brandwein et al., 2016) which has been unequivocally confirmed by our results. Furthermore, we could show that physicochemical interactions with fiber-based packaging materials contribute to the thriving environment for bacteria, rather than surface adhesion properties or the three dimensional cellulose fiber networks. The superiority of fiber-based packaging materials to plastic packaging regarding cross-contamination could already been shown (Siroli et al., 2017), but explained the observed antimicrobial effects only by the physical structure of the porous fiber material. In contrast, we disintegrated the packaging material and therefore provided optimal growth conditions for bacteria including appropriate growth temperature, shaking in Erlenmeyer flasks and optimal water availability (water activity of 1.0). Thus, our growth-favoring model appears to be more suitable to study metabolic and chemical interactions of microorganisms with packaging materials, but disregarding the physical structures. Only reduced shaking to 50 rpm during incubation was necessary to prevent floc formation,

TABLE 3 Phenotypes of tested bacterial strains on different CMC media and xylan medium.

Growth medium	*E. coli*	*S. aureus*	*B. cereus*	*C. firmus*	*N. circulans*	*B. subtilis*	*C. uda*
CMC medium A	(+)	(+)	7.7 mm	(−)	(+)	8.3 mm (12.3 mm)	2.7 mm
CMC medium B	(−)	(−)	(−)	(−)	(−)	(−)	(−)
Xylan medium	(+)	(+)	(+)	(−)	(+)	16.7 mm	8.7 mm

If visible colonies with clear halos were detected, the sizes of the halos are shown in mm. If a second, outer halo was visible, the size in mm is given in brackets. (+) indicates visible colonies without any halo on the respective growth medium, while (−) indicates no visible microbial growth.

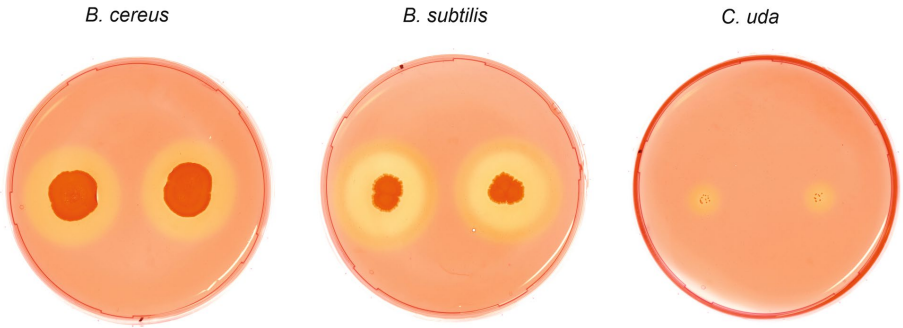

FIGURE 6
Cellulose degrading phenotypes of *Bacillus cereus*, *Bacillus subtilis* and *Cellulomonas uda*. Spot inoculation of *B. cereus*, *B. subtilis* and *C. uda* (control) on CMC medium A. Plates were stained with 0.1% Congo red solution to highlight CMC degradation indicated by clear halo formation. Two halos were observed for *B. subtilis*.

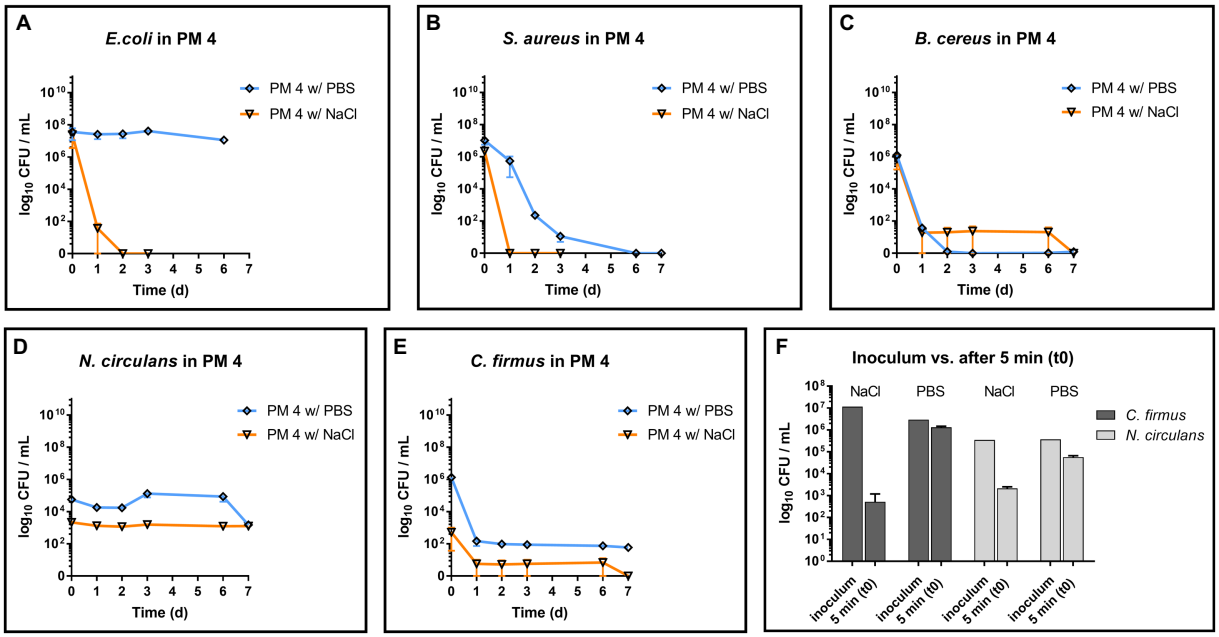

FIGURE 7
Influence of PBS and saline solution on microbial survival in PM 4. Comparison of microbial survival in PM 4 growth media based on PBS or saline solution (0.9% NaCl). Packaging material PM 4 was homogenized either with PBS (orange, pH = 7.40) or with saline solution (blue, pH=4.46) and inoculated with 5–7 $\log_{10}$ CFU/mL for survival monitoring of the test strains **(A–E)**. The mean with range is plotted. Additionally, the prepared inoculum and the bacterial counts after 5min (t0) in the packaging material medium PM 4 were compared for *C. firmus* and *N. circulans* **(F)**. The mean with standard deviation is plotted.

guaranteeing maximal access to fibers and other compounds at the expense of not maximizing oxygen supply. Although in everyday food storage water activities above 0.9 and temperatures above 30°C are rarely reached, the present study investigated the basic principles of growth of different microorganisms in fiber-based packaging materials in very growth promoting conditions. Since a potential contact with liquids, e.g., rain, condensation, should not be neglected and appropriate storage temperatures might fail, this work gives a fundamental insight into the interaction of bacteria with the packaging material itself for a general risk assessment. In general it has long been known that microorganisms can decompose fiber-based materials (Ntaikou et al., 2009), which is a key aspect for an ecological and sustainable packaging material. Our study could reveal that microbial growth in the fiber-based materials is possible, but it depends on highly specific interactions of certain microorganisms with certain types of packaging material. Just because a species can grow in one packaging material does not imply it will grow in another due to the vast variety of different packaging types. Interestingly, *E. coli* was the only species able to grow in a bleached fresh fiber medium. The isolates *C. firmus* and *N. circulans*, on the other side, could only grow in two materials that contained recycled fibers, and growth of *B. cereus* was restricted to a material composed entirely of recycled fibers. These three species, belonging to the Bacillaceae, are typical packaging inherent bacteria (Suihko et al., 2004; Lalande et al., 2014; Schmid et al., 2021) and appeared to be specifically adapted to the composition of the recycled fibers materials. Evaluation of spore germination is essential, since

endospore forming bacteria comprise the major part of packaging inherent bacteria (Väisänen et al., 1991; Suihko et al., 2004). As a matter of fact, these aerobic mesophilic spore-forming bacteria have no medical significance in most cases. From an industrial standpoint, however, germination and subsequent growth of packaging inherent bacteria could affect the product quality. Here again, spore germination and growth was associated with the secondary food packaging material made of 100% recycled fibers. This underlines the increased microbial integrity of fresh fiber products that come into direct contact with food compared to recycled packaging materials. This is also supported by the fact that increased recycling content correlates with increased bacterial load (Hladíková et al., 2015). The actual role of the fiber type, however, remains ambiguous, since manufacturing of recycled packaging materials also involves numerous additives and fillers such as starch and calcium carbonate (Hubbe and Gill, 2016). Unfortunately, the industry partners did not disclose the exact ingredients of the packaging materials only giving fiber-type and current application in the food packaging sector. Therefore, upcoming research should focus on the identification and the actual role of additives from a microbiological point of view. Furthermore, the negligible influence of the fibers is supported by the divergent cellulolytic and xylanolytic phenotypes of the tested bacteria, which did not allow any correlation with their growth potential. Since cellulose fibers are an integral part of fiber-based packaging materials, they can be denied a crucial role as a source of nutrients. The same applies to hemicelluloses, which are heteropolymers consisting of various sugar monomers. They are usually removed to varying degrees during the manufacturing of packaging materials and are also known as nutrients for microorganisms (Wedekind et al., 1988; Hu et al., 2013). However, the digestion of xylan was limited to *B. subtilis* indicating that hemicellulose digestion may not be a major contributor to microbial growth. Still, a hemicellulose contribution to microbial growth cannot be ruled out completely due to the exceptionally diverse class of hemicelluloses. More research on bacterial degradation of different hemicelluloses would be required, especially within complex materials. Methodologically, the specificity of CMC agar-based assays has been doubted (Johnsen and Krause, 2014). Nevertheless, it proved to be a valid screening tool, and we were able to demonstrate the independence of microbial growth from cellulolytic enzymes. Generally, the food packaging sector constantly strives for novel packaging strategies to extend shelf life, minimize cross-contamination and control microbial growth. This led to the continuous development of newly functionalized biomaterials, thin films and coatings to achieve antimicrobial food packaging. Novel approaches in active food packaging often use CMC, chitosan or poly lactic acid films, which are coupled with bioactive components such as ZnO, Ar or TiO_2 nanoparticles, or quaternary ammonium compounds (Li et al., 2017, 2018). Despite their antimicrobial effectiveness, these functionalization strategies are associated with high costs and product safety has hardly been evaluated. There have been only few studies evaluating the interaction of microorganisms with already established food packaging materials (Brandwein et al., 2016; Siroli et al., 2017). A more detailed investigation of these materials can contribute to finding the appropriate packaging material for different applications from a microbiological perspective. Furthermore, it can reveal new targets for potential functionalization and elucidate already existing properties typical for active food packaging, such as the prevention of microbial growth. In our study, we could observe the strongest growth using the packaging material consisting exclusively of recycled fibers (PM 3). However, according to the manufacturer, this packaging material is not intended for direct contact with food, so the risk of cross-contamination of food is not possible. On the other side, all packaging materials intended for direct food contact prevented the growth of *S. aureus* and *B. cereus*. Based on these findings, fiber-based food packaging materials can be developed to prevent microbial growth in the packaging itself. Nevertheless, food processing hygiene is much more crucial for food safety, than the negligible risk that emanates from the fiber-based packaging materials (Ekman et al., 2009). We also detected a low pH of 4.5, which resulted in reduced survival for all tested bacterial species in PM 4. Unfortunately, we were not able to find the cause of this low pH and possible sources are manifold. Nevertheless, lowering of the pH has been known for a long time and is still used in food preservation to prevent microbial growth. Taking into account the relevant standards for food packaging materials (European Parliament, 2004) and the technical requirements during production, adjustment of the pH could provide a cost-effective and consumer-safe functionalization strategy of already established packaging materials. The fact that buffered media did not compensate all growth inhibiting effects strongly suggests further antimicrobial compounds active in the packaging medium. This also supports the need for further investigation of fiber-based packaging materials to find cost-effective and sustainable solutions with active packaging properties. Evaluation of bacterial growth in packaging materials is essential for future risk assessment in the food packaging sector. Our study provides information on the growth capacities but it is limited in the mathematical description of distinct growth parameters, mostly due to the strongly diverging growth phenotypes with different lag, log and stationary phases for the test strain in the diverse growth media. The focus on qualitative growth assessment rather than quantitative growth analysis, along with the small sample size of packaging materials, also resulted in a limited statistical analysis of the data. Nevertheless, all experiments were performed in replicates and descriptive statistics are given. Based on the results of this study, upcoming research will therefore concentrate on the growth kinetics in fiber-based packaging materials, taking mathematical models for bacterial growth into account.

Data availability statement

The datasets presented in this study can be found in online repositories. The names of the repository/repositories and accession number(s) can be found at: https://www.ncbi.nlm.nih.gov/genbank/, OP422519, OP422520.

Author contributions

PS: conceptualization, methodology, data collection and analysis, validation, and writing – original draft. SM: conceptualization, and writing – review and editing. NP: methodology, data collection and analysis, and visualization. EK: methodology, data collection and analysis. SP: methodology, writing – review and editing. CK: funding acquisition, supervision, and writing – review and editing. All authors have approved the final version to be published. All authors are to be accountable for all aspects of the work in ensuring that questions related to the accuracy or integrity of any part of the work are appropriately investigated and resolved.

Funding

This work has been funded by the Christian Doppler Society, Austria (CD-Laboratory for Mass Transport through Paper). The financial support of the Austrian Federal Ministry of Labour and Economy and the National Foundation for Research, Technology and Development, Austria is acknowledged.

Acknowledgments

The authors thank Karin Zojer for intellectual support and research management.

Conflict of interest

The authors declare that the research was conducted in the absence of any commercial or financial relationships that could be construed as a potential conflict of interest.

Publisher's note

All claims expressed in this article are solely those of the authors and do not necessarily represent those of their affiliated organizations, or those of the publisher, the editors and the reviewers. Any product that may be evaluated in this article, or claim that may be made by its manufacturer, is not guaranteed or endorsed by the publisher.

References

Abdelmalek, F., Steinbüchel, A., and Rofeal, M. (2022). The hyperproduction of polyhydroxybutyrate using bacillus mycoides ICRI89 through enzymatic hydrolysis of affordable cardboard. *Polymers* 14:2810. doi: 10.3390/polym14142810

Altschul, S. F., Gish, W., Miller, W., Myers, E. W., and Lipman, D. J. (1990). Basic local alignment search tool. *J. Mol. Biol.* 215, 403–410. doi: 10.1016/S0022-2836(05)80360-2

Amore, A., Parameswaran, B., Kumar, R., Birolo, L., Vinciguerra, R., Marcolongo, L., et al. (2015). Application of a new xylanase activity from *Bacillus amyloliquefaciens* XR44A in brewer's spent grain saccharification. *J. Chem. Technol. Biotechnol.* 90, 573–581. doi: 10.1002/jctb.4589

Amore, A., Pepe, O., Ventorino, V., Birolo, L., Giangrande, C., and Faraco, V. (2013). Industrial waste based compost as a source of novel cellulolytic strains and enzymes. *FEMS Microbiol. Lett.* 339, 93–101. doi: 10.1111/1574-6968.12057

Asato, C. M., Gonzalez-Estrella, J., Jerke, A. C., Bang, S. S., Stone, J. J., and Gilcrease, P. C. (2016). Batch anaerobic digestion of synthetic military base food waste and cardboard mixtures. *Bioresour. Technol.* 216, 894–903. doi: 10.1016/j.biortech.2016.06.033

Azevedo, A. G., Barros, C., Miranda, S., Machado, A. V., Castro, O., Silva, B., et al. (2022). Active flexible films for food packaging: a review. *Polymers* 14:2442. doi: 10.3390/polym14122442

Brandwein, M., Al-Quntar, A., Goldberg, H., Mosheyev, G., Goffer, M., Marin-Iniesta, F., et al. (2016). Mitigation of biofilm formation on corrugated cardboard fresh produce packaging surfaces using a novel thiazolidinedione derivative integrated in acrylic emulsion polymers. *Front. Microbiol.* 7, 1–9. doi: 10.3389/fmicb.2016.00159

Brummer, V., Jurena, T., Hlavacek, V., Omelkova, J., Bebar, L., Gabriel, P., et al. (2014). Enzymatic hydrolysis of pretreated waste paper – Source of raw material for production of liquid biofuels. *Bioresour. Technol.* 152, 543–547. doi: 10.1016/j.biortech.2013.11.030

De Oliveira, W. Q., De Azeredo, H. M. C., Neri-Numa, I. A., and Pastore, G. M. (2021). Food packaging wastes amid the COVID-19 pandemic: trends and challenges. *Trends Food Sci. Technol.* 116, 1195–1199. doi: 10.1016/j.tifs.2021.05.027

Deshwal, G. K., Panjagari, N. R., and Alam, T. (2019). An overview of paper and paper based food packaging materials: health safety and environmental concerns. *J. Food Sci. Technol.* 56, 4391–4403. doi: 10.1007/s13197-019-03950-z

Ekman, J., Tsitko, I., Weber, A., Nielsen-Leroux, C., Lereclus, D., and Salkinoja-Salonen, M. (2009). Transfer of *Bacillus cereus* spores from packaging paper into food. *J. Food Prot.* 72, 2236–2242. doi: 10.4315/0362-028X-72.11.2236

European Parliament (2004). Regulation EC 1935/2004 on materials and articles intended to come into contact with food. Available at: https://eur-lex.europa.eu/LexUriServ/LexUriServ.do?uri=CONSLEG:2004R1935:20090807:EN:PDF%0Ahttps://eur-lex.europa.eu/legal-content/EN/ALL/?uri=CELEX:02004R1935-20090807

Gupta, R. S., Patel, S., Saini, N., and Chen, S. (2020). Robust demarcation of 17 distinct *Bacillus* species clades, proposed as novel *Bacillaceae* genera, by phylogenomics and comparative genomic analyses: description of *Robertmurraya kyonggiensis* sp. nov. and proposal for an emended genus bacillus limiting it only to the members of the subtilis and cereus clades of species. *Int. J. Syst. Evol. Microbiol.* 70, 5753–5798. doi: 10.1099/ijsem.0.004475

Hennekinne, J. A., De Buyser, M. L., and Dragacci, S. (2012). Staphylococcus aureus and its food poisoning toxins: characterization and outbreak investigation. *FEMS Microbiol. Rev.* 36, 815–836. doi: 10.1111/j.1574-6976.2011.00311.x

Hladíková, Z., Kejlová, K., Sosnovcová, J., Jírová, D., Vavrouš, A., Janoušek, S., et al. (2015). Microbial contamination of paper-based food contact materials with different contents of recycled fiber. *Czech J. Food Sci.* 33, 308–312. doi: 10.17221/645/2014-CJFS

Hol, F. J. H., Whitesides, G. M., and Dekker, C. (2019). Bacteria-in-paper, a versatile platform to study bacterial ecology. *Ecol. Lett.* 22, 1316–1323. doi: 10.1111/ele.13274

Hu, G., Fu, S., and Liumaki, H. (2013). Hemicellulose in pulp affects paper properties and printability. *Appita J.* 66, 139–144.

Hubbe, M. A., and Gill, R. A. (2016). Fillers for papermaking: a review of their properties, usage practices, and their mechanistic role. *Bioresources* 11, 2886–2963. doi: 10.15376/BIORES.11.1.2886-2963

International Organization for Standardization (2020). *Microbiology of Food and Animal Feeding Stuffs—Horizontal Method for the Enumeration of Presumptive Bacillus cereus—Colony-Count Technique at 30 Degrees C—Amendment 1: Inclusion of Optional Tests*. Geneva: International Organization for Standardization. 27.

Johnsen, H. R., and Krause, K. (2014). Cellulase activity screening using pure carboxymethylcellulose: application to soluble cellulolytic samples and to plant tissue prints. *Int. J. Mol. Sci.* 15, 830–838. doi: 10.3390/ijms15010830

Lalande, V., Barnabé, S., and Côté, J.-C. (2014). Comparison of the bacterial microbiota in a bale of collected cardboard determined by 454 pyrosequencing and clone library. *Adv. Microbiol.* 04, 754–760. doi: 10.4236/aim.2014.412082

Li, J., Cha, R., Mou, K., Zhao, X., Long, K., Luo, H., et al. (2018). Nanocellulose-based antibacterial materials. *Adv. Healthc. Mater.* 7, 1–16. doi: 10.1002/adhm.201800334

Li, W., Zhang, C., Chi, H., Li, L., Lan, T., Han, P., et al. (2017). Development of antimicrobial packaging film made from poly(lactic acid) incorporating titanium dioxide and silver nanoparticles. *Molecules* 22:1170. doi: 10.3390/molecules22071170

Maitz, S., Schmid, P. J., and Kittinger, C. (2022). Modelling and determination of parameters influencing the transfer of microorganisms from food contact materials. *Int. J. Environ. Res. Public Health* 19:2996. doi: 10.3390/ijerph19052996

Moschonas, G., Lianou, A., Nychas, G. J. E., and Panagou, E. Z. (2021). Spoilage potential of *Bacillus subtilis* in a neutral-pH dairy dessert. *Food Microbiol.* 95:103715. doi: 10.1016/j.fm.2020.103715

Norrrahim, M. N. F., Nurazzi, N. M., Jenol, M. A., Farid, M. A. A., Janudin, N., Ujang, F. A., et al. (2021). Emerging development of nanocellulose as an antimicrobial material: an overview. *Mater. Adv.* 2, 3538–3551. doi: 10.1039/d1ma00116g

Ntaikou, I., Koutros, E., and Kornaros, M. (2009). Valorisation of wastepaper using the fibrolytic/hydrogen producing bacterium *Ruminococcus albus*. *Bioresour. Technol.* 100, 5928–5933. doi: 10.1016/j.biortech.2009.06.019

Patel, S., and Gupta, R. S. (2020). A phylogenomic and comparative genomic framework for resolving the polyphyly of the genus *Bacillus*: proposal for six new genera of *Bacillus* species, *Peribacillus* gen. nov., *Cytobacillus* gen. nov., *Mesobacillus* gen. nov., *Neobacillus* gen. nov., *Metabacillu*. *Int. J. Syst. Evol. Microbiol.* 70, 406–438. doi: 10.1099/ijsem.0.003775

Patrignani, F., Siroli, L., Gardini, F., and Lanciotti, R. (2016). Contribution of two different packaging material to microbial contamination of peaches: implications in their microbiological quality. *Front. Microbiol.* 7:938. doi: 10.3389/fmicb.2016.00938

Poladyan, A., Margaryan, L., Trchounian, K., and Trchounian, A. (2020). Biomass and biohydrogen production during dark fermentation of *Escherichia coli* using office paper waste and cardboard. *Int. J. Hydrog. Energy* 45, 286–293. doi: 10.1016/j.ijhydene.2019.10.246

Relman, D. A. (1993). "Universal bacterial 16S rDNA amplification and sequencing" in *Diagnostic Molecular Microbiology: Principles and Applications*. eds. D. H. Persing, T. F. Smith, F. C. Tenover and T. J. White (Washington, DC: ASM Press), 489–495.

Schmid, P. J., Maitz, S., and Kittinger, C. (2021). *Bacillus cereus* in packaging material: molecular and phenotypical diversity revealed. *Front. Microbiol.* 12:698974. doi: 10.3389/fmicb.2021.698974

Siroli, L., Patrignani, F., Serrazanetti, D. I., Chiavari, C., Benevelli, M., Grazia, L., et al. (2017). Survival of spoilage and pathogenic microorganisms on cardboard and plastic packaging materials. *Front. Microbiol.* 8:2606. doi: 10.3389/fmicb.2017.02606

Stenfors Arnesen, L. P., Fagerlund, A., and Granum, P. E. (2008). From soil to gut: *Bacillus cereus* and its food poisoning toxins. *FEMS Microbiol. Rev.* 32, 579–606. doi: 10.1111/j.1574-6976.2008.00112.x

Suihko, M. L., Sinkko, H., Partanen, L., Mattila-Sandholm, T., Salkinoja-Salonen, M., and Raaska, L. (2004). Description of heterotrophic bacteria occurring in paper mills and paper products. *J. Appl. Microbiol.* 97, 1228–1235. doi: 10.1111/j.1365-2672.2004.02416.x

Suominen, I., Suihko, M. L., and Salkinoja-Salonen, M. (1997). Microscopic study of migration of microbes in food-packaging paper and board. *J. Ind. Microbiol. Biotechnol.* 19, 104–113. doi: 10.1038/sj.jim.2900424

Väisänen, O. M., Mentu, J., and Salkinoja-Salonen, M. S. (1991). Bacteria in food packaging paper and board. *J. Appl. Bacteriol.* 71, 130–133. doi: 10.1111/j.1365-2672.1991.tb02967.x

Väisänen, O. M., Weber, A., Bennasar, A., Rainey, F. A., Busse, H. J., and Salkinoja-Salonen, M. S. (1998). Microbial communities of printing paper machines. *J. Appl. Microbiol.* 84, 1069–1084. doi: 10.1046/j.1365-2672.1998.00447.x

Wedekind, K. J., Mansfield, H. R., and Montgomery, L. (1988). Enumeration and isolation of cellulolytic and hemicellulolytic bacteria from human feces. *Appl. Environ. Microbiol.* 54, 1530–1535. doi: 10.1128/aem.54.6.1530-1535.1988

Yang, S. C., Lin, C. H., Aljuffali, I. A., and Fang, J. Y. (2017). Current pathogenic *Escherichia coli* foodborne outbreak cases and therapy development. *Arch. Microbiol.* 199, 811–825. doi: 10.1007/s00203-017-1393-y

Zaidi, S., Vats, M., Kumar, N., Janbade, A., and Gupta, M. K. (2022). Evaluation of food packaging paper for microbial load and storage effect on the microbial activity of paper. *Packag. Technol. Sci.* 35, 569–577. doi: 10.1002/pts.2652

Zumsteg, A., Urwyler, S. K., and Glaubitz, J. (2017). Characterizing bacterial communities in paper production—troublemakers revealed. *Microbiology* 6, 1–6. doi: 10.1002/mbo3.487

frontiers | Frontiers in Microbiology

TYPE Original Research
PUBLISHED 27 January 2023
DOI 10.3389/fmicb.2023.1124770

OPEN ACCESS

EDITED BY
Changyu Zhou,
Ningbo University,
China

REVIEWED BY
Ruiming Luo,
Ningxia University,
China
Fangda Sun,
Northeast Agricultural University,
China
Kezhou Cai,
Hefei University of Technology, China

*CORRESPONDENCE
Honggang Tang
✉ zaastang@163.com

SPECIALTY SECTION
This article was submitted to Food Microbiology, a section of the journal Frontiers in Microbiology

RECEIVED 15 December 2022
ACCEPTED 13 January 2023
PUBLISHED 27 January 2023

CITATION
Zhang J, Zhao K, Li H, Li S, Xu W, Chen L, Xie J and Tang H (2023) Physicochemical property, volatile flavor quality, and microbial community composition of Jinhua fatty ham and lean ham: A comparative study. *Front. Microbiol.* 14:1124770. doi: 10.3389/fmicb.2023.1124770

Physicochemical property, volatile flavor quality, and microbial community composition of Jinhua fatty ham and lean ham: A comparative study

Jin Zhang[1], Ke Zhao[1], Huanhuan Li[1], Shuangxi Li[2], Weimin Xu[3], Lihong Chen[1], Jing Xie[4] and Honggang Tang[1]*

[1]State Key Laboratory for Managing Biotic and Chemical Threats to the Quality and Safety of Agro-Products, Institute of Food Science, Zhejiang Academy of Agricultural Sciences, Hangzhou, Zhejiang, China, [2]Xingzhi College, Zhejiang Normal University, Jinhua, Zhejiang, China, [3]Jinhua Jinnian Ham Co., Ltd., Jinhua, Zhejiang, China, [4]Zhejiang Institute of Product Quality and Safety Science, Hangzhou, Zhejiang, China

The physicochemical property, volatile flavor compounds, and microbial community structure of Jinhua fatty ham (FH) and lean ham (LH) were investigated and compared by high-throughput sequencing and HS-GC-IMS. Results showed that FH had higher pH and slightly lighter and yellower color than LH. Meanwhile, 33 volatile flavor compounds were identified from FH and LH, among which LH showed higher abundance of total alcohols and acids, but FH had generally richer aldehydes, ketones, esters, heterocyclic, and sulfur-containing compounds. Moreover, FH and LH did not have significant difference in α-diversity of bacterial community, but LH presented a much lower α-diversity of fungal community than FH. Besides, the dominant microorganisms (relative abundance >2%) in FH were *Ruminococcaceae* UCG-005, *Staphylococcus*, *Ruminococcaceae* UCG-014, *Meyerozyma*, and *Aspergillus* at the genus level, while in LH were *Staphylococcus*, *Psychrobacter*, *Halomonas*, *Propionicicella*, *Ruminococcaceae* UCG-005, *Meyerozyma*, *Yamadazyma*, and *Aspergillus*. Furthermore, the analysis of Pearson's correlation and metabolic network confirmed that the discriminative flavor compounds of FH were mainly β-oxidation and degradation products of fatty acids, while those of LH were mostly derived from the Strecker reaction or microbial metabolism of amino acids. The present study could help understand the potential pathway of characteristic microorganisms affecting flavor formation of fat-deficient dry-cured hams and provide theoretical supports for developing healthier fermented meat products.

KEYWORDS

Jinhua ham, fatty ham, lean ham, volatile flavor compound, bacterial community, fungal community, GC-IMS, high-throughput sequencing

1. Introduction

Chinese dry-cure ham is a traditional fermented meat product with a long history of over 1,000 years (Li et al., 2022). Jinhua ham, considered one of the most representative Chinese dry-cured hams, is widely prevalent around the world due to its unique flavor and abundant nutrients (Li W. et al., 2021; Wang et al., 2021). Jinhua hams are produced from fresh hind legs

of pigs through a long processing procedures, mainly including raw material selection, salting, dry-ripening, and post-ripening, which usually spend several months (Zhou et al., 2021a). The fats, proteins, and glycogens in raw hams can be degraded into large amounts of amino acids, fatty acids, and pyruvates during the dry-ripening, which further produce the characteristic flavor compounds of dry-cured hams through diverse chemical reactions, such as β-oxidation, deamination, Strecker degradation, and Millard reaction (Martínez-Onandi et al., 2017; Bosse et al., 2018; Shi et al., 2019). Hence, fat plays a crucial role in the formation of unique flavor of Jinhua hams. However, high-level fats or polyunsaturated fatty acids in meats are sensitive to oxidative deterioration, which are related with the rancid smell and may have a side effect on consumers' acceptance (Benet et al., 2015; Zhou et al., 2021b). In addition, the consumption of foods with high-level saturated fats could be associated with an increased risk of cholesterol-related cardiovascular pathologies (Trevisan et al., 1990; Benet et al., 2016). Therefore, the lean ham (LH), manufactured from the pork hind leg removed skin and fat tissues, are more and more popular among consumers, especially populations with health concerns. Nevertheless, the physicochemical property and flavor quality were rarely studied for LH, even though sufficiently reported for normal fatty hams (FH). Moreover, the effect of fat deficiency on the flavor characteristics of dry-cured hams was also not investigated yet.

On the other hand, the aforementioned complex reactions producing unique flavor compounds are dependent on the enzymatic actions of not only endogenous enzymes but also microbial enzymes (Petrova et al., 2015; Wang et al., 2021). Recent studies reported that various microorganisms could promote the formation of characteristic flavor and quality property of dry-cured hams by performing proteolysis, lipolysis, and oxidation activities (Toledano et al., 2019; Chen et al., 2021; Li et al., 2022). Meanwhile, several reports focused on the composition of microbial communities and relative content of volatiles in Jinhua FH (Ge et al., 2017; Wang et al., 2021; Deng et al., 2022). Moreover, the core microorganisms in Jinhua FH, such as *Staphylococcus*, *Lactobacillus*, *Debaryomyces*, and *Apiotrichum*, have been identified positively associated with the flavor compounds derived from the catabolism of amino acids, such as some branched aldehydes and heterocyclic compounds (Zhou et al., 2022). However, there is still a lack of comprehensive knowledge on microbial community of Jinhua LH. Furthermore, the potential metabolic pathway of core bacteria/fungi affecting flavor formation in LH was also not understood.

Therefore, the objective of this study was firstly, to compare the physicochemical property, volatile flavor quality, and microbial community composition of Jinhua FH and LH, and secondly, to explore the correlations and connections between core microbes and differential flavor compounds. The color, pH, water activity, chemical composition, and nitrite residue of both FH and LH were determined. The headspace-gas chromatography-ion mobility spectrometry (HS-GC-IMS) and high-throughput sequencing of 16S rRNA/ITS genes were also utilized to analyze volatile flavor profiles and bacterial/fungal communities, respectively. Furthermore, the analysis of correlation and metabolic network was applied for the exploration of relationship between core microorganisms and volatiles. The information obtained from this study could help understand the potential pathway of characteristic microorganisms influencing flavor formation of dry-cured hams under the condition of fat deficiency.

2. Materials and methods

2.1. Processing and sampling of Jinhua fatty ham and lean ham

The Jinhua hams used in the present study were prepared and sampled in Jinhua Jinnian Ham Co., Ltd (Zhejiang, China). Six fresh hind legs (14.5 ± 0.5 kg, pH = 5.9 ± 0.2) of domestic pigs (Large White × Landrace) were used to prepare Jinhua FH and LH following the procedures of Zhou et al. (2021a) with some modifications. For Jinhua FH, three whole hind legs were salted for 75 days with 0.014% $NaNO_2$ and 10% NaCl per leg, followed by soak cleaning for 1 day and sun-drying for 1 day. Subsequently, hind legs were dehydrated for 7 days in a dehydration plant, sun-dried for another day, and then ripened for 180 days in a dry-ripening room. During the ripening, the ambient temperature progressively increased from 5°C to 35°C, while the relative humidity gradually decreased from 85 to 65%. Afterward, legs were further post-ripened for about 30 days at room temperature (25°C), and the hams were finally obtained when the weight loss reached approximately 40% of the initial weight. For Jinhua LH, the skins and fat tissues were firstly trimmed off from the other three hind legs. The final hams were also obtained following the gradual procedures of salting, soak cleaning, sun-drying, dehydrating, secondary sun-drying, dry-ripening, and post-ripening, which were all performed under the same conditions with Jinhua FH. Furthermore, as described by Chen et al. (2021) with minor modifications, approximately 5 cm × 2 cm × 0.2 cm pieces were cut from the surface of the *biceps femoris* muscle of each ham, which were used for the fungal community determination. Meanwhile, about 20 g interior samples were taken from the central fraction (about 3–4 cm depth) of the *biceps femoris* muscle of each ham, which were used for the evaluation of physicochemical parameters, volatile flavor compounds, and bacterial community. All samples were vacuum-packaged and frozen at-80°C until further analysis.

2.2. Measurement of color, pH, and water activity (aw)

The color, pH and water a_w were measured following the methods of our previous studies (Li H. et al., 2021; Zhang et al., 2022) with minor modifications. The color of samples was directly detected using a colorimeter (NH310, 3NH Technology Co., Ltd., China), where the L, a^*, and b^* values represent lightness, redness/greenness, and yellowness/blueness, respectively. A white standard plate with the L, a^*, and b^* values of 99.46, 0.19, and −1.98, respectively, was used for calibration before color detection. The pH value was determined using a portable pH meter (Testo 205, Testo Instruments Co., Ltd., Shenzhen, China) equipped with a piercing pH probe and a temperature-compensated temperature probe. The a_w value was determined with an intelligent water activity meter (HD-4, Huake Instrument and Meter Co., Ltd., Wuxi, China).

2.3. Detection of chemical composition

The chemical composition of ham samples was detected as described by our previous study (Zhang et al., 2017) with minor modifications. Briefly, the total contents of moisture, protein, fat, and minerals were analyzed by the method of direct drying (GB/T 5009.3–2016), Kjeldahl

(ISO 5983-1997), Soxhlet extraction (ISO 1444-1996), and dry-ashing (ISO 5984-2002), respectively.

2.4. Estimation of nitrite residue

According to the method of Liu et al. (2019) with minor modifications, the content of residual nitrite was detected with a nitrite assay kit following the manufacturer's instruction (Nanjing Jiancheng Bioengineering Institute, Nanjing, China). Briefly, ham samples were dispersed into distilled water and filtrated, followed by the reaction with sulphanilamide solution and N-naphthyl-ethylenediamine dihydrochloride. The nitrite content was calculated based on the absorbance of supernatant at 550 nm, which was assayed using an ultraviolet–visible spectrophotometer (UV-1750, Shimadzu, Kyoto, Japan).

2.5. Determination of volatile flavor compounds

As described by Liu et al. (2020) with minor modifications, the volatile flavor compounds of ham samples were identified by a headspace-gas chromatography-ion mobility spectrometer (HS-GC-IMS; Flavorspec, G.A.S. Instrument, Germany) equipped with a SE-54 capillary column (15 m × 0.53 mm × 1 μM). Samples were firstly cut into approximately 1 cm × 1 cm × 1 cm cubes and minced by an analytical grinder (Aika Instrument Equipment Co., Ltd., Guangzhou, China). Then 2 g samples were put into a 20 ml headspace sampling vial and incubated at 60°C for 20 min. Afterward, 500 μL headspace was injected into the injector automatically with a heated syringe at 85°C. Subsequently, samples were transferred into the capillary column by high-purity nitrogen (>99.99%) at the following programmed flow rates: initially 2 ml/min for first 2 min, then 10 ml/min for 8 min, next 100 ml/min for 10 min, and eventually 150 ml/min for 5 min. Meanwhile, the temperature of column and drift tube was kept as 60°C and 45°C, respectively, and the flow rate of drift gas (nitrogen gas, >99.99% purity) was maintained as 150 mL/min.

The IMS data were analyzed using the instrumental laboratory analysis view (LAV) software with the Reporter, Gallery Plot, and Dynamic PCA plug-in applications. The volatile flavor compound was identified by comparing the retention index (RI) and drift time (DT) with the NIST library and IMS database retrieval software obtained from G.A.S. The intensities of these compounds were calculated based on the height of selected signal peaks.

2.6. Analysis of bacterial and fungal communities

The analysis of microbial communities, including the compositions of both fungi and bacteria, were performed by high-throughput sequencing following the procedures of Chen et al. (2021) and Wang et al. (2021) with some modifications. The total genome DNA of bacteria and fungi was extracted using a Cetyltrimethylammonium Bromide (CTAB) method following the manufacturer's instructions of the genomic DNA extraction kit. The V3-V4 hypervariable regions of bacterial 16S rRNA genes were amplified with the forward primer 5'-CCTAYGGGRBGCASCAG-3′ and reverse primer 5′-GGACTACNNGGGTATCTAAT-3′. The ITS1-1\u00B0F regions of fungal ITS genes were amplified with the forward primer 5′-CTTGGTCATTTAGAGGAAGTAA-3′ and reverse primer 5′-GCTGCGTTCTTCATCGATGC-3′. All PCR reactions were conducted in 30 μL reactions with 15 μL Phusion® High-Fidelity PCR Master Mix (New England Biolabs), 0.2 μM forward and reverse primers, and approximately 10 ng template DNA. PCR products were then mixed in equidensity ratios and purified through the Axy Prep DNA Gel Extraction Kit (AXYGEN; for bacteria) or Qiagen Gel Extraction Kit (Qiagen, Germany; for fungi).

The data sequencing was carried out according to the procedures of Wang et al. (2021) and Li et al. (2022) with some modifications. Sequencing libraries were generated using the NEB Next® Ultra™ DNA Library Prep Kit for Illumina (NEB, United States; for bacteria) or TruSeq® DNA PCR-Free Sample Preparation Kit (Illumina, United States; for fungi) following the manufacturer's recommendations and index codes were added. The library quality was evaluated on the Qubit@ 2.0 Fluorometer (Thermo Fisher Scientific) and Agilent Bioanalyzer 2,100 system. Then the library was sequenced on the Illumina Miseq/HiSeq2500 (for bacteria) or NovaSeq (for fungi) platform. Afterward, the QIIME (V1.9.1) quality controlled process was performed to filter raw reads to obtain high-quality clean reads. The reads were compared with the reference database (Silva database) using the UCHIME algorithm to detect chimera sequences, and the chimera sequences were removed to acquire the effective clean reads. The sequence analysis was performed using the UPARSE algorithms. Sequences with ≥97% similarity were assigned to the same operational taxonomic units (OTUs), and representative sequences for each OTU were screened for further annotation. The significance of differences in microbial communities was statistically analyzed based on the relative abundance of bacteria or fungi at various levels, mainly including phylum, genus, and species. The α-diversity was presented *via* the Shannon index, Simpson index, ACE index, Chao 1 index, and observed species, while the β-diversity was assayed by the principal coordinate analysis (PCoA).

2.7. Statistical analysis

All experiments were performed in triplicate with the results shown as average ± standard deviation. Tables were made by the Microsoft Excel 2016 software, while figures were drawn with the Origin V2021 (Origin-Lab, Northampton, United States) and Microsoft PowerPoint 2016. Analysis of variance (ANOVA) was performed using the SAS V8 software (SAS Institute Inc., Carry, United States), while analysis of Pearson's correlation and hierarchical cluster (HCA) was conducted by the plug-in applications in Origin V2021. Differences among mean values were established with the Duncan multiple range test. The significant difference was confirmed when $p < 0.05$.

3. Results and discussion

3.1. Differences In physicochemical properties

The physicochemical property of dry-cure ham was closely associated with the flavor quality and microbial diversity (Domínguez et al., 2022). The physicochemical parameters of internal samples from Jinhua FH and LH, including color, water activity (a_w), pH, chemical composition, and

nitrite residue, are shown in Table 1. It is clear that there is no significant distinction between the a^* values (redness) of FH and LH ($p > 0.05$). However, FH showed slightly higher L and b^* values than LH ($p < 0.05$), suggesting that the color of FH was slightly lighter and yellower than that of FH. This result may be attributed to their difference in the redox degree of proteins, especially the myoglobin and hemoglobin (Parolari et al., 2016). Specifically, myoglobin and hemoglobin are the main pigments responsible for the color of dry-cured hams (Parolari et al., 2016; Zhou et al., 2021b), and the lack of protection by fat and skin tissues might allow more myoglobins/hemoglobins in LH to be oxidized during dry-ripening, possibly resulting in the darker color of LH.

Besides, the a_w values of FH and LH were not obviously different ($p > 0.05$) and both far under 0.85, which was a low a_w that protects hams from most harmful microbes and meanwhile allows the growth of salt-consuming and flavor-generating bacteria/fungi (Chen et al., 2021). However, LH exhibited a remarkable lower pH than FH ($p < 0.05$). Bosse et al. (2018) reported that a pH of 6.0–6.2 would cause a higher microbial risk and reduced water diffusion ability in hams, while hams with pH of 5.6–6.0 have more desirable saltiness, color, and texture. The pH values of FH and LH were 6.08 ± 0.03 and 5.75 ± 0.04, respectively, suggesting that LH might has higher sensory quality and edible safety than FH. The distinct pH values of FH and LH was probably attributed to their distinction in the intensity of acids generated during ripening (Table 2; Figure 1).

Furthermore, these two hams also exhibited no significant difference in chemical compositions ($p > 0.05$). The moisture content of both FH and LH (around 31.5%) was similar with that of Mianning hams reported by Chen et al. (2021), which is low enough to prevent spoilage and improve quality of hams. This result was also consistent with the a_w data as mentioned above, since the water content is usually considered positively correlated with the water activity. Meanwhile, the minerals in hams can be mainly salts (Domínguez et al., 2022), hence FH and LH showed similar mineral contents (about 8.50%; $p > 0.05$) because of the same adding amount of NaCl during salting. Additionally, the nitrite residues were 1.13 ± 0.21 and 1.57 ± 0.12 for FH and LH, respectively, without marked distinction ($p > 0.05$) and far under the secure nitrite residue limits (30 mg/kg) for meat products in China (Chen et al., 2021). On the other hand, the pigments contributing to the rose-red color of dry-cured hams are mainly nitromyoglobins and nitrohemoglobins, which are the product of reactions between nitrites/nitrates and myoglobins/hemoglobins (Parolari et al., 2016). Therefore, the similar nitrite residue of FH and LH suggested a same nitrite consuming amount for the production of red pigments, which can be the main reason for their similar redness (a^* value) as mentioned above. Overall, the data shown in Table 1 indicate that LH had an obviously lower lightness, yellowness, and pH than FH, probably resulting from their discrimination in oxidation and fermentation products.

TABLE 1 Physicochemical parameters of internal samples from Jinhua FH and LH.

Physicochemical indexes	FH	LH
L	29.44 ± 0.89[a]	25.33 ± 0.36[b]
a^*	12.38 ± 0.11[a]	12.11 ± 0.27[a]
b^*	5.27 ± 0.83[a]	3.43 ± 0.85[b]
a_w	0.71 ± 0.09[a]	0.73 ± 0.01[a]
pH	6.08 ± 0.03[a]	5.75 ± 0.04[b]
Moisture (%)	31.90 ± 6.47[a]	31.37 ± 3.88[a]
Protein (%)	46.53 ± 3.75[a]	44.10 ± 1.87[a]
Mineral (%)	8.43 ± 1.05[a]	8.67 ± 1.06[a]
Fat (%)	4.60 ± 0.80[a]	3.23 ± 0.91[a]
Nitrite (mg/kg)	1.13 ± 0.21[a]	1.57 ± 0.12[a]

Different lowercases within the same row denote significant differences between Jinhua FH and LH ($p < 0.05$). FH, fatty ham; LH, lean ham.

3.2. Comparison of volatile flavor compounds

The volatile flavor profiles of internal samples from Jinhua FH and LH were analyzed by HS-GC-IMS and results are illustrated as a two-dimension spectra plot (Figure 2). The y-axis and x-axis in Figure 2 showed the retention time (RT) of GC and the relative drift time (DT) of ions, respectively (Liu et al., 2020). Meanwhile, the red line representing $x = 1.0$ was the reactive ion peak (RIP). Besides, each data point corresponded to a volatile flavor compound, and its color indicated the intensity of volatile (Li et al., 2019). Specifically, the blue and white colors represented a low intensity of volatiles, whereas the yellow and red colors showed a high intensity of compounds. It is exhibited that the two hams showed similar number of ion peaks within the DT range of 1.0–1.7 ms, suggesting that the numbers of main identified volatiles were not obviously different in FH and LH. However, the data points (ion peaks) of FH mostly showed a redder color or bigger size than those of LH, indicating that FH had an overall higher intensity of volatile flavor than LH.

Furthermore, to compare the finger-print of characteristic volatiles in FH and LH, the Gallery plot plug-in was utilized with results presented in Figure 3. Each row in Figure 3 represented a single volatile flavor compound, which could correspond to a single signal (monomer) or a pot (dimer) in the IMS spectra plot (Figure 2) depending on its concentration (Arroyo-Manzanares et al., 2018). As shown in Figure 3, a total of 33 volatile compounds were identified, which can be classified into 7 chemical families. In details, there were 7 alcohols, 8 ketones, 10 aldehydes, 4 esters, 2 acids, 1 heterocyclic compound, and 1 sulfur-containing compound. These findings were in accordance with the reports of Liu et al. (2020), Wang et al. (2021), and Li et al. (2022) on the volatile profiles of Jinhua hams.

The profiles of individual volatile flavor compounds were further analyzed with data shown in Table 2. Aldehydes are known as the major contributors to the unique flavor of fermented meats due to their high concentrations and low aroma thresholds (Liu et al., 2020; Wang et al., 2021). As exhibited in Table 2, hexanal, 2-methylbutanal, and 3-methylbutanal were the richest aldehydes in both FH and LH, followed by 2-methylpropanal (for FH) or phenylacetaldehyde (for LH), in accordance with the findings of Wang et al. (2021) on the volatiles of Jinhua hams. Hexanal is regarded as the major lipid oxidation product in dry-cured hams, and a low-content hexanal generally provides a pleasant grassy, fruity, and green odor (Benet et al., 2015; Domínguez et al., 2022). 2-methylbutanal, 3-methylbutanal, and 2-methylpropanal are all branched aldehydes, deriving from oxidative deamination and decarboxylation of valine, leucine, and isoleucine through Strecker degradation (Narváez-Rivas et al., 2014). Meanwhile, they are also medium-chain (C4-C9) aliphatic aldehydes, which were considered responsible for grassy, fatty, and/or nutty flavors of meat products (Liu et al., 2020; Wang et al., 2021). Furthermore, the abundances of most identified aldehydes were significantly lower ($p < 0.05$) or similar ($p > 0.05$) in LH compared with those in FH. Noteworthily, only

10.3389/fmicb.2023.1124770

TABLE 2 Intensities of 33 identified volatile flavor compounds from Jinhua FH and LH by HS-GC-IMS.

Volatile flavor compound	RI	RT (s)	DT (ms)	Intensity (V)		Odor description
				FH	LH	
Alcohols (7)						
1-Octen-3-ol (M)	984.1	564.06	1.159	503.76 ± 6.15[a]	274.88 ± 13.82[b]	Mushroom, earthy, green, oily, fungal, and raw chicken
1-Pentanol (M)	764.0	250.95	1.252	493.27 ± 12.62[a]	412.24 ± 11.95[b]	Fusel oil, sweet, and balsam
1-Pentanol (D)	761.8	248.94	1.504	199.36 ± 6.12[a]	105.39 ± 3.98[b]	
Ethanol (M)	460.0	102.79	1.047	1002.96 ± 11.62[a]	417.87 ± 6.27[b]	Strong alcoholic, ethereal, and medical
2-Propanol (M)	492.9	112.30	1.093	797.08 ± 20.78[b]	2096.11 ± 73.43[a]	Alcohol, musty, and woody
1-Hexanol (M)	868.8	364.51	1.639	71.06 ± 0.37[a]	30.14 ± 4.30[b]	Ethereal, fusel oil, fruity, alcoholic, and sweet green
3-Hexen-1-ol (M)	854.8	346.98	1.233	45.35 ± 3.40[b]	179.71 ± 2.83[a]	Fresh, green, cut grass, foliage vegetable, herbal, and oily
3-Hexen-1-ol (D)	855.1	347.34	1.515	27.70 ± 6.54[b]	95.37 ± 12.43[a]	
3-Methyl-1-butanol (M)	729.6	221.15	1.246	679.72 ± 7.45[b]	1049.00 ± 13.76[a]	Fusel oil, alcoholic, whiskey, fruity, and banana
3-Methyl-1-butanol (D)	732.4	223.45	1.488	990.89 ± 14.04[a]	787.58 ± 7.39[b]	
Ketones (8)						
3-Octanone (M)	990.4	577.91	1.303	159.31 ± 13.96[a]	72.22 ± 0.52[b]	Fresh, herbal, lavender, sweet, and mushroom
6-Methyl-5-hepten-2-one (M)	990.9	578.83	1.178	65.32 ± 2.46[a]	43.86 ± 3.84[b]	Citrus, green, musty, lemongrass, and apple
2-Octanone (M)	995.4	589.04	1.334	115.78 ± 6.85[a]	67.28 ± 2.40[b]	Earthy, weedy, natural woody, and herbal
2-Heptanone (M)	890.9	394.27	1.261	660.05 ± 11.70[a]	320.17 ± 15.8[b]	Fruity, spicy, sweet, herbal, coconut, and woody
2-Heptanone (D)	890.3	393.34	1.636	460.71 ± 20.68[a]	155.21 ± 1.46[b]	
3-Hydroxy-2-butanone (M)	706.1	202.82	1.051	511.53 ± 11.82[a]	320.74 ± 2.83[b]	Sweet, buttery, creamy, dairy, milky, and fatty
3-Hydroxy-2-butanone (D)	706.6	203.21	1.331	347.91 ± 6.76[a]	172.67 ± 2.35[b]	
2-Butanone (M)	582.2	142.82	1.061	852.91 ± 27.62[a]	712.45 ± 17.96[b]	Acetone-like, ethereal, fruity, and camphor
2-Butanone (D)	582.2	142.82	1.249	5370.31 ± 127.24[a]	2892.93 ± 88.18[b]	
Acetone (M)	489.2	111.19	1.122	4875.18 ± 109.71[a]	3946.4 ± 204.50[b]	Solvent, ethereal, apple, and pear
2-Pentanone (M)	684.0	187.89	1.376	299.59 ± 26.72[a]	370.21 ± 49.84[a]	Sweet, fruity, ethereal, wine, banana, and woody
Aldehydes (10)						
n-Nonanal (M)	1103.1	790.53	1.473	458.85 ± 18.37[a]	394.49 ± 28.14[b]	Waxy, aldehydic, rose, fresh, orris, orange, peel, fatty, and peely
Phenylacetaldehyde (M)	1046.9	678.37	1.253	838.99 ± 87.35[b]	1025.35 ± 21.09[a]	Green, sweet, floral, hyacinth, clover, honey, and cocoa
Benzaldehyde (M)	957.3	508.64	1.152	701.51 ± 14.23[a]	358.10 ± 3.70[b]	Strong, sharp, sweet, bitter, almond, and cherry
Benzaldehyde (D)	957.6	509.33	1.472	287.89 ± 18.00[a]	111.62 ± 11.07[b]	
Heptanal (M)	899.5	407.29	1.332	735.02 ± 10.05[a]	676.13 ± 63.83[a]	Fresh, aldehydic, fatty, green, herbal, wine-lee, and ozone
Heptanal (D)	898.7	406.05	1.700	339.87 ± 24.74[a]	364.63 ± 95.29[a]	

(Continued)

TABLE 2 (Continued)

Volatile flavor compound	RI	RT (s)	DT (ms)	Intensity (V)		Odor description
				FH	LH	
Hexanal (M)	789.8	275.65	1.564	3640.15 ± 347.86[a]	3153.10 ± 219.67[a]	Fresh, green, fatty, aldehydic, grass, leafy, fruity, and sweaty
Pentanal (M)	696.8	196.03	1.181	526.97 ± 25.28[a]	426.90 ± 12.33[b]	Fermented, bready, fruity, nutty, and berry
Pentanal (D)	693.4	193.58	1.422	337.35 ± 68.60[a]	457.12 ± 83.29[a]	
2-Methylbutanal (M)	661.6	176.87	1.403	3545.00 ± 9.58[a]	2102.76 ± 28.43[b]	Musty, cocoa, phenolic, coffee, nutty, malty, fermented, fatty, and alcoholic
3-Methylbutanal (M)	643.0	168.25	1.411	5331.26 ± 80.80[a]	3386.63 ± 13.16[b]	Ethereal, aldehydic, chocolate, peach, and fatty
Octanal (M)	1009.5	612.88	1.406	487.59 ± 18.22[a]	510.4 ± 63.07[a]	Aldehydic, waxy, citrus, orange, peel, green, herbal, fresh, and fatty
Octanal (D)	1009.0	612.04	1.831	61.05 ± 5.04[a]	69.99 ± 13.53[a]	
2-Methylpropanal (M)	550.3	131.08	1.107	1110.38 ± 27.14[a]	614.7 ± 4.31[b]	Fresh, aldehydic, floral, and green
2-Methylpropanal (D)	559.6	134.41	1.282	513.10 ± 60.84[a]	384.57 ± 8.87[b]	
Esters (4)						
γ-Butyrolactone (M)	915.5	433.14	1.086	172.75 ± 35.18[a]	172.77 ± 13.88[a]	Creamy, oily, fatty, and caramel
Ethyl acetate (M)	614.6	155.86	1.103	287.71 ± 9.74[a]	160.31 ± 7.09[b]	Ethereal, fruity, sweet, weedy, and green
Ethyl acetate (D)	618.8	157.63	1.338	477.6 ± 19.91[a]	213.95 ± 21.01[b]	
Butyl acetate (M)	808.2	294.23	1.237	93.36 ± 3.70[a]	65.08 ± 3.88[b]	Ethereal, solvent, fruity, and banana
Butyl acetate (D)	806.9	292.80	1.622	18.75 ± 8.54[a]	20.13 ± 3.71[a]	
Butyl propanoate (M)	908.9	422.32	1.281	24.65 ± 9.19[b]	43.59 ± 1.69[a]	Earthy, sweet, weak, and rose
Acids (2)						
Isovaleric acid (M)	837.4	326.20	1.208	450.36 ± 63.62[b]	643.21 ± 22.42[a]	Sour, stinky, feet, sweaty, cheese, and tropical
Isovaleric acid (D)	837.4	326.20	1.491	52.44 ± 8.41[b]	88.37 ± 3.49[a]	
2-Methylpropanoic acid (M)	750.8	239.03	1.162	174.86 ± 5.30[b]	477.95 ± 5.84[a]	Acidic, sour, cheese, dairy, buttery, and rancid
2-Methylpropanoic acid (D)	752.8	240.79	1.377	51.77 ± 9.65[b]	397.47 ± 9.53[a]	
Heterocyclic (1)						
2-Pentylfuran (M)	993.0	583.67	1.255	255.32 ± 17.21[a]	162.83 ± 13.59[b]	Fruity, green, earthy, beany, vegetable, and metallic
Sulfur-containing (1)						
Dimethyl disulfide (M)	746.1	234.96	0.970	237.54 ± 3.56[a]	71.35 ± 2.33[b]	Sulfurous, vegetable, cabbage, and onion

Different lowercases within the same row denote significant differences between Jinhua FH and LH ($p < 0.05$). FH, fatty ham; LH, lean ham; RI, retention index; RT, retention time; DT, drift time; M, monomer; D, dimer. The odor description of volatile flavor compounds was from the good scents company information system (www.thegoodscentscompany.com).

the phenylacetaldehyde showed a relatively higher richness in LH ($p < 0.05$). Phenylacetaldehyde is originated from the Strecker degradation of phenylalanine and might contribute to the spicy sensation of hams (García-González et al., 2008).

Ketones are another important flavor component in dry-cured meat products, and the high-intensity ketones are usually associated with the creamy, fruity, cooked, and spicy flavor characteristics (Zhu et al., 2018). The most abundant ketones in the two hams were 2-butanone and acetone ($p < 0.05$; Table 2). Acetone could be mainly transferred from acetyl-CoA, one of the major degradation products of glycogens in the muscle, and imparts a buttery taste and fruity aroma to meat products (Shi et al., 2019; Li W. et al., 2021). 2-butanone and other methyl ketones are produced *via* the decarboxylation of β-keto acids or the β-oxidation of saturated fatty acids, and act as precursors in the formation of fatty flavor during the ripening of meats (Pham et al., 2008; Shi et al., 2019). Besides, FH had significantly higher intensities in almost all identified ketones than LH

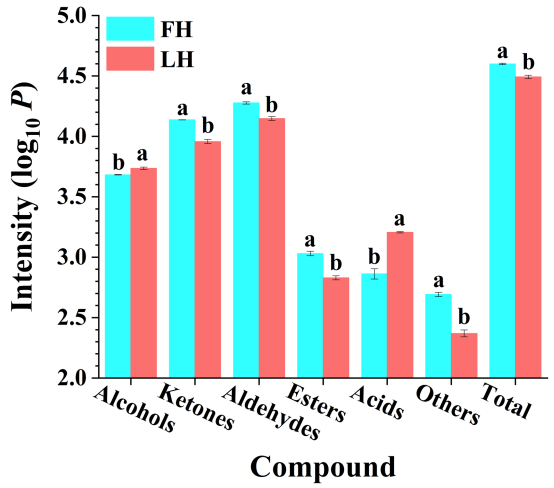

FIGURE 1
Comparison of volatile flavor compound intensities of Jinhua FH and LH in different chemical families. Different lowercases above the error bar denote significant differences between Jinhua FH and LH ($p<0.05$). FH, fatty ham; LH, lean ham. Log_{10} *P* is the logarithmic value of total intensity for compounds of each chemical family in HS-GC-IMS spectra.

($p<0.05$) excluding 2-pentanone. The 2-pentanone did not show noteworthy distinction between the two hams ($p>0.05$; Table 2).

Alcohols are considered contributing less to the aroma of hams because of their relatively higher odor thresholds than aldehydes and ketones, but they can also impart to an herbal, woody, and oily flavor at high concentrations (Liu et al., 2020). The linear-chain aliphatic alcohols are the oxidation products of lipids, whereas the branched alcohols are mostly reported as the microbial degradation products of corresponding branched aldehydes (Shi et al., 2019). It is clear in Table 2 that the most abundant alcohol was obviously distinct for the two hams, which was 2-propanol in LH but ethanol in FH. Meanwhile, most identified linear-chain alcohols showed a higher richness in FH ($p<0.05$), while 2-propanol, 3-methyl-1-butanol (monomer), and 3-hexen-1-ol presented higher abundances in LH ($p<0.05$).

Two short-chain fatty acids (SCFAs; C1-C6), isovaleric acid and 2-methylpropanoic acid, were also identified in both FH and LH, which probably originated from the deamination of amino acids or the secondary metabolism by microbes (Liu et al., 2020; Li et al., 2022). Interestingly, both the two identified acids were more abundant in LH ($p<0.05$; Table 2), which can be a key reason for its relatively lower pH ($p<0.05$; Table 1). These acids could contribute to a sour taste and cheese flavor, and neutralize some deleterious alkaline compounds in fermented meats such as amine and pyrazine (García-González et al., 2008; Liu et al., 2020). Esters were found with relatively high aroma thresholds, generated *via* the esterification between carboxylic acids and alcohols, and partially provided the sweet, fruit, and/or fatty flavors in meat products (Carrapiso et al., 2015). The predominant esters were ethyl acetate and γ-butyrolactone in both FH and LH. The intensity of γ-butyrolactone was similar in FH and LH ($p>0.05$), but the richness of ethyl acetate was relatively higher in FH than that in LH ($p<0.05$).

Moreover, only one heterocyclic compound, 2-pentylfuran, was found in the two hams, which was also determined as the most abundant furans in Chinese bone-less hams by Li et al. (2022). 2-pentylfuran is regarded as an odor-active compound with a green and fruity flavor in dry-cured hams (García-González et al., 2008). In addition, dimethyl disulfide was the only identified sulfur-containing volatile in the two hams, which was in line with the report of Liu et al. (2020) on Jinhua hams. This chemical family is generally products of sulfur-containing amino acid catabolism or microbial metabolism, and usually provides an unpleasant flavor with low odor threshold (Pérez-Santaescolástica et al., 2018). However, dimethyl disulfide has a vegetable aroma and important contribution to the characteristic flavors of cured meats (Liu et al., 2020). Besides, both 2-pentylfuran and dimethyl disulfide showed higher concentrations in FH than those in LH ($p<0.05$).

The total abundance of volatiles belonged to each chemical family was further summarized with results illustrated in Figure 1. It is shown that FH had significantly higher total intensity of ion peaks for volatiles than LH ($p<0.05$). On one hand, aldehydes were the most abundant volatiles among all chemical families for both FH and LH, followed by ketones and alcohols, which were consistent with the findings of Liu et al. (2020) and Li W. et al. (2021) on volatiles from various Chinese dry-cured hams. On the other hand, LH showed remarkably higher total intensities of acids and alcohols ($p<0.05$), whereas other types of volatiles were obviously less abundant for LH ($p<0.05$).

3.3. Analysis of bacterial community structure

The high-throughput sequencing of 16S rRNA genes was performed to investigate the bacterial community structures of Jinhua FH and LH. The α-diversity of bacteria from FH and LH, including Shannon, Simpson, ACE, and Chao 1 indexes, are shown in Table 3. Shannon and Simpson indexes represent the community diversity, and the ACE and Chao 1 indexes are associated with the community richness (Mu et al., 2020). It is clear that the two hams did not have significantly different α-diversities in terms of all indexes ($p>0.05$). Besides, the numbers of observed bacterial species in FH and LH were 1,058 ± 307 and 1,262 ± 71, respectively, without marked difference ($p>0.05$). These data indicate that FH and LH had an overall similar diversity and richness in bacterial communities.

Figure 4 compares the bacterial community structure of two hams at various levels, including phylum, genus, and species. As illustrated in Figure 4A, *Firmicutes* was the most abundant bacteria at the phylum level in FH with a relative abundance of 87.23% ($p<0.05$), followed by *Bacteroidetes* (6.06%) and *Proteobacteria* (3.46%; $p<0.05$). This result was in consistence with the reports of Wang et al. (2021) and Li et al. (2022) on the bacterial composition of Jinhua hams. However, the dominant bacterial phyla (>5%) in LH showed a greater variety, which included *Proteobacteria* (41.39%), *Firmicutes* (20.33%), *Cyanobacteria* (16.26%), *Actinobacteria* (8.92%), and *Bacteroidetes* (5.57%; $p<0.05$). Compared with the bacteria in FH, the richness of *Firmicutes* was sharply decreased in LH ($p<0.05$), but *Proteobacteria*, *Cyanobacteria*, *Actinobacteria*, *Chloroflexi*, and *ε-acteraeota* exhibited a significant elevation in relative abundance ($p<0.05$).

At the genus level (Figure 4B), *Ruminococcaceae* UCG-005 (22.39%), *Staphylococcus* (11.91%), and *Ruminococcaceae* UCG-014 (4.27%) were the dominant bacteria (>2%) in FH ($p<0.05$), while *Staphylococcus* (22.88%) and *Psychrobacter* (11.58%) were the richest bacterial genera in LH ($p<0.05$), followed by *Halomonas* (2.50%), *Propionicicella* (2.07%),

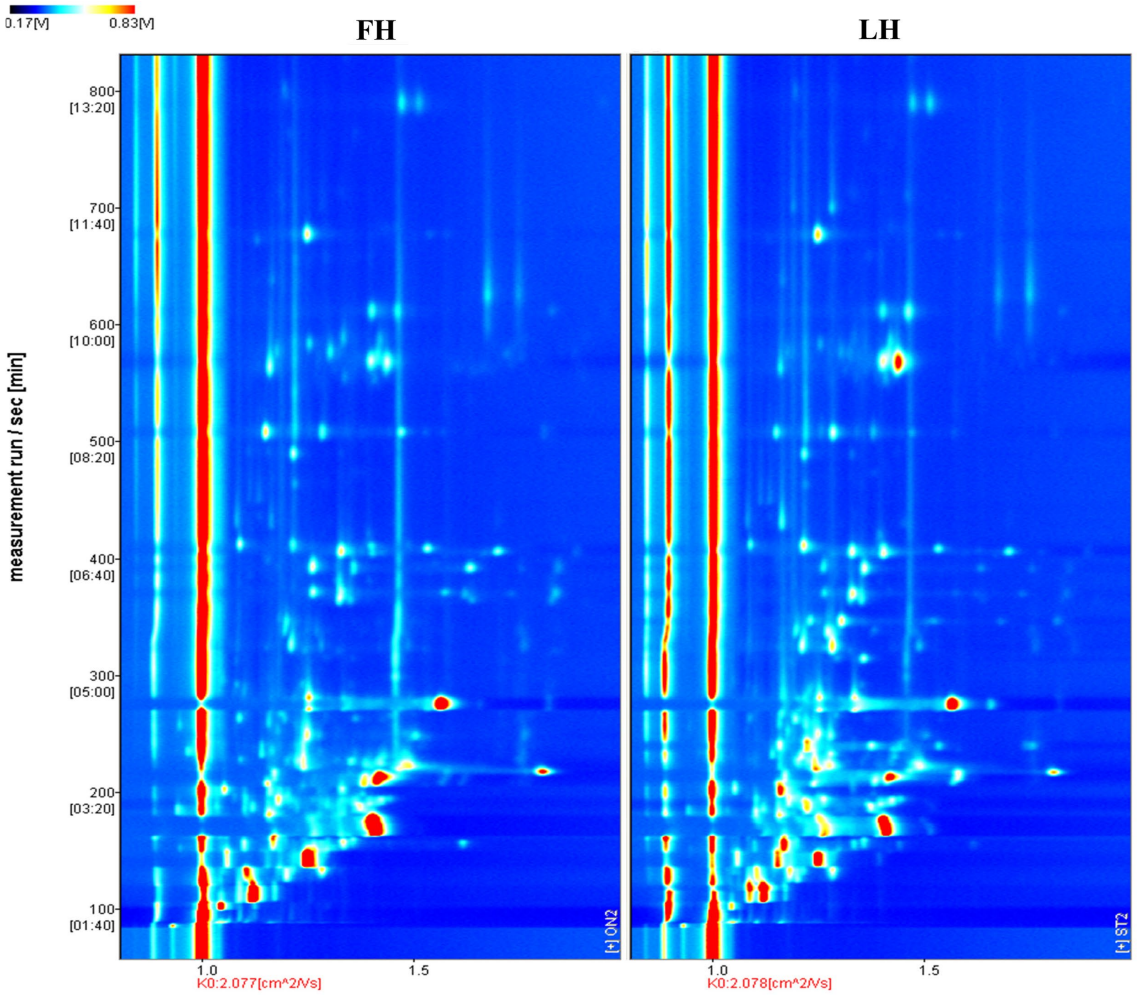

FIGURE 2
Comparison of volatile flavor profiles of Jinhua FH and LH with two-dimension HS-GC-IMS spectra. FH, fatty ham; LH, lean ham.

and *Ruminococcaceae* UCG-005 (2.02%; $p < 0.05$). Wang et al. (2021) reported that *Staphylococcus*, *Psychrobacter*, *Halomonas*, and unidentified *Ruminococcaceae* were among dominant bacterial genera of Jinhua hams ripened for different months, which were corresponded to our above findings. Furthermore, among the main bacterial genera with a relative abundance >1%, FH had richer *Ruminococcaceae* UCG-005, *Ruminococcaceae* UCG-014, *Bacteroides*, *Ruminococcaceae* NK4A214 group, and [*Ruminococcus*] torques group ($p < 0.05$), whereas LH showed higher richness of *Staphylococcus*, *Psychrobacter*, *Propionicicella*, *Ochrobactrum*, *Sphingomonas*, *Lactobacillus*, and *Halomonas* ($p < 0.05$).

At the species level (Figure 4C), the dominant bacteria (>1%) were *Staphylococcus* sp., *Ruminococcaceae* UCG-005 *sp.*, and *Ruminococcaceae* NK4A214 group sp. for FH ($p < 0.05$), whereas *Staphylococcus sp.*, *Ochrobactrum sp.*, *Psychrobacter pulmonis*, and *Halomonas subglaciescola* for LH ($p < 0.05$). On the other hand, among the core bacterial species with a richness >0.5%, the richness of *Ruminococcaceae* UCG-005 sp. and *Ruminococcaceae* NK4A214 group *sp.* were more abundant in FH ($p < 0.05$), while *Staphylococcus sp.*, *Ochrobactrum sp.*, *Psychrobacter pulmonis*, *Prevotella paludivivens*, and *Halomonas subglaciescola* presented a relatively higher richness in LH ($p < 0.05$).

3.4. Analysis of fungal community structure

The high-throughput sequencing of ITS genes was applied to analyze the fungal community structures of Jinhua FH and LH. The α-diversity of fungi from the two hams are exhibited in Table 4. Generally, FH presented much higher Shannon, ACE, and Chao 1 indexes than LH ($p < 0.05$). Moreover, the number of fungal species observed from FH was 697 ± 147, approximately 2.8 times of that observed from LH (246 ± 5; $p < 0.05$). These results reveal that both diversity and richness of fungal community in LH was dramatically reduced in comparison to FH.

Figure 5 illustrates the fungal community structure of FH and LH at the phylum, genus, and species level. As illustrated in Figure 5A, *Ascomycota* was the richest fungus phylum in FH and accounted for a relative abundance of 82.79%, followed by *Basidiomycota* (6.06%) and *Mortierellomycota* (2.66%; $p < 0.05$). Meanwhile, *Ascomycota* was the only dominant fungal phylum (>5%) in LH ($p < 0.05$), accounting for a much higher relative abundance (97.69%) than that in FH ($p < 0.05$). In accordance with this finding, Lin et al. (2020) and Chen et al. (2021) also found that *Ascomycota* was the absolutely predominant fungus at the phylum level in Laowo dry-cured hams and Mianning hams, respectively. Besides, the relative abundances of

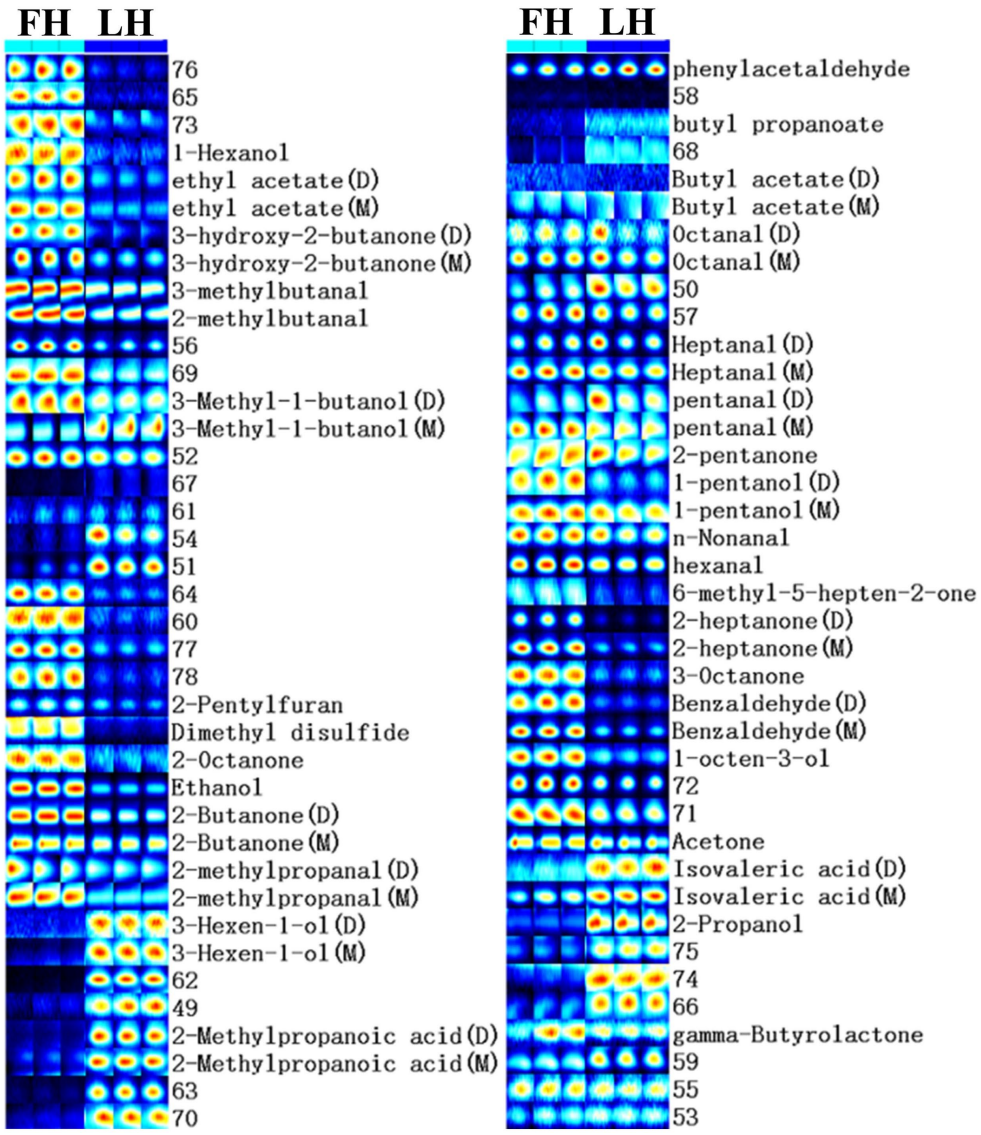

FIGURE 3
Gallery plot of characteristic flavor finger-print of Jinhua FH and LH determined by HS-GC-IMS. FH, fatty ham; LH, lean ham.

TABLE 3 α-diversity indexes of bacterial communities in Jinhua FH and LH.

α-diversity indexes	FH	LH
Shannon	5.24 ± 0.83[a]	5.23 ± 1.06[a]
Simpson	0.88 ± 0.07[a]	0.83 ± 0.11[a]
ACE	1314.42 ± 269.91[a]	1316.98 ± 62.12[a]
Chao1	1280.03 ± 274.09[a]	1344.48 ± 85.11[a]
Goods coverage	1.00 ± 0.00[a]	1.00 ± 0.00[a]
Observed species	1,058 ± 307[a]	1,262 ± 71[a]

Different lowercases within the same row denote significant differences in bacterial communities between Jinhua FH and LH ($p < 0.05$). FH, fatty ham; LH, lean ham.

many fungal phyla, mainly including *Basidiomycota*, *Rozellomycota*, *Chytridiomycota*, and *Glomeromycota* were significantly lower in LH than those in FH ($p < 0.05$).

At the genus level (Figure 5B), *Meyerozyma* (55.61%) was the most abundant fungus in FH ($p < 0.05$), followed by *Aspergillus* (11.67%; $p < 0.05$). While *Meyerozyma* (64.79%), *Yamadazyma* (17.76%), and *Aspergillus* (12.82%) were the dominant fungal genera (>2%) in LH ($p < 0.05$). Consistent with these findings, Lin et al. (2020) also found that *Yamadazyma*, *Meyerozyma*, and *Aspergillus* was the most abundant fungal genus in Laowo dry-cured hams ripened for 1–3 years, respectively. On the other hand, among the core fungal genera with a relative abundance >1%, the richness of *Fusarium*, *Debaryomyces*, *Marasmius*, and *Apiotrichum* were relatively higher in FH ($p < 0.05$), and *Yamadazyma* was the only more abundant fungus in LH ($p < 0.05$).

At the species level (Figure 5C), *Meyerozyma sp.*, *Aspergillus proliferans*, and *Yamadazyma triangularis* were all among the core fungi (>1%) of both FH and LH ($p < 0.05$). Besides, *Debaryomyces sp.* and *Apiotrichum sp.* were also the dominant fungi in FH ($p < 0.05$). Moreover, among the core fungal species with a relative abundance >0.5%, FH showed more abundant *Marasmius siccus*, *Debaryomyces sp.*, *Apiotrichum sp.*, *Archaeorhizomyces sp.*, and *Fusarium solani* ($p < 0.05$), whereas LH presented a higher relative abundance in *Yamadazyma triangularis* ($p < 0.05$).

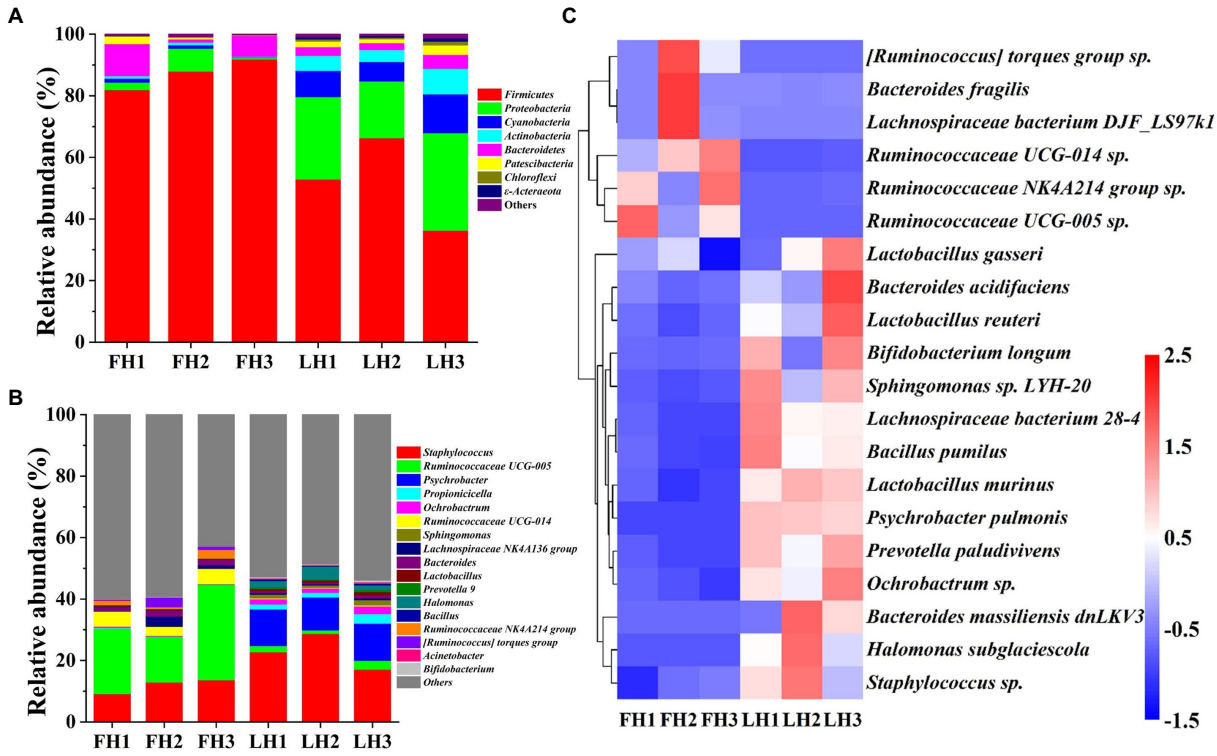

FIGURE 4
Bacterial community structure of Jinhua FH and LH at the phylum, genus, and species levels. (**A**) Relative abundance at the phylum level. (**B**) Relative abundance at the genus level. (**C**) Heatmap of HCA for the relative abundance of main species (top 20). The color gradation in panel **C** represents the Z-scores of corresponding relative abundances. FH, fatty ham; LH, lean ham.

TABLE 4 α-diversity indexes of fungal communities in Jinhua FH and LH.

α-diversity indexes	FH	LH
Shannon	3.58 ± 1.15^{a}	1.91 ± 0.03^{b}
Simpson	0.66 ± 0.17^{a}	0.56 ± 0.02^{a}
ACE	750.46 ± 161.03^{a}	277.53 ± 13.40^{b}
Chao1	742.63 ± 160.02^{a}	270.22 ± 13.81^{b}
Goods coverage	1.00 ± 0.00^{a}	1.00 ± 0.00^{a}
Observed species	697 ± 147^{a}	246 ± 5^{b}

Different lowercases within the same row denote significant differences in fungal communities between Jinhua FH and LH ($p < 0.05$). FH, fatty ham; LH, lean ham.

3.5. Correlations and connections between differential core microorganisms and discriminative volatile flavor compounds

Figure 6A shows the Pearson's correlations between 17 differential core microbial genera ($p < 0.05$ and relative abundance >1%; 12 bacterial genera, 2 yeast genera, and 3 mold genera) and 29 discriminative volatile flavor compounds ($p < 0.05$) in Jinhua FH and LH. Surprisingly, 12 of the 17 differential core microorganisms, including 10 bacterial genera and 2 yeast genera, showed significant correlations with the distinct volatiles ($p < 0.05$ and $|r| > 0.82$). Among these microbial genera, *Staphylococcus*, *Lactobacillus*, *Yamadazyma*, *Ochrobactrum*, and *Sphingomonas* were one type of microbes mainly positively correlating with acids, branched alcohols, and a few linear-chain alcohols (2-propanol and 3-hexen-1-ol) in the two hams ($p < 0.05$ and $r > 0.82$). *Staphylococcus* has been considered the most important factor in the sensory characteristics development of dry-cured hams, owning to its strong abilities of nitrate reductase, catalase, protease, and lipase (Landeta et al., 2013; Xiao et al., 2020). *Lactobacillus* could extend the shelf life of hams by inhibiting the growth of spoilage bacteria *via* its product lactic acid, which could be further utilized by other microorganisms for SCFA synthesis (Figure 6A; Table 1; Xiao et al., 2020; Hu et al., 2022). *Yamadazyma* has been reported positively related to the organic acid level and negatively associated with the amino acid content in hams (Lin et al., 2020; Mu et al., 2020), suggesting its potential capability of producing SCFAs from amino acids (Figure 6A). Furthermore, *Lactobacillus* and *Yamadazyma* were both core microorganisms with higher relative abundances in LH ($p < 0.05$; Figures 4B, 5B), which could be an important contributor to the relatively higher acid volatile level (Figure 1; Table 2) and lower pH (Table 1) of LH ($p < 0.05$), owning to their potential association with SCFA generation.

On the other hand, *Ruminococcaceae* UCG-005, *Psychrobacter*, *Ruminococcaceae* UCG-014, and *Debaryomyces* were another type of microorganisms that positively correlated with aldehydes, ketones, most linear-chain alcohols, esters, and the other two compounds (2-pentylfuran and dimethyl disulfide) in the two hams ($p < 0.05$ and $r > 0.82$). *Psychrobacter* is a common bacterium in low-temperature fermented foods with substantial proteolysis ability (Broekaert et al., 2013). Zhang et al. (2021) has reported that *Debaryomyces* could produce branched aldehydes, such as 2-methylbutanal and 3-methylbutanal, by utilizing amino acids. Furthermore, Flores et al. (2004) reported that *Debaryomyces*

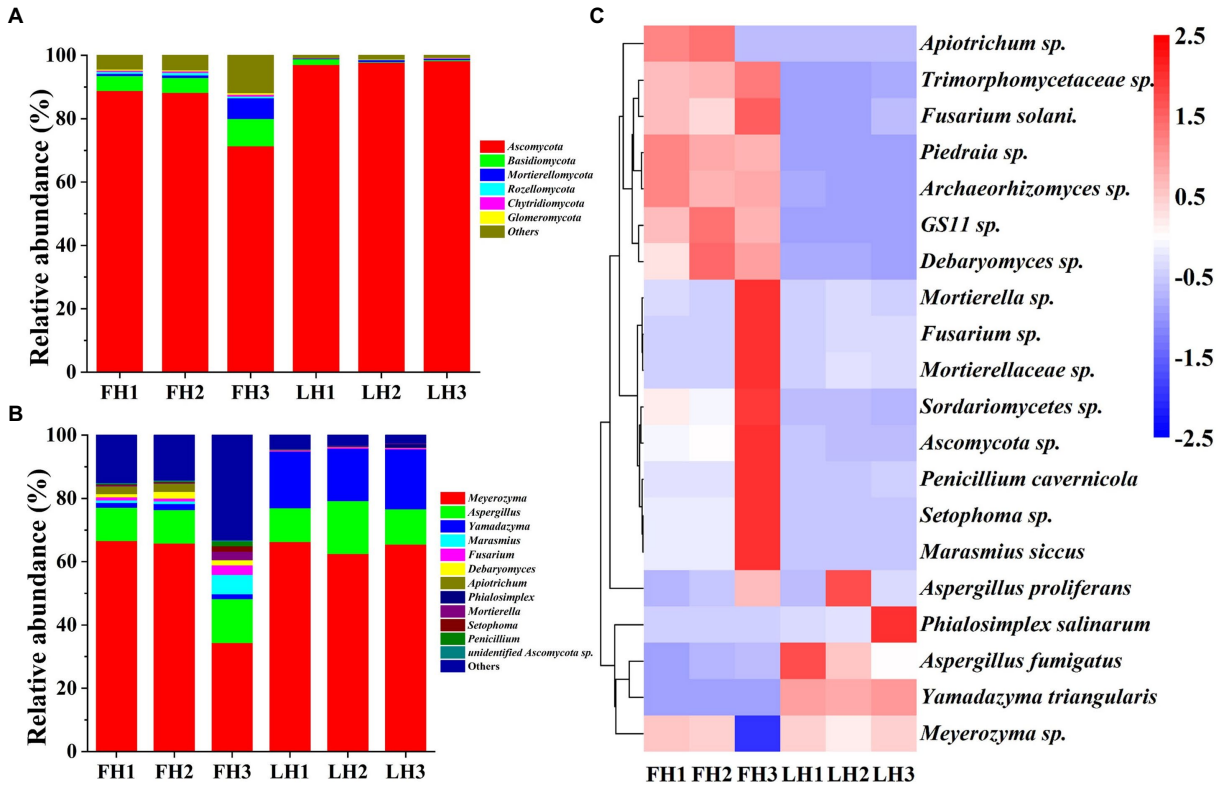

FIGURE 5
Fungal community structure of Jinhua FH and LH at the phylum, genus, and species levels. **(A)** Relative abundance at the phylum level. **(B)** Relative abundance at the genus level. **(C)** Heatmap of HCA for the relative abundance of main species (top 20). The color gradation in panel **C** represents the Z-scores of relative abundances. FH, fatty ham; LH, lean ham.

could promote the generation of ethyl esters in dry-fermented meats. The intensities of 2-methylbutanal, 3-methylbutanal, and ethyl acetate were all positively correlated with the richness of *Debaryomyces* (Figure 6A), which were consistent with their findings. Moreover, the role of *Ruminococcaceae* family was rarely reported in fermented meat products, but it is known with capacities of fat degradation and fatty acid β-oxidation (Baars et al., 2018), which might contribute to the high-level volatiles originated from fats in FH, such as methyl ketones, furans, and some liner-chain aldehydes/alcohols (Figure 6A).

According to the present data and associated previous reports (Chen et al., 2017; Shi et al., 2019; Mu et al., 2020; Li et al., 2022), the potential metabolic network of discriminative volatiles' formation under the involvement of core microorganisms in Jinhua FH and LH is further illustrated in Figure 6B. Briefly, the absence of fats significantly affected the microbial community structure and the flavor formation process in LH. By lipases from *Staphylococcus* and *Ruminococcaceae* in FH, fats can be degraded into fatty acids, which further generated methyl ketones and furans through decarboxylation and other reactions. Besides, the unsaturated fatty acids can be broken down through the β-oxidation by *Ruminococcaceae* to produce linear-chain aldehydes, which can be reduced to linear-chain alcohols and further esterified under the promotion of *Debaryomyces*. Whereas in LH, the protein metabolism was relatively enhanced due to the lack of fats and the action of characteristic core microbes. Under the proteolysis of *Staphylococcus* and *Psychrobacter*, more proteins were degraded into amino acids, which were then subjected to Strecker degradation and deamination for further generation of some aromatic aldehydes or linear-chained alcohols. Besides, the branched acids could be generated by *Yamadazyma* and some other microbes through utilizing amino acids or *Lactobacillus*-produced lactic acids. In summary, this metabolic network confirmed that the discriminative flavor compounds of FH were mainly β-oxidation and degradation products of fatty acids, whereas those of LH were mostly derived from the Strecker reaction or microbial metabolism of amino acids.

4. Conclusion

In conclusion, the lack of fats obviously influenced the microbial composition and flavor formation of LH, which further affected some physiochemical parameters. FH and LH did not show significant differences in redness, water activity, chemical composition, and nitrite residue, but FH had higher pH and a slightly lighter and yellower color. Besides, a total of 33 volatile flavor compounds were identified. FH and LH exhibited significant differences in 29 identified volatiles, among which LH showed higher total abundance of alcohols and acids, whereas FH had generally richer aldehydes, ketones, esters, heterocyclic compounds, and sulfur-containing compounds. Meanwhile, FH and LH also showed no significant difference in α-diversity of bacterial community, but LH had a both lower richness and diversity of fungal community than FH. The dominant microorganisms (>2%) were *Ruminococcaceae* UCG-005, *Staphylococcus*, *Ruminococcaceae* UCG-014, *Meyerozyma*, and *Aspergillus* in FH at the genus level,

10.3389/fmicb.2023.1124770

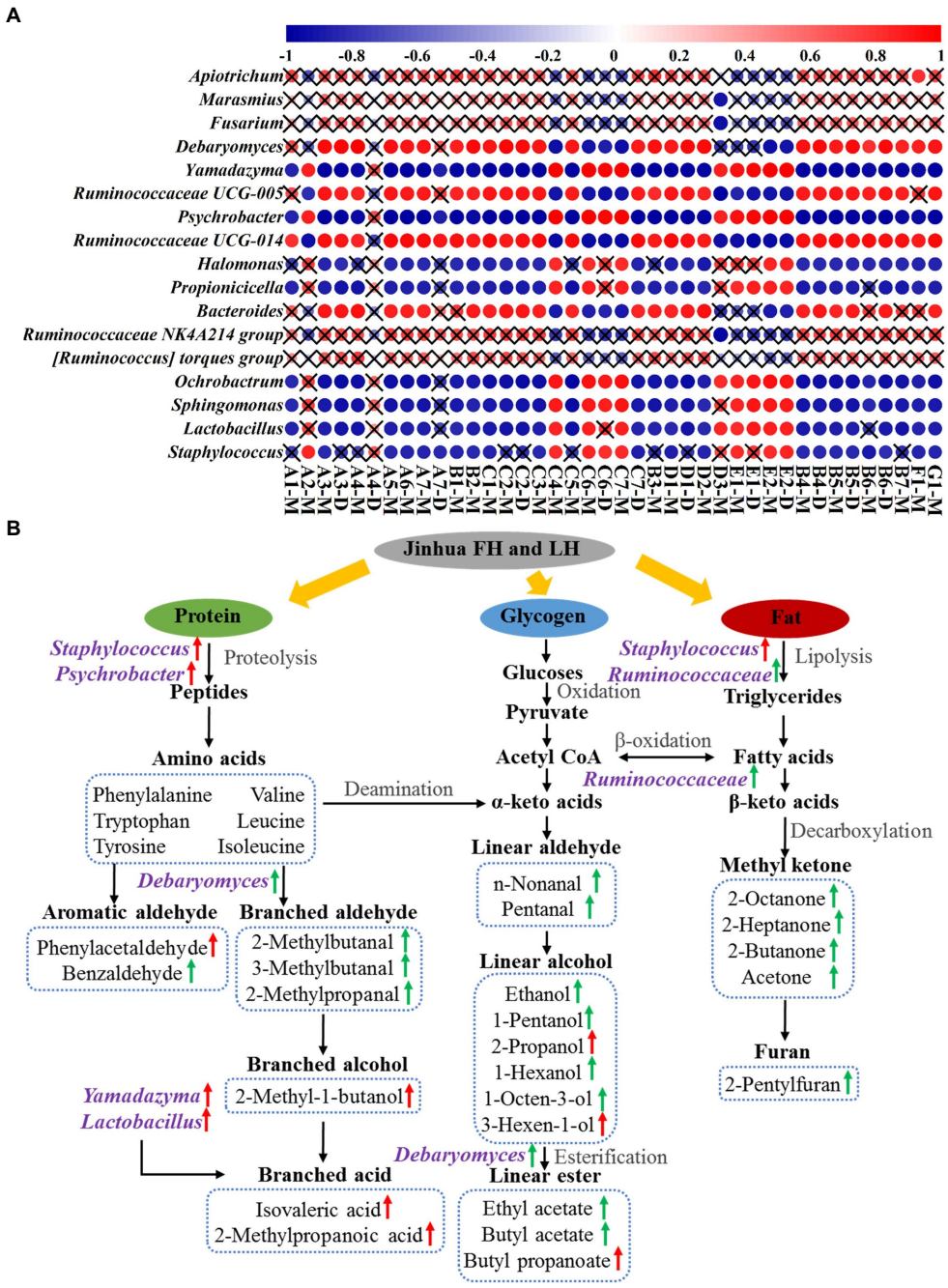

FIGURE 6
Pearson's correlations **(A)** and potential pathways **(B)** between differential core microorganisms and distinct volatile flavor compounds. The color gradation and circle size in panel **A** represent the correlation coefficient (r value), while the pattern without a "×" symbol indicates a significant correlation ($p<0.05$). The green and red arrows in panel **B** indicate an up-regulation in FH and LH, respectively. A1, n-nonanal; A2, phenylacetaldehyde; A3, benzaldehyde; A4, pentanal; A5, 2-methylbutanal; A6, 3-methylbutanal; A7, 2-methylpropanal; B1, 3-octanone; B2, 6-methyl-5-hepten-2-one; B3, 2-octanone; B4, 2-heptanone; B5, 3-hydroxy-2-butanone; B6, 2-butanone; B7, acetone; C1, 1-octen-3-ol; C2, 1-pentanol; C3, ethanol; C4, 2-propanol; C5, 1-hexanol; C6, 3-hexen-1-ol; C7, 3-methyl-1-butanol; D1, ethyl acetate; D2, butyl acetate; D3, butyl propanoate; E1, isovaleric acid; E2, 2-methylpropanoic acid; F1, 2-pentylfuran; G1, dimethyl disulfide; M, monomer; D, dimer.

whereas *Staphylococcus*, *Psychrobacter*, *Halomonas*, *Propionicicella*, *Ruminococcaceae* UCG-005, *Meyerozyma*, *Yamadazyma*, and *Aspergillus* for LH. The analysis of Pearson's correlation and metabolic network confirmed that the discriminative flavor compounds of FH were mainly β-oxidation and degradation products of fatty acids, while those of LH were mostly derived from the Strecker reaction or microbial metabolism of amino acids. Furthermore, *Staphylococcus*, *Yamadazyma*, *Ruminococcaceae*, *Debaryomyces*, *Lactobacillus*, and *Psychrobacter* might be the core microorganisms contributing to their differences in flavor characteristics and pH value. This work could help understand the potential pathway of characteristic microorganisms influencing flavor formation of fat-deficient dry-cured hams and provide theoretical supports for developing healthier fermented meat products.

Data availability statement

The data presented in the study are deposited in the Sequence Read Archive of National Center for Biotechnology Information repository (https://www.ncbi.nlm.nih.gov/sra), accession number PRJNA917481.

Author contributions

JZ: conceptualization, methodology, writing-original draft, writing-review and editing, visualization, and funding acquisition. KZ: data curation. HL: software. SL: validation. WX: resources. LC: funding acquisition. JX: formal analysis and resources. HT: conceptualization, resources, and funding acquisition. All authors contributed to the article and approved the submitted version.

Funding

This research was financially supported by the Zhejiang Key Research and Development Program (Nos. 2021C04024 and 2022C02060), Zhejiang Natural Science Foundation (No. LY21C200003), International Cooperation Fund of Zhejiang Academy of Agricultural Science (No. 10411040122GJ0101F), Young Professionals Promotion Funds of Zhejiang Academy of Agricultural Sciences (No. 2020R15R08E01), and Scientific Research Fund for Advanced Scholar of Zhejiang Academy of Agricultural Science (No. 3300002172744).

Acknowledgments

We thank Shanghai Applied Protein Technology Co., Ltd. Co., Ltd., Shanghai, China and GAS Instrument Co., Ltd., Germany for their assistance in the analysis of microbial communities and volatile flavor compounds, respectively.

Conflict of interest

WX is employed by Jinhua Jinnian Ham Co., Ltd (Jinhua, China).

The remaining authors declare that this research was conducted in the absence of any commercial or financial relationships that could be construed as a potential conflict of interest.

Publisher's note

References

Arroyo-Manzanares, N., Martín-Gómez, A., Jurado-Campos, N., Garrido-Delgado, R., Arce, C., and Arce, L. (2018). Target vs. spectral fingerprint data analysis of Iberian ham samples for avoiding labelling fraud using headspace-gas chromatography-ion mobility spectrometry. *Food Chem.* 246, 65–73. doi: 10.1016/j.foodchem.2017.11.008

Baars, A., Oosting, A., Lohuis, M., Koehorst, M., El Aidy, S., Hugenholtz, F., et al. (2018). Sex differences in lipid metabolism are affected by presence of the gut microbiota. *Sci. Rep.* 8, 1–11. doi: 10.1038/s41598-018-31695-w

Benet, I., Guàrdia, M. D., Ibañez, C., Solà, J., Arnau, J., and Roura, E. (2015). Analysis of SPME or SBSE extracted volatile compounds from cooked cured pork ham differing in intramuscular fat profiles. *LWT Food Sci. Technol.* 60, 393–399. doi: 10.1016/j.lwt.2014.08.016

Benet, I., Guàrdia, M. D., Ibañez, C., Solà, J., Arnau, J., and Roura, E. (2016). Low intramuscular fat (but high in PUFA) content in cooked cured pork ham decreased Maillard reaction volatiles and pleasing aroma attributes. *Food Chem.* 196, 76–82. doi: 10.1016/j.foodchem.2015.09.026

Bosse, R., Müller, A., Gibis, M., Weiss, A., Schmidt, H., and Weiss, J. (2018). Recent advances in cured raw ham manufacture. *Crit. Rev. Food Sci. Nutr.* 58, 610–630. doi: 10.1080/10408398.2016.1208634

Broekaert, K., Noseda, B., Heyndrickx, M., Vlaemynck, G., and Devlieghere, F. (2013). Volatile compounds associated with *Psychrobacter* spp. and *Pseudoalteromonas* spp., the dominant microbiota of brown shrimp (*Crangon crangon*) during aerobic storage. *Int. J. Food Microbiol.* 166, 487–493. doi: 10.1016/j.ijfoodmicro.2013.08.013

Carrapiso, A. I., Noseda, B., García, C., Reina, R., Del Pulgar, J. S., and Devlieghere, F. (2015). SIFT-MS analysis of Iberian hams from pigs reared under different conditions. *Meat Sci.* 104, 8–13. doi: 10.1016/j.meatsci.2015.01.012

Chen, Q., Kong, B., Han, Q., Xia, X., and Xu, L. (2017). The role of bacterial fermentation in lipolysis and lipid oxidation in Harbin dry sausages and its flavor development. *LWT Food Sci. Technol.* 77, 389–396. doi: 10.1016/j.lwt.2016.11.075

Chen, L., Wang, Z., Ji, L., Zhang, J., Zhao, Z., Zhang, R., et al. (2021). Flavor composition and microbial community structure of Mianning ham. *Front. Microbiol.* 11:623775. doi: 10.3389/fmicb.2020.623775

Deng, J., Xu, H., Li, X., Wu, Y., and Xu, B. (2022). Correlation of characteristic flavor and microbial community in Jinhua ham during the post-ripening stage. *LWT Food Sci. Technol.* 171:114067. doi: 10.1016/j.lwt.2022.114067

Domínguez, R., Pateiro, M., Teixeira, A., Perez-Alvarez, J. A., Santos, E. M., Trindade, M. A., et al. (2022). "Dry-cured ham" in *Production of traditional Mediterranean meat products*. ed. J. M. Lorenzo (New York, NY: Humana), 57–65. doi: 10.1007/978-1-0716-2103-5_7

Flores, M., Durá, M. A., Marco, A., and Toldrá, F. (2004). Effect of *Debaryomyces* spp. on aroma formation and sensory quality of dry-fermented sausages. *Meat Sci.* 68, 439–446. doi: 10.1016/j.meatsci.2003.04.001

García-González, D. L., Tena, N., Aparicio-Ruiz, R., and Morales, M. T. (2008). Relationship between sensory attributes and volatile compounds qualifying dry-cured hams. *Meat Sci.* 80, 315–325. doi: 10.1016/j.meatsci.2007.12.015

Ge, Q., Gu, Y., Zhang, W., Yin, Y., Yu, H., Wu, M., et al. (2017). Comparison of microbial communities from different Jinhua ham factories. *AMB Express* 7, 1–8. doi: 10.1186/s13568-017-0334-0

Hu, Y., Zhang, L., Wen, R., Chen, Q., and Kong, B. (2022). Role of lactic acid bacteria in flavor development in traditional Chinese fermented foods: a review. *Crit. Rev. Food Sci. Nutr.* 62, 2741–2755. doi: 10.1080/10408398.2020.1858269

Landeta, G., Curiel, J. A., Carrascosa, A. V., Muñoz, R., and De Las Rivas, B. (2013). Characterization of coagulase-negative staphylococci isolated from Spanish dry cured meat products. *Meat Sci.* 93, 387–396. doi: 10.1016/j.meatsci.2012.09.019

Li, W., Chen, Y. P., Blank, I., Li, F., Li, C., and Liu, Y. (2021). GC×GC-ToF-MS and GC-IMS based volatile profile characterization of the Chinese dry-cured hams from different regions. *Food Res. Int.* 142:110222. doi: 10.1016/j.foodres.2021.110222

Li, H., Chen, Y., Tang, H., Zhang, J., Zhang, L., Yang, X., et al. (2021). Effect of lysozyme and Chinese liquor on Staphylococcus aureus growth, microbiome, flavor profile, and the quality of dry fermented sausage. *LWT Food Sci. Technol.* 150:112059. doi: 10.1016/j.lwt.2021.112059

Li, Z., Wang, Y., Pan, D., Geng, F., Zhou, C., and Cao, J. (2022). Insight into the relationship between microorganism communities and flavor quality of Chinese dry-cured boneless ham with different quality grades. *Food Biosci.* 50:102174. doi: 10.1016/j.fbio.2022.102174

Li, M., Yang, R., Zhang, H., Wang, S., Chen, D., and Lin, S. (2019). Development of a flavor fingerprint by HS-GC–IMS with PCA for volatile compounds of Tricholoma matsutake singer. *Food Chem.* 290, 32–39. doi: 10.1016/j.foodchem.2019.03.124

Lin, F., Cai, F., Luo, B., Gu, R., Ahmed, S., and Long, C. (2020). Variation of microbiological and biochemical profiles of laowo dry-cured ham, an indigenous fermented food, during ripening by GC-TOF-MS and UPLC-QTOF-MS. *J. Agric. Food Chem.* 68, 8925–8935. doi: 10.1021/acs.jafc.0c03254

Liu, D., Bai, L., Feng, X., Chen, Y. P., Zhang, D., Yao, W., et al. (2020). Characterization of Jinhua ham aroma profiles in specific to aging time by gas chromatography-ion mobility spectrometry (GC-IMS). *Meat Sci.* 168:108178. doi: 10.1016/j.meatsci.2020.108178

Liu, P., Wang, S., Zhang, H., Wang, H., and Kong, B. (2019). Influence of glycated nitrosohaemoglobin prepared from porcine blood cell on physicochemical properties, microbial growth and flavor formation of Harbin dry sausages. *Meat Sci.* 148, 96–104. doi: 10.1016/j.meatsci.2018.10.008

Martínez-Onandi, N., Rivas-Cañedo, A., Ávila, M., Garde, S., Nuñez, M., and Picon, A. (2017). Influence of physicochemical characteristics and high pressure processing on the volatile fraction of Iberian dry-cured ham. *Meat Sci.* 131, 40–47. doi: 10.1016/j.meatsci.2017.04.233

Mu, Y., Su, W., Mu, Y., and Jiang, L. (2020). Combined application of high-throughput sequencing and metabolomics reveals metabolically active microorganisms during Panxian ham processing. *Front. Microbiol.* 10:3012. doi: 10.3389/fmicb.2019.03012

Narváez-Rivas, M., Gallardo, E., and León-Camacho, M. (2014). Chemical changes in volatile aldehydes and ketones from subcutaneous fat during ripening of Iberian dry-cured ham: Prediction of the curing time. *Food Res. Int.* 55, 381–390. doi: 10.1016/j.foodres.2013.11.029

Parolari, G., Aguzzoni, A., and Toscani, T. (2016). Effects of processing temperature on color properties of dry-cured hams made without nitrite. *Foods*, 5:33 33, doi: 10.3390/foods5020033.

Pérez-Santaescolástica, C., Carballo, J., Fulladosa, E., Garcia-Perez, J. V., Benedito, J., and Lorenzo, J. M. (2018). Effect of proteolysis index level on instrumental adhesiveness, free amino acids content and volatile compounds profile of dry-cured ham. *Food Res. Int.* 107, 559–566. doi: 10.1016/j.foodres.2018.03.001

Petrova, I., Aasen, I. M., Rustad, T., and Eikevik, T. M. (2015). Manufacture of dry-cured ham: a review. Part 1. Biochemical changes during the technological process. *Eur. Food Res. Technol.* 241, 587–599. doi: 10.1007/s00217-015-2490-2

Pham, A. J., Schilling, M. W., Mikel, W. B., Williams, J. B., Martin, J. M., and Coggins, P. C. (2008). Relationships between sensory descriptors, consumer acceptability and volatile flavor compounds of American dry-cured ham. *Meat Sci.* 80, 728–737. doi: 10.1016/j.meatsci.2008.03.015

Shi, Y., Li, X., and Huang, A. (2019). A metabolomics-based approach investigates volatile flavor formation and characteristic compounds of the Dahe black pig dry-cured ham. *Meat Sci.* 158:107904. doi: 10.1016/j.meatsci.2019.107904

Toledano, A. M., Jordano, R., Medina, L. M., and López-Mendoza, M. C. (2019). Behavior and effect of combined starter cultures on microbiological and physicochemical characteristics of dry-cured ham. *J. Food Sci. Technol.* 56, 122–131. doi: 10.1007/s13197-018-3465-7

Trevisan, M., Krogh, V., Freudenheim, J. L., Blake, A., Muti, P., Panico, S., et al. (1990). Diet and coronary heart disease risk factors in a population with varied intake. *Prev. Med.* 19, 231–241. doi: 10.1016/0091-7435(90)90024-E

Wang, Y., Li, F., Chen, J., Sun, Z., Wang, F., Wang, C., et al. (2021). High-throughput sequencing-based characterization of the predominant microbial community associated with characteristic flavor formation in Jinhua ham. *Food Microbiol.* 94:103643. doi: 10.1016/j.fm.2020.103643

Xiao, Y., Liu, Y., Chen, C., Xie, T., and Li, P. (2020). Effect of lactobacillus plantarum and staphylococcus xylosus on flavor development and bacterial communities in Chinese dry fermented sausages. *Food Res. Int.* 135:109247. doi: 10.1016/j.foodres.2020.109247

Zhang, J., He, S., Kong, F., Huang, S., Xiong, S., Yin, T., et al. (2017). Size reduction and calcium release of fish bone particles during nanomilling as affected by bone structure. *Food Bioprocess Technol.* 10, 2176–2187. doi: 10.1007/s11947-017-1987-z

Zhang, L., Huang, C., Johansen, P. G., Petersen, M. A., Poojary, M. M., Lund, M. N., et al. (2021). The utilization of amino acids by *Debaryomyces hansenii* and *Yamadazyma triangularis* associated with cheese. *Int. Dairy J.* 121:105135. doi: 10.1016/j.idairyj.2021.105135

Zhang, J., Zhu, L., Li, H., Tang, H., Yang, H., Zhao, K., et al. (2022). Effects of micro—/nano-scaled chicken bones on heat-induced gel properties of low-salt pork batter: physicochemical characteristics, water distribution, texture, and microstructure. *Food Chem.* 373:131574. doi: 10.1016/j.foodchem.2021.131574

Zhou, C. Y., Bai, Y., Wang, C., Li, C. B., Xu, X. L., Pan, D. D., et al. (2021a). 1H NMR-based metabolomics and sensory evaluation characterize taste substances of Jinhua ham with traditional and modern processing procedures. *Food Control* 126:107873. doi: 10.1016/j.foodcont.2021.107873

Zhou, C. Y., Pan, D. D., Cao, J. X., and Zhou, G. H. (2021b). A comprehensive review on molecular mechanism of defective dry-cured ham with excessive pastiness, adhesiveness, and bitterness by proteomics insights. *Compr. Rev. Food Sci. Food Saf.* 20, 3838–3857. doi: 10.1111/1541-4337.12779

Zhou, C., Xia, Q., Du, L., He, J., Sun, Y., Dang, Y., et al. (2022). Recent developments in off-odor formation mechanism and the potential regulation by starter cultures in dry-cured ham. *Crit. Rev. Food Sci. Nutr.* 4, 1–15. doi: 10.1080/10408398.2022.2057418

Zhu, C. Z., Zhao, J. L., Tian, W., Liu, Y. X., Li, M. Y., and Zhao, G. M. (2018). Contribution of histidine and lysine to the generation of volatile compounds in Jinhua ham exposed to ripening conditions via Maillard reaction. *J. Food Sci.* 83, 46–52. doi: 10.1111/1750-3841.13996

frontiers | Frontiers in Microbiology

TYPE Original Research
PUBLISHED 02 February 2023
DOI 10.3389/fmicb.2022.1118907

OPEN ACCESS

EDITED BY
Jinxuan Cao,
Beijing Technology and Business University, China

REVIEWED BY
Qian Chen,
Northeast Agricultural University, China
Jin Guofeng,
Beijing Technology and Business University, China

*CORRESPONDENCE
Hai Yu
✉ yuhai@yzu.edu.cn

SPECIALTY SECTION
This article was submitted to Food Microbiology, a section of the journal Frontiers in Microbiology

RECEIVED 08 December 2022
ACCEPTED 28 December 2022
PUBLISHED 02 February 2023

CITATION
Liu R, Ma Y, Chen L, Lu C, Ge Q, Wu M, Xi J and Yu H (2023) Effects of the addition of leucine on flavor and quality of sausage fermented by *Lactobacillus fermentum* YZU-06 and *Staphylococcus saprophyticus* CGMCC 3475.
Front. Microbiol. 13:1118907.
doi: 10.3389/fmicb.2022.1118907

Effects of the addition of leucine on flavor and quality of sausage fermented by *Lactobacillus fermentum* YZU-06 and *Staphylococcus saprophyticus* CGMCC 3475

Rui Liu[1], Yong Ma[1], Lei Chen[1], Chenyan Lu[1], Qingfeng Ge[1], Mangang Wu[1], Jun Xi[2] and Hai Yu[1]*

[1]School of Food Science and Engineering, Yangzhou University, Yangzhou, Jiangsu, China, [2]Changshou Characteristic Meat Product Processing and Engineering Research Center of Jiangsu, Jiangsu Changshou Group Co., Ltd., Rugao, Jiangsu, China

Methyl-branched aldehydes, especially 3-methylbutanal, have been reported to be perceived either as a malty or as a nutty/chocolate-like aroma and were considered an important flavor contributor in fermented meat products. Decomposition of leucine (Leu) by branched-chain amino acid transaminase (BACT) is a crucial step in the metabolism of Leu to 3-methylbutanal. This study was conducted to explore the effects of mixed-starter culture (*Lactobacillus fermentum* YZU-06 and *Staphylococcus saprophyticus* CGMCC 3475) and addition of Leu (0, 1, and 3 mM) on the flavor and quality of fermented sausages. The pH, water activity, texture profile analysis, color, counts of lactic acid bacteria (LAB) and staphylococci, peptide, and flavor compounds were detected during fermentation. The results showed that the starter culture group increased hardness, elasticity, the counts of LAB and staphylococci, peptide content, volatile flavor compounds, as well as the sensorial scores of sausage, while decreasing pH, a_w, and L^* and b^* values compared with the non-inoculation group. The mixed starter of adding with 3 mM Leu enhanced the content of 3-methylbutanal and overall flavor of fermented sausages. It is applicable to directionally produce methyl-branched aldehydes and improve the overall quality of fermented sausage by the addition of Leu and using starter of *L. fermentum* YZU-06 and *S. saprophyticus* CGMCC 3475.

KEYWORDS

fermented sausage, leucine, *Lactobacillus fermentum* YZU-06, 3-methylbutanal, flavor

1. Introduction

Fermentation is an important process of meat preservation and the development of meat products, among which fermented sausage is favored by consumers worldwide. The texture and flavor of sausage are developed during fermentation involving many physical, microbiological, and biochemical changes. Flavor is one of the most important attributes of fermented sausage, consisting of esters, aldehydes, alcohols, ketones, acids, terpenes, aromatic, and compounds

(Ammor et al., 2005; Baick and Kim, 2015). Branched-chain aldehydes are notably derived from precursors of branched-chain amino acids [BCAAs, i.e., leucine (Leu), isoleucine (Ile), and valine (Val)] that give the fermented sausage-rich aroma characteristics. Among them, the odor threshold is low for 3-methylbutanal, 0.06 ppm, followed by 2-methylbutanal (0.10 ppm), and 2-methylpropanal (0.10 ppm), which have been perceived as nutty and almond flavor in Hungarian Salami (Söllner and Schieberle, 2009). In addition, the presence of 3-methylbutanal, a degradation production of Leu, confers malt and chocolate aroma in fermented sausages (Smit et al., 2005). Olivares et al. (2009) determined the aroma-active compounds in fermented sausage at different processing stages and found that 3-methylbutanal was an important aroma contributor since the start of the ripening process. The relatively high concentrations of branched-chain aldehydes prominently contribute to the overall flavor of fermented sausage (Herranz et al., 2004).

Branched-chain amino acid transaminase (BCAT), the rate-limiting step of BCAA catabolism, is crucial to the biosynthesis of branched-chain aldehydes during fermentation (Afzal et al., 2012). The first step of synthetic branched-chain aldehydes is the formation of the corresponding α-ketoacids by the transamination reaction of BCAAs, which was catalyzed by BCAT. The α-ketoacid is subsequently decarboxylated and converted into its corresponding aldehydes (Afzal et al., 2012). The mutant of branched-chain aminotransferase gene (*bcaT*) in *Lactobacillus lactis* subsp. *cremoris* NCDO 763 would cause the subsequent decline in the production of intermediate keto acid (Yvon et al., 2000). Moreover, our previous study proved that *Lactobacillus fermentum* YZU-06 with high BCAT activity could be used for promoting BCAA metabolite synthesis in the myofibrillar protein model (Liu et al., 2022). From this perspective, the starter culture with high BCAT activity is able to contribute to the flavor of fermented meat products.

Flavor precursors are another essential factor in improving the aroma and quality of fermented meat products. Our previous study confirmed that the content of branched-chain aldehydes, alcohols, and acids, as well as texture properties, was improved by adding BCAAs in dry-cured fermented sausage (Wang et al., 2021). As an important precursor of flavor substances, protein is involved in the process of proteolysis to produce peptides and free amino acids (FAAs) (Yu et al., 2021). The application of protease can further promote proteolysis for better odor, flavor, texture, and general acceptability in dry fermented sausages (Bruna et al., 2002). In addition, lactic acid bacteria (LAB) have the ability to hydrolyze muscle proteins, contributing to flavor and/or aroma generation in products (Yu et al., 2020). Casaburi et al. (2008) reported that sarcoplasmic proteins were significantly degraded during sausage maturation by adding *Staphylococcus xylosus* and *L. curvatus*. Casaburi et al. (2006) found that *Staphylococcus saprophyticus* screened from fermented sausage was able to preferentially hydrolyze the N-terminal residue substrate, including leucine. The proteolytic ability of *S. saprophyticus* CGMCC 3475 has been confirmed in our previous work (data not shown). In this study, *S. saprophyticus* CGMCC 3475 was used to hydrolyze proteins and intended to release more aroma precursors (peptides and FAAs) for the flavor improvement of fermented sausage. Meanwhile, *L. fermentum* YZU-06 with both proteolytic and BCAT activity presented more BCAA metabolites of 3-methylbutanal and 2-methylbutanal than that of *L. plantarum* CGMCC18217 in myofibrillar protein model in our previous work (Liu et al., 2022). However, it is not clear whether the characteristic 3-methylbutanal can be directionally produced by adding exogenous Leu and *L. fermentum* YZU-06 in meat products. Therefore, the aim of this study was to evaluate the effects of *L. fermentum* YZU-06 in combination with *S. saprophyticus* CGMCC 3475 and the addition of Leu on the flavor and quality of sausage during the fermentation for the flavor development of a fermented product.

2. Materials and methods

2.1. Material preparation

L. fermentum YZU-06 and *S. saprophyticus* CGMCC 3475 were isolated from Jinhua ham and maintained at −80°C in de Man-Rogosa-Sharpe (MRS) medium containing 25% (v/v) glycerol. The strain of 1% (v/v) inoculum was activated twice and grown in 10 ml MRS broth at 37°C for 18 h before use. The bacterial cells were harvested by centrifugation at 6,000 × *g* for 10 min at 4°C. The pellet was washed three times with 0.1 M phosphate-buffered saline (PBS) solution (pH 7.0) and resuspended in PBS solution. Edible-grade Leu was purchased from Shanghong Biotech, Zhengzhou, China. Pork muscle and back fat were obtained from the carcasses aged for 24 h at 4°C in a commercial slaughter plant (Sushi Meat Co., Ltd., Huai'an, China). Glucose, salt, monosodium glutamate, spice powder, ginger powder, Daqu liquor, and distilled water were purchased from the Auchan's Market (Yangzhou, China).

2.2. Preparation of fermented sausages

The fermented sausages were manufactured in accordance with Ge et al. (2019) with some modifications. Lean pork (35 kg) and pork fat (15 kg) were minced and mixed with the following ingredients: glucose (7%), salt (3%), monosodium glutamate (0.2%), spice powder (0.1%), ginger powder (0.15%), Daqu liquor (2%), and distilled water (10%). The mixture was divided into the following nine groups. The inoculation density of the single bacteria starter (*L. fermentum* YZU-06) or mixed-starter culture (*L. fermentum* YZU-06 and *S. saprophyticus* CGMCC 3475 at a 2:1 ratio) was 10^7 CFU/g in the sausages. The first group without strains and Leu was assigned to the CK group. The groups added with 1 and 3 mM Leu were assigned to the CK-1 and CK-3 groups, respectively. The group fermented with *L. fermentum* YZU-06 was assigned to the G group. *L. fermentum* YZU-06 and Leu (1 and 3 mM) were added, designating as the G-1 and G-3 groups. The group inoculated with mixed-starter culture was assigned to the GQ group. The mixed-starter culture with different concentrations of Leu, including 1 and 3 mM, was added and named the GQ-1 group and GQ-3 group, respectively. Mixtures were filled in natural casings of 4 cm in diameter and 10 cm in length. Three independent batches of fermented sausages were prepared, and three sausages were performed in each batch. Sausages were placed in a fermentation room. In the first stage of fermentation, relative humidity (RH) and temperature were set to 95% and 30°C ± 0.5°C for 1 day. The temperature was adjusted to 16°C ± 0.5°C, and RH was successively decreased to 90, 87, and 85%. The duration for each RH was 2 days. The fermentation temperature in the third stage was 12°C ± 0.5°C, and RH was set at 85, 80, and 75%, and each RH condition was fermented for 7 days. The total ripening period was 28 days. Samples were taken from each group on days 1, 7, 14, 21, and 28 of fermentation.

2.3. pH value measurement

A digital pH value meter (Testo 205, Testo AG, Germany) was used to measure the pH value of fermented sausages after the casings were removed. Standard buffers of pH 4.0, 7.0, and 10.0 [Thermo Fisher Scientific (China) Co., Ltd., Shanghai, China] were used to calibrate the pH meter. The sausage samples (10 g) were homogenized with 50 ml distilled water for 10 s twice at 8,000 rpm on ice, with a 15 s interval between bursts. The pH was recorded and averaged from triplicate measurements.

2.4. Determination of water activity (a_w)

The a_w was determined using the a_w meter (Novasina AG, Novasina, Switzerland). Sausages (3 g) were minced and placed in the measuring chamber for 10 min at 24°C. The a_w value was recorded after the measurement was completed.

2.5. Texture profile analysis (TPA)

The TPA of fermented sausages was detected and referred to the method of Ge et al. (2019) with slight modifications. Fermented sausages were cut into cubes in the shape of 1 cm × 1 cm × 1 cm and then measured by the texture analyzer (TA-XT. plus, Stable Micro Systems, Godalming Surrey, UK), which was equipped with a stainless-steel cylinder probe (P/36 R, Stable Micro Systems, Godalming Surrey, UK). The sausage sample was compressed to 50% of its original height with a pretest speed of 2 mm/min, a test speed of 2 mm/min, and a post-test speed of 1 mm/min. Hardness (N), adhesion (mJ), cohesion (ratio), elasticity (mm), and chewiness (mJ) were recorded. The TPA attributes of each sausage sample were averaged from triplicate measurements.

2.6. Determination of color of fermented sausages

The color was determined using a colorimeter (Chroma Meter CR-400, Konica Minolta, Japan) and calibrated with a white ceramic tile. The instrumental color parameters, including L^*, a^*, and b^* values, of each sample were measured in triplicate from different sites.

2.7. Microbiological analysis

The microbiological analysis was performed according to Kaban and Kaya (2009) with slight modifications. A 10-g sausage was cut using a sterile knife and then transferred into a sterile plastic bag. The meat sample was homogenized with 90 ml sterile water using a homogenizer (80 microBiomaster, Seward, Britain) for 120 s with a 10 s interval between bursts. The serial 10-fold dilutions were prepared in sterile physiological water (0.85% NaCl). Appropriate dilution samples (0.1 ml) were poured or spread in duplicate on different growth media. LAB was enumerated on MRS agar (Hope Bio-Technology Co., Ltd., Qingdao, China) after 48 h at 30°C. *Staphylococcus* was determined on mannitol salt agar (Hope Bio-Technology Co., Ltd., Qingdao, China) after the incubation was carried out at 30°C for 48 h.

2.8. Peptide analysis

Peptides were determined according to the methodology described by Nie et al. (2014). The 3 g fermented sausage sample was homogenized with 27 ml of 15% TCA solution (w/v) using a homogenizer (T 18 digital, IKA group, Staufen, Germany) at 3,000 rpm for 60 s, followed by centrifugation at 12,000 × *g* for 10 min at 4°C. The content of soluble peptides in the supernatant was determined using a Stable Lowry Protein Assay Kit (C504051-1000, Shanghai Shenggong Co., Ltd., Shanghai, China) and expressed as μg/g sample.

2.9. Determination of volatile compounds

Volatile components were determined as described by Montanari et al. (2016) with some modifications. For each analysis, a 10 g sausage sample was minced and weighed into a 40 ml headspace vial, and methyl caprylate (0.68 mg/ml) was used as the internal standard solution by adding 20 μl into each headspace vial. A solid-phase microextraction needle covered with 75 μm carboxen/polydimethylsiloxane (CAR/PDMS Stable Flex) (Supelco, Steinheim, Germany) was exposed headspace of the sample for 45 min in the vial with 60°C water bath. After the adsorption of the volatile compounds, the fiber was injected and kept for 5 min in the inlet (230°C, splitless mode) of a gas-chromatograph-mass spectrometry (Trace ISQ, Thermo Scientific, Waltham, USA). The volatile compounds were separated using a 30 m × 0.25 mm × 0.2 μm capillary column (DB-WAX, Agilent, USA). The carrier gas was nitrogen (grade N_2 > 99.999%) at a constant flow rate of 3.0 ml/min. The temperature of the detector was maintained at 280°C. The oven temperature was initially kept at 40°C for 1 min, increased by 5°C/min up to 100°C for 8 min, and then 8°C/min up to 240°C for 5 min. The ionization mode was EI^+, and the electron energy was 70 eV. The scan time was 0.2 s, and the detector voltage was 500 V. The volatile compounds with similarities greater than 80% were shown by comparing the mass spectral data of the samples with those retrieved from digital libraries. The content of the aroma compound was expressed as relative content based on the internal standard.

2.10. Sensory evaluation

The sensory evaluation of fermented sausage was conducted with the method described by Valencia et al. (2006). There were 12 panelists (6 men and 6 women), aged between 20 and 35 years, majoring in Food Science at the School of Food Science and Engineering of Yangzhou University, Yangzhou, China. The panelist training, sensory room, and procedures of sensory evaluation were followed by the Chinese standard GB/T 22210-2008 (Criterion for sensory evaluation of meat and meat products). The sensory panelists received the training according to the nine-point scoring criteria (**Table 1**). The panelists were set in individual compartments, and all forms of communication were not allowed during the evaluation. Smoking, drinking, and eating were not allowed for at least 1 h before sensory analysis. The sample (0.3 cm thick) of each fermented sausage at room temperature was placed on a white ceramic plate labeled with a three-digit random code. Distilled water was provided to the

TABLE 1 The definition of sensory quality attributes for fermented sausage.

Scoring items	Scoring criteria	Score
Color (9)	The cut meat filling is shiny, the muscle is rosy red, and the surface is bright	7–9
	The cut surface is glossy, the fat is yellow, and the muscle is dark	4–6
	The meat filling is dull and the muscle is gray	1–3
Flavor (9)	It has the characteristic aroma of fermented sausage	7–9
	The aroma of fermented sausage is weak	4–6
	Poor aroma and peculiar smell	1–3
Texture (9)	The cut meat filling is tight, the lean meat is closely combined with the fat meat, and the boundary is clear	7–9
	The meat filling on the cut surface is loose, and the combination of lean meat and fat meat is not tight	4–6
	The section is completely loose and the center is softened	1–3
Taste (9)	Salty and sweet, pure sour taste, pleasant aftertaste	7–9
	The taste is not pure and there is less aftertaste	4–6
	Strong sour taste and unpleasant aftertaste	1–3

panelists to rinse their mouths to avoid cross-interference. All the data were collected and used for statistical analysis.

2.11. Statistical analysis

The data obtained from the experiment were analyzed using SAS V8 software (SAS Institute Inc., Cary, NC, USA). Physical, microbial, and quality characteristic data were evaluated using a mixed-model ANOVA using Leu concentration (0, 1, and 3 mM), starter treatments (non-starter, single-strain starter, and mixed-strain starter), and fermentation time that were set as the main effect factors and batches as the random factor. For the sensory evaluation, the random effects included sausage and sensory panel (session number, tasting order, and panelist number). The mean standard error of each treatment was used to describe the least significant difference of means after the data were subjected to the Bonferroni test ($P < 0.05$). A principal component analysis was performed using the statistical software SIMCA 14.1 (MKS Instruments AB Inc., Malmo, Sweden).

3. Results and discussion

3.1. pH and a_w changes

The change in pH values during sausage fermentation is shown in **Figure 1A**. The initial pH value of all treatment samples was approximately 5.94, showing no significant difference among treatments ($P > 0.05$). A declining trend in pH values was observed in the first 7 days and then increased during the later fermentation, which may be due to the buffering effect of the peptides, and amino acids from proteolytic degradation and the organic acids produced by LAB during fermentation (Essid and Hassouna, 2013). The pH value of fermented sausages in the GQ, GQ-1, and GQ-3 groups was lower than that of the groups with and without *L. fermentum* YZU-06 inoculation during the fermentation. By the end of fermentation, the lowest pH values (a mean of pH 5.16) were found in the mixed-starter groups, which was significantly lower than those of other groups ($P < 0.05$). This may be due to the combined effects of the acid produced by *Lactobacillus* and *Staphylococcus* (Sun et al., 2016), which may contribute to the inhibition of the growth of spoilage microorganisms and prolonged shelf life of fermented sausage production (Adams and Nicolaides, 1997).

Figure 1B shows a decreasing trend in a_w of sausage through the entire fermentation process. The high a_w values (0.96) of the samples were detected at the beginning of the processing and then a_w decreased gradually to the lower values ranging from 0.61 and 0.64 at the end of fermentation. The imbalance in humidity between the inside and outside of the sausages causes moisture loss (Olivares et al., 2010). Moreover, the denaturation of proteins as a result of the drop in pH during fermentation and the degradation of protein caused by microorganisms involved in fermentation likely decreased the water-holding capacity (Seleshe and Kang, 2021). The starter and fermentation time was shown to have a cross-impact on a_w value. The a_w of the inoculated group was significantly lower than that of the control groups during incubation ($P < 0.05$), which was consistent with the finding that the lowest a_w value in the dry fermented sausage was fermented by *L. plantarum* GM77 and *S. xylosus* GM92 (Kaban and Kaya, 2009). The results suggested that the inoculation treatments promoted the reduction of a_w, while the addition of Leu had a minimal effect on the a_w decline in sausage during fermentation.

3.2. Texture properties

As shown in **Figure 2A**, the hardness of the sausage increased significantly during 28 days of fermentation ($P < 0.05$). At the end of fermentation, the hardness of the inoculated groups was significantly higher than that of the control groups ($P < 0.05$), except for the CK-1 group. These results are in agreement with those found by Lorenzo and Franco (2012), who reported that the hardness was negatively related to a_w value in dry-cured foal sausages. On the contrary, the adhesion of sausages decreased at 28 days compared with the beginning of fermentation, and the adhesion of the inoculation groups was significantly higher than those of the CK and CK-1 groups ($P < 0.05$, **Figure 2B**). **Figure 2C** shows that no significant differences were observed in cohesion among treatment groups at 28 days ($P > 0.05$), and the addition of starter and Leu, as well as fermentation time, had no significant effects on cohesion ($P > 0.05$). Elasticity and chewiness increased with the fermentation time (**Figures 2D, E**). The starters are responsible for the fermentation of carbohydrates added to the mixture, leading to a decrease in the pH value. The acidification below the isoelectric point of muscle protein affects protein coagulation, which is responsible for the hardness and chewiness of the final product (Essid and Hassouna, 2013). The results of texture are consistent with the findings of Lorenzo and Franco (2012) that the change in TPA is attributed to the water loss in sausage during the maturing period.

3.3. Color changes

The changes in L^*, a^*, and b^* values of fermented sausages are shown in **Figure 3**. All samples exhibited the typical color

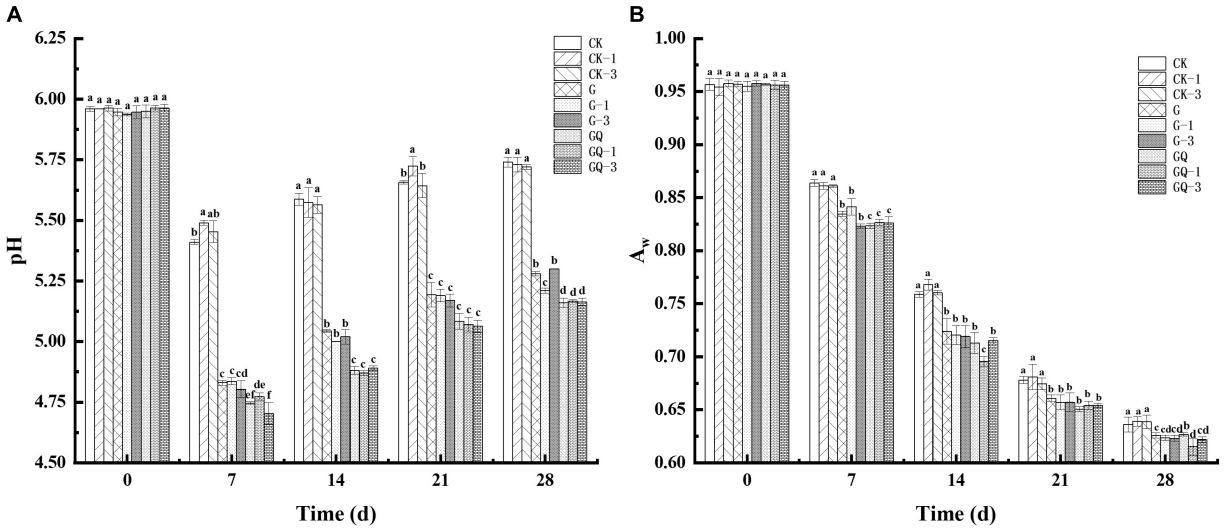

FIGURE 1
The pH values **(A)** and a_w **(B)** of fermented sausages among treatments during the fermentation for 0, 7, 14, 24, and 28 days. Different lowercase letters (a–f) indicate a significant difference between different treatment groups at the same fermentation time ($P < 0.05$). The group without starter culture and leucine was assigned to the CK group. The groups added with 1 and 3 mM of leucine without starter culture were assigned to the CK-1 and CK-3 groups, respectively. The group with *Lactobacillus fermentum* YZU-06 was assigned to the G group. The groups with *Lactobacillus fermentum* YZU-06 and different concentrations of leucine (1 and 3 mM) were named G-1 and G-3 groups, respectively. The fermented sausage with the mixed-starter cultures of *Lactobacillus fermentum* YZU-06 and *Staphylococcus saprophyticus* CGMCC 3475 was assigned to the GQ group. The groups with the mixed-starter cultures and different concentrations of leucine (1 and 3 mM) were named GQ-1 and GQ-3 groups, respectively.

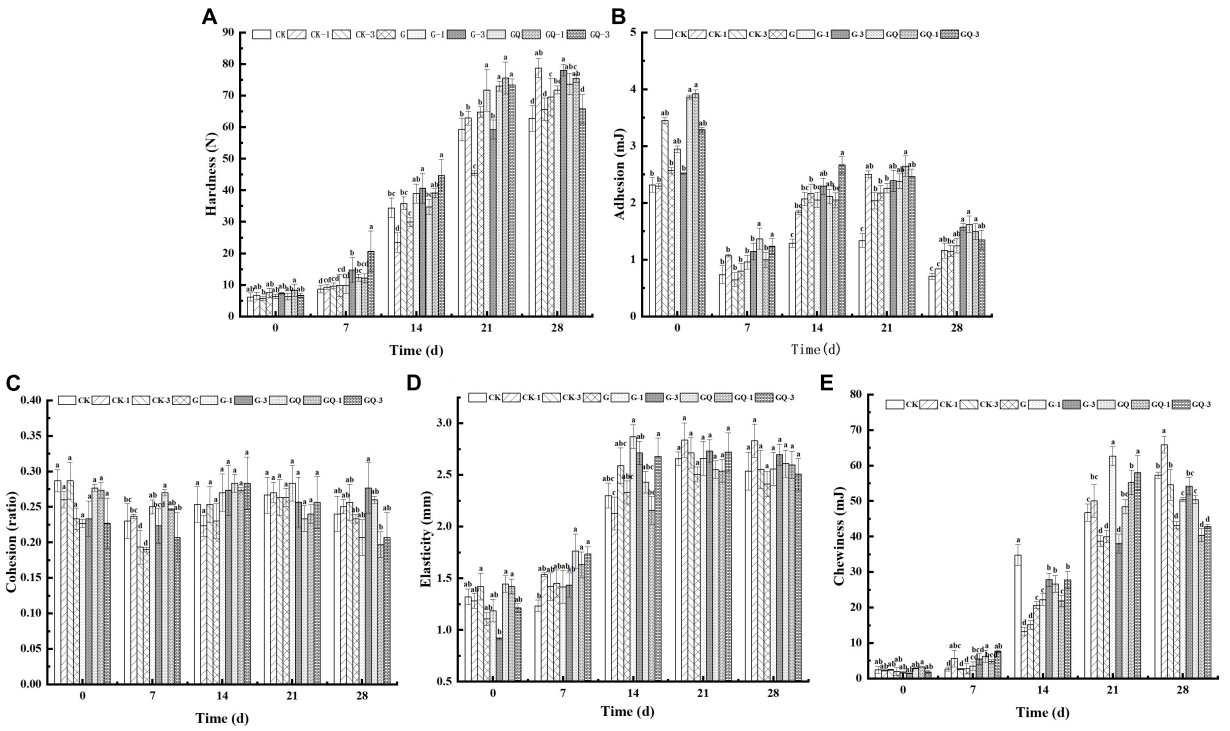

FIGURE 2
Changes in the texture of sausages, including hardness **(A)**, adhesion **(B)**, cohesion **(C)**, elasticity **(D)**, and chewiness **(E)**, among treatments during the fermentation for 0, 7, 14, 24, and 28 days. Different lowercase letters (a–d) indicate a significant difference between different treatment groups at the same fermentation time ($P < 0.05$). The group without starter culture and leucine was assigned to the CK group. The groups added with 1 and 3 mM of leucine without starter culture were assigned to the CK-1 and CK-3 groups, respectively. The group with *Lactobacillus fermentum* YZU-06 was assigned to the G group. The groups with *Lactobacillus fermentum* YZU-06 and different concentrations of leucine (1 and 3 mM) were named G-1 and G-3 groups, respectively. The fermented sausage with the mixed-starter cultures of *Lactobacillus fermentum* YZU-06 and *Staphylococcus saprophyticus* CGMCC 3475 was assigned to the GQ group. The groups with the mixed-starter cultures and different concentrations of leucine (1 and 3 mM) were named GQ-1 and GQ-3 groups, respectively.

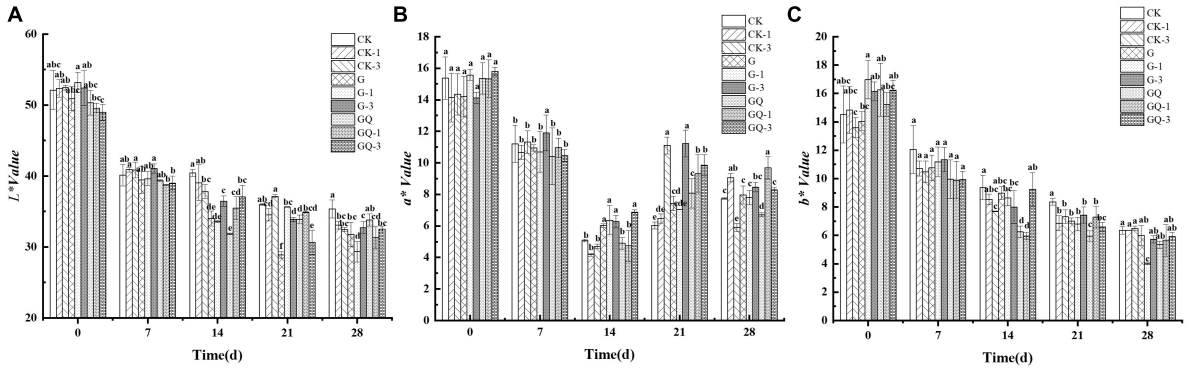

FIGURE 3
Changes in the color attributes of L^* **(A)**, a^* **(B)**, and b^* **(C)** in sausages among treatments during the fermentation for 0, 7, 14, 24, and 28 days. Different lowercase letters (a–f) indicate a significant difference between different treatment groups at the same fermentation time ($P < 0.05$). The group without starter culture and leucine was assigned to the CK group. The groups added with 1 and 3 mM of leucine without starter culture were assigned to the CK-1 and CK-3 groups, respectively. The group with *Lactobacillus fermentum* YZU-06 was assigned to the G group. The groups with *Lactobacillus fermentum* YZU-06 and different concentrations of leucine (1 and 3 mM) were named G-1 and G-3 groups, respectively. The fermented sausage with the mixed-starter cultures of *Lactobacillus fermentum* YZU-06 and *Staphylococcus saprophyticus* CGMCC 3475 was assigned to the GQ group. The groups with the mixed-starter cultures and different concentrations of leucine (1 and 3 mM) were named GQ-1 and GQ-3 groups, respectively.

characteristics of fermented sausages. The L^* value decreased from 51.11 to 32.01 in sausage during 28 days of fermentation ($P < 0.05$). At the end of fermentation, the L^* values of the G-1 and GQ-1 groups were 29.33 and 31.32, respectively, which were significantly lower than that of the other groups ($P < 0.05$). The average a^* value of the incubated samples decreased from 15.08 to 5.86 during 14 days of ripening and then increased to 8.15 at the end of the process. The b^* value in all treatment groups decreased from 15.11 to 5.76 during the ripening. The b^* value of the inoculated G-1 group was significantly lower than those of the control groups during 21–28 days of fermentation ($P < 0.05$). Color plays an important role in consumers' sensory perception of fermented sausage. Casaburi et al. (2007) found that the L^* value of sausages decreased throughout the entire fermentation period. Likewise, the decrease in L^* value of Suck sausage within 15 days of maturation led to a decrease in gloss, which was consistent with the report by Kayaardı and Gök (2004). The decrease in a^* value could be the denaturation of nitroso-erythropoietin due to the production of lactic acid. This result was in agreement with the findings of Ge et al. (2019), who found that the change in a^* value in the *L. plantarum* NJAU-01 group was in the same trend as this study. The Spanish dry-cured sausages showed a decreasing trend in b^* value during the maturation stages (Pérez-Alvarez et al., 1999). The decrease in b^* value was probably due to the consumption of oxygen by microorganisms, resulting in a decrease in oxygenated myoglobin, which was an important component of the yellow coloration.

3.4. Changes in the count of LAB and staphylococci

The change in LAB counts in the sausages during fermentation is shown in **Figure 4A**. The addition of Leu had no significant effects on the initial LAB counts ($P > 0.05$). At the initial fermentation stage, the counts of MRS solid media in the sausage groups inoculated with LAB were about 7.17–7.27 lg CFU/g, and the counts in the control groups were 4.13–4.22 lg CFU/g. The inoculated groups with starter cultures reached the highest level of LAB (8–9 lg CFU/g) at 7 or 14 days of fermentation. After 7 days of fermentation, the counts of LAB in the GQ, GQ-1, and GQ-3 groups were lower than that of the G, G-1, and G-3 groups. However, at the end of the fermentation, the counts of LAB in the GQ, GQ-1, and GQ-3 groups were significantly higher than that in the G, G-1, and G-3 groups and the control groups ($P < 0.05$). This indicated that *L. fermentum* YZU-06 and *S. saprophyticus* CGMCC 3475 were well adapted to the environment and propagated rapidly during sausage fermentation. The addition of a starter inhibited the growth of undesirable bacteria, and the mixed starter promoted better growth of LAB (Essid and Hassouna, 2013). The low pH and a_w values may contribute to the decrease in the count of LAB in the fermented sausage at the end of ripening (Samelis et al., 1998).

Figure 4B shows the changes in the counts of staphylococci in the sausages during fermentation. The initial counts of staphylococci were 5.21–5.23 lg CFU/g in the sausages of GQ, GQ-1, and GQ-3 groups and 4.61–5.06 lg CFU/g in the sausages of LAB inoculated and control groups, respectively. The counts of staphylococci increased to 6.64–7.13 lg CFU/g, 5.62–6.36 lg CFU/g, and 6.53–6.84 lg CFU/g in inoculated staphylococci, inoculated LAB, and control groups at 7 days of fermentation, respectively. After the completion of the fermentation, the counts of staphylococci decreased to 3.80–4.45 lg CFU/g. The reduction in staphylococci during the last 2 weeks of maturation in sausages indicated that staphylococci were less competitive and inhibited by the intensive growth of LAB and a lower pH value (Casaburi et al., 2008).

3.5. Peptide content

The content of soluble peptides derived from the fermented sausages at the end of fermentation is shown in **Figure 5**. The peptide contents of GQ, GQ-1, and GQ-3 groups with the mixed starter and supplemented with Leu were significantly higher than the control groups CK, CK-1, and CK-3 ($P < 0.05$). The increase in total peptides indicated protease activity, mainly deriving from the action of microorganisms and endogenous muscle enzymes (Visessanguan et al., 2004). The higher total peptide content of the mixed inoculated

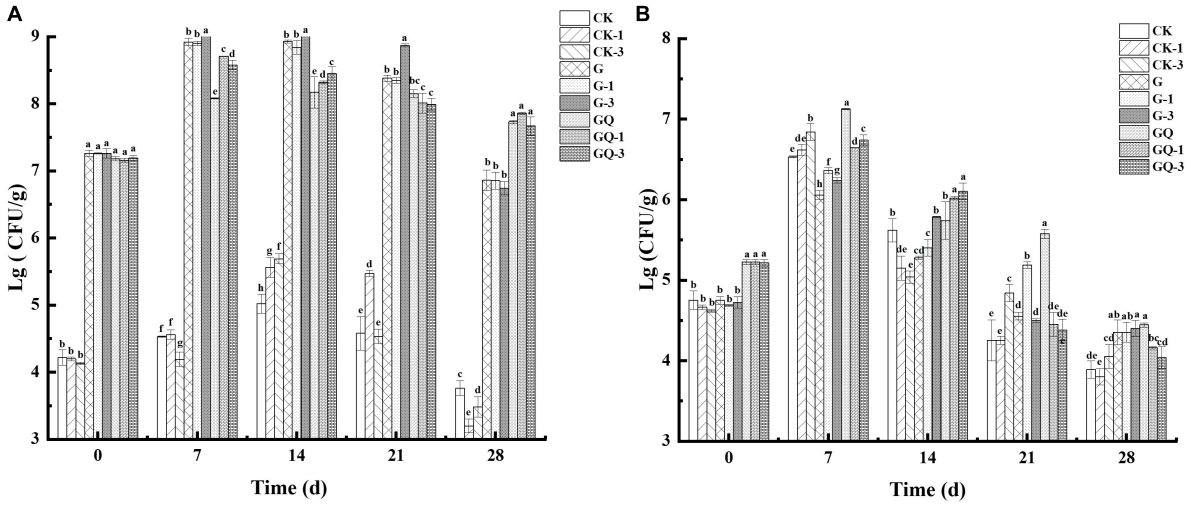

FIGURE 4
Changes in viable counts of LAB **(A)** and *staphylococcus* **(B)** in sausages among treatments during the fermentation for 0, 7, 14, 24, and 28 days. Different lowercase letters (a–h) indicate a significant difference between different treatment groups at the same fermentation time ($P < 0.05$). The group without starter culture and leucine was assigned to the CK group. The groups added with 1 and 3 mM of leucine without starter culture were assigned to the CK-1 and CK-3 groups, respectively. The group with *Lactobacillus fermentum* YZU-06 was assigned to the G group. The groups with *Lactobacillus fermentum* YZU-06 and different concentrations of leucine (1 and 3 mM) were named G-1 and G-3 groups, respectively. The fermented sausage with the mixed-starter cultures of *Lactobacillus fermentum* YZU-06 and *Staphylococcus saprophyticus* CGMCC 3475 was assigned to the GQ group. The groups with the mixed-starter cultures and different concentrations of leucine (1 and 3 mM) were named GQ-1 and GQ-3 groups, respectively.

group indicated a higher degree of protein degradation, which also showed that the higher content of the substance can be used as the precursor of flavor compounds. These peptides can be further decomposed by enzymes to produce some low-molecular-weight compounds, including amino acids, aldehydes, organic acids, and ammonia, which are potential flavor volatile (Díaz et al., 1993). For example, 3-methylbutanal, as a metabolite of BCAAs, can interact with different sulfur compounds derived from methionine and cysteine to form bacon flavor and improve sausage flavor (Riebroy et al., 2008). In addition, the rate of protein hydrolysis usually depends on many factors, including the nature of the meat microbiota and processing conditions. As reported by Visessanguan et al. (2004), the low pH value stimulated the hydrolysis of myofibrillar protein to form FAAs.

3.6. Volatile compounds

The identification of volatile components in fermented sausages at 28 days is shown in **Figure 6**. As shown in **Figures 6A**, total of 62 volatile compounds were determined and grouped into seven classes as shown in **Supplementary Table 1**, including esters (22), alcohols (11), aldehydes (8), acids (8), alkanes (4), olefins (5), ketones (2), and other compounds (2). Among them, 32, 47, and 43 compounds were detected in CK, CK-1, and CK-3 groups, respectively, while more than 49 compounds were detected in the inoculation group. The relative content of flavor substances in each treatment group is shown in **Figure 6B**. The main volatile flavor substances in fermented sausage were esters, aldehydes, alcohols, acids, and other compounds. These volatile compounds were mainly derived from fat oxidation, amino acid catabolism, carbohydrate fermentation, microbial activity, and spices (Kaban and Kaya, 2009). The principal component analysis (PCA) of flavor compounds among treatment groups at 28 days of sausage fermentation is shown in **Figure 6C**. It was found that the control groups, including CK, CK-1, and CK-3, were localized in the third quadrant and clearly scattered from the inoculated groups. Moreover, the inoculated groups of *L. fermentum*

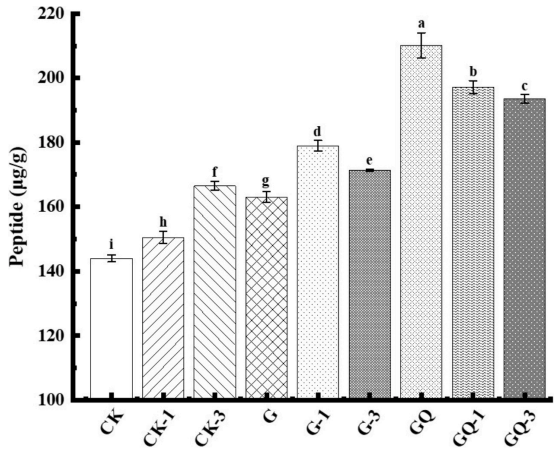

FIGURE 5
Peptide content of sausage among treatments at the end of fermentation (28 days). Different lowercase letters (a–i) indicate a significant difference between different treatment groups ($P < 0.05$). The group without starter culture and leucine was assigned to the CK group. The groups added with 1 and 3 mM of leucine without starter culture were assigned to the CK-1 and CK-3 groups, respectively. The group with *Lactobacillus fermentum* YZU-06 was assigned as the G group. The groups with *Lactobacillus fermentum* YZU-06 and different concentrations of leucine (1 and 3 mM) were named G-1 and G-3 groups, respectively. The fermented sausage with the mixed-starter cultures of *Lactobacillus fermentum* YZU-06 and *Staphylococcus saprophyticus* CGMCC 3475 was assigned to the GQ group. The groups with the mixed-starter cultures and different concentrations of leucine (1 and 3 mM) were named GQ-1 and GQ-3 groups, respectively.

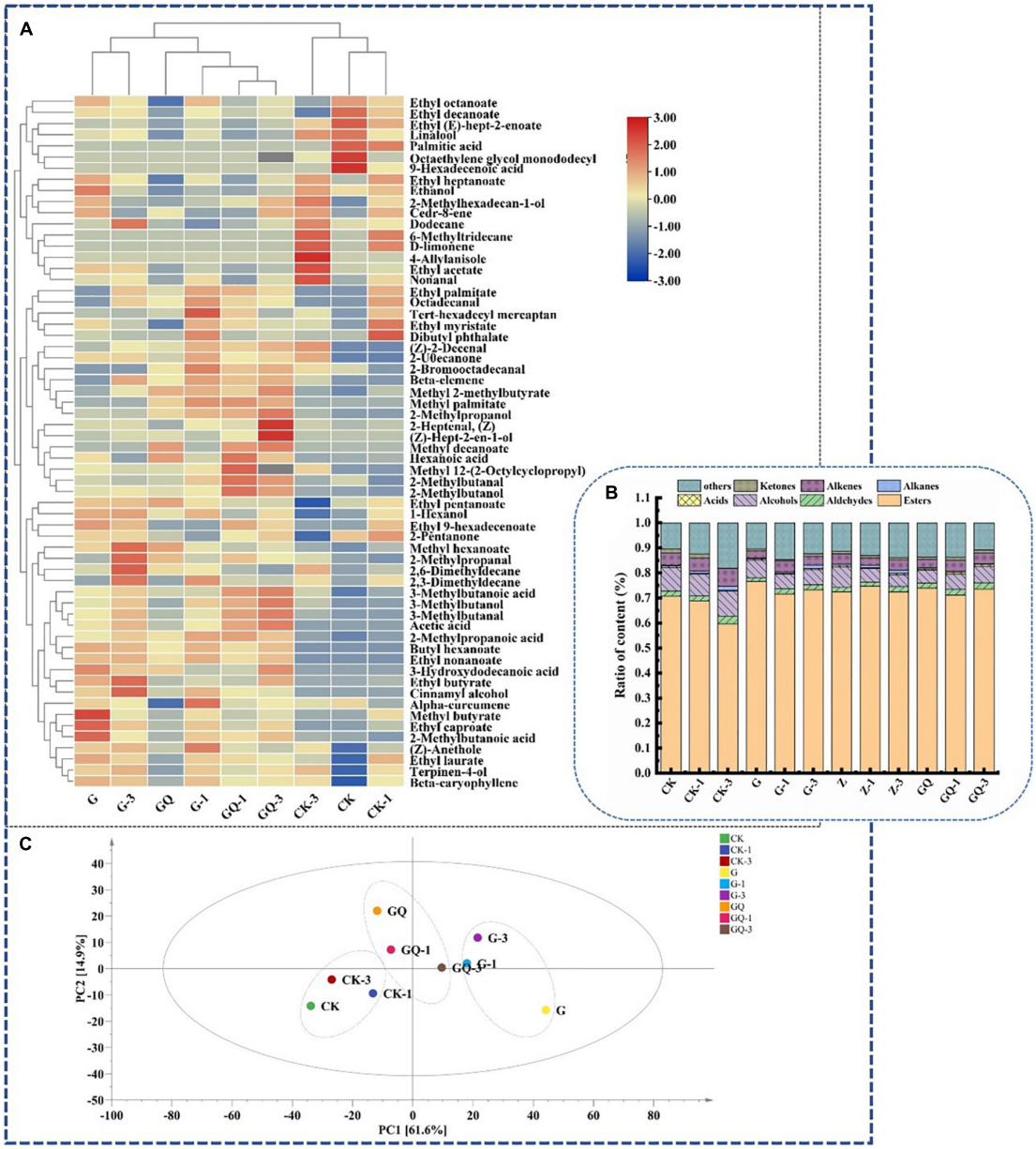

FIGURE 6
The flavor profiles of fermented sausages, including heatmap **(A)**, composition of sausage flavors in the different groups **(B)**, and principal component analysis of flavor substances among treatments **(C)** at the end of fermentation (28 days). The group without starter culture and leucine was assigned to the CK group. The groups added with 1 and 3 mM of leucine without starter culture were assigned to the CK-1 and CK-3 groups, respectively. The group with *Lactobacillus fermentum* YZU-06 was assigned to the G group. The groups with *Lactobacillus fermentum* YZU-06 and different concentrations of leucine (1 and 3 mM) were named G-1 and G-3 groups, respectively. The fermented sausage with the mixed-starter cultures of *Lactobacillus fermentum* YZU-06 and *Staphylococcus saprophyticus* CGMCC 3475 was assigned to the GQ group. The groups with the mixed-starter cultures and different concentrations of leucine (1 and 3 mM) were named GQ-1 and GQ-3 groups, respectively.

YZU-06 (G groups) and mixture starter of *L. fermentum* YZU-06 and *S. saprophyticus* CGMCC 3475 (GQ groups) also showed different distributions of the PCA mapping points. The amounts of volatile compounds in samples inoculated with mixture starters (GQ group 2,863.85 μg/kg, GQ-1 group 3,033.21 μg/kg, GQ-3 group 3,585.83 μg/kg) were higher than those in the control groups (average value of 2,807.53 μg/kg). Thus, it is indicated that the addition of Leu and mixed starter plays an important role in enriching the types and contents of flavor substances in fermented sausage.

The 3-methylbutanal/butanal/butyrate were derived from catabolism of Leu (Beck et al., 2004; Yu et al., 2020), and these compounds were the focus of attention in this study. The addition of 3 mM Leu and mixed-starter culture resulted in higher branched-chain aldehyde/alcohol/acid in the GQ group than that of the other groups ($P < 0.05$). Among them, the content of 3-methylbutanal (17.53 μg/kg) in the GQ-3 group was five times higher than that in the group CK (3.47 μg/kg) and 1.3 times higher than that of the G-3 group. The amount of 3-methylbutanol (5.48 μg/kg) and 2-methylpropanol (1.92 μg/kg) produced by the GQ-3 group was significantly higher than the other groups ($P < 0.05$). Microbial fermentation promoted the conversion of muscle proteins to FAAs in fermented sausages. BCAAs can be converted into α-keto

TABLE 2 Scores of sensory evaluation of sausages among different treatments.

Time (d)	Group									SE	*P*-value		
	CK	CK-1	CK-3	G	G-1	G-3	GQ	GQ-1	GQ-3		Strain	BCAAs	Strain*BCAAs
Color	6.23^{c}	6.53^{c}	6.68^{bc}	7.16^{ab}	7.28^{ab}	7.33^{a}	7.50^{a}	7.46^{a}	7.76^{a}	0.04	<0.05	0.22	0.89
Flavor	7.10^{b}	7.15^{b}	7.18^{b}	7.60^{ab}	7.83^{a}	7.95^{a}	8.23^{a}	8.00^{a}	8.03^{a}	0.02	<0.05	0.88	0.66
Texture	7.43^{a}	7.35^{ab}	7.20^{ab}	6.79^{c}	7.05^{b}	7.43^{a}	6.90^{c}	7.05^{b}	7.54^{a}	0.14	0.32	0.10	0.18
Taste	7.25^{b}	7.13^{c}	7.10^{c}	7.15^{c}	7.68^{ab}	7.70^{ab}	7.75^{ab}	7.85^{a}	7.90^{a}	0.07	<0.05	0.54	0.54

*Indicates the interaction between strains and branched-chain amino acids. Different superscript letters (a–c) indicate a significant difference among treatment groups ($P < 0.05$).

acids by microbial transaminases, which was the first rate-limiting step for the conversion of BCAAs to branched aldehydes. As an important intermediate, α-keto acids can be further transformed into various flavor compounds through non-oxidative decarboxylation or oxidative dehydrogenation (Smit et al., 2004). Aldehydes can be converted into the corresponding alcohols and carboxylic acids by alcohol dehydrogenase and aldehyde dehydrogenase, respectively (Chen et al., 2015). 2-Methylpropanal produced by valine can be oxidized to 2-methylpropionic acid by aldehyde dehydrogenase or reduced to 2-methylpropanol by alcohol dehydrogenase, respectively. Moreover, 2- and 3-methylbutanal produced by Leu and Ile can be oxidized to 2- and 3-methylbutanal by aldehyde dehydrogenase or reduced to 2- and 3-methylbutanol by alcohol dehydrogenase. These compounds produce malt, fruity, and sweaty flavors, which were identified as the key volatile compounds in cured ham and cured loin (Bosse et al., 2021). In addition, the most abundant aldehydes in fermented sausage were non-anal formed by the oxidation of N-9 polyunsaturated fatty acids, which delivered the smell of carnation, citrus, and laurel (Olivares et al., 2011).

Esters are low-odor threshold compounds and give fermented sausage fruit aroma (Sun et al., 2010). Ester was the most abundant in the G group. Ethyl butyrate and methyl 2-methylbutyrate were mostly detected in the inoculated groups and related to the post-esterification of methyl branched-chain by transmination of microbial metabolism of BCAAs (Schmidt and Berger, 1998). Ethyl butyrate in the G-3 group (2,969.18 μg/kg) and methyl 2-methylbutyrate in GQ-3 group (5.23 μg/kg) were significantly higher than that of the other groups ($P < 0.05$). In addition, many esters identified in the present study were ethyl esters, which produced fruity odors (Chen et al., 2017). The high content of ethyl compounds may be due to the decomposition of carbohydrates by *L. fermentum* YZU-06. Sun et al. (2010) showed that ethanol played an important role in the flavor of Cantonese sausage. In the present study, ethanol was identified to have the highest content in alcohols, among which the GQ group had the lowest ethanol content.

Acids have great implications on the flavor development of sausage, including acetic acid and hexanoic acid, which are derived from the degradation of carbohydrates (Liu et al., 2003). The GQ-3 group exhibited significantly higher 3-methylbutanoic acid (9.12 μg/kg) than the other treatment groups ($P < 0.05$). Ketones could be produced mainly through lipid oxidation, microbial fermentation, and carbohydrate catabolism. Two ketones were detected, of which 2-pentanone was produced by microbial β-oxidation in the presence of *Staphylococcus* (Leroy et al., 2006). Hydrocarbons, including four alkanes and five alkenes, were also detected in the volatile flavor substances of sausages, which may be the product of lipid auto-oxidation. However, the presence of alkanes might not be an important contributor to the flavor due to their high threshold value (Latorre-Moratalla et al., 2011). The alkenes, including α-curmene, D-limonene, β-caryophyllene, cedarene, and β-elemene, may be obtained from spices such as onion and ginger powder and spice powder (Montanari et al., 2016).

3.7. Sensory analysis

A sensory analysis is essential for meat products to meet consumer demand and recognition (Ruiz-Capillas et al., 2021). As shown in **Table 2**, no significant difference was found in texture scores among the inoculated groups of *L. fermentum* YZU-06 only and mixed-starter groups ($P > 0.05$), while the color scores in the mixed-starter groups were significantly higher than that of the control groups ($P < 0.05$). The inoculated groups, except the G group, showed significantly higher overall flavor scores than those in the control groups ($P < 0.05$). Two inoculated groups (GQ-1 and GQ-3) presented greater taste scores than those of the control groups ($P < 0.05$). This was attributed to the fact that the inoculation of the starter could promote the hydrolysis of protein and the subsequent release of peptides and FAA for the development of flavor and taste during fermentation (Hu et al., 2022). Taken together, the addition of starter and Leu significantly improved the sensory quality of the sausage.

7. Conclusion

The primary outcome of this study was to develop the fermented sausage by directional production of 3-methylbutanal *via* Leu supplement and the selected culture, *L. fermentum* YZU-06 and *S. saprophyticus* CGMCC 3745. The combination of Leu and strain applied to fermented sausage provides a novel strategy to not only improve the diversity of flavor compounds, but also the overall quality of the fermented sausage. Therefore, *L. fermentum* YZU-06 has great potential as a starter for the production of fermented meat products. The mechanism of flavor development is the interaction between protein, lipids, microorganisms, spices, external environment, and processing parameters and needs to be further studied.

Data availability statement

The original contributions presented in this study are included in the article/**Supplementary material**,

further inquiries can be directed to the corresponding author.

Author contributions

HY and RL: conceptualization and resources. YM: methodology, investigation, and writing the original draft preparation. MW: software. RL, HY, and QG: validation. CL: formal analysis, writing, reviewing, and editing. RL: data curation. JX: supervision. HY: funding acquisition. All authors have read and agreed to the published version of the manuscript.

Funding

This research was funded by the National Natural Science Foundation of China (nos. 31901610 and 32172276), the Qing Lan Project of Yangzhou University, the High-Level Talent Support Program of Yangzhou University, and the Key R&D Project of the Science and Technology Department of Jiangsu Province (BE2022333), as well as the cooperation of Yangzhou and Yangzhou University in the Construction of Science and Technology Innovation Platform Project (no. YZ2020267).

Conflict of interest

JX was employed by the Jiangsu Changshou Group Co., Ltd.

The remaining authors declare that the research was conducted in the absence of any commercial or financial relationships that could be construed as a potential conflict of interest.

Publisher's note

All claims expressed in this article are solely those of the authors and do not necessarily represent those of their affiliated organizations, or those of the publisher, the editors and the reviewers. Any product that may be evaluated in this article, or claim that may be made by its manufacturer, is not guaranteed or endorsed by the publisher.

Supplementary material

The Supplementary Material for this article can be found online at: https://www.frontiersin.org/articles/10.3389/fmicb.2022.1118907/full#supplementary-material

References

Adams, M. R., and Nicolaides, L. (1997). Review of the sensitivity of different foodborne pathogens to fermentation. *Food Control* 8, 227–239. doi: 10.1016/S0956-7135(97)00016-9

Afzal, M. I., Delaunay, S., Paris, C., Borges, F., Revol-Junlles, A. M., and Cailliez-Grimal, C. (2012). Identification of metabolic pathways involved in the biosynthesis of flavor compound 3-methylbutanal from leucine catabolism by *Carnobacterium maltaromaticum* LMA 28. *Int. J. Food Microbiol.* 157, 332–339. doi: 10.1016/j.ijfoodmicro.2012.05.010

Ammor, S., Dufour, E., Zagorec, M., Chailou, S., and Chevallier, I. (2005). Characterization and selection of *Lactobacillus sakei* strains isolated from traditional dry sausage for their potential use as starter cultures. *Food Microbiol.* 22, 529–538. doi: 10.1016/j.fm.2004.11.016

Baick, S. C., and Kim, C. H. (2015). Assessment of characteristics and functional properties of *Lactobacillus* Species isolated from Kimchi for dairy use. *Korean J. Food Sci. Anim. Resour.* 35, 339–349. doi: 10.5851/kosfa.2015.35.3.339

Beck, H. C., Hansen, A. M., and Lauritsen, F. R. (2004). Catabolism of leucine to branched-chain fatty acids in *Staphylococcus xylosus*. *J. Appl. Microbiol.* 96, 1185–1193. doi: 10.1111/j.1365-2672.2004.02253.x

Bosse, R., Wirth, M., Weiss, J., and Gibis, M. (2021). Effect of storage temperature on volatile marker compounds in cured loins fermented with *Staphylococcus carnosus* by brine injection. *Eur. Food Res. Technol.* 247, 233–244. doi: 10.1007/s00217-020-03621-w

Bruna, J. M., Fernandez, M., Ordonez, J. A., and Hoz, L. D. L. (2002). Enhancement of the flavour development of dry fermented sausages by using a protease (Pronase E) and a cell-free extract of *Penicillium camemberti*. *J. Sci. Food Agric.* 82, 526–533. doi: 10.1002/jsfa.1073

Casaburi, A., Aristoy, M. C., Cavella, S., Monaco, R. D., Ercolini, D., Toldra, F., et al. (2007). Biochemical and sensory characteristics of traditional fermented sausages of Vallo di Diano (Southern Italy) as affected by the use of starter cultures. *Meat Sci.* 76, 295–307. doi: 10.1016/j.meatsci.2006.11.011

Casaburi, A., Monaco, R. D., Cavella, S., Toldra, F., Ercolini, D., and Villanai, F. (2008). Proteolytic and lipolytic starter cultures and their effect on traditional fermented sausages ripening and sensory traits. *Food Microbiol.* 25, 335–347. doi: 10.1016/j.fm.2007.10.006

Casaburi, A., Villani, F., Toldrá, F., and Sanz, Y. (2006). Protease and esterase activity of staphylococci. *Int. J. Food Microbiol.* 112, 223–229. doi: 10.1016/j.ijfoodmicro.2006.04.008

Chen, Q., Kong, B., Han, Q., Xia, X. F., and Xu, L. (2017). The role of bacterial fermentation in lipolysis and lipid oxidation in Harbin dry sausages and its flavour development. *LWT Food Sci. Technol.* 77, 389–396. doi: 10.1016/j.lwt.2016.11.075

Chen, Q., Liu, Q., Sun, Q., Kong, B.H., and Xiong, Y.L. (2015). Flavour formation from hydrolysis of pork sarcoplasmic protein extract by a unique LAB culture isolated from Harbin dry sausage. *Meat Sci.* 100, 110–117. doi: 10.1016/j.meatsci.2014.10.001

Díaz, O., Fernandez, M., Fernando, G. D. G. D., Hoz, L. D. L., and Ordonez, J. A. (1993). Effect of the addition of pronase E on the proteolysis in dry fermented sausages. *Meat Sci.* 34, 205–216. doi: 10.1016/0309-1740(93)90028-G

Essid, I., and Hassouna, M. (2013). Effect of inoculation of selected *Staphylococcus xylosus* and *Lactobacillus plantarum* strains on biochemical, microbiological and textural characteristics of a Tunisian dry fermented sausage. *Food Control* 32, 707–714. doi: 10.1016/j.foodcont.2013.02.003

Ge, Q. F., Pei, H. J., Liu, R., Chen, L., Gao, X. Q., Gu, Y. B., et al. (2019). Effects of *Lactobacillus plantarum* NJAU-01 from Jinhua ham on the quality of dry-cured fermented sausage. *LWT Food Sci. Technol.* 101, 513–518. doi: 10.1016/j.lwt.2018.11.081

Herranz, B., Fernández, M., Hierro, E., Bruna, J. M., Ordonez, J. A., and Hoz, L. D. L. (2004). Use of *Lactococcus lactis* subsp. Cremoris NCDO 763 and α-ketoglutarate to improve the sensory quality of dry fermented sausages. *Meat Sci.* 66, 151–163. doi: 10.1016/S0309-1740(03)00079-2

Hu, Y. Y., Zhang, L., Wen, R. X., Chen, Q., and Kong, B. H. (2022). Role of lactic acid bacteria in flavor development in traditional Chinese fermented foods: A review. *Crit. Rev. Food Sci. Nutr.* 62, 2741–2755. doi: 10.1080/10408398.2020.1858269

Kaban, G., and Kaya, M. (2009). Effects of *Lactobacillus plantarum* and *Staphylococcus xylosus* on the quality characteristics of dry fermented sausage "sucuk". *J. Food Sci.* 74, S58–S63. doi: 10.1111/j.1750-3841.2008.01014.x

Kayaardı, S., and Gök, V. (2004). Effect of replacing beef fat with olive oil on quality characteristics of Turkish soudjouk (sucuk). *Meat Sci.* 66, 249–257. doi: 10.1016/S0309-1740(03)00098-6

Latorre-Moratalla, M. L., Bosch-Fusté, J., Bover-Cid, S., Aymerich, T., and Vidal-Carou, M. C. (2011). Contribution of enterococci to the volatile profile of slightly-fermented sausages. *LWT Food Sci. Technol.* 44, 145–152. doi: 10.1016/j.lwt.2010.06.033

Leroy, F., Verluyten, J., and Vuyst, L. D. (2006). Functional meat starter cultures for improved sausage fermentation. *Int. J. Food Microbiol.* 106, 270–285. doi: 10.1016/j.ijfoodmicro.2005.06.027

Liu, R., Lu, C. Y., Wang, Y. Y., Shen, Y. H., Ge, Q. F., Wu, M. G., et al. (2022). Characterization of a lactic acid bacteria using branched-chain amino acid transaminase and protease from Jinhua Ham and application in myofibrillar protein model. *Meat Sci.* 191:108852. doi: 10.1016/j.meatsci.2022.108852

Liu, S. Q., Holland, R., and Crow, V. L. (2003). The potential of dairy lactic acid bacteria to metabolise amino acids via non-transaminating reactions and endogenous transamination. *Int. J. Food Microbiol.* 86, 257–269. doi: 10.1016/S0168-1605(03)00040-0

Lorenzo, J. M., and Franco, D. (2012). Fat effect on physico-chemical, microbial and textural changes through the manufactured of dry-cured foal sausage lipolysis, proteolysis and sensory properties. *Meat Sci.* 92, 704–714. doi: 10.1016/j.meatsci.2012.06.026

Montanari, C., Bargossi, E., Gardini, A., Lanciotti, R., Magnani, R., Gardini, F., et al. (2016). Correlation between volatile profiles of Italian fermented sausages and their size and starter culture. *Food Chem.* 192, 736–744. doi: 10.1016/j.foodchem.2015.07.062

Nie, X. H., Lin, S. L., and Zhang, Q. L. (2014). Proteolytic characterisation in grass carp sausage inoculated with *Lactobacillus plantarum* and *Pediococcus pentosaceus*. *Food Chem.* 145, 840–844. doi: 10.1016/j.foodchem.2013.08.096

Olivares, A., Navarro, J. L., and Flores, M. (2009). Establishment of the contribution of volatile compounds to the aroma of fermented sausages at different stages of processing and storage. *Food Chem.* 115, 1464–1472. doi: 10.1016/j.foodchem.2009.01.083

Olivares, A., Navarro, J. L., and Flores, M. (2011). Effect of fat content on aroma generation during processing of dry fermented sausages. *Meat Sci.* 87, 264–273. doi: 10.1016/j.meatsci.2010.10.021

Olivares, A., Navarro, J. L., Salvador, A., and Flores, M. (2010). Sensory acceptability of slow fermented sausages based on fat content and ripening time. *Meat Sci.* 86, 251–257. doi: 10.1016/j.meatsci.2010.04.005

Pérez-Alvarez, J. A., Sayas-Barberá, M. E., Fernández-López, J., and Aranda-Catala, V. (1999). Physicochemical characteristics of Spanish-type dry-cured sausage. *Food Res. Int.* 32, 599–607. doi: 10.1016/S0963-9969(99)00104-0

Riebroy, S., Benjakul, S., and Visessanguan, W. (2008). Properties and acceptability of Som-fug, a Thai fermented fish mince, inoculated with lactic acid bacteria starters. *LWT Food Sci. Technol.* 41, 569–580. doi: 10.1016/j.lwt.2007.04.014

Rouhi, M., Sohrabvandi, S., and Mortazavian, A. M. (2013). Probiotic fermented sausage: Viability of probiotic microorganisms and sensory characteristics. *Crit. Rev. Food Sci. Nutr.* 53, 331–348. doi: 10.1080/10408398.2010.531407

Ruiz-Capillas, C., Herrero, A. M., Pintado, T., and Delgado-Pando, G. (2021). Sensory analysis and consumer research in new meat products development. *Foods* 10:429. doi: 10.3390/foods10020429

Samelis, J., Metaxopoulos, J., Vlassi, M., and Pappab, A. (1998). Stability and safety of traditional Greek salami-a microbiological ecology study. *Int. J. Food Microbiol.* 44, 69–82. doi: 10.1016/S0168-1605(98)00124-X

Schmidt, S., and Berger, R. G. (1998). Aroma compounds in fermented sausages of different origins. *LWT Food Sci. Technol.* 31, 559–567. doi: 10.1006/fstl.1998.0420

Seleshe, S., and Kang, S. N. (2021). Effect of different *Pediococcus pentosaceus* and *Lactobacillus plantarum* strains on quality characteristics of dry fermented sausage after completion of ripening period. *Food Sci. Anim. Resour.* 41:636. doi: 10.5851/kosfa.2021.e21

Smit, B. A., Engels, W. J. M., Wouters, J. T. M., and Smit, G. (2004). Diversity of L-leucine catabolism in various microorganisms involved in dairy fermentations, and identification of the rate-controlling step in the formation of the potent flavour component 3-methylbutanal. *Appl. Microbiol. Biotechnol.* 64, 396–402. doi: 10.1007/s00253-003-1447-8

Smit, G., Smit, B. A., and Engels, W. J. M. (2005). Flavour formation by lactic acid bacteria and biochemical flavour profiling of cheese products. *FEMS Microbiol. Rev.* 29, 591–610. doi: 10.1016/j.fmrre.2005.04.002

Söllner, K., and Schieberle, P. (2009). Decoding the key aroma compounds of a Hungarian-type salami by molecular sensory science approaches. *J. Agric. Food Chem.* 57, 4319–4327. doi: 10.1021/jf900402e

Sun, Q. X., Chen, Q., Li, F. F., Zheng, D. M., and Kong, B. H. (2016). Biogenic amine inhibition and quality protection of Harbin dry sausages by inoculation with *Staphylococcus xylosus* and *Lactobacillus plantarum*. *Food Control* 68, 358–366. doi: 10.1016/j.foodcont.2016.04.021

Sun, W. Z., Zhao, Q. Z., Zhao, H. F., and Zhao, M. M. (2010). Volatile compounds of Cantonese sausage released at different stages of processing and storage. *Food Chem.* 121, 319–325. doi: 10.1016/j.foodchem.2009.12.031

Valencia, I., Ansorena, D., and Astiasarán, I. (2006). Nutritional and sensory properties of dry fermented sausages enriched with n-3 PUFAs. *Meat Sci.* 72, 727–733. doi: 10.1016/j.meatsci.2005.09.022

Visessanguan, W., Benjakul, S., Riebroy, S., and Thepkasikul, P. (2004). Changes in composition and functional properties of proteins and their contributions to Nham characteristics. *Meat Sci.* 66, 579–588. doi: 10.1016/S0309-1740(03)00172-4

Wang, Y. Q., Liu, R., Ge, Q. F., Wu, M. G., Xu, B. C., Xi, J., et al. (2021). Effects of branched-chain amino acids and *Lactobacillus plantarum* CGMCC18217 on volatiles formation and textural properties of dry-cured fermented sausage. *Int. J. Food Sci. Technol.* 56, 374–383. doi: 10.1111/ijfs.14652

Yu, D., Feng, M. Q., Sun, J., Xu, X. L., and Zhou, G. H. (2020). Protein degradation and peptide formation with antioxidant activity in pork protein extracts inoculated with *Lactobacillus plantarum* and *Staphylococcus simulans*. *Meat Sci.* 160:107958. doi: 10.1016/j.meatsci.2019.107958

Yu, D., Feng, M., and Sun, J. (2021). Influence of mixed starters on the degradation of proteins and the formation of peptides with antioxidant activities in dry fermented sausages. *Food Control* 123:107743. doi: 10.1016/j.foodcont.2020.107743

Yvon, M., Chambellon, E., Bolotin, A., and Roudot-Algaron, F. (2000). Characterization and role of the branched-chain aminotransferase (BcaT) isolated from *Lactococcus lactis* subsp. Cremoris NCDO 763. *Appl. Environ. Microbiol.* 66, 571–577. doi: 10.1128/AEM.66.2.571-577.2000

frontiers | Frontiers in Microbiology

TYPE Original Research
PUBLISHED 09 February 2023
DOI 10.3389/fmicb.2023.1124546

OPEN ACCESS

EDITED BY
Jinxuan Cao,
Beijing Technology and Business University, China

REVIEWED BY
Chan Zhang,
Beijing Technology and Business University, China
Hongkai Zhu,
Tea Research Institute (CAAS), China
Xinlin Wei,
Shanghai Jiao Tong University, China

*CORRESPONDENCE
Yao Zou
✉ zouyao82@163.com
Ming-zhi Zhu
✉ mzzhucn@hotmail.com
Wei Xu
✉ xuweianti@sicau.edu.cn

SPECIALTY SECTION
This article was submitted to Food Microbiology, a section of the journal Frontiers in Microbiology

RECEIVED 15 December 2022
ACCEPTED 23 January 2023
PUBLISHED 09 February 2023

CITATION
Liao S-y, Zhao Y-q, Jia W-b, Niu L, Bouphun T, Li P-w, Chen S-x, Chen W, Tang D-d, Zhao Y-l, Zou Y, Zhu M-z and Xu W (2023) Untargeted metabolomics and quantification analysis reveal the shift of chemical constituents between instant dark teas individually liquid-state fermented by *Aspergillus cristatus*, *Aspergillus niger*, and *Aspergillus tubingensis*. *Front. Microbiol.* 14:1124546.
doi: 10.3389/fmicb.2023.1124546

Untargeted metabolomics and quantification analysis reveal the shift of chemical constituents between instant dark teas individually liquid-state fermented by *Aspergillus cristatus*, *Aspergillus niger*, and *Aspergillus tubingensis*

Si-yu Liao[1], Yi-qiao Zhao[1], Wen-bao Jia[1], Li Niu[2], Tunyaluk Bouphun[3], Pin-wu Li[1], Sheng-xiang Chen[1], Wei Chen[1], Dan-dan Tang[1], Yue-ling Zhao[1], Yao Zou[1]*, Ming-zhi Zhu[2]* and Wei Xu[1]*

[1]College of Horticulture, Tea Refining and Innovation Key Laboratory of Sichuan Province, Sichuan Agricultural University, Chengdu, China, [2]Key Laboratory of Tea Science of Ministry of Education, National Research Center of Engineering Technology for Utilization of Functional Ingredients from Botanicals, College of Horticulture, Hunan Agricultural University, Changsha, China, [3]Faculty of Science and Agricultural Technology, Rajamangala University of Technology Lanna Lampang, Lampang, Thailand

Instant dark teas (IDTs) were individually liquid-state fermented using the fungi *Aspergillus cristatus*, *Aspergillus niger*, and *Aspergillus tubingensis*. To understand how the chemical constituents of IDTs were affected by the fungi, samples were collected and measured by liquid chromatography-tandem mass-tandem mass spectrometry (LC-MS/MS). Untargeted metabolomics analysis revealed that 1,380 chemical constituents were identified in positive and negative ion modes, and 858 kinds of chemical components were differential metabolites. Through cluster analysis, IDTs were different from the blank control, and their chemical constituents mostly included carboxylic acids and their derivatives, flavonoids, organooxygen compounds, and fatty acyls. And the metabolites of IDTs fermented by *A. niger* and *A. tubingensis* had a high degree of similarity and were classified into one category, which showed that the fungus used to ferment is critical to the formation of certain qualities of IDTs. The biosynthesis of flavonoids and phenylpropanoid, which involved nine different metabolites such as p-coumarate, p-coumaroyl-CoA, caffeate, ferulate, naringenin, kaempferol, leucocyanidin, cyanidin, and (-)-epicatechin, were significant pathways influencing the quality formation of IDTs. Quantification analysis indicated that the *A. tubingensis* fermented-IDT had the highest content of theaflavin, theabrownin, and caffeine, while the *A. cristatus* fermented-IDT had the lowest content of theabrownin, and caffeine. Overall, the results provided new insights into the relationship between the quality formation of IDTs and the microorganisms used in liquid-state fermentation.

KEYWORDS

instant dark teas, fungi, liquid-state fermentation, metabolome, quantification analysis

1. Introduction

Dark tea is a typical post-fermented tea in China, including Yunnan Pu-erh tea, Hunan Fu-brick tea, Shaanxi Fu-brick tea, Hubei Qing-brick tea, Sichuan Kang-brick tea, and Guangxi Liu-bao-tea (Lin et al., 2021), which is associated with diverse health benefits, such as inhibiting fat deposition, antioxidant, anti-diabetic, anti-cancer, cardiovascular protective, gastrointestinal protective, hepatoprotective, neuroprotective, photoprotective, and sleep regulation (Peng et al., 2014; Lin et al., 2021; Wu et al., 2021; Wei et al., 2022). In pile-fermentation, which is a kind of solid-state fermentation and the key process to forming the unique characteristics of dark tea (Li et al., 2018; Xu et al., 2022b), the microorganism is critical to the quality formation. Chinese dark teas produced *via* different crafts house different microbial communities. *A. cristatus*, which also known as *Eurotium cristatum* (Hubka et al., 2013), is considered the dominant microorganism and plays a key role in the quality formation of Fu-brick tea (Zhu et al., 2020; Wang et al., 2021), contributing to increasing the levels of volatile organic compounds with stale and floral aromas (Xiao et al., 2022). *A. niger* and *A. tubingensis* are the major fungi among Pu-erh tea manufacturers (Abe et al., 2008; Haas et al., 2013; Wang et al., 2015).

Instant dark teas (IDTs), a novel type of tea beverage, are traditionally manufactured using dark tea that has been solid-state fermented, water-extracted, filtered, condensed, and dried (Lu et al., 2015). Additionally, the other way to process instant dark tea is by having microorganisms ferment tea soup, which has the advantages of stability, rapidity, avoiding mixed microbial contamination, and mild manufacturing conditions (Hsu et al., 2002). In previous studies, IDTs were inoculated with *A. cristatus*, *A. niger*, or *A. tubingensis* for liquid-state fermentation, showing completely different main chemical constituents and sensory qualities (Lu et al., 2015; Wang Q. et al., 2018; Chen et al., 2021; Ma et al., 2021; Wang et al., 2021; Jun et al., 2022). The metabolic pathways, which were critical to the sensory qualities of the IDTs, have unclear relationships with microorganisms.

Metabolomics is an effective tool for explaining the effects of metabolites in tea fermented by microorganisms (Cai et al., 2022). Metabolomics analysis showed that certain microorganisms have important effects on the transformation of metabolites and flavor formation during pile-fermentation (Shi et al., 2021; Li et al., 2022). The previous experiment reveals that *A. cristatus* is critical to the formation of certain qualities of IDT during liquid-state fermentation, using untargeted and targeted metabolomics (An et al., 2021). However, it is unclear how the qualities of IDTs are influenced by the effects of several dominant microorganisms.

In our study, IDTs were fermented in a liquid-state by the fungi (*A. cristatus*, *A. niger*, and *A. tubingensis*), which were isolated from Fu-brick tea and raw dark tea and identified by phylogenetic analysis. To evaluate the safety of IDTs, ochratoxin and citrinin concentrations were tested using high performance liquid chromatography (HPLC). The content of the main chemical components of IDTs was determined. Metabolites of IDTs were analyzed by ultra-high performance liquid chromatography-hybrid quadrupole time-of-flight/Mass spectrometry (UHPLC-QTOF-MS) and liquid chromatography-tandem mass-tandem mass spectrometry (LC-MS/MS) based untargeted metabolomics. This study has advanced our knowledge regarding how the characteristics of IDTs formed by fermenting in the liquid state.

2. Materials and methods

2.1. Materials and chemical reagents

Green tea was used as the raw material for liquid-state fermentation and provided by Mabian Wenbin Tea Industry Co., Ltd. (Sichuan, China). Fu-brick tea and raw dark tea were used to isolate the fungal strains provided by Hunan Haoming Tea Industry Food Co., Ltd. (Hunan, China).

Ochratoxin A (OTA), Ochratoxin B (OTB), and Citrinin (CIT) standards were purchased from Pribolab Pte. Ltd. (Qingdao, China). Chromatographic-grade methanol, acetonitrile, and glacial acetic acid were provided by Chengdu Kelong Co., Ltd. (Chengdu, China).

2.2. Fungal strains

The strains of Q4, Q54, and ZM1 were isolated from a Fu-brick tea and a raw dark tea and identified using morphological and phylogenetic analysis of fungal internally transcribed spacer (ITS) and partial β-tubulin (*BenA*) gene sequences (Ma et al., 2022), with the identification method as previously reported (Yu et al., 2020). Strains were preserved on potato dextrose agar (PDA) at 4°C. The spore suspensions of the strains were prepared with sterile water and adjusted to 4.0×10^6 CFU/mL for the next liquid-state fermentation.

2.3. Tea liquid-state fermentation

Under aerobic conditions, liquid-state fermentation was carried out in a shaking incubator (YS-100B, Changzhou, China). Green tea was infused in distilled water (liquid-to-solid ratio of 60:1 mL/g) and sterilized at 121°C for 20 min. The sterilized tea soup was inoculated with 2% (v/v) spore suspensions and fermented at 25°C with a shaking speed of 190 rpm. Three replicates were set for each treatment, and the blank control was inoculated with the same amount of sterile water. Because of the difference in growth characteristics between the strains, the fermentation duration for *A. cristatus* was 132 h, while the fermentation duration for the other two strains was 72 h. After fermentation ended, the mixtures were, respectively, filtered by multilayer gauze to remove mycelia. The filtrates were centrifuged further at 5,000 rpm for 15 min to obtain instant dark tea (IDTs), which were stored at −80°C in the following experiment.

2.4. Determinations of ochratoxins and citrinin

Instant dark teas were filtered by 0.22 μm aqueous filter membrane and then detected the content of ochratoxins and citrinin by HPLC (1260, Agilent, USA). Ochratoxin A (OTA) and ochratoxin B (OTB) were separated using a Phenomenex C_{18} (5 μm, 150 × 4.6 mm) column loaded with water-glacial acetic acid (98:2 v/v) (phase A) and acetonitrile (phase B), with isocratic elution (50:50). Citrinin (CIT) was separated by Phenomenex C_{18} (5 μm, 250 × 4.6 mm) column, using the mobile phase of acetonitrile-isopropanol-phosphoric acid (35:10:55 v/v).

2.5. Determination of main chemical compounds

The contents of tea polyphenols, tea pigments (theaflavins, thearubigins, and theabrownin), and amino acids were determined using spectrophotometry, as previously described (Wang et al., 2011, 2014). The content of caffeine was determined using ultraviolet spectrophotometry in GB/T 8312-2013, and the content of organic acids were determined using acid-base indicator titration in GB/T 12456-2021.

2.6. Metabolomics

2.6.1. Metabolites extraction

The IDTs samples were thawed at 4°C. Then 100.0 μL of samples fermented by different fungal strains were individually extracted with 300 μL of methanol, 20 μL of internal standard substances were added, vortexed for 30 s, ultrasonically treated for 10 min (incubated in ice water), and incubated for 1 h at −20°C to precipitate proteins. The sample was then centrifuged for 15 min at 4°C, 13,000 rpm. Transfer the supernatant (200 μL) into a 2 mL LC/MS glass vial, take 20 μL from each sample and pool them as QC samples, and take 200 μL supernatant for UHPLC-QTOF-MS analysis.

2.6.2. LC-MS/MS analysis

LC-MS/MS analysis was performed using an HPLC system (1290, Agilent Technologies) with a UPLC BEH Amide column (1.7 μm, 2.1 × 100 mm) coupled to a Triple TOF 5600 (Q-TOF, AB Sciex) at a flow rate of 0.5 mL·min^{-1}. Mobile phase A consisted of 25 mM NH_4OAc and 25 mM NH_4OH in water (pH = 9.75), and mobile phase B was composed of acetonitrile. The gradient program was as follows: 0 min, 95% B; 7 min, 65% B; 9 min, 40% B; 9.1 min, 95% B; 12 min, 95% B. The injection volume was 3 μL. The Triple TOF mass spectrometer was used for its ability to acquire MS/MS experiments. In this mode, the acquisition software (Analyst TF 1.7, AB Sciex) continuously evaluated the full scan survey MS data as it collected and triggered the acquisition of MS/MS spectra depending on preselected criteria. In each cycle, 12 precursor ions whose intensities were greater than 100 were chosen for fragmentation at collision energy (CE) of 30 V (15 MS/MS events with product ion accumulation time of 50 ms each). ESI source conditions were set as follows: Ion source gas 1 at 60 Psi, Ion Spray Voltage Floating (ISVF) 5,000 or −4,000 V in positive or negative modes, respectively.

2.6.3. Data preprocessing and annotation

MS raw data (.d) files were converted to the mzXML format using ProteoWizard and processed by R package XCMS (version 3.2). The preprocessing results generated a data matrix that consisted of the retention time (RT), mass-to-charge ratio (m/z) values, and peak intensity. The R package CAMERA was used for peak annotation after XCMS data processing. An in-house MS2 database was applied to the identification of metabolites.

2.7. Statistical analysis

All tests were repeated triple times, and data were expressed as means with standard deviation (SD). Duncan's one-way ANOVA (for ≥ 3 samples) was carried out using the SPSS 27.0 software (SPSS Inc. Chicago, IL, USA). Differences were considered statistically significant when the *p*-value was less than 0.05. The principal component analysis (PCA), heat map, different metabolite screening (fold change ≥ 2.0, *P* value ≤ 0.05, and variable importance in projection value ≥ 1.0), functional annotation, and enrichment analysis of differential metabolite KEGG were performed using BMK Cloud[1]. Based on the metabolism classification information provided by the HMDB database[2], the annotated differential metabolism in IDTs samples is statistically mapped. The clusterProfiler, an R packager specially used for enrichment analysis of GO and KEGG, was used to enrich and analyze the annotation results of the differential metabolite KEGG[3] by using the hypergeometric test method to draw an enrichment network diagram.

3. Results and discussion

3.1. Strains

When cultured on PDA plates, the mycelia of strains Q4, Q54, and ZM1 were golden, white, and white, respectively, and the conidial areas were dark blonde, black, and dark green, respectively. Through the colony morphology and phylogenetic analysis, strains Q4, Q54, and ZM1 were identified as *A. cristatus* (the ITS and partial *BenA* gene sequences were deposited in GenBank under accession numbers OQ135132 and OQ136613, respectively), *A. niger* (the ITS and partial *BenA* gene sequences were deposited in GenBank under accession numbers OQ121833 and OQ136614, respectively), and *A. tubingensis* (the ITS and partial *BenA* gene sequences were deposited in GenBank under accession numbers OQ121834 and OQ136615, respectively) stains, respectively (**Figure 1**). Considering the safety of IDTs fermented by the strains (Blanc et al., 1995; O'Brien et al., 2005; Malir et al., 2016), the mycotoxins (OTA, OTB, and CIT) were tested by HPLC and results shown that were below limit of detection (**Supplementary Table 1**).

3.2. Changes in chemical components in IDTs

The composition and contents of chemical components determine the sensory of IDTs. In this study, the contents of chemical components in IDTs samples fermented by *A. niger* (IDTB), *A. cristatus* (IDTC), and *A. tubingensis* (IDTD) were listed in **Table 1**. The contents of tea polyphenols (tea polyphenols, TPs), amino acids (amino acids, AA), and organic acids (organic acids, OA) were reduced under the function of the microorganisms.

TPs are the main water-soluble substances in tea (Senanayake, 2013) and the sources of tea soup convergence, whose possible consumption ways were as follows: one part provided energy for the survival of microorganisms, while the other part was converted into their oxidation products under the action of microorganisms. During fermentation, enzymes secreted by microorganisms converted TPs

1 https://www.biocloud.net
2 https://hmdb.ca/
3 https://www.genome.jp/kegg

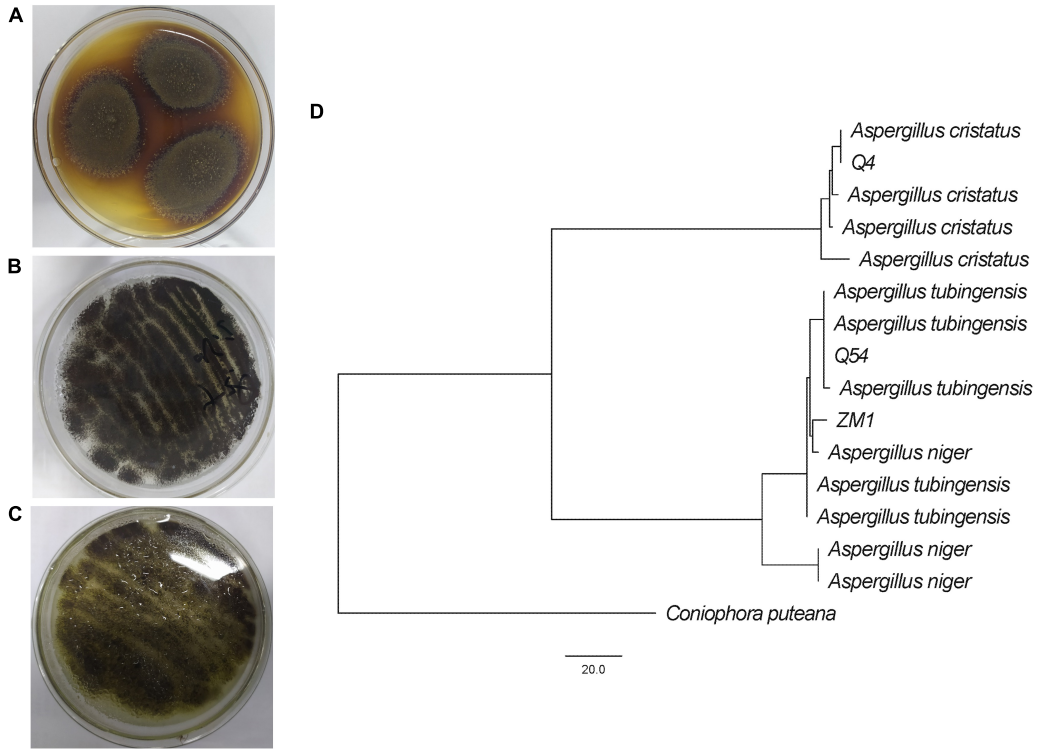

FIGURE 1
Identification of *A. cristatus* (Q4) **(A)**, *A. tubingensis* (Q54) **(B)**, and *A. niger* (ZM1) **(C)**, including colony morphology on PDA plates and molecular phylogenetic analysis **(D)**.

TABLE 1 Chemical constituents of instant dark teas fermented in liquid-state by *A. cristatus*, *A. niger*, and *A. tubingensis*.

Chemical constituents (mg/mL)	Instant dark teas samples			
	IDTA	IDTB	IDTC	IDTD
Tea polyphenols	2.050 ± 0.191^{A}	0.928 ± 0.144^{BC}	0.877 ± 0.445^{C}	1.184 ± 0.199^{B}
Amino acids	0.473 ± 0.104^{A}	0.109 ± 0.186^{D}	0.177 ± 0.114^{C}	0.204 ± 0.085^{B}
Caffeine	0.028 ± 0.001^{B}	0.029 ± 0.001^{B}	0.016 ± 0.001^{C}	0.031 ± 0.001^{A}
Theaflavin	0.029 ± 0.021^{AB}	0.0048 ± 0.002^{C}	0.001 ± 0.006^{BC}	0.038 ± 0.001^{A}
Thearubigins	0.655 ± 0.080^{A}	0.583 ± 0.159^{A}	0.092 ± 0.0021^{B}	0.384 ± 0.450^{AB}
Theabrownins	0.464 ± 0.021^{B}	0.388 ± 0.060^{BC}	0.309 ± 0.020^{C}	0.651 ± 0.087^{A}
Tea pigments	1.148 ± 0.041^{A}	0.934 ± 0.223^{A}	0.410 ± 0.014^{B}	0.658 ± 0.181^{B}
Malic acid	26.353 ± 8.595^{A}	5.243 ± 1.355^{B}	23.450 ± 2.978^{A}	10.832 ± 3.582^{B}
Acetic acid	23.600 ± 7.697^{A}	4.567 ± 1.266^{B}	21.000 ± 2.666^{A}	9.700 ± 3.207^{B}
Tartaric acid	29.500 ± 9.622^{A}	5.733 ± 1.570^{B}	26.250 ± 3.333^{A}	12.125 ± 4.010^{B}
Citric acid	25.173 ± 8.211^{A}	4.780 ± 1.409^{B}	22.400 ± 2.844^{A}	10.347 ± 3.422^{B}
Citric acid monohydrate	27.533 ± 8.980^{A}	5.267 ± 1.514^{B}	24.500 ± 3.111^{A}	11.317 ± 3.742^{B}
Lactic acid	35.400 ± 11.546^{A}	7.267 ± 1.804^{B}	31.500 ± 4.000^{A}	14.550 ± 4.812^{B}
Total organic acids	220.267 ± 71.842^{A}	43.200 ± 11.538^{B}	196.000 ± 24.887^{A}	90.533 ± 29.939^{B}

The different fermentation treatments of instant dark tea were the blank control (IDTA), *Aspergillus niger* (IDTB), *Aspergillus cristatus* (IDTC), and *Aspergillus tubingensis* (IDTD). Data are shown as mean values ± standard deviation. The letters A, B, C (superscript) represent the degree of significant difference in data. The values marked with different uppercase letters within a given row were significantly different ($p < 0.05$).

into quinones first, then further oxidized and polymerized to form tea pigments (Wang Q. et al., 2018). Tea pigments, including theaflavins (theaflavins, TFs), thearubigins (thearubigins, TRs), and theabrownins (theabrownins, TBs), are the reason for color changes in tea soup after fermentation and have the characteristics of anti-atherosclerosis, anti-obesity, and maintain muscle health (Gong et al., 2010; Liu et al., 2016; Xu et al., 2022a). Compared to IDT prepared by blank control (IDTA), IDTB had the highest content of TRs, IDTD had the highest content of TPs, TFs, and TBs, while IDTC had the lowest content of TPs, TFs, and TRs ($p < 0.05$). These data

indicated that *A. tubingensis* could efficiently utilize TPs and catalyze the transformation from TPs to TFs and TBs, while *A. cristatus* had a weak ability to catalyze the oxidation of TPs but consumed the highest contents of TPs in IDTs fermented by fungi. Our study showed that the mellow mouthfeel of IDTs would better format with the degradation of TPs and the formation of tea pigments under the action of microorganisms (Wang Y. et al., 2018).

The purine alkaloids in teas typically include caffeine, theobromine, and theophylline, and caffeine contributes to tea's stimulant properties (Wang Q. et al., 2018). The caffeine content of IDTD was significantly higher than the other IDTs ($p < 0.05$), considering that certain secretions from *A. tubingensis* can promote the production of caffeine or the inability of *A. tubingensis* in liquid-state fermentation to use the caffeine originally present in tea soup. The high content of caffeine in IDTD should allow it to be a better stimulant than the other IDTs. Instead, the caffeine content of IDTC was lowest in the IDTs ($p < 0.05$), which indicated that the caffeine originally present in tea soup could be significantly consumed or degraded through liquid-state fermentation by *A. cristatus*. Therefore, IDTC had a more mellow mouthfeel in the IDTs and *A. cristatus* had the potential to develop tea beverages with low content of caffeine. A recent study showed that the content of caffeine increased during the liquid-state fermentation by *A. cristatus* (An et al., 2021), which is different from our results. This may be caused by the difference in microorganisms. Additionally, there was no significant difference in caffeine content between IDTA and IDTB ($p < 0.05$), showing that *A. niger* had no significant effect on caffeine metabolism. This indicated the fungal species (*A. niger*, *A. tubingensis*, and *A. cristatus*) are responsible for caffeine metabolism, which can affect the caffeine content through different microbial pathways.

AA can help to form the mellow taste of tea (An et al., 2021). The level of AA in IDTs fermented by fungi was significantly lower than the corresponding level in IDTA ($p < 0.05$). In IDTs fermented by fungi, the level of AA in IDTB was the lowest but it in IDTD was the highest ($p < 0.05$), which showed that *A. niger* could significantly consume AA originally, but *A. tubingensis* had the weakest ability to consume AA in the strains used to produce IDTs. This may be because AA, one of the readily metabolize nutrients in tea soup (Wang Q. et al., 2018), were abundantly used during fungal growth.

OA were key constituents in tea leaves that influence the tea quality (Xu et al., 2013). In this study, the contents of OA in IDTs were determined, including malic acid, tartaric acid, acetic acid, citric acid, citric acid monohydrate, and lactic acid. The levels of OA in IDTB and IDTD were higher than the corresponding levels in IDTA and IDTC, and there were no significant differences in the organic levels between IDTA and IDTC. This indicated that *A. cristatus* could cause a better biological activity of IDT than *A. niger* and *A. tubingensis*.

3.3. Metabolomics analysis of IDTs

3.3.1. PCA analysis and vene diagram

Through non-target metabolomics technology, a total of 1,380 chemicals were detected in the IDTs (A refers to the IDT was produced by the blank control; B refers to IDT was fermented by *A. niger*; C refers to IDT was fermented by *A. cristatus*; D refers to IDT was fermented by *A. tubingensis*) in positive and negative modes (**Supplementary Table 2**), including 858 metabolites which closely related to the quality formation of IDTs (**Figure 2B**). The PCA differentiated the four IDTs samples (**Figure 2A**), indicating that there were significant differences between the IDTs fermented by the strains and the blank control. The principal components of IDTB and IDTD were similar, which were quite different from the principal components of IDTC, for the close biological relationship between *A. niger* and *A. tubingensis* (Juhász et al., 2004).

The compounds with FC value greater than 2.0, *P* value less than 0.05, and VIP value greater than 1.0 were defined as differential metabolites among IDTs samples. Compared with the blank control (**Figure 2B**), 858 metabolites were clustered after trimming and filtering, and 562 core metabolites were shared by the IDTs fermented by different strains. Additionally, compared with the IDTB and IDTD, the total number of metabolites in IDTC was the minimum, but the number of exclusive metabolites in IDTC was the maximum. There is the least number of similar metabolites between the IDTC and IDTD. This implied that the microorganisms used for liquid-state fermentation are critical to the quality formation of IDTs.

3.3.2. Heatmap and histogram of differential metabolites

Heatmap was used to visualize the differences of metabolites among IDTs fermented by dissimilar strains, in which each column represents an IDT sample and each row represents a metabolite (**Figure 3A**). *Via* thermogram analysis, the metabolites polymerization in IDTs is divided into three categories. Compared with the blank control, the expression of categories I substance was significantly upregulated in IDTB and IDTD, while the expression of categories II substance was only upregulated significantly in IDTC. For the category III substance, it was significantly downregulated in IDTs fermented by the three stains, indicating that there was consistency in the transformation of the metabolites of IDTs under the function of the three fungi strains. According to the similarity in metabolite classification, the composition of metabolites of IDTB and IDTD, confirms our previous conclusion. Therefore, in the heatmap diagram, IDTB and IDTD were classified into one category, and IDTC belonged to one group with them for the metabolites of it were significantly different from IDT produced by the blank control.

Based on the metabolites classification information provided by the HMDB databases, the annotated differential metabolism in IDTs is statistically mapped (**Figure 3B**), and the number of substances species was more than 20 were considered as the key metabolites. The diagram showed that the key metabolites in IDTs production were carboxylic acids and their derivatives, flavonoids, organooxygen compounds, and fatty acyls. It was different for the order of the number of these key metabolites in IDTs fermented by dissimilar strains. And the key metabolites numbers in IDTC showed more differences than it in IDTB and IDTD, which had the largest number of carboxylic acids and their derivatives and the smallest number of fatty acids. Besides, for the other two key metabolites, the number of flavonoids in IDTC was smaller than it in the other two IDTs fermented by fungi. This indicated that flavonoids and carboxylic acids and their derivatives were more used by *A. cristatus* in the instant dark tea production process. This may be due to the relatively low utilization of organooxygen compounds and fatty acyls by *A. cristatus*, or *A. cristatus* can promote the synthesis of these two metabolites, which needs further experimental verification.

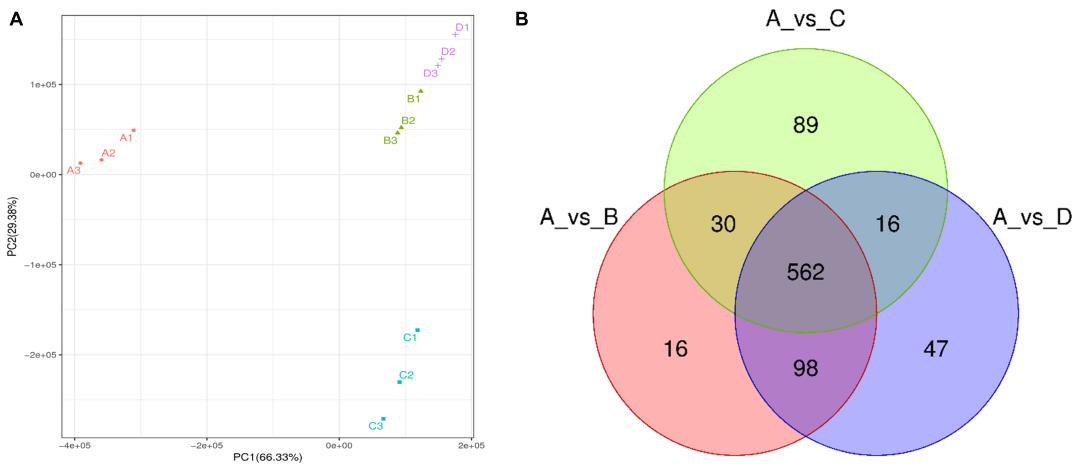

FIGURE 2
The metabolomics data were subjected to principal component analysis (PCA) **(A)** and Vene diagram **(B)** of differential metabolites in IDTs. The different fermentation treatments of instant dark tea were the blank control [A], *Aspergillus niger* [B], *Aspergillus cristatus* [C], and *Aspergillus tubingensis* [D].

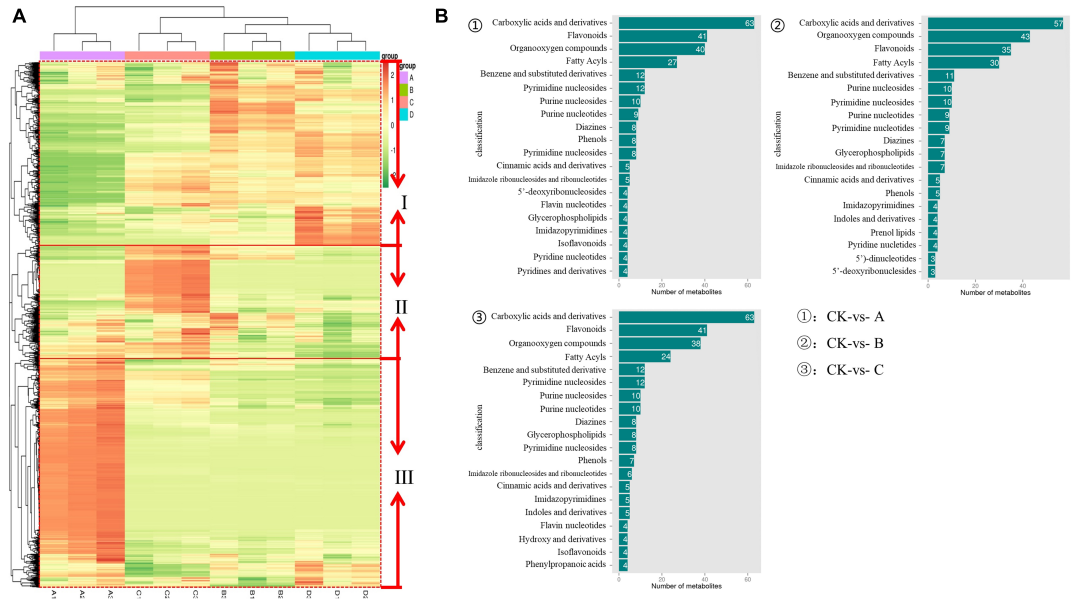

FIGURE 3
The metabolomics data were subjected to heatmap analysis **(A)** and column diagram differential metabolites **(B)** in IDTs. In the heatmap, a color-coded scale grading from orange to green represented the metabolites from high to low. The different fermentation treatments of instant dark tea were the blank control [A], *Aspergillus niger* [B], *Aspergillus cristatus* [C], and *Aspergillus tubingensis* [D].

3.3.3. Analysis of enrichment network and metabolic pathway of metabolites

The enrichment network of metabolites in IDTs is drawn in Figure 4, along with heat dots representing the levels of associated metabolites. The results showed the main metabolic pathway in IDTs fermented by the strains. The main pathways in IDTs were as follows: IDTB involved aminobenzoate degradation, biosynthesis of phenylpropanoids, flavonoid biosynthesis, nicotinamide metabolism, and valine, leucine and isoleucine degradation; IDTC involved biosynthesis of phenylpropanoids, biosynthesis of various secondary metabolites metabolites-part 2, flavonoid biosynthesis, purine metabolism, and valine, leucine and isoleucine degradation; IDTD involved biosynthesis of phenylpropanoids, degradation of aromatic compounds, flavonoid biosynthesis, metabolism of xenobiotics by cytochrome P450, and toluene degradation.

In this study, the biosynthesis of flavonoids and phenylpropanoids was the mutual metabolic pathway in IDTs fermented by the three stains, including the largest number of metabolites for their biggest size of the node. The metabolites in flavonoid biosynthesis were a comprehensive decline under the function of the strains, indicating that the flavonoid substances in tea soup were transformed and utilized with the influence of microorganisms. IDTs fermented by microorganisms can obtain a mild taste because flavonoid is one of the sources of the astringent sense of tea soup. Flavonoid is also one of the main components of tea polyphenols (He et al., 2020), so it may be the central carbon source for microbial growth provided by the tea soup. Besides, expect

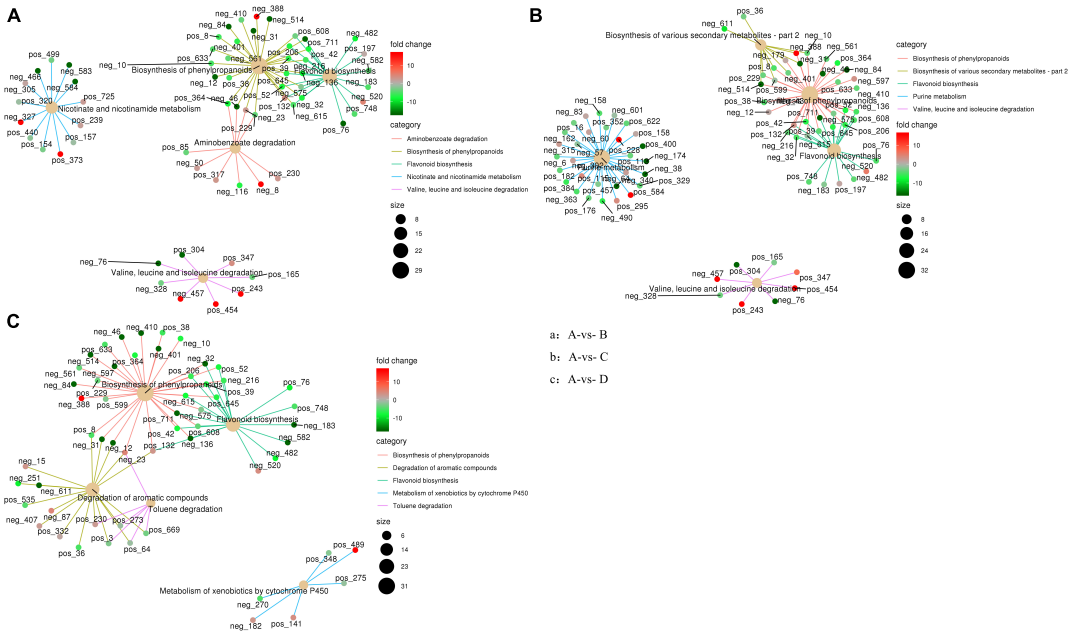

FIGURE 4
Enrichment network diagram of differential metabolites in IDTs. Pictures respectively represent metabolites pathways between IDT produced by blsnk control and IDTs fermented by fungi. The light-yellow node refers to the associated metabolic pathway, and its size of it indicates the number of metabolites included by these pathways. The dots connected with the node refer to the specific metabolites annotated to the pathway, along with the color depth indicating the difference multiple taking the value of log 2. The different fermentation treatments of instant dark tea were the blank control [A], *Aspergillus niger* [B], *Aspergillus cristatus* [C], and *Aspergillus tubingensis* [D].

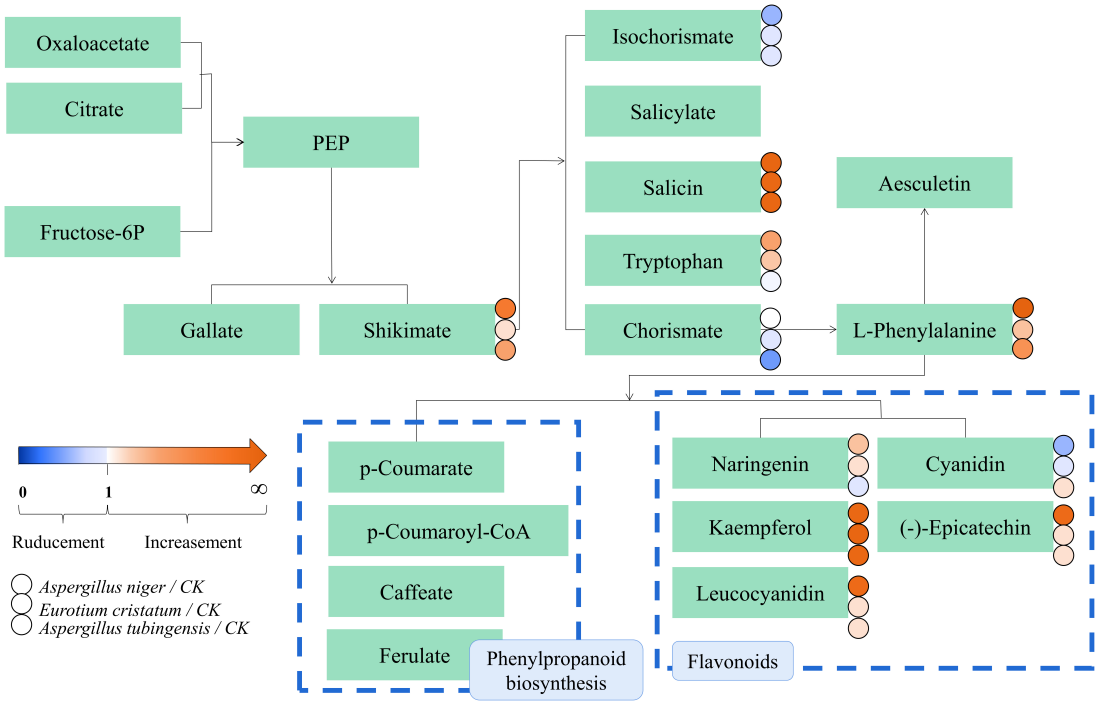

FIGURE 5
metabolic pathway diagram of the differential metabolites in IDTs. The dots represent the relative content of metabolites between the IDT fermented by microorganisms and the bank control. The dots represent the relative content of metabolites between IDT produced by blank control and IDTs fermented by fungi. The color-coded scale grading from orange to blue represented the metabolites from high to low. The different fermentation treatments of instant dark tea were the blank control [A], *Aspergillus niger* [B], *Aspergillus cristatus* [C], and *Aspergillus tubingensis* [D].

the synthesis of chorismite, the metabolites of phenylpropanoids biosynthesis have significantly risen under the function of the strains. Phenylalanine is the precursor of phenylpropanoid biosynthesis and is eventually converted into flavanols and flavonol glycosisdes through the flavonoid biosynthesis pathway after catalysis by a series of enzymes (Wu et al., 2020; Sun et al., 2022). In our previous

study, we certified that amino acid contents were significantly reduced under the action of microorganisms. This indicated that the transformation from phenylpropanoids to phenylpropanoid was promoted and the biosynthesis pathway of flavonoid from phenylpropanoid was inhibited, with the effects of microbial extracellular enzymes in the liquid-state fermentation system.

The degradation of valine, leucine, and isoleucine was a collective metabolic pathway in IDTs fermented by *A. niger* and *A. cristatus*, with the metabolites of (s)-3-hydroxyisobutyl-CoA, and (s)-b-aminoisobutyric acid significantly rose and the metabolites of methylcrotonyl-CoA slightly rose. For IDTD, the metabolism of caffeic acid was significantly decreased in the degradation of its aromatic compounds of the IDT. Caffeic acid is a phenolic compound, with the activity of antioxidant, anti-inflammatory, and anti-carcinogenic (Espíndola et al., 2019). Therefore, IDTD may have certain healthcare functions.

The possible metabolic pathways for the quality formation of IDTs fermented by microorganisms were drawn in **Figure 5**, along with color-coded dots representing the levels of the associated metabolites. There were 22 substances differentially expressed in the metabolic transformation pathway shown in **Figure 5**. In the diagram, the biosynthesis of phenylpropanoid and flavonoids were also the main metabolic pathway influencing the quality formation of IDTs, like our previous results. There were nine differential metabolites in the pathways: p-coumarate, p-coumaroyl-CoA, caffeate, ferulate, naringenin, kaempferol, leucocyanidin, cyanidin, and (-)-epicatechin, which may be driven by extracellular enzymes secreted by microorganisms.

As mentioned above, microorganisms are critical to the qualities of IDTs in liquid-state fermentation, for their function in the transformation of water-soluble substances in tea soup. In our study, the transformation and utilization of flavonoids and phenylpropanoid have high consistency under the function of *A. niger*, *A. cristatus*, and *A. tubingensis* in the process of liquid-state fermentation, which indicated that single fungus fermentation is conducive to targeted changes in the content of certain substances and developing functional tea products or guiding the production of instant dark tea products according to market demand.

4. Conclusion

This study explored the relationship between the quality formation of instant dark teas (IDTs) and the dominant microorganisms (*A. niger*, *A. cristatus*, and *A. tubingensis*) used for liquid-state fermentation, and revealed the main metabolic pathways during fermentation. The fermentation of IDTs by the dominant microorganisms caused the degradation of tea polyphenols, amino acids, and organic acids. Especially, the IDT fermented by *A. tubingensis* had the highest content of theaflavins, theabrownins, and caffeine, while the IDT fermented by *A. cristatus* had the lowest content of theabrownins and caffeine. Metabolic results revealed that 22 metabolites were identified as key metabolites responsible for differential metabolic pathways among IDTs fermented by strains. And the biosynthesis of flavonoids and phenylpropanoids were the key metabolic pathways in the quality formation of IDTs, with nine differential metabolites including p-coumarate, p-coumaroyl-CoA, caffeate, ferulate, naringenin, kaempferol, leucocyanidin, cyanidin, and (-)-epicatechin. Our results advance our insights into the metabolic changes in the quality formation of IDTs processed by liquid-state fermentation using *A. niger*, *A. cristatus*, and *A. tubingensis*.

Data availability statement

The data presented in our study are deposited in the https://www.ncbi.nlm.nih.gov/ repository, accession numbers: OQ135132, OQ121833, OQ121834, OQ136613, OQ136614, and OQ136615.

Author contributions

S-YL and Y-QZ participated in conceptualization, methodology, software, formal analysis, investigation, data curation, and visualization. W-BJ participated in software and investigation. TB participated in adding and editing and reviewing all parts of the manuscript. P-WL and S-XC participated in resources and validation. LN, WC, D-DT, Y-LZ, and YZ participated in conceptualization and methodology. M-ZZ participated in review and editing. WX participated in conceptualization, writing—review and editing, and funding acquisition. All authors contributed to the article and approved the submitted version.

Funding

This work was supported by Sichuan Province S&T Project (2021ZHFP0021, 2022ZHXC0022, 2023YFH0025, and 2023YFN0010) and Ya'an Yucheng District School Cooperation Project (2022).

Conflict of interest

The authors declare that the research was conducted in the absence of any commercial or financial relationships that could be construed as a potential conflict of interest.

Publisher's note

Supplementary material

The Supplementary Material for this article can be found online at: https://www.frontiersin.org/articles/10.3389/fmicb.2023.1124546/full#supplementary-material

References

Abe, M., Takaoka, N., Idemoto, Y., Takagi, C., Imai, T., and Nakasaki, K. (2008). Characteristic fungi observed in the fermentation process for Puer tea. *Int. J. Food Microbiol.* 124, 199–203. doi: 10.1016/j.ijfoodmicro.2008.03.008

An, T., Chen, M., Zu, Z., Chen, Q., Lu, H., Yue, P., et al. (2021). Untargeted and targeted metabolomics reveal changes in the chemical constituents of instant dark tea during liquid-state fermentation by *Eurotium cristatum*. *Food Res. Int.* 148:110623. doi: 10.1016/j.foodres.2021.110623

Blanc, P. J., Laussac, J. P., Bars, J. L., Bars, P. L., Loret, M. O., Pareilleux, A., et al. (1995). Characterization of monascidin A from *Monascus* as citrinin. *Int. J. Food Microbiol.* 27, 201–203. doi: 10.1016/0168-1605(94)00167-5

Cai, H., Zhong, Z., Li, Z., Zhang, X., Fu, H., Yang, B., et al. (2022). Metabolomics in quality formation and characterization of tea products: A review. *Int. J. Food Sci. Technol.* 57, 4001–4014. doi: 10.1111/ijfs.15767

Chen, Q., Zhang, M., Chen, M., Li, M., Zhang, H., Song, P., et al. (2021). Influence of *Eurotium cristatum* and *Aspergillus niger* individual and collaborative inoculation on volatile profile in liquid-state fermentation of instant dark teas. *Food Chem.* 350:129234. doi: 10.1016/j.foodchem.2021.129234

Espíndola, K. M. M., Ferreira, R. G., Narvaez, L. E. M., Rosario, A. C. R. S., Silva, A. H. M., da Sliva, A. G. B., et al. (2019). Chemical and pharmacological aspects of caffeic acid and its activity in Hepatocarcinoma. *Front. Oncol.* 9:541. doi: 10.3389/fonc.2019.00541

Gong, J., Peng, C., Chen, T., Gao, B., and Zhou, H. (2010). Effects of theabrownin from Pu-erh Tea on the metabolism of serum lipids in rats: Mechanism of action. *J. Food Sci.* 75, H182–H189. doi: 10.1111/j.1750-3841.2010.01675.x

Haas, D., Pfeifer, B., Reiterich, C., Partenheimer, R., Reck, B., and Buzina, W. (2013). Identification and quantification of fungi and mycotoxins from Pu-erh tea. *Int. J. Food Microbiol.* 166, 316–322. doi: 10.1016/j.ijfoodmicro.2013.07.024

He, H.-F., Wei, K., Yin, J., and Ye, Y. (2020). Insight into tea flavonoids: Composition and chemistry. *Food Rev. Int.* 37, 812–823. doi: 10.1080/87559129.2020.1721530

Hsu, F.-L., Wang, P.-M., Lu, S.-Y., and Wu, W.-T. (2002). A combined solid-state and submerged cultivation integrated with adsorptive product extraction for production of *Monascus* red pigments. *Bioprocess Biosyst. Eng.* 25, 165–168. doi: 10.1007/soo449-002-0291-z

Hubka, V., Kolařík, M., Kubátová, A., and Peterson, S. W. (2013). Taxonomic revision of *Eurotium* and transfer of species to *Aspergillus*. *Mycologia* 105, 912–937. doi: 10.3852/12-151

Juhász, A., Láday, M., Gácser, A., Kucsera, J., Pfeiffer, I., Kevei, F., et al. (2004). Mitochondrial DNA organisation of the mtDNA type 2b of *Aspergillus tubingensis* compared to the *Aspergillus niger* mtDNA type 1a. *FEMS Microbiol. Lett.* 241, 119–126. doi: 10.1016/j.femsle.2004.10.025

Jun, J., Zhang, M., An, T., Zu, Z., Song, P., Chen, M., et al. (2022). Preparation of instant dark tea by liquid-state fermentation using sequential inoculation with *Eurotium cristatum* and *Aspergillus niger* : Processes optimization, physiochemical characteristics and antioxidant activity. *LWT Food Sci. Technol.* 162:113379. doi: 10.1016/j.lwt.2022.113379

Li, J., Wu, S., Yu, Q., Wang, J., Deng, Y., Hua, J., et al. (2022). Chemical profile of a novel ripened Pu-erh tea and its metabolic conversion during pile fermentation. *Food Chem.* 378:132126. doi: 10.1016/j.foodchem.2022.132126

Li, Q., Chai, S., Li, Y., Huang, J., Luo, Y., Xiao, L., et al. (2018). Biochemical components associated with microbial community shift during the pile-fermentation of primary dark tea. *Front. Microbiol.* 9:1509. doi: 10.3389/fmicb.2018.01509

Lin, F., Wei, X., Liu, H., Li, H., Xia, Y., Wu, D., et al. (2021). State-of-the-art review of dark tea: From chemistry to health benefits. *Trends Food Sci. Technol.* 109, 126–138. doi: 10.1016/j.tifs.2021.01.030

Liu, J., Peng, C., Gao, B., and Gong, J. (2016). Serum metabolomics analysis of rat after intragastric infusion of Pu-erh theabrownin. *J. Sci. Food Agric.* 96, 3708–3716. doi: 10.1002/jsfa.7556

Lu, H., Yue, P., Wang, Y., Fu, R., Jiang, J., and Gao, X. (2015). Optimization of submerged fermentation parameters for instant dark tea production by *Eurotium cristatum*. *J. Food Process. Preserv.* 40, 1–11. doi: 10.1111/jfpp.12694

Ma, Y., Jiang, B., Liu, K., Li, R., Chen, L., Liu, Z., et al. (2022). Multi-omics analysis of the metabolism of phenolic compounds in tea leaves by *Aspergillus luchuensis* during fermentation of pu-erh tea. *Food Res. Int.* 162:111981. doi: 10.1016/j.foodres.2022.111981

Ma, Y., Ling, T., Su, X., Jiang, B., Nian, B., Chen, L., et al. (2021). Integrated proteomics and metabolomics analysis of tea leaves fermented by *Aspergillus niger*, *Aspergillus tamarii* and *Aspergillus fumigatus*. *Food Chem.* 334:127560. doi: 10.1016/j.foodchem.2020.127560

Malir, F., Ostry, V., Pfohl-Leszkowicz, A., Malir, J., and Toman, J. (2016). Ochratoxin A: 50 years of research. *Toxins* 8:191. doi: 10.3390/toxins8070191

O'Brien, E., Prietz, A., and Dietrich, D. R. (2005). Investigation of the teratogenic potential of ochratoxin A and B using the FETAX system. *Birth Defects Res.* 74, 417–423. doi: 10.1002/bdrb.20054

Peng, Y., Xiong, Z., Li, J., Huang, J., Teng, C., Gong, Y., et al. (2014). Water extract of the fungi from Fuzhuan brick tea improves the beneficial function on inhibiting fat deposition. *Int. J. Food Sci. Nutr.* 65, 610–614. doi: 10.3109/09637486.2014.898253

Senanayake, S. P. J. N. (2013). Green tea extract: Chemistry, antioxidant properties and food applications – a review. *J. Funct. Foods* 5, 1529–1541. doi: 10.1016/j.jff.2013.08.011

Shi, J., Ma, W., Wang, C., Wu, W., Tian, J., Zhang, Y., et al. (2021). Impact of various microbial-fermented methods on chemical profile of dark tea using a single raw tea material. *J. Agric. Food Chem.* 69, 4210–4222. doi: 10.1021/acs.jafc.1c00598

Sun, Z., Chen, D., Zhu, L., Zhao, Y., Lin, Z., Li, X., et al. (2022). A comprehensive study of the differences in protein expression and chemical constituents in tea leaves (*Camellia sinensis* var. sinensis) with different maturity using a combined proteomics and metabolomics method. *Food Res. Int.* 157:111397. doi: 10.1016/j.foodres.2022.111397

Wang, Q., Belščak-Cvitanović, A., Durgo, K., Chisti, Y., Gong, J., Sirisansaneeyakul, S., et al. (2018). Physicochemical properties and biological activities of a high-theabrownins instant Pu-erh tea produced using *Aspergillus tubingensis*. *LWT Food Sci. Technol.* 90, 598–605. doi: 10.1016/j.lwt.2018.01.021

Wang, Q., Gong, J., Chisti, Y., and Sirisansaneeyakul, S. (2014). Bioconversion of tea polyphenols to bioactive theabrownins by *Aspergillus fumigatus*. *Biotechnol. Lett.* 36, 2515–2522. doi: 10.1007/s10529-014-1632-0

Wang, Q., Gong, J., Chisti, Y., and Sirisansaneeyakul, S. (2015). Fungal isolates from a Pu-Erh type tea fermentation and their ability to convert tea polyphenols to theabrownins. *J. Food Sci.* 80, M809–M817. doi: 10.1111/1750-3841.12831

Wang, Q., Peng, C., and Gong, J. (2011). Effects of enzymatic action on the formation of theabrownin during solid state fermentation of Pu-erh tea. *J. Sci. Food Agric.* 91, 2412–2418.

Wang, X., Li, X., Liu, B., Long, F., Wei, J., Zhang, Y., et al. (2021). Comparison of chemical constituents of Eurotium cristatum -mediated pure and mixed fermentation in summer-autumn tea. *LWT Food Sci. Technol.* 143:111132. doi: 10.1016/j.lwt.2021.111132

Wang, Y., Zhang, M., Zhang, Z., Jiang, J., Gao, X., and Yue, P. (2018). Multiple responses optimization of instant dark tea production by submerged fermentation using response surface methodology. *J. Food Sci. Technol.* 55, 2579–2586. doi: 10.1007/s13197-018-3178-y

Wei, Y., Xu, J., Miao, S., Wei, K., Peng, L., Wang, Y., et al. (2022). Recent advances in the utilization of tea active ingredients to regulate sleep through neuroendocrine pathway, immune system and intestinal microbiota. *Crit. Rev. Food Sci. Nutr.* 32, 1–29. doi: 10.1080/10408398.2022.2048291

Wu, L., Huang, X., Liu, S., Liu, J., Guo, Y., Sun, Y., et al. (2020). Understanding the formation mechanism of oolong tea characteristic non-volatile chemical constitutes during manufacturing processes by using integrated widely-targeted metabolome and DIA proteome analysis. *Food Chem.* 310:125941. doi: 10.1016/j.foodchem.2019.125941

Wu, W., Hu, Y., Zhang, S., Liu, D., Li, Q., Li, Y., et al. (2021). Untargeted metabolomic and lipid metabolism-related gene expression analyses of the effects and mechanism of aged Liupao tea treatment in HFD-induced obese mice. *R. Soc. Chem. Advances* 11, 23719–23800. doi: 10.1039/d1ra04438a

Xiao, Y., Huang, Y., Chen, Y., Zhu, M., He, C., Li, Z., et al. (2022). Characteristic fingerprints and change of volatile organic compounds of dark teas during solid-state fermentation with *Eurotium cristatum* by using HS-GC-IMS, HS-SPME-GC-MS, E-nose and sensory evaluation. *LWT Food Sci. Technol.* 169:113925. doi: 10.1016/j.lwt.2022.113925

Xu, J., Wei, Y., Huang, Y., Weng, X., and Wei, X. (2022a). Current understanding and future perspectives on the extraction, structures, and regulation of muscle function of tea pigments. *Food Sci. Nutr.* 7, 1–23. doi: 10.1080/10408398.2022.2093327

Xu, J., Wei, Y., Li, F., Weng, X., and Wei, X. (2022b). Regulation of fungal community and the quality formation and safety control of Pu-erh tea. *Comp. Rev. Food Sci. Food Safe* 21, 4546–4572. doi: 10.1111/1541-4337.13051

Xu, Y., Zhong, X., Yin, J., Yuan, H., Tang, P., and Du, Q. (2013). The impact of Ca2+ combination with organic acids on green tea infusions. *Food Chem.* 139, 944–948. doi: 10.1016/j.foodchem.2013.01.025

Yu, Y., Zhao, Y., Zeng, Y., Xu, R., and Xu, W. (2020). Application of BenA Combined with ITS Sequence in the Identification of Golden Flower. *J. Tea Commun.* 47, 255–261.

Zhu, M., Li, N., Zhou, F., Jian, O., Liu, D., Xu, W., et al. (2020). Microbial bioconversion of the chemical components in dark tea. *Food Chem.* 312:126043. doi: 10.1016/j.foodchem.2019.126043

frontiers | Frontiers in Microbiology

TYPE Original Research
PUBLISHED 15 February 2023
DOI 10.3389/fmicb.2023.1135912

OPEN ACCESS

EDITED BY
Zhihong Sun,
Inner Mongolia Agricultural University, China

REVIEWED BY
Guozhong Zhao,
Tianjin University of Science and Technology, China
Zhuang Guo,
Hubei University of Arts and Science, China

*CORRESPONDENCE
Shuliang Liu
✉ lsliang999@163.com

SPECIALTY SECTION
This article was submitted to Food Microbiology, a section of the journal Frontiers in Microbiology

RECEIVED 02 January 2023
ACCEPTED 27 January 2023
PUBLISHED 15 February 2023

CITATION
Liu A, Ou Y, Shu H, Mou T, Li Q, Li J, Hu K, Chen S, He L, Zhou J, Ao X, Yang Y and Liu S (2023) Exploring the role of Sichuan Baoning vinegar microbiota and the association with volatile flavor compounds at different fermentation depths.
Front. Microbiol. 14:1135912.
doi: 10.3389/fmicb.2023.1135912

Exploring the role of Sichuan Baoning vinegar microbiota and the association with volatile flavor compounds at different fermentation depths

Aiping Liu[1], Yixue Ou[1], Haojie Shu[1], Tianyu Mou[1], Qin Li[1], Jianlong Li[1], Kaidi Hu[1], Shujuan Chen[1], Li He[1], Jiang Zhou[2], Xiaolin Ao[1], Yong Yang[1] and Shuliang Liu[1]*

[1]College of Food Science, Sichuan Agricultural University, Ya'an, Sichuan, China, [2]Sichuan Baoning Vinegar Co., Ltd., Langzhong, Sichuan, China

Cereal vinegar is usually produced through solid-state fermentation, and the microbial community plays an important role in fermentation. In this study, the composition and function of Sichuan Baoning vinegar microbiota at different fermentation depths were evaluated by high-throughput sequencing combined with PICRUSt and FUNGuild analysis, and variations in volatile flavor compounds were also determined. The results revealed that no significant differences (p>0.05) were found in both total acid content and pH of vinegar *Pei* collected on the same day with different depths. There were significant differences between the bacterial community of samples from the same day with different depths at both phylum and genus levels (p<0.05), however, no obvious difference (p>0.05) was observed in the fungal community. PICRUSt analysis indicated that fermentation depth affected the function of microbiota, meanwhile, FUNGuild analysis showed that there were variations in the abundance of trophic mode. Additionally, differences in volatile flavor compounds were observed in samples from the same day with different depths, and significant correlations between microbial community and volatile flavor compounds were observed. The present study provides insights into the composition and function of microbiota at different depths in cereal vinegar fermentation and quality control of vinegar products.

KEYWORDS

cereal vinegar, high-throughput sequencing, microbiota, Sichuan Baoning vinegar, volatile flavor compounds

1. Introduction

Vinegar is a popular traditional acidic condiment and preservative with a long history (Li et al., 2015). Production of vinegar is usually divided into liquid-state fermentation and solid-state fermentation according to the fermentation type (Haruta et al., 2006; Li et al., 2022). In Europe, vinegar is mainly produced by liquid-state fermentation using fruits as raw materials; in Asia such as China, Japan, and Korea vinegar is mainly produced by solid-state fermentation using cereals as raw materials (Lynch et al., 2019; Yuan et al., 2021). Compared to liquid-state fermentation, solid-state fermentation involves more complex microbiota, leading to more abundant flavor (Wu et al., 2019; Gao et al., 2022). However, in order to enhance production

yield and efficiency, two-stage liquid–solid fermentation is also utilized by Chinese vinegar manufacturers (Liu et al., 2022). Sichuan Baoning vinegar, as representative of Sichuan bran vinegar, is one of the four traditionally famous vinegars in China (Chen et al., 2016). Sichuan Baoning vinegar differs from other vinegars in the following aspects: use of uncooked wheat bran as the primary raw material and Daqu (great koji) incorporated with Chinese herbs as the saccharifying agent; complete solid-state fermentation; an open fermentation process, with saccharification, alcohol fermentation, and acetic acid fermentation carried out simultaneously. The lactic acid content in Baoning vinegar was higher, leading to a more soft taste (Liu et al., 2022).

As is known, the processing of vinegar relies on a variety of microorganisms, and both culture-dependent (Wu et al., 2010; Vegas et al., 2013) and culture-independent (Kong et al., 2022; Sengun et al., 2022) methods have been employed to study the microbiota during vinegar fermentation. Due to the open fermentation of cereal vinegar, the microbiota succession may be affected by environmental factors and microorganisms from raw materials, processing equipment, and surrounding environment. The contents of ethanol, titratable acid, and reducing sugar, rather than temperature, were reported to be the major environmental factors shaping the microbiota of Zhenjiang aromatic vinegar (Huang et al., 2022). Meanwhile, fermentation depth may also impose an effect on solid-state fermentation since the depth of the substrate can affect the magnitude of temperature and oxygen gradients (Rathbun and Shuler, 1983; Ridder et al., 1999). The volatile flavor compounds are reliable quality indicators of vinegar. The relationship between volatile flavor compounds and microbial community has been confirmed (Wang et al., 2022; Zhang et al., 2022). However, little is known about the effects of fermentation depth on the microbiota and volatile flavor compounds of cereal vinegar.

In the present study, amplicon-based high-throughput sequencing was applied to explore the composition and function of Sichuan Baoning vinegar microbiota at the upper and lower layers. Meanwhile, the relationship between microbiota and volatile flavor compounds was studied, expecting to provide insights into the fermentation mechanism and quality control of cereal vinegar.

2. Materials and methods

2.1. Sampling

The vinegar *Pei* samples (the fermentation mixture before leaching) were collected from Sichuan Baoning Vinegar Co., Ltd. (Langzhong, Sichuan, China) between July 2022 and August 2022. The production of Baoning vinegar was carried out as reported by Liu et al. (2021), and samples (obtained approximately 0.5 ~ 1 h before mixing, except for the 1st day's sample obtained ~ 1 h after mixing) on days 1, 5, 9, 13, 17, 21, 24, and 27 from the upper (5 ~ 40 cm from the top) and lower (70 ~ 110 cm from the top) layers were collected using the five-point sampling method (four corners and center of each layer), respectively. Samples from the same layer were mixed, and excess vinegar *Pei* was removed by the quadrate method. Afterward, 300 ~ 400 g of vinegar *Pei* was sealed in sterile Ziplock bags at −40°C. Samples are identified based on the sampling day and the layer (U = upper, L = lower), e.g., U1 indicates upper layer samples collected on day 1. The total acid content of vinegar *Pei* was recorded as reported by Liu et al. (2020), and pH was determined using a pH meter (PHS–3CB; Shanghai Yueping Scientific Instrument Co., Ltd., Shanghai, China).

2.2. Miseq sequencing

Each sample was divided into three portions and sent to Majorbio (Shanghai, China) for bacterial and fungal diversity analysis using the Illumina Miseq system, e.g., sample U1 was sequenced with three portions identified as U1_1, U1_2, and U1_3. Specifically, primers 338F (5′-ACTCCTACGGGAGGCAGCAG′) and 806R (5′-GGACTACHV GGGTWTCTAAT-3′) were used to amplify the V3–V4 regions of bacterial 16S rDNA, while fungal internal transcribed spacer (ITS) regions were amplified using primers ITS1F (5′-CTTGGTCATTTA GAGGAAGTAA-3′) and ITS2R (5′-GCTGCGTTCTTCATCGATGC-3′; Zeng et al., 2022).

2.3. Bioinformatics analysis

After sequencing, PE reads were spliced according to the overlap relationship using Flash (version 1.2.11), and then trimming, quality control, and assessment of raw reads were conducted by fastp (version 0.19.6). Similar sequences were clustered into the same operational taxonomy unit (OTU) with a 97% sequence identity. The OTU number of each sample was employed to assess species richness. The sequences were evaluated for alpha-diversity (Mothur, version 1.30.2) and beta-diversity (Qiime, version 1.9.1). Linear discriminant analysis (LDA) effect size (LEfSe) was used to analyze the different species at different fermentation depths using LEfSe software (version 1.0), and an LDA score ≥ 2.0 was set to indicate important biomarkers in samples. Microbial functions were annotated by PICRUSt2 (version 2.2.0) for the 16S rDNA OTU and FUNGuild (version 1.0) for the ITS OTU.

2.4. Volatile flavor compounds analysis

The volatile flavor compounds were tested as previously reported (Liu et al., 2020) using gas chromatography–mass spectrometry (GC–MS; 5975C/6890 N; Agilent, United States) with an elastic capillary vessel column (HP-5MS, 30 m × 0.25 mm i.d., 0.25 μm film thickness). After comparing with the NIST 2020 library, compounds with a similarity index higher than 80% were employed for analysis. After normalization of all peak areas, the relative content of each compound was calculated based on its peak area compared to all peak areas.

2.5. Statistical analysis

The total acid, pH, and volatile flavor compounds of vinegar *Pei* samples were analyzed with three independent replicates and expressed as mean ± SD. The relationship between total acid, pH, and microbial community structure was analyzed by RDA/CCA. Spearman's rank correlation coefficient was used to analyze the relationship between volatile flavor compounds and microbiota. Statistical comparative analysis between two groups was performed by t-test using SPSS 27.0 (SPSS, Chicago, IL, United States) unless otherwise specified.

3. Results and discussion

3.1. Microbiota analysis

3.1.1. Alpha diversity

Alpha diversity indices, including shannon, chao, and coverage, were calculated in different samples (Supplementary Table S1). The coverage of sequences was over 0.999, indicating sufficient authenticity and depth of sequencing (Zhao et al., 2022). The shannon and chao values in the bacterial and fungal communities were similar between most of vinegar *Pei* from the same day with different fermentation depths. As revealed by shannon indice, the bacterial community diversity of the upper layer was lower than that of the lower layer on day 13 ($p < 0.05$), but it was higher between day 17 to 24 ($p > 0.05$), especially on day 27 ($p < 0.05$). As revealed by chao value, the bacterial richness exhibited an opposite trend after day 17, and significant differences were observed on days 24 and 27. For the fungal community, the richness of the upper layer was significantly lower than that of the lower layer on day 17 ($p < 0.05$), but it became higher after day 24, especially on day 27 ($p < 0.05$). The diversity of the fungal community in both layers was similar, except for day 5.

3.1.2. Beta diversity

The principal coordinates analysis (PCoA) at genus level based on the Bray-Curtis distance indicated that the first two principal components make up 81.56 and 5.26% of the total variance contribution ratio in the bacterial community (Figure 1A), whereas the first two principal components make up 81.41 and 7.30% of the total variance contribution ratio in the fungal community (Figure 1B). There were significant differences in the bacterial community of samples from different depths at genus level ($p < 0.05$), but few differences were observed in the fungal community ($p > 0.05$). The unweighted pair-group method with arithmetic mean (UPGMA) distance analysis on genus level revealed that most of the samples from the same day with different depths were separated (Figures 1C,D).

3.1.3. Bacterial and fungal communities

A total of 194 OTUs were obtained based on 97% similarity threshold, and 7 fungal phyla, 13 fungal classes, 38 fungal orders, 58 fungal families, and 94 fungal genera were detected in vinegar *Pei* samples from both fermentation layers. At the phylum level, Firmicutes, Proteobacteria, and Actinobacteriota all possessed the highest abundance through the fermentation in both fermentation depths, which was similar to our previous report, but the abundance of Cyanobacteria, Bacteroidetes, and Deinococcus-Thermus was lower in the present study (Liu et al. (2021)). The abundance of Proteobacteria and Actinobacteriota was a little higher in the upper layer while that of Firmicutes was higher in the lower layer (Figures 2A–C). At the genus level, similar to our previous report (Liu et al., 2022), *Lactobacillus*, *Bacillus*, and *Acetobacter* were the top 3 genera through the fermentation in both fermentation depths (Figures 2D,E), but the abundance of *Lactobacillus* (74.98%) and *Bacillus* (11.14%) was higher in the lower layer while the abundance of *Acetobacter* (7.94%) was higher in the upper layer (Figure 2F). On the first day of fermentation, *Bacillus* was the predominant (28.64%), followed by *Lactobacillus* (14.35%) and *Streptomyces* (14.11%), which was different from previous reports (Liu

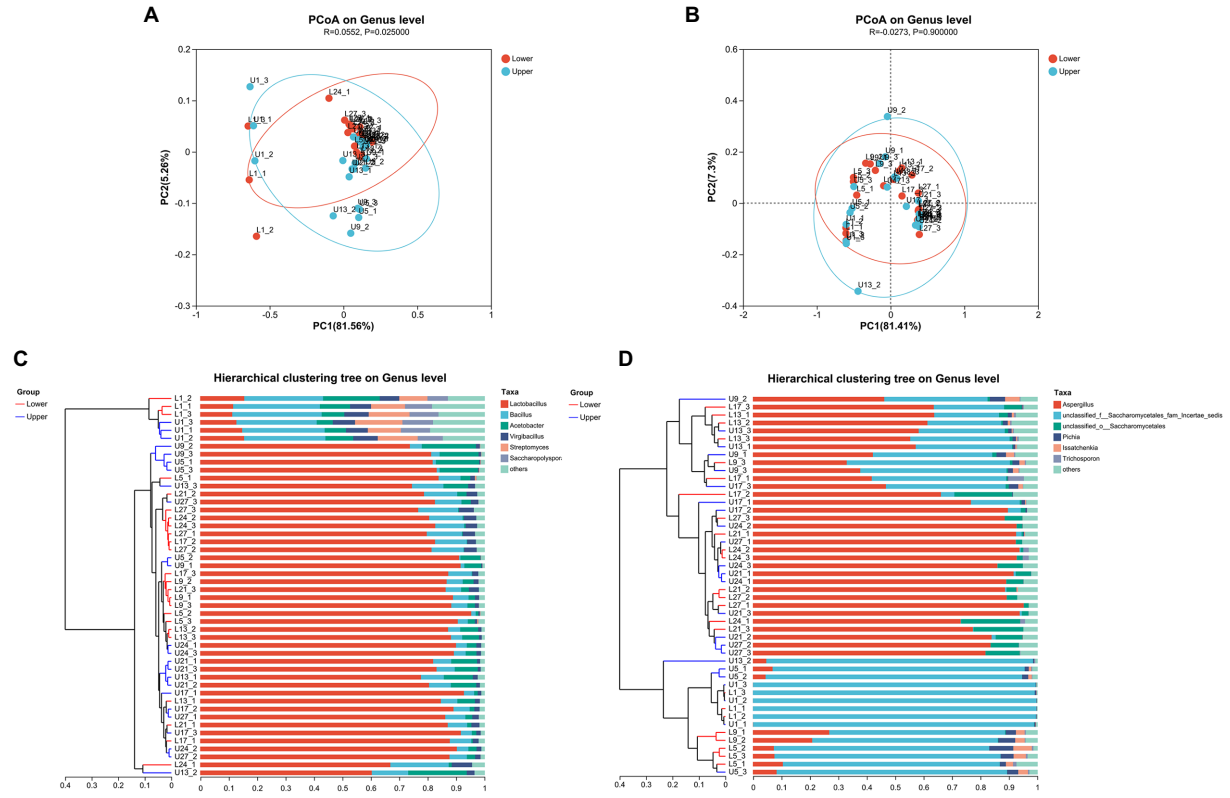

FIGURE 1
Principal coordinates analysis (PCoA) **(A)** and unweighted pair-group method with arithmetic mean (UPGMA) **(C)** analysis of bacterial community structure; PCoA **(B)** and UPGMA **(D)** analysis of fungal community structure.

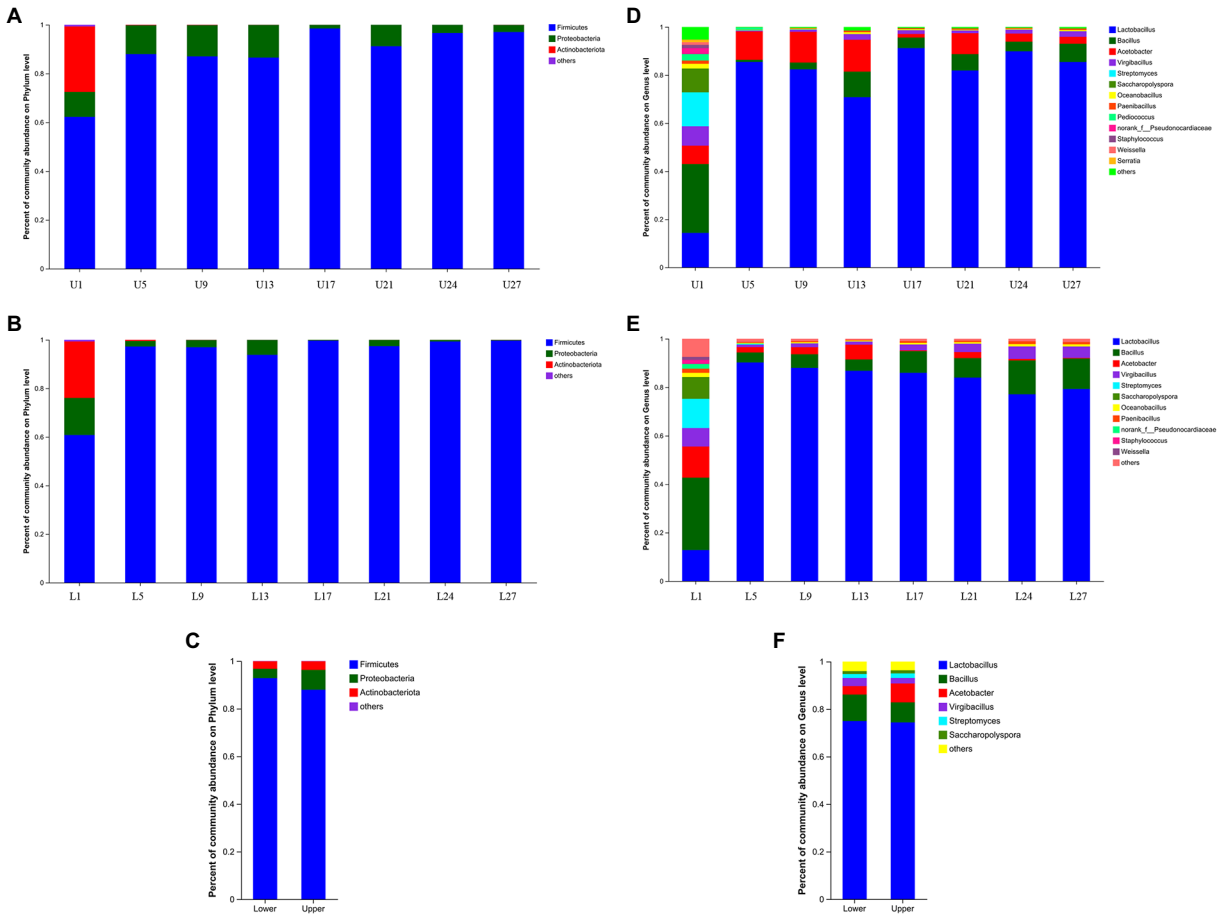

FIGURE 2
Relative abundance of the bacterial community structure. **(A)** The upper layer at phylum level, **(B)** the lower layer at phylum level, **(C)** the upper and lower layers at phylum level, **(D)** the upper layer at genus level, **(E)** the lower layer at genus level, **(F)** the upper and lower layers at genus level.

et al. (2021); Liu et al., 2022) and the reason might lie in the differences in environmental factors and microorganisms from materials, processing equipment, and surrounding environment. Afterward, *Lactobacillus* was predominant, ranging from 70.83 to 91.23% in the upper layer and 77.13 to 90.24% in the lower layer, respectively, which was not in agreement with the results of Zhenjiang aromatic vinegar and Shanxi mature vinegar (Huang et al., 2022; Kou et al., 2022). Generally, the abundance of *Lactobacillus* showed an increasing and then decreasing trend during the fermentation in the lower layer whereas no regular pattern was observed in the upper layer. The abundance of *Acetobacter* also changed without a regular pattern, but it was the highest on day 13 in both fermentation depths.

A total of 649 OTUs were obtained based on 97% similarity threshold, and 9 fungal phyla, 30 fungal classes, 69 fungal orders, 166 fungal families, and 316 fungal genera were detected in vinegar *Pei* samples from both fermentation layers. At the phylum level, Ascomycota and Basidiomycota possessed the highest abundance through fermentation in both fermentation depths, and the abundance of Ascomycota was far higher than that of Basidiomycota, which agreed with the study by Ai et al. (2019). Notably, the abundance of Ascomycota was higher in the lower layer (Figures 3A–C). At the genus level, *Aspergillus* was the predominant, followed by unclassified_f__Saccharomycetales_fam_Incertae_sedis, unclassified_o__Saccharomycetales, *Pichia* and *Apiotrichum* in the upper layer, while the predominant genera in the lower layer were *Aspergillus*, unclassified_f__Saccharomycetales_fam_Incertae_sedis, unclassified_o__Saccharomycetales, *Pichia* and *Issatchenkia* (Figures 3D,E). Generally, the abundance of *Aspergillus* increased with the fermentation, while unclassified_f__Saccharomycetales_fam_Incertae_sedis showed a decreasing trend. The changing trend of unclassified_o__Saccharomycetales, *Pichia*, and *Issatchenkia* were different in the upper and lower layers. The primary difference in the upper and lower layers was that the abundance of *Aspergillus* (48.30%), *Pichia* (1.49%), and *Issatchenkia* (1.11%) was higher at the lower layer (Figure 3F), which might be caused by more accessible oxygen in the upper layer.

Linear discriminant analysis effect size analysis (logarithmic LDA scores threshold of 2) was performed to identify bacterial (Figure 4A) and fungal (Figure 4B) taxa with significant abundance differences in different layers. *Virgibacillus*, *Paenibacillus*, *Oceanobacillus*, and 12 other bacterial genera were significantly enriched in the lower layer, while bacterial genera *Acetobacter* and *Kroppenstedtia* were significantly enriched in the upper layer. Fungal genus *Botrytis* was significantly enriched in the lower layer.

Analysis of similarities (ANOSIM; Supplementary Table S2) indicated that no significant differences were observed in the bacterial community of samples from the same day with different fermentation depths at OTU level ($p > 0.05$), however, there were significant

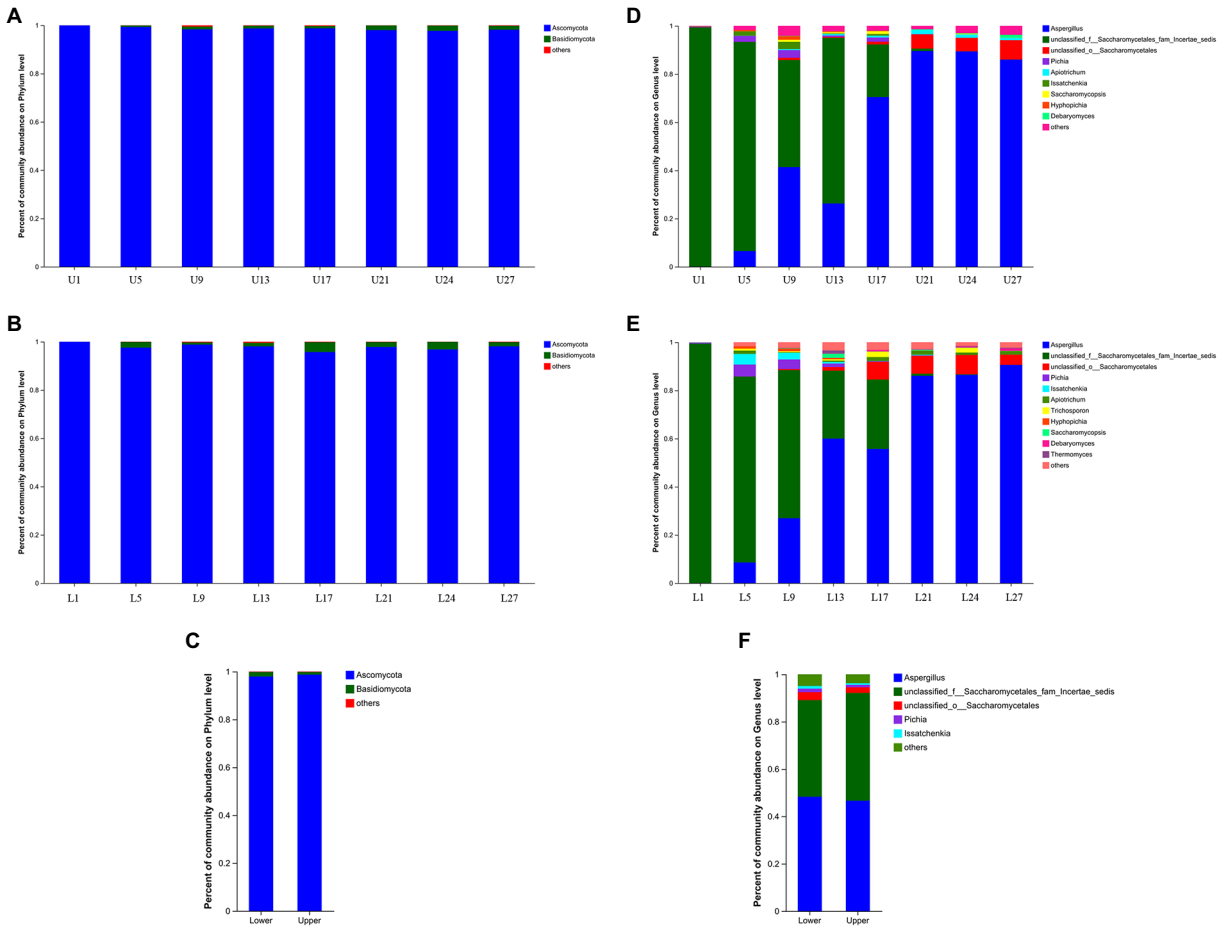

FIGURE 3
Relative abundance of the fungal community structure. **(A)** The upper layer at phylum level, **(B)** the lower layer at phylum level, **(C)** the upper and lower layers at phylum level, **(D)** the upper layer at genus level, **(E)** the lower layer at genus level, **(F)** the upper and lower layers at genus level.

differences between the bacterial community of samples from the same day with different fermentation depths at both phylum and genus levels ($p < 0.05$). As for the fungal community, no significant differences were observed in samples from different fermentation depths at OTU, phylum, and genus levels ($p > 0.05$).

3.1.4. PICRUSt and FUNGuild functional prediction

PICRUSt2 was applied to predict the bacterial function, and 6 types of biological metabolic pathways, including metabolism, genetic information processing, environmental information processing, human diseases, cellular processes, and organismal systems, were obtained by comparing with the KEGG database. Forty-four subfunctions were observed in the analysis of the secondary functional layer of the predicted genes, and differences were found between samples on the same day with different fermentation depths, especially for cell motility, circulatory system, and excretory system, etc. (Figure 5A). Metabolism was the primary pathway, and carbohydrate, amino acid, and energy metabolism of the microbiota were predicted (Figure 5B). As can be seen, more variations were observed at the third level. As for carbohydrate metabolism, the most obvious difference was in starch and sucrose metabolism.

FUNGuild was used to predict the function of the fungal community. As illustrated in Figure 5C, eight trophic modes were classified, and the "unassigned" was defined as OTUs that were not matched with any taxa. Saprotroph was the primary trophic mode throughout the fermentation, with relative abundance ranging from 93.88 to 99.72%. Saprotroph-symbiotroph was the second most abundant trophic mode in samples from day 1 to 13, while the type of the second most abundant trophic mode varied after day 17.

3.2. Content of total acid and pH of vinegar *Pei*

As shown in Figure 6, the total acid content increased with the fermentation in both layers, while pH showed a decreasing trend. Notably, there was no significant difference ($p > 0.05$) in both total acid content and pH of vinegar *Pei* collected on the same day with different depths, which might indicate a good processing control on vinegar production to some extent. RDA/CCA revealed that total acid and pH significantly affected the microbial community, and these two factors together explained 84.64 and 60.39% of the bacterial and fungal communities variation at genus level, respectively (Supplementary Figures S1A,C). The correlation between pH/total acid content and the top 10 abundant genera was evaluated by the spearman correlation heatmap. Both pH and total acid content were significantly correlated with bacterial genera *Acetobacter*, *Streptomyces*, *Saccharopolyspora*, and *Pediococcus* (Supplementary Figure S1B), while

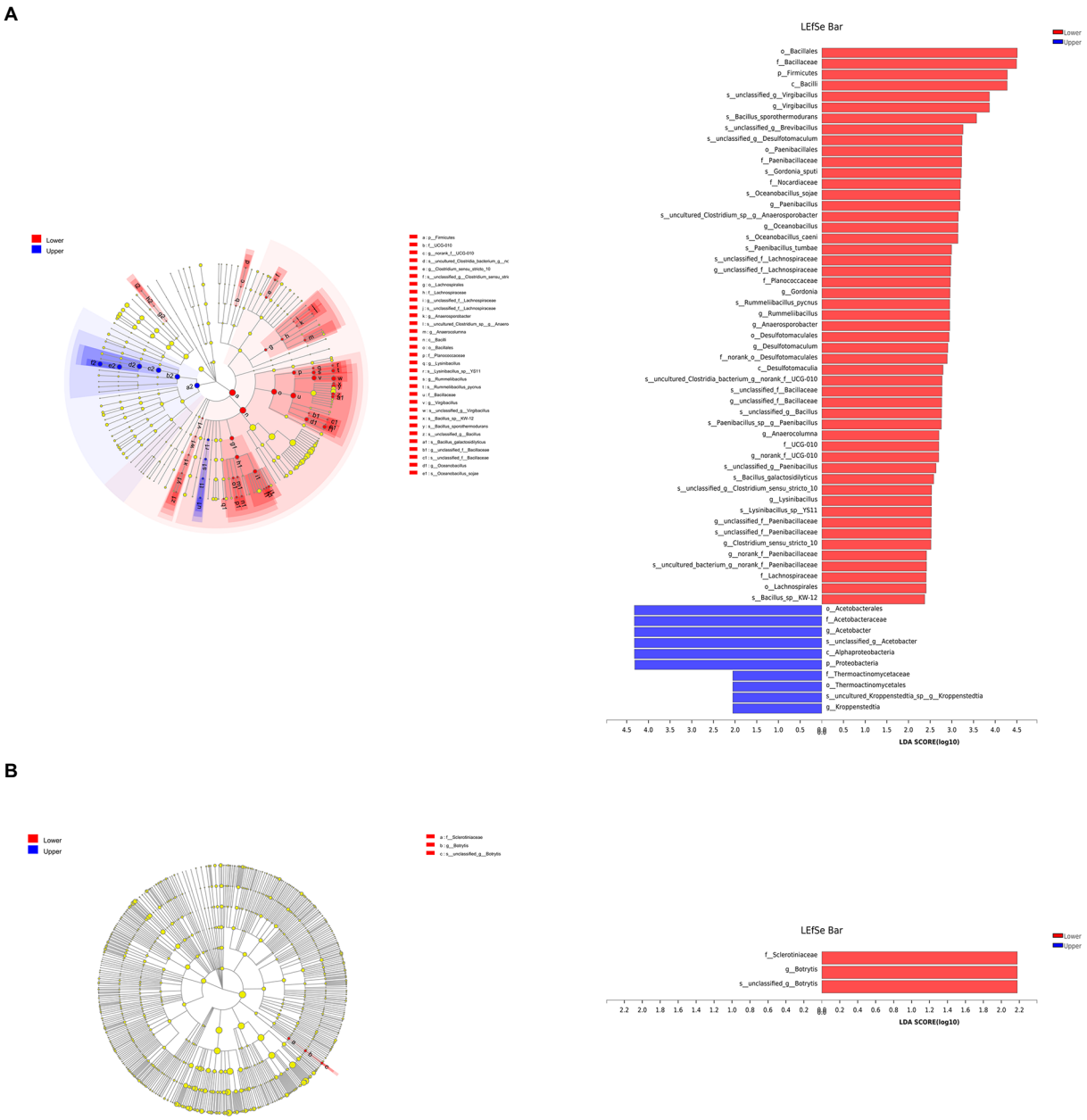

FIGURE 4
The bacterial **(A)** and fungal **(B)** communities of vinegar *Pei* were analyzed through Linear discriminant analysis effect size (LEfSe) to determine the optimal characteristic taxa.

significant correlations were observed between pH/total acid content and all the 10 most abundant fungal genera except *Trichisporon* and *Saccharomycopsis* (Supplementary Figure S1D; $p < 0.001$).

3.3. Volatile flavor compounds

The number of six common types of volatile flavor compounds, including esters, acids, alcohols, carbonyls, heterocyclic, and olefines, as well as their relative percentage composition were shown in Table 1. There were certain differences in both the number of volatile flavor compounds and their relative percentage composition between samples from the same day with different depths. Obvious differences were observed in the relative contents of acids and alcohols, which were primarily introduced by the content of acetic acid and phenethyl alcohol, respectively. Both the type and percentage of ester compounds were the most abundant throughout fermentation, with the relative percentage composition ranging from 26.97 to 50.25% after day 1, which agreed with the result by Jiang et al. (2019). Similar to the report by Gong et al. (2021), the relative content of alcohols was the second highest. After the beginning of fermentation, obvious differences in the relative percentage composition of ester compounds and acid compounds were observed on day 13, whereas that of alcohol compounds and carbonyl compounds were observed on days 9 and 9–13, respectively. Ethyl octanoate, ethyl acetate, ethyl caproate, phenethyl acetate, and ethyl phenylacetate, detected in various vinegars (Ríos-Reina et al., 2020; Pothimon et al., 2022; Xu et al.,

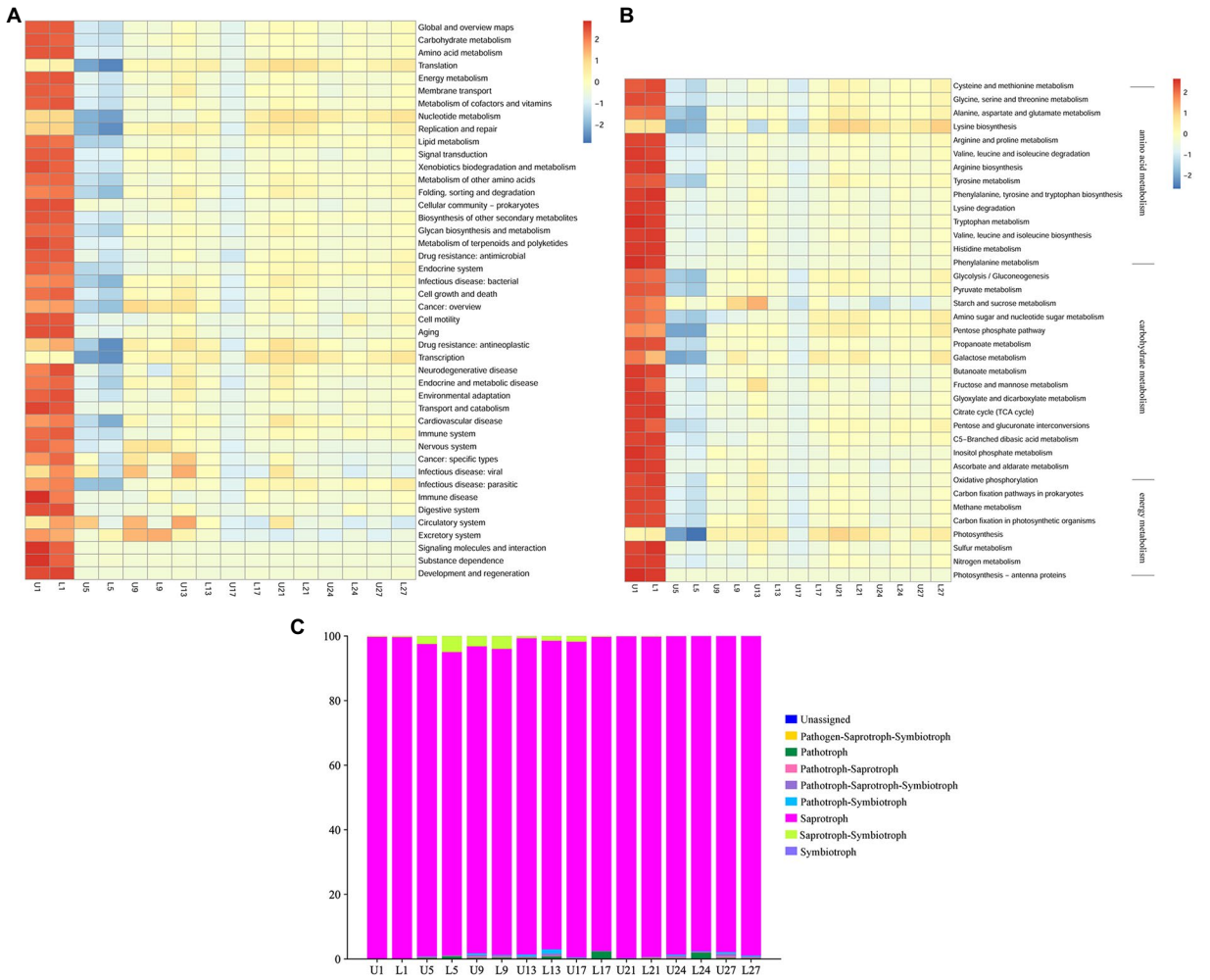

FIGURE 5
Heatmap showing the hierarchical clustering of predicted KEGG Orthologs functional profiles of the bacterial community at level 2 **(A)** and level 3 (carbohydrate, amino acid, and energy metabolism) **(B)**; Relative abundance of predicted trophic mode of fungi **(C)**.

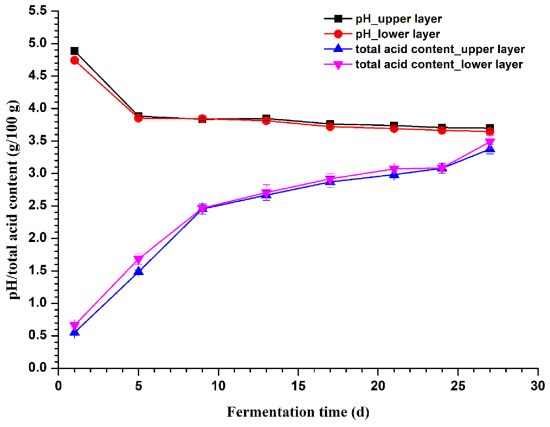

FIGURE 6
Changes in pH and total acid content of vinegar *Pei* during fermentation.

2022), were esters with high relative percentage. Tetramethyl pyrazine, a characteristic flavor and bioactive compound in vinegar (Li et al., 2016; Liu et al., 2021), was detected in vinegar *Pei* from both depths, and there was no significant difference in its relative content ($p > 0.05$). Notably, phenols such as 2-methoxy-5-methylphenol and 4-ethyl-2-methoxy-phenol, rarely reported in cereal vinegar, were produced, and 4-ethyl-2-methoxy-phenol was detected throughout the fermentation. Observable differences in their relative percentage were found between samples from the same day with different depths (data not shown).

The correlation between volatile flavor compounds and the 10 most abundant genera was revealed by the spearman correlation heatmap (Figure 7). Esters and acids showed significant correlations with *Bacillus*, *Virgibacillus*, *Oceanobacillus*, *Paenibacillus*, *Rummeliibacillus*, and *Trichosporon*. *Acetobacter* was significantly positively correlated with olefins, carbonyls and heterocyclic compounds ($p < 0.05$). Alcohols showed a significant correlation with *Pediococcus*, *Aspergillus*, *unclassified_f__Saccharomycetales_fam_Incertae_sedis*, *unclassified_o__Saccharomycetales*, *Pichia*, *Saccharopolyspora*, *Rummeliibacillus*, *Issatchenkia*, *Monascus*, and *Hyphopichia* ($p < 0.05$).

4. Conclusion

Significant differences between the bacterial community of samples from the same day with different fermentation depths at both phylum

TABLE 1 Number of volatile flavor compounds and their relative percentage composition (n/%) during vinegar fermentation.

Sample	Esters		Acids		Alcohols		Carbonyls		Heterocyclic		Olefines	
	Type	Percentage	Type	Percentage	Type	Percentage	Type	Percentage	Type	Percentage	Type	Percentage
U1	13	15.77 ± 0.76	6	35.31 ± 3.83	4	4.11 ± 0.68	10	4.19 ± 0.43	5	7.34 ± 1.04	1	3.88 ± 1.08
L1	17	14.05 ± 4.38	5	14.78 ± 4.96	7	23.31 ± 4.54	9	6.64 ± 1.09	4	8.87 ± 1.58	1	3.70 ± 0.18
U5	29	50.25 ± 4.65	5	1.05 ± 0.40	10	18.84 ± 3.55	7	5.66 ± 1.48	3	3.34 ± 1.39	1	0.42 ± 0.36
L5	22	48.33 ± 0.81	7	5.09 ± 1.50	10	16.60 ± 2.40	5	3.65 ± 0.71	2	7.52 ± 0.38	1	0.42 ± 0.42
U9	29	45.84 ± 3.64	7	13.84 ± 0.36	14	13.63 ± 4.00	7	5.41 ± 1.27	3	5.82 ± 1.54	3	0.81 ± 0.80
L9	27	35.81 ± 4.56	6	13.03 ± 5.18	15	27.20 ± 2.37	2	2.54 ± 0.69	3	3.71 ± 0.56	0	–
U13	21	26.97 ± 1.27	7	22.28 ± 5.27	15	20.34 ± 194	7	8.22 ± 0.43	4	5.30 ± 2.82	0	–
L13	25	45.48 ± 3.62	6	6.71 ± 0.74	11	19.85 ± 3.78	5	2.77 ± 0.48	2	6.24 ± 1.17	0	–
U17	25	31.23 ± 2.77	6	16.31 ± 7.39	13	20.94 ± 2.53	4	3.48 ± 0.68	3	4.28 ± 0.57	0	–
L17	21	28.89 ± 1.34	7	12.72 ± 3.21	13	18.09 ± 1.16	4	3.16 ± 0.92	3	4.29 ± 0.27	0	–
U21	24	36.45 ± 4.23	8	23.06 ± 1.69	17	23.42 ± 2.07	9	5.88 ± 3.01	1	0.68 ± 0.13	0	–
L21	24	32.60 ± 2.19	7	12.32 ± 0.84	14	22.28 ± 6.92	4	3.35 ± 1.14	3	3.73 ± 0.01	0	–
U24	24	40.60 ± 2.81	5	12.58 ± 7.44	13	22.13 ± 3.58	5	4.10 ± 0.40	2	4.08 ± 1.05	0	–
L24	23	35.83 ± 10.54	7	12.37 ± 2.73	13	28.35 ± 9.06	2	2.53 ± 0.05	2	3.02 ± 0.63	0	–
U27	26	42.00 ± 1.71	7	10.39 ± 4.89	14	23.87 ± 5.23	5	4.12 ± 0.70	3	2.38 ± 0.71	0	–
L27	27	39.79 ± 3.12	7	7.80 ± 1.50	15	27.90 ± 4.14	8	3.34 ± 0.58	2	1.42 ± 0.77	1	0.28 ± 0.24

-, not detected.

10.3389/fmicb.2023.1135912

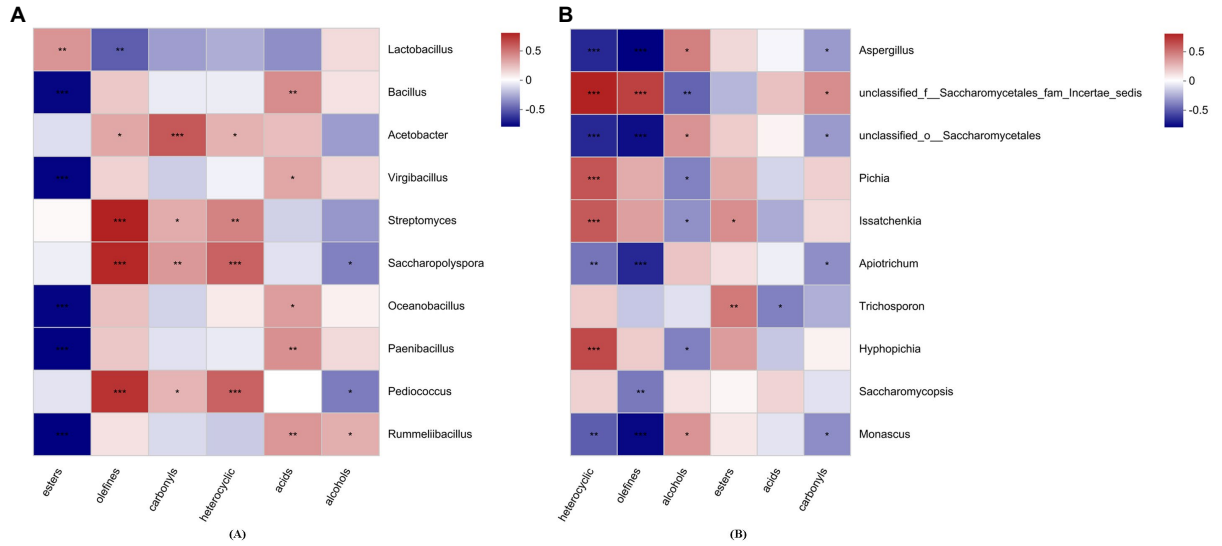

FIGURE 7
The correlation between volatile flavor compounds and the top 10 bacterial **(A)** and fungal **(B)** genera. *p <0.05, **p <0.01, ***p <0.001.

and genus levels were observed ($p < 0.05$), whereas no significant difference was observed in the fungal community. *Acetobacter* and *Kroppenstedtia* were significantly enriched in the upper layer. The function of microbiota was altered according to PICRUSt analysis, and the number of volatile flavor compounds and their relative percentage composition were affected by the microbial community at different depths. However, no significant difference was observed in total acid content. To the best of our knowledge, this has been the first study trying to explore the effects of fermentation depth on vinegar fermentation, which will provide insights into the quality control of cereal vinegar production. The changes in other vinegar quality attributes and detailed mechanisms under the effects of fermentation depth on microbiota composition and function need further study.

Data availability statement

The raw data supporting the conclusions of this article will be made available by the authors, without undue reservation.

Author contributions

AL: conceptualization, writing—original draft, writing—review and editing, and funding acquisition. YO, HS, and TM: methodology and data curation. QL, JL, KH, SC, and LH: writing—original draft. JZ: suggestions and resources. XA and YY: writing—review and editing. SL: writing—review and editing and supervision. All authors contributed to the article and approved the submitted version.

Funding

We appreciate the financial support from the Science and Technology Department of Sichuan Province (No. 2022NSFSC0116 and No. 2020YFN0133).

Conflict of interest

JZ is employed by Sichuan Baoning Vinegar Co., Ltd.

The remaining authors declare that the research was conducted in the absence of any commercial or financial relationships that could be construed as a potential conflict of interest.

Publisher's note

All claims expressed in this article are solely those of the authors and do not necessarily represent those of their affiliated organizations, or those of the publisher, the editors and the reviewers. Any product that may be evaluated in this article, or claim that may be made by its manufacturer, is not guaranteed or endorsed by the publisher.

Supplementary material

The Supplementary material for this article can be found online at: https://www.frontiersin.org/articles/10.3389/fmicb.2023.1135912/full#supplementary-material

References

Ai, M., Qiu, X., Huang, J., Wu, C., Jin, Y., and Zhou, R. (2019). Characterizing the microbial diversity and major metabolites of Sichuan bran vinegar augmented by Monascus purpureus. *Int. J. Food Microbiol.* 292, 83–90. doi: 10.1016/j.ijfoodmicro.2018.12.008

Chen, H., Chen, T., Giudici, P., and Chen, F. (2016). Vinegar functions on health: constituents, sources, and formation mechanisms. *Compr. Rev. Food Sci. Food Saf.* 15, 1124–1138. doi: 10.1111/1541-4337.12228

Gao, H., Zhao, Y., Wang, W., Xu, D., Sun, Y., Li, J., et al. (2022). Unraveling the chemosensory characteristics of typical Chinese commercial rice vinegars with multiple strategies. *Food Anal. Methods* 15, 1922–1935. doi: 10.1007/s12161-022-02260-z

Gong, M., Zhou, Z., Liu, S., Zhu, S., Li, G., Zhong, F., et al. (2021). Dynamic changes in physico-chemical attributes and volatile compounds during fermentation of Zhenjiang vinegars made with glutinous and non-glutinous japonica rice. *J. Cereal Sci.* 100:103246. doi: 10.1016/j.jcs.2021.103246

Haruta, S., Ueno, S., Egawa, I., Hashiguchi, K., Fujii, A., Nagano, M., et al. (2006). Succession of bacterial and fungal communities during a traditional pot fermentation of rice vinegar assessed by PCR-mediated denaturing gradient gel electrophoresis. *Int. J. Food Microbiol.* 109, 79–87. doi: 10.1016/j.ijfoodmicro.2006.01.015

Huang, T., Lu, Z. M., Peng, M. Y., Liu, Z. F., Chai, L. J., Zhang, X. J., et al. (2022). Combined effects of fermentation starters and environmental factors on the microbial community assembly and flavor formation of Zhenjiang aromatic vinegar. *Food Res. Int.* 152:110900. doi: 10.1016/j.foodres.2021.110900

Jiang, Y., Lv, X., Zhang, C., Zheng, Y., Zheng, B., Duan, X., et al. (2019). Microbial dynamics and flavor formation during the traditional brewing of Monascus vinegar. *Food Res. Int.* 125:108531. doi: 10.1016/j.foodres.2019.108531

Kong, H., Kim, S. H., Jeong, W. S., Kim, S. Y., and Yeo, S. H. (2022). Microbiome analysis of traditional grain vinegar produced under different fermentation conditions in various regions in Korea. *Foods* 11:3573. doi: 10.3390/foods11223573

Kou, R., Li, M., Xing, J., He, Y., Wang, H., and Fan, X. (2022). Exploring of seasonal dynamics of microbial community in multispecies fermentation of Shanxi mature vinegar. *J. Biosci. Bioeng.* 133, 375–381. doi: 10.1016/j.jbiosc.2022.01.003

Li, S., Li, P., Feng, F., and Luo, L. X. (2015). Microbial diversity and their roles in the vinegar fermentation process. *Appl. Microbiol. Biotechnol.* 99, 4997–5024. doi: 10.1007/s00253-015-6659-1

Li, S., Li, P., Liu, X., Luo, L., and Lin, W. (2016). Bacterial dynamics and metabolite changes in solid-state acetic acid fermentation of Shanxi aged vinegar. *Appl. Microbiol. Biotechnol.* 100, 4395–4411. doi: 10.1007/s00253-016-7284-3

Li, Q., Li, L., Zhu, H., Yang, F., Xiao, K., Zhang, L., et al. (2022). Lactobacillus fermentum as a new inhibitor to control advanced glycation end-product formation during vinegar fermentation. *Food Sci. Hum. Wellness* 11, 1409–1418. doi: 10.1016/j.fshw.2022.04.031

Liu, L., Hu, H., Yu, Y., Zhao, J., Yuan, L., Liu, S., et al. (2021). Characterization and identification of different Chinese fermented vinegars based on their volatile components. *J. Food Biochem.* 45:e13670. doi: 10.1111/jfbc.13670

Liu, A., Pan, W., Li, S., Li, J., Li, Q., He, L., et al. (2022). Seasonal dynamics of microbiota and physicochemical indices in the industrial-scale fermentation of Sichuan Baoning vinegar. *Food Chem. X* 16:100452. doi: 10.1016/j.fochx.2022.100452

Liu, A., Peng, Y., Ao, X., Pan, W., Chen, S., He, L., et al. (2020). Effects of Aspergillus Niger biofortification on the microbial community and quality of Baoning vinegar. *LWT* 131:109728. doi: 10.1016/j.lwt.2020.109728

Liu, A., Wang, R., Li, J., Li, Q., He, L., Chen, S., et al. (2021). Multiple rounds of Aspergillus Niger biofortification confer relatively stable quality with minor changes of microbial community during industrial-scale Baoning vinegar production. *Food Res. Int.* 150:110768. doi: 10.1016/j.foodres.2021.110768

Lynch, K. M., Zannini, E., Wilkinson, S., Daenen, L., and Arendt, E. K. (2019). Physiology of acetic acid bacteria and their role in vinegar and fermented beverages. *Compr. Rev. Food Sci. Food Saf.* 18, 587–625. doi: 10.1111/1541-4337.12440

Pothimon, R., Krusong, W., Daetae, P., Tantratian, S., and Gullo, M. (2022). Determination of antifungal volatile organic compounds of upland rice vinegar and their inhibition effects on Aspergillus flavus in dried chili pepper. *Food Biosci.* 46:101543. doi: 10.1016/j.fbio.2022.101543

Rathbun, B. L., and Shuler, M. L. (1983). Heat and mass transfer effects in static solid–substrate fermentations: design of fermentation chambers. *Biotechnol. Bioeng.* 25, 929–938. doi: 10.1002/bit.260250405

Ridder, E. R., Nokes, S. E., and Knutson, B. L. (1999). Optimization of solid-state fermentation parameters for the production of xylanase by Trichoderma longibrachiatum on wheat bran in a forced aeration system. *Trans. ASAE* 42, 1785–1790. doi: 10.13031/2013.13342

Ríos-Reina, R., Segura-Borrego, M. P., Morales, M. L., and Callejón, R. M. (2020). Characterization of the aroma profile and key odorants of the Spanish PDO wine vinegars. *Food Chem.* 311:126012. doi: 10.1016/j.foodchem.2019.126012

Sengun, I. Y., Kilic, G., Charoenyingcharoen, P., Yukphan, P., and Yamada, Y. (2022). Investigation of the microbiota associated with traditionally produced fruit vinegars with focus on acetic acid bacteria and lactic acid bacteria. *Food Biosci.* 47:101636. doi: 10.1016/j.fbio.2022.101636

Vegas, C., González, Á., Mateo, E., Mas, A., Poblet, M., and Torija, M. J. (2013). Evaluation of representativity of the acetic acid bacteria species identified by culture-dependent method during a traditional wine vinegar production. *Food Res. Int.* 51, 404–411. doi: 10.1016/j.foodres.2012.12.055

Wang, D., Wang, M., Cao, L., Wang, X., Sun, J., Yuan, J., et al. (2022). Changes and correlation of microorganism and flavor substances during persimmon vinegar fermentation. *Food Biosci.* 46:101565. doi: 10.1016/j.fbio.2022.101565

Wu, J., Gullo, M., Chen, F., and Giudici, P. (2010). Diversity of Acetobacter pasteurianus strains isolated from solid-state fermentation of cereal vinegars. *Curr. Microbiol.* 60, 280–286. doi: 10.1007/s00284-009-9538-0

Wu, Q., Min, Y., Xiao, J., Feng, N., Chen, Y., Luo, Q., et al. (2019). Liquid state fermentation vinegar enriched with catechin as an antiglycative food product. *Food Funct.* 10, 4877–4887. doi: 10.1039/C8FO01892H

Xu, S., Ma, Z., Chen, Y., Li, J., Jiang, H., Qu, T., et al. (2022). Characterization of the flavor and nutritional value of coconut water vinegar based on metabolomics. *Food Chem.* 369:130872. doi: 10.1016/j.foodchem.2021.130872

Yuan, X., Chen, X., Virk, M. S., Ma, Y., and Chen, F. (2021). Effects of various rice-based raw materials on enhancement of volatile aromatic compounds in Monascus vinegar. *Molecules* 26:687. doi: 10.3390/molecules26030687

Zeng, Y., Wang, Y., Chen, Q., Xia, X., Liu, Q., Chen, X., et al. (2022). Dynamics of microbial community structure and enzyme activities during the solid-state fermentation of Forgood Daqu: a starter of Chinese strong flavour Baijiu. *Arch. Microbiol.* 204:577. doi: 10.1007/s00203-022-03198-w

Zhang, X., Zhang, X., Yan, Y., Liu, Y., Zhao, X., Xu, H., et al. (2022). Relationship between flavor compounds and changes of microbial community in the solid fermented vinegar. *Biosci. Biotech. Bioch.* 86, 1581–1589. doi: 10.1093/bbb/zbac143

Zhao, Y., Suyama, T., Wu, Z., and Zhang, W. (2022). Characterization of variations and correlations between flavor metabolites and microbial communities of industrial paocai brine during fermentation. *J. Food Process. Preserv.* 46:e16859. doi: 10.1111/jfpp.16859

frontiers | Frontiers in Microbiology

TYPE Review
PUBLISHED 22 February 2023
DOI 10.3389/fmicb.2023.1120659

OPEN ACCESS

EDITED BY
Jinxuan Cao,
Beijing Technology and Business University, China

REVIEWED BY
Zheng Han,
Shanghai Academy of Agricultural Sciences, China
Zhaowei Zhang,
Oil Crops Research Institute (CAAS), China

*CORRESPONDENCE
Tunyaluk Bouphun
tunyaluk@rmutl.ac.th
Yao Zou
zouyao82@163.com

†These authors have contributed equally to this work and share first authorship

SPECIALTY SECTION
This article was submitted to Food Microbiology, a section of the journal Frontiers in Microbiology

RECEIVED 10 December 2022
ACCEPTED 01 February 2023
PUBLISHED 22 February 2023

CITATION
Xu W, Zhao Y-q, Jia W-b, Liao S-y, Bouphun T and Zou Y (2023) Reviews of fungi and mycotoxins in Chinese dark tea. *Front. Microbiol.* 14:1120659. doi: 10.3389/fmicb.2023.1120659

Reviews of fungi and mycotoxins in Chinese dark tea

Wei Xu[1†], Yi-qiao Zhao[1†], Wen-bao Jia[1], Si-yu Liao[1], Tunyaluk Bouphun[2]* and Yao Zou[1]*

[1]College of Horticulture, Tea Refining and Innovation Key Laboratory of Sichuan Province, Sichuan Agricultural University, Chengdu, China, [2]Faculty of Science and Agricultural Technology, Rajamangala University of Technology Lanna Lampang, Lampang, Thailand

The fermentation is the main process to form the unique flavor and health benefits of dark tea. Numerous studies have indicated that the microorganisms play a significant part in the fermentation process of dark tea. Dark tea has the quality of "The unique flavor grows over time," but unscientific storage of dark tea might cause infestation of harmful microorganisms, thereby resulting in the remaining of fungi toxins. Mycotoxins are regarded as the main contributor to the quality of dark tea, and its potential mycotoxin risk has attracted people's attention. This study reviews common and potential mycotoxins in dark tea and discusses the possible types of masked mycotoxins in dark tea. A summary of the potential risks of mycotoxins and masked mycotoxins in dark tea is presented, intending to provide a reference for the prevention and risk assessment of harmful fungi in dark tea.

KEYWORDS

dark tea, mycotoxins, fungi, contamination, masked mycotoxins

1. Introduction

Dark tea, one of the six major tea groups, is a post-fermented tea that is produced by solid-state fermentation involving microorganisms (Wang et al., 1991a). In recent years, it has been proven that dark tea produces many specific products that are not found in other teas during processing, for which the damp-heat effect and microbial extracellular enzymes are accountable (Wang et al., 1991b; Qi et al., 2004; Chen and Qi, 2010). Different kinds of dark tea have been found to have their own dominant fungal strains during the processes of fermentation and storage (Xiong, 2017), and parts of these strains can synthesize fungal toxins.

Mycotoxins widely existed in all kinds of food, which is a serious threat to human health and safety, which has become one of the most important issues in the field of food safety (Bhat et al., 2010; Medina et al., 2015, 2017; Haque et al., 2020; Martínez-Culebras et al., 2021; Zhang et al., 2021). Mycotoxins are secondary metabolites produced by fungi that may be harmful to humans when ingested, inhaled, or in contact with skin (Marin et al., 2013). Fungi of many genera produce fungal toxins, mainly *Aspergillus*, *Penicillium*, *Alternaria*, *Fusarium*, and *Claviceps* genus (Murugesan et al., 2015; Jiang et al., 2018; Wang G. et al., 2020). The common fungal toxins are aflatoxins (AFTs), ochratoxins (OTs), deoxynivalenol (DON), fumonisins (FUMs), zearalenone (ZEN), patulin (PAT), and Citrinins (CITs) (Haque et al., 2020; Vargas Medina et al., 2021). There are also masked mycotoxins that have been overlooked in previous testing and assessment (Tan et al., 2016). The main dominant microorganisms and potentially contaminating mycotoxins in dark tea are shown in Figure 1. Recent evidence suggests that mycotoxins were detected in fermented tea (Liu et al., 2016; Mo et al., 2016; Hu et al., 2019; Xu W. et al., 2019), which indicated that there is indeed a possibility that dark tea is contaminated with mycotoxins during the production and processing as well as storage processes.

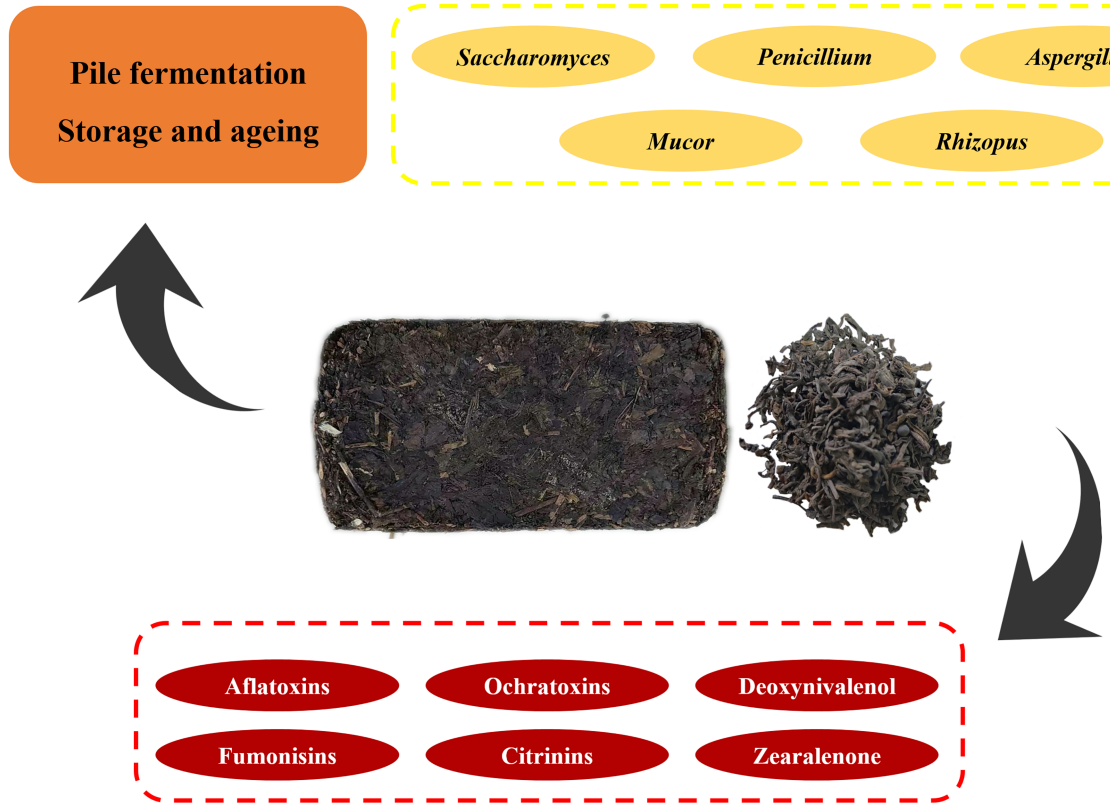

FIGURE 1
The main dominant microorganisms and potentially contaminating mycotoxins in dark tea.

There exist several methods for measuring the mycotoxins, for instance: thin-layer chromatography (TIC)(Zhao et al., 2016), enzyme-linked immunosorbent assay (ELISA)(Li et al., 2016; Zhang, 2017; Zhu et al., 2017), high performance liquid chromatography (HPLC) (Kong et al., 2014; Li and He, 2020; Iqbal et al., 2021), liquid chromatography–tandem mass spectrometry (LC–MS/MS) (Kresse et al., 2019; York et al., 2020), and gas chromatography (GC) (Li et al., 2000; Lin et al., 2013). The currently existing measuring methods of mycotoxins have trouble detecting the masked mycotoxins in dark tea (Tan et al., 2016). Therefore, we need to pay more attention to the safety of dark tea during production and storage to ensure the health and safety of consumers. This paper reviews the contamination status and contamination levels of common mycotoxin species in dark tea, also speculates on the masked mycotoxins that may exist in dark tea, and discusses the main microbial sources of mycotoxin production in dark tea and the possible ways to cause mycotoxin contamination processes in dark tea, which may provide a reference for food safety policymakers and researchers.

2. Common fungal toxins in dark tea

2.1. Aflatoxin

Aflatoxins (AFTs) are a class of secondary metabolites produced by *Aspergillus parasiticus* and *Aspergillus flavus* (Piekkola et al., 2012). Aflatoxins are readily produced by *Aspergillus flavus* under relatively high air humidity and temperature conditions (Yu et al., 2004). Aflatoxins can be classified into several types, such as B_1, B_2, G_1, and G_2. Among them, aflatoxin B_1 (AFB_1) is the most toxic and has been classified as a class I carcinogen by the World Health Organization Cancer Research Unit (Yogendrarajah et al., 2015).

Currently, numerous studies have indicated that there is a risk of aflatoxins in dark tea. Liu et al. (2016) used high performance liquid chromatography–tandem mass spectrometry (HPLC–MS) for testing 10 samples of Pu-erh tea, among which AFB_1 was detected in two samples at 3.1 μg/kg and 7.5 μg/kg, respectively. Wu J. (2013) used HPLC to detect AFB_1 in seven samples at concentrations greater than 5 μg/kg in 60 samples of Pu-erh tea. Cui et al. (2020) examined 158 dark tea samples by liquid chromatography-mass spectrometry, two of which tested positive for aflatoxins. One Kangzhuan tea contained 2.07 μg/kg of AFB_1; the other Fuzhuan tea contained four aflatoxins at concentrations of AFB_1: 1.24 μg/kg, AFB_2: 0.78 μg/kg, AFG_1: 0.81 μg/kg, AFG_2: 1.04 μg/kg. The previous reports have shown that dark tea has the possibility of being contaminated with aflatoxins, but levels and detection rates of aflatoxins are very low, so the risk exposure level of aflatoxin in dark tea is very low. Aflatoxin, as a highly toxic carcinogen, has always been a great concern for tea consumers. Therefore, the most effectively way to prevent dark tea from being contaminated by exogenous aflatoxin during processing and storage is an issue worthy of attention and consideration.

2.2. Ochratoxins

Ochratoxin (OTs) is a group of secondary metabolites produced by fungi *Aspergillus* and *Penicillium* (Wang et al., 2018). Ochratoxins were first isolated by Vander Merwe from the metabolites of

Aspergillus ochraceus (Van der Merwe et al., 1965). Ochratoxin is classified into several types based on its structure, including A, B, C, and, with ochratoxin A (OTA) ranking first. Available studies have demonstrated that OTA is nephrotoxic, hepatotoxic, immunotoxic, genotoxic, neurotoxic, and teratogenic (Chen et al., 2018). It is classified by the International Agency for Research on Cancer (IARC) as a renal carcinogen in animals and a probable carcinogen in humans. OTA contaminates a variety of crops and teas (Zhang, 2017; Deng et al., 2020; He et al., 2020; Zhao et al., 2022), with the main OTA-producing fungi differing depending on environmental conditions. The main fungi that produce OTA are shown in Table 1 (Sánchez-Hervás et al., 2008; Iqbal et al., 2014; Wang et al., 2016; Deng et al., 2020). Only parts of some strains of *Aspergillus niger* have the ability to produce OTA. There are differences in the ability to synthesize OTA on different substrates and under different environmental conditions (Deng et al., 2020).

Many researchers have tested OTA in dark tea using various testing techniques, and the results are detailed in Table 2. Combined with the above results, it can be observed that OTA in dark tea has a certain exposure risk. Many *Aspergillus* spp. fungi are dominant in the processing of dark tea, which is closely related to the formation of dark tea sensory quality (Wu J., 2013; Xiong, 2017). On the other hand, Fungi of the genus *Penicillium* have been detected during the storage of dark tea (Haas et al., 2013). OTA-producing fungi have similar strains to the dominant fungi in dark tea solid-state fermentation and storage As a result, there is a risk of OTA exposure during both the processing and storage of dark tea. The dominant strains in dark tea during the solid-state fermentation process are similar to many OTA-producing strains, but OTA is not only present in dark tea samples. OTA has been found in black and green tea samples, according to some studies (Santos et al., 2009; Malir et al., 2014). This indicates that the source of OTA in dark tea has two possibilities, therefore we should pay much more attention to fungal production of toxicity and exogenous contamination. And Zhao Z. et al. (2021) and Zhou et al. (2015a,b) isolated OTA-producing strains from dark tea samples.

TABLE 1 The main fungi producing OTA.

Genus	Species
Aspergillus	*A. niger, A. carbonarius, A. ochraceus, A. affinis, A. terreus, A. fumigatus, A. versicolor, A. tubingensis, A. petrakii, A. sclerotiorum, A. westerdii. A. tubingensis, A. petrakii, A. sclerotiorum, A. westerdijkiae, A. alliaceus, A. sulphureus, A. melleu, A. parasiticus, A. sulphureus, A. melleu, A. sulphureus. A. parasiticus, A. welwitschiae*
Penicillium	*P. verrucosum, P. variabile, P. nordicum, P. cyclopium, P. chrysogenum, P. polonicum, P. viridicatum*

2.3. Citrinin

Citrinin (CIT) was originally isolated from cultures of *Penicillium citrinum* by Hetherington and Raistrick (1931). CIT is a well-known hepatorenal toxin that causes functional and structural kidney damage as well as debilitation of liver metabolism (Flajs and Peraica, 2009; Vidal et al., 2018). In recent years, CIT has received much attention due to its toxic effects on mammals and its widespread presence in foods, where it is usually found together with OTAs (Silva et al., 2021). The main CIT-producing fungi are similar to the OTA-producing ones, mainly *Penicillium* and *Aspergillus* fungi (Sengling Cebin Coppa et al., 2019).

The kidney is the main target organ for the toxic effects of CIT, and there are also reports of CIT effects on the liver and bone marrow (Magan and Olsen, 2004). CIT is a fungal toxin widely present in food, and there is a possibility that dark tea is contaminated with CIT. Li and He (2020) examined 113 tea samples of Liupao tea from different years by HPLC, 37 positive CIT samples with a CIT content of 7.8–206.1 μg/kg were detected. Zhou et al. (2015a,b) isolated an OTA-producing *Penicillium chrysogenum* dominant strain from Pu-erh tea by inoculating it on raw dark tea with 35% moisture content at 30°C for 25 days, and the CIT content was 26.30 μg/kg.

Since the majority of OTA-producing fungi can produce CIT (Silva et al., 2021), OTA was also detected in many tea samples, which forced us to consider whether OTA-producing fungi in dark tea will also produce CIT. Bugno et al. (2006) isolated 10 genera of molds from herbs, 89.9% of the fungi were *Aspergillus* and *Penicillium* spp., and 21.97% of both *Aspergillus* and *Penicillium* spp. were able to produce CIT. Two hundred and sixty strains of *Penicillium* spp. were isolated from cereals and fruits by Andersen et al. (2004), and 85% of *Penicillium* spp. were able to produce CIT. In recent years, many other researchers have isolated and identified *Penicillium citrinum* from dark tea. Haas et al. (2013) isolated and identified two strains of

TABLE 2 OTA detection in dark tea samples.

Dark tea types	Method	Positive rate	Contents (μg/kg)	References
Wet storage fermented dark tea	ELISA	100%	Less than 50	Liu et al. (2011)
Pu-erh Tea	HPLC	11%	0.65–94.7	Haas et al. (2013)
Pu-erh tea, etc.	HPLC–MS/MS	4%	0.22–0.44	Mo et al. (2016)
Pu-erh tea, Fu tea, etc.	UPLC–MS /MS	4%	4.2	Liu et al. (2016)
Pu-erh tea, etc.	UPLC-MS /MS	8%	0.9–6.7	Liu et al. (2017)
Pu-erh Tea	LC-MS/MS	0%	ND	Hu et al. (2019)
Pu-erh tea, Liupao tea, etc.	HPLC	1.85%	34.9–36.8	Ye et al. (2020)
Dark tea	HPLC	9.2%	2.51–12.62	Zhao et al. (2022)

Penicillium citrinum from traditional Pu-erh tea loose tea, three strains in organic Pu-erh tea loose tea, and three strains in tightly pressed Pu-erh tea, respectively. Su (2018) isolated and identified 34 fungal strains from four commercially available dark tea samples, including four strains of *Penicillium oryzae*. Zhao (2012) and Hu et al. (2020) isolated and identified *Penicillium citrinum* from 'flowering' of Fuzhuan tea and finished dark tea, respectively. *Aspergillus* spp. and *Penicillium* spp. fungi are very common in the production and processing of dark tea. *Penicillium citrinum* is also more common in dark tea. Therefore, there is a certain risk exposure level for CIT in dark tea, which poses potential health hazards to consumers. There are relatively few studies on CIT in dark tea samples, and there is almost no standard limit on the amount of CIT in dark tea.

2.4. Deoxynivalenol

Deoxynivalenol (DON), also known as vomitoxin, is named for its ability to cause vomiting in pigs. This is a secondary metabolite produced by *toxigenic Fusarium* species and others, combined with the high rate of contamination in both cereals and their products (Chen et al., 2017; Csikós et al., 2020; Wang and Wang, 2021; Yang et al., 2021). DON is potentially harmful to both humans and animals when it enters the food chain, such as causing loss of appetite, immunosuppression, nausea, and vomiting, and has been classified as a Class III carcinogen by the European Union (Pereira et al., 2019).

Although DON is mostly detected in cereals and their products, the researchers have not paid sufficient attention to it. In recent years, it has been reported that tea also has the possibility of being contaminated by DON. Yan (2019) examined 61 fermented dark tea samples, and DON was detected in three samples, including one Pu-erh tea with 8.6 μg/kg and two Hunan dark tea with 70.1 and 299.5 μg/kg, respectively. Hu et al. (2019) examined 174 Pu-erh tea samples, DON was detected in 30.63% of the samples. Although the content of DON in the detected dark tea samples is far below the limit, we should pay much more attention to DON, which can protect the health of consumers and promote the sustainable development of dark tea.

2.5. Masked mycotoxins

Masked mycotoxins, usually conjugated mycotoxins, are mycotoxin derivatives formed by microbial transformation, degradation, hydrolysis, reduction, glycosylation, formylation, etc. Most masked mycotoxins are less toxic or non-toxic than their original mycotoxins. However, some masked mycotoxins are not completely transformed and degraded, and under some specific conditions, these masked mycotoxins can be reconverted to mycotoxins under certain conditions (Berthiller et al., 2013; Tan et al., 2016).

The detection of masked mycotoxins is relatively cumbersome. In the initial studies, the "indirect method" was usually used as a quantitative method to detect the amount of masked mycotoxins. With the constant development of analytical techniques, the direct detection of masked mycotoxins has become more common. Currently, commonly used direct detection methods include LC–MS/MS and ELISA. LC–MS/MS method has been widely used for the detection of mycotoxin residues in cereals, grains, oils, and other foods for its high selectivity and sensitivity (Lozowicka et al., 2022). LC–MS/MS can simultaneously detect different components in mixed samples, so that masked mycotoxins, their prototypes, metabolites, and even different types of mycotoxins can be quantified simultaneously. Vendl et al. (2009) used LC–MS/MS to simultaneously quantify DON and ZON prototypes and their eight masked mycotoxins in cereal foods. Due to the shortage of commercial standards, studies on the quantitative analysis of masked mycotoxins are significantly limited. However, ELISA may respond to masked mycotoxins (Berthiller et al., 2013). The mycotoxins detection studies in tea, where results of the test by ELISA were mostly positive for mycotoxins (Santos et al., 2009; Liu, 2011), also forced us to think, whether there are also masked mycotoxins in tea.

Also, the detection of mycotoxins exposure levels in dark tea is mainly for their prototypes and little attention has been paid to the risk of masked mycotoxins. There are only a few reports on the preparation of standards, anabolic pathways of masked mycotoxins (Tan et al., 2016), which is the reason that masked mycotoxins deserve further attention and research. The common masked mycotoxins are masked trichothecenes, masked ZEN, masked fumonisins, masked OTA etc. Table 3 shows the common masked mycotoxins in naturally contaminated foods.

In addition to these masked mycotoxins detected in naturally contaminated food, there are also masked mycotoxins that have been identified but not yet observed in naturally contaminated food. All of the prototypes of mycotoxins mentioned above have been found in dark tea. Whether it forms masked mycotoxins in the same condition. Whether the masked mycotoxins are harmful to consumers. These questions force us to investigate more in the future.

3. Microbial sources of fugal toxins in Chinese dark tea

Dark tea belongs to the post-fermented tea category, and microorganisms participate and play an equally important role in its production and processing. Many researchers have isolated and identified the dominant microorganisms from the production and processing of dark tea as well as from the finished tea, and the more common dominant microbial genera are shown in Table 4.

As can be seen from Table 4, fungi of the genera *Aspergillus* and *Penicillium* play a very significant role in the processing of dark tea. There has been a lot of research on the dominant microorganisms of different types of dark tea, but there has been little research on whether these dominant microorganisms can produce fungus-derived toxins.

3.1. *Aspergillus*

Many *Aspergillus* spp. fungi are the dominant species in the production and processing of dark tea and have a strong relationship with the formation of dark tea quality (Jiang, 2012a; Wu J., 2013; Xiong, 2017). At present, only *Eurotium cristatum* has been specified by the Chinese national standard as the physicochemical index of Fuzhuan tea.

There are parts of fungi in the genus *Aspergillus* that produce mycotoxins, such as *Aspergillus flavus*, *Aspergillus fumigatus*, *Aspergillus niger*, and *Aspergillus versicolor*.

TABLE 3 Common masked mycotoxins.

Classify	Masked mycotoxin	Contaminated food	References
Masked trichothecenes	DON-3-glucoside	Wheat; malts; maize	Savard (1991)
	DON-3-glucoside; DON-15-glucoside	Wheat; maize	Berthiller et al. (2005)
	DON-3-glucoside	Wheat	Kluger et al. (2015)
	DON-3-glucoside	Beer	Kostelanska et al. (2009)
	3-AcDON; 15-AcDON; DON-3-glucoside	Wheat	Palacios et al. (2017)
	T-2 toxin 3-O-glucoside; HT-2 toxin 3-O-glucoside	Wheat; oat	Busman et al. (2011)
	T-2 toxin-di-glucoside; HT-2 toxin-di-glucoside	Corn powder	Nakagawa et al. (2013)
	T2-3-glucoside; HT2-3-glucoside; HT2-4-glucoside	Wheat; oats	Lattanzio et al. (2012)
Masked ZEN	Z14G	Wheat	Schneweis et al. (2002)
	Z14S	Wheat flour; bran flakes	Vendl et al. (2010)
	α-ZEL； β-ZEL; Z14G; α-ZELG; β-ZELG; Z14S	Wheat; maize; wheat; oats etc	De Boevre et al. (2012)
Masked fumonisins	HFB1	Corn flakes	Kim et al. (2003)
	HFBs	Maize	Dall Asta et al. (2009)

During the fermentation of dark tea, the number of *Aspergillus* spp. is always in a dominant position. The fungi *Aspergillus* spp. have an essential contribution to the quality formation of dark tea. For example, *Aspergillus niger* metabolism can produce organic acids and enzymes that have a variety of hydrolytic enzymes, including oxidases, glycosidases, and proteases, which can hydrolyze polysaccharides, fats, proteins, and cellulose into monosaccharides, amino acids, and some soluble carbohydrates, so that the biochemical components in the tea can be easily leached out and enhance the thickness of the tea broth. *Aspergillus niger* is a comparatively safe industrial fungus that was recognized worldwide in the 20th century and is a commonly used industrial fermentation strain. However, in recent years, there have been plenty of studies finding that some strains of *Aspergillus niger* could produce mycotoxins. Although only a few *Aspergillus niger* fungi are able to produce mycotoxins, we absolutely need to pay more attention to them.

3.2. *Penicillium*

Fungi of the genus *Penicillium* are also frequently detected during dark tea processing and in finished dark tea (Haas et al., 2013). It is widely used in the processing and storage of dark tea production.

There are more than 600 species of fungi in the genus *Penicillium*, and their morphological characteristics are generally similar to each other. Many researchers have also isolated and identified *Penicillium* spp. fungi from dark tea, as shown in Table 5, and *Penicillium* spp. fungi that may produce fungal toxins are shown in Table 6.

3.3. Other genus

Li (2019) isolated fungi of the genus *Rhizoctonia* from Ya'an Tibetan Tea. Zhao (2012) isolated one strain of *Fusarium* spp., one strain of *Trichoderma* and three strains of *Mucor* spp. from the 'flowering' processing of Fuzhuan tea. Wu et al. (2021) isolated *Fusarium equiseti*, *Alternaria*, and *Cladosporium cladosporioides* from Fuzhuan tea. Wen et al. (2012) isolated *Mucor* spp. and *Rhizoctonia* spp. from Liupao tea fermentation samples. All of the above fungi have the ability to produce mycotoxins, but few researchers have paid attention to them previously. These are the questions and directions that we need to pay close attention to in the future, whether these fungi can produce mycotoxins on tea substrates or not.

These fungal genera that have been isolated and identified as having the potential to cause adverse health effects to consumers are *Fusarium*, *Xylaria*, *Streptomyces*, and, *Trichoderma* spp. The fungi of the genus *Fusarium* mainly include *Fusarium graminearum*, *Fusarium verticillioides*, *Fusarium nivale*, *Fusarium tricinctum*, and *Fusarium equiseti* etc. (Zu et al., 2021). These fungi may produce toxic secondary metabolites such as trichothecenes, zearalenone, moniliformin, and butenolide (Huang et al., 2017). Some strains of *Trichoderma* such as *T. reesei* and *T. viride* are capable of producing gliotoxin, which belongs to the Tricothecenes (Mao and Zhang, 2018). Some strains of *Alternaria* can produce a variety of mycotoxins such as alternariol (AOH), alternariolmethylether (AME), and tenuazonicacid (TeA) (López et al., 2016). *Mucor* spp. is also a pathogenic fungus, often causing mold in food, Mucor can enter the body through the respiratory tract, digestive tract, or skin, causing blood clots and tissue necrosis (Yang and Liu, 2021).

In summary, many researchers have isolated and identified the microorganisms from dark tea. Therefore, a plentiful toxin-producing source has been discovered. The isolation and identification of toxin-producing fungi in dark tea require us to think highly of the safety of dominant fungi in the processing of dark tea and avoid the infestation of toxicity-producing fungi. We need to pay further attention to whether these fungi produce mycotoxins and whether they can cause health effects in consumers. Only a small number of researchers have paid attention to the toxicity-producing properties and isolating conditions of dark tea. However, in order to ensure the safety of dark tea production, research on the infestation of harmful fungi in dark tea is unquestionably required.

4. Possible contamination pathway

The initial production process of dark tea can be roughly divided into fixing, rolling, pile fermentation, and drying. Dark tea can be mainly classified into Hunan Fuzhuan tea, Sichuan Kangzhuan tea,

10.3389/fmicb.2023.1120659

TABLE 4 Common dominant genus in dark tea.

Type of dark tea	Dominant genus	References
Kangzhuan tea	*Aspergillus, Penicillium, Saccharomyces*	Fu and Guinian (2008)
Kangzhuan tea	*Aspergillus, Mucor, Mycobacterium, Rhizopus*	Xu (2010)
Kangzhuan tea	*Aspergillus, Penicillium, Saccharomyces*	Zheng (2013)
Sichuan dark tea	*Aspergillus, Penicillium, Saccharomyces, Rhizopus*	Jiang (2012b)
Ya'an Tibetan tea	*Aspergillus, Penicillium, Rhizopus*	Li (2019)
Pu-erh tea	*Aspergillus, Penicillium, Saccharomyces, Rhizopus*	Zhou et al. (2004)
Pu-erh tea	*Aspergillus, Saccharomyces*	Dong et al. (2009)
Pu-erh tea	*Aspergillus, Arxula*	Wang Q. et al. (2020)
Pu-erh tea	*Aspergillus, Penicillium, Saccharomyces*	Bi et al. (2014)
Pu-erh tea	*Aspergillus, Penicillium, Saccharomyces*	Zhang et al. (2012)
Pu-erh tea	*Aspergillus, Saccharomyces*	Hu (2013)
Pu-erh tea	*Aspergillus, Saccharomyces*	Peng and Yu (2011)
Fuzhuan tea	*Aspergillus, Penicillium*	Zhang et al. (2010)
Fuzhuan tea	*Aspergillus, Penicillium*	Zhao H. et al. (2021)
Fuzhuan tea	*Aspergillus*	Ruan (2015)
Fuzhuan tea	*Aspergillus, Penicillium*	Hu (2012)
Fuzhuan tea	*Aspergillus, Penicillium*	Liu et al. (2011)
Fuzhuan tea	*Aspergillus*	Yang et al. (2020)
Fuzhuan tea	*Aspergillus, Penicillium*	Wu et al. (2021)
Liupao tea	*Aspergillus, Penicillium*	Wen et al. (2012)
Liupao tea	*Aspergillus*	Chen R. et al. (2016)
Liupao tea	*Aspergillus*	Ou et al. (2017)

TABLE 5 Common *Aspergillus* spp. and *Penicillium* spp. fungi in dark tea.

Type of dark tea	Species	References
Ya'an Tibetan tea	*Aspergillus niger, Aspergillus fumigatus, Aspergillus miscellaneous, Penicillium citrinum*	Li (2019)
Fuzhuan tea during 'flowering'	*Aspergillus niger, Aspergillus fumigatus, Aspergillus confusus*	Zhao (2012)
Brick tea	*Aspergillus pseudogalactiae*	Wang et al. (2015)
Fuzhuan tea	*Aspergillus costiformis Kong& Qi, Aspergillus niger and Aspergillus oryzae*	Wu et al. (2021)
Fuzhuan tea	*Aspergillus sojae, Penicillium purpurogenum, Penicillium chrysogenum*	Liu et al. (2011)
Liupao tea	*Aspergillus chevalieri, Aspergillus restrictus, Aspergillus tubingensis,*	Chen R. et al. (2016)
Liupao tea	*Aspergillus niger, Aspergillus tubingensis, Aspergillus fumigatus, Aspergillus oryzae, Aspergillus sydowii, Aspergillus ochraceus, Aspergillus tamarii and Aspergillus sloerotiorum, Penicillium citrinum, Penicillium chrysogenum, Penicillium oxalicum, Penicillium chermesinum, Penicillium meleagrinum*	Xu (2014)
Sichuan dark tea	*Aspergillus niger, Penicillium citrinum, Penicillium crustosum, Penicillium brevicompactum, penicillium georgiense, penicillium brocae*	Xiong (2017)
Liupao tea	*Penicillium jiangxiense*	Ou et al. (2017)
Dark tea	*Aspergillus niger, Aspergillus tabinum, Aspergillus carbonarius, Aspergillus nidulans, Aspergillus ochraceus, Penicillium verrucosum*	Zhao Z. et al. (2021)

Hubei Qingzhuan tea, Guangxi Liupao tea, Yunnan ripe Pu-erh tea, and Shaanxi Fuzhuan tea, etc., and their main manufacture processes are shown in Figure 2.

Each origin of dark tea has its own unique processing process. Fermentation and storage are the main ways for dark tea to be infested by harmful fungi, and if it is infested by toxicity-producing fungi during processing, it is likely to lead to the contamination of dark tea with fungal toxins.

4.1. Pile fermentation

The pile fermenting process is crucial in defining the quality of dark tea. The essence of fermentation is the enzymatic reaction of extracellular enzymes produced by the secretion of dominant microorganisms and the action of moist heat (heat of microbial respiration and metabolism) combined.

A series of complex transformations occur to form the unique flavor quality of dark tea (Wang et al., 1991a). During processing, high temperature and high humidity conditions are favorable for microbial growth and the metabolic transformation of black tea, but if the dark tea is contaminated with harmful fungi during the pile fermentation, then there is a risk that the dark tea will be contaminated with fungal toxins.

The microorganisms in the fermentation process are the more abundant stage in the whole dark tea production process (Zhang et al., 2017; Xu Z. et al., 2019). Wen et al. (2012) isolated *Aspergillus niger*, *Aspergillus oryzae*, and *Aspergillus glaucus* from Liupao tea fermentation samples. Wang Q. et al. (2020) and Dong et al. (2009) isolated *Aspergillus niger*, *Aspergillus tamarii*, *Aspergillus fumigatus*, *Aspergillus clavatus*, *Aspergillus oryzae*, *Aspergillus glaucus*, *Aspergillus terreus*, *Aspergillus candidus*, *Aspergillus wentii* var. *fumeus*, *Aspergillus penicillioides*, *Aspergillus aureolatus*, *Aspergillus egyptiacus*, *Aspergillus foetidus*, *Aspergillus japonicus Saito var. japonicus*, *Aspergillus restrictus Smith*, etc., from the fermentation process of Pu-erh tea.

4.2. Storage

Dark tea is a kind of post-fermented tea with the characteristic that "flavor improves with ages," and its flavor is unique. The change of the inner material component of dark tea is intimately related to temperature, humidity, and age (Chen Y. et al., 2016). Therefore, during the storage process, dark tea is always changing silently, and the degree is accountable for the storage conditions. Mildew and deterioration of the dark tea are brought on by improper storage, thus leading to the contamination of dark tea by fungal toxins.

Dark tea during storage is probably infested with harmful fungi due to high humidity conditions and thus. Xu et al. (2016) investigated mycotoxin residues under natural moldy and exogenous inoculation with toxin-producing *Aspergillus flavus* conditions by artificial high humidity mold-promoting culture, and all three mycotoxins were not detected in naturally moldy dark tea samples, while AFB_1 was detected in tea samples with exogenous inoculation with *Aspergillus flavus* strains. Zhong et al. (2010) isolated and identified a total of one *Aspergillus* strain, three *Penicillium* strains, and one *Rhizopus* strain for the fungal populations present in the storage of Ya'an Tibetan tea. Zhou et al. (2015a,b) isolated and identified a strain of *Aspergillus niger* from aged Pu-erh tea for solid-state fermentation of Pu-erh tea, and OTA was detected in the fermented Pu-erh tea samples, which proved that this strain of *Aspergillus niger* has the ability to produce OTA. In Li's finding, total of 218 fungi was isolated from Liupao tea, and some of these strains, such as *Aspergillus ochraceus*, *Aspergillus oryzae*, *Penicillium citrinum*, and *Penicillium chrysogenum* can produce CIT (Li et al., 2020). Zhao et al. (2021) isolated 560 fungal strains from dark tea samples, including seven species of *Penicillium* spp. and 13 species of *Aspergillus* spp., and 20 species of other genera. Six different species of isolated fungi were identified had the ability to produce OTA. Nearly all strains belonging to species of *Aspergillus carbonarius*, *Aspergillus ochraceus*, *Aspergillus nidulans* and *Penicillium verrucosum* were capable of producing OTA, but only part of *Aspergillus niger* and *Aspergillus tubingensis* can produce OTA. Zhao et al. (2022) isolated 18 strains of *Aspergillus* spp. and *Penicillium* spp. fungi from dark tea samples of different years, and one *Aspergillus niger* was found to have the ability to produce OTA. Although dark tea has the characteristic of "flavor improves with ages," if it is not stored properly, it may becomeinfested with harmful fungi and thus become moldy or produce fungal toxins that are harmful to human health.

TABLE 6 *Penicillium* fungi that may produce fungal toxins in dark tea.

Fungi	Fungal toxin of possible production
Penicillium citrinum	Citrinin (Guo et al., 2019)
Penicillium chrysogenum	Citrinin; Patulin (Zhou et al., 2015a)
Penicillium purpurogenum	Citrinin (Chai et al., 2012)
Penicillium viridicatum	Ochratoxin A; Citrinin (Pitt, 1987)
Penicillium verrucosum	Ochratoxin A (Zhao Z. et al., 2021); Citrinin (Bragulat et al., 2008)

The possibility of dark tea being contaminated by fungi, which warns that dark tea enterprises need to concentrate on the contamination of harmful microorganisms during the production process. It's necessary to constantly pay attention to the changes in environmental conditions during the storage of dark tea to prevent it from being contaminated by fungi during the storage process. The standardized of the production of dark tea is urgently needed to

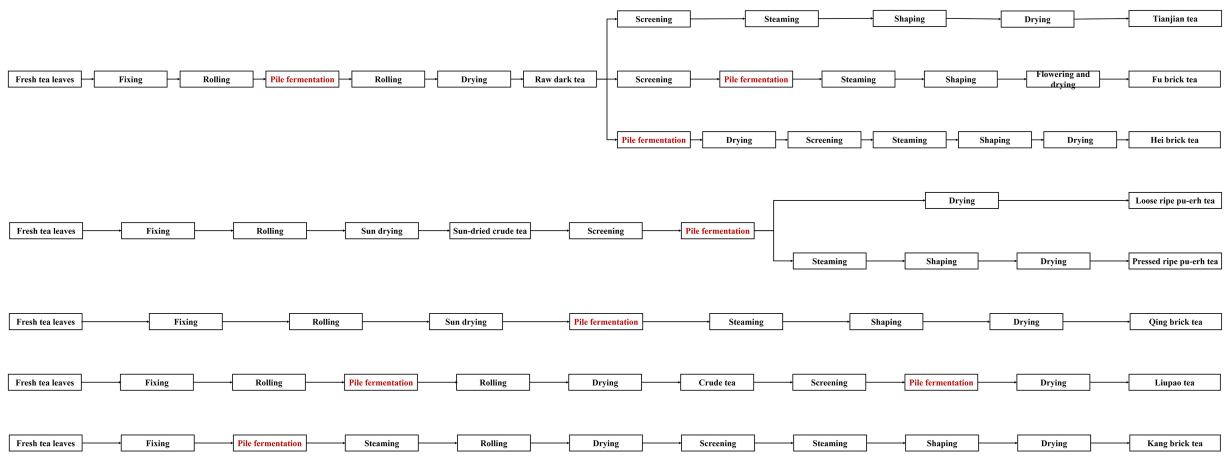

FIGURE 2
The main manufacture processing of various dark tea.

ensure the safety of the dark tea production, processing, and storage environments, which is the guarantee for the prosperous development of the dark tea industry.

5. Discussion

Dark tea is potentially contaminated with toxin-producing fungi (Jiang et al., 2018; Deng et al., 2020). Microorganisms in dark tea play an important part in the formation of dark tea sensory quality, while some microorganisms can lead to tea fungal toxin contamination (Xin and Liang, 2020). During the processing of dark tea, extracellular enzyme catalysis by microorganisms is the dominant factor, thus promoting the transformation of dark tea quality and forming its unique flavor. Existing microbial studies on dark tea have identified *Aspergillus* spp. as the dominant fungal group in the fermentation process of dark tea. However, from the perspective of food safety, *Aspergillus* spp. fungi can produce a variety of fungal toxins, such as: aflatoxin, ochratoxin, citrinin, and vomitoxin (Sengun et al., 2008; Bräse et al., 2009; Zhao et al., 2017; Li et al., 2021). In recent years, the debate on whether dark tea contaminated with harmful fungi can produce fungal toxins has become more intense. Public opinion often emerges that tea contains fungal contaminants that can cause cancer, and some scholars have also reported studies on dark tea being contaminated by fungal toxins (Liu et al., 2016, 2017; Cui et al., 2020; Li et al., 2020; Zhao et al., 2022), which has had a huge impact on the development of the industry.

Dark tea has increased the risk of mycotoxins contamination due to the involvement of fungi during the microbial and hygrothermal dominated solid-state fermentation process. Zhou et al. (2015a,b), Zhang et al. (2016) ,and Zhao Z. et al. (2021) have isolated toxin-producing fungi from dark tea, but the detection rate and content of mycotoxins in tea were far below expectations. Zhao et al. (2015) suggested that in the solid-state fermentation process, there is a possibility of the presence of antagonistic microorganisms that inhibit the growth of harmful fungi and the production of mycotoxins. The results of some other studies have shown that certain endogenous components in tea are capable of inhibiting fungal toxin production (Wu Q., 2013; Li H. et al., 2015; Guo, 2018).

At the same time, the tea matrix composition is highly complex and specific, containing abundant tea pigments, polyphenols, caffeine, and other substances, which are the material basis for the health functions of tea, and such secondary metabolites also have the ability to stop or inhibit mycotoxin production by mycorrhizal fungi in the presence of fungal contamination (Zhao et al., 2017; Jiang et al., 2018). In a study of aflatoxin production by *Aspergillus flavus* using tea substrates, results showed that aqueous extracts from Yunnan Big Leaf tea had a significant inhibitory effect on the synthesis of aflatoxins, they speculated that the tea extract may have inhibited aflatoxin synthesis by modulating the expression of *aflR* (Li H. et al., 2015). In recent years, it has also been found that there is a close relationship between aflatoxin biosynthesis and oxidative stress, and that the presence of antioxidants inhibits the synthesis of AFB_1 (Wu Q., 2013; Zhao, 2014; Guo, 2018). All these studies show that the active substances in tea have the ability to inhibit the production of toxins from mycotoxins, but there is a limit to the inhibitory effect of active substances on harmful fungi, and what we need is to completely and effectively avoid contamination of tea with harmful mycotoxins to effectively and efficiently protect the safety of consumers.

There are many studies on mycotoxins in dark tea, and most of the findings suggest that the level of mycotoxin exposure in dark tea is insufficient to threaten the health of tea consumers (Liu et al., 2016; Mo et al., 2016; Hu et al., 2019). The results of mycotoxin detection in dark tea are inconsistent due to different sources of dark tea samples as well as different methods of determination. Results of ELISA were mostly positive for mycotoxins (Santos et al., 2009; Li W. et al., 2015), while LC–MS/MS results were mostly negative, with only a few positive cases present. The possible reasons for this situation are due to the results for ELISA are probably false positive, and LC–MS/MS results seem more reliable. The complexity of the tea matrix, the conversion of polyphenols to pigment substances such as theaflavins and thearubigins during the fermentation of dark tea by the action of moist heat and microbial extracellular enzymes (Jiang, 2012a; Zhang, 2015; Ji et al., 2016), which can affect the results of ELISA.

If the sample pretreatment method is not appropriate and the interferences, such as tea pigment substances are not removed, the ELISA or HPLC assay will easily show false positives due to the interference of pigment substances. Another possible reason is that the mycotoxins in tea transform themselves or combine with certain substances in tea to form masked mycotoxins that are difficult to detect. At present, the reliable mycotoxin detection methods commonly used in dark tea products are high performance HPLC and HPLC-MS, but if the mycotoxin forms are masked by certain substances in dark tea under specific conditions, it is difficult to be detected by the above two methods. Due to the complexity of the tea matrix and the instability of certain mycotoxins, the formation of masked mycotoxins in dark tea also has a greater possibility.

So far, there are more studies on the exposure of mycotoxins in tea, but there are fewer studies on the exposure, toxicity, and contamination status of masked mycotoxins. The results of some reports have shown that some of the masked mycotoxins may re-release their prototypes after entering the digestive systems of humans and animals, posing serious potential safety hazards to food. The toxicity of many masked mycotoxins may be much lower than their prototypes or even non-toxic, but if they react again in the human body, then there will be a greater safety risk. Therefore, it is necessary to conduct basic research on the formation, regulatory mechanisms, contamination status, and detection methods of the major masked mycotoxins in tea to provide a scientific basis for effective prevention, control, and safety supervision of masked mycotoxins in tea.

The most effective way to prevent mycotoxin contamination in dark tea is to avoid the infestation of harmful microorganisms during production, processing, and storage, as well as to eliminate mycotoxin production from the source. It is urgent to perform a precise screening of beneficial microorganisms and avoid harmful microbial infestation, which is also an effective way to prevent fungal toxin contamination in dark tea. It is also the direction of future efforts by dark tea producers.

Author contributions

WX and YZ: conceptualization, investigation, draft reviewing, and editing. Y-qZ: conceptualization, investigation, data curation, writing

– original draft preparation, and writing – review and editing. W-bJ: conceptualization, investigation, and data curation. S-yL: conceptualization and investigation. TB: draft reviewing, revision, and editing. All authors contributed to the article and approved the submitted version.

Funding

This work was supported by Sichuan Province S&T Project (2021ZHFP0021, 2022ZHXC0022, 2023YFH0025, and 2023YFN0010) and Ya'an Yucheng District School Cooperation Project (2022).

Conflict of interest

The authors declare that the research was conducted in the absence of any commercial or financial relationships that could be construed as a potential conflict of interest.

Publisher's note

All claims expressed in this article are solely those of the authors and do not necessarily represent those of their affiliated organizations, or those of the publisher, the editors and the reviewers. Any product that may be evaluated in this article, or claim that may be made by its manufacturer, is not guaranteed or endorsed by the publisher.

References

Andersen, B., Smedsgaard, J., and Frisvad, J. C. (2004). *Penicillium expansum*: consistent production of patulin, chaetoglobosins, and other secondary metabolites in culture and their natural occurrence in fruit products. *J. Agric. Food Chem.* 52, 2421–2428. doi: 10.1021/jf035406k

Berthiller, F., Crews, C., Dall'Asta, C., Saeger, S. D., Haesaert, G., Karlovsky, P., et al. (2013). Masked mycotoxins: a review. *Mol. Nutr. Food Res.* 57, 165–186. doi: 10.1002/mnfr.201100764

Berthiller, F., Dall'Asta, C., Schuhmacher, R., Lemmens, M., Adam, G., and Krska, R. (2005). Masked mycotoxins:determination of a deoxynivalenol glucoside in artificially and naturally contaminated wheat by liquid chromatography–tandem mass spectrometry. *J. Agric. Food Chem.* 53, 3421–3425. doi: 10.1021/jf047798g

Bhat, R., Rai, R. V., and Karim, A. A. (2010). Mycotoxins in food and feed: present status and future concerns. *Compr. Rev. Food Sci. Food Saf.* 9, 57–81. doi: 10.1111/j.1541-4337.2009.00094.x

Bi, Y., Luo, Y., Fan, Z., and Shi, S. (2014). Isolation and identification of fungi in fu-hei fermentation of pu-erh tea. *Modern Agric. Sci. Technol.* 624, 279–281. doi: 10.3969/j.issn.1007-5739.2014.10.174

Bragulat, M., Martinez, E., Castella, G., and Cabanes, F. (2008). Ochratoxin a and citrinin producing species of the genus penicillium from feedstuffs. *Int. J. Food Microbiol.* 126, 43–48. doi: 10.1016/j.ijfoodmicro.2008.04.034

Bräse, S., Encinas, A., Keck, J., and Nising, C. F. (2009). Chemistry and biology of mycotoxins and related fungal metabolites. *Chem. Rev.* 109, 3903–3990. doi: 10.1021/cr050001f

Bugno, A., Almodovar, A. A. B., Pereira, T. C., Pinto, T. J. A., and Sabino, M. (2006). Occurence of toxigenic fungi in hcrbal drugs. *Braz. J. Microbiol.* 37, 47–51. doi: 10.1590/S1517-83822006000100009

Busman, M., Poling, S. M., and Maragos, C. M. (2011). Observation of t-2 toxin and ht-2 toxin glucosides from *Fusarium sporotrichioides* by liquid chromatography coupled to tandem mass spectrometry (LC-MS/MS). *Toxins* 3, 1554–1568. doi: 10.3390/toxins3121554

Chai, Y., Cui, C., Li, C., Wu, C., Tian, C., and Hua, W. (2012). Activation of the dormant secondary metabolite production by introducing gentamicin-resistance in a marine-derived *Penicillium purpurogenum* g59. *Mar. Drugs* 10, 559–582. doi: 10.3390/md10030559

Chen, R., Hao, B., Tian, H., Li, S., Ma, Y., and Wang, C. (2016). Distribution of fungal strains and molecular identification of Eurotium cristatum in liupao tea. *Food Sci. Technol.* 41, 19–23. doi: 10.13684/j.cnki.spkj.2016.04.004

Chen, Y., Li, S., Liu, Z., and Huang, J. (2016). Research progress on aging mechanism of dark tea. *Hunan Agric. Sci.* 12, 118–122. doi: 10.16498/j.cnki.hnnykx.2016.012.035

Chen, W., Li, C., Zhang, B., Zhou, Z., Shen, Y., Liao, X., et al. (2018). Advances in biodetoxification of ochratoxin a-a review of the past five decades. *Front. Microbiol.* 9:1386. doi: 10.3389/fmicb.2018.01386

Chen, Y., and Qi, G. (2010). Research progress on the quality formation mechanism of Kang brick tea. *Tea in Fujian.* 32, 8–12.

Chen, L., Yu, M., Wu, Q., Peng, Z., Wang, D., Kuča, K., et al. (2017). Gender and geographical variability in the exposure pattern and metabolism of deoxynivalenol in humans: a review. *J. Appl. Toxicol.* 37, 60–70. doi: 10.1002/jat.3359

Csikós, V., Varró, P., Bódi, V., Oláh, S., Világi, I., and Dobolyi, A. (2020). The mycotoxin deoxynivalenol activates gabaergic neurons in the reward system and inhibits feeding and maternal behaviours. *Arch. Toxicol.* 94, 3297–3313. doi: 10.1007/s00204-020-02791-6

Cui, P., Yan, H., Granato, D., Ho, C., Ye, Z., Wang, Y., et al. (2020). Quantitative analysis and dietary risk assessment of aflatoxins in Chinese post-fermented dark tea. *Food Chem. Toxicol.* 146:111830. doi: 10.1016/j.fct.2020.111830

Dall Asta, C., Mangia, M., Berthiller, F., Molinelli, A., Sulyok, M., Schuhmacher, R., et al. (2009). Difficulties in fumonisin determination: the issue of hidden fumonisins. *Anal. Bioanal. Chem.* 395, 1335–1345. doi: 10.1007/s00216-009-2933-3

De Boevre, M., Di Mavungu, J. D., Maene, P., Audenaert, K., Deforce, D., Haesaert, G., et al. (2012). Development and validation of an lc-ms/ms method for the simultaneous determination of deoxynivalenol, zearalenone, t-2-toxin and some masked metabolites in different cereals and cereal-derived food. *Food Addit. Contam. Part A* 29, 819–835. doi: 10.1080/19440049.2012.656707

Deng, X., Tu, Q., Wu, X., Huang, G., Shi, H., Li, Y., et al. (2020). Research progress on the safety risk of ochratoxin a in tea. *Sci. Technol. Food Ind.* 1-10, 405–412. doi: 10.13386/j.issn1002-0306.2020070080

Dong, K., Xiong, X., and Lan, Z. (2009). Analysis of microbial taxa during fermentation of pu-erh tea. *Modern Agric. Sci. Technol.* 01, 164–165. doi: 10.3969/j.issn.1007-5739.2009.01.108

Flajs, D., and Peraica, M. (2009). Toxicological properties of citrinin. *Arch. Ind. Hyg. Toxicol.* 60, 457–464. doi: 10.2478/10004-1254-60-2009-1992

Fu, R., and Guinian, Q. (2008). Study of microorganism in kangzhuan tea in Sichuan province. *Jiangsu Agric. Sci.* 5, 231–234. doi: 10.3969/j.issn.1002-1302.2008.05.080

Guo, R. (2018). *Inhibition and Mechanism of Tea Polyphenol Monomers on afb1 Production by Aspergillus flavus*. Master's thesis. Xi An: Shaanxi University of Science and Technology.

Guo, W., Zhao, M., Chen, Q., Huang, L., Mao, Y., Xia, N., et al. (2019). Citrinin produced using strains of *Penicillium citrinum* from liupao tea. *Food Biosci.* 28, 183–191. doi: 10.1016/j.fbio.2019.01.015

Haas, D., Pfeifer, B., Reiterich, C., Partenheimer, R., Reck, B., and Buzina, W. (2013). Identification and quantification of fungi and mycotoxins from pu-erh tea. *Int. J. Food Microbiol.* 166, 316–322. doi: 10.1016/j.ijfoodmicro.2013.07.024

Haque, M. A., Wang, Y., Shen, Z., Li, X., Saleemi, M. K., and He, C. (2020). Mycotoxin contamination and control strategy in human, domestic animal and poultry: a review. *Microb. Pathog.* 142:104095. doi: 10.1016/j.micpath.2020.104095

He, S., Li, H., Li, B., Han, X., Jiang, H., Jin, Y., et al. (2020). Advances in the toxic effects and toxicogenic mechanism of ochratoxin a. *Shanghai J. Anim. Husbandry Vet. Med.* 4, 9–12. doi: 10.14170/j.cnki.cn31-1278/s.2020.04.004

Hetherington, A. C., and Raistrick, H. (1931). On the production and chemical constitution of a new yellow colouring matter, citrinin, produced from glucose by penicillium citrinum thom. *Philos. Trans. R. Soc. Lond. Ser B* 220, 269–297.

Hu, Z. (2012). *Flora Diversity and Fermentation Process Codition of Fuzhuan Brick-Tea in h Unan Area*. Master's thesis. Changsha: Hunan Agricultural University.

Hu, J. (2013). *Dynamic Analysis of Pile-Fermentation Process for Pu-erh Tea at Different Seasons*. Master's thesis. Guangzhou: South China University of Technology.

Hu, Z., Liu, S., Xu, Z., Liu, S., and Wen, X. (2020). Sequencing and analysis of the complete mitochondrial genome of *Penicillium citrinum* in Hunan Yiyang dark tea. *J. Tea Sci.* 40, 830–844. doi: 10.13305/j.cnki.jts.2020.06.010

Hu, L., Shi, Z., Zhao, L., Liu, X., Dong, Y., Jiang, M., et al. (2019). Simultaneous detection and analysis of 16 kinds of mycotoxins in pu-erh tea. *Acta Agric. Zhejiangensis* 31, 1700–1708.

Huang, X., Wang, S., Mao, D., Miao, S., and Shen, J. (2017). Research progress on toxicity of fusarium mycotoxins. *J. Food Saf. Qual.* 8, 3117–3128. doi: 10.3969/j.issn.1004-874X.2013.15.042

Iqbal, S. Z., Mumtaz, A., Mahmood, Z., Waqas, M., Ghaffar, A., Ismail, A., et al. (2021). Assessment of aflatoxins and ochratoxin a in chili sauce samples and estimation of dietary intake. *Food Control* 121:107621. doi: 10.1016/j.foodcont.2020.107621

Iqbal, S. Z., Nisar, S., Asi, M. R., and Jinap, S. (2014). Natural incidence of aflatoxins, ochratoxin a and zearalenone in chicken meat and eggs. *Food Control* 43, 98–103. doi: 10.1016/j.foodcont.2014.02.046

Ji, J., Yuan, D., Liu, F., Yang, Y., Chen, X., Hao, R., et al. (2016). Research progress in formation mechanism of fuzhuan brick tea quality. *Food and Drug* 18, 52–60. doi: 10.3969/j.issn.1672-979X.2016.01.015

Jiang, Y. (2012a). *Study on the Influence of Advantage Fungi to Its Quality Components in the Process of Piled-Fermentation of Sichuan Brick Tea*. Master's Thesis. Yaan: Sichuan Agriculture University.

Jiang, Y. (2012b). *Study on the Influence of Advantage Fungi to Its Quality Components in the Process of Piled-Fermentation of Sichuan Brick Tea*. Master's Thesis. Yaan: Sichuan Agricultural University.

Jiang, Y., Xu, W., and Zhu, Q. (2018). Research progress and discussion on fungal contamination of dark tea. *J. Tea Sci.* 38, 227–236. doi: 10.13305/j.cnki.jts.2018.03.002

Kim, E. K., Scott, P. M., and Lau, B. P. Y. (2003). Hidden fumonisin in corn flakes. *Food Addit. Contamin.* 20, 161–169. doi: 10.1080/0265203021000035362

Kluger, B., Bueschl, C., Lemmens, M., Michlmayr, H., Malachova, A., Koutnik, A., et al. (2015). Biotransformation of the mycotoxin deoxynivalenol in fusarium resistant and susceptible near isogenic wheat lines. *PLoS One* 10:e119656. doi: 10.1371/journal.pone.0119656

Kong, W., Wei, R., Logrieco, A. F., Wei, J., Wen, J., Xiao, X., et al. (2014). Occurrence of toxigenic fungi and determination of mycotoxins by hplc-fld in functional foods and spices in China markets. *Food Chem.* 146, 320–326. doi: 10.1016/j.foodchem.2013.09.005

Kostelanska, M., Hajslova, J., Zachariasova, M., Malachova, A., Kalachova, K., Poustka, J., et al. (2009). Occurrence of deoxynivalenol and its major conjugate, deoxynivalenol-3-glucoside, in beer and some brewing intermediates. *J. Agric. Food Chem.* 57, 3187–3194. doi: 10.1021/jf803749u

Kresse, M., Drinda, H., Romanotto, A., and Speer, K. (2019). Simultaneous determination of pesticides, mycotoxins, and metabolites as well as other contaminants in cereals by lc-lc-ms/ms. *J. Chromatogr. B* 1117, 86–102. doi: 10.1016/j.jchromb.2019.04.013

Lattanzio, V. M. T., Visconti, A., Haidukowski, M., and Pascale, M. (2012). Identification and characterization of new Fusarium masked mycotoxins, T2 and HT2 glycosyl derivatives, in naturally contaminated wheat and oats by liquid chromatography-high-resolution mass spectrometry. *J. Mass Spectrom* 47, 466–475. doi: 10.1002/jms.2980

Li, X. (2019). *Isolation and Identification of Main Microorganisms in Finished Ya'an Tibetan Tea*. Master's Thesis. Yaan: Sichuan Agricultural University.

Li, D., and He, J. (2020). Determination of aflatoxin in lycium barbarum by hplc. *Farm Prod. Process.* 23, 54–56. doi: 10.16693/j.cnki.1671-9646(X).2020.12.016

Li, J., Li, X., Qi, Y., Tian, X., Zhang, J., and Long, S. (2016). Detection of aflatoxin b_1 in soy sauce by enzyme linked immunosorbent assay. *J. Food Saf. Qual.* 7, 4735–4739. doi: 10.19812/j.cnki.jfsq11-5956/ts.2016.12.005

Li, Z., Mao, Y., Teng, J., Xia, N., Huang, L., Wei, B., et al. (2020). Evaluation of mycoflora and citrinin occurrence in chinese liupao tea. *J. Agric. Food Chem.* 68, 12116–12123. doi: 10.1021/acs.jafc.0c04522

Li, W., Nong, R., Shen, Y., Li, J., Ran, Y., Chen, J., et al. (2021). Determination of ochratoxin a in pu-erh tea by ultra performance liquid chromatography-tandem mass spectrometry. *J. Food Saf. Qual.* 12, 2240–2245. doi: 10.19812/j.cnki.jfsq11-5956/ts.2021.06.029

Li, H., Tan, Y., Chen, Z., Qu, J., Chen, Y., and Fang, X. (2015). Effect of Yunnan large-leaf *Camellia sinensis* extract on growth and aflatoxin production of *Aspergillus flavus*. *Modern Food Sci. Technol.* 31, 101–106. doi: 10.13982/j.mfst.1673-9078.2015.11.017

Li, W., Xu, K., Xiao, R., Yin, G., and Liu, W. (2015). Development of an hplc-based method for the detection of aflatoxins in pu-erh tea. *Int. J. Food Prop.* 18, 842–848. doi: 10.1080/10942912.2014.885043

Li, D., Zhou, H., Li, Q., and Meng, X. (2000). Wide caliber gas-chromatography to detect the content of t-2 toxin in grain. *Chin. J. Endemiol.* 1, 71–72. doi: 10.3760/cma.j.issn.1000-4955.2000.01.024

Lin, Y., Chen, J., Wu, B., Li, C., Liu, Q., and Xie, J. (2013). Determination of t-2 and ht-2 toxins in cereal grains by solid phase extraction and gas chromatography-tandem mass spectrometry. *Mil. Med. Sci.* 37, 381–384. doi: 10.7644/j.issn.1674-9960.2013.05.015

Liu, Q. (2011). Elisa method for the determination of mycotoxin contamination of fermented tea and plant spices. *China Trop. Med.* 11, 1381–1382.

Liu, Y., Chen, J., Tan, G., Liu, Z., and Li, X. (2017). Determination of ten mycotoxins in fermented dark tea by quechers-ultra-high-performance liquid chromatography-tandem mass spectrometry. *Modern Food Sci. Technol.* 33, 280–288. doi: 10.13982/j.mfst.1673-9078.2017.7.039

Liu, Y., Tan, G., Liu, Z., Li, X., and Chen, J. (2016). Determination of various mycotoxins in fermented tea by ultra-high performance liquid chromatography-tandem mass spectrometry. *Modern Food Sci. Technol.* 32, 322–327. doi: 10.13982/j.mfst.1673-9078.2016.8.049

Liu, S., Zhao, Y., Lei, C., Dong, M., Peng, X., and Xiaomei, Z. (2011). A preliminary research on separation and identification of the fungi form xiang-yi fuzhuan tea. *Hubei Agric. Sci.* 50, 1765–1769. doi: 10.3969/j.issn.0439-8114.2011.09.013

López, P., Venema, D., de Rijk, T., de Kok, A., Scholten, J. M., Mol, H. G. J., et al. (2016). Occurrence of alternaria toxins in food products in the Netherlands. *Food Control* 60, 196–204. doi: 10.1016/j.foodcont.2015.07.032

Lozowicka, B., Iwaniuk, P., Konecki, R., Kaczynski, P., Kuldybayev, N., and Dutbayev, Y. (2022). Impact of diversified chemical and biostimulator protection on yield, health status, mycotoxin level, and economic profitability in spring wheat (Triticum aestivum L.) cultivation. *Agronomy* 12:258. doi: 10.3390/agronomy12020258

Magan, N., and Olsen, M. (2004). *Mycotoxins in Food: Detection and Control*. Cambridge: Elsevier Science & Technology.

Malir, F., Ostry, V., Pfohl-Leszkowicz, A., Toman, J., Bazin, I., and Roubal, T. (2014). Transfer of ochratoxin a into tea and coffee beverages. *Toxins* 6, 3438–3453. doi: 10.3390/toxins6123438

Mao, L., and Zhang, C. (2018). Detection of gliotoxin in cucumber by high performance liquid chromatography. *J. Zhejiang Agric. Sci.* 59, 1603–1606. doi: 10.16178/j.issn.0528-9017.20180932

Marin, S., Ramos, A. J., Cano-Sancho, G., and Sanchis, V. (2013). Mycotoxins: occurrence, toxicology, and exposure assessment. *Food Chem. Toxicol.* 60, 218–237. doi: 10.1016/j.fct.2013.07.047

Martínez-Culebras, P. V., Gandía, M., Boronat, A., Marcos, J. F., and Manzanares, P. (2021). Differential susceptibility of mycotoxin-producing fungi to distinct antifungal proteins (AFPS). *Food Microbiol.* 97:103760. doi: 10.1016/j.fm.2021.103760

Medina, A., Akbar, A., Baazeem, A., Rodriguez, A., and Magan, N. (2017). Climate change, food security and mycotoxins: do we know enough? *Fungal Biol. Rev.* 31, 143–154. doi: 10.1016/j.fbr.2017.04.002

Medina, Á., Rodríguez, A., and Magan, N. (2015). Climate change and mycotoxigenic fungi: impacts on mycotoxin production. *Curr. Opin. Food Sci.* 5, 99–104. doi: 10.1016/j.cofs.2015.11.002

Mo, J., Gong, Q., Zhou, H., Bai, X., Tan, J., Peng, Z., et al. (2016). Determination of ochratoxin a in tea by high performance liquid chromatography-tandem mass spectrometry. *J. Food Saf. Qual.* 7, 182–187. doi: 10.19812/j.cnki.jfsq11-5956/ts.2016.01.037

Murugesan, G. R., Ledoux, D. R., Naehrer, K., Berthiller, F., Applegate, T. J., Grenier, B., et al. (2015). Prevalence and effects of mycotoxins on poultry health and performance, and recent development in mycotoxin counteracting strategies. *Poult. Sci.* 94, 1298–1315. doi: 10.3382/ps/pev075

Nakagawa, H., Sakamoto, S., Sago, Y., and Nagashima, H. (2013). Detection of type a trichothecene di-glucosides produced in corn by high-resolution liquid chromatography-orbitrap mass spectrometry. *Toxins* 5, 590–604. doi: 10.3390/toxins5030590

Ou, H., Deng, X., Zhang, L., Zhang, J., Ma, S., and Qiu, R. (2017). Isolation and identification of dominant microorganisms of liupao tea before and after steaming. *Guangdong Agric. Sci.* 44, 129–135. doi: 10.16768/j.issn.1004-874X.2017.02.020

Palacios, S. A., Erazo, J. G., Ciasca, B., Lattanzio, V. M. T., Reynoso, M. M., Farnochi, M. C., et al. (2017). Occurrence of deoxynivalenol and deoxynivalenol-3-glucoside in durum wheat from Argentina. *Food Chem.* 230, 728–734. doi: 10.1016/j.foodchem.2017.03.085

Peng, X., and Yu, M. (2011). Isolation and identification of culturable microorganisms in a 10-year-old fermented pu-erh tea. *Food Sci.* 32, 196–199.

Pereira, L. T. P., Putnik, P., Iwase, C. H. T., and de Oliveira Rocha, L. (2019). Deoxynivalenol: insights on genetics, analytical methods and occurrence. *Curr. Opin. Food Sci.* 30, 85–92. doi: 10.1016/j.cofs.2019.01.003

Piekkola, S., Turner, P. C., Abdel-Hamid, M., Ezzat, S., El-Daly, M., El-Kafrawy, S., et al. (2012). Characterisation of aflatoxin and deoxynivalenol exposure among pregnant egyptian women. *Food Addit. Contamin Part A.* 29, 962–971. doi: 10.1080/19440049.2012.658442

Pitt, J. I. (1987). Penicillium viridicatum, penicillium verrucosum, and production of ochratoxin a. *Appl. Environ. Microbiol.* 53, 266–269. doi: 10.1128/aem.53.2.266-269.1987

Qi, G., Tian, H., Liu, A., and Shi, Z. (2004). Studies on the quality chemical components in Sichuan brick tea. *J. Tea Sci.* 04, 266–269. doi: 10.3969/j.issn.1000-369X.2004.04.008

Ruan, L. (2015). *Predominant Fungi and Its Effect on Quality of Fu Brick Tea in Different Seasons and Districts*. Master's thesis. Changsha: Hunan Agricultural University.

Sánchez-Hervás, M., Gil, J. V., Bisbal, F., Ramón, D., and Martínez-Culebras, P. V. (2008). Mycobiota and mycotoxin producing fungi from cocoa beans. *Int. J. Food Microbiol.* 125, 336–340. doi: 10.1016/j.ijfoodmicro.2008.04.021

Santos, L., Marín, S., Sanchis, V., and Ramos, A. J. (2009). Screening of mycotoxin multicontamination in medicinal and aromatic herbs sampled in Spain. *J. Sci. Food Agric.* 89, 1802–1807. doi: 10.1002/jsfa.3647

Savard, M. E. (1991). Deoxynivalenol fatty acid and glucoside conjugates. *J. Agric. Food Chem.* 3, 570–574.

Schneweis, I., Meyer, K., Engelhardt, G., and Bauer, J. (2002). Occurrence of zearalenone-4-β-d -glucopyranoside in wheat. *J. Agric. Food Chem.* 50, 1736–1738. doi: 10.1021/jf010802t

Sengling Cebin Coppa, C. F., Mousavi Khaneghah, A., Alvito, P., Assunção, R., Martins, C., Eş, I., et al. (2019). The occurrence of mycotoxins in breast milk, fruit

products and cereal-based infant formula: a review. *Trends Food Sci. Technol.* 92, 81–93. doi: 10.1016/j.tifs.2019.08.014

Sengun, I., Yaman, D., and Gonul, S. (2008). Mycotoxins and mould contamination in cheese: a review. *World Mycotoxin J.* 1, 291–298. doi: 10.3920/WMJ2008.x041

Silva, L. J. G., Pereira, A. M. P. T., Pena, A., and Lino, C. M. (2021). Citrinin in foods and supplements: a review of occurrence and analytical methodologies. *Foods* 10:14. doi: 10.3390/foods10010014

Su, Q. (2018). *Fungal Solid-State Fermentation Teas and Its Teadenol-Producing Potentiality*. Master's Thesis. Kunming: Yunnan University.

Tan, Y., Liu, N., Zhu, R., and Wu, A. (2016). Major types of masked mycotoxins and state-of-the-art methodological advance for their detection. *Sci. Sin. Chim.* 46, 251–256. doi: 10.1360/N032015-00205

Van der Merwe, K. J., Steyn, P. S., Fourie, L., and Scott, D. B. (1965). Ochratoxin a, a toxic metabolite produced by *Aspergillus ochraceus* with. *Nature* 205, 1112–1113. doi: 10.1038/2051112a0

Vargas Medina, D. A., Bassolli Borsatto, J. V., Maciel, E. V. S., and Lanças, F. M. (2021). Current role of modern chromatography and mass spectrometry in the analysis of mycotoxins in food. *TrAC Trends Anal. Chem.* 135:116156. doi: 10.1016/j.trac.2020.116156

Vendl, O., Berthiller, F., Crews, C., and Krska, R. (2009). Simultaneous determination of deoxynivalenol, zearalenone, and their major masked metabolites in cereal-based food by lc–ms–ms. *Anal. Bioanal. Chem.* 395, 1347–1354. doi: 10.1007/s00216-009-2873-y

Vendl, O., Crews, C., Macdonald, S., Krska, R., and Berthiller, F. (2010). Occurrence of free and conjugated fusarium mycotoxins in cereal-based food. *Food Addit. Contamin. Part A* 27, 1148–1152. doi: 10.1080/19440041003801166

Vidal, A., Mengelers, M., Yang, S., De Saeger, S., and De Boevre, M. (2018). Mycotoxin biomarkers of exposure: a comprehensive review. *Compr. Rev. Food Sci. Food Saf.* 17, 1127–1155. doi: 10.1111/1541-4337.12367

Wang, Q., Peng, W., Yang, R., Zhao, M., Jiang, X., Zhang, J., et al. (2020). Community structure of culturable microbes during the fermentation of pu-erh tea. *Food Ferment. Indus.* 46, 88–93. doi: 10.13995/j.cnki.11-1802/ts.024150

Wang, Z., Shi, Z., Liu, Z., Huang, J., Shi, L., Wen, Q., et al. (1991a). Discussion on the mechanism of quality and flavor formation of dark tea. *J. Tea Sci.* 1-9, 288–296.

Wang, Z., Shi, Z., Liu, Z., Huang, J., and Wen, Q. (1991b). Discussion on the mechanism of quality and flavor formation of fuzhuan brick tea. *J. Tea Sci.* S1, 49–55.

Wang, L., Tan, G., Pan, Q., Peng, X., Zhang, W., Pang, M., et al. (2015). Two species of *Aspergillus* forming yellow cleistothecia popularly known as"golden flower" in dark brick tea of China. *Mycosystema* 34, 186–195. doi: 10.13346/j.mycosystema.130275

Wang, Y., and Wang, S. (2021). Research advance of the occurrence, toxicity and metabolism of modified deoxynivalenol contaminated in grains. *Food Sci. Technol.* 46, 321–327. doi: 10.13684/j.cnki.spkj.2021.02.049

Wang, Y., Wang, L., Liu, F., Wang, Q., Selvaraj, J., Xing, F., et al. (2016). Ochratoxin a producing fungi, biosynthetic pathway and regulatory mechanisms. *Toxins* 8:83. doi: 10.3390/toxins8030083

Wang, Y., Wang, L., Wu, F., Liu, F., Wang, Q., Zhang, X., et al. (2018). A consensus ochratoxin a biosynthetic pathway: insights from the genome sequence of *Aspergillus ochraceus* and a comparative genomic analysis. *Appl. Environ. Microbiol.* 84, e1009–e1018. doi: 10.1128/AEM.01009-18

Wang, G., Wang, Y., Zhang, H., Zhang, C., Yang, B., Huang, S., et al. (2020). Factors that affect the formation of mycotoxins: a literature review. *Mycosystema* 39, 477–491. doi: 10.13346/j.mycosystema.190334

Wen, Z., Shi, R., He, Y., Wu, P., Pan, B., and Liang, S. (2012). Research on variation of microbial communities of liupao tea during pile fermentation. *Jo. Anhui Agric. Sci.* 40, 1009–1011. doi: 10.13989/j.cnki.0517-6611.2012.02.041

Wu, J. (2013). *Study on Pu'er tea Quality Formation and State of Mycotoxins During the Aging Process*. Nanchang: Nanchang University.

Wu, Q. (2013). *Study on Components of Inhibiting Production of Aflatoxin in Tea and Related Characteristic*. Yangling: Northwest Agriculture and Forestry University.

Wu, J., Lyu, J., Hu, X., and Shi, C. (2021). Changes of molds in jingwei fuzhuan brick tea during fermentation. *Modern Food Sci. Technol.* 37, 79–86. doi: 10.13982/j.mfst.1673-9078.2021.2.0789

Xin, Y., and Liang, P. (2020). Status quo and prevention and control of tea pollution. *Tea Fujian* 42, 14–16.

Xiong, Y. (2017). *Study on Microbial Diversity of Sichuan Dark Tea During Post-Fermentation and Airborne Microbial in Fermentation Workshop*. Master's Thesis. Yaan: Sichuan Agricultural University.

Xu, W. (2010). *Identification of Fungal Colonization of Sichuan Kangzhuan Tea During Pile-Fermentaion*. Master's Thesis. Yaan: Sichuan Agricultural University.

Xu, S. (2014). *Fungal Community Analysis of Liupao Tea*. Master's Thesis. Nanning: Guangxi University.

Xu, W., Jiang, Y., Tian, S., and Zhu, Q. (2019). Analysis of quality components and mycotoxins residues in mildewed raw dark tea with high humidity by liquid chromatography and mass spectrometry. *Food Sci.* 40, 293–298. doi: 10.7506/spkx1002-6630-20181106-064

Xu, W., Wu, D., Jiang, Y., and Zhu, Q. (2016). Microbial research on black tea:the community composition and food safety analysis. *J. Food Saf. Qual.* 7, 3541–3552. doi: 10.19812/j.cnki.jfsq11-5956/ts.2016.09.021

Xu, Z., Wu, L., Liu, S., Huang, H., Dong, M., and Zhao, Y. (2019). Review for development of microbial diversity during dark tea fermentation period. *J. Biol.* 36, 92–95. doi: 10.3969/j.issn.2095-1736.2019.03.092

Yan, P. (2019). *Study on the Toxicity and Exposure Levels of Deoxynivalenol and Its Derivatives in Wheat and Maize*. Master's Thesis. Wuhan: Wuhan Polytechnic University.

Yang, Z., and Liu, Z. (2021). Advances in the diagnosis and treatment of trichinosis. *Chinese J. Intern. Med.* 11, 1013–1016. doi: 10.3760/cma.j.cn112138-20210224-00159

Yang, J., Zeng, X., Pu, H., Yang, X., and He, Z. (2020). Investigation of the microbial diversity and community structure in Shaanxi Fu brick tea. *Food Ferment. Indus.* 46, 50–57. doi: 10.13995/j.cnki.11-1802/ts.022055

Yang, J., Zhao, X., Zhang, G., and Guo, J. (2021). Effect and advances in research of deoxynivalenol on intestinal health of livestock and poultry. *China Feed* 09, 87–92. doi: 10.15906/j.cnki.cn11-2975/s.20210917

Ye, Z., Wang, X., Fu, R., Yan, H., Han, S., Gerelt, K., et al. (2020). Determination of six groups of mycotoxins in chinese dark tea and the associated risk assessment. *Environ. Pollut.* 261:114180. doi: 10.1016/j.envpol.2020.114180

Yogendrarajah, P., Devlieghere, F., Njumbe Ediage, E., Jacxsens, L., De Meulenaer, B., and De Saeger, S. (2015). Toxigenic potentiality of *Aspergillus flavus* and *Aspergillus parasiticus* strains isolated from black pepper assessed by an lc-ms/ms based multi-mycotoxin method. *Food Microbiol.* 52, 185–196. doi: 10.1016/j.fm.2015.07.016

York, J. L., Magnuson, R. H., and Schug, K. A. (2020). On-line sample preparation for multiclass vitamin, hormone, and mycotoxin determination in chicken egg yolk using lc-ms/ms. *Food Chem.* 326:126939. doi: 10.1016/j.foodchem.2020.126939

Yu, J., Bhatnagar, D., and Cleveland, T. E. (2004). Completed sequence of aflatoxin pathway gene cluster in *Aspergillus parasiticus*. *FEBS Lett.* 564, 126–130. doi: 10.1016/S0014-5793(04)00327-8

Zhang, C. (2015). *Variation of Ann Tea Polyphenols and Its Extraction and Isolation During Processing and Storage*. Master's Thesis. Hefei: Anhui Agricultural University.

Zhang, M. (2017). *Study on Rapid Detection of Ochratoxins Contamination in Food by Immunological Methods*. Master's Thesis. Yangling: Northwest Agriculture and Forestry University of Science and Technology.

Zhang, Y., Huang, Y., Liang, Y., Ji, X., and Hu, X. (2017). Research progress on pile fermentation of dark tea. *Food Mach.* 33, 216–220. doi: 10.13652/j.issn.1003-5788.2017.03.044

Zhang, H., Li, H., and Mo, H. (2010). Microbial population and antibacterial activity in fuzhuan brick tea. *Food Sci.* 31, 293–297.

Zhang, Y., Skaar, I., Sulyok, M., Liu, X., Rao, M., and Taylor, J. W. (2016). The microbiome and metabolites in fermented pu-erh tea as revealed by high-throughput sequencing and quantitative multiplex metabolite analysis. *PLoS One* 11:e157847. doi: 10.1371/journal.pone.0157847

Zhang, J., Xia, Z., Zhang, X., Zheng, D., and Zhou, Y. (2021). Overview of quality and safety standards for rice in China. *China Rice* 27, 77–83. doi: 10.3969/j.issn.1006-8082.2021.04.016

Zhang, Y., Zhao, S., Liang, H., Li, W., Zhao, T., and Li, C. (2012). Changes of fungal community in puer tea fermentation. *China Brewing* 31, 122–125. doi: 10.3969/j.issn.0254-5071.2012.01.037

Zhao, R. (2012). *Study the Development of the Microorganism and the Quality of Fu Brick Tea During the Processing*. Master's Thesis. Guangdong, China: Hunan Agricultural University.

Zhao, X. (2014). Mechanistic study on the inhibition of aflatoxin biosynthesis by gallic acid based on rna-seq data. Paper presented at the Compilation of Papers and Abstracts of the 9th Congress and Symposium of Guangdong Genetics Society From.

Zhao, Z. J., Hu, X. C., and Liu, Q. J. (2015). Recent advances on the fungi of pu-erh ripe tea. *Int. Food Res. J.* 22:1240.

Zhao, H., Huang, S., Shi, L., and Wang, Y. (2021). Isolation and identification of preponderant strains of fu brick tea and primary study on fermentation of low grade green tea. *Food Sci.* 43, 89–95.doi: 10.7506/spkx1002-6630-20210415-211

Zhao, Y., Jia, W., Liao, S., Xiang, L., Chen, W., Zou, Y., et al. (2022). Dietary assessment of ochratoxin a in chinese dark tea and inhibitory effects of tea polyphenols on ochratoxigenic *Aspergillus niger*. *Front. Microbiol.* 13:1073950. doi: 10.3389/fmicb.2022.1073950

Zhao, X., Li, R., Zhou, C., Zhang, J., He, C., Zheng, Y., et al. (2016). Separation and purification of deoxynivalenol (don) mycotoxin from wheat culture using a simple two-step silica gel column chromatography. *J. Integr. Agric.* 43, 89–95. doi: 10.1016/S2095-3119(15)61098-X

Zhao, Z., Lou, Y., Shui, Y., Zhang, J., Hu, X., Zhang, L., et al. (2021). Ochratoxigenic fungi in post-fermented tea and inhibitory activities of *bacillus* spp. from post-fermented tea on ochratoxigenic fungi. *Food Control* 126:108050. doi: 10.1016/j.foodcont.2021.108050

Zhao, M., Ma, Y., Chen, L., and Lv, C. (2017). Not only pu-erh tea, all foods are at risk of aflatoxin contamination. *Pu-erh.* 107, 68–71.

Zheng, Y. (2013). Identification of fungal population in the pile fermentation process of kangzhuan tea. *J. Anhui Agric. Sci.* 41, 1261–1264. doi: 10.13989/j.cnki.0517-6611.2013.03.023

Zhong, T., Qi, G. X. W., Chen, S., and Li, J. (2010). Ldentification of fungal populations during the storage period of tibetan tea. *Guizhou Agric. Sci.* 38, 101–103. doi: 10.3969/j.issn.1001-3601.2010.10.031

Zhou, C., Chen, W., Mu, R., Wu, Z., and Zhang, M. (2015a). Research on function and safety of *Penicillium chrysogenum*, a preponderant fungus during the fermentation process of pu'er tea. *Guangdong Agric. Sci.* 42, 21–24. doi: 10.3969/j.issn.1004-874X.2015.06.004

Zhou, C., Chen, W., Wu, Z., Zhang, M., Guan, J., Li, T., et al. (2015b). Research on identification, function and safety of *Aspergillus niger*, a preponderant fungus during the fermentative process of pu'er tea. *J. Food Saf. Qual.* 6, 1006–1010. doi: 10.19812/j.cnki.jfsq11-5956/ts.2015.03.048

Zhou, H., Li, J., Zhao, L., Han, J., Yang, X., Yang, W., et al. (2004). Study on main microbes on quality formation of Yunnan puer tea during pile-fermentation process. *J. Tea Sci.* 03, 212–218. doi: 10.13305/j.cnki.jts.2004.03.012

Zhu, L., Zhang, Z., and Xie, F. (2017). Determination of aflatoxin b1 in Chinese moon cake by enzyme-linked immunosorbant assay. *Farm Prod. Process.* 10, 56–58. doi: 10.16693/j.cnki.1671-9646(X).2017.05.044

Zu, Z., Tian, S., and Qian, Y. (2021). Research progress of fusarium toxin contaminated grain and animal feed. *Guangdong Feed.* 30, 49–51.

frontiers | Frontiers in Microbiology

TYPE Original Research
PUBLISHED 16 March 2023
DOI 10.3389/fmicb.2023.1110720

OPEN ACCESS

EDITED BY
Wei Zhao,
Jiangnan University,
China

REVIEWED BY
Feng Zhang,
Affiliated Hospital of Jiangnan University,
China
Shi Wu,
Guangdong Academy of Science,
China

*CORRESPONDENCE
Xiaomei Yan
✉ yanxiaomei@icdc.cn
Haibin Wang
✉ wanghb811@163.com
Zilong He
✉ hezilong@buaa.edu.cn

†These authors share first authorship

SPECIALTY SECTION
This article was submitted to
Food Microbiology,
a section of the journal
Frontiers in Microbiology

RECEIVED 29 November 2022
ACCEPTED 27 February 2023
PUBLISHED 16 March 2023

CITATION
Guo Y, Yu X, Wang J, Hua D, You Y, Wu Q, Ji Q, Zhang J, Li L, Hu Y, Wu Z, Wei X, Jin L, Meng F, Yang Y, Hu X, Long L, Hu S, Qi H, Ma J, Bei W, Yan X, Wang H and He Z (2023) A food poisoning caused by ST7 *Staphylococcal aureus* harboring *sea* gene in Hainan province, China.
Front. Microbiol. 14:1110720.
doi: 10.3389/fmicb.2023.1110720

A food poisoning caused by ST7 *Staphylococcal aureus* harboring *sea* gene in Hainan province, China

Yahui Guo[1,2,3†], Xiaojie Yu[4†], Jixiao Wang[4], De Hua[4], Yuanhai You[2], Qingbo Wu[4], Qinglong Ji[5], Jianzhong Zhang[2], Liefei Li[4], Yuan Hu[2], Zhonghui Wu[4], Xiaoyue Wei[2], Lianqun Jin[6], Fanliang Meng[2], Yuhua Yang[2], Xiaofeng Hu[6], Lijin Long[2], Songnian Hu[7], Heyuan Qi[8], Juncai Ma[7,8], Wenwen Bei[4], Xiaomei Yan[2]*, Haibin Wang[1,3]* and Zilong He[9]*

[1]Baotou Medical College, Inner Mongolia University of Science and Technology, Baotou, China, [2]Chinese Center for Disease Control and Prevention, National Institute for Communicable Disease Control and Prevention, Beijing, China, [3]Beijing Chaoyang District Center for Disease Control and Prevention, Beijing, China, [4]Hainan Provincial Center for Disease Control and Prevention, Haikou, China, [5]Chinese Academy of Inspection and Quarantine, Beijing, China, [6]Chinese PLA Center for Disease Control and Prevention, Beijing, China, [7]State Key Laboratory of Microbial Resources, Institute of Microbiology, Chinese Academy of Sciences, Beijing, China, [8]Microbial Resource and Big Data Center, Institute of Microbiology, Chinese Academy of Sciences, Beijing, China, [9]Beijing Advanced Innovation Center for Big Data-Based Precision Medicine, Interdisciplinary Innovation Institute of Medicine and Engineering, School of Engineering Medicine, Beihang University, Beijing, China

ST7 *Staphylococcus aureus* is highly prevalent in humans, pigs, as well as food in China; however, staphylococcal food poisoning (SFP) caused by this ST type has rarely been reported. On May 13, 2017, an SFP outbreak caused by ST7 *S. aureus* strains occurred in two campuses of a kindergarten in Hainan Province, China. We investigated the genomic characteristics and phylogenetic analysis of ST7 SFP strains combined with the 91 ST7 food-borne strains from 12 provinces in China by performing whole-genome sequencing (WGS). There was clear phylogenetic clustering of seven SFP isolates. Six antibiotic genes including *blaZ, ANT (4')-Ib, tetK, lnuA, norA,* and *lmrS* were present in all SFP strains and also showed a higher prevalence rate in 91 food-borne strains. A multiple resistance plasmid pDC53285 was present in SFP strain DC53285. Among 27 enterotoxin genes, only *sea* and *selx* were found in all SFP strains. A ΦSa3int prophage containing type A immune evasion cluster (*sea, scn, sak*, and *chp*) was identified in SFP strain. In conclusion, we concluded that this SFP event was caused by the contamination of cakes with ST7 *S. aureus*. This study indicated the potential risk of new emergencing ST7 clone for SFP.

KEYWORDS

staphylococcus food poisoning, sequence type 7, whole-genome sequencing, enterotoxin A, prophage, plasmids

Introduction

Food-borne disease (FBD) caused by microorganisms is a major concern for food safety and it is a global health problem that is harmful to humans. *Staphylococcus aureus* an ubiquitous Gram-positive bacterium and a common causative pathogen of food poisoning (Hennekinne et al., 2012). A total of 314 outbreaks of staphylococcal food poisoning (SFP) were reported in

China between 2011 and 2016, involving 5,196 cases and 1 death (Liu et al., 2018). In 2020, the National Foodborne Disease Outbreak Surveillance System in China reported 4,662 outbreaks with confirmed etiology, of which bacterial pathogens were the most common cause of illnesses (41.7%) and *S. aureus* ranked third among the causative bacteria (75 outbreaks and 954 illnesses) (Li et al., 2021). The incubation period of SFP is 0.5–8 h, and the common symptoms are nausea and vomiting, with or without abdominal pain, dizziness, diarrhea, shivering, general weakness, and moderate fever (Hennekinne et al., 2012).

Staphylococcus aureus can produce different Staphylococcal enterotoxins (SEs)and SE-like (SEl) toxins. It was reported less than 1 μg of SE can cause SFP (Pinchuk et al., 2010). The most common SEs are SEA, SEB, SEC, SED and SEE, accounting for approximately 95% of SFP outbreaks (Bastos et al., 2017). Most of the SEs and SEl toxins are located on the mobile genetic elements (MGEs) (such as plasmids, prophages, genomic islands, and pathogenicity islands) or next to the staphylococcal cassette chromosome (Argudin et al., 2010). Among them, SEA and SEP are carried by prophages (Argudin et al., 2010).

ST7 *S. aureus* is an important circulating clone in China. ST7 is one of the most commonly isolated STs from the nasal swabs of healthy individuals and occupational livestock workers in China (Yan et al., 2015; Ye et al., 2015). ST7 is also the dominant type in healthy and diseased pigs, and environment (pigpen gates, soil, and ground), followed by ST398 and ST9 in China (Yan et al., 2014; Zhou et al., 2020). ST7 strains can cause a variety of diseases both in animals and humans. ST7 clones are common cause of bovine mastitis (Li et al., 2017). Among the human-related diseases, ST7 clones commonly cause skin and soft tissue infections, bacteremia, pneumonia, and musculoskeletal infection, especially in children (Gu et al., 2016; Li et al., 2018; Wu et al., 2018). Most importantly, ST7 is the dominant type in a variety of foods, such as ready-to-eat foods and vegetables (Liao et al., 2018; Rong et al., 2018).

At present, ST6, ST943, ST5, ST59, ST81, and ST8 were the predominant types of *S. aureus* that caused food poisoning outbreaks in many countries (Cha et al., 2006; Suzuki et al., 2014; Li et al., 2018; Chen and Xie, 2019; Lv et al., 2021). Untill now, outbreaks of ST7 food poisoning have been only reported in Shijiazhuang and Guangzhou in China (Lv et al., 2021; Zhou et al., 2022). On May 13, 2017, an SFP outbreak caused by ST7 *S. aureus* strains occurred in two campuses of a kindergarten in Hainan Province, China, involving 26 children and one adult. ST7, as a new emerging SFP clone, is not well characterized up to now. In this study, we aimed to investigate the genomic characteristics of these ST7 strains, by using whole-genome sequencing (WGS). In particular, we analyzed the SFP strains for virulence, drug resistance, prophages, plasmid, and defense systems. Moreover, we conducted phylogenetic analysis of these SFP strains along with the 91 ST7 strains isolated from food in 12 provinces of China.

Materials and methods

Epidemiological investigation

On May 13, 2017, an outbreak of food poisoning in campuses A and B of a kindergarten in the Hainan Province, China was investigated. The outbreak involved 26 children and one adult. The symptoms had appeared after consumption of breakfast. The most common symptoms were vomiting (27/27, 100%), followed by periumbilical abdominal pain (14/27, 51.85%), and fever (3/27, 11.11%). The incubation period for symptoms was 1–3 h. The cakes purchased from a cake shop were suspected of being related to the SFP. The leftover food and anal swabs of patients were collected for bacterial isolation. All samples were processed based on *S. aureus* isolation methods for foods according to the national standards in China (GB/T 4789.10–2017). Five *S. aureus* strains were isolated from leftover cake and lean porridge in campus A, the cream from cake shop, and leftover cake in campus B, while two strains from patients were isolated from campus A.

Bacterial collection

Ninety-one food-borne ST7 *S. aureus* strains were collected from 12 provinces of China between 2006 and 2019 (Supplementary Figure S1). All the strains in the study were confirmed by PCR detection for *nuc* and *mecA* (Merlino et al., 2002).

Antimicrobial susceptibility testing

The minimum inhibitory concentrations (MICs) of cefoxitin, linezolid, clindamycin, erythromycin, doxycycline, gentamicin, penicillin, rifampicin, sulfamethoxazole, tigecycline, ciprofloxacin, tetracycline, vancomycin, fusidic acid, quinupristin/dalfopristin, daptomycin, teicoplanin, florfenicol, tiamulin, and nitrofurantoin for 7 SFP strains were determined by microdilution method. *S. aureus* ATCC29213 was used as the quality control strain. The MICs values were interpreted according to Clinical and Laboratory Standard Institute (CLSI) Performance Standards for Antimicrobial Susceptibility Testing (31st edition).

DNA extraction, genome sequencing, assembly, and annotation

Genomic DNA was extracted from pure cultures using a commercial kit (QIAGEN, Germany) and quantified by Qubit 4.0 (USA Invitrogen ABI). Genomic DNA was sequenced using Illumina NovaSeq PE150 by the Beijing Novogene Bioinformatics Technology Co. Ltd. All sequences were preprocessed by READFQ V10 (Chen et al., 2018) to delete data with mass value ≤20. Clean data were assembled using SPAdes V3.13 (Bankevich et al., 2012), from which only contigs greater than 500 bp in length were selected for further analysis. The Nanopore Oxford MinION platform was used for three strains, i.e., DC53285, DC53206, and DC52998 (You et al., 2018). Unicycler v0.5.0 (Wick et al., 2017) was used for genome assembly based on ONT long reads and Illumina short reads. All genomes were annotated by Prokka V1.14.5 (Seemann, 2014). The closed genome was confirmed by PCR (Supplementary Table S4).

Phylogenetic analysis

The genomes of seven SFP strains, 91 food-borne strains, and seven ST7 published sequences from NCBI (Supplementary Table S1)

were included in the phylogenetic analysis. DC51277 (CC7-ST943) was used as an outgroup. The core genome was extracted by Roary 3.13.0 (Page et al., 2015). Maximum-likelihood phylogenetic trees were constructed using RAxML V8.2.12 (Stamatakis, 2014) based on 2,387 core genes (shared by >99% of *S. aureus* isolates) and the evolutionary tree was visualized by ITOL[1] (Letunic and Bork, 2019).

Multilocus sequencing typing (MLST), detection of virulence, resistance, restriction-modification genes (R-M), prophage, and plasmid

MLST was performed by PubMLST[2] website. VFDB and CARD libraries were downloaded to construct the local database, and the search within blastp was conducted with parameters of >80% identity and >80% coverage. According to the copy number of virulence and resistance genes, heatmap was drawn using the heatmap package of R V4.1.2. (Chan, 2018). To better assess the carriage rate of virulence genes, our data were compared with the data of a previously published manuscript (Slingerland et al., 2020), in which genome of 10,288 *S. aureus* strains were included. Statistical analysis was performed by Chi-squared test for independence using SPSS Statistics 25.0 (IBM). p values <0.05 were considered indicative of statistical significance.

R-M genes were searched on Restriction-Modification Finder 1.1.[3] *hsdM* and *hsdS* were verified by PCR (Supplementary Table S4). CRISPR-cas genes were searched on CRISPRCas Finder (Couvin et al., 2018).

The prophage structure of four strains was compared, including one SFP strain (DC53285) and three non-SFP strains which carried *sea* (DC53206, DC52998, and DC52929). Prophages and plasmids were identified by PHASTER[4] and PlasmidFinder.[5] The prophage and plasmid nucleotide sequences were compared with sequences in the GenBank database using BLASTN[6] and were visualized by Easyfig (Sullivan et al., 2011). The closed plasmid was confirmed by PCR (Supplementary Table S4).

Results

Phylogenetic analysis of SFP strains and non-SFP strains

The 106 genomic sequences (incuding one outgroup sequence) in this study shared 2,387 core genes. The phylogenetic tree can be mainly divided into two clusters (Figure 1). The tree demonstrated that the SFP outbreak strains isolated from the food matrix (DC53286, DC53288, DC53289, DC53349, and DC53362) clustered together with those of the human cases (DC53284 and DC53285) in a single clade carried by one branch in cluster 1. Further analysis of SFP strains in the phylogenetic tree showed that food isolates from campus A were closly clustered with campus B, and the cream from cake shop closly clustered with patient isolates from campus A.

The geographically clustered stains were from Hainan, Anhui, and Jilin Provinces in cluster 1 and 2, respectively. These strains were mainly isolated from meat with adjacent isolation years. The one NCBI sequence from human in Zhejiang Province in China that was closly clustered with Chinese isolates from food matrix in cluster 1. In cluster 2, six NCBI human sequences of foreign countries clustered as a subclade with an imported food isolate from Uruguay and a few food isolates from China.

Phenotype and genotype of antibiotic resistance

All SFP isolates were methicillin-sensitive *S. aureus* (MSSA) and only resistant to penicillin and tetracycline. The heatmap showed the same resistance gene profiles of the seven SFP strains, all of which carried one copy of *blaZ, tetK, ANT (4')-Ib*, and *lnuA, lmrS*, and *norA* gene (Figure 2).

In this study, 91 food-borne strains carried a total of 15 resistance genes. Six antibiotic genes showed a higher prevalence rate, i.e., *norA, lmrS, blaZ, ANT (4')-Ib, tetK*, and *lnuA* (Supplementary Table S2). Only two strains carried two copies of resistance genes, which were *AAC (6')-Ie-APH (2")-Ia, catA*, and *blaZ*, respectively (Figure 2). No special antibiotic genes were observed for the 7 SFP strains compared with 91 food-borne strains.

Combined with phylogenetic tree, *ermC, lnuA, ANT (4 ')-Ib,* and *tetK* were mainly distributed in cluster 1 strains ($p < 0.05$). And most of strains were from poultry and livestock meat in Anhui, Hainan, and Yunnan Province. While *AAC (6 ')-Ie-APH (2")-Ia* and *ermB* genes were mainly found in cluster 2 strains ($p < 0.05$), and most of which were from poultry and livestock meat in Jilin and Gansu Province (Supplementary Table S2; Figure 1).

Distribution of virulence genes

All SFP isolates had the same virulence gene profile (Figure 3; Supplementary Table S3). Among the 27 enterotoxin genes, only *sea* and *selx* were found in all SFP strains. The *chp*, *sak*, *scn*, *lukD, lukE, lukS-PV*, and *lukF-PV* were also present in all SFP strains.

The 91 non-SFP isolates showed a significantly higher prevalence rate of ten virulence genes, i.e., *fnbA, fnbB, sdrD, lukD, lukE, sep, lukF-PV, lukS-PV, sak*, and *sdrE* compared with the reference data ($p < 0.05$). Six virulence genes (*tsst-1, sea, sec, sel, chp*, and *sspB*) had a lower prevalence rate ($p < 0.05$, Supplementary Table S3). Almost all the virulence genes were one copy, except for *eap/map*, *hysA*, and *nuc.*

Genomic structure of prophage carrying sea

One SFP strain (DC53285) and three non-SFP strains (DC53206, DC52998, and DC52929) were selected for the prophage structure analysis. The identified prophages of DC53285, DC53206, DC52998,

1 https://itol.embl.de
2 https://pubmlst.org/
3 https://cge.cbs.dtu.dk/services/Restriction-ModificationFinder/
4 http://phaster.ca/
5 https://cge.food.dtu.dk/services/PlasmidFinder/
6 http://blast.ncbi.nlm.nih.gov/blast

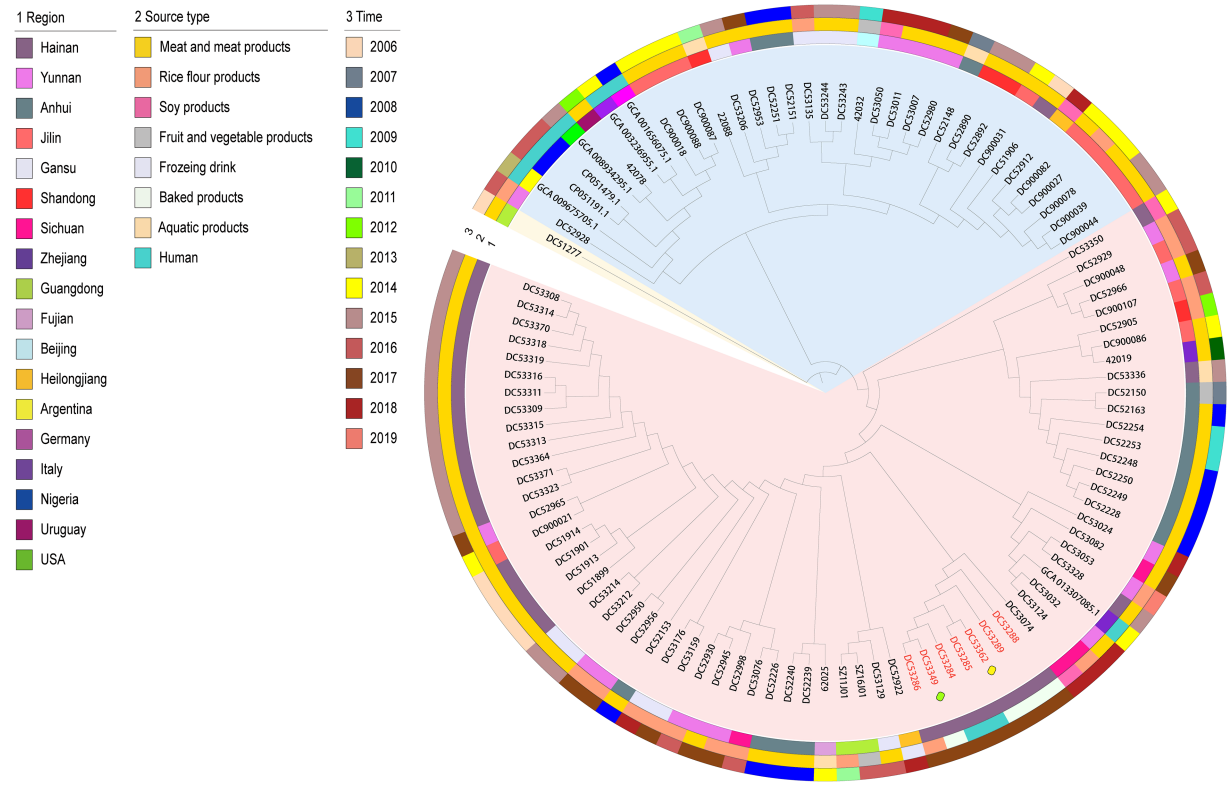

FIGURE 1
Maximum-likelihood phylogenetic tree based on 2,387 core genes of the 106 *S. aureus* isolates. The outgroup ST943 strain is indicated in yellow bottom; cluster 1 and 2 is shown in red and blue bottom, respectively. Isolates from food poisoning are indicated by red text. The yellow and green boxes represent strains from the cake shop and campus B, respectively. The remaining SFP strains are from campus A. Region, time, and source type are indicated by means of numbers and the colored rings. NCA_013307085.1, GCA_001656075.1, GCA_003236955.1, GCA_008934295.1, GCA_009675705.1, CP051191, and CP051479 are sequences from NCBI.

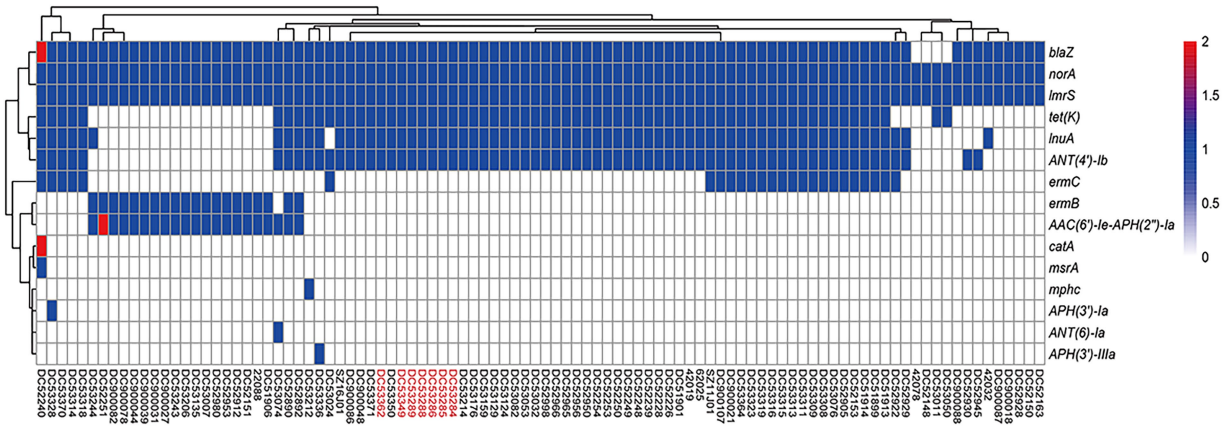

FIGURE 2
Heatmap of copy number of resistance genes of ST7 *S. aureus* strains. The gene copy number 0, 1, 2 are shown in white, blue, and red bottom, respectively. Isolates from food poisoning are indicated by red text.

and DC52929 were 42,263 bp, 47,075 bp, 46,733 bp, and 47,230 bp in length and contained 67, 67, 68, and 68 coding sequences (CDSs), respectively. They were all integrated within the *hlb* and belonged to ΦSa3int integrase gene group. Overall, the structure of DC53285 shared 98.97% of nucleotide sequence identity and 85% coverage with ΦNM3 (NC_008617.1), and shared 96.87% identity and 78% coverage with SA1014ruMSSAST7 (NC_048710.1) (Figure 4). DC52929 prophage showed low nucleotide similarity with the above three prophages. Type A immune evasion cluster (IEC) genes (*sea, sak, chp*, and *scn*) were found in DC53285, DC53206, and DC52998 prophage, while type D IEC genes (*sea, sak, and scn*) were found in DC52929. The *lukF*-PV and *lukS*-PV were located downstream of the four prophages (Figure 4).

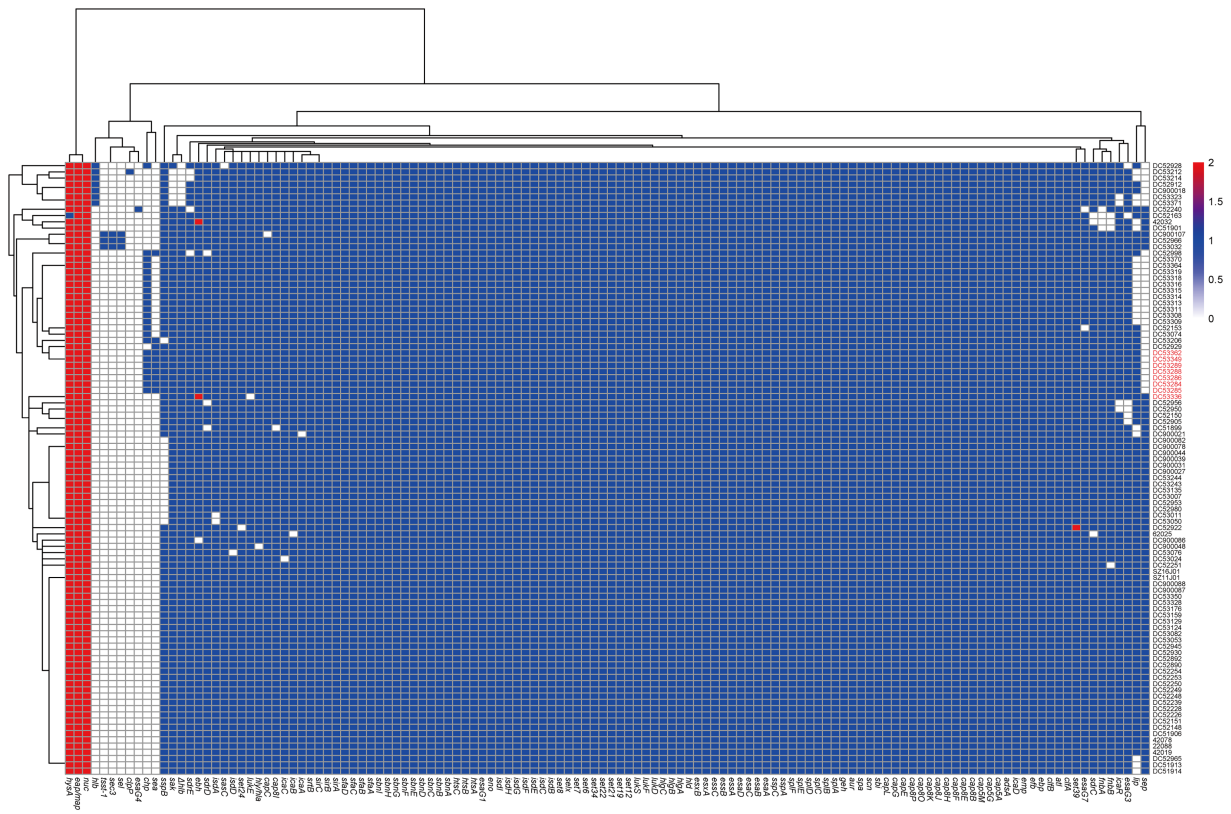

FIGURE 3
Heatmap of copy number of virulence genes of ST7 *S. aureus* strains. The gene copy number 0, 1, 2 are shown in white, blue, and red bottom, respectively. Isolates from food poisoning are indicated by red text. *Δhlb* is indicated truncated *hlb* gene.

ST7 SFP strain carried a multi-antibiotic resistant plasmid

A multiple resistance plasmid pDC53285 was present in the SFP strain DC53285. The complete sequence of pDC53285 was 35,024 bp in size and had a G+C content of 29% (accession no. NMDC60045017). Sequence analysis identified 43 CDSs. pDC53285 carried four antibiotic resistance genes, including *ANT(4′)-Ib, tetK, lunA,* and *blaZ*. Plasmid pDC53285 shared 99% coverage (99.97% nucleotide identity) with the plasmid MJ015 (NZ_CP038185.1) from Zhejiang Province in NCBI database. The genetic structure of pDC53285 also showed high nucleotide similarity (71% identity) and the main ORF features with two plasmids pSR02 (NZ_CP048645) and pMW2 (NZ_CM007996). The 1–18,870 bp and 33,717–35,024 bp regions of pDC53285 were highly equivalent to the 1–16,494 bp, and 24,746–26,055 bp regions of plasmid pSR02. The pDC53285 plasmid retained around two-thirds of the genes from pSR02, mainly including *ANT(4′)-Ib, tetK*, *lunA*, *oriT* (the origin of transfer site), and a relaxase protein. The 18,853–25,717 bp region of pDC53285 was highly equivalent to the 2,173–20,100 bp region of pMW2, mainly including *blaZ* and a relaxase protein. The two relaxase protein encoding genes belonged to MOB_V family (Figure 5A). Further sequence analysis showed that the two plasmids (pMW2 and pSR02) harbored a 17 bp upstream homologous region and an 835 bp downstream homologous region (Figure 5B).

ST7 SFP isolates carry intact type I and IV restriction-modification (RM) systems

All SFP strains contained complete type I and type IV RM systems. Analysis of CRISPR-cas system revealed that none of the SFP strains carried CRISPR-cas system encoding genes.

Discussion

In this study, we used WGS to investigate *S. aureus* involved in the outbreak in Hainan Province, China. We confirmed seven ST7 SFP isolates with a clear phylogenetic clustering in cluster 1. Further analysis of SFP strains in the phylogenetic tree showed that food isolates from campus A were closly clustered with campus B, and the cream from cake shop closly clustered with patient isolates from campus A. Therefore, we concluded that this SFP event was caused by the contamination of cakes from cake shop with *S.aureus* carrying *sea*. The strain isolated from the porridge was also related with this SFP, which may be due to cross contamination of porridge with cakes. SFP investigations have typically relied on epidemiological data and molecular typing; however, WGS is increasingly used in recent years (Mossong et al., 2015; Durand et al., 2018; Nouws et al., 2021). In this study, we also confirmed that WGS can be a high discriminative tool to support epidemiological outbreak-investigations.

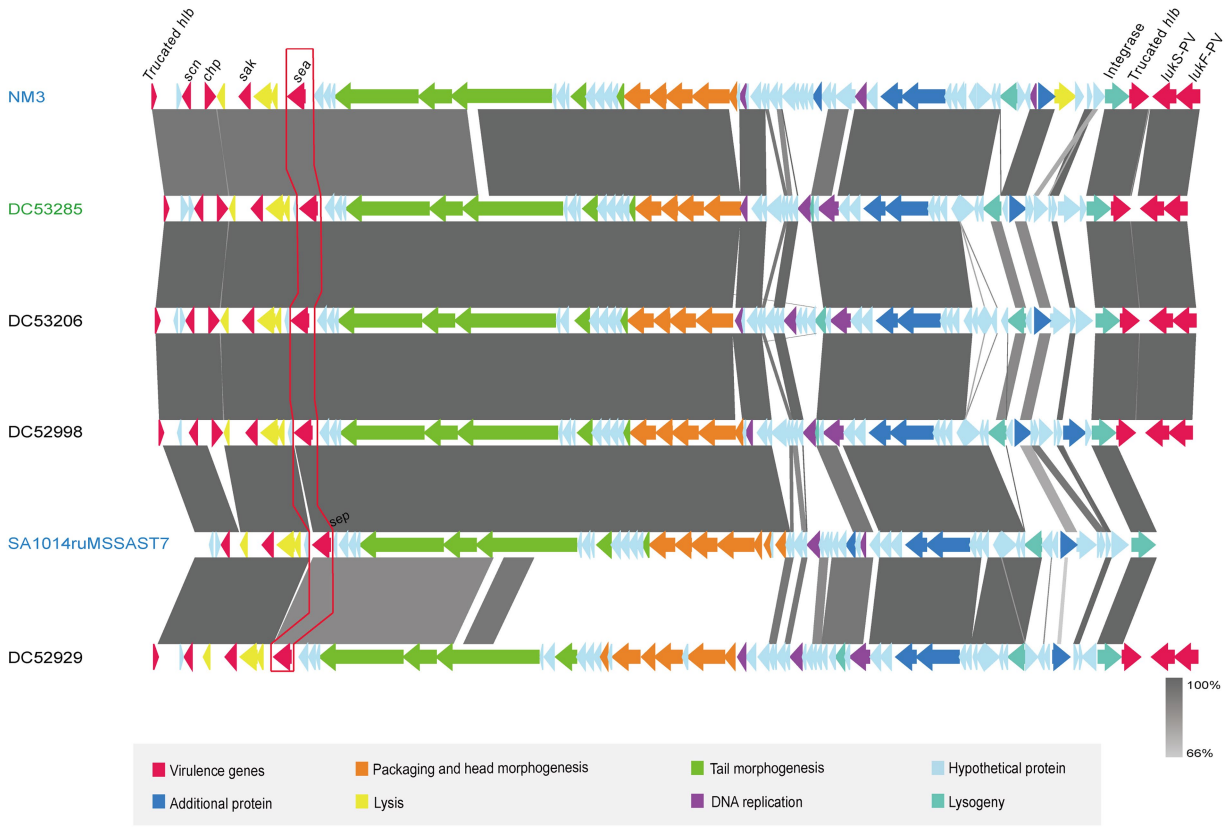

FIGURE 4
Architecture of prophages from ST7 SFP and non-SFP strains, and similar regions in phage from NM3 and SA1014ruMSSAST7. Corresponding CDSs are colored as indicated. SFP strain DC53285 is shown in green, and non-SFP strains DC53206, DC52998, and DC52929 are shown in black. NM3 (NC_008617.1) and SA1014ruMSSAST7 (NC_048710.1) from NCBI are shown in blue. The nucleotide similarities in the structure are indicated by grey shading.

SEA was the main cause of food poisoning caused by ST7 *S. aureus* in this study. SEA, alone or in association with other SE(s), is the most frequently involved (>75%) in SFP outbreaks worldwide (Hennekinne et al., 2012; Guillier et al., 2016). The *sea* is the most frequently identified enterotoxin gene in China (Yan et al., 2012; Chen and Xie, 2019) and is always located on the prophage (Argudin et al., 2010), which formed the IEC together with the different combinations of *scn, chp, sak*, and *sep* (van Wamel et al., 2006). All SFP isolates in this study carried ΦSa3int prophages belonging to the family *Siphoviridae* and genus *Biseptimavirus*. In addition, type A IEC, including *sea, scn, sak*, and *chp* gene were found on the ΦSa3int prophages. Studies have shown that the main difference between human and animal strains of *S. aureus* is that human strains always carry IEC (McCarthy and Lindsay, 2013). Thus, the real source of the contamination of cakes in this study was probably human based on the IEC type of the SFP strains. However, we do not have strains isolated from the staff in the cake shop to support this inference. The prophage of SFP strain DC53285 showed high nucleotide similarity with NM3(NC_008617.1) which was carried by ST254 (CC8) *S. aureus*. Phage ΦphiNM3 has been reported in different MLST type strains, including ST1, ST5, ST7, ST8, ST30, ST72, ST109, and ST508 (Nepal et al., 2021). Therefore, the ΦSa3int prophage of SFP strains may have been exchanged by horizontal gene transfer (HGT) from the same or different ST strains. A previous study found a significantly higher prevalence of ΦNM3 in chronic rhinosinusitis patients with high disease severity compared to those with low disease severity (Nepal et al., 2021). This implies that the prophage of SFP strains can increase the pathogenicity of strains.

A multiple resistant plasmid pDC53285 with *rep5a* was found in ST7 SFP strain. pDC53285 carried *oriT* and relaxase protein, which were similar to that in plasmid pMW2 and pSR02. The conjugative mobilization plasmids usually have a Type-IV secretion apparatus, an origin of transfer (*oriT*) site, and a relaxase protein. Interestingly, it has recently been demonstrated that mobilization transfer can be carried out through the relaxase-*in trans* mechanism for the plasmid only with *oriT* and relaxase protein, and it is a frequent event that most *S. aureus* plasmids have evolved to take advantage of (O'Brien et al., 2015; Ramsay et al., 2016). Therefore, the plasmid pDC53285 in this study may be a mobilizable plasmid through the relaxase-*in trans* mechanism of mobilization. pDC53285 showed the highest nucleotide similarity with the plasmid carried by MJ015 (NZ_CP038185.1), which is an MSSA ST7 strain isolated from a patient in Zhejiang, China. Therefore, pDC53285 may potentially be a mobilizable plasmid through a horizontal transfer manner. Further studies should investigate the distribution of pDC53285 in Chinese strains. Based on the genetic structure of pDC53285, it is speculated that pDC53285 was generated as a result of fusion between plasmids pSR02 and pMW2. On further comparative analysis, two plasmids (pMW2 and pSR02) were found to harbor a 17 bp upstream homologous region

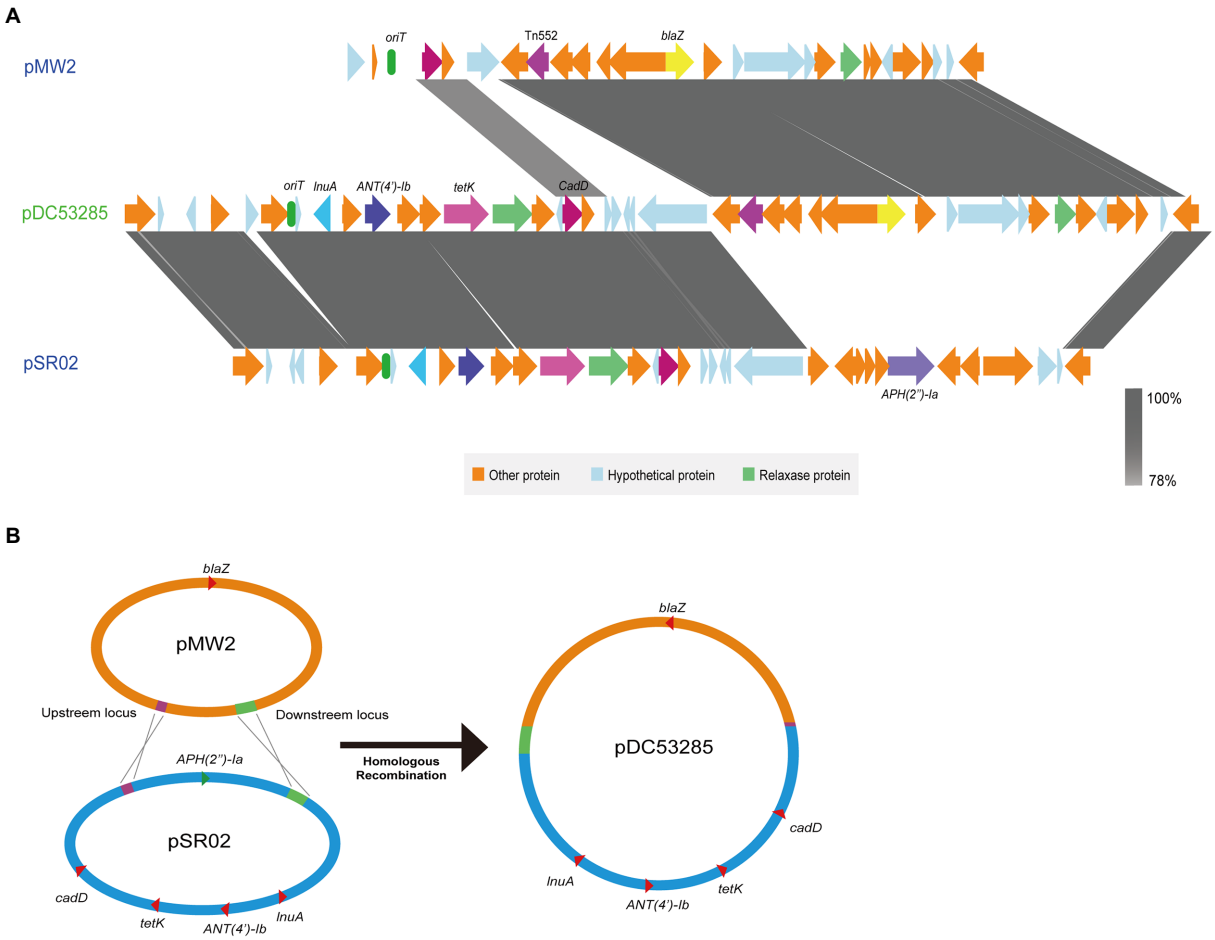

FIGURE 5
(A) Structure of pDC53285 from ST7 SFP strain and similar regions in plasmid pMW2 (AP004832.1) and pSR02(CP048645.1). Corresponding CDSs are colored as indicated. The nucleotide similarities in the structure are indicated by grey shading. **(B)** Illustration of the process of evolution of pMW2 (AP004832.1) and pSR02(CP048645.1) to pDC53285.

and an 835 bp downstream homologous region, facilitating homologous recombination of the two plasmids, and resulting in formation of a 35,024 bp integrated multi-antibiotic resistance plasmid. The same recombination mechanism was reported for a conjugative virulence plasmid, p15WZ-82_Vir, from a clinical *Klebsiella variicola* strain (Yang et al., 2020).

ANT(4')-Ib, also called *aadD2*, encoding an aminoglycoside 4′-O-nucleotidyltransferase was first described in *Bacillus clausii* and rarelly reported in *S. aureus*(Bozdogan et al., 2003; Ullah et al., 2021). In this study, the high prevalence of *ANT (4')-Ib,* together with *blaZ, tetK,* and *lnuA* were found in ST7 food-borne and SFP strains. It may be that these food-borne strains carry the similar multiple resistant plasmid as SFP strains as well. These antibiotic resistance genes were mainly distributed in strains of cluster 1 and closely associated with region and poutry/livestorck-derived foods. Whether these resistance genes originated in local poutry/livestorck associated strains is worth to be further investigated.

The *sep* gene is always located on the prophage and can also cause SFP (Omoe et al., 2005; Chiang et al., 2008; Argudin et al., 2010). The carriage rate of *sep* carried by ST7 *S. aureus* in this study (69.4%, 68/98) was much higher than that in previous studies (Omoe et al., 2005; Bania et al., 2006; Chiang et al., 2008; Wang et al., 2021). Therefore, the ST7 strains isolated from food in this study are at high risk of causing SFP. This is the first study to identify a high carriage rate of *lukFS*-PV (100%, 98/98) in the ST7 *S. aureus*. The *lukFS*-PV plays an important role in pathogenicity in the context of bacteremia, keratitis, skin and soft tissue infections, and other related diseases (Sueke et al., 2013; Knudsen et al., 2016; Xiao et al., 2019). Such a high carriage rate of *lukFS*-PV among ST7 isolates is liable to increase the risk and severity of diseases.

In summary, we concluded that this SFP event was caused by the contamination of cakes from cake shop with ST7 *S. aureus*. The food poisoning was found to be caused by enterotoxin A and a type A IEC (*sea, scn, chp, and sak*) was located on the ΦSa3int prophage. Six antibiotic genes including *blaZ, ANT (4')-Ib, tetK, lnuA, norA,* and *lmrS* were present in all SFP strains and also showed a higher prevalence rate in 91 food-borne strains. In addition, a multi-resistant plasmid pDC53285 was found in ST7 SFP strains, which may act as a vector for the dissemination of antimicrobial resistance among strains. Due attention should be accorded to the high prevalence rate of *sep, lukF*-PV, and *lukS*-PV in ST7 strains isolated from food, which is liable to increase the risk of SFP and other diseases.

Limitations

Because this is a retrospective study, samples from the staff in the cake shop, food handlers, and environment in the canteen in the kindergarten were not available. It is difficult to conclude whether the contamination comes from human.

Data availability statement

'The data presented in the study are deposited in the NCBI repository, accession number PRJNA917243, and modified BioSample Accession is available in the Supplementary material.

Ethics statement

This study was approved by Ethical Committee of National Institute for Communicable Disease Control and Prevention Chinese Center for Disease Control and Prevention (approval No. ICDC-202111). The patients/participants provided written informed consent to participate in this study.

Author contributions

All authors listed have made a substantial, direct, and intellectual contribution to the work and approved it for publication.

Funding

This work was supported by the National Natural Science Foundation of China (Grant No. 81873959), Key R&D Program of China (2018YFC1603800) and The National Key R&D Program of China (2021YFC2301000).

Conflict of interest

The authors declare that the research was conducted in the absence of any commercial or financial relationships that could be construed as a potential conflict of interest.

Publisher's note

All claims expressed in this article are solely those of the authors and do not necessarily represent those of their affiliated organizations, or those of the publisher, the editors and the reviewers. Any product that may be evaluated in this article, or claim that may be made by its manufacturer, is not guaranteed or endorsed by the publisher.

Supplementary material

The Supplementary material for this article can be found online at: https://www.frontiersin.org/articles/10.3389/fmicb.2023.1110720/full#supplementary-material

References

Argudin, M. A., Mendoza, M. C., and Rodicio, M. R. (2010). Food poisoning and *aureus* enterotoxins. *Toxins (Basel)* 2, 1751–1773. doi: 10.3390/toxins2071751

Bania, J., Dabrowska, A., Bystron, J., Korzekwa, K., Chrzanowska, J., and Molenda, J. (2006). Distribution of newly described enterotoxin-like genes in *Staphylococcus aureus* from food. *Int. J. Food Microbiol.* 108, 36–41. doi: 10.1016/j.ijfoodmicro.2005.10.013

Bankevich, A., Nurk, S., Antipov, D., Gurevich, A. A., Dvorkin, M., Kulikov, A. S., et al. (2012). SPAdes: a new genome assembly algorithm and its applications to single-cell sequencing. *J. Comput. Biol.* 19, 455–477. doi: 10.1089/cmb.2012.0021

Bastos, C. P., Bassani, M. T., Mata, M. M., Lopes, G. V., and da Silva, W. P. (2017). Prevalence and expression of staphylococcal enterotoxin genes in *Staphylococcus aureus* isolated from food poisoning outbreaks. *Can. J. Microbiol.* 63, 834–840. doi: 10.1139/cjm-2017-0316

Bozdogan, B., Galopin, S., Gerbaud, G., Courvalin, P., and Leclercq, R. (2003). Chromosomal aadD2 encodes an aminoglycoside nucleotidyltransferase in *Bacillus clausii*. *Antimicrob. Agents Chemother.* 47, 1343–1346. doi: 10.1128/AAC.47.4.1343-1346.2003

Cha, J. O., Lee, J. K., Jung, Y. H., Yoo, J. I., Park, Y. K., Kim, B. S., et al. (2006). Molecular analysis of *Staphylococcus aureus* isolates associated with staphylococcal food poisoning in South Korea. *J. Appl. Microbiol.* 101, 864–871. doi: 10.1111/j.1365-2672.2006.02957.x

Chan, B. K. C. (2018). Data Analysis Using R Programming. *Adv. Exp. Med. Biol.* 1082, 47–122. doi: 10.1007/978-3-319-93791-5_2

Chen, Q., and Xie, S. (2019). Genotypes, enterotoxin gene profiles, and antimicrobial resistance of *Staphylococcus aureus* associated with foodborne outbreaks in Hangzhou, China. *Toxins (Basel)* 11:307. doi: 10.3390/toxins11060307

Chen, S., Zhou, Y., Chen, Y., and Gu, J. (2018). Fastp: an ultra-fast all-in-one FASTQ preprocessor. *Bioinformatics* 34, i884–i890. doi: 10.1093/bioinformatics/bty560

Chiang, Y. C., Liao, W. W., Fan, C. M., Pai, W. Y., Chiou, C. S., and Tsen, H. Y. (2008). PCR detection of staphylococcal enterotoxins (SEs) N, O, P, Q, R, U, and survey of SE types in *Staphylococcus aureus* isolates from food-poisoning cases in Taiwan. *Int. J. Food Microbiol.* 121, 66–73. doi: 10.1016/j.ijfoodmicro.2007.10.005

Couvin, D., Bernheim, A., Toffano-Nioche, C., Touchon, M., Michalik, J., Néron, B., et al. (2018). CRISPRCasFinder, an update of CRISRFinder, includes a portable version, enhanced performance and integrates search for Cas proteins. *Nucleic Acids Res.* 46, W246–W251. doi: 10.1093/nar/gky425

Durand, G., Javerliat, F., Bes, M., Veyrieras, J. B., Guigon, G., Mugnier, N., et al. (2018). Routine whole-genome sequencing for outbreak investigations of *Staphylococcus aureus* in a National Reference Center. *Front. Microbiol.* 9:511. doi: 10.3389/fmicb.2018.00511

Gu, F. F., Chen, Y., Dong, D. P., Song, Z., Guo, X. K., Ni, Y. X., et al. (2016). Molecular epidemiology of *Staphylococcus aureus* among patients with skin and soft tissue infections in two Chinese hospitals. *Chin. Med. J.* 129, 2319–2324. doi: 10.4103/0366-6999.190673

Guillier, L., Bergis, H., Guillier, F., Noel, V., Auvray, F., and Hennekinne, J.-A. (2016). Dose-response modelling of staphylococcal enterotoxins using outbreak data. *Procedia Food Sci.* 7, 129–132. doi: 10.1016/j.profoo.2016.05.002

Hennekinne, J. A., De Buyser, M. L., and Dragacci, S. (2012). *Staphylococcus aureus* and its food poisoning toxins: characterization and outbreak investigation. *FEMS Microbiol. Rev.* 36, 815–836. doi: 10.1111/j.1574-6976.2011.00311.x

Knudsen, T. A., Skov, R., Petersen, A., Larsen, A. R., and Benfield, T.Danish Staphylococcal Bacteremia Study (2016). Increased age-dependent risk of death associated with lukF-PV-positive *Staphylococcus aureus* bacteremia. *Open Forum Infect. Dis.* 3:ofw220. doi: 10.1093/ofid/ofw220

Letunic, I., and Bork, P. (2019). Interactive tree of life (iTOL) v4: recent updates and new developments. *Nucleic Acids Res.* 47, W256–W259. doi: 10.1093/nar/gkz239

Li, H., Li, W., Dai, Y., Jiang, Y., Liang, J., et al. (2021). Characteristics of settings and etiologic agents of foodborne disease outbreaks–China, 2020. *China CDC Wkly* 3, 889–893. doi: 10.46234/ccdcw2021.219

Li, T. M., Lu, H. Y., Wang, X., Gao, Q. Q., Dai, Y. X., Shang, J., et al. (2017). Molecular characteristics of *Staphylococcus aureus* causing bovine mastitis between 2014 and 2015. *Front. Cell. Infect. Microbiol.* 7:127. doi: 10.3389/fcimb.2017.00127

Li, S. G., Sun, S. J., Yang, C. T., Chen, H. B., Yin, Y. Y., Li, H. N., et al. (2018). The changing pattern of population structure of *Staphylococcus aureus* from bacteremia in China from 2013 to 2016: ST239-030-MRSA replaced by ST59-t437. *Front. Microbiol.* 9:332. doi: 10.3389/fmicb.2018.00332

Liao, F., Gu, W. P., Yang, Z. S., Mo, Z. S., Fan, L., Guo, Y. D., et al. (2018). Molecular characteristics of *Staphylococcus aureus* isolates from food surveillance in Southwest China. *BMC Microbiol.* 18:91. doi: 10.1186/s12866-018-1239-z

Liu, J. K., Bai, L., Li, W. W., Han, H. H., Fu, P., Ma, X. C., et al. (2018). Trends of foodborne diseases in China: lessons from laboratory-based surveillance since 2011. *Front. Med.* 12, 48–57. doi: 10.1007/s11684-017-0608-6

Lv, G., Jiang, R., Zhang, H., Wang, L., Li, L., Gao, W., et al. (2021). Molecular characteristics of *Staphylococcus aureus* from food samples and food poisoning outbreaks in Shijiazhuang, China. *Front. Microbiol.* 12:652276. doi: 10.3389/fmicb.2021.652276

McCarthy, A. J., and Lindsay, J. A. (2013). *Staphylococcus aureus* innate immune evasion is lineage-specific: a bioinfomatics study. *Infect. Genet. Evol.* 19, 7–14. doi: 10.1016/j.meegid.2013.06.012

Merlino, J., Watson, J., Rose, B., Beard-Pegler, M., Gottlieb, T., Bradbury, R., et al. (2002). Detection and expression of methicillin/oxacillin resistance in multidrug-resistant and non-multidrug-resistant *Staphylococcus aureus* in Central Sydney, Australia. *J. Antimicrob Chemother.* 49, 793–801. doi: 10.1093/jac/dkf021

Mossong, J., Decruyenaere, F., Moris, G., Ragimbeau, C., Olinger, C. M., Johler, S., et al. (2015). Investigation of a staphylococcal food poisoning outbreak combining case-control, traditional typing and whole genome sequencing methods, Luxembourg, June 2014. *Euro Surveill.* 20:30059. doi: 10.2807/1560-7917.ES.2015.20.45.30059

Nepal, R., Houtak, G., Shaghayegh, G., Bouras, G., Shearwin, K., Psaltis, A. J., et al. (2021). Prophages encoding human immune evasion cluster genes are enriched in *Staphylococcus aureus* isolated from chronic rhinosinusitis patients with nasal polyps. *Microb Genom* 7:726. doi: 10.1099/mgen.0.000726

Nouws, S., Bogaerts, B., Verhaegen, B., Denayer, S., Laeremans, L., Marchal, K., et al. (2021). Whole genome sequencing provides an added value to the investigation of staphylococcal food poisoning outbreaks. *Front. Microbiol.* 12:750278. doi: 10.3389/fmicb.2021.750278

O'Brien, F. G., Yui Eto, K., Murphy, R. J., Fairhurst, H. M., Coombs, G. W., Grubb, W. B., et al. (2015). Origin-of-transfer sequences facilitate mobilisation of non-conjugative antimicrobial-resistance plasmids in *Staphylococcus aureus*. *Nucleic Acids Res.* 43, 7971–7983. doi: 10.1093/nar/gkv755

Omoe, K., Hu, D. L., Takahashi-Omoe, H., Nakane, A., and Shinagawa, K. (2005). Comprehensive analysis of classical and newly described staphylococcal superantigenic toxin genes in *Staphylococcus aureus* isolates. *FEMS Microbiol. Lett.* 246, 191–198. doi: 10.1016/j.femsle.2005.04.007

Page, A. J., Cummins, C. A., Hunt, M., Wong, V. K., Reuter, S., Holden, M. T., et al. (2015). Roary: rapid large-scale prokaryote pan genome analysis. *Bioinformatics* 31, 3691–3693. doi: 10.1093/bioinformatics/btv421

Pinchuk, I. V., Beswick, E. J., and Reyes, V. E. (2010). Staphylococcal enterotoxins. *Toxins (Basel)* 2, 2177–2197. doi: 10.3390/toxins2082177

Ramsay, J. P., Kwong, S. M., Murphy, R. J., Yui Eto, K., Price, K. J., Nguyen, Q. T., et al. (2016). An updated view of plasmid conjugation and mobilization in staphylococcus. *Mob. Genet. Elements* 6:e1208317. doi: 10.1080/2159256X.2016.1208317

Rong, D. L., Wu, Q. P., Wu, S., Zhang, J. M., and Xu, M. F. (2018). Distribution and drug resistance and genotyping of *Staphylococcus aureus* contamination in ready-to-eat food and vegetables in some parts of China. *Acta Microbiol Sin.* 58, 314–323. doi: 10.13343/j.cnki.wsxb.20170144

Seemann, T. (2014). Prokka: rapid prokaryotic genome annotation. *Bioinformatics* 30, 2068–2069. doi: 10.1093/bioinformatics/btu153

Slingerland, B., Vos, M. C., Bras, W., Kornelisse, R. F., De Coninck, D., van Belkum, A., et al. (2020). Whole-genome sequencing to explore nosocomial transmission and virulence in neonatal methicillin-susceptible *Staphylococcus aureus* bacteremia. *Antimicrob. Resist. Infect. Control* 9:39. doi: 10.1186/s13756-020-0699-8

Stamatakis, A. (2014). RAxML version 8: a tool for phylogenetic analysis and post-analysis of large phylogenies. *Bioinformatics* 30, 1312–1313. doi: 10.1093/bioinformatics/btu033

Sueke, H., Shankar, J., Neal, T., Winstanley, C., Tuft, S., Coates, R., et al. (2013). lukSF-PV in *Staphylococcus aureus* keratitis isolates and association with clinical outcome. *Invest. Ophthalmol. Vis. Sci.* 54, 3410–3416. doi: 10.1167/iovs.12-11276

Sullivan, M. J., Petty, N. K., and Beatson, S. A. (2011). Easyfig: a genome comparison visualizer. *Bioinformatics* 27, 1009–1010. doi: 10.1093/bioinformatics/btr039

Suzuki, Y., Omoe, K., Hu, D. L., Sato'o, Y., Ono, H. K., Monma, C., et al. (2014). Molecular epidemiological characterization of *Staphylococcus aureus* isolates originating from food poisoning outbreaks that occurred in Tokyo, Japan. *Microbiol. Immunol.* 58, 570–580. doi: 10.1111/1348-0421.12188

Ullah, N., Dar, H. A., Naz, K., Andleeb, S., Rahman, A., Saeed, M. T., et al. (2021). Genomic Investigation of Methicillin-Resistant Staphylococcus aureus ST113 Strains Isolated from Tertiary Care Hospitals in Pakistan. *Antibiotics (Basel)*. 10:1121. doi: 10.3390/antibiotics10091121

van Wamel, W. J., Rooijakkers, S. H., Ruyken, M., van Kessel, K. P., and van Strijp, J. A. (2006). The innate immune modulators staphylococcal complement inhibitor and chemotaxis inhibitory protein of *Staphylococcus aureus* are located on beta-hemolysin-converting bacteriophages. *J. Bacteriol.* 188, 1310–1315. doi: 10.1128/JB.188.4.1310-1315.2006

Wang, W., Baker, M., Hu, Y., Xu, J., Yang, D., Maciel-Guerra, A., et al. (2021). Whole-genome sequencing and machine learning analysis of *Staphylococcus aureus* from multiple heterogeneous sources in China Reveals Common Genetic Traits of Antimicrobial Resistance. *mSystems* 6:e0118520. doi: 10.1128/mSystems.01185-20

Wick, R. R., Judd, L. M., Gorrie, C. L., and Holt, K. E. (2017). Unicycler: resolving bacterial genome assemblies from short and long sequencing reads. *PLoS Comput. Biol.* 13:e1005595. doi: 10.1371/journal.pcbi.1005595

Wu, S., Huang, J., Wu, Q., Zhang, J., Zhang, F., Yang, X., et al. (2018). *Staphylococcus aureus* isolated from retail meat and meat products in China: incidence, antibiotic resistance and genetic diversity. *Front. Microbiol.* 9:2767. doi: 10.3389/fmicb.2018.02767

Xiao, N., Yang, J., Duan, N., Lu, B., and Wang, L. (2019). Community-associated *Staphylococcus aureus* PVL(+) ST22 predominates in skin and soft tissue infections in Beijing, China. *Infect. Drug Resist.* 12, 2495–2503. doi: 10.2147/IDR.S212358

Yan, X., Song, Y., Yu, X., Tao, X., Yan, J., Luo, F., et al. (2015). Factors associated with *Staphylococcus aureus* nasal carriage among healthy people in northern China. *Clin. Microbiol. Infect.* 21, 157–162. doi: 10.1016/j.cmi.2014.08.023

Yan, X., Wang, B., Tao, X., Hu, Q., Cui, Z., Zhang, J., et al. (2012). Characterization of *Staphylococcus aureus* strains associated with food poisoning in Shenzhen, China. *Appl. Environ. Microbiol.* 78, 6637–6642. doi: 10.1128/AEM.01165-12

Yan, X., Yu, X., Tao, X., Zhang, J., Zhang, B., Dong, R., et al. (2014). *Staphylococcus aureus* ST398 from slaughter pigs in Northeast China. *Int. J. Med. Microbiol.* 304, 379–383. doi: 10.1016/j.ijmm.2013.12.003

Yang, X. M., Ye, L. W., Chan, E. W. C., Zhang, R., and Chen, S. (2020). Tracking recombination events that occur in conjugative virulence plasmid p15WZ-82_Vir during the transmission process. *mSystems* 5:20. doi: 10.1128/mSystems.00140-20

Ye, X., Liu, W., Fan, Y., Wang, X., Zhou, J., Yao, Z., et al. (2015). Frequ ency-risk and duration-risk relations between occupational livestock contact and methicillin-resistant *Staphylococcus aureus* carriage among workers in Guangdong, China. *Am. J. Infect. Control* 43, 676–681. doi: 10.1016/j.ajic.2015.03.026

You, Y., Davies, M. R., Protani, M., McIntyre, L., Walker, M. J., and Zhang, J. (2018). Scarlet fever epidemic in China caused by streptococcus pyogenes serotype M12: Epidemiologic and molecular analysis. *EBioMedicine* 28, 128–135. doi: 10.1016/j.ebiom.2018.01.010

Zhou, Y., He, Y. Y., Wang, F. W., He, P., Hou, S. P., Tao, X., et al. (2022). Molecular characterization of *Staphylococcus aureus* ST6 and ST7 isolates from food-borne illness outbreaks. *Zhonghua Yu Fang Yi Xue Za Zhi* 56, 178–184. doi: 10.3760/cma.j.cn112150-20210712-00670

Zhou, Y., Li, X., and Yan, H. (2020). Genotypic characteristics and correlation of epidemiology of *Staphylococcus aureus* in healthy pigs, diseased pigs, and environment. *Antibiotics (Basel)* 9:839. doi: 10.3390/antibiotics9120839

frontiers | Frontiers in Microbiology

TYPE Original Research
PUBLISHED 27 April 2023
DOI 10.3389/fmicb.2023.1126940

OPEN ACCESS

EDITED BY
Hongshun Yang,
Jiangnan University (Shaoxing) Industrial Technology Research Institute, China

REVIEWED BY
Soraya Chaturongakul,
Mahidol University, Thailand
Nicolas Guiliani,
University of Chile, Chile
Shaojuan Lai,
Henan University of Technology, China

*CORRESPONDENCE
Mark Gomelsky
✉ gomelsky@uwyo.edu

†PRESENT ADDRESS
Li-Hong Chen,
College of Horticulture and Plant Protection, Inner Mongolia Agricultural University, Hohhot, China

‡These authors share first authorship

RECEIVED 18 December 2022
ACCEPTED 11 April 2023
PUBLISHED 27 April 2023

CITATION
Fulano AM, Elbakush AM, Chen L-H and Gomelsky M (2023) The *Listeria monocytogenes* exopolysaccharide significantly enhances colonization and survival on fresh produce. *Front. Microbiol.* 14:1126940. doi: 10.3389/fmicb.2023.1126940

The *Listeria monocytogenes* exopolysaccharide significantly enhances colonization and survival on fresh produce

Alex M. Fulano[1‡], Ahmed M. Elbakush[2‡], Li-Hong Chen[1†] and Mark Gomelsky[1*]

[1]Department of Molecular Biology, University of Wyoming, Laramie, WY, United States, [2]Faculty of Veterinary Medicine, Tripoli University, Tripoli, Libya

Fresh produce contaminated with *Listeria monocytogenes* has caused major listeriosis outbreaks in the last decades. Our knowledge about components of the listerial biofilms formed on fresh produce and their roles in causing foodborne illness remains incomplete. Here, we investigated, for the first time, the role of the listerial Pss exopolysaccharide (EPS) in plant surface colonization and stress tolerance. Pss is the main component of *L. monocytogenes* biofilms synthesized at elevated levels of the second messenger c-di-GMP. We developed a new biofilm model, whereby *L. monocytogenes* EGD-e and its derivatives are grown in the liquid minimal medium in the presence of pieces of wood or fresh produce. After 48-h incubation, the numbers of colony forming units of the Pss-synthesizing strain on pieces of wood, cantaloupe, celery and mixed salads were 2–12-fold higher, compared to the wild-type strain. Colonization of manmade materials, metals and plastics, was largely unaffected by the presence of Pss. The biofilms formed by the EPS-synthesizing strain on cantaloupe rind were 6–16-fold more tolerant of desiccation, which resembles conditions of whole cantaloupe storage and transportation. Further, listeria in the EPS-biofilms survived exposure to low pH, a condition encountered by bacteria on the contaminated produce during passage through the stomach, by 11–116-fold better than the wild-type strain. We surmise that *L. monocytogenes* strains synthesizing Pss EPS have an enormous, 10^2–10^4-fold, advantage over the non-synthesizing strains in colonizing fresh produce, surviving during storage and reaching small intestines of consumers where they may cause disease. The magnitude of the EPS effect calls for better understanding of factors inducing Pss synthesis and suggests that prevention of listerial EPS-biofilms may significantly enhance fresh produce safety.

KEYWORDS

foodborne pathogen, listeriosis, food safety, c-di-GMP, desiccation, acid stress, biofilm, vegetable and fruit

Introduction

Listeria monocytogenes is one of the most notorious foodborne pathogens. Listeriosis, a severe systemic illness caused by this bacterium, affects primarily the elderly, pregnant women, newborns, and the immune compromised individuals. While the number of listeriosis cases is relatively modest, e.g., approximately 1,600 cases per annum in the USA, mortality rates are extremely high, 15−20% (Centers for Disease Control and Prevention, 2022). This justifies the "zero *L. monocytogenes* tolerance" policy of the US Department of Agriculture (Archer, 2018), which means that large shipments of ready-to-eat food products that are contaminated or suspected to be contaminated with *L. monocytogenes* are often recalled. The high socioeconomic costs associated with contaminated food make *L. monocytogenes* the third "most expensive" pathogen in the USA among all bacterial, viral, and eukaryotic foodborne pathogens (Hoffmann and Ahn, 2021).

While traditional sources of listerial contamination have included ready-to-eat meat, poultry, seafood, and dairy products, the number of listeriosis outbreaks associated with contaminated fresh produce has been growing (Zhu et al., 2017). Major outbreaks in the recent years have been caused by contaminated cantaloupes (also known as rock melons), celery, packaged salads, bean sprouts, caramelized apples, and frozen vegetables (Centers for Disease Control and Prevention, 2022; NSW Government). Among these outbreaks, the 2011 cantaloupe-associated outbreak stands out. It affected people in 28 states resulting in 33 fatalities and one miscarriage, making it one of the highest mortality food-poisoning incidents in the modern US history. That outbreak involved whole cantaloupes contaminated with *L. monocytogenes* at a Colorado cantaloupe processing facility (McCollum et al., 2013). Currently, we poorly understand what factors may have contributed to *L. monocytogenes* colonization of the whole cantaloupes, and helped bacteria survive on the inhospitable surface of cantaloupe rind during extended periods of storage and transportation throughout the USA. This situation applies to other kinds of fresh produce, which impedes our ability to prevent fresh produce-associated listeriosis outbreaks (Marik et al., 2020).

On the surfaces of various materials bacteria grow in biofilms, where aggregated cells are surrounded by the secreted extracellular matrix that enhances their survival (Costerton et al., 1999; Flemming and Wingender, 2010; Flemming et al., 2016). In the environment, listeria, which is frequently associated with the decaying plant matter (Welshimer and Donker-Voet, 1971; Fenlon, 1986; Ivanek et al., 2007; Freitag, 2009), likely grows in biofilms as well, yet we do not know composition of listerial biofilms in the environment. The studies of plant-associated biofilms in various other bacteria revealed that the extracellular biofilm matrix comprises exopolysaccharide (EPS), extracellular DNA (eDNA), fimbriae/pili and amyloid fibers (Flemming and Wingender, 2010; Limoli et al., 2015; Karygianni et al., 2020). Fimbriae/pili and amyloid fibers were never observed in *L. monocytogenes*. eDNA is an abundant component of listerial biofilms on various materials (Harmsen et al., 2010; Zetzmann et al., 2015). The role of EPS as component of plant-associated listerial biofilms has not been studied, until this work. The presence of EPS in biofilms formed by various listerial strains was inferred via indirect methods (Borucki et al., 2003; Hefford et al., 2005; Combrouse et al., 2013; Tiensuu et al., 2013), yet until recently, the ability of *L. monocytogenes* to synthesize EPS has remained controversial (Renier et al., 2011).

Our earlier work (Chen et al., 2014) uncovered the ability of *L. monocytogenes* to synthesize EPS, designated Pss, when cellular levels of the second messenger, cyclic dimeric GMP (c-di-GMP), are elevated. The Pss EPS is a unique polymer composed of the repeating trisaccharide unit, {4)-β-ManpNAc-(1−4)-[α-Galp-(1−6)]-β-ManpNAc-(1-}, and is the only cell-attached, insoluble, EPS synthesized by listeria (Köseoğlu et al., 2015). In liquid media, Pss causes cell aggregation, clumping but does not promote attachment to glass or polystyrene materials (Chen et al., 2014). The second messenger c-di-GMP, that activates Pss synthesis, controls EPS synthesis and production of other biofilm components not only in listeria, but in a variety of bacteria (Römling et al., 2013). At present, environmental factors that turn on c-di-GMP synthesis in *L. monocytogenes* are unknown, therefore, Pss synthesis is induced by genetic means, e.g., by expressing a heterologous c-di-GMP synthase, diguanylate cyclase (DGC), or by inactivating c-di-GMP phosphodiesterases (PDEs) that hydrolyze c-di-GMP (Chen et al., 2014). The rise in cellular c-di-GMP levels is conveyed to the Pss biosynthetic apparatus by the c-di-GMP-effector protein, PssE, whose gene is encoded within the *pssA-E* biosynthesis operon (Chen et al., 2014).

To investigate the role of Pss in *L. monocytogenes* colonization of plant surfaces, we developed a listeria-plant biofilm model that involves incubation of the autoclaved wood coupons (disks), as substitutes for partially degraded wood present in the environment, in the minimal medium inoculated with listeria. We also used pieces of fresh produce in place of wood coupons. The plant material was incubated in liquid medium to allow not only bacterial attachment but also biofilm formation. We used the EGD-e wild-type strain and its derivatives that express varying EPS levels. Strain Δ*pdeB/C/D* constitutively expresses EPS because it lacks c-di-GMP-specific PDEs, PdeB, PdeC and PdeD (Chen et al., 2014). Strain Δ*pdeB/C/D*Δ*pssC* contains elevated c-di-GMP levels but carries a mutation in the gene encoding the key Pss biosynthetic enzyme, glycosyltransferase PssC, which impairs Pss synthesis (Köseoğlu et al., 2015). Yet another strain, engineered in this work, lacks all DGCs and PDEs, Δ*pdeB/C/D* Δ*dgcA/B/C*, is devoid of c-di-GMP and therefore, impaired in Pss synthesis.

We found that the Pss EPS promotes *L. monocytogenes* colonization of wood, cantaloupe rind and pulp, celery, and lettuce, but does not affect colonization of abiotic, manmade materials. We also found that listeria growing in the EPS-biofilms on plant surfaces are much more tolerant of desiccation and acid stress. The enhanced colonization of plant matter, increased tolerance of desiccation and acid stress (conditions that mimic, respectively, fresh produce storage and exposure to stomach acid following produce consumption), may give *L. monocytogenes* EPS-biofilms enormous advantage in causing foodborne illness. Results of this work imply that *L. monocytogenes* EPS-biofilms may present a serious problem for fresh produce industry.

Results

EPS strongly promotes *L. monocytogenes* colonization of the surfaces of wood but not manmade materials

To study listerial biofilms on plant surfaces, we departed from the commonly used models. First, instead of growing *L. monocytogenes* in rich media that contains peptides, amino acids, lipids, and nucleotides or nucleic acids, we switched to minimal medium containing glucose as carbon source, because such medium better approximates conditions under which listeria interact with plant matter in nature and in fresh produce processing facilities. Second, we incubated autoclaved wood coupons (as substrates mimicking partially degraded wood in the environment) and sterilized pieces of fresh produce in the liquid medium inoculated with *L. monocytogenes* for extended period, 48 h, to allow biofilm formation.

Following incubation, a significant fraction of biomass of the Pss EPS-synthesizing Δ*pdeB/C/D* strain was attached to the wood coupons (**Figures 1A, B**). This contrasted poor colonization of surfaces of the manmade materials, i.e., stainless steel, aluminum or acrylic (**Figures 1A, B**). This finding is consistent with our earlier observations that listerial EPS-aggregates formed in liquid medium poorly attach to polystyrene and glass surfaces (Chen et al., 2014). To test if surface roughness, as opposed to the nature of the material, played a major role in attachment, we scratched the surfaces of manmade materials thus bringing surfaces roughness closer to the roughness of the wood coupons. This did not improve bacterial attachment (not shown), suggesting that EPS-synthesizing listeria strongly prefer wood over manmade materials.

In contrast to the voluminous biofilms formed on wood coupons by the Pss-synthesizing strain, 48-h old biofilms of the wild-type strain, EGD-e, or the Δ*pdeB/C/D*Δ*pssC* mutant impaired in EPS synthesis were not visible to the naked eye (**Figures 1A, B**). To quantify attached cells, the biofilm biomass was scraped off from the surface of wood coupons, vigorously vortexed in liquid medium, and serial dilutions were plated for enumerating colony forming units (CFUs). **Figure 1C** shows that the Pss EPS strongly, by at least fourfold, promotes colonization of wood coupons. Because prior to biomass scraping, loosely associated aggregates were removed by rinsing in sterile medium, the reported fold-difference is an underestimate.

To assess whether preference for wood is specific to the (unknown) tree species from which coupons were made, we tested coupons made from three known tree types. The EPS-synthesizing strain showed improved attachment to all tested wood coupons, albeit to varying extent (**Figure 2**). Therefore, listerial Pss increases attachment to various kinds of wood.

The Pss EPS increases *L. monocytogenes* colonization of fresh produce

Next, we investigated the role of the Pss EPS in listerial colonization of fresh produce using produce types that were

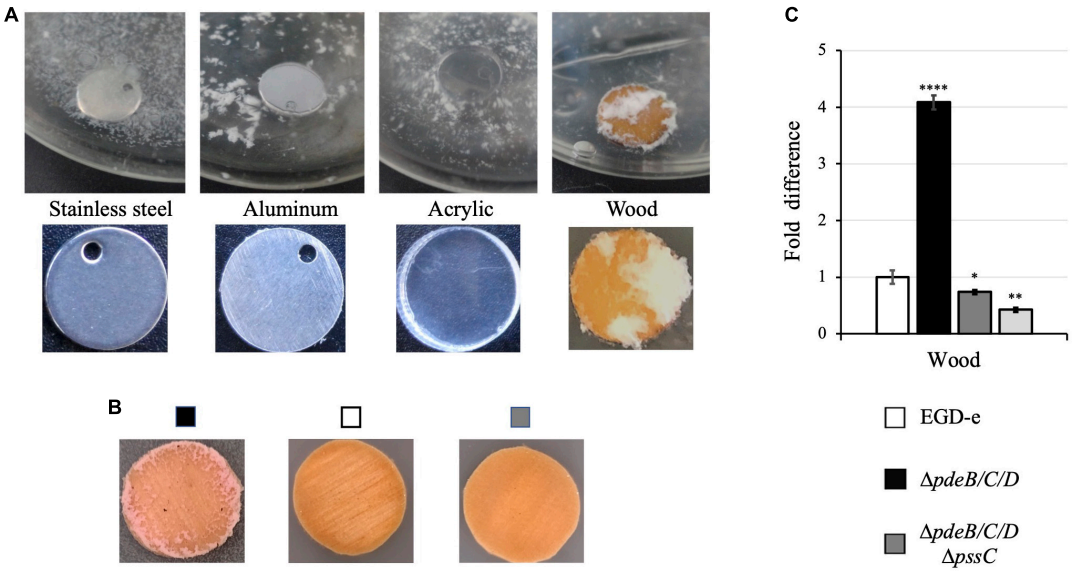

FIGURE 1
The listerial Pss EPS enhances colonization of wood but not manmade materials. *L. monocytogenes* strains were grown in liquid HTM/GY medium at 30°C for 48 h in the presence of coupons (disks) made from wood and manmade materials. **(A)** The EPS-synthesizing strain (Δ*pdeB/C/D*) grown in the presence of coupons made from stainless steel, aluminum and acrylic, and (unknown tree) wood forms voluminous biofilms only on wood coupons. **(B)** The EPS-synthesizing strain, but not wild type or the EPS-impaired strain (Δ*pdeB/C/D*Δ*pssC*), form biofilms on wood coupons. All strains express red fluorescent protein mScarlet, which turns biomass pink (**Table 1**; Bindels et al., 2017). **(C)** Comparison of the CFU numbers in biofilms formed by various strains on the wood coupons following removal of the loosely attached biomass by rinsing. Shown are fold-differences compared to the wild type (EGD-e). The average CFU numbers of the wild type were 8.0×10^8 CFU per coupon. Data are from three independent experiments with at least two replicates in each experiment. Error bars represent standard deviations. Significant differences, compared to EGD-e, are indicated as follows: $^*P < 0.05$, $^{**}P < 0.01$, and $^{****}P < 0.0001$.

TABLE 1 Strains and plasmids used in this study.

Strain and plasmid	Relevant genotype or description	References or source
Strains		
Escherichia coli		
DH10β	Strain used for plasmid maintenance	New England BioLabs
Listeria monocytogenes		
EGD-e	Wild type	ATCC BAA-679*
Δ*pdeB/C/D*	EGD-e containing deletions in the *pdeB, pdeC* and *pdeD* genes	Chen et al., 2014
Δ*pdeB/C/D*Δ*pssC*	Δ*pdeB/C/D* and in-frame deletion in *pssC*	Köseoğlu et al., 2015
Δ*pdeB/C/D*Δ*dgcA/B/C*	c-di-GMP null mutant	This study
Plasmids		
pAM-mScarlet	pAM101-derived vector containing the mScarlet gene under the P_{veg} promoter, Cm^r	This study
pKSV7-Δ*dgcA/B*	Plasmid for in-frame deletion of *dgcAB*	Chen et al., 2014
pKSV7-Δ*dgcC*	Plasmid for in-frame deletion of *dgcC*	Chen et al., 2014

*ATCC, American Type Culture Collection.

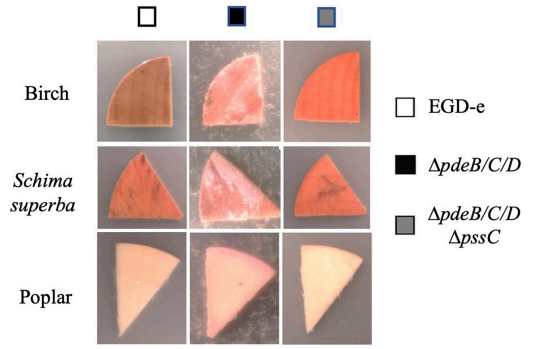

FIGURE 2
The listerial EPS-enhanced colonization of wood from various tree species. Coupon pieces from three tree species (birch, *Schima superba* and poplar) show higher colonization by the *L. monocytogenes* EPS-synthesizing strain (Δ*pdeB/C/D*), compared to the wild type (EGD-e) and EPS-impaired strain (Δ*pdeB/C/D*Δ*pssC*). The pink color of the biomass is due to the expressed mScarlet protein. Wood pieces were incubated in the HTM/GY minimal medium in the presence of listeria for 48 h at 30°C.

associated with the past listeriosis outbreaks. We tested the role of Pss in biofilm formation on cantaloupe rind, the cause of major listeriosis outbreaks in the US and Australia (McCollum et al., 2013; NSW Government, 2018), as well as on cut pieces of fresh produce, which caused the majority of listeriosis outbreaks (Marik et al., 2020; Centers for Disease Control and Prevention, 2022). Sterilized pieces of approximately the same sizes were inoculated with *L. monocytogenes* in flasks containing minimal medium at 30°C.

After 48-h incubation, the EPS-synthesizing strain formed visible biofilms on cantaloupe rind (Figure 3A). Such biofilms were also visible on the surfaces of celery and lettuce (Figure 3A), most prominently on the cutting edges. No biofilms were visible on the pieces of produce grown in the presence of the wild-type and EPS-impaired strains (Figure 3A). Biofilms of the EPS-synthesizing strain contained ~2–12-fold higher CFUs, compared to the wild type, and ~4–22-fold higher, compared to the EPS-impaired strain (Figure 3B), suggesting that EPS strongly promotes colonization of various plant surfaces. The effect of EPS on colonization of cantaloupe rind versus pulp was stronger (12-fold versus 2-fold) (Figure 3B), suggesting that plant surface composition and roughness play important roles in EPS-dependent *L. monocytogenes* colonization.

In the experiments described above, minimal media contained glucose as a carbon source. To mimic conditions at cantaloupe storage and processing facilities, where water/moisture may be present, but carbon source is likely absent or limiting, we repeated the experiment using minimal medium lacking glucose. Residual bacterial growth under those conditions was possible due to the juice leaking from cantaloupe pieces. The lack of glucose in the medium significantly, by almost 10^3-fold, decreased colonization of cantaloupe rind (7.4×10^6 versus 7.0×10^9 CFU, Figures 3B, C). However, the trend in surface colonization was preserved, i.e., the EPS-synthesizing strain colonized cantaloupe rind several-fold more efficiently than the wild-type or the EPS-impaired strains (Figure 3C).

For a closer look at the biofilms on cantaloupe rind, we employed scanning electron microscopy (SEM). All strains formed extracellular appendages on cantaloupe rind, which may represent a combination of eDNA, nanotubes and flagella (Figure 4) and will not be discussed further. The biofilms formed by the EPS-synthesizing strain showed abundant EPS matrix in which listeria were embedded (Figure 4). We were unable to unambiguously determine if the wild type formed any Pss. It showed somewhat higher attachment to plant matter, compared to the EPS-impaired strain, Δ*pdeB/C/D*Δ*pssC* (Figures 1C, 3B), however, whether this was due to low levels of Pss is unclear.

The EPS-biofilms enhance *L. monocytogenes* tolerance to desiccation

Earlier we showed that the Pss EPS enhances *L. monocytogenes* tolerance to desiccation, when cell aggregates grown in liquid medium were compared to planktonically grown cells (Chen et al., 2014). Desiccation is the condition experienced by listeria during storage of fresh produce, such as whole cantaloupes, at the processing facilities and transportation to supermarkets and consumer homes and restaurants (Esbelin et al., 2018). To assess the role of the Pss EPS-biofilms on fresh produce surfaces in desiccation tolerance, we subjected the 48-h old biofilms formed on cantaloupe rind to drying on air at room temperature for up to 3 weeks. For ease of comparisons, we adjusted CFUs of surface-attached bacteria of all strains to approximately the same initial values by mechanically removing ~90% biofilm of the EPS-synthesizing strain (Figure 3B) prior to the desiccation experiment. We realize that much thinner EPS-biofilms likely resulted in our underestimating the magnitude of desiccation tolerance benefits rendered by the Pss EPS.

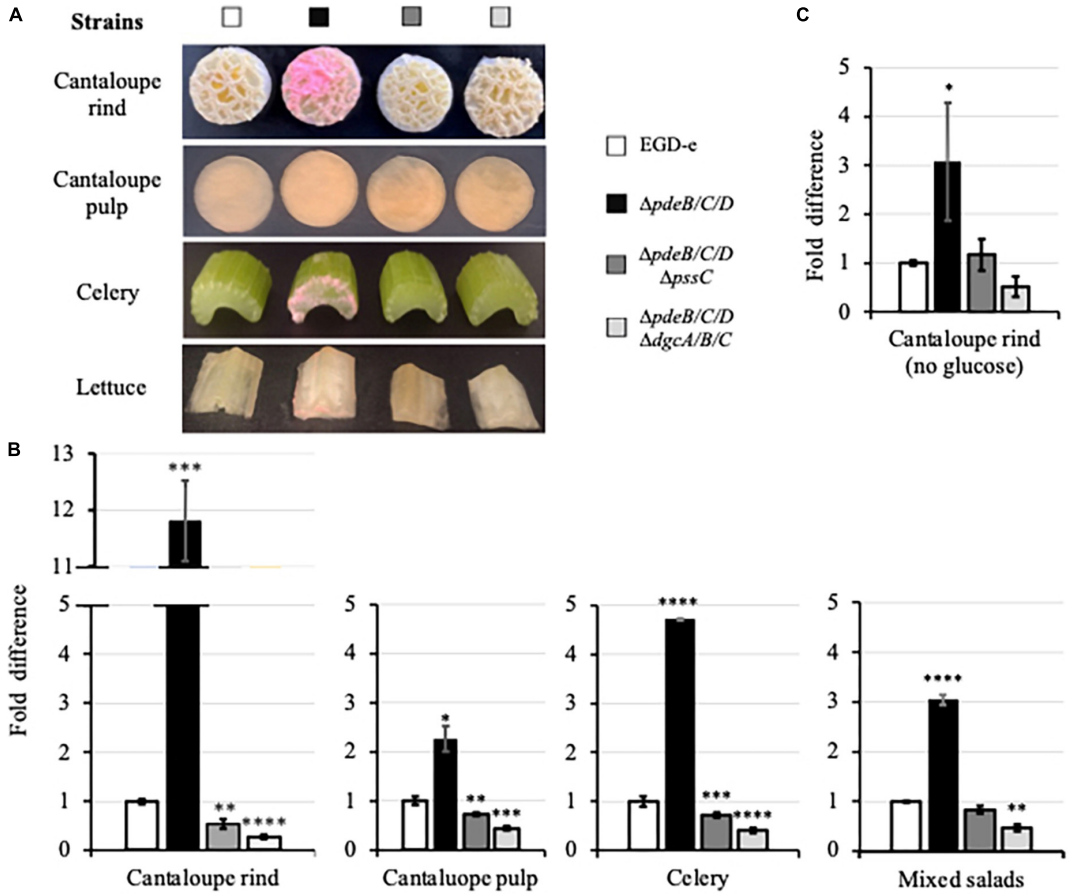

FIGURE 3
The EPS-enhanced colonization of the pieces of fresh produce. **(A)** Pieces of cantaloupe (containing or lacking rind), celery and Iceberg lettuce (a component of mixed salad) following incubation in the HTM/GY medium with *L. monocytogenes* for 48 h at 30°C. The biomass appears pink due to the expressed mScarlet protein. **(B)** Comparison of the CFUs of *L. monocytogenes* in biofilms formed on the fresh produce pieces incubated in the HTM/GY medium. Shown are fold-differences compared to the wild type (EGD-e). The average CFU numbers for the wild type were 7.0×10^9 CFU per cantaloupe rind, 1.2×10^{10} CFU per cantaloupe pulp, 1.9×10^8 CFU per piece of celery, and 8.0×10^8 CFU per three pieces (lettuce, carrot, cabbage) of mixed salad. Error bars represent standard deviations. **(C)** Comparison of the *L. monocytogenes* CFUs in biofilms formed on cantaloupe rind in the HTM medium lacking glucose and yeast extract. The average CFUs of the wild type was 7.4×10^6 CFU per cantaloupe rind. In all figures, data are from three independent experiments with at least two replicates in each experiment. Standard deviations are shown on the graph as error bars. Significant differences, compared to the wild type, are indicated as follows: *$P < 0.05$; **$P < 0.01$; ***$P < 0.001$, and ****$P < 0.0001$.

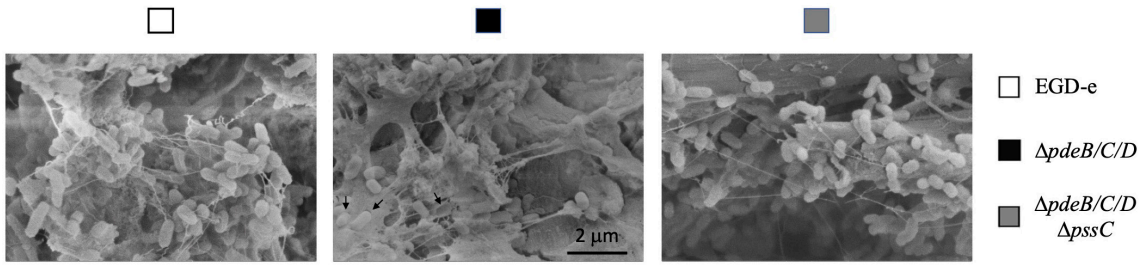

FIGURE 4
The SEM images of *L. monocytogenes* biofilms formed on cantaloupe rind. Bacterial cells embedded in the EPS matrix and presumed empty shells around bacteria removed during sample preparation (black arrows) are seen in the EPS-synthesizing strain but not in the wild type and EPS-impaired strains. Magnification, 40,000×.

After 7 days, CFUs decreased in the wild type from 100 to ∼10%, in the EPS-impaired strain to ∼7.4%, and in the EPS-synthesizing strain to 74%, i.e., by ∼10, ∼13, and 1.35-fold, respectively, (Figure 5). During prolonged desiccation, the EPS-synthesizing strain continued to maintain significant survival advantage over other strains (Figure 5). Desiccation tolerance in this strain was 6–16-fold higher, compared to the wild type, over the whole 3 week time course. This implies that the listerial

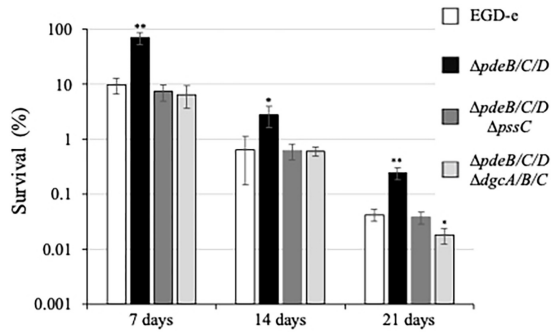

FIGURE 5
Survival under desiccation of the *L. monocytogenes* biofilms. The 48-h old biofilms formed on cantaloupe coupons containing rind and pulp (diameter, 20 mm; depth 4 mm) were placed in Petri dishes rind up and allowed to dry on open air. A coupon was cut into four quarters. One quarter was used for enumeration of initial CFUs, other quarters were subjected to desiccation and withdrawn on days 7, 14, and 21 days, respectively. Following withdrawal, the coupon quarters were rehydrated, homogenized, and subjected to CFU enumeration. For each strain, survival was calculated based on the initial CFU number of that strain on day 0 (assigned to 100%). Prior to the experiment, ~90% of the biofilm biomass of the EPS-synthesizing strain, Δ*pdeB/C/D*, was removed from rind to bring the initial CFU numbers close to those of other strains. The average initial CFUs per coupon quarter for all strains were within the range of (1.1–3.4) × 10^8. Significant differences, compared to EGD-e, are indicated as follows: $^*P < 0.05$ and $^{**}P < 0.01$.

EPS-biofilms formed on fresh produce could survive storage and transportation of fresh produce much better than biofilms formed by the strains not synthesizing Pss.

The EPS-biofilms enhance *L. monocytogenes* tolerance of acid stress

Prior to reaching hospitable small intestine, the site of the gastrointestinal tract where *L. monocytogenes* causes disease, it faces the challenge of stomach (gastric) acid. To mimic the process of consumption of the contaminated produce, we tested acid stress survival of the listerial biofilms formed on the cut fresh produce. For this experiment, we switched from cantaloupe rind as a model to cantaloupe pulp and celery, because rind is not consumed. The pieces of pulp and celery containing 48-h old listerial biofilms were exposed to acid stress, approximating pH of the stomach acid, i.e., pH 1.5—3.5 (Marieb and Hoehn, 2018). One stress regimen involved a 15-min exposure of the produce pieces to pH 2.5. Another regimen involved a 15-min exposure to pH 5.0, followed by 15 min at pH 2.5 (Guerreiro et al., 2022).

As shown in **Figures 6A, B**, exposure to pH 5 alone resulted in only moderate decreases in bacterial survival in all strains. However, exposure to pH 2.5 uncovered a large difference in survival, i.e., ~20% for the EPS-synthesizing strain versus ~1.8% for the wild type and ~1.4% for the EPS-impaired strain (**Figure 6A**). Thus gives the EPS-synthesizing strain an ~11-fold survival advantage over the wild type. Similarly, after a two-step regimen (pH 5.0, then pH 2.5), ~1% of the EPS-synthesizing strain survived but only ~0.085% of the wild type and ~0.081% of the EPS-impaired strain, thus revealing an ~12-fold advantage of the EPS-synthesizing strain over the wild type. Similar results were obtained when listerial survival in biofilms on the celery pieces was measured (**Figure 6B**), i.e., ~25% survival of the EPS-synthesizing strain versus ~2% for the wild type and ~1.7% for the EPS-impaired strain following exposure to pH 2.5, and ~4.7% versus 0.04% and 0.03% survival following a two-step regimen. Thus, the EPS-synthesizing strain has a 12—116-fold survival advantage on celery pieces, compared to the wild-type. These results suggest that from ~11- to ~116-fold higher number of *L. monocytogenes* in the EPS-biofilms on cut fresh produce could survive exposure to stomach acid, compared to the biofilms lacking Pss EPS.

EPS is the primary c-di-GMP-dependent factor responsible for enhanced *L. monocytogenes* plant surface colonization and survival

In *L. monocytogenes*, EPS synthesis is the dominant, albeit not the only phenotype associated with the elevated c-di-GMP levels (Chen et al., 2014; Elbakush et al., 2018). In other bacteria, elevated c-di-GMP levels, in addition to upregulating EPS synthesis, affect such biofilm components as protein adhesins, pili, and fimbria (Römling et al., 2013). To access the impact of c-di-GMP-dependent factors other than Pss EPS that contribute to listerial colonization and survival on plant matter, we constructed the *L. monocytogenes* c-di-GMP null strain, Δ*pdeB/C/D*Δ*dgcA/B/C*. In addition to lacking c-di-GMP-specific PDEs, this mutant also lacks all DGCs involved in c-di-GMP synthesis (Chen et al., 2014). We found that the c-di-GMP null mutant behaved similarly to the high c-di-GMP strain impaired in Pss synthesis, Δ*pdeB/C/D* Δ*pssC*, in survival assays (**Figures 5**, **6**), thus suggesting that Pss is the key factor affecting stress tolerance. In plant surface colonization assays the c-di-GMP null strain appeared somewhat, ~2-fold, inferior, compared to the Δ*pdeB/C/D* Δ*pssC* strain (**Figures 1C**, **3B, C**). From these experiments, it is evident that the Pss EPS is the dominant c-di-GMP-dependent factor affecting listerial colonization of plant matter and stress tolerance.

Discussion

In this study, we investigated the role of the Pss EPS in *L. monocytogenes* colonization of plant surfaces. We discovered that Pss significantly, from 2 to 12-fold, improves colonization of diverse plant matter, from different kinds of wood to cantaloupe rind, cantaloupe pulp, celery, and lettuce. Pss has little or no effect on colonization of non-plant, manmade materials (**Figures 1**–**3**). While the ability of several kinds of EPS to facilitate attachment to plant surfaces has been reported in various bacteria (Danhorn and Fuqua, 2007; Yaron and Römling, 2014; Castiblanco and Sundin, 2016), this is the first report describing such function of the *L. monocytogenes* Pss EPS.

Colonization efficiency depended on the properties of plant surface. The Pss EPS had the largest effect on rough, fiber-rich surfaces of wood and netted cantaloupe rind, and the smallest –

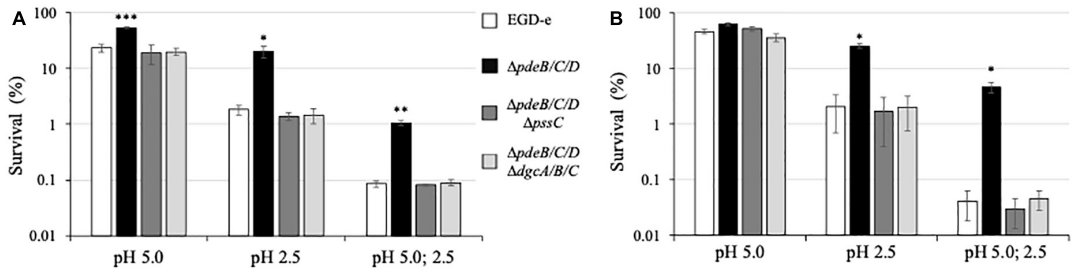

FIGURE 6
Survival under acid stress of the *L. monocytogenes* biofilms. The 48-h old biofilms formed on pieces of cantaloupe pulp **(A)** and celery **(B)** were exposed for 15 min to pH 5.0 or pH 2.5, or sequentially to pH 5.0 (15 min) and pH 2.5 (15 min). Following medium neutralization, cantaloupe and celery pieces were collected, homogenized, and CFU were enumerated. For each strain, survival percentages were calculated based on the initial CFU prior to exposure to acid (assigned to 100%). The average initial CFUs for all strains were within the range of (5.3–7.3) $\times 10^9$ per cantaloupe pulp piece and (1.1–1.4) $\times 10^9$ per celery piece. Significant differences, compared to EGD-e, are indicated as follows: $^*P < 0.05$, $^{**}P < 0.01$, and $^{***}P < 0.001$.

on smooth surfaces of cantaloupe pulp (Figure 3B). More EPS-biofilms were formed on the edges than on the smooth surfaces of the same produce (Figure 3A). Because strains used in this study grow at the same rate, differences in colonization reflect differences in initial surface attachment, therefore Pss is involved in attachment to plant matter. While we did not directly interrogate the mechanism of Pss-mediated plant surface binding, the ability of Pss to bind to diverse plant matter, but not to manmade materials, and bind better to fiber-rich surfaces of wood and cantaloupe rind suggests that Pss interacts with the insoluble plant (ligno)cellulose fibers. Only few additional factors promoting attachment to plant matter are known in *L. monocytogenes*. One of these is functional flagella. They enhance initial attachment to plant surfaces in some *L. monocytogenes* strains (Lemon et al., 2007; Gorski et al., 2009). Another factor is a cellulose binding protein, Lcp (LMOf2365_0859). Strain *L. monocytogenes* F2365 attached to cantaloupe rind, lettuce, and spinach better than the *lcp* mutant by several-fold (Bae et al., 2013). Lmo0842, an Lcp homolog, is encoded in the EGD-e genome and may have the same function. Note, however, that voluminous Pss EPS synthesized by the Δ*pdeB/C/D* strain likely masked surface proteins, including Lmo0842. Because the EPS-synthesizing strain is impaired in motility (Chen et al., 2014), Pss also likely negated the effects of flagella.

In addition to enhancing colonization, the Pss EPS strongly protected *L. monocytogenes* grown in the EPS-biofilms on the surfaces of fruit and vegetables against desiccation and acid stresses. These stresses are arguably most relevant from the standpoint of fresh produce safety because they mimic, respectively, conditions of produce storage and transportation, and passage of the contaminated produce pieces through the stomach following consumption. In our experimental setup, EPS-biofilms showed a 6—16-fold increase in desiccation tolerance (Figure 5), and a 11—116-fold increase in acid stress survival (Figure 6). The findings that listerial EPS-biofilms are much more tolerant to stresses are in line with the role of EPS-biofilms in other bacteria (Mao et al., 2006; Deka et al., 2019). These findings are also consistent with our earlier observations that clumps of the Δ*pdeB/C/D* strain formed in liquid media are much more tolerant of desiccation and exposure to harmful chemicals, compared to planktonically grown cells (Chen et al., 2014).

To estimate the overall effect that the *L. monocytogenes* EPS on safety of such produce as cantaloupes, we combined the effects of Pss on produce colonization (Figures 1C, 3B, C; 2—12-fold increase in CFUs), ability to survive during storage and transportation (Figure 5, 6—16-fold increase in desiccation tolerance) and ability to survive stomach acid exposure (Figure 6, 11—116-fold increase in acid stress survival). By multiplying the low- and high-end values, we estimate that the EPS-synthesizing strain has an enormous, 10^2- to 10^4-fold, advantage over EPS-impaired strains in reaching the small intestine of consumers where they may cause disease. If desiccation is not part of processing, the advantage would remain very large. Note that these numbers may be underestimates, because the bulk (~90%) of the EPS-biofilms was removed prior to the desiccation experiment, in order to bring pre-desiccation CFUs of all strains to the same range. Further, the 48-h biofilms tested in this study may not have fully developed protective potential, compared to older biofilms (Hingston et al., 2013; Chen et al., 2020). We surmise that the enormous advantage imparted by EPS to listeria on fresh produce makes EPS an extremely problematic factor from the standpoint of fresh produce safety.

The key question not addressed in this work is how often listerial EPS-biofilms are formed on plant matter, including fresh produce. On the one hand, *Listeria* are frequently associated with the decaying plant matter in nature (Welshimer and Donker-Voet, 1971; Fenlon, 1986; Ivanek et al., 2007; Freitag, 2009). The benefits rendered by Pss regarding enhanced colonization and stress tolerance point to the high likelihood that EPS is synthesized on plant matter. Further, the *pssA-E* operon encoding the Pss EPS biosynthetic machinery is part of the core *L. monocytogenes* genome, deciphered from 1,696 genomes of strains isolated from diverse sources and geographic locations (Moura et al., 2016). Strong conservation of the *pssA-E* operon in the genomes of pathogenic and non-pathogenic listeria supports the notion that Pss is important for environmental survival (Chen et al., 2014). On the other hand, the Pss EPS has been unambiguously detected only in the *L. monocytogenes* strains with artificially elevated c-di-GMP levels, either via mutations (e.g., Δ*pdeB/C/D*) or via expression of a foreign DGC (Chen et al., 2014). Under the conditions used in this study, the wild type, EGD-e, showed no solid evidence of Pss. If it was synthesized, the amounts were not readily detectable by SEM (Figure 4) and were low to make a major difference in

colonization and stress survival, compared to the EPS-impaired strains (**Figures 1C**, **3**, **5**, **6**). It is of course possible that EGD-e is not an optimal strain for investigating EPS synthesis, because it has been propagated under the laboratory conditions for several decades (Murray et al., 1926). Such maintenance is known to select against biofilm phenotypes resulting in domesticated strains (McLoon et al., 2011). *L. monocytogenes* strains isolated from the recent fresh produce outbreaks may therefore offer more relevant insights into EPS synthesis.

Additional factors that may have obscured EPS presence in *L. monocytogenes* biofilms concern experimental design of most studies of listerial attachment to plant matter. *L. monocytogenes* in these studies was usually grown in rich liquid media, spotted on the surfaces of fresh produce, and allowed to dry. Bacterial biofilms and survival were then investigated over time at different environmental conditions, such as temperature and humidity (Marik et al., 2020). This setup undervalues time needed for planktonic, single-cell bacteria from liquid medium to switch to the surface-attached, biofilm lifestyle, when EPS synthesis is expected to take place (Römling et al., 2013). Further, rich media used in those studies may not adequately mimic conditions under which listerial biofilms are formed on plant matter, whether in the environment or in fresh produce processing facilities. It is also important to note that the majority of listerial biofilm studies involved manmade materials used in food processing, such as stainless steel, aluminum, rubber, glass, and plastics (Blackman and Frank, 1996; Bonaventura et al., 2008; Lee et al., 2017). The extracellular biofilm matrices on these materials contain mostly eDNA and secreted proteins (Blackman and Frank, 1996; Rieu et al., 2008; Harmsen et al., 2010; Ferreira et al., 2014; Guilbaud et al., 2015; Zetzmann et al., 2015; Oloketuyi and Khan, 2017; Rodríguez-López et al., 2018), and biofilm forming capacity is highly dependent on specific strains and experimental conditions (Borucki et al., 2003; Cherifi et al., 2017; Lee et al., 2017; Gorski et al., 2021; Gray et al., 2021). The lack of EPS under these conditions is consistent with the results of this work that showed that Pss does not affect colonization of manmade materials (Chen et al., 2014; **Figure 1**).

To better understand the role of the *L. monocytogenes* Pss EPS in nature and in fresh produce industry, we need to uncover environmental factors that increase c-di-GMP levels and thus turn on Pss synthesis. Having a Pss-specific probe would also be helpful for detecting Pss EPS on plant matter. Work in these areas is ongoing, as is the search for compounds that inhibit formation of EPS-biofilms. Even if such biofilms are formed on fresh produce only by some strains and only under specific conditions, from the standpoint of fresh produce safety, the 10^2-10^4-fold advantage that EPS may render *L. monocytogenes* in causing foodborne illness seems too large to ignore.

Materials and methods

Bacterial strains, plasmids, and growth conditions

Strains and plasmids used in this study are listed in **Table 1**. The c-di-GMP null strain, Δ*pdeB/C/D* Δ*dgcA/B/C*, was constructed from strain Δ*pdeB/C/D* using sequential deletion of *dgcA/B* (with the help of pKSV7-Δ*dgcAB*) and *dgcC* (with the help of pKSV7-Δ*dgcC*), as described earlier (Chen et al., 2014). Plasmid pAM-mScarlet expressing the red fluorescent protein mScarlet (Bindels et al., 2017) was constructed to enhance visualization of *L. monocytogenes* on the surfaces of wood and fresh produce. The mScarlet gene was synthesized with *L. monocytogenes*-optimized codons (Twist Bioscience) and cloned downstream of the strong *Bacillus subtilis* Pveg promoter (Guiziou et al., 2016) in the pAM101-derived vector (Fujimoto and Ike, 2001). The listerial strains were grown in the liquid minimum HTM medium (Tsai and Hodgson, 2003) containing 3% glucose and 0.2% yeast extract, HTM/GY, at 30°C under shaking (220 rpm). When strains containing pAM-mScarlet were used, the media was supplemented with 10 μg/mL chloramphenicol (Cm). For enumerating CFUs, cultures were routinely plated onto Brain Heart Infusion (BHI) agar (Millipore Sigma, Burlington, MA, United States) and incubated at 37°C for 36 h.

Preparation and treatment of coupons used in biofilm experiments

All coupons (disks for do-it-yourself arts and crafts projects) were purchased on from various vendors, including coupons made from unspecified wood (32 mm diameter × 1.2 mm thickness, Woodpile), birch (50 mm × 8 mm, Woodpeckers), poplar (50 mm × 2.5 mm, Juvale), *Schima superba* (38 mm × 4 mm, Axe Sickle), stainless steel (38 × 1.55 mm, PH Pandahall, CA, USA), aluminum (38 × 1.55 mm, RPM Stamping Blanks, Rose Metal Products, Springfield, MO, USA), and acrylic (25.4 × 1.8 mm, Tupalizy, PTC-Office). Prior to use, all non-wood coupons were immersed in 70% ethanol for 20 min for disinfection, rinsed twice in sterile deionized water and air dried. The wood coupons were autoclaved (121°C, 30 min). In some experiments, prior to sterilization, surfaces of steel, aluminum and acrylic coupons were roughened up by a scrapper to imitate surface roughness of wood coupons.

The overnight *L. monocytogenes* cultures were diluted 1:100 into 10 mL HTM/GY medium in 125-mL flasks and grown at 30°C until optical density of ∼ 0.4 at 600 nm. Sterile wood coupons or pieces of fresh produce were added at this point and cultivation was continued for 48 h. The coupons were subsequently withdrawn and rinsed twice in sterile HTM to remove loosely attached biofilms. The biomass attached to the coupons and produce pieces was thoroughly scrapped off into HTM medium using a sterile scalpel, and the suspensions were vortexed. Serial dilutions were plated onto BHI agar plates and grown at 37°C for 36 h followed by CFU enumeration.

Preparation and inoculation of pieces of fresh produce

Whole cantaloupes, celery, and mixed salads (Iceberg lettuce, red cabbage, carrots) used in this study were purchased from local

(Laramie, WY) retail stores. Cantaloupe coupons (20 mm × 4 mm) were obtained by using a cork borer. Some pieces were cut out to contain rind, others were cut out to contain cantaloupe pulp only. Celery was cut in pieces of varying lengths from similar sized stocks. Prior to processing, fresh produce was thoroughly washed. Cutout pieces were sterilized by complete submersion into 8.25% sodium hypochlorite (CloroxPro, Clorox Professional Products Company) in the 50-mL centrifuge tubes placed on a rocker platform for 20 min. Following sterilization, fresh produce pieces were submerged in 50-mL sterile distilled water overnight and subsequently rinsed in fresh sterile distilled water. Sterile pieces were added to listerial cultures, as described above for coupons.

Following 48-h incubation, produce pieces were aseptically removed from the cultures and rinsed by dipping in three sequential beakers with sterile HTM media. To measure listerial colonization, cantaloupe rind was carefully separated from pulp and processed separately, while the remaining pulp was discarded. To measure colonization of cantaloupe pulp, pulp-only pieces lacking rind were used. The produce pieces were mechanically macerated in the Stomacher bags in 5 mL HTM medium and homogenized for 10 min at high speed (Stomacher® 80 Biomaster, Seward, UK). The serial dilutions of the homogenates were plated onto BHI agar plates for CFU enumeration.

SEM analysis of listeria-plant biofilms

Small (5 mm diameter x 1 mm thickness) pieces of cantaloupe rind containing *L. monocytogenes* biofilms were used for SEM (Scanning Electron Microscope FEI Quanta 250). Briefly, rind pieces were fixed for 2 h in 2% glutaraldehyde-PBS buffer at room temperature, followed by dehydration steps in a series of ethanol baths (10 min each) containing 25, 50, 75, 95, and 100% (3 times) ethanol, and postfixed by incubation with 1% osmium tetroxide in PBS for 1 h in the dark. The samples were then dried using Balzers Critical Point Dryer (CPD 020) before coating with gold-palladium, as described earlier (Muravnik et al., 2016).

Desiccation survival of *L. monocytogenes* in biofilms on cantaloupe rind

Rind-containing cantaloupe pieces were removed from the liquid *L. monocytogenes* cultures after 48-h incubation. To adjust biomass levels to approximately the same initial cell numbers, the voluminous EPS-biofilms of the Δ*pdeB/C/D* strain were gently brushed off cantaloupe rind, resulting in the removal of ∼ 90% biomass. Coupons were then aseptically cut into four equal-sized quarters. One quarter was used to determine initial CFU (day 0) following homogenization in Stomacher. The remaining quarters were placed on sterile blotting paper in open Petri dishes and kept at room temperature inside the biological safety cabinet with the switched off blower. After 7, 14, and 21 days of storage the quarters were placed in Stomacher bags with 5 mL HTM medium, soaked for 1 h, homogenized and serial dilutions were plated for CFU enumeration.

Acid stress survival of *L. monocytogenes* in biofilms on celery pieces

Biofilms formed on the pieces of celery and cantaloupe pulp were used in acid stress experiments. The sizes of celery pieces were adjusted to have similar initial number of listeria in biofilms, as follows: 20 mm (EGD-e), 5 mm (Δ*pdeB/C/D*), 22 mm (Δ*pdeB/C/D*Δ*pssC*), and 24 mm (Δ*pdeB/C/D*Δ*dgcA/B/C*). The 4-mm thick cantaloupe pulp pieces had the following diameters: 18 mm (EGD-e), 15 mm (Δ*pdeB/C/D*), 19 mm (Δ*pdeB/C/D*Δ*pssC*), and 20 mm (Δ*pdeB/C/D*Δ*dgcA/B/C*). Following 48-h incubation in liquid *L. monocytogenes* cultures, celery or cantaloupe pulp pieces were removed and placed in HTM/GY acidified to pH 5.0 or 2.5 with hydrochloric acid for 15 min at 37°C. A preconditioning protocol involved exposing celery pieces to pH 5.0 for 15 min followed by exposure to pH 2.5 for additional 15 min, as described (Guerreiro et al., 2022). The acid was neutralized to pH 7.0 by addition of the sodium hydroxide solution, celery pieces were homogenized, and serial dilutions were plated for CFU enumeration.

Statistical analysis

Microsoft Excel was used for data processing analysis and presentation. The bar charts display a mean ± standard deviation (SD) from three independent experiments, each of which had at least two replicates. Unpaired Student's *t*-tests were performed using Prism 9 for Mac (GraphPad). Significant differences, compared to the wild type, EGD-e, are indicated in all figures as follows: *, $P < 0.05$; **, $P < 0.01$; ***, $P < 0.001$, and ****, $P < 0.0001$.

Data availability statement

The raw data supporting the conclusions of this article will be made available by the authors, without undue reservation.

Author contributions

AF performed the experiments, analyzed the data, and wrote the manuscript. AE performed the experiments and analyzed the data. L-HC constructed the *L. monocytogenes* c-di-GMP null strain. MG conceived, designed, coordinated the research, and wrote the manuscript. All authors contributed to the article and approved the submitted version.

Funding

This work was supported by USDA-NIFA-AFRI-1946224 and in part by the NIFA HATCH Program via the University of Wyoming Agriculture Experimental Station grant WYO-583-17 and Integrated Microscopy Core is supported by NIH P20 GM121310.

Acknowledgments

We acknowledge Dr. Zhaojie Zhang (Integrated Microscopy Core) and Dr. Tyler C. Brown (Materials Characterization Laboratory) at the University of Wyoming for technical support in SEM studies, and Kiet Tran for the pAM-mScarlet plasmid.

Conflict of interest

The authors declare that the research was conducted in the absence of any commercial or financial relationships that could be construed as a potential conflict of interest.

Publisher's note

All claims expressed in this article are solely those of the authors and do not necessarily represent those of their affiliated organizations, or those of the publisher, the editors and the reviewers. Any product that may be evaluated in this article, or claim that may be made by its manufacturer, is not guaranteed or endorsed by the publisher.

References

Archer, D. L. (2018). The evolution of FDA's policy on *Listeria monocytogenes* in ready-to-eat foods in the United States. *Curr. Opin. Food Sci.* 20, 64–68. doi: 10.1016/j.cofs.2018.03.007

Bae, D., Seo, K. S., Zhang, T., and Wang, C. (2013). Characterization of a potential *Listeria monocytogenes* virulence factor associated with attachment to fresh produce. *Appl. Environ. Microbiol.* 79, 6855–6861. doi: 10.1128/AEM.01006-13

Bindels, D., Haarbosch, L., Weeren, L., Postma, M., Wiese, K., Mastop, M., et al. (2017). mScarlet: a bright monomeric red fluorescent protein for cellular imaging. *Nat. Methods* 14, 53–56. doi: 10.1038/nmeth.4074

Blackman, I. C., and Frank, J. F. (1996). Growth of *Listeria monocytogenes* as a biofilm on various food-processing surfaces. *J. Food Prot.* 59, 827–831. doi: 10.4315/0362-028X-59.8.827

Bonaventura, G. D., Piccolomini, R., Paludi, D., D'Orio, V., Vergara, A., Conter, M., et al. (2008). Influence of temperature on biofilm formation by *Listeria monocytogenes* on various food-contact surfaces: relationship with motility and cell surface hydrophobicity. *J. Appl. Microbiol.* 104, 1552–1561. doi: 10.1111/j.1365-2672.2007.03688.x

Borucki, M. K., Peppin, J. D., White, D., Loge, F., and Call, D. R. (2003). Variation in biofilm formation among strains of *Listeria monocytogenes*. *Appl. Environ. Microbiol.* 69, 7336–7342. doi: 10.1128/aem.69.12.7336-7342.2003

Castiblanco, L. F., and Sundin, G. W. (2016). New insights on molecular regulation of biofilm formation in plant-associated bacteria. *J. Integr. Plant Biol.* 58, 362–372. doi: 10.1111/jipb.12428

Centers for Disease Control and Prevention (2022). Available online at: https://www.cdc.gov/listeria/. (accessed February 6, 2022).

Chen, L., Köseoğlu, V., Güvener, Z., Myers-Morales, T., Reed, J., Orazio, S., et al. (2014). Cyclic di-GMP-dependent signaling pathways in the pathogenic firmicute *Listeria monocytogenes*. *PLoS Pathog.* 10:e1004301. doi: 10.1371/journal.ppat.1004301

Chen, X., Thomsen, T. R., Winkler, H., and Xu, Y. (2020). Influence of biofilm growth age, media, antibiotic concentration and exposure time on *Staphylococcus aureus* and *Pseudomonas aeruginosa* biofilm removal in vitro. *BMC Microbiol.* 20:264. doi: 10.1186/s12866-020-01947-9

Cherifi, T., Jacques, M., Quessy, S., and Fravalo, P. (2017). Impact of nutrient restriction on the structure of *Listeria monocytogenes* biofilm grown in a microfluidic system. *Front. Microbiol.* 8:864. doi: 10.3389/fmicb.2017.00864

Combrouse, T., Sadovskaya, I., Faille, C., Kol, O., Guérardel, Y., and Midelet-Bourdin, G. (2013). Quantification of the extracellular matrix of the *Listeria monocytogenes* biofilms of different phylogenic lineages with optimization of culture conditions. *J. Appl. Microbiol.* 114, 1120–1131. doi: 10.1111/jam.12127

Costerton, J. W., Stewart, P. S., and Greenberg, E. P. (1999). Bacterial biofilms: a common cause of persistent infections. *Science* 284, 1318–1322. doi: 10.1126/science.284.5418.1318

Danhorn, T., and Fuqua, C. (2007). Biofilm formation by plant-associated bacteria. *Annu. Rev. Microbiol.* 61, 401–422. doi: 10.1146/annurev.micro.61.080706.093316

Deka, P., Goswami, G., Das, P., Gautom, T., Chowdhury, N., Boro, R., et al. (2019). Bacterial exopolysaccharide promotes acid tolerance in *Bacillus amyloliquefaciens* and improves soil aggregation. *Mol. Biol. Rep.* 46, 1079–1091. doi: 10.1007/s11033-018-4566-0

Elbakush, A. M., Miller, K. W., and Gomelsky, M. (2018). CodY-mediated c-di-GMP-dependent inhibition of mammalian cell invasion in *Listeria monocytogenes*. *J. Bacteriol.* 200:e457. doi: 10.1128/JB.00457-17

Esbelin, J., Santos, T., and Hébraud, M. (2018). Desiccation: an environmental and food industry stress that bacteria commonly face. *Food Microbiol.* 69, 82–88. doi: 10.1016/j.fm.2017.07.017

Fenlon, D. R. (1986). Growth of naturally occurring *Listeria* spp. in silage: a comparative study of laboratory and farm ensiled grass. *Grass Forage Sci.* 41, 375–378. doi: 10.1111/j.1365-2494.1986.tb01828.x

Ferreira, V., Wiedmann, M., Teixeira, P., and Stasiewicz, M. J. (2014). Listeria monocytogenes persistence in food-associated environments: epidemiology, strain characteristics, and implications for public health. *J. Food Prot.* 77, 150–170. doi: 10.4315/0362-028X.JFP-13-150

Flemming, H. C., and Wingender, J. (2010). The biofilm matrix. *Nat. Rev. Microbiol.* 8, 623–633. doi: 10.1038/nrmicro2415

Flemming, H. C., Wingender, J., Szewzyk, U., Steinberg, P., Rice, S. A., and Kjelleberg, S. (2016). Biofilms: an emergent form of bacterial life. *Nat. Rev. Microbiol.* 14, 563–575. doi: 10.1038/nrmicro.2016.94

Freitag, N. E. (2009). Complete transcriptional profile of an environmental pathogen. *Future Microbiol.* 4, 779–782. doi: 10.2217/fmb.09.56

Fujimoto, S., and Ike, Y. (2001). pAM401-based shuttle vectors that enable overexpression of promoterless genes and one-step purification of tag fusion proteins directly from *Enterococcus faecalis*. *Appl. Environ. Microbiol.* 67, 1262–1267. doi: 10.1128/AEM.67.3.1262-1267.2001

Gorski, L., Duhé, J. M., and Flaherty, D. (2009). The use of flagella and motility for plant colonization and fitness by different strains of the foodborne pathogen *Listeria monocytogenes*. *PLoS One* 4:e5142. doi: 10.1371/journal.pone.0005142

Gorski, L., Walker, S., Romanolo, K. F., and Kathariou, S. (2021). Growth and survival of attached *Listeria* on lettuce and stainless steel varies by strain and surface type. *J. Food Prot.* 84, 903–911. doi: 10.4315/JFP-20-434

Gray, J., Chandry, P. S., Kaur, M., Kocharunchitt, C., Fanning, S., Bowman, J., et al. (2021). Colonisation dynamics of *Listeria monocytogenes* strains isolated from food production environments. *Sci. Rep.* 11:12195. doi: 10.1038/s41598-021-91503-w

Guerreiro, D. N., Pucciarelli, M. G., Tiensuu, T., Gudynaite, D., Boyd, A., Johansson, J., et al. (2022). Acid stress signals are integrated into the σB - dependent general stress response pathway via the stressosome in the food-borne pathogen *Listeria monocytogenes*. *PLoS Pathog.* 18:e1010213. doi: 10.1371/journal.ppat.1010213

Guilbaud, M., Piveteau, P., Desvaux, M., Brisse, S., and Briandet, R. (2015). Exploring the diversity of *Listeria monocytogenes* biofilm architecture by high-throughput confocal laser scanning microscopy and the predominance of the honeycomb-like morphotype. *Appl. Environ. Microbiol.* 81, 1813–1819. doi: 10.1128/AEM.03173-14

Guiziou, S., Sauveplane, V., Chang, H., Clert, C., Declerck, N., Jules, M., et al. (2016). A part toolbox to tune genetic expression in *Bacillus* subtilis. *Nucl. Acids Res.* 44, 7495–7508. doi: 10.1093/nar/gkw624

Harmsen, M., Lappann, M., Knøchel, S., and Molin, S. (2010). Role of extracellular DNA during biofilm formation by *Listeria monocytogenes*. *Appl. Environ. Microbiol.* 76, 2271–2279. doi: 10.1128/AEM.02361-09

Hefford, M. A., Aoust, S., Cyr, T. D., Austin, J. W., Sanders, G., Kheradpir, E., et al. (2005). Proteomic and microscopic analysis of biofilms formed by *Listeria monocytogenes* 568. *Can. J. Microbiol.* 51, 197–208. doi: 10.1139/w04-129

Hingston, P. A., Stea, E. C., Knøchel, S., and Hansen, T. (2013). Role of initial contamination levels, biofilm maturity and presence of salt and fat on desiccation survival of *Listeria monocytogenes* on stainless steel surfaces. *Food Microbiol.* 36, 46–56. doi: 10.1016/j.fm.2013.04.011

Hoffmann, S., and Ahn, J. W. (2021). *Updating economic burden of foodborne diseases estimates for inflation and income growth, ERR-297*. Department of Agriculture, Economic Research Service. Available online at: https://www.ers.usda.gov/webdocs/publications/102640/err-297.pdf?v=1403.6 (accessed March 18, 2023).

Ivanek, R., Gröhn, Y. T., and Wiedmann, M. (2007). *Listeria monocytogenes* in multiple habitats and host populations: review of available data for mathematical modeling. *Food. Pathog. Dis.* 3, 319–336. doi: 10.1089/fpd.2006.3.319

Karygianni, L., Ren, Z., Koo, H., and Thurnheer, T. (2020). Biofilm matrixome: extracellular components in structured microbial communities. *Trends Microbiol.* 28, 668–681. doi: 10.1016/j.tim.2020.03.016

Köseoğlu, V., Heiss, C., Azadi, P., Topchiy, E., Güvener, Z., Lehmann, T., et al. (2015). *Listeria monocytogenes* exopolysaccharide: origin, composition, biosynthetic machinery, and c-di-GMP-dependent regulation. *Mol. Microbiol.* 96, 728–743. doi: 10.1111/mmi.12966

Lee, B. H., Hébraud, M., and Bernardi, T. (2017). Increased adhesion of *Listeria monocytogenes* strains to abiotic surfaces under cold stress. *Front. Microbiol.* 8:2221. doi: 10.3389/fmicb.2017.02221

Lemon, K. P., Higgins, D. E., and Kolter, R. (2007). Flagellar motility is critical for *Listeria monocytogenes* biofilm formation. *J. Bacteriol.* 189, 4418–4424. doi: 10.1128/JB.01967-06

Limoli, D. H., Jones, C. J., and Wozniak, D. J. (2015). Bacterial extracellular polysaccharides in biofilm formation and function. *Microbiol. Spectr.* 3:11. doi: 10.1128/microbiolspec.MB-0011

Mao, Y., Doyle, M. P., and Chen, J. (2006). Role of colanic acid exopolysaccharide in the survival of enterohaemorrhagic *Escherichia coli* O157:H7 in simulated gastrointestinal fluids. *Lett. Appl. Microbiol.* 42, 642–647. doi: 10.1111/j.1472-765X.2006.01875.x

Marieb, E. N., and Hoehn, K. (2018). *Human anatomy and physiology*. Londonp: Pearson Education.

Marik, C. M., Zuchel, J., Schaffner, D. W., and Strawn, L. K. (2020). Growth and survival of *Listeria monocytogenes* on intact fruit and vegetable surfaces during postharvest handling: a systematic literature review. *J. Food. Prot.* 83, 108–128. doi: 10.4315/0362-028X.JFP-19-283

McCollum, J. T., Cronquist, A. B., Silk, B. J., Jackson, K. A., Connor, K. A., Cosgrove, S., et al. (2013). Multistate outbreak of listeriosis associated with cantaloupe. *N. Engl. J. Med.* 369, 944–953. doi: 10.1056/NEJMoa121583

McLoon, A. L., Guttenplan, S. B., Kearns, D. B., Kolter, R., and Losick, R. (2011). Tracing the domestication of a biofilm-forming bacterium. *J. Bacteriol.* 193, 2027–2034. doi: 10.1128/JB.00722-08

Moura, A., Criscuolo, A., Pouseele, H., Maury, M., Leclercq, A., Tarr, C., et al. (2016). Whole genome-based population biology and epidemiological surveillance of *Listeria monocytogenes*. *Nat. Microbiol.* 2:16185. doi: 10.1038/nmicrobiol.2016.185

Muravnik, L. E., Kostina, O. V., and Shavarda, A. L. (2016). Glandular trichomes of tussilago farfara (senecioneae, asteraceae). *Planta* 244, 737–752. doi: 10.1007/s00425-016-2539-x

Murray, E. G. D., Webb, R. A., and Swann, M. B. R. (1926). A disease of rabbits characterised by a large mononuclear leucocytosis, caused by a hitherto undescribed bacillus *Bacterium monocytogenes*. *J. Pathol.* 29, 407–439. doi: 10.1002/path.1700290409

NSW Government, (2018). *Department of primary industries. listeria outbreak investigation. summary report for the melon industry*. Available online at: https://www.foodauthority.nsw.gov.au/sites/default/files/_Documents/foodsafetyandyou/listeria_outbreak_investigation.pdf (accessed March 18, 2023).

Oloketuyi, S. F., and Khan, F. (2017). Inhibition strategies of *Listeria monocytogenes* biofilms-current knowledge and future outlooks. *J. Basic Microbiol.* 57, 728–743. doi: 10.1002/jobm.201700071

Renier, S., Hébraud, M., and Desvaux, M. (2011). Molecular biology of surface colonization by *Listeria monocytogenes*: an additional facet of an opportunistic gram-positive foodborne pathogen. *Environ. Microbiol.* 13, 835–850. doi: 10.1111/j.1462-2920.2010.02378.x

Rieu, A., Briandet, R., Habimana, O., Garmyn, D., Guzzo, J., and Piveteau, P. (2008). *Listeria monocytogenes* EGD-e biofilms: no mushrooms but a network of knitted chains. *Appl. Environ. Microbiol.* 74, 4491–4497. doi: 10.1128/AEM.00255-08

Rodríguez-López, P., Rodríguez-Herrera, J. J., Vázquez-Sánchez, D., and López, C. M. (2018). Current knowledge on *Listeria monocytogenes* biofilms in food-related environments: incidence, resistance to biocides, ecology and biocontrol. *Foods* 7:E85. doi: 10.3390/foods7060085

Römling, U., Galperin, M. Y., and Gomelsky, M. (2013). Cyclic di-GMP: the first 25 years of a universal bacterial second messenger. *Microbiol. Mol. Biol. Rev.* 77, 1–52. doi: 10.1128/MMBR.00043-12

Tiensuu, T., Andersson, C., Rydén, P., and Johansson, J. (2013). Cycles of light and dark co-ordinate reversible colony differentiation in *Listeria monocytogenes*. *Mol. Microbiol.* 87, 909–924. doi: 10.1111/mmi.12140

Tsai, H. N., and Hodgson, D. A. (2003). Development of a synthetic minimal medium for *Listeria monocytogenes*. *Appl. Environ. Microbiol.* 69, 6943–6945. doi: 10.1128/AEM.69.11.6943-6945.2003

Welshimer, H. J., and Donker-Voet, J. (1971). Listeria monocytogenes in nature. *Appl. Microbiol.* 21, 516–519. doi: 10.1128/am.21.3.516-519.1971

Yaron, S., and Römling, U. (2014). Biofilm formation by enteric pathogens and its role in plant colonization and persistence. *Microb. Biotechnol.* 7, 496–516. doi: 10.1111/1751-7915.12186

Zetzmann, M., Okshevsky, M., Endres, J., Sedlag, A., Caccia, N., Auchter, M., et al. (2015). DNase-sensitive and -resistant modes of biofilm formation by *Listeria monocytogenes*. *Front. Microbiol.* 6:1428. doi: 10.3389/fmicb.2015.01428

Zhu, Q., Gooneratne, R., and Hussain, M. (2017). *Listeria monocytogenes* in fresh produce: outbreaks, prevalence and contamination levels. *Foods* 6:21. doi: 10.3390/foods6030021

Frontiers in Microbiology

Explores the habitable world and the potential of microbial life

The largest and most cited microbiology journal which advances our understanding of the role microbes play in addressing global challenges such as healthcare, food security, and climate change.

Discover the latest Research Topics

See more →

Frontiers

Avenue du Tribunal-Fédéral 34
1005 Lausanne, Switzerland
frontiersin.org

Contact us

+41 (0)21 510 17 00
frontiersin.org/about/contact